

V.N. Goncharskiy, N.I. Kalashnikov
and S.K. Kuzovkin

**Technical
Fundamentals
of
Aeroelectrical
Exploration**

NATIONAL AERONAUTICS
AND SPACE ADMINISTRATION
1974

TECHNICAL FUNDAMENTALS OF AEROELECTRICAL EXPLORATION

V.N. Goncharskiy, N.I. Kalashnikov and S.K. Kuzovkin

Translation of: Tekhnicheskiye Osnovy Aeroelektroz-
vedki, Kiev, "Naukova Dumka" Press, 1969, 380 pages.

NATIONAL AERONAUTICS AND SPACE ADMINISTRATION
WASHINGTON, D.C. 20546 FEBRUARY 1974

TT 71 - 53151

NASA TT F - 15,402 /

TECHNICAL FUNDAMENTALS OF AEROELECTRICAL
EXPLORATION (Tekhnicheskiye Osnovy
aeroelektrozvedki)
"Naukova Dumka" Press, Kiev, 1969, 380 pp.

Goncharovskiy, V.N. et al

Translated from Russian

Prepared for the National Science Foundation, Washington, D.C.
and National Aeronautics & Space Administration by Dr. Ismail Saad.

C O N T E N T S

<u>P A R T - I</u>		<u>PAGE</u>
1.	Chapter I - Classification and General Characteristics of Methods Applied in Airborne Electric Prospecting.	7
2.	Chapter II Methods of Airborne Electric Prospecting which use Harmonic Electromagnetic Field.	34
3	Chapter III Primary Harmonic Electromagnetic Field Used in Aerial Electric Prospecting.	66
4.	Chapter IV Some Data Regarding Normal and Anomalous Fields and Practical Results of Survey.	105
5.	Chapter V Quantities Measurable by Aerial Electric Prospecting.	146
 <u>P A R T II</u>		
6.	Chapter VI Principles of Planning Units and the Elements of Apparatus in Aerial Electric Prospecting - Generating Units.	171
7.	Chapter VII Construction Principles of Magnetic Fields Detectors.	214
8.	Chapter VIII Transmission of Signal of the Main Phase to the Measuring Apparatus of the BDK Method.	246
9.	Chapter IX Interferences in Amplitude and Phase Measurements and the Methods for Reducing Their Effect.	265
10.	Chapter X Construction Principles of the Measuring Apparatus	348
11.	Chapter XI Compensation of the Primary Field Signal in the Method of Induction.	466
12.	Chapter XII Recording of Measurable Parameters.	547
13.	Chapter XIII Measuring Errors and Increasing Accuracy of Measuring Instruments	573
14.	Chapter XIV Examples of Construction of Apparatus for Aerial Electric Prospecting.	661

ABSTRACT

The monograph correlates results of many years work of various Scientific Research Institutes of the Soviet Union, in particular of the Physico-mechanical Institute of the Academy of Sciences of the Uzbek SSR, as well as of these in other countries, in the sphere of methods and apparatus development for the geophysical serial electric prospecting of useful minerals. It presents an estimate of the primary electromagnetic fields. Gives analysis of interferences of various origins, affecting the receiving-measuring channel. Discusses electric compensation methods of the primary field signal, etc.

It is meant for specialists of general and geophysical instruments engineering and geophysical electric prospecting. It should also be useful for students of corresponding trades.

Ch. Editor B.I. Blazhkevitch

Dr. of Techn.Sciences.

FOREWORD

In the general complex of geophysical investigations, both in USSR and in other countries, the importance of aerial geophysical prospecting progressively increases.

At present the following methods are being applied in the aerial geophysical prospecting: photosurveying, magnetic prospecting, gamma-ray and gravity surveys and electric prospecting (6, 9, 26, 27, 51, 103, 142, 158, 240). Each one of the indicated methods has its own characteristics and limits of application. Magnetic prospecting and gamma-ray survey could be rated as the most highly developed method, gravity survey as the least. During the last decade electric prospecting has become widely adopted in airborne geophysical investigations.

The aerial geophysical investigations were initially conducted in Soviet Union in 1939 by A.A. Legatchev and A.T. Mainbered, who used magnetometer in experimenting during a flight (26). In 1939 the All Union Geological Institute (VSEGEI) has founded the first aeromagnetic party in the world.

In other countries the airborne geophysical investigations have begun considerably later. Specially in USA this type of investigations were not conducted until 1946.

Aerial geophysical prospecting has the advantages of low cost, high speed of operations, possibility of investigating roadless areas as well as inaccessible areas ground-work and continuity and objectivity of measuring results. The shortcomings of these methods are complexity of operations in high mountain conditions and difficulty of horizontal alignment in these localities.

The initial development of aerial electric prospecting was begun only in the fifties. The idea of creating this type of methods for prospecting was nascent as far back as the thirties-forties (168, 202, 203). However, the realization was hampered by non-availability, at that times, of high-response noiseproof measuring apparatus, capable of operating in flying conditions.

The first practical attempt to switch over from ground electric prospecting to airborne was undertaken in 1946 in Canada by "Lundberg Exploration Co." Investigations on a small scale were carried out by means of generating and receiving apparatus, but the results obtained were found to be inconclusive.

The most successful, apparently, was the apparatus of another Canadian firm "Internation Nickel Co." With the use of this firm's apparatus a discovery was made in 1950 of massive sulphides deposit in New Brunswick (Canada). Then in 1955 appeared the apparatus of the swedish firm "ABEM", the apparatus of "American metal and Co.", two-frequency apparatus of the Canadian firm "Aeromagnetic Service Ltd., Toronto" and others. The indicated apparatus was operated, as a rule, by the induction method with the use of harmonic fields (6, 158, 258, 263, 267).

The typical features of the first developments outside of USSR were their advertisement and "secrecy". Each firm or company advertised its own version of aereoelectric prospecting, without any serious analysis of its realistic possibilities. Recently the curtain of secrecy has been to some extent lifted (166, 167, 211, 254, 263), but not enough for an exact concept of principles in design of the apparatus, nor of the methods applied for interpretation of obtained results.

In the Soviet Union the aerial electric prospecting is developing systematically. It's scientific fundamentals and industrial applications are coordinated by the Ministry of Geology of USSR and Academy of Sciences

of USSR.

Scientific organisations of the Institute of Earth's physics (IKZ) of the Academy of Sciences of USSR, Moscow State University (MGU), All Union Scientific Research Institute of Methods and Technique of Geophysical prospecting (VITR) of the Ministry of Geology of USSR, All Union Scientific Research Institute of Prospecting Geophysics (VIRG) of the Ministry of Geology of USSR and others, are resolving theoretical questions and problems of interpretation, and substantiating spheres of application and the possibility of applying airborne electric prospecting for geological mapping and exploration of useful minerals.

The co-workers association of the Physico-Mechanical Institute of the Science Academy of Uzbek SSR (formerly Institute of Mechanical Engineering and Automatics of the Academy of Sciences of Uzbek SSR) is actively participating in the development of apparatus for aerial electric prospecting. As a result of extensive scientific research, many important questions relating to the methods and technique of electric prospecting have been resolved. Principles have been laid down for designing, generating and measuring apparatus for certain methods, which have found application in the national geophysical practice.

The first method-testing aerial electric prospecting in USSR was conducted in 1957-59 in the area of Maidan-Villa r.st. of Shepetovsky District in Khmel'nitsky region of Uzbek SSR. The tests were conducted by two methods - method of infinitely long cable (BOK) and method of induction (plane version with an out-board gondola) (89, 102, 103, 105, 123, 132). Using experience of the testing and production work of aerial electro-prospecting apparatus, many organisations began intensive development of known and new versions of the indicated methods. Thus, VITR has developed a version of induction method with the use of revolving magnetic field (VMP), Institute of automatics and electrometry of the Academy of Sciences of USSR has suggested a method of aerial electro-prospecting with the use of the natural magnetic field of

Earth*, etc.

In the development of various systems of apparatus for airborne electric prospecting primary consideration was paid to experience accumulated, as a rule, in small organizations. As a result many methods were suggested with various technical indices and sets of apparatus with many types of characteristics (competence of generating unit, response of receiving unit, working frequencies, etc.).

At present the number of methods for airborne electric prospecting has attained several scores. It should be mentioned, that the induction method has the highest rate of development (63, 66, 67, 117, 181, 234, 263).

In the national development of aerial electro-prospecting, the work of Western Khazakstan and Novosibirsky geophysical combines is of high theoretical and practical value.

During the last few years many scientific works have begun classifying the results of aerogeophysical survey (41, 42, 63, 66, 69, 117, 216). Attempts were made to determine application limits of aerial electro-prospecting, specify problems resolvable by its means and to analyse the possibility of combining it with other aerogeophysical methods. Some major problems regarding data interpretation have been resolved. However, none of these works pay enough attention to the principles of instrument engineering, typical requirements of devices in flying conditions and many other problems.

*The same institute has developed and produced a set of devices for BDK method (method of infinitely long cable), different from those produced in Uzbek SSR and Ministry of geology of USSR (105, 118).

The number of problems resolvable by airborne electric prospecting continuously increases. Therefore it has become necessary to correlate the main data, relating to technical fundamentals of airborne electric prospecting generally and airborne electric prospecting with harmonic field in particular. The aims of the presented monograph is to systematise the technical fundamentals of the method with harmonic field.

The authors are sincerely grateful to Dr. B.I. Blaszhkevitch for his valuable advice in the preparation of manuscript.

Any critical remarks and suggestions should be sent to the following address: L'vov, ul. Mauchnaia, 5, Fiziko-mekhanicheski institut AN Usbek SSR.

.....

PART ONE
PHYSICAL FUNDAMENTALS OF AIRBORNE ELECTRIC
PROSPECTING WITH HARMONIC FIELD.

Chapt. I - CLASSIFICATION AND GENERAL CHARACTERISTICS OF METHODS APPLIED
IN AIRBORNE ELECTRIC PROSPECTING.

1. Problems of airborne electric prospecting.

Experience has proved the effectivity and economical expediency of this method, specially in inaccessible locality. It is being successfully applied in detecting and tracing of sulphide ore, electric mapping of large areas, the search of fresh water, problems of applied geology, etc. (163, 166, 170, 190, 201, 202, 209, 263).

Same as all the other geophysical methods of prospecting for useful minerals, airborne electric prospecting finds a wide range of application in combination with other aerogeophysical and ground methods of exploration (26, 166, 169, 184, 202). In some cases it may resolve independent problems, in others it gives the basic or auxiliary information in the interpretation of field material (6, 8, 190). But sometimes its application may be found altogether irrational (51, 202).

Diversity of problems facing airborne electric prospecting, variability of geological and physical conditions, in which it may be used as a form of aerial geophysical exploration, require different means for the study of measurable parameters, methods of interpretation and, moreover, assume existence of several already worked out methods of airborne electric prospecting.

For a resolution of a certain problem the choice of method for airborne electric prospecting is predetermined by two main criteria. The first is connected with physical properties and dimensions of the typical conductive body, which is being sought, the second - with geological

conditions, topography or with chemical and physical features of the exploration area. Effectivity of airborne electric prospecting is determined also by rational selection of method for aerial investigations and correct interpretation of obtained results.

From reconnaissance and mapping to detailed exploration from the air of limited areas in the search for purely ore objects - is the range of problems resolvable by airborne electric prospecting. However for concrete geological conditions the number of these problems is, of course, limited and is subject for special investigations.

Unfortunately upto now, questions regarding development of concrete and specific problems, resolvable by airborne electric prospecting independently or in combination with other geophysical methods have not as yet been clearly formulated and are not elucidated, neither by special literature, nor by any text books, which limits to a certain extent its application.

Concretisation of problems, resolvable by airborne electric prospecting is at present of approximate nature. In spite of the considerable scope of work, carried out in various geological conditions, the obtained data are interpreted mainly qualitatively. However this gap will be filled up with accumulation of experimental material and resolution of a number of theoretical problems and questions of mechanical interpretation of survey results.

Before characterising the range of problems, resolvable by airborne electric prospecting, let's point out the main advantages of utilizing variable electromagnetic fields in geophysics.

1. More complete resolution of inverse geophysical problem, i.e. discrete determination of the physical properties of the source of anomaly and its

geometrical parameters (in airborne electric prospecting development of these questions is still in the initial stage).

2. Amplitude-phase measuring of electromagnetic fields in a wide range of frequencies with the aim of classifying geophysical anomalies of ore and rock products (this advantage is widely applied in practice).

Application of frequency characteristics is most important in composite geological-geophysical conditions in the presence of highly conductive cover of variable thickness and also non-uniform enclosing rocks (it is precisely because of this, that multifrequency detailed survey on anomalous sections, detected during explorations, is considered to be a necessary stage of field work).

3. Possibility of exploring certain types of ore, lacking the continuous galvanic conductivity.

The main disadvantages of using variable electromagnetic fields in geophysics include discovery side-by-side with highly conductive ore, anomalies of large quantities of rock products; comparative complexity of fields, which hampers theoretical calculations in resolving inverse geophysical problems; appearance of distorting effect of surface non-uniformities with increasing frequency of the field.

At present the variable current electric prospecting utilizes electromagnetic fields with frequency from tens cycles per second to hundreds of kilocycles. Low frequency airborne electric prospecting of objects with very high electric conductivity has certain advantages over the high frequency one. The most important of these is the considerable depth of investigations, i.e. the possibility of detecting deep-seated conductive bodies. The high frequency airborne electric prospecting is worth while on objects of comparatively high resistance. It should be pointed out, that both the advantages and disadvantages of using variable magnetic fields in airborne

electric prospecting become more perceptible with higher frequency of electromagnetic oscillations.

Various versions of devices for airborne electric prospecting by method of induction with one or two airborne apparatus have become quite popular. Conditions, in which eddy currents are generated in conductive body under the effect of primary field, built-up by the generator frame, depend in this method on relationship between the generator frame and the deep-seated conductive body. At the

It is a known fact (180), that with horizontal position of generator frame the maximum bond exists in the case, when the conductive body (bed) is also occurring horizontally or at a flat slant in relation to horizon. But with the vertical generator frame maximum bond exists with a body bedded at depth in a vertical plane, and specially, when the plane of the vertical generator frame is parallel to the plane or the strike of this body.

Therefore, depending on the problem of exploration it is possible to apply different versions of aeroinduction with the use of vertical and horizontal generator frames. Thus, in the search for sulphides, specially in the areas of Pre-Cambrian Shield, it should be kept in view, that an overwhelming majority of massive sulphides occur vertically. In this case generator frame, mounted in vertical plane, will have a maximum bond with the conductive object. It means, that the aerial method for prospecting should have a vertical set up (horizontal direction of magnetic moment) of the generator frame, etc.

In the opinion of majority of authors (7, 203, 209), the induction method could be more expediently used in resolving problems of geological mapping and recognizing exploration of areas with possible mineralization, since very often these are the areas with wide anomalies of considerably greater magnitude than the ore areas, which are invariably connected with massives of rocks, forming large structural shapes. Problems of geological

mapping are related to the problem of discovering areas, where it is possible to apply other aerogeo-physical method and to carry out ground explorations of one or another type of useful minerals.

Similar problems could be more or less resolved by aerial method of infinitely long cable (BDK) and of radiokip. For instance, airborne electric prospecting by BDK method has greater mapping possibilities than the induction method. This may be explained primarily by the possibility of conducting small scale survey at comparatively low altitude of flight and by the nature of the field, formed by the land group. The advantages of BDK method increase considerably with the use of helicopters in the search for ore deposits in extremely rugged region. Application of helicopter versions of airborne induction method is limited by the dependence of survey results (specially with amplitude determinations) on the altitude of helicopter's flight in these conditions.

The aerial radioactive method of prospecting should be used combined with other airborne geophysical methods for exploration of useful minerals. Physical and technical prerequisites of suitable conditions for airborne electric prospecting by radioactive method are assumed to be the following (202, 204): sufficiently high difference in electric conductivity of the sought for geological object and enclosing rocks; uniformity and constant thickness of overburden and its high resistivity; non-presence on working profiles of electric transmission or communication lines, pipe-lines, railway lines and other man-made conductors.

It follows then, that airborne electric prospecting by radioactive method could be used in resolving problems of geological mapping, detecting zones of tectonic dislocations and, sometimes, in suitable conditions, for exploring and tracing of sulphide ore bodies. Successful application of this method is also possible in resolving problems of applied geology and hydro-geology.

Such is the general outline of the range of problems, which are being resolved at present by means of airborne electric prospecting. Undoubtedly, in time the limits of its application will widen. Its methods will become more perfect and will assure effective resolution, both of general and concrete geophysical problems.

2. Classification of methods.

Geophysical investigations are divided into surface, subsurface and aerial. A place of importance among the latter is taken by aerial electric prospecting, development rate of which has considerably increased during the last 10-15 years. During this time considerable number of methods and their modifications for this type of prospecting have been developed, sometimes so similar in their physical principles and practical application, that it is difficult to select operative methods either for the resolution of general, or specific problems of geophysical investigations.

Classification of geophysical investigation methods, which from a common theoretical point of view present a picture of the present state of airborne electric prospecting as a whole, will make it possible to determine ways for development and improvement of the methods themselves, as well as of the schemes of installations and apparatus for their practical implementation.

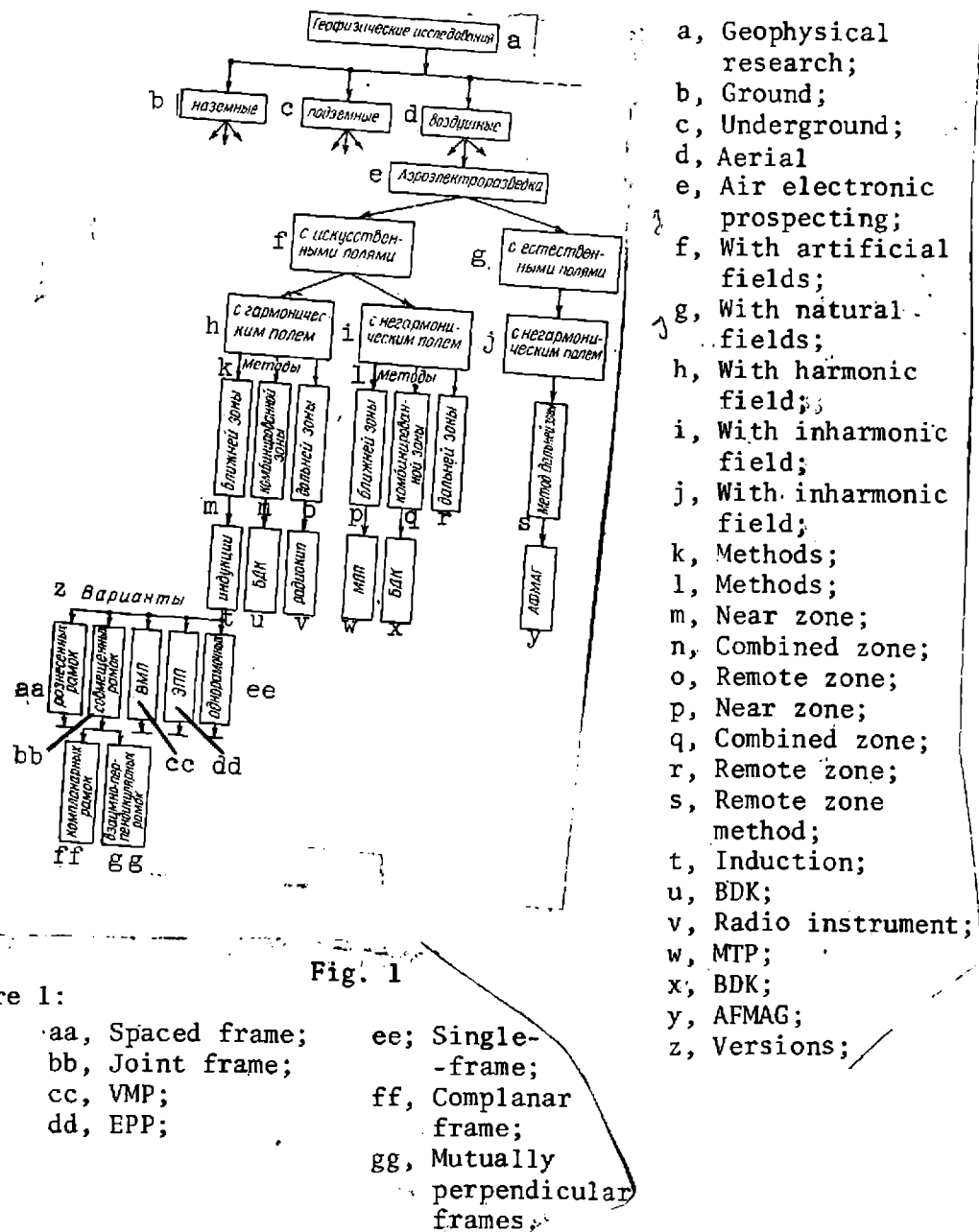
To resolve this problem N.I. Kalashnikov and S.K. Kuzovkin have based classification of the modern methods of geophysical investigations on the following distinctive criteria:

1. Type of the applied sources of electromagnetic field.
2. Time and nature of the radiated electromagnetic field.
3. Interpretation methods of the survey's results.
4. Technique of survey (geometry of installation, i.e. disposition

* See book "Geophysical apparatus, 33. "Nedra", Leningrad, 1967.

system of the sources and receivers of the field; excitation methods of the primary field sources and the methods for investigating variations of this field, etc.

On basis of the first classification sign methods of the airborne electric prospecting could be divided into two large groups: methods using artificial electromagnetic field, and methods using the natural electromagnetic field.(fig.1).



In construction of apparatus, development of methods and technique for interpretation of survey results the significance is of the second classification sign. Nature of the radiated electromagnetic field specifies, on one hand, construction of the generating and receiving devices of the first group of methods, and on the other - determines methods for measuring parameters of this field and specifies a number of characteristic features for the conduct of survey and interpretation of its results, as well as for plotting schemes of apparatus for one or another method of airborne electric prospecting.

From the time nature of the radiated electromagnetic fields practically all methods of the first group (with artificial electromagnetic fields) could be reduced to two subgroups: 1) methods using harmonic field; 2) methods using non-harmonic electromagnetic field. It is logical, that in the group of methods with natural fields there is only one subgroup with non-harmonic fields, which, as we know, are built-up by far away thunderstorms.

In defining the third classification sign, it should be mentioned, that all the methods of airborne electric prospecting are based on the properties of only the variable electromagnetic field. These properties for normal and anomalous fields, used in the airborne electric prospecting, are analysed theoretically in three zones; near, combined and remote.* Accordingly the methods suggested are in principle distinct from each other in theoretical premises, as well as in the interpretation methods of survey results; induction method, which uses nearest zone to emitter of harmonic field; radio method using the furthest zone; method of combined zone - airborne electric prospecting by BDK method.

*The zone, where ^{wave}length of electromagnetic wave λ is considerably greater than distance r between the emitter and receiver of electromagnetic field, is denoted as the near, zone with $\lambda \ll r$ - furthest and the zone, where $\lambda \gg r$ or $\lambda \leq r$, - combined.

The fourth classification sign could form a basis for apparatus modification or a version of some definite method of aerial electro-prospecting. In ^{much} as this sign is of technical, and not theoretical nature, the number of apparatus modifications and method versions is unlimited, which is confirmed by practical experience. For instance, the highest number of versions pertains to the subgroup of methods using harmonic field of the nearest zone. The electromagnetic primary and anomalous fields in the zone of induction, even though dependent to a considerable extent on the geometry of the system, can be depicted in their majority by simple terms, convenient for using comparatively simple methods for interpretation of survey results. However not every geometry system of the generating and receiving frames location in space has unambiguous exploration possibilities (depth, resolving power, efficiency, etc.) and moreover not every geometry could be easily realised by the present technical means.

Application of different versions of the nearest zone method, when the use is of one aircraft and outboard gondola, two aircrafts apparatus with combined generating and receiving frames or with their discrete set up, indicate, that the interest aroused by this method is as great as ever (66, 67, 117, 132, 180, 181).

Thus, the most highly developed are the methods of airborne electric prospecting with artificially built-up electromagnetic harmonic fields. The natural non-harmonic fields can be applied only with methods of the remote zone, since the flight of aircraft in the vicinity of the thunderstorm center is dangerous.

Certain difficulties of theoretical and constructional nature are present in the use of non-harmonic fields. Possibilities of methods with this type of fields are not as yet fully discovered. Therefore the subgroup of methods using the non-harmonic fields happens to be less developed, although the

premises are there for their intensified development with accumulation of experimental data.

The diversity of methods and their variants of airborne prospecting indicate, on one hand, their wide range of application, and on the other - that at the present development stage of geophysical investigations technique they are still far from perfect. It should be mentioned, that till the 60-s many airborne electro-prospecting methods and the pertinent apparatus were being developed on premise, that they will simultaneously resolve two problems of geophysical investigations: geophysical mapping and exploration of purely ore bodies (8, 42, 201, 209, 251). But in practice the effectivity of one or another method was evaluated, unfortunately, only by resolution of one of the indicated individual problems and not always objectively.

Our problem is to throw some light on the main aspects of the airborne electric prospecting with the use of only the harmonic field. However to get the general idea of this method as a whole it would be expedient to analyse characteristics of other methods also and of their exploration possibilities.

3. Brief description of methods.

In ground electric prospecting with the use of artificial electromagnetic fields the emitters applied are of various types. The field is usually excited by means of a long wire grounded at the ends, coil or loop fed by alternate current, also by means of antenna of broadcasting radio-stations. In the first case the coupling of field source with earth is voltaic, in other - inductive.

In airborne electric prospecting the emitters of electromagnetic field are the same as in surface electric prospecting. The field emitters could be fed by harmonic and non-harmonic currents. The more prevalent are the generators of harmonic current, but the non-harmonic current generators may also be used, if current impulse, for instance, has a rectangular shape (31, 254, 263).

In distinction from those used in surface electric prospecting, field receivers in airborne electric prospecting, due to continuous motion of apparatus in the air, should not have voltaic coupling with the ground. Receivers of magnetic and electric fields could generally be broad-band. But most often the receivers, specially of magnetic field, are tuned in to resonance on working frequency of the field emitter. In this case even with non-harmonic current of the emitter these methods may be used only for the study of a narrow spectrum of signals near some frequency of non-harmonic current source.

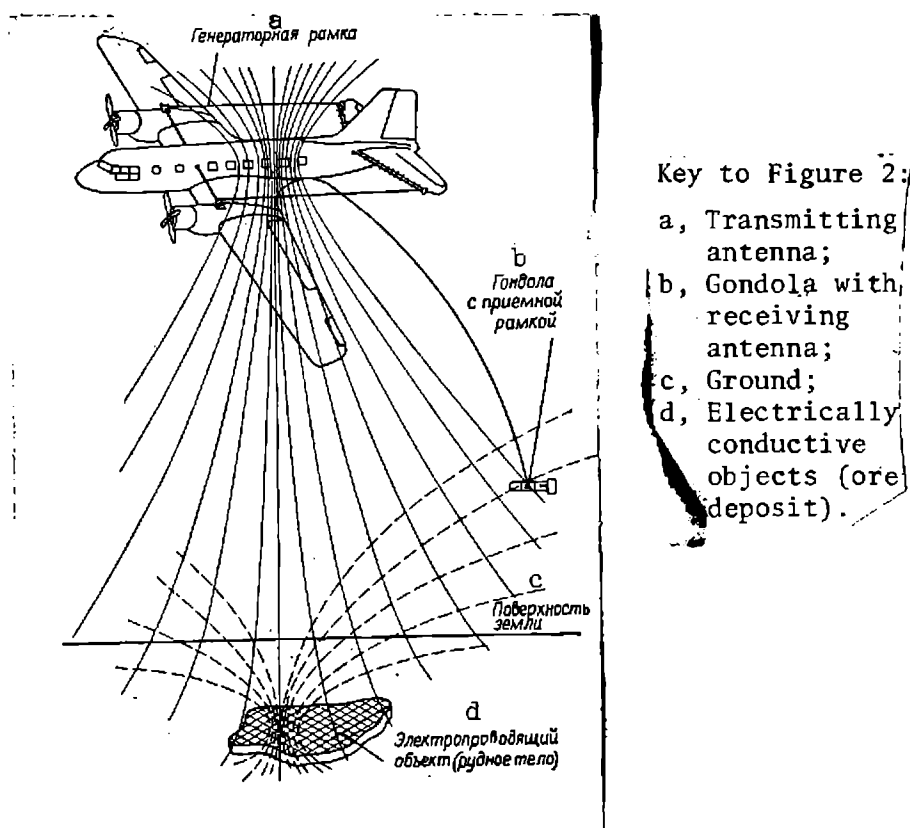


Fig. 2.

Among the methods of the nearest zone the most popular is the induction method, in which as an emitter of harmonic electromagnetic field the application is of a multiturn framework, stretched above the fuselage of aircraft or set up in special outboard gondolas. In this case the receivers of magnetic field are the multiturn inductance coils with core or without, set up usually in the outboard gondola.

Diagram showing the principle of airborne electric prospecting by induction method and the outside view of the plane in air with the set up electroprospecting station is shown in Fig. 2.

The primary magnetic field is built-up around the plane and in the ground with conductive ore body by means of the generating frame. During the aircraft flight this field pierces the ore body and the ground, composed of rocks with similar or different from ore body conductivity, and builds up within them eddy currents. Intensity variation of these currents, recorded in flight along a profile, depends on the conductivity ratio of ore body and the adjacent beds, and the currents themselves build-up the so called secondary field of the same frequency as the primary. At the point of gondola's location the receivers of magnetic field receive the resultant field, while the measuring instruments, set up on the plane, record parameters of signal from this field after its preliminary electric compensation.

In relation to conductance of bodies, encountered within the working profile, there is variation of the intensity and phase of the electric signal, induced in the receiver of field; this is marked as anomaly on record diagrams.

The vector diagram, showing interdependence between the intensity vectors of primary \vec{H}_1 , secondary \vec{H}_2 and resultant \vec{H}_p fields, is shown in Fig. 3. Here \vec{H}_{2a} - vector of active component, and \vec{H}_{2p} - vector of reactive component of the secondary field (direction of vector \vec{H}_1 is taken as the

starting, i.e. the system of coordinates is determined by the current direction in the field's source).

Fig. 3.

Conditions, in which eddy currents are build-up in conductive body under the effect of the existing primary magnetic field, depend largely on the interdependence between the field emitter and the deep-seated conductive body. Inasmuch as the overwhelming majority of massive sulphide formations is usually vertically bedded (see para 1 of the present chapter), the optimum location plane of the loops of field sources is vertical. With this orientation of the primary field source the effect of flat-bedded conductive bodies, including rock products (bogs lakes and surface deposits), is reduced to a minimum.

Thus, the position of generating frames and field receivers can generally be various. However in practice orientation of the generating frames is being often determined only by the type of utilized aircraft and the maximum area of the frame that it can provide (increasing magnetic moment).

The simplified structural diagram of two-frequencies apparatus for the aerial induction method is shown in Fig. 4. The exciter of the field is the rectangular primary frame 4, stretched between the center of airplane wing and stabilizer. The frame consists of two sections, joined into common band. Each section is fed from a corresponding competent amplifier 2, deriving excitation on working frequency of a double-frequency generator 1 with quartz crystal control.

The receiving coils 6, tuned to resonance, and the preliminary (gondola) amplifier 7 are set up in gondola, which is towed by the plane on a wire cable about 150 m in length. Signals of both frequencies, transmitted from the output of gondola amplifier along the cable, are fed to compensator 8.

Compensating voltage from selection circuit of compensating signal 3 is also fed in here. By amplitude and phase adjustment of the compensating voltage compensation is attained of intensified electromotive force, induced in each receiving coil on working frequencies of the apparatus. At the output of compensator the signal of working frequency is separated and amplified by selective amplifier 9, after which it enters into phase indicator blocks 11 and phase response voltmeter 13-15.

The basic signal for the phase-indicator is the voltage of driving oscillator preliminarily combined by means of phase-shifter 5 with signal phase at the output of the selective amplifier. Amplitude, phase and the component are recorded by registers 10, 12 and 16 respectively.

The circuit of phase voltmeter is based on the circuit of synchronous detector. With the reactive component recording of the measurable signal (after compensation) the supporting voltage, fed to signal, makes a phase-turn at 90° in relation to signal phase. In this type of circuit the output voltage is automatically compensated by servo mechanism 14 and 15.

The apparatus is fed from the electric circuit of the aircraft by transforming the direct current into alternate. The airborne electric prospecting with airborne instruments is usually carried out at an altitude of 150 m by parallel profiling. The length of each profile is 50-100 km. Distance between profiles is determined by the scale of the geophysical survey.

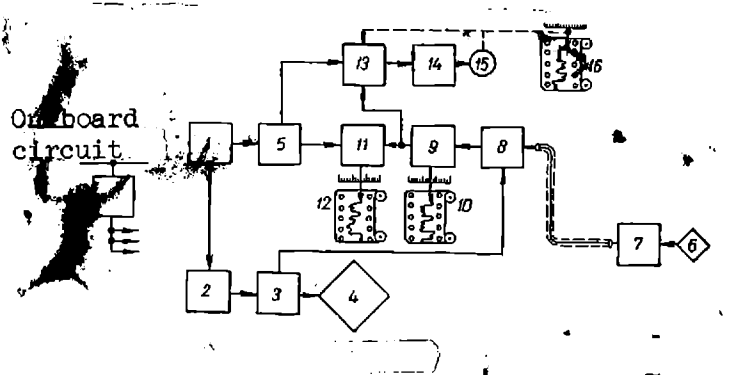


Fig. 4.

Depth of the airborne electric prospecting by induction method is determined by the following factors: a) working frequency, stop-down of which increases the depth (98, 251); b) distance between the source and receiver of the field, i.e. by the carrying about of the frames (with an increased within certain limits carrying the primary field considerably decreases, which produces an increased response of the instruments to anomalous variations of the field); c) vertical distance to conductive body; d) sensitivity of receiving and measuring instruments, etc.

Increase in the actual response of devices, meant for work in conditions of considerable interferences of various origin, including those, specified by the method selected, is the most difficult problem. In certain systems, developed abroad, the response of receiving and measuring devices is upto 0.001-0.0015% of the primary field magnitude (263). This type of high response (several hundreds of times greater than that of ground devices) will permit localisation of fine conductive bodies. If the apparatus is practically without inertialess, which is quite possible with harmonically time-varying primary field, the aerial geophysical survey could be carried out at aircraft speed upto 200-250 km/hr. In this case one of the decisive factors is the time, which enhances effectivity of airborne electric prospecting 100-200 times as compared to ground methods.

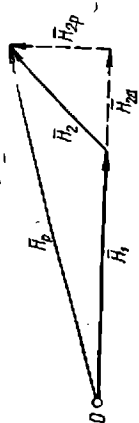


FIG. 3.

As an example of combined zone method, in which the primary field is built-up by means of current in cable grounded at both ends, may serve the BDK method (6, 30, 103, 216). In this method the measuring instruments are set up on the aircraft, and the generating jointly with cable - on the ground. Parameter measuring of the electromagnetic field of the cable is carried out within an area covered by the normal work zone of measuring apparatus. The nature of the field is affected by the medium, in which the cable field is distributed. By measuring field parameters from the air, it is possible to study properties of the medium, which composes the investigation

area, i.e. to resolve the problem of airborne electric prospecting (75).

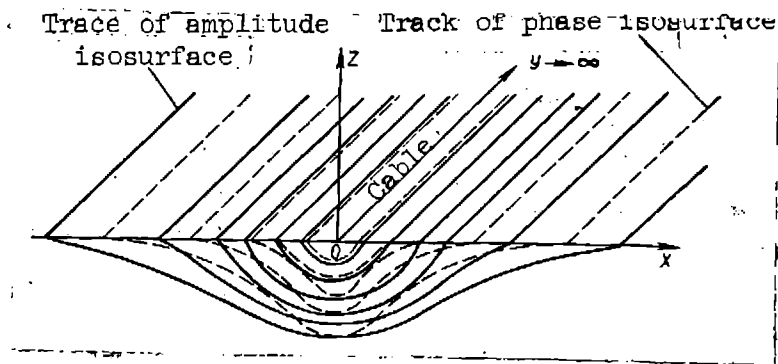


Fig. 5.

Typical nature of the field of infinite length cable is shown in Fig. 5, according to which the highest density of amplitude and phase isoplanes is evident near the cable; with the removal from cable along the OX line, density of lines decreases. Therefore, the measuring range of the field's parameters along the OX line should be considerable and should depend primarily on the distance to cable, on which the apparatus will function normally. In other directions (OY), (OZ) this relationship is weaker.

a, UHF radio station; b, 100-150 MHz; c, UHF radio station; d, 2.3-3.2 MHz; e, Detector receiver and phase meter; f, Radio transmitter for carrier signal; g, Carrier signal receiver; h, Voltmeter; i, Module; j, mkV;

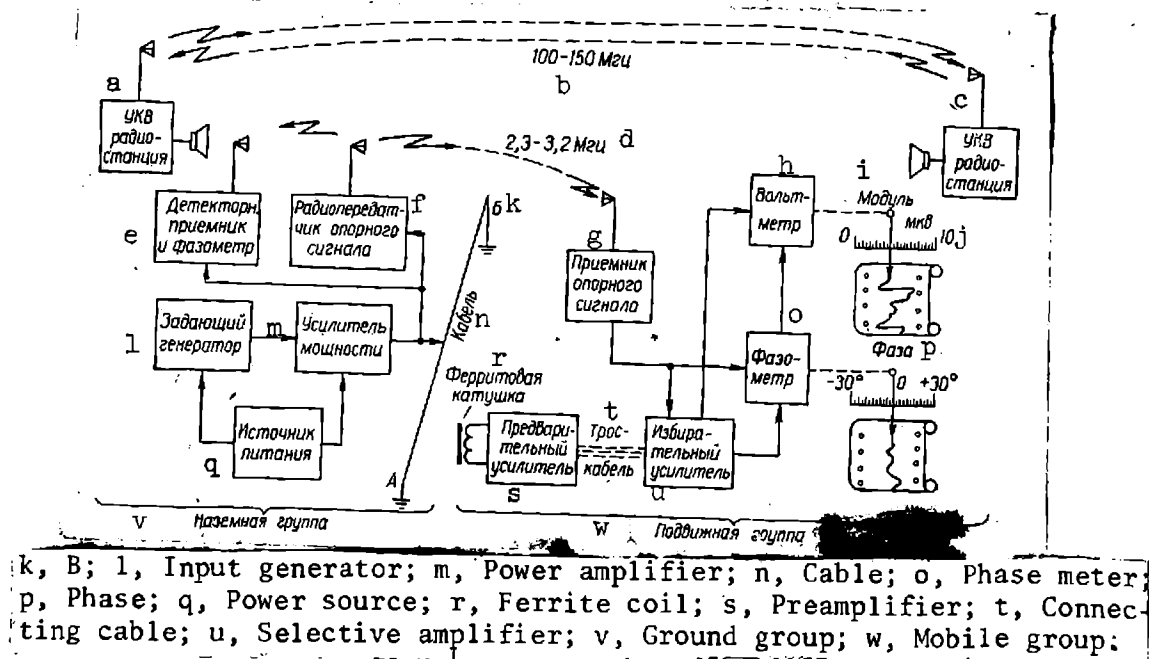


Fig. 6.

Block diagram of apparatus, used in airborne electric prospecting by BDK method is shown in Fig. 6 (the ferrite coil and preliminary amplifier of the mobile group set are taken out into outboard gondola on connecting wire).

The ground group with the generating apparatus is usually placed in the center of the survey area. To both sides of the ground group an insulated cable is laid out over 10 km in length. The initial point of cable pieces is joined to the input of power amplifier, and the ends are grounded by means of dowels at points A and B (see Fig. 6). To build up the electromagnetic field, alternate harmonic current, produced by the generating apparatus, is put through the cable. Investigations of electromagnetic field are implemented by means of measuring instruments of the mobile group. Fig. 7 shows helicopter MI-4, equipped with BDK devices. The flights are across the cable along parallel profiles (line OX, see Fig. 5).

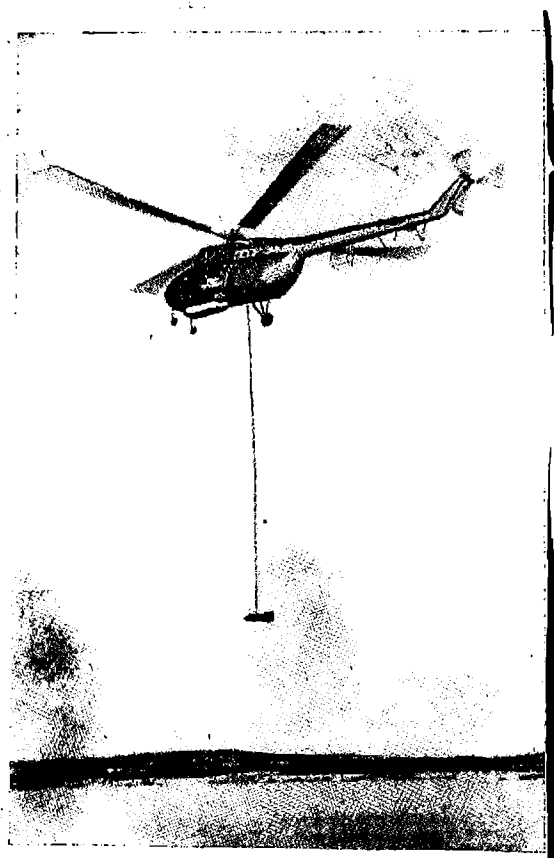


Fig. 7.

Power of the ground group apparatus is supplied by the mobile power plant. For the study of amplitude-phase characteristics of the electromagnetic field from the air, the apparatus is provided with a transmitter of key signal of ultrashort wave length range. The phase of the key signal emitted into the air, is controlled by phase-indicator, to which the signals are fed from the shunt, out-in sequentially to cable, and demodulated signal of working frequency from the output of detector. For command communication the ground and mobile groups are provided with ultrashort wave length radiostations (in frequency band 100-150 megacycles per second).

Apparatus of the mobile group provides for the reception and demodulation of the key signal (by means of signal pickup), reception of the investigation electromagnetic field (by means of ferrite coil), as well as determination and recording of amplitude and phase of e.m.f., induced in the coil by the field (by means of measuring devices).

During the flight the apparatus records "normal" field of the cable and its anomalies, which are intercorrelated at adjacent profiles.

In airborne electric prospecting by remote zone methods, which study fields of broadcasting and special radio-stations, the use is made of ordinary or special radioreceivers-registers of special appliances, assembled according to the circuits of devices for measuring amplitude-phase characteristics of the field. Survey technique is not different from the above described, but the interpretation methods differ considerably (204, 221, 222).

The problem of enhancing effectivity of airborne electric prospecting of the near zone with artificially excited harmonic fields is closely related with the resolution of two main problems. The first consists in assuring sufficiently accurate measurements of the very weak secondary fields intensity in the presence of artificially built-up primary fields, which in many cases have considerable intensity (sometimes exceeding many times the intensity of secondary fields). The second problem is to provide an effective safe-guard of

measuring instruments from interferences, arising with random changes during the flight of the reciprocal position and orientation of the source and field detector.

These problems are resolved by methods of airborne electric prospecting with non-harmonic fields, i.e. by methods, which permit to divide in time the effects on detector of primary and secondary fields. This division is possible if the source of primary field is energized by rectangular impulses (e.g. by direct current impulses) and the specifics are studied of the setting up process of electromagnetic field in-between the next impulses. The nature of this setup is specified by the non-uniformity of sections at the point of determinations. In the practice of geophysical investigations this method is called the field set up method or the method of transient processes (MPP)(31, 62, 263).

The specific feature of the MPP is its multifrequency, as the rectangular current impulse shows itself as a sum of harmonic oscillations with various amplitudes and phases.* Nature determination of the field's setting up at different times after the moment, when exciter impulse ceases, permits direct division of obtained anomalies into these of ore and rock products.

The ore anomalies are characterised by a drawn out setting up process, the rock product anomalies - by its quick damping. Therefore measurements made during the first moments after termination of impulse, assume presence in the area mainly of rock product anomalies. Measurements taken later indicate the presence of purely ore objects or mineralized deposits.

Thus the transient process method is one of the most promising. The MPP apparatus is being developed in USSR, as well as abroad. However, as

*Resolution of a direct problem, i.e. calculations of magnetic field, are carried out the most simply and expeditiously by spectral method, principle of which is the presentation of periodic sequence of rectangular impulses as Fourier series.

some works indicate (75, 218, 254), development of different versions of the non-harmonic field method encounters considerable technical difficulties.

Firstly, due to the presence in the vicinity of field source of considerable metallic mass of the aircraft it is difficult to assure in the generator frame steep fronts of current impulses, specially of the rear ones. Secondly, it is difficult to design field detector, which would in fact be inertialess. This is necessary even if only to prevent, in the presence of current impulse within the source of primary field, accumulation in field detector of electromagnetic energy from this current (field). Thirdly, it is technically difficult to produce measuring device, capable of assuring cut-in of field detector exactly at the termination moments of current impulses in the source and determination of the initial setting up of excited field.

In development of apparatus of foreign firms ("Input", "Selco", etc.) the principle used is the setting up of electromagnetic field. Thus, in the apparatus "Input" (1959) the application is of a large horizontal generator frame, set up above the aircraft, through which current is transmitted during 1.5 msec. The detector of electromagnetic field is set up in the gondola horizontally and at a perpendicular to the direction of the flight. The gondola is towed by a 150 m wire cable. The measurements are carried out 0; 400 and 1200 msec after cessation of impulse. Since after the cessation of impulse eddy currents and the secondary electromagnetic fields, built-up by them, decay, the system actually investigates decay characteristics of electromagnetic field at different times at three points of reading.* It is obvious, that with changing geometry of source-detector system there is no methodical interference in this version of the near zone method.

* The apparatus of "Input" system additionally records amplitude at the start of reading from two receiving frames - horizontal and vertical.

It is possible to suggest other versions of the system, similar to that analyzed, but the technical difficulties in their implementation are quite considerable (61, 108, 254, 263). Therefore, there is still a lot that has to be done towards the development of apparatus and interpretation technique of obtained results.

With development and widespread use in aviation of methods for locating various objects, based on the reflection from them of electromagnetic energy signals there was an emergence of airborne electric prospecting by radiolocation (75,210). However, the technical realization of this method also faces considerable difficulties. First of all the requirement is of competent impulses, period of which does not exceed fractions of microsecond. This is explained by the fact, that the period of impulse should be shorter than its travel time from the energy emitter to object and from the object to locator, as the operation of device is based on utilizing radio-echo. The reflected signal should not return before the radiation of probing impulse will terminate. The propagation velocity of radio-waves is high, therefore with possible competence and existing designs of receiving and measuring devices, when the altitude of survey cannot be considerable, and the objects are comparatively close, the emission time of signal should comprise an extremely small fraction of a second, i.e. the apparatus has to be ^{of} high-frequency.

The use of radio-location method is also hampered by high absorption of high frequency electromagnetic oscillations energy by rocks, as a result of which level of the useful reflected signal, i.e. the energy level of electromagnetic, wave, reflected from conductive body, is found to be too low. It is assumed, that this can be avoided by stacking of useful signals. Therefore, the stacking of reflected (secondary) signals or division of probing and reflected signals according to the ~~phase~~^{phase} provides a possibility of detecting and recording of locally bedded conductive bodies (46, 710). This

75, 210). This assumes, that the objects of geophysical investigations are stationary and, thus, all the prerequisites for the realisation of the method are present during a flight.

For the airborne electric prospecting it is possible to utilize the event of self- and reciprocal induction between the oscillating circuit and the conductive body. In this case the oscillating circuit could function simultaneously as the low frequency source of the primary magnetic field (for an assured magnetic coupling with the object) and the pickup, in which e.m.f. of self- or reciprocal induction. The efficiency of this method is determined by the obtained parameter stability of the ^{proper*} oscillating circuit and of the measuring device, as well as by the extent of compensation in measuring circuit of primary voltage on the oscillating circuit. Since in this case there are no changes in geometry of source - field detector system (no methodical interference), it is quite possible to attain, without any considerable difficulties, a high degree of compensation, at the subtraction factor (see para 3, chapt. II) comprises $10^{-5} - 10^{-6}$. Moreover, there is an actual possibility of measuring both the e.m.f. of self-induction and e.m.f. of reciprocal induction. In addition it is possible to measure variations, under the effect of conductive bodies, of total (active and reactive) resistance of oscillating circuit or its natural resonance frequency and its Q-factor (234).

*The experience of manufacturing low-frequency oscillating circuits shows, that the stability of their parameters in time and with temperature variations of the surrounding medium could be very high, if special care is taken for thermo-stabilization and compensation of the circuit's components.

During the last few years in USSR and abroad the application has become wide-spread of methods, based on the utilization of natural electromagnetic fields (106, 169, 234, 269). Their development and practical application are of considerable interest for geophysical investigations, since this eliminates the presence in the set of instruments of quite bulky and inefficient in respect of energy generating devices. In this case the weight and overall size of apparatus becomes considerably reduced, which makes its production and operation cost less, and the output higher.

The origin of natural electromagnetic fields is not yet fully known. However it is possible to assert, that the main source of these fields is the lightening discharge (109, 156, 195). Since these, as a rule, originate at a great distance from the place of operations, it is possible to assume, that these sources of primary field are practically at an infinitely remote distance. In this case the intensity of electromagnetic field is considerable even at a distance of several thousands kilometers from the center of thunder-storm (173, 195), i.e. source competency of natural electromagnetic field is immeasurably higher than that of powerful radio-stations. Due to considerable signal level of natural electromagnetic fields, the depth of investigations appreciably increases, geometry disruption of source-detector system does not affect the results, also there are other advantages, important for electric prospecting.

The nature of the lightening field is impulsive, and not steady harmonic; the frequency spectrum, in which the main part of energy is concentrated, comprises 60 cycles - 30 kilo cycles per second (270). Investigations show, that at a distance of over 5000 km from the source the maximum amplitude of the signal is evident on frequencies 60-70 ^{Hertz} cps (112). The intensity of electromagnetic field within the frequency band 10-100 ^{Hertz} cps

comprises approximately 10^{-5} a/m, and within the band of over 100 cps - from 10^{-6} to 10^{-9} a/m.

It is a well known fact, that electromagnetic energy, released during thunder storms, expands along a spherical wave-guide, limited by Earth surface and the base of ionosphere. With travelling along the uniform surface, the vertical component of the magnetic field attenuates considerably faster than the horizontal. As a result with great distance from the energy source (thousands of kilometers) the variable magnetic field, if its propagation is above a uniform and isotropic medium, becomes horizontally polarized. Thus, in area of geophysical survey the operations are usually with practically plane wave, having only the horizontal magnetic component (268, 270) If along the travel path of this type of wave there is a geoelectric anomaly, i.e. a body of electroconductibility, different from that of surrounding medium, reflection of the wave will cause the appearance of the vertical component of magnetic field. In this case it may be assumed, that the dip of polarization plane will depend on the conductivity of those sections of earth's surface, above the measurements are being conducted. Thus, from the nature of variations of the vertical component of natural electromagnetic field of Earth it is possible to judge the electric anomalies and to define areas, promising for exploration of useful minerals.

There are several versions of airborne electric prospecting using natural electromagnetic field. One of these is based on measuring absolute values of the field's characteristics. However due to the fact, that the intensity of electromagnetic field at any point of space could increase during a short period some tens of times (upto 40 db), practical application of this method is difficult. Taking this into account, the measuring is of those parameters of electromagnetic field, which are very little affected by

short-period, diurnal and annual variations, yet at the same time are extremely variable with the presence in the area of conductive bodies.

It may be assumed, that with sufficient averaging the total electromagnetic field, i.e. in the presence of conductive body, has a certain elliptic polarization. In this connection, the parameters, which are not dependent on the intensity of primary field, will be the following: small axis ratio of the elliptically polarized field to big axis, dip of the big axis and the inclination of polarization plane towards the horizon, also the semiaxis ratio of ellipsoid projection onto vertical plane and the angle of gradient of the big semiaxis of ellipsoid's projection towards the horizon (106).

In Canada development has been accomplished of the AFMAG apparatus, which serves for measuring the angle of gradient of the natural electromagnetic field polarization plane (aircraft version) (169, 269). The shortcoming of this method is a rather low intensity of the natural field. Moreover it is subject to seasonal and diurnal variations. The use of this apparatus in northern latitudes from 30 to 60 is only possible during summer (June-August and partially in September) for 3-5 hrs. Obviously with the presence in the area of lightning discharges the AFMAG method is inapplicable.

One of the AGMAG modifications provides for the location of detector in the outboard gondola, towed by wire-cable at a distance of 60-90 m from the plane. The angle of gradient in polarization plane is measured on frequencies of 90 and 340 ^{Hertz} ~~Hz~~ by means of two reciprocally perpendicular receiving frames, the planes of which are at an angle of 45° to direction of flight (169, 263). With a uniform and isotropic medium the signals,

taken off from the two frames, are equal, since the polarization plane is horizontal. But if the medium is non-uniform, the polarization plane has a definite angle of gradient towards the horizon, therefore the signals in the frames are not equivalent. The measurable difference of signals in this frames is compared and interpreted in conversion to angles of gradient. Ratio of low and high amplitude signals is used for comparing conductivity of anomalous objects. The direction of flight is across the strike of regional geological structures. Besides the plane version there is also a helicopter version of AFMAG. In this model the working frequencies are 150 and 590 Hertz.

The apparatus for measuring the true polarization ellipsoid is rather complex. Therefore it seems more expedient to develop apparatus for measuring projection parameters of ellipsoid onto vertical plane. In this case the ratio of semiaxis and the angle of gradient of the big axis to horizon can be measured even by means of two reciprocally perpendicular detectors, located in vertical plane. The work in this direction has only just begun. Institute of automatics and electrometry of the Academy of Sciences of USSR developed apparatus of LFM-3 type (ground version), meant for measuring the above indicated parameters, and also phase-shifting between signals, excited by total field (natural Earth field and geoelectrical anomaly field) in vertical and horizontal detectors (106).

It is presumed, that the apparatus LFM-3, set up on helicopter MI-4 or plane of the AN-2 type, will be used for the aerial version of the

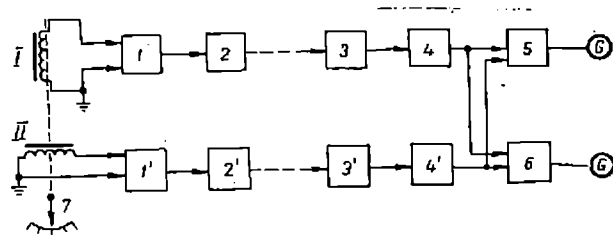


Fig. 8.

analyzed method for geophysical prospecting. To reduce the vibrations and the energy noise of the aircraft, the field detectors and some other part elements of the apparatus will be placed in the outboard gondola. The measurable parameters will be the amplitude ratio of signals, induced in two reciprocally perpendicular field detectors, angle of gradient of the polarization plane and the voltage phase-shift at the output detectors with their position fixed in respect of the flight direction. The main specifications of the airborne version of LFM-3 are similar to these of ground apparatus: working frequencies 80; 160; 240; 480; and 960 Hertz; measuring limits of polarization plane angle of gradient $\pm 45^\circ$; measuring limits of phase-shift between signals in vertical and horizontal frames $\pm 20^\circ$; amplitude values of measurable fields $10^{-4} - 10^{-7}$ a/m. The apparatus is implemented on semiconducting elements.

The block-diagram of the airborne version of LFM-3 apparatus is shown in Fig. 8. The block of input elements consists of two reciprocally perpendicular frames I-II (vertical and horizontal) with ferrite coils, elements of frame tuning into resonance for five fixed frequencies 1-1' and two preliminary amplifiers 2-2'. Signals, transmitted along the cable, are fed into measuring block, containing selective 3-3' and wideband 4-4' amplifiers, ratio-measuring device 5 and phase-indicator 6. Parameter reading may be implemented by measuring devices G (or registrators), cut-in to outputs of the ratio-measure and phase-indicator. The reciprocal perpendicularity set up of the frames is controlled by angle gauge 7.

CHAPTER II.

METHODS OF AIRBORNE ELECTRIC PROSPECTING, WHICH USE HARMONIC ELECTROMAGNETIC FIELD.

1. The nearest zone method (airborne electric prospecting by induction method).

The nearest zone method is based on studying the effect of currents, induced in ore bodies or in any other conductive bodies occurring within the top layers of the earth crust, on the primary electromagnetic field, generated artificially by alternate harmonic current of the oscillating frame, fixed on the aircraft or in the outboard gondola. This effect is defined by the varying magnitude and direction of the resultant field vector, i.e. by the field's anomalies (70, 263). The defined anomalies make it possible to resolve the inverse geophysical problem: the position of the geological objects, causing these anomalies, is identified and their qualitative appraisal is then carried out.

In airborne electric prospecting the direct carriers of information regarding the analysis of the electromagnetic field are the electro-motive forces, induced in detectors. Usually they are the multiturn induction coils with ferromagnetic cores or without them (see chapt. VII). When investigations are conducted by the nearest zone method, these detectors are set up mostly in the outboard gondola, occasionally directly on the aircraft (263).

The main problem of the measuring-recording instruments is to separate from signals, information connected with the secondary field, induced in field detectors, and to eliminate the effect of the primary field signal on the indications of these instruments.

At present there are many versions of the nearest zone method. They differ in the geometry of the source-detector system, method of electric compensation, the number of used aircraft, etc. According to the latter,

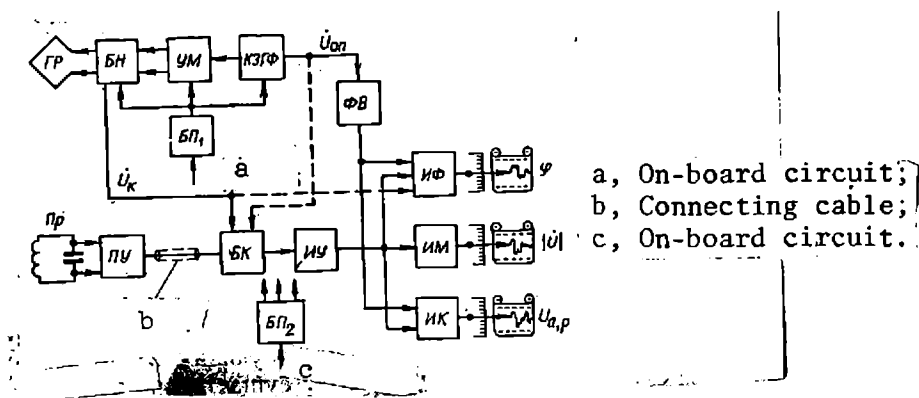
all versions of the method are divided into two large groups. The first group unifies versions concerned with the use of only one aircraft (plane or helicopter). The second group includes those requiring two aircrafts: one for the source, and one for the field detector.

Another distinguishing feature of the different versions of the nearest zone method is the number of magnetic field detectors, their disposition and orientation in respect of the field's source, and also the use of detectors in determination of the output values.

Versions of the first group: 1) the field's source is directly on the plane, and the detector in the outboard gondola, towed by wire-cable (21, 63, 103, 117, 123, 263); one plane with the use of rotating magnetic field (VMP) and outboard gondola for disposition of field detectors (117, 234); 3) the source and the detector are firmly fixed on the aircraft relatively close to each other (28, 263); 4) the source and the detector are firmly fixed in the outboard gondola of large size (117, 263, 264); 5) the receiving frame is coplanar or reciprocally perpendicular in the center of the oscillating frame (117), etc.

Versions of the second group: 1) circular rotating magnetic field (234); 2) linear polarization field (236, 237).

The block diagram of the apparatus, shown in Fig. 9, corresponds to the majority of versions in the first group. The exciter of the field is the oscillating frame ΓP , fed through its block of tuning to resonance $\bar{B} H$ by power amplifier $Y M$, which is excited on the working frequency from the master oscillator with quartz crystal control of frequency $K3 \Gamma \Phi$. The signal of working frequency, received by tuned to resonance field detector Πp and amplified by the preliminary amplifier Πy , is fed into the block of electric compensation $\bar{B} K$. The compensating voltage U_k , obtained either from



БН block or from $K3\sqrt{\phi}$ is also fed in the same block. By adjusting the amplitude and the phase of voltage U_k the necessary compensation of the signal, excited in the field detector by primary or resultant field is obtained.

From the output of the compensator the signal is fed into selective amplifier HY , in which the outside noises are suppressed. From the output of HY the signal is fed into circuits of measuring modulus HM , phase $H\Phi$

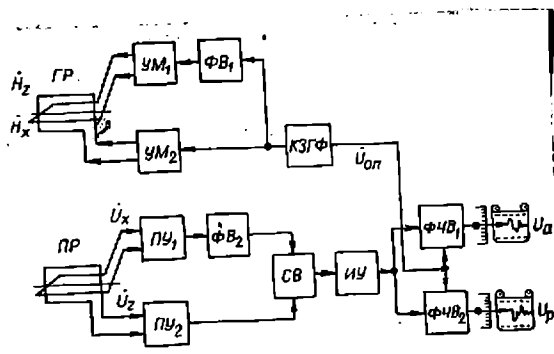


Fig. 10.

and component $\mathcal{H} K$. For phase-response instruments, the key signal U_0 is the output voltage $K3\Gamma\Phi$, previously combined by phase inverter ΦB with current phase in the oscillating frame. The recording devices are cut into meter outputs. The energy source of the apparatus is the power supply system of the plane, fed through blocks $\mathcal{E}\Pi_1$ and $\mathcal{E}\Pi_2$.

The block diagram of the apparatus for single-plane version of VMP is shown in Fig. 10. The reciprocally perpendicular oscillating frames ΓP are fed from power amplifiers YM_1 and YM_2 , which are excited by master oscillator $K3\Gamma\Phi$, and the exciting voltage to one of the power amplifiers, for instance YM_1 , is fed with phase-shift at 90° , implemented in phase-inverter ΦB_1 . In this way the feed of the oscillating frames by currents with phase-shift at 90° is attained. The reciprocally perpendicular receiving frames ΠP , tuned into resonance, are out into preliminary amplifiers ΠY_1 and ΠY_2 , the output signals of which are fed into the subtraction circuit CB. One of the output signals, for instance the signal of amplifier ΠY_1 , passes first through phase-inverter ΦB_2 , where it acquires the 90° phase-shift. The signal of imbalance from the output of the subtraction circuit is fed to the selective amplifier $\mathcal{H} Y$, and then to phase-response voltmeters $\Phi \mathcal{H} B_1$ and $\Phi \mathcal{H} B_2$ which measure the active and reactive component of this signal. The key signal U_{on} is the voltage of the master oscillator.

The block diagram of the oscillating group in the apparatus of a two-plane version of VMP is practically undistinguishable from that in Fig. 10. But the group of measuring instruments could be modified in various ways, depending on the measurable parameters of the imbalance signal. The supporting voltage for phase-response meters is the voltage of one of the measuring channels, for instance, the output voltage of amplifier ΠY_2 .

In some modifications of a two-plane pattern of VMP, the application is of a ratio circuit, instead of subtracting circuit, and the quantities measured are the imbalance of the circuit and the phase-shift between the signals taken (234, 236). In the instruments of the version with lineally polarized field, the oscillating portion is plotted according to the block diagram of one of the channels in the VMP apparatus, meant for the excitation of horizontal or vertical oscillating frame. The measuring part of the version under analysis and the VMP are similar, except for the orientation of the reciprocally perpendicular receiving frames.

The use of the outboard gondola in individual versions of the nearest zone aerial method causes some difficulties. These difficulties are most clearly evident in conditions of undulating relief and windy weather: the results are affected by the interferences caused by the variations of primary field signal generated due to the vibrations of the gondola (technical interferences). The vibrations of the gondola are intensified by windy weather and in conditions which contribute to the formation of air pockets. The latter circumstance is of importance to aerial electro-prospecting, as the useful signal cannot sometimes be measured on account of the magnitude of this type of interference (see para 6, Chapter IX).

To eliminate this deficiency, versions were worked out (for plane and helicopter), with the exclusion of the outboard gondola. In this case the receiving frames are placed directly on the aircraft in a firmly fixed streamlined unit. The rational disposition of the oscillating and receiving frames on the plane or helicopter assures considerable reduction in the noise caused by changes in the geometry of the system of vibrations. The minor depth of prospecting is compensated to some extent by the high response of the apparatus, the low altitude of the flight and the high mobility of the aircraft. These versions have also other positive qualities

and are, therefore, quite promising for carrying out large-scale (detailed) survey (63, 117).

Let us examine briefly the main versions of the apparatus for the aerial method of the nearest zone and its salient characteristics:

1. Versions in which the field detector is located in the outboard gondola, towed by aircraft by means of wire cable from 20 to 100-150 m in length. In this case the perception is of the vertical or the horizontal component of the primary field* and the recording is of its variations, caused by the secondary field effect; the drift angle of the gondola is $45-90^{\circ}$. The same pattern was used for the national devices of AERIC and AERI-2 type (21, 102, 117, 123), in which the drift angle of the gondola does not exceed 65° .

In the plane or helicopter version, when the drift angle of the gondola is 90° , the source and field detector are "firmly" fixed on one aircraft (28).

2. "Canadian"(plane) version, when the field detector, sensing horizontal component of the primary field, is located in the gondola with drift angle 45° . According to the testimonials of foreign firms, this version is more successful than any of the preceding ones (63).

3. Helicopter version, when the oscillating and receiving frames are located on the same vertical line, i.e., the drift angle of the gondola is approximately zero. This version is applied with a comparatively low speed of horizontal flight.

* By the vertical component of the primary field is meant the component in the direction of the magnetic moment of oscillating dipole, vertically oriented (horizontal oscillating frame), and by the horizontal component - the component perpendicular to the vertical and located in the plane of flight.

4. Version without an outboard gondola with source and field detector located at opposite ends of the plane's wings, i.e. at a comparatively short distance (28, 235), and other similar versions (233, 262, 263, 265), for instance, the helicopter version of "Canadian Aero Sikorsky Helicopter" (263). In this modification the range of frames has been increased in order to enhance the depth of investigations. With this aim the big oscillating frame, placed perpendicularly to the direction of the flight, and the receiving frame, which measures the vertical component of the field, were set up on special brackets in the nose and tail respectively, of "Sikorsky-55" helicopter (Fig. 11). The distance between frames covered 18 m. The devices measured active and reactive components of the signal, excited by the vertical component of the primary field on frequency of 390 cps.

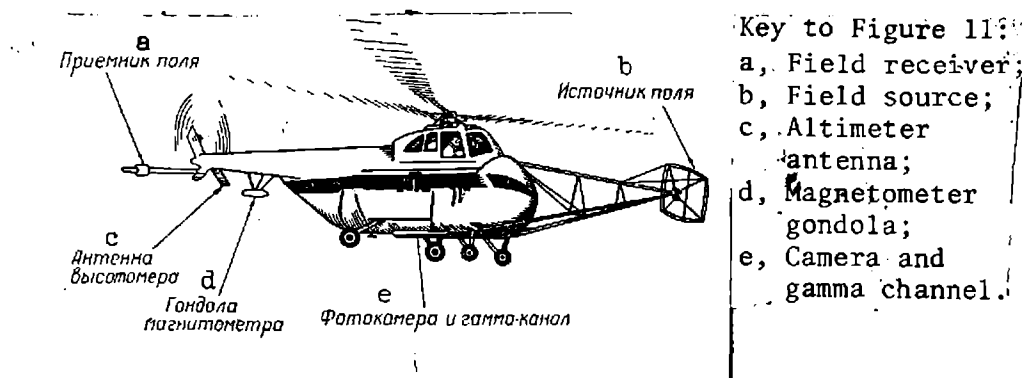
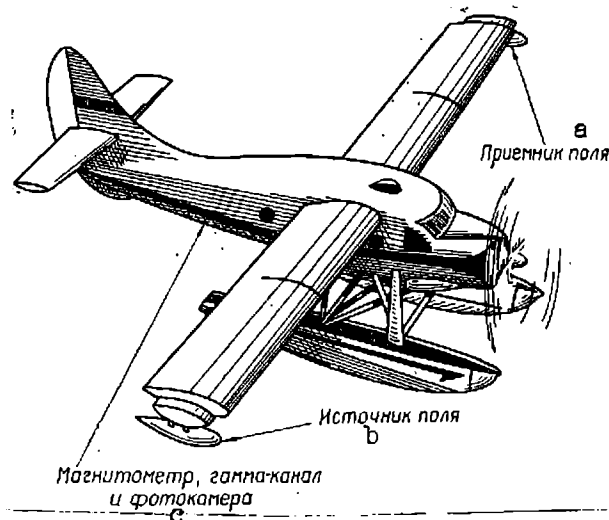


Fig. 11.

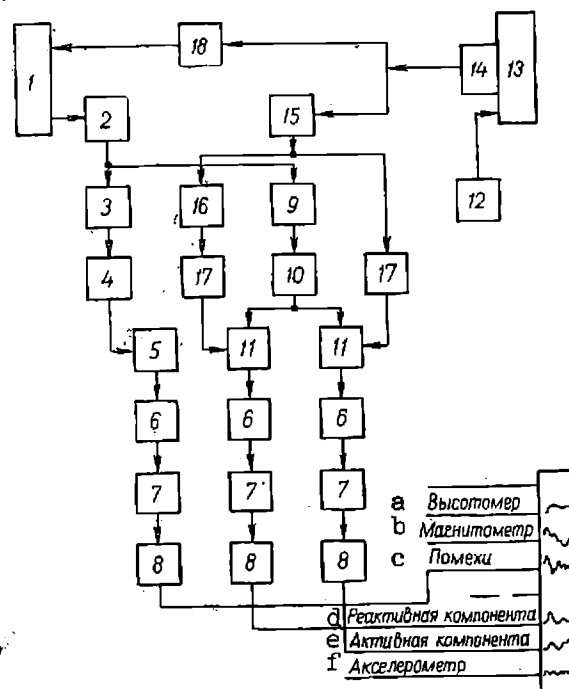
Notable among the plane versions is the "Canadian Aero Otter" (263), mounted on a hydroplane "Otter" (Fig. 12). This apparatus measures active and reactive components of the vertical or horizontal constituent of the field on frequency 320 cps. The oscillating and receiving frames are set up on the ends of wings; the distance between them is 18.6 m.



Key to Figure 12:
a, Field receiver;
b, Field source;
c, Magnetometer,
gamma channel
and camera.

Fig. 12.

Another example of the apparatus for the plane version of the induction method in the first group with a rigid position of the source and the field detector is the Mullard apparatus (28), a block diagram of which is shown in Fig. 13.



Key to Figure 13:
a, Altimeter;
b, Magnetometer;
c, Noise;
d, Reactive
component;
e, Active
component;
f, Accelerometer.

Fig. 13.

The primary electromagnetic field is generated by the current in oscillating frame 13, set up in the same way as the detector of the magnetic field (receiving frame) 1, at the ends of plane wings. The frame is fed by an alternate current of working frequency from the oscillator 12. Cut into the circuit of this frame is a small frame 14 of compensating and key signals, from which voltage is taken for compensation of e.m.f., induced in the magnetic field detector 1 by the oscillating frame field. The setting of the required amplitude and of the initial phase of compensating voltage is implemented by the balance circuit 18, consisting of an attenuator and a phase-inverter. The signal is compensated during a flight at high altitude, which excludes the effect of any ground conductors. Therefore, the decompensation signal at the output of the field detector, which appears during the flight at normal altitude, is taken in this apparatus as useful (anomalous).

The anomalous signal enters, through preliminary amplifier 2, band filter 9 and linear amplifier 10, into inputs of phase-response detectors ($\Phi\Pi$) 11. The output voltages of $\Phi\Pi$ are proportional, respectively, to the active and reactive components of the anomalous signal, being in phase and quadrature with the current in the oscillating frame. To ensure for this condition the supporting voltage, frame 14 taken off through filter 15 is fed into one of the phase-response detectors through phase-shifting circuit 16 and amplifier 17 and into the other - only through amplifier.

The output signals of the phase-response detectors pass through integrating circuits 6, coordination hookups 7 and are then fed to amplifiers 8 of the eight-channel recorder, one channel of which is used for recording noises. With this aim the signal from the output of preliminary amplifier 2 is fed into detector 5 through band filter 3 and linear amplifier 4. Then, similarly, with the preceding registration patterns (blocks 6-8),

the signal enters the recorder. The other channels are used for recording magnetometer, accelerometer or radiometer data, time-breaks and orienting-points.

The apparatus operates on frequency 320 cps. The recording of atmospherics is done on frequency 268 cps. To separate weak anomalies, adjustment of the frequency pass band (integrator 6) is provided.

5. One-plane version of a circular rotating magnetic field. This type of magnetic field is generated by aircraft located on two reciprocally perpendicular oscillating frames 1 (point O), in which the currents are phase-shifted at 90° . Two receiving reciprocally perpendicular frames 2, the planes of which are parallel to the planes of the oscillating frames, are located in the outboard gondola (point P), towed by wire-cable (Fig.14). The signal, sensed by one of the receiving frames, turned in phase at 90° and is subtracted from the signal, sensed by the second receiving frame. In this way the reciprocal compensation of signals, excited in both the receiving frames by the primary field is attained. Inasmuch as the anomalous effects along the vertical and horizontal constituents of the secondary field differ substantially (8, 117, 200), the reciprocal compensation, with the presence in the flight area of conductive objects, is broken off. The measurements of the difference of signals, excited by the primary field, and also of the phase-shifts between them are taken.

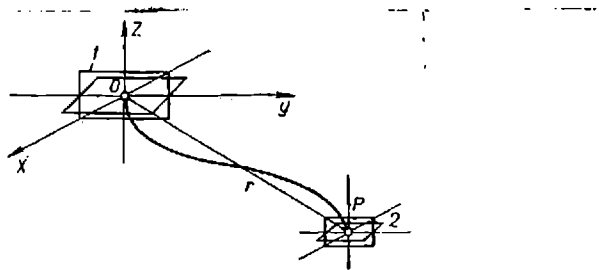


Fig. 14.

This version of the aerial induction method was developed by the Swedish firm "Bolindens Gruv. A.B." (267). Distortions of the circular field, caused by the metal parts of the plane or by its body, are eliminated by adjustment of the angle between the planes of oscillating frames and the control of the current phase in one of them. The reciprocal compensation of direct signals, induced in receiving frames by the primary field, is effected by subtraction from the signal, sensed by the vertical frame, of the signal perceived by the horizontal frame signal phase is preliminarily shifted by 90°). The working frequency is 3600 cps. The apparatus measures and records the active and the reactive components of the signal, induced in receiving frames by the resultant field.

The block diagram of one of the modifications of the rotating magnetic field patterns, developed in Sweden, is shown in Fig. 15 (211). The oscillating device contains two similar reciprocally perpendicular oscillating frames 2 and 3, energized from oscillator 1, through devices 4 and 5, which provide the current-shift in frames 2, 3 by 90° and control the intensity of these currents. The receiving unit has frames 6 and 7, one of which is horizontal and the other vertical. The pivotal axis yy in the

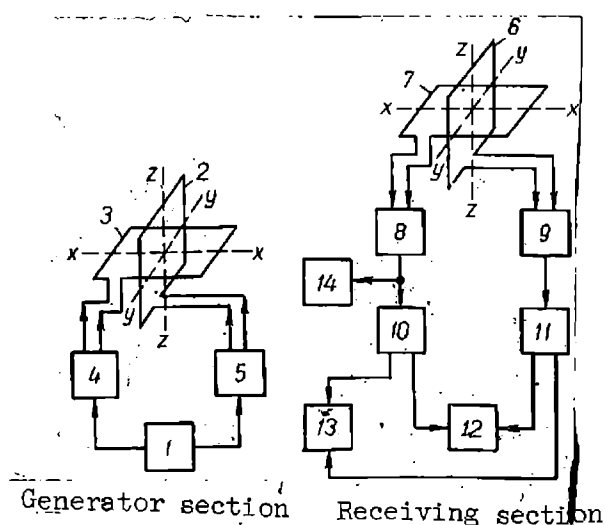


Fig. 15.

system of oscillating and receiving frames should coincide as precisely as possible. Both frames of the receiving unit are out into phase-inverters 10 and 11 through preliminary amplifiers 8 and 9. The phase-inverters shift voltages, induced in these frames, by 90° . The difference of voltages (block 12) and their phase-shift (block 13) in their initial state (after blocks 10 and 11) should be equal to zero. To outputs of blocks 12 and 13 are cut in devices for recording the amplitude and the phase-shift with the appearance of the secondary field from a conductive object. The higher anomalous signal will be induced in vertical frame 6, in the horizontal it slightly varies; therefore, the intensity of voltage at the output of this frame may serve as a measure of the normal field. Indicator 14 records the amplitude of voltage at the output of frame 7, and since it varies in inverse proportion to the cube of the distance between the oscillating and receiving frames, it is used for distance-determination between them. Receiving frames and preliminary amplifiers are placed in the outboard gondola, towed by the plane. The altitude of flight is 120 m. The length of the wire cable is 50 or 150 m. The working frequency is 880 cps.

The compensation stability of the direct signal with the varying geometry of the system in this version is not very high, whereas the apparatus is quite complex. Therefore, it never became popular and was eventually transformed into a two-plane version.

6. Versions with combined oscillating and receiving frames are meant for large-scale. Surveys on a previously investigated area. The small space between the frames decreases the depth of investigations. However, their mobility is high, flight altitude comparatively low and the applied apparatus gives a higher response, which to some extent compensates for the reduced depth.

The "Aeromagnetic Survey Ltd." have developed an apparatus in which the oscillating and receiving frames are located in one large gondola, transported by helicopter (258). The frames are placed perpendicularly to the axis of the gondola; the distance between them is about 9 m. The diameter of the frames is approximately 0.6 m. The working frequency is 4000 cps. With some modification of the apparatus (two vertical receiving frames were located on the same axis with the horizontal oscillating frame on both its external sides) a sufficiently high and more reliable compensation of the direct signal was attained.

The "American Metals Helicopter Co." (263) has developed an apparatus fitted on helicopter "Bell." The oscillating and receiving frames are in the gondola. The apparatus measures the active and the reactive constituents of imbalance signal on frequency 1000 cps (two different frequencies may also be used). The axis of the frames is common and their planes are reciprocally perpendicular.

In the Soviet Union these versions of the nearest zone aeromethod were not developed.

7. Helicopter version, when two field detectors, meant for the reception of the vertical or horizontal constituent of the field, are placed into the outboard gondola of large dimensions on both sides of the horizontal oscillating frame also placed there. The source and field detectors are firmly fixed one with the other (63). Plane and helicopter

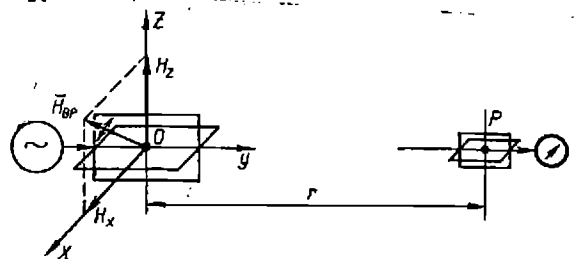


Fig. 16.

versions have also been developed; in these the receiving frame is placed either coplanar or reciprocally perpendicular in the center of the primary (oscillating) frame (117, 263 and others).

Versions of the circular rotating magnetic field and linearly polarized field belong, as has been pointed out, to the second group, which uses two aircrafts. Let us briefly analyse these versions.

1. The version of the circular rotating magnetic field is implemented by means of two planes, flying one behind the other in the same direction at a distances of 100-300 m. On one of the planes are set up the oscillating frames, similar to those in the one-plane version, and on the other, in outboard gondola - two reciprocally perpendicular receiving frames, the planes, of which are parallel to those of the oscillating frames (Fig. 16).

With equal amplitude of magnetic moments of the oscillating frames, the resultant vector of the primary magnetic field at points, lying on the flight axis of the plane carrying the oscillating frames, revolves around this axis within a plane perpendicular to the axis, with angular velocity equal to angular frequency of the exciter current. In other words, the field at these points is polarized in a circle. The outboard gondola with the receiving frames, transported by the second plane with the wire cable 20-30 m in length, should be on the flight axis of the first plane.* It is obvious that, with a uniform external medium, the inducement in receiving frames will be of alternate voltage U_x and U_z , multiple values of which U_x and U_z are equal in modulus, but differ in amplitude by 90° . Therefore,

* From the navigational point of view it would be more convenient if the plane with the measuring apparatus and the outboard gondola would fly first, i.e. be the leading one, and the plane with the oscillating devices - second (following)(211).

if one of these voltages is turned into the corresponding direction by 90° and subtracted from the other, the resultant signal will be equal to zero.

The appearance near the given set up of conductive body will disrupt the attained balance. In this case the apparatus will be measuring parameters of imbalance signal $\Delta U = U_x - jU_z$ (its amplitude, phase, active and reactive components)/260, 265/. It is also possible to measure difference $U_x - U_z$ or U_x/U_z ratio of the virtual values of these voltages and phase-shift between them.

The most significant advantages of this version:- sufficiently stable compensation of the primary field signal, which is theoretically not upset with distance variation between frames, and also the high spread of frames, possible within the range of 200-400 m, permitting increase in the tangible response and depth of the method. Therefore this version of the near-zone aeromethod is referred as the most effective /117, 211, 234/. Its main shortcomings:/ simultaneous use of two planes in conditions of complicated navigation and the difficulty of setting up in practical conditions an exactly circular rotating magnetic field.

In 1959-1961, the All Union Scientific Research Institute of Methods and Technique of Prospecting (VITR) made and tested three sets of apparatus for the rotating magnetic field (working frequencies of apparatus - 2450, 1225 and 612.5 cps). The first was meant for plane LI-2, the second and third - for planes AN-2 /230, 234/.

The block diagram of generating devices in the two-plane version of the rotating magnetic field is practically the same as the diagram of the one-plane version. But the instrument, meant for measuring the intensity parameters of imbalance U , could be made in various modifications, depending on which parameters of imbalance signal it is required to measure amplitude, phase or components /231/. Fig. 17 a shows outside view of the generating assembly of the RMF (rotating magnetic field) apparatus, and

Fig. 17 - b of the measuring assembly.

However, considering that in the two-plane version of RMF it is difficult to maintain the co-axial alignment of the source and field detector, it was suggested that the double rotating magnetic field (DRMF)/227/ be used.

The substance of the DRMF version consists of the following. Currents of two frequencies - the working and the auxiliary are passed through oscillating frames. The second frequency should be considerably lower than the first as, with sufficiently low frequencies, anomalous effects are hardly present in the induction methods of aerial electric prospecting /99/. Currents of various frequencies may energize also discrete frames, which should be firmly interconnected. In this way, there is a build-up of two rotating magnetic fields, having identical configuration in non-conductive medium. These fields are generated in two receiving frames of two frequencies e.m.f. The intensities of working frequency, obtained from two reciprocally perpendicular receiving frames, similar to frames of the RMF version, are reciprocally subtracted after division by frequency filters and phase-shift in one of them at 90° , and the residual intensity is rectified (this applies also to the intensity of auxiliary frequency). For receiving fields of various frequencies, it is possible to use also different frames, tuned in resonance at working frequencies, provided there is a rigid connection between them. In this case the dividing frequency filters are not required.

By fixing a definite ratio between the intensities of exciting currents of the working and auxiliary frequencies in oscillating frames and adjustment of the receiving unit's response on the working and auxiliary frequencies, an equal intensity of rectified voltages in channels of both the frequencies is attained. Apparently, this equality is not upset at any

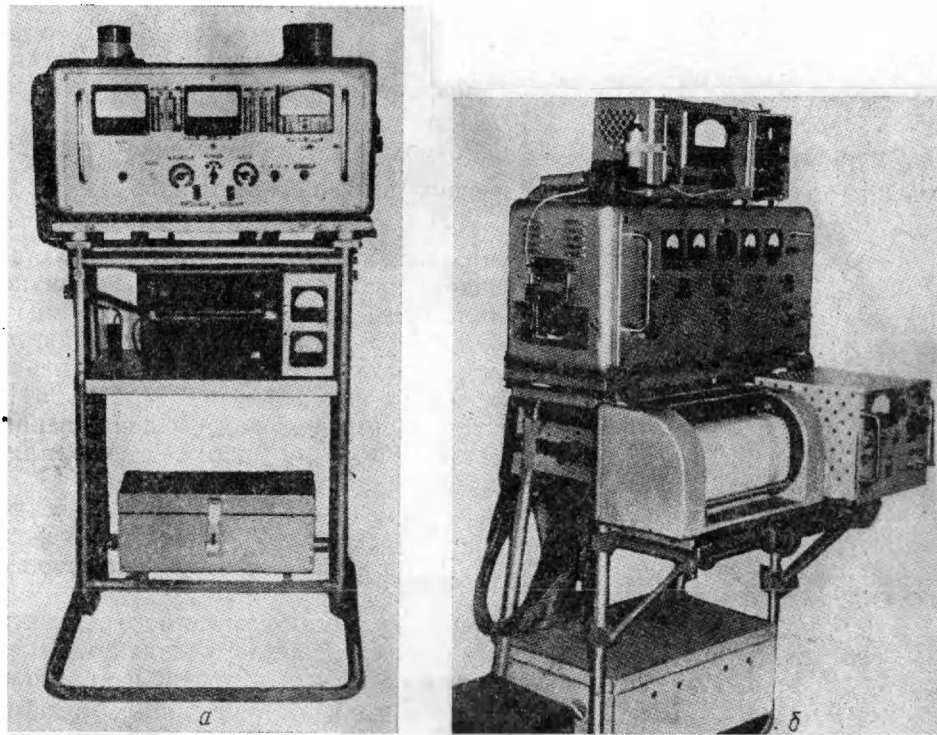


Fig. 17.

point of space, if the fields of the working and auxiliary frequencies have identical configuration. The rectified voltages are fed to the device meant for measuring out put. Thus, false anomalies, connected with reciprocal position-variation of oscillating and receiving frames, are eliminated in the non-conductive body.

Ore and other conductive bodies generate an anomalous field on the working frequency, and not at all on sufficiently low auxiliary frequency. This considerably simplifies separation of anomalies from ore bodies, when the false anomalies, are eliminated due to disruption of coaxial position of the source and field detectors.

Thus, the essential thing seems to be the application of two rotating fields, radiated by common emitter or two firmly joined emitters, and a common field detector or two firmly joined detectors, placed on the axis of the rotating fields and insensitive to fields with circular polarization, to shifting of the field detector relatively to the source along the axis of the rotating fields and to the slowing of the field detector around this axis. Response to objects with higher conductivity could be intensified due to the increased response of measuring apparatus, since the unstable position and inaccuracy of orientation of the field detectors practically do not contribute to the appearance of false anomalies.

However, it should be mentioned that the apparatus of DRMF method is quite complex and expensive in making and use.

2. The version of the linearly polarized field was tested in 1962 by the All Union Scientific Research Institute of Technique and Methods. The apparatus for this version is based on that for the rotating magnetic field [236, 237]. One plane carries horizontal oscillating frame, and the other an outboard gondola with two receiving frames. The perpendiculars of the frames are located in the flight plane YOZ and inclined at an angle of 45° to vertical line, i.e., axis OZ (Fig. 18). The receiving frames are

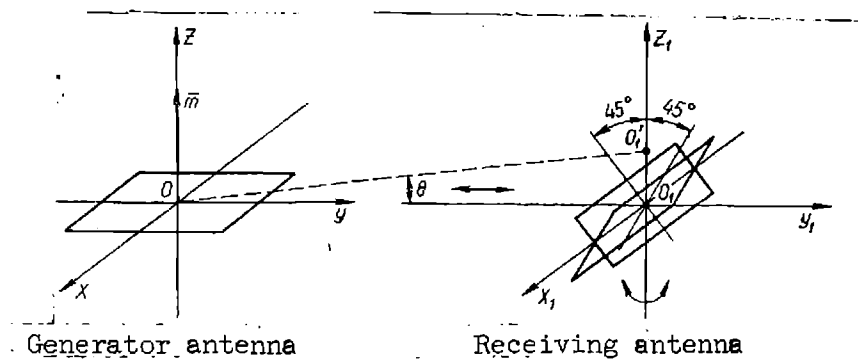
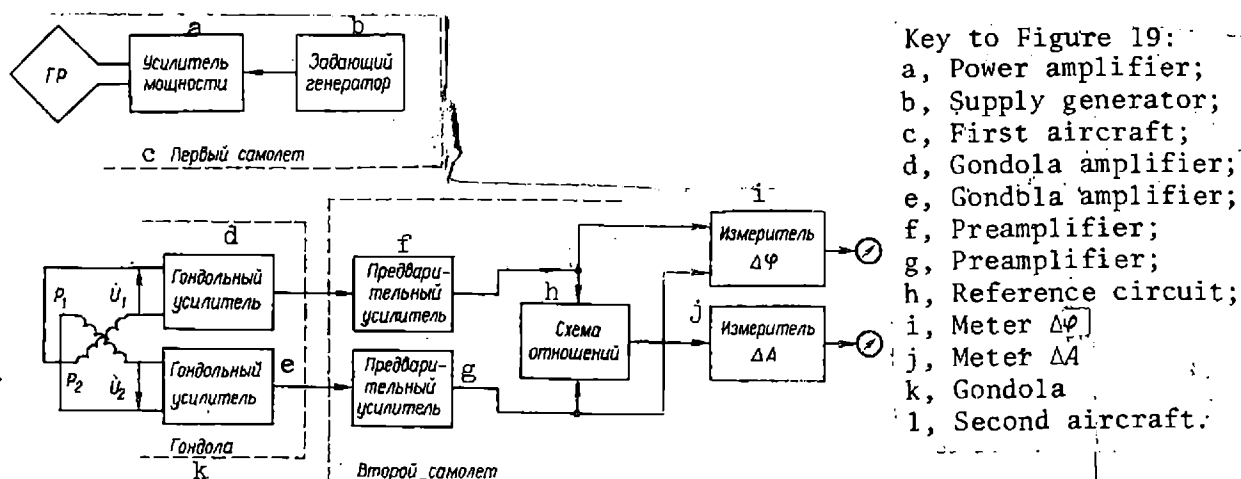


Fig. 18.

relatively oscillating, so that their center would be on the flight axis of the first plane. The block diagram of the apparatus is shown in Fig. 19.

The significant difference between this version and that of the rotating magnetic field is that this one has only oscillating frame and there is no necessity of generating the rotating magnetic field. The generating portion of the apparatus for the lineally polarized field could be constructed from the block diagram of one of the channels in the apparatus of the rotating magnetic field. For instance, it is possible to use one channel of the generating unit and the oscillating horizontal frame with vertical frame out-off. But the measuring devices of this version are similar to those of the rotating magnetic field. The measuring is of the same difference of signals excited in the field detectors of the oscillating frame and of the phase-angle between these signals. The field detectors remain the same, but their orientation in space relating to the oscillating frame and the vertical line (in the outboard gondola) varies.

In measuring voltage ratio in measuring devices of rotating magnetic field version the cut-in, instead of subtracting device, if the hookup for measuring amplitude ratio of signals, i.e. the measurements are taken of the so called amplitude parameter A /231, 234/.



Key to Figure 19:
a, Power amplifier;
b, Supply generator;
c, First aircraft;
d, Gondola amplifier;
e, Gondola amplifier;
f, Preamplifier;
g, Preamplifier;
h, Reference circuit;
i, Meter $\Delta\varphi$;
j, Meter ΔA ;
k, Gondola;
l, Second aircraft.

Fig. 19.

If the receiving frames are placed as shown in Fig. 18, and the geometry of the system is not upset, then with linear polarization of the primary field and absence of the secondary one it is possible to assume that e.m.f. in both the frames are excited by the vertical constituent of the primary field $H_B = H_z$; therefore, they are equivalent in value and have no phase-shift.

Theoretical calculations and tests have shown that this version has considerably greater technical error than the version of the rotating magnetic field. However the generator portion of this version is much simpler than in the above. The smallest technical error will be in the version with the vertical oscillating frame (horizontal dipole).

Thus, it follows that the two-plane versions of near-zone method are effective in respect of the optimum space selection between the source and the field detector. In a number of cases their application is complicated by the necessity for a simultaneous piloting of two planes with an exactly fixed position of one in relation to the other; moreover, in these cases the cost of the geophysical survey increases considerably.

2. The combined zone method.

The first information regarding the aerial electric prospecting in the combined zone (BDK method: or method of infinitely long cable) was the advertising communication of Lundberg in 1955 / 257/. The result of this communication was that for the search of useful minerals a method was applied, based on the study of electromagnetic field of the alternate current, flowing along a straight cable, grounded at both ends. The principle of this method consists of the following /158/. Two cables, 30 km in length, are laid on the ground and alternate current of 400 and 1000 cps frequency is passed through this cable from the ground generating group. The receiving-

measuring two-frequency apparatus of the mobile group is placed on the plane. Field parameters of the cable are measured simultaneously on two frequencies with the plane flying across the cable lying on the ground. Later on there was a communication, from the "Bolindens Gruv. A.B." Co. of Sweden and from other companies /6, 256, 267/ about the apparatus for the method of infinitely long cable.

In the USSR, the development of the infinitely long cable method and its apparatus began in 1955 /102, 103, 216, 218/. The first successful tests were conducted, in 1957, in the Maidan-Vilsky section of graphitized gneiss. In 1958, the Academy of Sciences of Uzbek SSR made and tested, in productive conditions, a set of apparatus AERA-58.

The substantial advantage of aerial electric prospecting by the combined zone method is the low response of the apparatus to flat-bedded conductors. Moreover, the system of current inlet into ground (when long grounded cable is applied) is in itself such better in comparison with other methods of aerial electric prospecting.

The disadvantage of the combined zone method is the necessity of laying out cable on the ground and the setting up in its vicinity of the land group of devices. However, the experience of utilising airborne electro-prospecting station testifies to the fact that this kind of opinion is more of a formal than objective nature, since it does not take into account the specifics of applying aerial geophysical prospecting generally and in inaccessible areas in particular /190, 216/. Moreover, the cost of 1 run. km of survey by the combined zone method is not high. Thus in the northern areas of the Kolsky peninsula, or in north-western Kazakhstan, the cost of aerial exploration by the method of infinitely long cable is found to be several times lower than the cost of the ground survey, whereas implementation is much faster. In these areas the cost of 1 run. km of large-scale mapping

is 10 - 15 roubles.

As field emitter in the apparatus of the combined zone method, so far only a long straight grounded cable is applied; no other emitters are applied. Since the parameters of the electromagnetic field vary quite sharply in space, there is no compensation of the primary field in this method..

The main problem of the measuring-recording apparatus in the infinitely long cable method is the measuring and recording of the amplitude and phase characteristics of normal and anomalous magnetic fields of the emitter from e.m.f., induced in the magnetic field detector (of multi-turn type of coil with core). For phase measuring, the measuring and recording devices get radio-transmitted information from the ground regarding the current phase in the source. The magnetic field detectors are most often set up in the outboard gondola. They are very seldom placed on the aircraft.

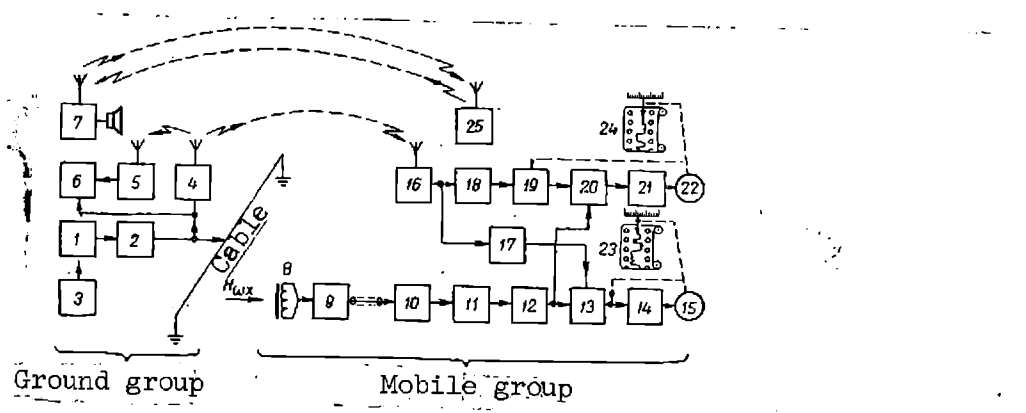


Fig. 20.

Fig. 20 shows a block diagram in greater detail than in Fig. 6, which explains certain specifics in the apparatus development for the infinitely long cable method. As pointed out above, the set of devices consists of two sections - the ground group, generating the electromagnetic field on one of the working frequencies and sending radio signals, modulated by supporting

voltage, and the mobile group, which measures and records field parameters, e.g. $H\omega_x$.

The electromagnetic field on the working frequency is generated by cable energized by a competent tube oscillator 2. The oscillator is provided with a capacitance block, by means of which the inductive reaction of the cable is being compensated. With the breaking of the cable a relay operates in the oscillator device, which disconnects the cable from the output terminals of the oscillator. For the ~~excitation~~ of oscillator 2, a master oscillator 2 has been provided, the frequency of which is controlled by quartz crystal. The energy-source of the ground apparatus is the portable power plant 3.

The key signal, coinciding in phase with the current in the cable, is transmitted to the mobile group by means of radio-station 4. Phase-control of the key signal, emitted into ether, is implemented by means of detector 5 and phase indicator 6. The latter is energized by two voltages - from shunt, connected in series with the cable, and by demodulated signal of low frequency from the output of detector 5.

For the command communication between the ground and mobile groups, radio-stations 7 and 25 have been included in the set of apparatus for aerial electro-prospecting. The mobile group measures and records the phase-angle and one of the components (active or reactive) of e.m.f., excited in receiving coil 8, which perceives the horizontal constituent of the cable's magnetic field $H\omega_x$. The output voltage of the coil enters wide-band amplifier 9, signal from which is transmitted along the connecting cable into preliminary amplifier 10, attenuator 11 and selective amplifier 12. Thereafter the signal is fed into two channels of measuring and recording - the channel of measuring and recording of components 13-15 and 23 and the channel of measuring and recording of phase 18-22, 24.

For the recording of components, use is made of direct measuring circuit, based on phase-response detector 13 (see para 4, chapt. X). The supporting voltage is the signal, received and rectified by radio-receiver 16. In order to measure and record quadrature components at all the four quadrants, a device is applied in the apparatus (not shown in figure), in which the phase-angle of the supporting voltage could vary by jumps of 90° within the limits of 360 elect degrees. To exclude during survey the effect of level variations of the supporting voltage, the latter is confined, in device 17, by a two-sided limiter and fed in the shape of rectangular impulses to the circuit of phase-response detector 13.

The constant potential at the output of detector 13, proportional to active or reactive component, is measured by automatic compensator (14, 15, 23). Block 14 cuts in the circuit of alternate current amplifier with transformation and reverse circuit of connection on constant current. At the output of alternate current the amplifier is out in control winding of reversible motor 15. Recording of the measurable parameter is implemented on a chart of recorder 23 by a carriage with writer, mechanically connected with motor 15.

The phase is measured by means of quasicompensation (see paras 2 and 2, chapt XII). For this, the measurable signal from the output of selective amplifier 12 is fed to similar phase-response circuit 20 of the phase measuring channel. The supporting voltage, after passing through amplifier-limiter 18 and phase-inverter 19, is fed to this circuit from key signal detector 16. Voltage from the output of phase response circuit 20 enters the amplifier of alternate current with transformation 21 and the control winding of reversible motor 22. This meter operates phase-inverter 19, till such time as the voltage at the output of circuit 20 becomes equivalent to zero.

The phase-angle is read from recorder dial 24 by the position of the phase-inverter's variable elements.

The set of mobile group devices includes also the outboard gondola, a device for its let down (with wire cutter), a marker of time breaks and landmarks on the charts of recorders, etc. The source of energy for the mobile group apparatus is the power line of the aircraft, fed through special dynamoelectric transformers.

It has been mentioned that the first set of the AERA-58 apparatus was made in 1958 in the Academy of Sciences of Ukrainian SSR. From the same block diagram in 1963 the All Union Scientific Research Institute of Methods and Technique of Prospecting made a small batch of serial apparatus for the infinitely long cable (ILC) method, which records components and phase.

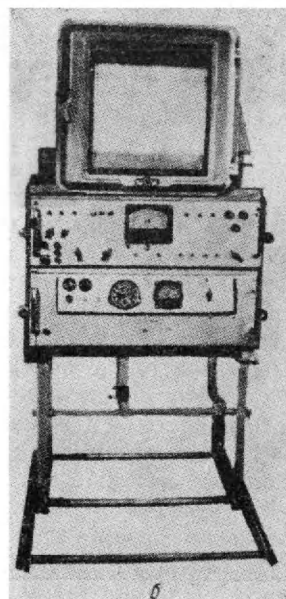
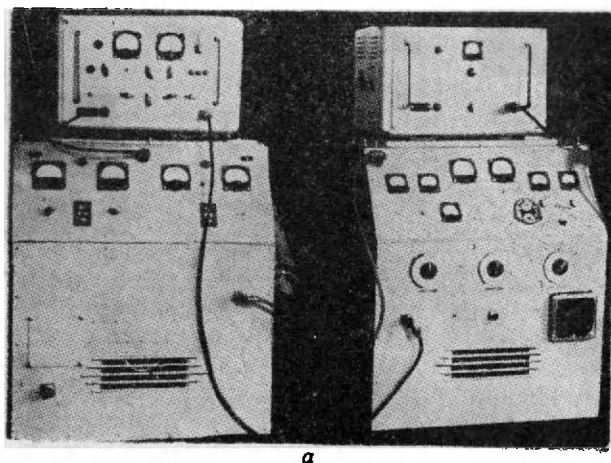


Fig. 21.

Fig. 21 - a shows the external appearance of the generating unit of the above apparatus, and Fig. 21 - b the appearance of measuring device. A modernized two-track automatic potentiometer EPP-09 is used as a recorder. The measuring system and the system of key signal detector jointly with the power-source are mounted in two blocks, set up on a split frame in the common housing. This type of construction resembles the apparatus of aeromagnetic stations.

The oscillating apparatus of the above set is distinct in construction from the similar apparatus AERA-58. It is more convenient for use in field conditions and is easily transportable by helicopter.

In 1959, the Institute of Automatics and Electrometry of the Academy of Sciences of the USSR began developing and, later on, constructed a set of devices for the infinitely long cable method, which measures amplitude, phase and components of the signal taken /118/. The measuring system of the apparatus is based on synchronous-quadratic reception /152/.

In 1960, the Academy of Sciences of Ukrainian SSR produced a few devices of the AERA-2 type for aerial electroprospecting by the infinitely long cable (ILC) method. In contrast to AERA-58 this apparatus measures and records amplitude and phase of e.m.f., induced in the magnetic field detectors by the cable field. The construction and block diagram of this apparatus have been described in work /90/ (see Para 3, chapt. XIV).

Except ILC apparatus, no other versions have been developed for the combined zone. Information of foreign firms regarding this apparatus is only of advertising nature. But the fact is well known that the apparatus of ILC method is widely used abroad.

3. The remote zone method (radiocomparison and control).

The idea of using electromagnetic fields of broadcasting radio-stations for geophysical investigations originated as far back as the

twenties. Subsequently, Soviet scientists /63, 168, 202, 204/ and those of other countries /255, 266/ have investigated in theory and confirmed on practice the possibility and expediency of utilizing for geophysical purposes the electromagnetic fields of remote, comparatively high-frequency broadcasting radio-stations. This trend of geophysical investigations has shaped into an independent method of radio-comparison and control, and of radio-waves mapping or profiling. At present for the study of the field's phase characteristics some investigators suggest the use of fields of special radio-stations, which emit non-modulated signals.

Thus it follows that the radio-comparison and control method is based on studying field intensity of remote, broadcasting radio-stations comparatively of high-frequency (long wave, transmitting in frequency band 150-400 kcps.), and also of special radio-stations (mainly superlong wave, operating in frequency band 80-120 and 10-30 kcps). This method, in comparison with the induction method, has a number of virtues. As we know, in induction method the measurements are effected in the near zone, when the distance between the source and the field detector is usually very much less than the wave length. The field's composition in this zone is quite complex and the field's intensity, which is most important, decreases with the distance considerably quicker than in the remote (wave) zone, due to which it is considerably more difficult to define relatively minor anomalies within the zone of sharply varying field. At the same time, in the near zone the attenuation of the field with depth occurs much quicker. This means that various non-uniformities on the surface appear in considerably greater degree than those in the subsurface. At great distances from the emitting radio-stations, i.e. in the wave zone, the field of these stations is sufficiently uniform. With the propagation of surface radio-waves, the

electromagnetic field penetrates partially the stratum of the top layers of the earth's crust (in the first approximation proportionally to their resistivity). Therefore, knowing the nature of distribution of intensity of the magnetic field on both sides of the interface air-ground in relation to electric properties of rocks, it is possible to perceive the geoelectric composition of the investigation area.

The depth of the radio-comparing and control method, depending on the resistivity value of cover-rocks, may comprise several to scores of meters. If the resistivity of cover rocks is 50-300 ohm, the depth will be within 10-20 m. Using fields of superlong wave radio-stations (10-30 kcps), the depth correspondingly increases 3-3.5 times /219/.

The main shortcomings of this method: limited depth; possible distortions of the anomalous pattern of the field due to short time variations of the radiostations field (specially in the northern areas and also during the ionospheric disturbances and magnetic storms); effect of conductors of non-geological origin (power and telephone lines, metal structures, etc.); effect of highly rugged ground; signal modulation effect of radiostations; difficulty of exact quantitative interpretation of measuring results. However, by maintaining certain techniques some of these deficiencies could be avoided by obtaining positive effect even in difficult conditions.

The ground version of the radio-comparing and radio control method - its theory, systems of applied apparatus, the technique and results of field work are most fully described in /202, 221/. The experience of productive application of this method in various areas of our country testifies to its extensive possibilities in defining and mapping contacts of various rocks, zones of tectonic dislocations, ore bodies, quartz veins, lens of underground waters, etc. The devices applied for ground work by this method are PINP-1 and PINP-2/222/.

The development of the aerial version of this method is quite promising, since, according to the physical principles of this method, this version should have certain advantages over the aerial versions of the induction method. The main merits of the method: no effect from the varying altitude of flight, since the use is of the remote zone, and the possibility of flying at an altitude of a few hundred meters without any appreciable decrease in exploration possibilities of the method.

In working out the aerial version of the radio-comparing and control method special attention should be paid to the construction of the apparatus, the choice of measurable constituents of the field and the mode of their measuring, and also to the development of rational methods for measuring and interpretation of the results obtained.

By applying the ordinary measuring device of the field's intensity in ground conditions it is easy to determine the amplitudes of all the constituents of the magnetic field, as well as the azimuth and the angle of gradient of its vector. In the aerial version of this method, with continuous measuring in motion simultaneous recording of several enumerated parameters is rather difficult. Therefore, at present the apparatus of the aerial version of the radio-comparing and control method records one measurable parameter. This parameter is usually the mean level of one of the components of the electric or magnetic field.

In 1957, the All Union Scientific Research Institute of Methods, and Technique of Prospecting (VITR) carried out experiments with the use of the helicopter version of the aerial RCC (radio-comparing and control) method. Helicopter MI-4. The devices were made in Moscow State University on the base of interference gauge IP-12. The initial experiments gave negative results. However, in 1960-61, positive results were obtained by means of the same

devices.

The geophysical laboratory of the All Union Scientific Research Institute of Hydrogeology and Engineering Geology of the Ministry of Geology, USSR, used the helicopter version of the aerial RCC method for exploring lenses of fresh water in the desert areas of Kara-Kum. The results of these investigations were also positive. During the experiments, determinations were made of the optimum altitude of flight. It was found that, in the search for large objects, such as lenses of fresh water, occurring among saline ground waters, the flight altitude had hardly any effect on the survey results. The limit flight altitude could be taken as 1000 m. Due to variation of the field's intensity with removal from radio station on extensive source of survey, corrections have to be inserted for variations of the normal field.

To obtain the greatest geophysical information, it is desirable to study with the use of the aerial versions of RCC method the phase composition of electromagnetic fields. Phase measuring provides the possibility of dividing the fixed anomalies into ore and rock products. However, the measuring is hampered by the time variations in phase structure of broadcasting stations fields, necessity to measure phases without a key signal from the source of the field, etc. Attempts were made to compensate the latter by using additional ground radio-station, which would transmit the key signal. However, this type of system was found to be rather complicated and the possibilities of its application limited. A method was suggested of amplitude-phase measuring of radio stations fields by comparing values of the measurable constituents of the field in the anomalous zone with the corresponding values in non-complicated and was not developed practically. More promising may be assumed the relative phase-measuring by means of two combined reciprocally perpendicular receiving frames, similar to those applied in the AFMAG apparatus. If the axes of these frames are placed in horizontal plane, ratio determination of voltages induced in frames, will

make it possible to record the angle of the direction finder. With the location of receiving frames axes in vertical plane, it is possible to measure the angle of gradient of the magnetic field vector. To reduce the level of noise from the electric equipment of aircraft, the receiving frames should be placed in the outboard gondola.

Also of interest in the aerial RCC method is the manner of measuring phases, as suggested by G.F. Ignatiev /78/. The principle consists of the following.

A device is set up on the plane for receiving signals from the ground radiostation, consisting of receiver 1 (Fig.22), two master quartz oscillators 2 and 3 and the system of automatic frequency tuning (AFT). The AFT system consists of synchronous phase detector 4, circuit breaker 5, amplifier of mismatching 6 and electric motor 7, coupled with condenser 9, which periodically tuned in resonance with the received signal the quartz master oscillators 2 and 3 with accuracy upto phase. The phase-shifts are measured by means of the phase-control system, cut in turn by turn to both the oscillators, consisting of synchronous detector 10, circuit breaker 11, amplifier of mismatching 12 and electric motor 7, coupled with phase-inverter 8. The phase-inverter 8 is, in its turn, coupled with transducer (not shown in the figure), which is responsible for the cut-in of the pen for recording the phase-shift between the voltage of master oscillator and the received signal. The given method allows the obtaining of higher-quality geophysical information due to the fact that electric properties of the geological section are being determined not from signal amplitudes of broadcasting and special radio-stations of the long wave band, but from the variation of phase-shifts between the signal of radiostation and the signals of master oscillators.

set up on the aircraft. Phase-information is more stable against interference than the amplitude information and less dependent on non-geological factors. Unfortunately, this method has not so far been tested in practice.

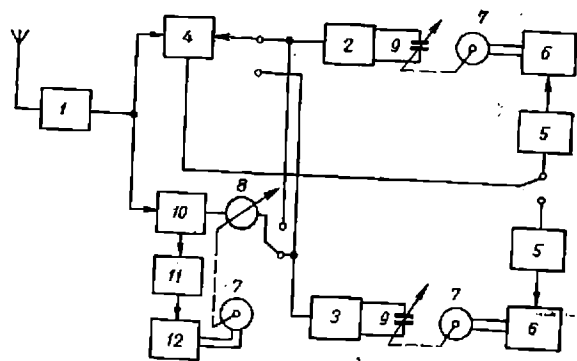


Fig. 22.

Thus, the expediency should be pointed out once more of the further development of method, verification of theory, perfection of apparatus, etc., in order to produce quicker commercial samples of apparatus for geophysical exploration by the aerial RCC method, the potentiality of which has been proved by the investigations (106, 202) carried out.

Chapter - III - PRIMARY HARMONIC ELECTROMAGNETIC FIELDS,
USED IN AERIAL ELECTRIC PROSPECTING.

1. Formulation of problem.

For constructing a perfect apparatus and developing an investigation method, in aerial electric prospecting, it is most important to have, besides information as to the chosen geometry of system, competence of generating response in receiving apparatus, noise level in detectors of electromagnetic field, and also data of primary and secondary electromagnetic fields.

In order to provide a sufficiently complete picture of primary electromagnetic fields, used in aerial electric prospecting with harmonic field, this chapter will discuss fields of a single oscillating dipole, of circular frame with current and circular rotating magnetic field, applied in near zone methods (induction methods), field of rectilinear infinitely long cable, applied in methods of combined zone (BDK method), and the field of long wave broadcasting and special radio stations, used in methods of remote zone (radio-comparing and control method).

The relationships, shown below, for parameters of primary fields, used in near, combined and remote zones, make it possible to define the specifics of these fields (these specifics are of significance only in aerial electric prospecting).

Moreover, analysis of the structure of primary fields, within location zone of receiver, artificially excited by various types of exciters, should provide answers also to questions as to the parameters which are possible to be determined and the kind of shielding against noise that should be provided for receiving and measuring devices in these cases.

The main groups of electromagnetic events, studied by methods of aerial electric prospecting, correspond to particular form of Maxwell's

series of equations (18, 83). In the near and combined zones Maxwell's equations for time harmonic electromagnetic field are usually written in complex form as follows(75,162):

$$\begin{aligned} \operatorname{rot} H &= j \omega \epsilon E + \vec{Q}; \\ \operatorname{rot} E &= - j \omega \mu H; \\ D &= \epsilon H; \\ B &= \mu H. \end{aligned} \quad (III.1)$$

For a quasi stationary field or a field, in which the variation processes pass sufficiently slowly, the right/hand portion of the second Maxwell equation (III.1) differs from zero, i.e. the given equation depicts in differential form the law of electromagnetic induction.

The series of equations (III.1) is resolved, ordinarily, with an estimate of boundary conditions and idealization of lower half-space as a uniform medium, and taking into account geometry of system in real aerial survey.

In remote zone wave type expansion of electromagnetic field takes place, which can be determined by Umov-Poynting vector, directed along the movement of propagating wave (52):

$$\vec{S} = \vec{E}H, \quad (III.2)$$

where H^* - conjugated complex of magnetic field intensity.

In this case:

$$\begin{aligned} E &= E_m e^{j(\omega t + \psi_1)} = E_m e^{j \omega t}, \\ H &= H_m e^{j(\omega t + \psi_2)} = H_m e^{j \omega t}, \end{aligned} \quad (III.3)$$

where E_m and H_m - complex tension amplitudes of electric and magnetic field respectively.

$$E_m = E_m e^{j \psi_1} \text{ and } H_m = H_m e^{j \psi_2}.$$

Resolution of the series of equations (III.1) - (III.3) with certain allowances permits, for practical purpose with sufficient accuracy to characterise methods of aerial electric prospecting with harmonic field and their versions. In particular too many allowances are allowed in the use of near zone method, the number of versions of which used in the aerial electric prospecting is considerable. For instance, primary field of induction aeromethod, excited by oscillating frame located in the aircraft, is analyzed on assumption, that this frame and aircraft are both in uniform medium (air) at an altitude, where the effect of earth surface could be ignored without any detriment to accuracy of calculations (69, 132).

It should be pointed out, that in near zone versions field detector could be located in relation to oscillating frame outside the contour, formed by turns of oscillating frame, and at distances considerably exceeds dimensions of contour (spread out frames), as well as within this contour or in its immediate vicinity (combined frames). Accordingly, the approach to deduction of relationships, characterising electromagnetic field at the point of field detector could also be ambiguous: the oscillating frame could either be taken as magnetic dipole, or as a closed loop (circular turn) with current.

In aerial versions of induction method with source and field detector spread out in space, the oscillating frame is frequently located in horizontal plane parallel to ground surface (see para 1, chapter II). But, if the application is of more composite construction of the oscillating frame, e.g., as in the version of rotating magnetic field, then out of the two frames, generating this field, one should be located in the horizontal plane, and the other - in vertical. Field detectors in these versions are

invariably placed in outboard gondola, towed by plane or helicopter by means of wire cable. The gondola is placed in vertical plane passing through the aircraft in direction of its motion. Orientation of field detectors in relation to oscillating frame varies in accordance with the chosen version.

In deduction of relationships, which determine the primary field in the near zone for versions with the spread out in space source and field detector, the consideration is only of induction zone. Primary field can be taken as quasi-stationary and the effect of electromagnetic field expansion need not be taken into account ('162). Simultaneously the zone in the immediate vicinity of the field's source is excluded, which permits to consider this source, i.e., oscillating frame, as magnetic dipole, characterised by a certain magnetic moment \bar{m} . Therefore, the oscillating frame, in this condition could be presented as a point source (point magnetic dipole) with magnetic moment $\bar{m} = km_z$, modulus of which is

$$m_z = /i/ wS, \sigma_{AB} \cdot m^2, \quad (III.4)$$

and the direction coincides with axis OZ, as shown in Fig. 23.

In formula (III.4) i , w , S - are respectively current, number of turns and the area of the frame. It is assumed, that the current in oscillating frame is harmonic time function, i.e. $i = I_m \sin(\omega t + \psi_i)$, and is shown by complex amplitude:

$$I_m = I_m e^{j\psi_i}, \quad (III.5)$$

and magnetic moment of dipole \bar{m}_z with positive values of current in oscillating frame is directed along the positive semi axis OZ.

The adopted conditions are satisfied also in the case of rigid fixing of source and field detector on one aircraft with comparatively less

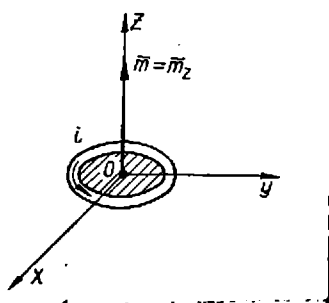


Fig. 23.

space between them, but only if the geometrical dimensions of the source and detector are considerably less than this spacing (i.e. less than the spread between the frames). If, on the other hand, the receiving frames are arranged in the immediate vicinity of the oscillating frame, then in the estimate of the primary field it is necessary to take into account the configuration of the oscillating frame. The intensity of the magnetic field is, generally, calculated from more composite formulas, containing elliptic integrals of Bessel's functions. Only with disposition of receiving frame, within the plane of oscillating frame, but outside its contours, will there be the constituent of primary field, parallel to axis OZ (the other constituents are not present), calculations of which present no difficulties.

In the aerial version of induction method, when the receiving frame is disposed within the oscillating one, the primary field is calculated by methods, applied in determination of intensity of magnetic field of circular current near the center of the circular turn, etc.

In calculations of the field in aerial BDK method there are some specifics. First a resolution of wave equation has to be found, which or the lines of space at certain points has the type of property, that when approaching them the field strives towards infinity in a certain way.

Then follows determination of the field's behavior in the vicinity of these points for unambiguous determination of the nature of the finite, but insignificant in geometrical dimensions source, which generates the field of the indicated composition (30, 75).

In estimations of remote zone in aerial electric prospecting, no special allowances are allowed.

2. Magnetic field of a single oscillating dipole in uniform space.

Let's take an oscillating dipole with magnetic moment \vec{m} , situated in uniform space and having a random orientation in respect of the adopted system of coordinates. The dipole of oscillating point with random direction of magnetic moment is in the center O of rectangular system of coordinates, as shown in Fig. 24. In this case for magnetic moment \vec{m} of dipole we get the following equation:

$$\vec{m} = \vec{i}m_x + \vec{j}m_y + \vec{k}m_z = \vec{m}_x + \vec{m}_y + \vec{m}_z, \quad (\text{III.6})$$

where \vec{m}_x , \vec{m}_y and \vec{m}_z - constituents of the moment on axes of coordinates, $\vec{m}_x = \vec{i}m_x$; $\vec{m}_y = \vec{j}m_y$; $\vec{m}_z = \vec{k}m_z$; \vec{i} , \vec{j} and \vec{k} - single vectors (orts).

Vector magnitude of magnetic moment, i.e. its modulus

$$m = |\vec{m}| = \sqrt{m_x^2 + m_y^2 + m_z^2}, \quad (\text{III.7})$$

and the angles α , β and γ , formed by the positive direction of axes OX, OY and OZ with vector \vec{m} , are determined by relationships

$$\cos \alpha = \frac{m_x}{m}; \cos \beta = \frac{m_y}{m}; \cos \gamma = \frac{m_z}{m}. \quad (\text{III.8})$$

If magnetic moment of dipole is oriented along axis OZ, according to most of the aerial induction methods (see Fig.23), then $m_x = m_y = 0$, $m_z = iwS$, $\vec{m} = \vec{k}m_z = \vec{m}_z$ (see term (III.4)).

Now let's pass on to the analysis of magnetic field, generated by this dipole at the arbitrary point P of a uniform space, and determine the perceptible by field detector constituents at this point. For calculation of the field we use vector constituents of magnetic field intensity H_x, H_y, H_z (in Cartesian coordinates) and H_r, H_φ, H_θ (in spherical coordinates).

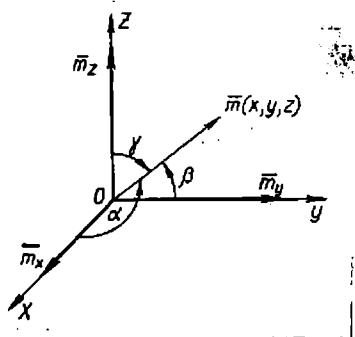


Fig. 24.

Vector of magnetic field at point P, by radius-vector \vec{r} (Fig. 25), will be accordingly [198/

$$\vec{H} = \frac{3(\vec{m} \cdot \vec{r})\vec{r}}{4\pi r^5} - \frac{\vec{m}}{4\pi r^5}. \quad (\text{III.9})$$

In spherical coordinates the terms for constituents of vector \vec{H} at the given point P have the following form [83, 162/:

radial constituent

$$H_r = \frac{2m_z \cos \theta}{4\pi r^3}; \quad (\text{III.10})$$

tangential constituent

$$H_\theta = \frac{m_z \sin \theta}{4\pi r^3}; \quad (\text{III.11})$$

azimuthal constituent

$$H_\varphi = 0, \quad (\text{III.12})$$

where r, θ and φ - spherical coordinates of point P in relation to origin O, located in the center of oscillating frame (see Fig. 25).

Due to symmetry in respect of axis OZ / equations (III.10) - (III.12)/, expressed by the independence of the constituents H_r , H_θ and H_φ from angle φ , the selection of the zero or meridional plane, in respect of which the azimuth reading is being taken, could be arbitrary. Therefore, if this is not stipulated, we will assume, that the given plane passes through axis OX , and the point P is in the plane YOZ .

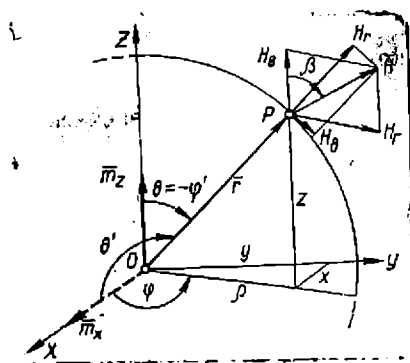


Fig. 25.

In these conditions the perceptible in arial induction method will be either vertical or horizontal constituent of the primary magnetic field (with one receiving frame) or both simultaneously (with two receiving frames). In Fig.25 the vertical constituent H_v is parallel to magnetic moment of dipole, and the horizontal H_h is perpendicular. To ensure the reception of the chosen constituent of the field, each receiving frame is given a corresponding spatial position. Therefore, in order to find the intensity of e.m.f., induced in receiving frame of one or another constituent of primary or resultant field, it is necessary to have terms for determination of vector \vec{H} modulus of the primary magnetic field intensity as a whole, as well as of its constituents - vertical H_v and horizontal H_h - as functions of the oscillating frame magnetic moment and coordinates of the location point of receiving frame in the chosen system of coordinates.

Vector modulus

$$/ \bar{H} / = \sqrt{H_r^2 + H_\theta^2}, \quad (\text{III.13})$$

Substituting in this equation terms (III.10) and (III.11) and implementing simple conversions, we get

$$/ H / = \frac{m_z}{4\pi r^3} \sqrt{\frac{5}{2} + \frac{3}{2} \cos 2\theta} = \frac{m_z}{8\pi r^3} \sqrt{10 + 6 \cos 2\theta}. \quad (\text{III.14})$$

On the basis of Fig. 25 when the terms (III.10) and (III.11) for vertical and horizontal constituents are taken into account, we find the following parities:

$$\begin{aligned} H_v &= H_z = H_r \cos \theta - H_\theta \sin \theta; \\ H_h &= H_y = H_r \sin \theta + H_\theta \cos \theta \end{aligned} \quad (\text{III.15})$$

Substituting in equation (III.15) terms (III.10) and (III.11) and implementing simple conversions, we obtain

$$\begin{aligned} H_v &= \frac{m_z}{8\pi r^3} (1 + 3 \cos 2\theta); \\ H_h &= \frac{m_z}{8\pi r^3} 3 \sin 2\theta. \end{aligned} \quad (\text{III.15a})$$

We bring in signs

$$\frac{1}{2} (1 + 3 \cos 2\theta) = F_1(\theta); \quad \frac{3}{2} \sin 2\theta = F_2(\theta).$$

Then

$$\begin{aligned} H_v &= \frac{m_z}{4\pi r^3} F_1(\theta); \\ H_h &= \frac{m_z}{4\pi r^3} F_2(\theta). \end{aligned} \quad (\text{III.16})$$

Angle between field vector \bar{H} and dipole axis

$$\beta = \text{arctg} \frac{H_h}{H_v} = \text{arctg} \frac{3 \sin 2\theta}{1 + 3 \cos 2\theta}. \quad (\text{III.17})$$

If we follow the variation progress of relationships $F_1(\theta)$ and $F_2(\theta)$, which enter into formulas (III.16), with angle θ variation from 0 to 180° , we would get the directivity pattern of vertical and horizontal constituents of the intensity vector of the primary magnetic field in horizontal oscillating frame (Figs.26 and 27). With the set m_z and r it is possible to determine from these relationships the intensity and sign of the constituents H_v and H_h for any point of space surrounding the oscillating frame.

The directivity curves (see Figs.26, 27) are symmetrical in relation to axis OY and OZ. Therefore, change of direction of oscillating frame magnetic moment to the opposite does not change the directivity pattern. This is of significance for further correlation.

Let us pass on to deduction of relations determining the constituents H_x , H_y and H_z of the intensity vector in magnetic field of oscillating dipole for the arbitrary observation point P (Fig. 28). Formulas of transition from spherical coordinates to Cartesian retaining signs taken in Fig. 28 we write as follows:

$$\left. \begin{aligned} x &= r \sin \theta \cos \varphi; \quad r = \sqrt{x^2 + y^2 + z^2}, \\ y &= r \sin \theta \sin \varphi; \quad \varphi = \arctg \frac{y}{x} \\ z &= r \cos \theta; \quad \theta = \arctg \frac{\sqrt{x^2 + y^2}}{z} \end{aligned} \right\} \quad (\text{III.18})$$

From Fig. 25 and 28 it follows, that

$$H_x = H_h \cos \varphi; \quad H_y = H_h \sin \varphi; \quad H_z = H_v. \quad (\text{III.19})$$

Substituting in equations (III.19) values of constituents H_h and H_v according to formulas (III.15) and (III.16), we get the terms for

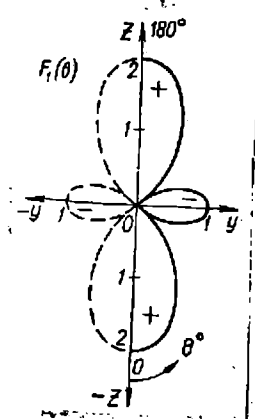


Fig. 26

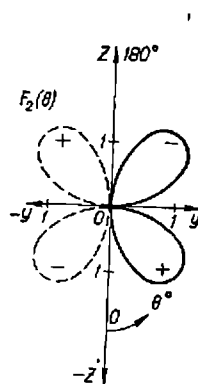


Fig. 27

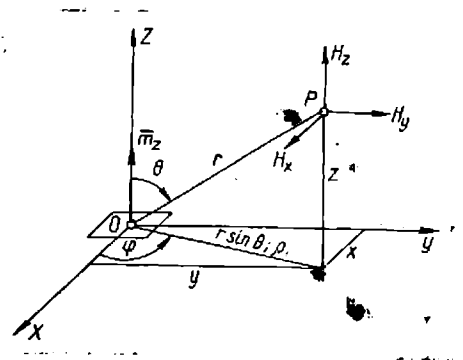


Fig. 28

constituents H_x , H_y and H_z as functions of spherical coordinates:

$$\begin{aligned} H_x &= \frac{m_z}{8 \pi r^3} 3 \sin 2 \theta \cos \varphi; \\ H_y &= \frac{m_z}{8 \pi r^3} 3 \sin 2 \theta \sin \varphi; \\ H_z &= \frac{m_z}{8 \pi r^3} (1 + 3 \cos 2 \theta) \end{aligned} \quad (III.20)$$

Since

$$\sin \varphi = \frac{y}{\sqrt{x^2 + y^2}}; \quad \cos \varphi = \frac{x}{\sqrt{x^2 + y^2}}$$

then

$$\begin{aligned} H_x &= \frac{m_z}{8 \pi r^3} 3 \sin 2 \theta \frac{x}{\sqrt{x^2 + y^2}}; \\ H_y &= \frac{m_z}{8 \pi r^3} 3 \sin 2 \theta \frac{y}{\sqrt{x^2 + y^2}}; \\ H_z &= \frac{m_z}{8 \pi r^3} (1 + 3 \cos 2 \theta) \end{aligned} \quad (III.21)$$

Let us express $\sin 2 \theta$ and $\cos 2 \theta$ in terms of Cartesian coordinates

Using trigonometric conversions $\sin 2 \theta = 2 \sin \theta \cos \theta = 2 \frac{\operatorname{tg} \theta}{1 + \operatorname{tg}^2 \theta}$

and $\cos 2 \theta = \cos^2 \theta - \sin^2 \theta = \frac{2}{1 + \operatorname{tg}^2 \theta} - 1$, we find

$$\sin 2\theta = \frac{2z \sqrt{x^2 + y^2}}{x^2 + y^2 + z^2}; \quad \cos 2\theta = \frac{z^2 - x^2 - y^2}{x^2 + y^2 + z^2} \quad (\text{III.22})$$

Substituting in equations (III.21) the determined values $\sin 2\theta$ and $\cos 2\theta$, we finally obtain

$$\left. \begin{aligned} H_x &= \frac{3m_z}{4\pi (x^2 + y^2 + z^2)^{5/2}} xz = \frac{3m_z}{4\pi r^5} xz \\ H_y &= \frac{3m_z}{4\pi (x^2 + y^2 + z^2)^{5/2}} yz = \frac{3m_z}{4\pi r^5} yz \\ H_z &= \frac{m_z}{4\pi (x^2 + y^2 + z^2)^{5/2}} (2z^2 - x^2 - y^2) \\ &= \frac{m_z}{4\pi r^5} (3z^2 - r^2), \end{aligned} \right\} \quad (\text{III.23})$$

$$\text{as } 2z^2 - x^2 - y^2 = 3z^2 - (x^2 + y^2 + z^2) = 3z^2 - r^2.$$

For the intensity vector modulus of magnetic field of dipole we write

$$|\vec{H}| = \sqrt{H_x^2 + H_y^2 + H_z^2}. \quad (\text{III.24})$$

Substituting in equation (III.24) values of constituents from terms (III.23), we find the value for modulus in terms of Cartesian coordinates;

$$|\vec{H}| = \frac{m_z}{4\pi r^5} \sqrt{(x^2 + y^2) + z(5x^2 + 5y^2 - 4z^2)} \quad (\text{III.24a})$$

Since

$$r = \sqrt{z^2 + y^2 + x^2},$$

then

$$|\vec{H}| = \frac{m_z}{4\pi r^3} \sqrt{\frac{3z^2}{r^2} + 1}. \quad (\text{III.24b})$$

In terms of cylindrical coordinated vector modulus will be

$$/H/ = \frac{m_z}{4\pi(\rho^2+z^2)^{3/2}} \sqrt{\frac{3z^2}{\rho^2+z^2} + 1}. \quad (\text{III.24c})$$

Similarly deductions are made for constituent determination of the intensity of the field in oscillating dipole with magnetic moment, directed along axes OX and OY.

For instance, for dipole \bar{m}_x with magnetic moment directed along axis OX ($m_y = m_z = 0$, $m = \bar{m}_x = \bar{m}_x$), constituents for the same observation point P in spherical coordinates (see Fig.25) with denotation of the new polar distance by θ' will be written as:

$$\left. \begin{aligned} H_r &= \frac{2m_x \cos \theta'}{4\pi r^3} ; \\ H_{\theta} &= \frac{m_x \sin \theta'}{4\pi r^3} ; \\ H_{\phi} &= 0. \end{aligned} \right\} \quad (\text{III.25})$$

(the azimuthal constituent H_{ϕ} due to symmetry of the field in relation to axis OX will not be present). Constituent H_x , H_y and H_z of the same dipole in Cartesian coordinates will be obtained as

$$\left. \begin{aligned} H_x &= \frac{m_x}{4\pi r^5} (3x^2 - r^2); \\ H_y &= \frac{3m_x}{4\pi r^5} xy; \\ H_z &= \frac{3m_x}{4\pi r^5} xz. \end{aligned} \right\} \quad (\text{III.25a})$$

For modulus of magnetic field intensity vector we will get equation:

$$\begin{aligned} /H/ &= \frac{m_x}{4\pi(x^2+y^2+z^2)^{5/2}} \sqrt{x^2(4x^2+5y^2+5z^2)+(y^2+z^2)^2} \\ &= \frac{m_x}{4\pi r^3} \sqrt{\frac{3x^2}{r^2} + 1}. \end{aligned} \quad (\text{III.26})$$

with $\theta = 90^\circ$), in spite of the fact, that at these points magnitude of the vertical constituent will be maximum. In this case it would be better to compensate the constant interference by electric means.

According to Fig. 27, the best geometry for measuring horizontal component of resultant field with rigid fixing of receiving frame will have the set up with drift angle being zero or 90° . However, these points evince the highest dependence of H_h on angle θ , therefore, the instability of interference here is also maximum. At $\theta = 45^\circ$ the horizontal component is maximum and the unstability of interference is minimum. Hence, points with angle θ , equal to zero or 90° for vertical constituent and $\theta = 45^\circ$ for horizontal are the most acceptable for placing field detectors, since at these points interference from changes in the system's geometry is minimal.

Hence it follows, that it is possible to plan several patterns for the apparatus of induction method (single-plane or helicopter) with the spread in space of oscillating and receiving frames. The different patterns are determined by the location point of receiving element in respect of the field source, as shown in Fig. 29:

- 1) $\theta \approx 0$ (point P_1) - helicopter pattern, when transducer (oscillating frame and detector (receiving frame) are located on one vertical line;
- 2) $\theta \approx 45^\circ$ (point P_2) - "Canadian" pattern;
- 3) $\theta \approx 65^\circ$ (point P_3) - induction method pattern, realized, for instance, in apparatus AERI-2;
- 4) $\theta \approx 90^\circ$ (point P_4) - plane and helicopter pattern, when the transducer and detector are at the same altitude.

3. Magnetic field of oscillating frame in the form of a circular turn with current.

Let us analyze the basic means of determining the intensity components of the primary field near the oscillating frame in case, when this frame could be takes as circular with turn radius R and energized by current with complex amplitude I_m . We assume, that the distance between the frames is comparatively less (radius of oscillating frame is slightly less than the center interval of oscillating and receiving frames). This type of set up refers to patterns of aerial induction method with combined frames.

We use the cylindrical coordinates ρ, φ, z . Axis OZ we direct along the axis of circular field, and the center of turn place at the origin of coordinates, as shown in Fig. 30. In this case, as we know, the field of circular current does not depend on coordinate φ .

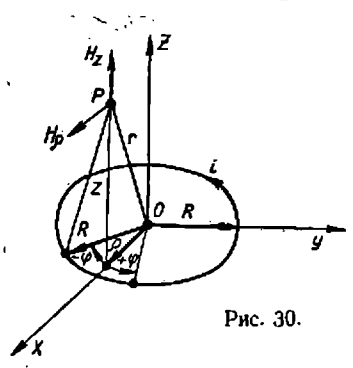


Fig. 30.

In the case under analysis the vector potential \vec{A} is perpendicular to plane ρOZ , i.e. it has only one constituent A_φ , which is determined by relationship /297/:

$$A_\varphi = \frac{\mu_0 I_m}{4\pi} \int_0^\pi \frac{2R \cos \varphi d\varphi}{R^2 + \rho^2 + z^2 - 2R\rho \cos \varphi} = \frac{\mu_0 R I_m}{2\pi} \int_0^\pi \frac{\cos \varphi d\varphi}{R^2 + \rho^2 + z^2 - 2R\rho \cos \varphi} =$$

$$= \frac{\mu_0 I_m}{\pi k} \left(\frac{1}{\rho} \right)^{\frac{1}{2}} \left[\left(1 - \frac{1}{2}k^2 \right) K - E \right], \quad (\text{III.27})$$

where $k^2 = 4R \rho [(R + \rho)^2 + z^2]$; K and E - functions R and ρ ,
determinable by total elliptic integrals of the first and second kind.

Since $\vec{B} = \mu_0 \vec{H} = \text{rot } \vec{A}$ and $\vec{H} = \frac{1}{\mu_0} \text{rot } \vec{A}$, then from relationship
(III.25) it is possible to determine constituents of magnetic field
intensity:

$$\left. \begin{aligned} H_\rho &= \frac{I_m w}{2\pi} \cdot \frac{z}{\rho [(R+\rho)^2 + z^2]^{\frac{3}{2}}} \left[-K + \frac{R^2 + \rho^2 + z^2}{(R-\rho)^2 + z^2} E \right]; \\ H_z &= \frac{I_m w}{2\pi} \cdot \frac{1}{[(R+\rho)^2 + z^2]^{\frac{3}{2}}} \left[K + \frac{R^2 - \rho^2 - z^2}{(R-\rho)^2 + z^2} E \right]; \end{aligned} \right\} \quad (\text{III.28})$$

$$H_\phi = 0.$$

If $\rho^2 + z^2 \gg R^2$, then

$$\left. \begin{aligned} H_\rho &= \frac{3R^2 I_m w}{4r^{5/2}}; \\ H_z &= \frac{R^2 I_m w}{4r^3} \left(2 - \frac{3\rho^2}{r^2} \right); \end{aligned} \right\} \quad (\text{III.28a})$$

$$H_\phi = 0.$$

If in these conditions the receiving frame is placed in the plane
of the oscillating frame, but outside its contour ($z = 0$), it receives the
vertical component, since the primary field has only one component - H_z ,
parallel to axis OZ ($H = H_\phi = 0$), which could be determined from ratio

$$H_z = \frac{I_m w}{2\pi \rho (R + \rho)} \left[K + \frac{R^2 - \rho^2}{(R - \rho)^2} E \right]. \quad (\text{III.29})$$

At $\rho = 0$, i.e. on the axis of the frame's turn, the field also has
only one component, directed along the axis OZ :

$$H_{z_0} = \frac{R^2 I_m w}{2r^3} = \frac{R^2 / m w}{2(R^2 + z^2)^{3/2}} \cdot \frac{R^2 I_m w}{2z^2}. \quad (\text{III.30})$$

In the case of receiving frame, being in plane and within the contour of oscillating frame, but not in the center, the component of the primary field will be determined by ratio (52)

$$H_z = \frac{I_m w}{\pi R(1-k^2)} \int_0^{\pi/2} \sqrt{1 - (k \sin \psi)^2} d\psi, \quad (\text{III.31.})$$

where $k = \frac{r}{R} < 1$ (r - distance from the center of turn to point P, at which the primary field is being determined (position center of the receiving frame)).

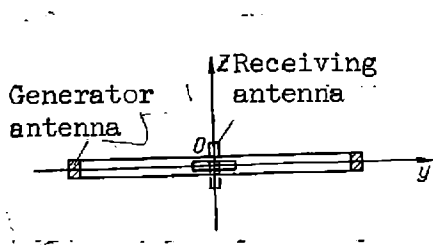


Fig. 31.

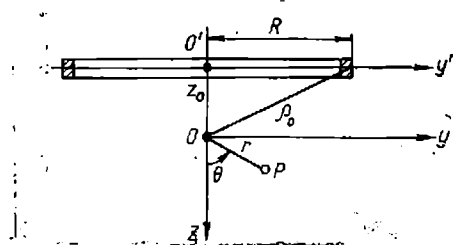


Fig. 32.

The determined integral in equation (III.31) - total elliptical integral of the second kind $E(k, \frac{\pi}{2})$ is determinable from table according to the value that, $k = \sin \alpha/2$.

In the center of the frame's turn, when $k = \frac{r}{R} = 0$ (coordinate $r = 0$), we have $E(k) = 1.57$ (29). Therefore, from formula (III.31) we find:

$$H_z = \frac{I_m w}{3.14 R(1-0)} \cdot 1.57 = \frac{I_m w}{2R}.$$

Thus in the center of the circular turn:

$$H_{z_0} = \frac{I_m w}{2R}. \quad (\text{III.31a})$$

Components of the primary field could be determined from somewhat different formulas on condition, that the center of the field is

arbitrarily displaced in relation to the center of oscillating frame.

Here are the basic relations for the calculations of primary magnetic field at point of field detector for this case.

For convenience of calculations we assume, that the oscillating frame has the shape of a circular loop of radius R with number of turns w and is energized by harmonic current, shown by a complex amplitude I_m , and the size of receiving frame (coil) is immensely less than that of the oscillating frame. The field detector receives either H_y or H_z component, depending on his position with respect to the oscillating frame (Fig.31).

If we take the circular loop axis $O'Z$ for the initial axis of coordinates, as shown in Fig. 32, then for points on axis OY with $\theta = 90^\circ$ and $r = y$ (r - length of radius-vector, θ - polar distance to point P), formulas for complex amplitudes H_y and H_z of horizontal $H_y(t)$ and vertical $H_z(t)$ components of the field's intensity H with accuracy upto terms of the second order of smallness (higher precision in components determination is practically inexpedient) would have the following appearance /128, 252/:

$$H_y = 0,75 I_m w \frac{R^2 z_0 y}{\rho_o^5} \left\{ 1 - \frac{5}{8} \cdot \frac{y^2}{4} (3R^2 - 4z_0^2) \right\}; \quad (\text{III.32})$$

$$H_z = 0,5 I_m w \frac{R^2}{\rho_o^3} \left(1 + \frac{3}{4} \cdot \frac{y^2}{\rho_o^4} (R^2 - 4z_0^2) \right),$$

where $z_0 = OO'$.

At the origin of coordinates, at point O , we have

$$H_y = 0; \quad H_{z_0} = \frac{0,5 I_m R^2 w}{\rho_o^3},$$

i.e., we arrive at the term corresponding to the formula (III. 30)

In case $Z_0 = 0$ that is to say $P_0 = R$; in the centre of the obtained generating frame (at point O).

$$H_y = 0; H_{z_0} = \frac{0,5 I_m w}{R},$$

i.e. we arrive at the term, corresponding to formula (III.31a).

4. Circular rotating magnetic field

Let us deduce the principal relations for magnitude and direction determination of the intensity vector of rotating magnetic field \vec{H}_{rot} in a uniform space. Position of axes and oscillating frames (dipoles with magnetic moments \vec{m}_x and \vec{m}_z) is shown in Fig. 33. We carry out calculations for arbitrary point P with Cartesian coordinates X, Y and Z.

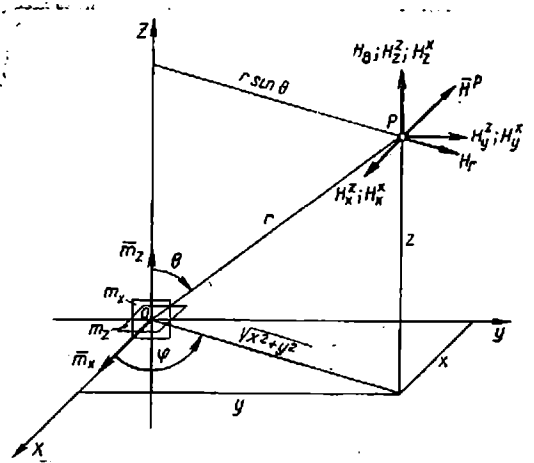


Fig. 33.

The sources of the field - dipoles \vec{m}_x and \vec{m}_z - are placed at the origin of coordinates. In the case of rotating magnetic field moduli of the magnetic moments of these dipoles will be /130/:

$$\begin{aligned} m_z &= m_0 \cos \omega t; \\ m_x &= m_0 \sin \omega t; \end{aligned} \quad (III.33)$$

where according to equation (III.4) $m_0 = I_w S$

The intensity components of the field of dipoles \bar{m}_z and \bar{m}_x on lines of coordinates OX, OY and OZ are determined from formulas (III.23) and (III.25a) respectively.

The resultant intensity components of rotating magnetic field \bar{H}^P are determined as sums of corresponding intensity components of fields, generated discretely by dipoles with moments \bar{m}_x and \bar{m}_z :

$$H_x^P = H_x^x + H_x^z; \quad H_y^P = H_y^x + H_y^z; \quad H_z^P = H_z^x + H_z^z.$$

Therefore, according to equations (III.23) and (III.25a) we get:

$$\left. \begin{aligned} H_x^P &= \frac{m_x}{4\pi r^3} \left(\frac{3x^2}{r^2} - 1 \right) + \frac{3m_z}{4\pi r^5} xz; \\ H_y^P &= \frac{3}{4\pi r^5} y (m_x x + m_z z); \\ H_z^P &= \frac{3m_x}{4\pi r^5} xz + \frac{m_z}{4\pi r^3} \left(\frac{3z^2}{r^2} - 1 \right). \end{aligned} \right\} \quad (III.34)$$

Substituting in equation (III.34) x, y and z from formulas (III.18), we get the terms for components of vector \bar{H}^P as functions of spherical coordinates:

$$\left. \begin{aligned} H_x^P &= \frac{m_x}{4\pi r^3} (3 \sin^2 \varphi \cos^2 \theta - 1) + \frac{3m_z}{4\pi r^3} \sin \theta \cos \theta \cos \varphi; \\ H_y^P &= \frac{3m_x}{4\pi r^3} \sin^2 \theta \sin \varphi \cos \varphi + \frac{3m_z}{4\pi r^3} \sin \theta \cos \theta \sin \varphi; \\ H_z^P &= \frac{3m_x}{4\pi r^3} \sin \theta \cos \theta \cos \varphi + \frac{m_z}{4\pi r^3} (3 \cos^2 \theta - 1). \end{aligned} \right\} \quad (III.35)$$

Substituting m_x and m_z from formulas (III.33) in (III.35), we get:

$$\begin{aligned} H_x^P &= a_x \cos \omega t - b_x \sin \omega t; \\ H_y^P &= a_y \cos \omega t - b_y \sin \omega t; \\ H_z^P &= a_z \cos \omega t - b_z \sin \omega t, \end{aligned} \quad (III.36)$$

where

$$\left. \begin{aligned} a_x &= \frac{3m_0}{4\pi r^3} \sin \theta \cos \theta \cos \varphi; \\ a_y &= \frac{3m_0}{4\pi r^3} \sin \theta \cos \theta \sin \varphi; \\ a_z &= \frac{m_0}{4\pi r^3} (3 \cos^2 \theta - 1); \end{aligned} \right\} \quad (\text{III.37})$$

$$\left. \begin{aligned} b_x &= \frac{m_0}{4\pi r^3} (3 \sin^2 \theta \cos^2 \varphi - 1); \\ b_y &= \frac{3m_0}{4\pi r^3} \sin^2 \theta \sin \varphi \cos \varphi; \\ b_z &= \frac{3m_0}{4\pi r^3} \sin \theta \cos \theta \cos \varphi. \end{aligned} \right\} \quad (\text{III.37-a})$$

Vector \bar{H}^P could be shown as

$$\bar{H}^P = \bar{a} \cos \omega t - \bar{b} \sin \omega t \quad (\text{III.38})$$

where

$$\bar{a} = \bar{i}a_x + \bar{j}a_y + \bar{k}a_z; \quad \bar{b} = \bar{i}b_x + \bar{j}b_y + \bar{k}b_z \quad (\text{III.39})$$

With an estimate of equations (III.37) and (III.37-a) we get

$$\left. \begin{aligned} |\bar{a}| &= \frac{m_0}{4\pi r^3} \sqrt{3 \cos^2 \theta + 1}; \\ |\bar{b}| &= \frac{m_0}{4\pi r^3} \sqrt{3 \sin^2 \theta \cos^2 \varphi + 1} \end{aligned} \right\} \quad (\text{III.40})$$

In accordance with parity (III.38) vector \bar{H} can be taken as a sum of two vectors (30):

$$\bar{M}_1 = \bar{a} \cos \omega t; \quad \bar{M}_2 = -\bar{b} \sin \omega t, \quad (\text{III.41})$$

moduli of which oscillate harmonically with the same frequency. These oscillations are shifted in phase at 90° .

It is well known, that addition of fields of two vectors with different directions, moduli of which vary harmonically with the same frequency and phase-shift, different to zero, produces the so called elliptically polarized field. The end of resultant vector of this type of field describes in space an ellips, lying in plane, determinable by direction of vectors \bar{a} and \bar{b} , which are its semi-axes.

If simultaneously $|\bar{a}| = |\bar{b}|$ and $\angle \bar{a}\bar{b} = 0$, there would be a circular rotating magnetic field. This condition is met, when $\theta = \varphi = 90^\circ$, i.e. at points on line OY (or line OZ), when $|\bar{a}| = |\bar{b}| = \frac{m_0}{4\pi r^3}$. In this case the plane, on which lie vectors \bar{a} and \bar{b} , is perpendicular to line OY (or OZ). At any other point the curve described by resultant vector, is an ellips. The modulus of resultant vector is determinable from equation.

$$|\vec{H}^P| = \sqrt{(H_x^P)^2 + (H_y^P)^2 + (H_z^P)^2}. \quad (\text{III.42})$$

Substituting in equation (III.42) values H_x^P , H_y^P and H_z^P from equations (III.34) and taking into account parities (III.33), after appropriate conversions and simplifications, we find the modulus of resulting vector in Cartesian coordinates:

$$|\vec{H}^P| = \frac{m_0}{4\pi r^3} \sqrt{\frac{3(x \sin t - z \cos \omega t)^2}{r^2} + 1}. \quad (\text{III.42a})$$

Substituting in equation (III.42a) values H_x^P , H_y^P and H_z^P from equations (III.35), we get the value of vector \vec{H}^P in spherical coordinates:

$$|\vec{H}^P| = \frac{m_0}{4\pi r^3} \sqrt{3 \sin^2 \theta \cos^2 \varphi \sin^2 \omega t + 3 \cos^2 \theta \cos^2 \omega t + 1}. \quad (\text{III.42b})$$

The angles of gradient of this vector pertaining to lines OX, OY and OZ respectively are as follows:

$$\alpha = \arccos \frac{H_x^P}{|\vec{H}^P|}; \quad)$$

$$\beta = \arccos \frac{H_y^p}{\sqrt{H}/P}; \quad) \quad (\text{III.43})$$

$$\gamma = \arccos \frac{H_z^p}{\sqrt{H}/P} . \quad)$$

For determining position of polarization plane in space in Cartesian coordinates it is necessary to determine the directing cosines of angles, formed by perpendicular to this plane and the lines of coordinates.

The single vector of the ellips plane perpendicular can be determined from formula:

$$\bar{n} = \frac{(\bar{b}\bar{a})}{/(\bar{b}\bar{a})/}, \quad (\text{III.44})$$

where $(\bar{b}\bar{a})$ -vector product.

Therefore, from formulas (III.44) and (III.36) we get:

$$\left. \begin{aligned} \cos \alpha &= \cos (\bar{n}, \bar{X}) = \frac{b_y a_z - b_z a_y}{q}; \\ \cos \beta &= \cos (\bar{n}, \bar{Y}) = \frac{b_z a_x - b_x a_z}{q}; \\ \cos \gamma &= \cos (\bar{n}, \bar{Z}) = \frac{b_x a_y - b_y a_x}{q}, \end{aligned} \right\} \quad (\text{III.45})$$

where $\cos \alpha$, $\cos \beta$ and $\cos \gamma$ - directive cosines;

$$q = /(\bar{b}\bar{a})/ = \sqrt{(b_y a_z - b_z a_y)^2 + (b_z a_x - b_x a_z)^2 + (b_x a_y - b_y a_x)^2}. \quad (\text{III.46})$$

Having substituted in parities (III.45), (III.46) values $a_x, a_y, a_z, b_x, b_y, b_z$ from equations (III.37), (III.37a) and carried out appropriate trigonometric conversions, we finally obtain:

$$\left. \begin{aligned} \cos \alpha &= \frac{3 \sin^2 \theta \sin \varphi \cos \varphi}{\sqrt{4 - 3 \sin^2 \theta \sin^2 \varphi}}; \\ \cos \beta &= \frac{2 - 3 \sin^2 \theta \sin^2 \varphi}{\sqrt{4 - 3 \sin^2 \theta \sin^2 \varphi}}; \end{aligned} \right\} \quad (\text{III.47})$$

$$\cos Y = \frac{3 \sin \theta \cos \theta \sin \varphi}{\sqrt{4 - 3 \sin^2 \theta \sin^2 \varphi}} \quad)$$

The obtained equations make it possible to calculate primary field at the placement point of receiving frames P (Fig.33) for a single-plane pattern of induction aeromethod with the use of circular rotating magnetic field. This pattern is not free from the effect of changes in geometry of the system, as confirmed by some of the authors (e.g./117/). Even on condition of ensuring the required angle, between the oscillating frames, polarization plane of the circular VMP* at point P will not be perpendicular to line OY (or OZ). Therefore, the effect of angles θ and φ on polarization plane dip will not be eliminated. Moreover, even with perpendicularity of vectors \vec{a} and \vec{b} (phase shift of e.m.f. in reception frames by $\frac{\pi}{2}$) moduli $|\vec{a}|$ and $|\vec{b}|$, on the basis of equation (III.40), are not reciprocally equivalent, i.e. vector of resulting field describes an ellipsis with rotation around its axis. Thus, e.m.f. induced in receiving frames after obtaining time shift of one of them by $\frac{\pi}{2}$, also will not be reciprocally equivalent in amplitude and their reciprocal compensation will be disturbed.

In order to obtain move-out of signals equal to zero, it would be necessary to lead in, besides the phase-invertor, also amplifier with conversion factor other than one (this factor is the function of coordinates) or to change the intensity of current in one of the oscillating frames.

For a two-plane pattern of VMP (see Fig.16) the rotating field will be circular along the line OY, when conditions $|\vec{a}| = |\vec{b}| = \frac{m_0}{4 \pi r^3} \cdot \theta = \varphi = 90^\circ$

* VMP = rotating magnetic field.

are satisfied. The plane, in which lie vectors \bar{a} and \bar{b} , is in this case perpendicular to line OY, i.e. - flight line of the first plane.

The resultant vector of magnetic field, retaining its modulus invariable, rotates around the flight axis of the aircraft with oscillating frame at angular velocity, equal to angular frequency of the current, which excites the field. With the similar parameters of receiving frames and the presence of a uniform medium in the area of flight, the primary field will induce in receiving frames variable voltages similar in amplitude, but shifted in phase by 90° . Since one of these voltages by means of a special phase-invertor turns in phase at 90° and is subtracted from the other, the resultant output signal will be equal to zero.

According to the symmetry of the spread, shown in Fig. 16, with only the primary field present some changes in rotation angle of oscillating and receiving frames around the axis OY, and also the simultaneous variation of current amplitudes or initial phases in both the oscillating frames will not result in appreciable change in the balance attained. Only in the presence of a secondary field distance variation between the mobile objects will slightly change the value of unbalanced signal.

On the basis of determining characteristics of the near zone aeromethods (induction aeromethod) given in chapter II and relations obtained in paras 2-4 of chapter III for calculations of primary field at the point of field detector a summary Table 1 has been composed.

Data of Table 1 permit to determine the relative magnitude of mechanical error in the analyzed patterns of induction aeromethod. Knowing parameters of field detector it would also be possible to calculate the absolute value of mechanical interference. The value of this

interference for the patterns of the first group (see para 1 Chapter II), except the single-plane pattern of VMP, is determined directly from formulas for the value of primary field component, received by detector. For the single-plane version of VMP of the first group and versions of second group the magnitude of interference is indirectly directed from formulas, which take into account the difference (ratio) of signals, induced in detectors by the received components of the field. In both the cases the value of mechanical interference depends on parameters of the primary fields sources and coordinates of field detectors (their position in relation to field source). Practical methods for determination of mechanical interferences are discussed in chapters IX and XIII.

5. Field of the rectilinear infinitely long cable.

The field of infinitely long cable with assumption of the uniformity of earth was initially calculated by Fok and Bursian (213); the field of finite length cable is discussed in works (41,42).

In aerial electroprospecting in calculations of the cable field the analysis is, usually, of its quasistationary approximation. It is assumed, that for air the wave number $k_0 = 0$, and for earth:

$$k = \frac{\omega}{c} \sqrt{\epsilon - j \frac{2\pi\sigma}{\omega}} \approx (1 - j) 2\pi \sqrt{\frac{f}{10}}, \text{ KM}^{-1},$$

where ρ - specific resistivity of earth, OM . M;

f - frequency of exciting field, cps.

Constituents of the cable's magnetic field \bar{H} is found from the values of vector-potential \bar{A} ($\bar{H} = \text{rot}, \bar{A}$). It is convenient to resolve this problem in relative dimensionless coordinates according ^{to} Dmitriev (68, 69):

$$\xi_1 = \left| \vec{k} \right| x = 2 \sqrt{2\pi} \frac{x}{\lambda}; \quad \xi_2 = \left| \vec{k} \right| z = 2 \sqrt{2\pi} \frac{z}{\lambda},$$

where λ - wave length within the earth; x, z - coordinates (see Figs.5 and 41).

Expressing constituents of the cable's magnetic field in terms of horizontal component of vector-potential A_y , directed along the cable, we get:

$$\begin{aligned} \dot{H}_x &= 10^{-3} \frac{\sqrt{2}}{\lambda} I \frac{\partial \dot{A}_y}{\partial \xi_2} \\ \dot{H}_y &= 0; \\ \dot{H}_z &= 10^{-3} \frac{\sqrt{2}}{\lambda} I \frac{\partial \dot{A}_y}{\partial \xi_1} \end{aligned} \quad (\text{III.48})$$

where I - current in cable, a.

A_y value is determinable with fulfilment of the following conditions:-

$$\Delta A_y = 0 \text{ at } \xi_2 > 0 \quad (\text{III.49})$$

$$\Delta A_y - jA_y = 0 \text{ at } \xi_2 < 0;$$

$$A_y \text{ and } \frac{\partial A_y}{\partial \xi_2} \text{ are continuous at } \xi_2 = 0$$

Along the cable $A_y \approx \ln r$ at $\xi_1 = 0$, $\xi_2 = 0$; in infinity $A = 0$.

As a result we get:

$$\begin{aligned} A_y &= 2 \int_0^\infty e^{-\xi_2 t} \frac{\cos \xi_1 t dt}{t + \sqrt{t^2 + j}} \text{ at } \xi_2 > 0; \\ A_y &= 2 \int_0^\infty e^{\xi_2 \sqrt{t^2 + j}} \frac{\cos \xi_1 t dt}{t + \sqrt{t^2 + j}} \text{ at } \xi_2 < 0. \end{aligned} \quad (\text{III.50})$$

With an estimate of equations (III.48) and (III.49) for the constituents of magnetic field above the ground surface we have the following

expressions:

$$\left. \begin{aligned} \dot{H}_x &= 10^{-3} \frac{2\sqrt{2}}{\lambda} I \int_0^{\infty} e^{-\xi_2 t} \frac{\cos \xi_1 t}{t + \sqrt{t^2 + j}} dt; \\ H_z &= -10^{-3} \frac{2\sqrt{2}}{\lambda} I \int_0^{\infty} e^{-\xi_2 t} \frac{\sin \xi_1 t}{t + \sqrt{t^2 + j}} dt. \end{aligned} \right\} \text{(III.51)}$$

Integrals in equations (III.51) are shown in the form of series and are determined by term-by-term integration.^(*)

If the field is analysed at $\frac{x}{\lambda} \gg 1$, then in the indicated expansion, with sufficient accuracy for practical purpose, it is possible to be restricted to the first term only.

Thus, far from the cable constituents H_x, H_z on the basis of equations (III.51) and (68) could be shown as:

$$\begin{aligned} \dot{H}_x &= -10^{-3} \frac{2I}{\lambda} \cdot \frac{(1-j)}{\xi_1^2}; \\ H_z &= -10^{-3} \frac{4I}{\lambda} \cdot \frac{[\xi_2 - j(\sqrt{2} + \xi_2)]}{\xi_1^2} \end{aligned} \quad \text{(III.52)}$$

If moduli $\left| \frac{H_z}{H_x} \right|$ are compared, we get equation:

$$\left| \frac{H_z}{H_x} \right| = \frac{2\sqrt{\xi_2^2 + \sqrt{2}} \xi_2 + 1}{\xi_1} \quad \text{(III.53)}$$

which testifies to the fact, that modulus $\left| \dot{H}_z \right|$ decreases with distance r considerably faster than $\left| \dot{H}_x \right|$. Therefore, in aerial electric prospecting by BDK method, when the investigation has to be carried out on as large as possible area with one laying of cable, it would be more economical to measure constituent H_x and not H_z .

(*) Integrals of type $\int_0^{\infty} \cos \xi_1 t F(t) dt$ and $\int_0^{\infty} \sin \xi_1 t F(t) dt$ on

Experience shows, that in resolving the technical problems in aerial electric prospecting, it is sufficient to use the approximate formulas (III.52), which are true for the central profile with cable of infinite and finite length /68, 216/. In other cases it would be more rational to use precise formulas (III.51) or curves obtained on analogue specially for problems of aerial electric prospecting /41/.

6. The field of long-wave broadcasting stations and radio-stations of special designation.

Methods of the high-frequency aerial electroprospecting (distant zone of sub-group with harmonic field) are based, as pointed out, on studying certain parameters of electromagnetic fields, in particular of the fields of long-wave broadcasting radio-stations and of other radio-stations within the area of investigation map.

In geophysical aerelectro-prospecting by radio-comparing and control the use is made of surface radio-waves, propagating above the ground surfaces and partially enveloping it due to diffraction. In certain conditions the effect of ionosphere and diffraction could be ignored, assuming, that the atmosphere is a uniform medium, and the ground surface

(continued from the back page)

condition, that function $F(t)$ and its derivatives are converted into zero at infinity, should be shown as (68):

$$\int_0^{\infty} \cos \xi_1 t F(t) dt = \sum_{n=1}^{\infty} (-1)^n \frac{F^{(2n-1)}(0)}{\xi_1^{2n}} ;$$

$$\int_0^{\infty} \sin \xi_1 t F(t) dt = \sum_{n=0}^{\infty} (-1)^n \frac{F^{(2n)}(0)}{\xi_1^{(2n+1)}} .$$

flat. This permits to assume, that the propagation of radio-waves depends only on electrical properties of rocks composing section of earth crust, chosen for the geophysical investigations.

Long radio-waves (in air $\lambda_0 > 3000$ m), applied in radio control method, are characterised by comparatively low absorption in the earth. Moreover, due to refraction they are capable of easily enveloping the earth surface. Starting from a distance of 60-200 km from the source, radio-waves are to a certain extent affected by space-wave, reflected from the layer of ionosphere, the altitude of which in day-time is 70 km, and at night - 85-90 km. At minor distances the surface wave is predominant. This permits to calculate the field's intensity from formulas of ideal radio-channel.

The space-wave affects the field's intensity at the point of reception, which results in errors of non-geological origin. Usually at night the intensity of the field is higher than during the day. However, according to numerous data, the field is more stable during the morning and partially during the daylight hours, i.e., at the usual time of implementing aerogeophysical investigations, at 150-200 km from the source.

The superlong waves, with frequencies less than 25 kcps with propagation at considerable distances are well reflected from the lower ionized layers both at night and during the day. Due to this and minor damping with reflection from the earth this type of waves propagate to greater distances in the unique wave guide, formed by earth surface and ionosphere. The field of superlong waves is distinct by the stability of amplitude and phase. However, even in superlong waves their regular variation is evident with changing distance and transition from day to night. The significant positive quality of these waves is the possibility of deeper penetration into sea water.

Results of investigating propagation of long and superlong waves are given in detail in the work /173/; the obtained data should be estimated in aeroelectro-prospecting in distant zone.

It may be assumed, that generally the problem of investigating propagation of radio-waves from the set properties of emitter is reduced to the following: determination of the main initial parameters - location, thickness, actual height of antenna and emitter's wave length; study of the medium's properties along the selected track - conductivity, dielectric permeability ϵ , magnetic permeability μ^* and determination at reception point of intensity vectors of electric E and magnetic \vec{H} fields (their amplitudes, phases, orientation in space, etc.), and also of Umov's and Pointing vector.

Questions regarding theory of radio-waves propagation in application to some problems of geophysics have been analysed by Sommerfield, Van der Pol, V.A. Fok, L.I. Mandelstamp, P.D. Papalexi /149, 214/ and others. The more detailed analysis of radio-waves propagation and anomalous changes of electromagnetic fields in application to ground and aerial electro-prospecting by radio-control method is given in works /201, 202/.

Let us present briefly these most significant aspects of the theory of radio-waves propagation and characteristic features of electro-magnetic field at point of observation.

It is well known, that for surface radio-waves (long and medium) field intensity of radio-station signal at any point of the wave zone,

*It is assumed, that within wave range, used for geophysical purposes, parameters σ , ϵ and μ are not dependent on the signal frequency.

situated within r kilometers from transmitter with P kilowatt power, may be shown by Shuleikin - Van der Pol formula /72/:

$$E_c = \frac{245 \sqrt{PD}}{r} \quad W, M \quad V/M, \quad (III.54)$$

where D - directive gain of antenna; W - dimensionless multiplier, characterizing energy absorption of electromagnetic waves and dependent on wave length and the nature of absorbing action of semi-conductive soil; if there are no loss of $W = 1$.

If there is an emitter in the shape of oscillator on transmitting side, field density could be determined from the following type of relation /247/:

$$E_c = \frac{120 \pi h_e I_A}{\lambda_0 r} \cos \theta \quad MV/M, \quad (III.55)$$

where h_e - virtual altitude of oscillator, km; I_A - highest intensity of current in oscillator, a; θ - angular height of the observation point in respect of oscillator.

From this relation it follows, that the field in distant (wave) zone decreases inversely proportional to distance from its source.

Geophysical investigations by radio control method are conducted within a limited area with base points and at considerable distance from the source of electromagnetic field. In this case the electromagnetic wave in the area of investigations may be taken as plane wave.

In medium with certain conductivity σ and permeability ϵ the field decreases with increasing distance from its source according to exponential decay:

$$E = E_0 e^{-\frac{2 \pi f}{c} \beta r} \sin \omega \left(t - \frac{\alpha}{c} r \right); \quad (III.56)$$

$$H = H_0 e^{-\frac{2 \pi f}{c} \beta r} \sin \omega \left(t - \frac{\alpha}{c} r \right).$$

where coefficients of phase and damping respectively will be /75/

$$\alpha = \sqrt{\epsilon \mu} \sqrt{\frac{1}{2} + \frac{1}{2} \sqrt{1 + \left(\frac{4\pi\sigma}{\epsilon\omega}\right)^2}};$$

$$\beta = \sqrt{\epsilon \mu} \sqrt{\frac{1}{2} - \frac{1}{2} \sqrt{1 + \left(\frac{4\pi\sigma}{\epsilon\omega}\right)^2}};$$
(III,57)

ω = working circular frequency.

Omitting in equations (III.56) the time multiple and bringing in absorption factor:

$$b = \frac{2\pi f}{c} \beta, \quad (III.58)$$

we arrive at the well known relations /18, 202, 247/:

$$E = E_0 e^{-br};$$

$$H = H_0 e^{-br}$$
(III.59)

Since $\frac{c}{\alpha}$ - propagation velocity of electromagnetic wave in direction of propagation,

$$\frac{c}{\alpha} = v, \quad (III.60)$$

where c - velocity of light, km/sec, then equation (III.60) determines the length of electromagnetic wave in medium:

$$\lambda = \frac{v}{f} = \frac{c}{\alpha f} = \frac{\lambda_0}{\alpha}. \quad (III.61)$$

Parameter $\frac{2\sigma}{\epsilon f}$ ($\frac{4\pi\sigma}{\omega\epsilon} = \frac{2\sigma}{\epsilon f}$) in formulas for factors α and β is equivalent to ratio of conductivity current to displacement current in medium under investigation.

If $\frac{2\sigma}{\epsilon f} \gg 1$, the medium may be taken as conductive. When $\frac{2\sigma}{\epsilon f} \ll 1$, the medium in its properties approaches dielectric.

The absorption factors for plane wave and velocity of its propagation vs. frequency f and conductivity σ at constant and known

value ϵ (for rocks $\epsilon \approx 10$) are given in /200, 202/.

In the presence of two media - uniform and isotropic, the nature of plane changes. The earth-air interface introduces certain distortions into electromagnetic wave front, i.e. one portion of it is reflected from the interface, and another is refracted and passes inward of the second medium. This results in changing orientation of vectors \vec{E} and \vec{H} in respect of interface, moreover, there will be two extreme cases of their orientation.

The first case - vector \vec{E} lies within a plane, which passes through Umov-Pointing vector and is perpendicular to interface. In this case there is normal polarization or polarization within the propagation plane.

Second case - vector \vec{H} lies within a plane passing through Umov-Pointing vector and perpendicular to the plane of interface. Here the polarization is abnormal, i.e. perpendicular to propagation plane.

The intermediate cases of polarization could be easily reduced to above two extreme cases by expanding vectors \vec{E} and \vec{H} on two axes. For geophysical investigations in distant zone the application is of normal or near to normal polarization.

Analysis of two extreme cases of change in orientation of vectors \vec{E} and \vec{H} shows, that with high angle φ between the vertical (line OZ) and the trend of incident wave, amplitudes of reflected waves are almost equivalent to those on incident, and the phase shift between them strives towards 180° . Investigations of fields of remote radio stations confirm the indicated theoretical deductions.

For normally polarized wave in air medium of distant zone the following relation is true between the horizontal E_x and vertical E_z components of electric field density vector:

$$\frac{E_x}{E_z} = \frac{1}{\sqrt{\epsilon_2 + j \left(\frac{2 \sigma_2}{f} \right)}} \quad (\text{III. 62})$$

where the term under the root - composite dielectric permeability of medium (the index 2 refers to earth medium).

Assuming, that for the air = 1 and $\mu = 1(75)$, we have

$$\bar{H}_y = - \bar{E}_z. \quad (\text{III. 63})$$

If the predominant within the earth are the displacement currents, then

$$\frac{|E_{x_1}|}{|E_{z_1}|} = \frac{|E_{z_1}|}{\sqrt{\epsilon_2 \mu_2}} \quad (\text{III. 64})$$

and if the conductive, then

$$E_{x_1} = \frac{1 - j}{2 \sqrt{\frac{2 \sigma_2}{f}}} E_{z_1}, \quad (\text{III. 65})$$

where index 1 refers to air medium.

Thus amplitude ratio is

$$\frac{|E_{x_1}|}{|E_{z_1}|} = \sqrt{\frac{f}{2 \sigma_2}}, \quad (\text{III. 66})$$

and the phases will be shifted at an angle of 45° , which is natural to the usual geological environment at these wave lengths.

Theoretical investigations show, that with adopted initial conditions (infinite extension, uniformity and isotropy of media) the vertical component of the electric field density vector is greater than horizontal at the air-earth interface. Therefore, the electromagnetic wave may be assumed to be plane-polarized * /162/. In this case vector \bar{E} on the surface

*The meaning of the term "plane" wave is the fact, that at any plane $z = \text{const}$ at a given time instant the phase of the process is constant, i.e. the oscillations throughout the plane are cephasal.

of earth is inclined forward at an angle:

$$\theta = \arctg \frac{E_{x_1}}{E_{z_1}} = \arctg \sqrt{\frac{f}{2 \cdot \sigma}} \quad (\text{III.67})$$

The relations (III.64) - (III.67) permit to draw some very significant conclusions for geophysical survey.

1. The Umov-Poynting vector, rigidly horizontal with propagation along the ideally conductive surface, in the presence of conductive anomalies acquires a vertical component, directed downward.

2. If in normal field horizontal component of electric field density vector is low, then in the presence of conductive anomaly it considerably increases. This permits to enhance the depth of investigations, as the reaction of conductive body within the earth, shown by variations of horizontal component, will seem more clearly defined on the background of the lower value of primary magnetic field.

3. Within the earth the horizontal component of the electric field density vector, i.e. $E_{z_2} \ll E_{x_2}$ is predominant.

4. From formula (III.67) it follows, that the slope of wave front, and therefore the loss within the earth increase with increasing frequency f and decrement of conductivity (due to increase of induction currents, which hamper penetration of electromagnetic energy within the earth.

The magnetic constituent of electromagnetic field in normal conditions (i.e. in a uniform half-space) is always rigidly horizontal, regardless of the conductivity of rocks. The vertical constituent of magnetic field is even in a greater degree than horizontal component of electric field, will be free of the primary field effect. Since vector H is horizontal,

the Umov-Pointing vector is vertical and directed downward. The amplitude decrease of electric and magnetic components of Umov-Pointing vector with depth occurs in the same way as in the case of unlimited space. It should be mentioned, that the slope of wave front is above the earth surface upto altitude in the order of $2-3 \lambda_0$. Higher up vector \vec{E} acquires an exactly vertical direction.

If the application is of horizontal oscillator, then on the flat surface of ideally conductive earth the intensity of electric field could be determined from the following formulas:

horizontal component in equatorial plane

$$E_r = \frac{240 \pi h_e I_A \sqrt{r_1 r_2}}{\lambda_0^2 r^2}, \text{ M } \cancel{B}/\text{M}, \quad (\text{III.68})$$

where r_1 and r_2 - altitude respectively of the radiation and reception points, km;

vertical component within the wave area

$$E_b = \frac{120 h_e I_A \sin \theta}{\lambda_0 \sqrt{\epsilon_2}}, \text{ M } \cancel{B}/\text{M}, \quad (\text{III.69})$$

where ϵ_2 - composite dielectric constant of the top layers of earth crust, determinable from relation

$$\epsilon = \epsilon \left(1 + j \frac{4\pi\sigma}{\epsilon \omega} \right); \quad (\text{III.70})$$

θ - angle between direction to observation point and the perpendicular to axis of horizontal oscillator.

With considerable removal from transmitter the vertical component is many times greater than horizontal and is used as an object of investigations in geophysical aeroelectric prospecting.

As has been pointed out, the radio-wave with passage above the earth

surface becomes partially damped, as in actual conditions the rocks along the propagation path of the radio-wave have a finite conductivity. In this case the damping of radio-wave is accounted for by introduction of a special factor or the absorption function $I_s(\rho)$, which depends on distance to field emitter, electric properties of rocks and frequency of oscillations:

$$E = E_0 I_s(\rho) = \frac{A}{\lambda_0 r} I_s(\rho), \quad (\text{III.71})$$

where A - certain constant quantity.

Parameter ρ , which characterises the absorption function, is denoted as numerical distance and is determinable by relation /202/:

$$\rho = \frac{\pi r \sqrt{(\epsilon - 1)^2 + \left(\frac{2\sigma}{f}\right)^2}}{\lambda_0 [\epsilon^2 + \left(\frac{2\sigma}{f}\right)^2]} = \text{Sr.} \quad (\text{III.72})$$

If $\sigma \ll \epsilon f$, i.e. in rocks invariably it is, then

$$\rho \approx \frac{\pi r}{\lambda_0} \cdot \frac{1}{\sqrt{\epsilon^2 + \left(\frac{2\sigma}{f}\right)^2}} \quad (\text{III.72a})$$

If the predominant within the earth are the currents of displacement, i.e. $\frac{2\sigma}{\epsilon f} \ll 1$, then

$$\rho = \frac{\pi r}{\lambda_0} \cdot \frac{1}{\epsilon} \quad (\text{III.72b})$$

But if $\frac{2\sigma}{\epsilon f} \gg 1$, then

$$\rho = \frac{\pi r}{\lambda_0} \cdot \frac{f}{2\sigma} \quad (\text{III.72c})$$

The numerical distance is determinable from formulas or by means of special, previously calculated, curves /202/. For determination of function $I_s(\rho)$ it is possible to use also the approximate equation

$$I_s(\rho) = \frac{2 + 0.3\rho}{2 + \rho + 0.6\rho^2} \quad (\text{III.73}).$$

CHAPTER IV - SOME DATA REGARDING NORMAL AND ANOMALOUS
FIELDS AND PRACTICAL RESULTS OF SURVEY.

1. Normal field in aerial methods of the near zone.

The geoelectric irregularities of the top layers of the earth crust are always disposed within the surrounding rocks (or media), which are, with rare exceptions, conductive laminations distorting the artificially generated primary field and cause the appearance of so called false anomalies. Therefore, in aerial electro-prospecting, same as in the ground one, a field has to be operated, which is a sum of the field of primary field source and of the field, generated by cover deposits of the earth surface. This field is denoted as normal, assuming that it is actually normal only in the absence of the disturbing object - the subject of geophysical investigation. In other conditions, an anomalous field, generated by the primary field source, cover deposits and conductive object will exist. Therefore, in aerial methods of the near zone, meant invariably for detecting and investigating the local geoelectric irregularities (metallization, ore bodies etc.), the normal is taken to be the field above a medium, not containing these irregularities, i.e.

$$\overline{H}_h = \overline{H}_1 + \overline{H}_{med.} \quad (IV.1)$$

From the analysis data of normal fields in aerial electro-prospecting it is possible to obtain some information regarding the effect of surrounding medium on the anomalous field and to determine the nature of false anomalies, emerging due to variation (along the survey profile) of the surrounding medium's parameters.

Calculations of the field, reflected from the earth surface (surrounding medium) component of normal field in aerial methods of the near zone, - same as calculations of anomalous fields, require highly complex mathematical computations. The pertinent investigations were conducted in the Soviet

Union, as well as in other countries and are sufficiently well elucidated in (38,47).

Let's take as an example the pattern of induction method of aerial electric prospecting with the source and detector of the field spread out in space. The most simple case of the surrounding medium generating in the presence of primary field source (magnetic dipole or any other source) normal field, is the uniform half-space. In this case two very rigid limitations are applied to the surrounding medium: the conductivity is assumed to be zero, and the primary field is taken as uniform (i.e. $\vec{H}_1 = \text{const}$). The first limitation determines the second, since from Maxwell's equations (see paral chapt. III) it follows, that $\text{rot } \vec{H} = \gamma \vec{E}$, i.e. the uniform field is only possible at $\gamma = 0$.

In actual conditions the conductivity of the surrounding medium is always different from zero, and the utilized fields are non-uniform and only in a few cases are near to them. The admissible simplifications ($\gamma \text{ med.} \approx 0$; $\vec{H}_1 \approx \text{const}$) permit a whole series of typical specifications in the induction method of aerial electric prospecting being defined and analysed.

Let the source of primary field be at altitude h above the uniform half-space with the conductivity of the medium γ (or its specific resistivity ρ). The surface of half-space we take as plane $z = 0$ (Fig.34). In the case of magnetic dipole with harmonic current by reading of field phase from the current phase in the source it is possible to assume (see paral, chapt. III), that

$$\vec{E}_m = E_m e^{j\omega t}; \vec{H}_m = H_m e^{j\omega t}.$$

In this the applied fields satisfy Maxwell's equations, which we write as

$$\left. \begin{aligned} \text{rot } \vec{H} &= j \frac{k^2}{k_0} \vec{E}; \\ \text{rot } \vec{E} &= -jk_0 \vec{H}; \\ \text{div } \vec{H} &= 0; \\ \text{div } \vec{E} &= 0. \end{aligned} \right\} \quad (\text{IV.2})$$

where k - wave number in the air, $k = k_0 \frac{\omega}{c}$, km^{-1} , at $z > 0$,
 $k = k_1 \approx (1 - j) k_0 \frac{3 \cdot 10^5}{\sqrt{10} \rho f}$, km^{-1} , at $z < 0$ (ρ - specific resistivity ohm m, f - field frequency, cps) (69).

The components of electromagnetic field \vec{H} and \vec{E} could be shown in terms of Hertz magnetic vector $\vec{\Pi}$, which is a function of coordinates and time and fully depicts the electric and magnetic sides of the wave process.

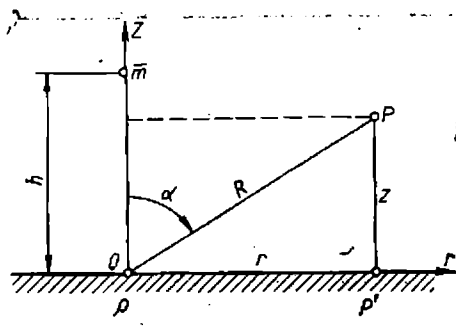


Fig. 34.

Vector $\vec{\Pi}$ is subject to wave equation (52), which ensues from the first Maxwell equation for the case of ideal dielectric ($v = c$; $\epsilon \mu = \frac{1}{c^2}$). Therefore, it is possible to write

$$\Delta \vec{\Pi} + k^2 \vec{\Pi} = 0. \quad (\text{IV.3})$$

where $k = k_0$ at $z > 0$; $k = k_1$ at $z < 0$.

At the location point of the field's source ($r = 0$, $z = h$) Hertz vector has this feature: $\vec{\Pi} \sim \frac{1}{r}$, while on the interface the marginal

conditions are maintained as a continuity of $\bar{\Pi}$ and $\frac{\partial \bar{\Pi}}{\partial z}$.

Assuming that in the cylindrical coordinates (z, r, φ) the conducting medium takes up half-space $z < 0$, and its boundary coincides with plane $z = 0$ (see Fig.34), let the magnetic field source also be in the area $z = h > 0$. The intermediate zone $(0 < z < h)$ is taken up by non-conductive and non-magnetic medium (air). In this case vector $\bar{\Pi}$ for vertical magnetic dipole could be shown in terms of integrals from the fundamental functions of the set problem (69):

$$\begin{aligned} \bar{\Pi} &= \int_0^\infty J_0(qr) e^{-\sqrt{q^2 - k_0^2}(z-h)} \frac{q dq}{\sqrt{q^2 - k_0^2}} + \\ &+ \int_0^\infty J_0(qr) e^{-\sqrt{q^2 - k_0^2}(z+h)} f(q) \frac{q dq}{\sqrt{q^2 - k_0^2}} \quad \text{at } z > 0; \quad (\text{IV.4}) \\ \bar{\Pi} &= \int_0^\infty J_0(qr) e^{\sqrt{q^2 - k_0^2} z - \sqrt{q^2 - k_0^2} h} \varphi(q) \frac{q dq}{\sqrt{q^2 - k_0^2}} \quad \text{at } z < 0. \end{aligned}$$

where $J_0(qr)$ - Bessel's function of the first series of zero order from argument qr ; q - factor of damping in direction r ; $\sqrt{q^2 - k_0^2}$ - factor of damping in direction z ; $f(q)$ and $\varphi(q)$ - functions determinable by marginal conditions.

Substituting these terms in marginal conditions, we get the initial equations for the determination of functions $f(q)$ and $\varphi(q)$:

$$1 + f(q) = \varphi(q); \quad \sqrt{q^2 - k_0^2} (1 - f(q)) = \sqrt{q^2 - k_1^2} \varphi(q).$$

Hence

$$\begin{aligned} f(q) &= \frac{\sqrt{q^2 - k_0^2} - \sqrt{q^2 - k_1^2}}{\sqrt{q^2 - k_0^2} + \sqrt{q^2 - k_1^2}}; \quad (\text{IV.5}) \\ \varphi(q) &= \frac{2\sqrt{q^2 - k_0^2}}{\sqrt{q^2 - k_0^2} + \sqrt{q^2 - k_1^2}}. \end{aligned}$$

Substituting the obtained values $f(q)$ and $\varphi(q)$ in formulas (IV.4), we find

$$\begin{aligned} \Pi &= \frac{e^{-jk_0 R}}{R} + \\ &+ \int_0^{\infty} J_0(qr) e^{-\sqrt{q^2 - k_0^2}(z+h)} \frac{(\sqrt{q^2 - k_0^2} - \sqrt{q^2 - k_1^2}) q dq}{(q^2 - k_0^2 + q^2 - k_1^2) q^2 - k_0^2} \text{ at } z > 0; \\ \Pi &= 2 \int_0^{\infty} J_0(qr) e^{-\sqrt{q^2 - k_1^2} z - \sqrt{q^2 - k_0^2} h} \frac{q dq}{\sqrt{q^2 - k_0^2} + \sqrt{q^2 - k_1^2}} \text{ at } z < 0. \end{aligned} \quad \dots (IV.6)$$

where $R = \sqrt{(z-h)^2 + r^2}$.

By placing $k_0=0$, we obtain the terms for the determination of constituents of the magnetic field ($H_\varphi = 0$) in quasistationary zone:

$$H_r = m \left\{ \frac{3r(z-h)}{R^5} + \int_0^{\infty} J_1(qr) e^{-q(z+h)} \frac{q - \sqrt{q^2 - k_1^2}}{q + \sqrt{q^2 - k_1^2}} q^2 dq \right\}; \quad (IV.7)$$

$$H_z = m \left\{ \frac{2(r-h)^2 - r^2}{R^5} + \int_0^{\infty} J_0(qr) e^{-q(z+h)} \frac{q - \sqrt{q^2 - k_1^2}}{q + \sqrt{q^2 - k_1^2}} q^2 dq \right\} \quad (IV.8)$$

If for the unit of length (distance) we take the wave length in earth

$$\Lambda = \frac{2\pi}{R \cdot k_1} = \frac{2\pi}{k_0^3 \cdot 10^5} \sqrt{10\rho} f = 10^3 \sqrt{\frac{10\rho}{f}} \text{ , M,}$$

and replace in integrals (IV.7) and (IV.8) the variable $q = \frac{2\sqrt{2}\pi}{\Lambda} t$, we will be converted to dimensionless distances $\xi_1 = \frac{r}{\Lambda}$ and $\xi_2 = \frac{z+h}{\Lambda}$.

As a result we obtain:

$$H_r = m \left\{ \frac{3r(z-h)}{R^5} + \frac{16\sqrt{2}\pi}{\Lambda^3} \int_0^\infty J_1(2\sqrt{2}\pi \xi_1 t) e^{-2\sqrt{2}\pi \xi_2 t} \frac{t - \sqrt{t^2 + j}}{t + \sqrt{t^2 + j}} t^2 dt \right\};$$

$$H_z = \dots (IV.9)$$

$$= m \left\{ \frac{2(z-h)^2 - r^2}{R^5} + \frac{16\sqrt{2}\pi}{\Lambda^3} \int_0^\infty J_0(2\sqrt{2}\pi \xi_1 t) e^{-2\sqrt{2}\pi \xi_2 t} \frac{t - \sqrt{t^2 + j}}{t + \sqrt{t^2 + j}} t^2 dt \right\}.$$

Assuming that the field detector is situated at point P at invariable distance $R = \sqrt{(z-h)^2 + r^2}$ from the point source of the reflected field, which is at point O, and denoting by α the angle between the vertical and the straight connecting source and field detector (see Fig.34), we get

$$z - h = -R \cos \alpha; \quad z + h = 2h - R \cos \alpha; \quad r = R \sin \alpha.$$

In this case formulas (IV.9) will have the following appearance:

$$H_r = m \left\{ \frac{1.5 \sin 2\alpha}{R^3} + \frac{16\sqrt{2}\pi}{\Lambda^3} \int_0^\infty J_1(2\sqrt{2}\pi \frac{R}{\Lambda} \sin \alpha t) e^{-2\sqrt{2}\pi \frac{2h-R \cos \alpha}{\Lambda} t} \frac{t - \sqrt{t^2 + j}}{t + \sqrt{t^2 + j}} t^2 dt \right\}$$

$$H_z = m \left\{ \frac{0.5 + 1.5 \cos \alpha}{R^3} + \frac{16\sqrt{2}\pi}{\Lambda^3} \int_0^\infty J_0(2\sqrt{2}\pi \frac{R}{\Lambda} \sin \alpha t) e^{-2\sqrt{2}\pi \frac{2h-R \cos \alpha}{\Lambda} t} \frac{t - \sqrt{t^2 + j}}{t + \sqrt{t^2 + j}} t^2 dt \right\} \dots (IV.10)$$

The first terms in formulas (IV.10) are the constituents of the primary field dipole, the second - those of the reflected field.

The variation nature of constituents H_{1r} and H_{1z} of the primary field is shown in relative units to distance R and angle α in Fig.35. The actual Re and imaginary. Im portions of both the constituents of the reflected field are shown in relation to α and Λ at $R = 100$ m and $h = 150$ m

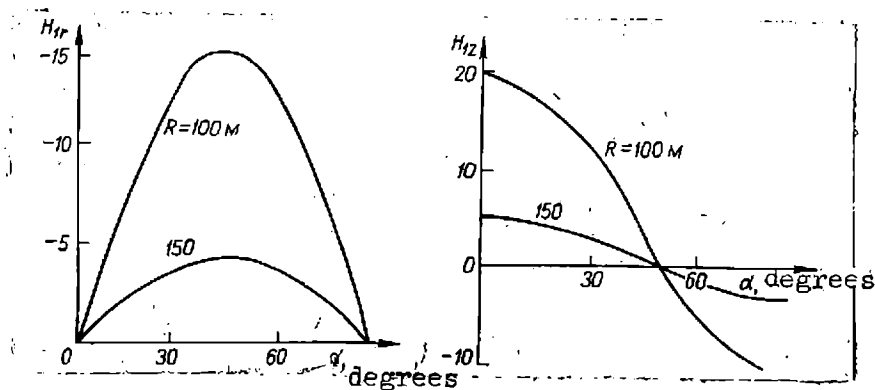


Fig. 35

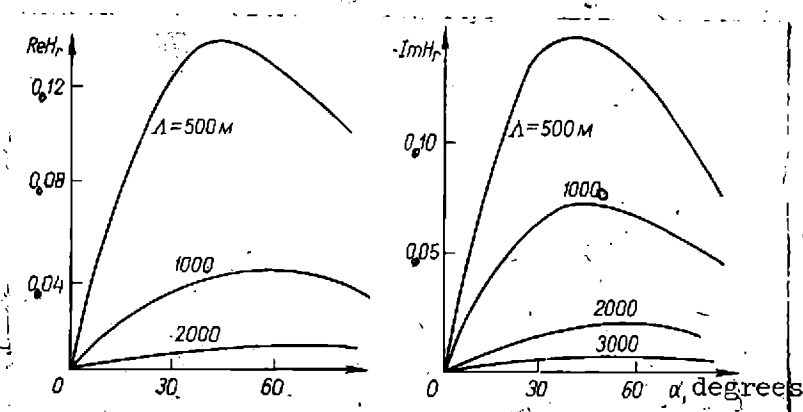


Fig. 36

in Fig. 36 and 37 respectively (69). According to these figures, the primary field is considerably larger than the reflected one^(*), which decreases with the increasing wave length in earth Λ , i.e. with increment of specific resistivity.

The magnitude of the reflected field is affected during the survey by decrement of sp. resistivity of the surface layers of earth, which thereby determine the useful signal, i.e. the anomalous effect in aerial electric prospecting.

The curves in Figs. 35-37 show that at the high altitude of survey the effect of the uniform earth surface is negligible. With low altitudes of

(*) the field densities on curves, in a/m, can be obtained by multiplying them by factor $4\pi \cdot 10^{-13} ISw$, where I - current, a; S - area, m^2 .

150-200 m this effect is quite perceptible and the magnitude of the reflected field is composed of several percents of the primary one. The altitude of flight along the survey route affects the magnitude of the reflected field, thereby causing interference during the measurements. The altitude variation of the flight is equivalent to the emergence of anomalous field variations (the reflected field attains 10-15% of the primary, i.e., it is of the same order with the anomalous field the magnitude of which is determined by the presence of insignificant geoelectric irregularities). Therefore, maintenance of a constant altitude of survey in relation to the earth surface determines to a considerable degree the quality of results obtained in aerial electroprospecting.

2. Anomalous fields in near zone methods.

In the aerial methods of the near zone, the anomalous (or secondary) field is that due to the presence in the top layers of the earth crust of mainly local geoelectric irregularities. It is determined by electrical parameters of the geoelectric irregularities, its shape (sphere, cylinder, plate, semiplate, etc.) and size, working frequency and the type of set up applied for the near zone method. Thus, the estimate of anomalous field is a very difficult problem, depending on many factors. For some forms of geoelectric irregularity, likely to be met with in practice, and a number of patterns for the aerial method of the near zone, for instance, the induction method, these problems are resolved in (69, 75, 239, 251).

Let us take the general case of determination of a secondary field of the simplest, most frequently encountered type of the conductive body - a sphere of radius a .

In the center O of spherical coordinates we place the spherical conductor of radius a , and at point O' - the primary field source, for

instance, the magnetic dipole \vec{m} with an arbitrary trend of magnetic moment. The distance between the center of the sphere and dipole we take equal to b . The surrounding sphere, enclosing the medium for conveniences of calculations, we will assume as the ideal dielectric ($\gamma = 0, \mu = 1$). Axis

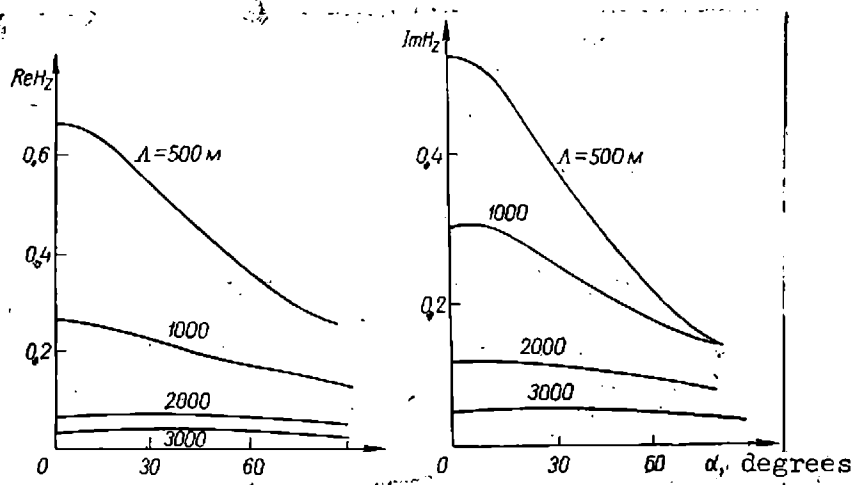


Fig.37

OZ we direct through point O' , axis OX - along the projection of the dipole moment onto plane XOY (Fig.38).

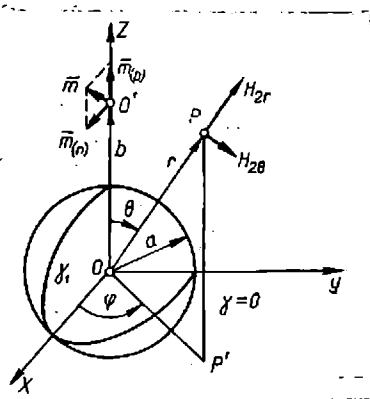


Fig.38

The magnetic dipole with an arbitrary trend of magnetic moment could be extended into two dipoles - transverse \vec{m}_t (\vec{m}_t), parallel to plane XOY, and vertical (radial) \vec{m}_z (\vec{m}_z), directed along axis OZ. Each dipole

generates at point P corresponding constituents of the secondary field, which could be shown as quickly-converging series at ratio $\frac{a^2}{br} \ll 1$ (63).

For the vertical dipole $m(p)$ we have two constituents of the secondary field-radial H_{2r} and tangential $H_{2\theta}$, which are determinable by the following relations (63, 185, 261):

$$H_{2r}^{(p)} = - 2Dm_{(p)} \frac{a^3}{4\pi b^3 r^3} \left[\cos \theta + 3 \frac{a^2}{br} (3 \cos^2 \theta - 1) + \right. \\ \left. + 3 \frac{a^4}{b^2 r^2} (5 \cos^2 \theta - 3) \cos \theta + \dots \right]; \quad (IV.11)$$

$$H_{2\theta}^{(p)} = - Dm_{(p)} \frac{3}{4\pi b^3 r^3} \sin \theta \left[1 + 6 \frac{a^2}{br} \cos \theta + \right. \\ \left. + \frac{9}{2} \cdot \frac{a^4}{b^2 r^2} (5 \cos^2 \theta - 1) + \dots \right]; \quad (IV.12)$$

$$H_{2\varphi}^{(p)} = 0. \quad (IV.13)$$

where D - composite factor, determinable by the conductive body parameter $v = \sqrt{j\gamma \mu \omega a^2}$ (251).

The first terms of expansion characterise the field of magnetic dipole with moment $m_{(p)} D \frac{a^3}{4\pi b^3}$, provisionally placed in the center of the conductive sphere and oriented on axis OZ opposite to the exciting dipole with moment $m_{(p)}$. The other terms of expansion:- fields of magnetic multipoles, which quickly attenuate, if the source and observation point are sufficiently distant from the center of the sphere.

For the transverse dipole $m(\Pi)$.

$$H_{2r}^{(n)} = Dm_{(n)} \frac{a^3}{4\pi b^3 r^3} \cos \varphi \sin \theta \left[1 + 6 \frac{a^2}{br} \cos \theta + \right. \\ \left. + \frac{9}{2} \cdot \frac{a^4}{b^2 r^2} (5 \cos^2 \theta - 1) + \dots \right]; \quad \dots (IV.14)$$

$$H_{2\theta}^{(n)} = -\frac{1}{2} Dm_{(n)} \frac{a^3}{4\pi b^3 r^3} \cos \varphi \left[\cos \theta + 4 \frac{a^2}{br} \cos 2\theta + \right. \\ \left. + \frac{9}{2} \cdot \frac{a^4}{b^2 r^2} (15 \cos^2 \theta - 11) + \dots \right]; \quad \dots (IV.15)$$

$$H_{2\varphi}^{(n)} = \frac{1}{2} Dm_{(n)} \frac{a^3}{4\pi b^3 r^3} \sin \varphi \left[1 + 4 \frac{a^2}{br} \cos \theta + \right. \\ \left. + \frac{9}{4} \cdot \frac{a^4}{b^2 r^2} (5 \cos^2 \theta - 1) + \dots \right] \quad \dots (IV.16)$$

In formulas (IV.14)-(IV.16) the first terms of expansion also characterise the field of magnetic dipole, conventionally placed in the center of the conductive sphere and oriented along the line OX opposite to the exciting field of transversal dipole. The moment of this dipole is half that of the radial and is $\frac{1}{2} Dm_{(n)} \frac{a^3}{4\pi b^3}$ (transverse dipole generates in the center of the conductive sphere half the field density).

Equations (IV.11)-(IV.16) were obtained on the assumption that the sphere is a good conductor, the radius of the sphere is small as compared to the wave length of the exciting field in confining medium ($\Lambda \gg a$), and the source of the field (magnetic dipole) is at a distance from the sphere which is less than the wave length in medium ($\Lambda \gg b, \Lambda \gg r$). With the frequencies used in aerial electroprospecting and the resistivity of enclosing medium upto hundreds and thousands of ohm/m, these conditions are fully satisfied.

If the direction of the magnetic dipole moment \bar{m} of the field's source coincides with plane ZOY, the azimuthal component of transverse dipole $H_{2\varphi}^{(\Pi)}$ converts into zero; hence, the transverse dipole, same as the radial, will have only two constituents - $H_{2r}^{(\Pi)}$ and $H_{2\theta}^{(\Pi)}$.

The convergence of the series of given expansions is determinable by ratio $\frac{a^2}{br}$. The higher is the denominator, the quicker is the convergence of the series.

Therefore, with the sphere considerably remote from the source of the primary field and from the location point of the field detector (observation point) the number of terms in each series could be reduced, for instance, to one (the first). This is true, if the dimensions of the sphere comprise two-three scores of meters, and the distance upto the point of observation is over 50 m. This assumption is almost always fulfilled in aerial electroprospecting by the method of the near zone. In this case, the primary field may also be taken as uniform. With these assumptions formulas (IV.11)-(IV.15) take the following form:

$$H_{2r}^{(p)} \approx -2 D_m(p) \frac{a^3}{4\pi b^3 r^3} \cos \theta; \quad \dots (IV.17)$$

$$H_{2\theta}^{(p)} \approx -D_m(p) \frac{a^3}{4\pi b^3 r^3} \sin \theta; \quad \dots (IV.18)$$

$$H_{2r}^{(\Pi)} \approx D_m(\Pi) \frac{a}{4\pi b^3 r^3} \sin \theta; \quad \dots (IV.19)$$

$$H_{2\theta}^{(\Pi)} \approx -\frac{1}{2} D_m(\Pi) \frac{a^3}{4\pi b^3 r^3} \cos \theta. \quad \dots (IV.20).$$

In the determination of the secondary field in the aerial induction method from formulas (IV.11)-(IV.16) and (IV.17)-(IV.20) the divergence does not exceed more than a few per cent.

If it is assumed that the primary magnetic field \vec{H}_{10} is uniform and vertical (i.e. the fields lines of the force are parallel to axis OZ) and the spherical conductor of the radius a lies in non-conductive medium (see Fig.38), then formulas for the constituents of the resultant field at the point of its reception are determined by the well known relations (185, 189, 251), obtainable from approximate formulas (IV.17)-(IV.18):

$$H_r = H_{10} \left(1 - \frac{D a^3}{4 \pi r^3} \right) \cos \theta; \quad \dots(IV.21)$$

$$H_\theta = - H_{10} \left(1 - \frac{D a^3}{8 \pi r^3} \right) \sin \theta; \quad \dots(IV.22)$$

$$H_\varphi = 0. \quad \dots(IV.23)$$

The transition from spherical coordinates to the Cartesian for the determination of vertical and horizontal components of the secondary and resultant fields, usually perceived by field detectors in the setup of the aerial induction method, does not present any difficulties (see para 2, chapt.V).

For non-isometric bodies the estimate of secondary fields is more difficult (77, 251). However, with certain allowances it may be simplified. For example, if it is assumed that the cylindrical conductor of radius a and finite extent is situated in the non-conductive medium ($\gamma = 0$) and is excited by the uniform field $\vec{H}_{10} = \vec{H}_{z_0}$, the formulas for the determination of components the resultant field at reception point will be written as simple relations.

Let us place the origin of cylindrical coordinates on the axis of the circular cylinder and direct axis OZ parallel to the moment of the oscillating dipole, as shown in Fig.39. Let us assume also that the reception point P with coordinates r and φ lies in plane ZOY. In this case the field's components at point P will be written as (185, 251):

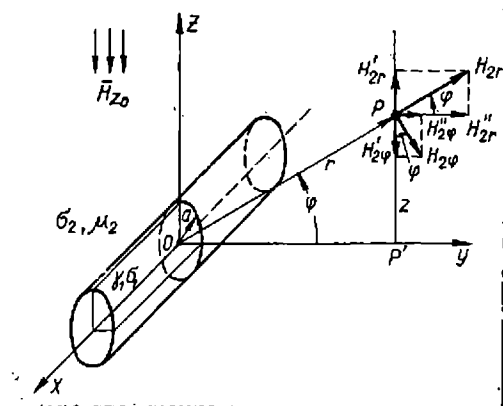


Fig.39

$$H_r = H_{10} \left(1 + T \frac{a^2}{r^2} \right) \cos \varphi; \quad \dots(\text{IV.24})$$

$$H_\varphi = H_{10} \left(1 - T \frac{a^2}{r^2} \right) \sin \varphi; \quad \dots(\text{IV.25})$$

$$H_x = 0. \quad \dots(\text{IV.26})$$

Here function T - composite quantity (98, 172).

$$T = \frac{I_2(v)}{I_0(v)} \quad \dots(\text{IV.27})$$

where $I_2(v)$ and $I_0(v)$ - Bessel's functions respectively of the whole (second) and zero series from argument $v = \sqrt{j\omega\mu\gamma} a^2$.

For the horizontal and vertical components of the secondary field we get the following terms

$$H_{2z} = H'_{2r} - H'_2 \varphi \quad \dots(28)$$

$$H_{2y} = H''_{2r} + H''_2 \varphi$$

where $H'_{2r} = H_{2r} \sin \varphi; \quad H''_{2r} = H_{2r} \cos \varphi;$
 $H'_2 = H_2 \varphi \cos \varphi; \quad H''_2 = H_2 \sin \varphi.$

Hence

$$H_{2z} = H_{2r} \sin \varphi - H_2 \varphi \cos \varphi; \quad H_{2y} = H_{2r} \cos \varphi + H_2 \varphi \sin \varphi.$$

After substitution of H_{2r} and $H_2 \varphi$ taken from formulas (IV.24) and (IV.25), we get

$$H_{2z} = H_{zo} T \frac{a^2}{r^2} \sin 2 \varphi; \quad (IV. 29)$$

$$H_{2y} = H_{zo} T \frac{a^2}{r^2} \cos 2 \varphi. \quad (IV.30)$$

The components of the resulting field will be

$$H_z = H_{\text{B}} = H_{iz} + H_{2z} \text{ and } H_y = H_h = H_{iy} + H_{2y},$$

In the same way the analysis of the anomalous secondary fields in patterns of aerial induction method for bodies of other shapes is carried out (38, 75, 172).

3. Anomalous and normal fields in BDK method (infinitely long cable method).

In the BDK method the field of the exciter source - long grounded cable - in principle determines the normal field also. To take the latter as a sum of source fields and as caused by the cover deposits of the earth surface, as is done for the near zone methods (see para 1, chapt. IV), has apparently no sense in the BDK method. Therefore, to describe the behavior of the normal field in the BDK method it is possible to use relations, given in work (68), or formulas (III.51), (III.52). Let us write them down in a simplified form (42, 48, 75).

In the cable zone, where $x > \frac{5}{\pi} \sqrt{\frac{5\rho}{f}}$, amplitudes of components H_x , H_z and the corresponding phase angles φ_{H_x} , φ_{H_z} will be determined in the Cartesian coordinates, on the basis of equations (III.52), by the following relations:

$$H_z = 1.13 \frac{I}{x^2} \sqrt{\frac{\rho}{f}} \cdot 10^{-4}, \text{ a/M};$$

$$H_z = 0.8 \frac{I}{x^3} \frac{\rho}{f} \sqrt{1 + 4z \sqrt{\frac{\rho}{f}} + 8z^2 \frac{\rho}{f}}, 10^{-3}, \text{ a/M}; \quad \dots(\text{IV.31})$$

$$\varphi_{H_x} = - \arctg 1, \text{ pa}\partial;$$

$$\varphi_{H_z} = \arctg \left(1 + 0.5 \frac{\sqrt{\frac{\rho}{f}}}{z} \right) \cdot \text{pa}\partial.$$

Thus, the field density of the long cable depends on the current intensity I , its frequency f , resistivity of the earth $(*)\rho$ and distance from the cable x . The intensity of the field vs. altitude of survey z is defined in the first approximation by the behavior of characteristics H_z and φ_{H_z} .

From equations (IV.31) it follows that the phase characteristic $\varphi_{H_x} = \frac{5}{4}\pi$ in the middle zone of the cable field does not depend on field parameters. But the phase characteristic φ_{H_z} depends on altitude, resistivity of the earth and frequency.

Therefore, with the removal from the cable the normal field of horizontal component H_x dampens more slowly than the normal field of component H_z ; thus it is possible with a certain response of the measuring instruments to withdraw to a considerable distance from the cable.

(*) Here besides the resistance of the cable wire, the intermediate resistance of the grounding electrodes is also taken into consideration.

In the determination of parameters of the measuring instruments, it is necessary to know the minimum densities of the fields in various geological conditions in a given frequency band and nominal (attainable in field conditions) cable current. These parameters may be determined from formulas (III.52) or from curves given in (69, 89, 216). One of these curves is known in Fig.40, where the variation range of ρ is taken from 10 to 10^4 OM. M, the operating frequency 1000 cps, and the nearest to cable zone ($x < 2-5$ km depending on ρ) is plotted from more exact formulas than (IV.31).

From Fig.40 it follows that with the increment of ρ within the indicated limits, i.e. 10^3 times, the field H_x increases approximately 30-40 times in distance from cable zone. It is interesting to note that at a distance of 10-20 km from the cable at $I = 1$ A, $f = 1000$ pcs and $\rho = 10$ OM. M the amplitude of H_x comprises only about 10^{-7} A/m.

Fig.41 shows the variation curves of horizontal components at 5 km length of the cable obtained by calculations (1) and experiments (2.3) and showing application limits of formula (IV.31).

The normal field of the cable is characterised by the variation of its gradient $\frac{dH_x}{dx}$. It is well known that, on the operation profile, the gradient varies on an average from 10^{-2} A/m² near the cable to 10^{-5} A/m² far from it (89). This causes some difficulties in devising measuring instruments, specially these with analogue recording of parameters (89, 103). Due to the restricted quick-action of analogue recorders it is very difficult to ensure (even at the minimum speed of the flight) the normal amplitude recording of the cable field in the near zone, where its gradient is comparatively high. The same is evident during the component and phase measuring^(*). Therefore, in aerial electric prospecting by the BDK method

(*) Phase gradient comprises on an average 50-90 degr/km close to the cable, gradually reducing to several degrees per 1 km in distance from the cable zone.

there is an existence of the so called "non-operative" zone^(*) not over 1 km in width at both sides of the cable.

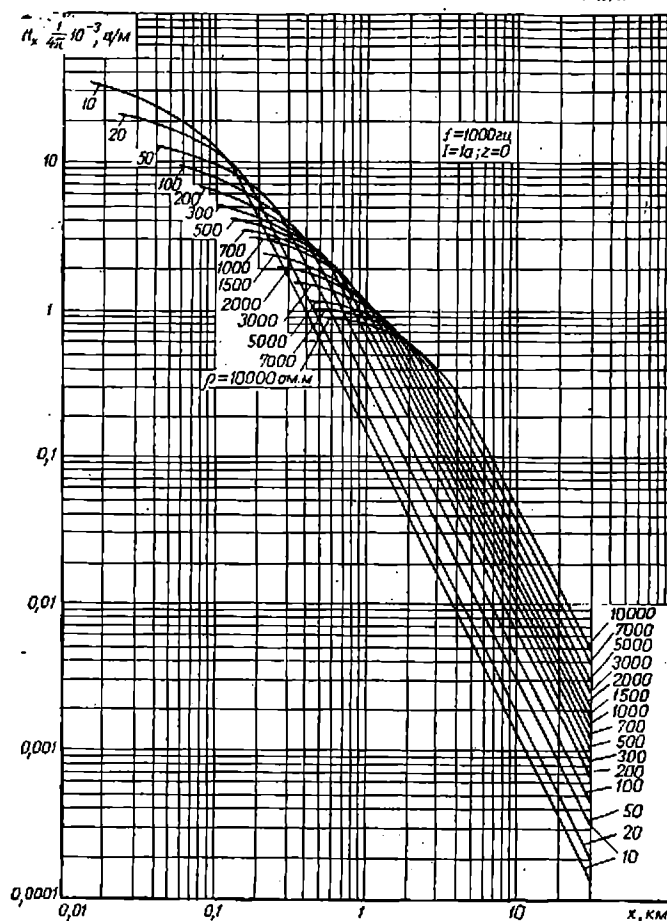


Fig.40

The normal and anomalous fields of the cable generally depend on frequency in a very complex manner. The same regular behavior of normal fields above a uniform lower half-space is that with the increment of frequency the zone of comparatively high gradients of the magnetic field parameters becomes gradually narrower on approaching the cable. In the middle zone, where formulas (IV.31) held true, the component H_x decreases

(*) The "non-operative" zone may be excluded in the use of instruments with digital quick-acting registers.

decreases with the rising frequency in inverse proportion to \sqrt{f} . In the same zone with a uniform lower half-space phase response ϕH_x is independent of frequency.

Thus, according to the regularities pointed out, the sensitivity of measuring devices to the magnetic field in the BDK method should vary due to considerable and irregular variation of the normal field density with increasing distance from the cable. Moreover, with the rise of the operating frequencies, the sensitivity of devices should increase.

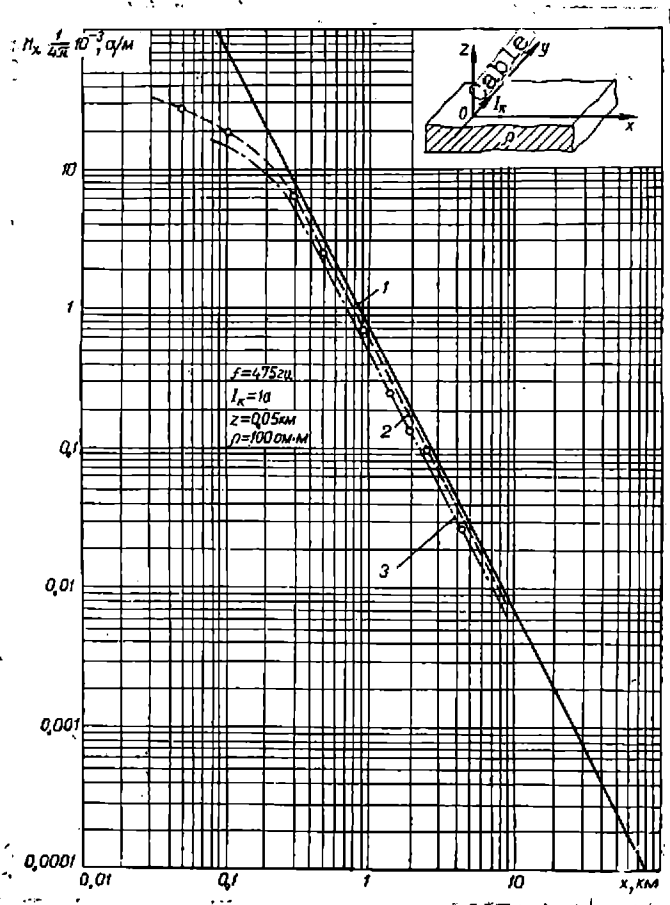


Fig.41

With the varying excitation frequency of the primary field, the anomalous fields are characterised by even more complex relationships than

the normal ones. Anomaly component, amplitudes and phases have diverse relationships due to their dissimilar frequency response. Given below, as an example are the anomalies of amplitude H_x and phase φH_x vs. frequency f , obtained in the actual survey conditions (216):

Frequency, cps.....	244	488	976	1952
Amplitude anomaly, %..	55	28	24	31
Phase anomaly, degr.....	25.2	18.6	13.2	13

According to these data, side by side with the usual decrement of anomaly with the rise of frequency within the 244-976 cps band, there is evidence of its amplitude increment on frequency 1952 cps. Because of this optimum, frequencies have to be selected for each geological area in order to obtain high effectivity of aerial electric prospecting by the BDK method. Hence in the development of devices, provision should be made for multi-frequency principle of field investigations (89, 108, 216, 251).

The altitude of survey is also of importance in the BDK method. However, its effect on survey results is considerably less than in the near zone method. The comparatively low relation of anomaly to altitude is explained by the fact that the cable field in zone $x \gg \frac{5}{\pi} \sqrt{\frac{5\rho}{f}}$ is actually a plane wave front (38).

Experience shows that, in prospecting by the BDK method the anomalies are very well defined upto 100 m altitude, gradually damping at an altitude of 300 m and above.

The normal cable field H_x at altitude range 50-300 m, retains its value for a whole number of geological areas with an error of less than 10%. With increasing altitude of survey the width of the anomaly of field parameters increases. Therefore, in the actual conditions, the altitude

of flight rarely exceeds 150 m (216, 218). As an example, showing variation of amplitude-phase response of the field vs. altitude, Table 2 gives the data of amplitude anomaly above a sulphide deposit (216).

TABLE 2

Earth-surface field detec- tor distance m	f r e q u e n c y, cps			
	244		976	
	Amplitude anomaly %	Width of anomaly m	Amplitude anomaly, %	Width of anomaly m
35	57	230	64	300
100	21	270	33	310
200	16	350	24	400
300	11	380	11	480

4. Results of Survey by Induction Method.

Operations in Maidan-Vila area (Khmelnitsky region) with AERIS apparatus.

The first experimental method-testing operations with the AERIS apparatus for aerial electric prospecting by the induction method were conducted in May-June, 1959. The exploratory possibilities of the aerial induction method were checked in Maidan-Villa area on the section of graphitized-gneiss deposits. This section is situated on the north-western edge of the Ukrainian crystalline massif, where the crystalline basement rocks in the form of granite ($\rho = 500-1000$ ohm/m), pitching westward, are overlain by sedimentary formations of Paleozoic, Mesozoic and Cenozoic ages. Deposits of graphitized gneiss, containing 2-4% of graphite, have low resistivity (ohm units/m) and occur in the section in the form of several layers 5-40 m in thickness with steep dipping. The main band of graphitized gneiss was 1000-1500 m in width and 20 km in length. Sedimentary deposits, shown by sandy-argillaceous formations with average $\rho = 30-50$ ohm/m, have thickness in the operation area from 10 to 40 m (216). In spite of the

presence of graphitized gneiss with high conductivity as disturbing objects, shielding the lower bedrocks, hinder effective application in this section of the aerial induction method. However, due to the near base, where the apparatus for this method is being developed, this area was nevertheless selected for the initial experiments and method-testing.

The flights of plane with the AERIS apparatus were carried out along previously chosen profiles with marked prominent features. In flying past these, the operators on a signal from the navigator marked them on tapes of registers. To obtain authentic data, the flights were conducted in calm weather early in the morning, when the bumping of the gondola was practically imperceptible. The altitude of flight was usually 150 m and was maintained by radio altimeter. Measurements along the profile were executed during straight and reverse flying.

The testing of the exploratory effectivity of the method was divided into two stages: the first provided for testing on one frequency, the second simultaneously on two.

In the single-frequency survey, the measuring was of the modulus, phase and reactive signal component at each operating frequency of devices. The measuring was executed both with the application of electric compensation of the primary field signal and without it. To check the operation stability of the apparatus and the correctness of the applied measuring technique, all recording was doubly repeated. Serving as control was the reproducibility of results with the same conditions of flight (same speed, altitude, intensity of oscillating frame, etc.).

During the field work it was found that the recorded curves of modulus, phase and reactive component of the signal showed also the zone of

graphitized gneiss and surface irregularities. The results of the second measuring in single-frequency survey showed little divergence from the first (see Fig.183). It was also found that the sensitivity of the method increase with three - and four-fold electric compensation of the primary field signal. Moreover, it was determined that the graphitized gneiss are more clearly marked on frequencies of devices 244, 488 and 976 cps. On frequencies 7812 and 3906 cps the fixing is of surface irregularities (changing topography, peat, bogs, etc.). Thus the verification was obtained of the differentiation in frequencies of anomalies from conducting objects of the type of graphitized gneiss and surface irregularities.

Method-testing and production operations with the AERIS apparatus, were carried out in Kazkhstan and Southern Urals in June-September, 1959 from the base of Jezkazgansky geophysical party of Kazgeofiztrest.

The aim of experimenting, method and production testing was to check the possible application of the aerial induction method for explanation of ore deposits and geophysical mapping.

The section of Jezkazgansky ore area, allotted for experiments, was broken up into profiles, situated parallel to each other at 1-2 km distance. The aerial geophysical survey was conducted in the following order: first in sections, investigated by the ground geophysical survey and the geological structure of the top layers of earth crust has been established; then in places of the given area, where the ground explorations have not so far been conducted or not on a full scale. The aerial geophysical survey by the induction method aimed at confirming the presence of known boundaries of the anomalous zones and to extend these boundaries.

The signals of the secondary field were measured by modulus, phase and reactive component. All the measurements were carried out with and without compensation of the primary field. The extent of compensation, as a rule, did not exceed 8-10 times. As an example, Fig.42 shows modulus recording curves of two adjacent profiles with different geological section ($f = 488$ cps, $h = 150$ m).

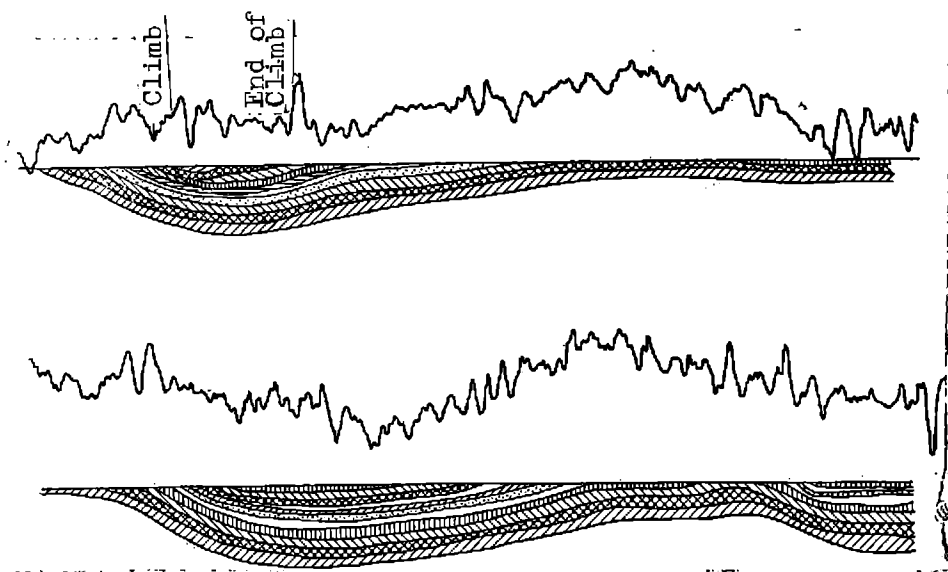


Fig.42

In order to obtain the best results, the survey was conducted during morning hours. The duration of the survey was on an average 3-3.5 hrs. The length of the profile usually did not exceed 50-60 km. The geological results of the survey were found to be quite satisfactory.

During the method-testing operations in the Southern Ural area, the selection was of copper pyrite deposit in an area of comparatively smooth relief. The ore bodies, which here have the shape of lenticular or sheet-like deposits of steep dipping, are confined to the brachianticlinal fold, defined on the surface as a low ridge, composed of secondary quartzites.

According to the data of ground investigations, the resistivity of the massive ore is very low, less than 1 ohm/m, and of impregnation ore - comparatively high, from 20-30 to 200-300 ohm/m. The resistivity of the surrounding rocks, depending on their composition and extent of metamorphisation, varies from 300 to 2000 ohm/m. Loose deposits have resistivity of a few scores of ohm per m.

The flight conditions were the same as in the Jezkazgansky area.

Fig.43 shows the survey results on one of the profiles (a - modulus recording, b - phase recording altitude of flight 150 m).

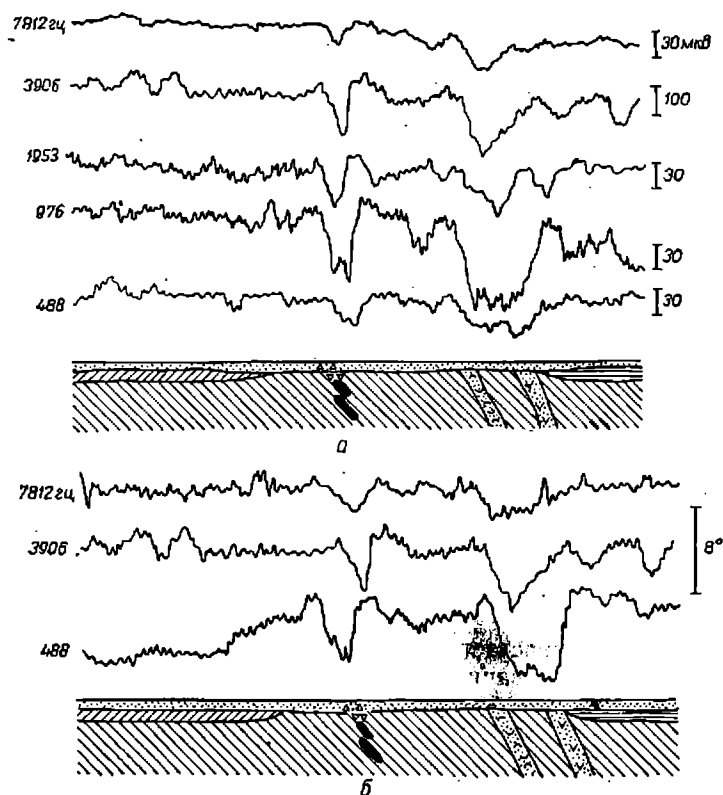


Fig.43

According to the given data, amplitude anomalies on operating frequencies comprise respectively 12; 24; 17; 16; and 11% of the normal field. The highest amplitude anomaly is evident on frequency 976 cps, and

in phase - on frequency 488 cps. It may be assumed that in this case the source of the first anomaly (middle of curve) is not the ore deposit itself (total shading), but to a considerable extent the supra ore zone (triangles) of oxidized ore and weathering crust material confining effusions. The second anomaly (on the right side of the chart) is formed by steeply-dipping layers of tuff of mixed composition and major thickness with parameters similar to those of the ore body. On higher frequencies, the shielding effect of detrital deposits is felt and the anomalies dampen.

Thus, it is possible to state that aerial electric prospecting by the induction method can give positive results in the search for sulphide ore deposits. However, it is impossible to determine the cause of anomaly appearance by aerial electric prospecting alone. It would be necessary to carry out multi-frequency electric prospecting on the ground, as well as investigations by other methods of geophysical exploration (magnetic prospecting, gravity survey, etc.).

Operations in the Area of Maidan-Villa Station with Devices AERI-2.

The first tests of the AERI-2 devices were carried out in November-December, 1961. The geological environment of the area is characterised by the section shown in Fig.44-b (1-Neogene, 2-Gneiss, 3-Granite, 4-graphitized gneiss). The resistivity of detrital deposits is upto 100 ohm/m, of graphitized gneiss - 1-10 ohm/m. On frequency 243 cps (Fig.44-a), in the survey with three-fold compensation of the primary field signal, clear results were obtained of anomalous zones on phase and reactive component curves. The zone of graphitized gneiss is marked on the diagrammatic tape by phase anomaly (φ) of about 10" and reactive component (U_p) of 30 mkw. Neogene deposits are marked by anomalous variations of phase within 15-25", and of reactive component - 20-25 mkw. In the

survey without compensation on frequency 1949 cps, high values are evident above the Neogene deposits of measurable parameters (Fig.44-b).

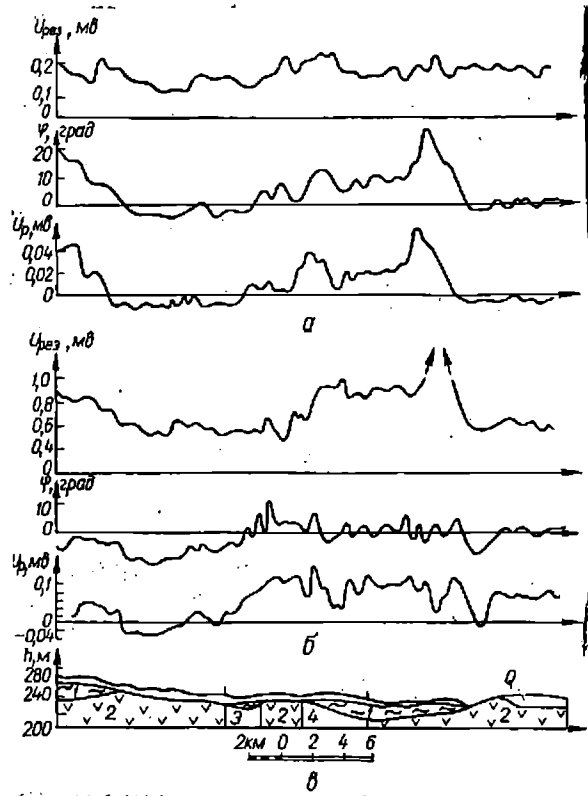


Fig.44

Fig.45 shows the recording of modulus $U_{res.}$, phase φ and reactive component U_r with simultaneous double-frequency survey on frequencies 487 cps (continuous line $I_r = 11 \mu$) and 1949 cps (dotted line, $I_r = 9 \mu$) with two-fold compensation of the primary field signal ($h = 200$ m, $v = 250$ km/hr in relatively calm weather). According to the data shown, the anomalous variations of the field are more defined on frequency 487 cps than on 1949 cps. In the area of landmark "Traverse Maidan-Villa", the recording of all parameters shows anomaly, connected with the presence of a section of conductive graphitized gneiss.

Configuration of the curves, in repeated flights along the route, practically coincides. Fig.46 shows curves of repeated recordings on one route at frequency 487 cps ($I_r = 10^4$) with three-fold compensation, which indicates satisfactory convergence of results, in particular of phase and reactive component, even with poor meteorological conditions.

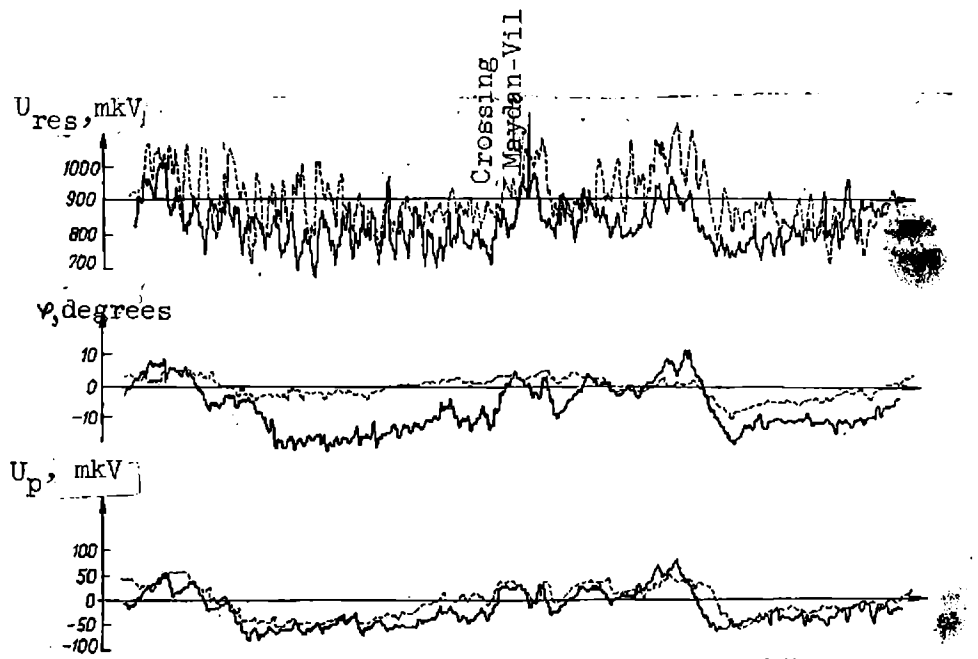


Fig.45

Experimental Operations on Pyrite-Pyrrhotite deposit of Karelia (34)

The geological environment of the indicated deposit is conducive to the application of electric prospecting methods; the ore zone is composed of highly conductive shales (graphitized and chlorite-aktinilitic), in which lenses of sulphuric pyrite, with resistivity of a few tenths of ohm/m and thickness 20-30 m occur. The surrounding crystalline rocks have resistivity of 1000 ohm/m. The thickness of detrital deposits in the area does not exceed 5-10 m, and the resistivity of the detritus comprises about

200 ohm/m. The results of measuring in the section (frequency 487 cps with two-three-fold compensation) are shown by curves in Fig.47 (1-surrounding rocks, 2- ore zone). The survey route shown in Fig.47-a, is laid along the extent of the ore zone several km in length. Above the ore zone is an anomaly upto 100 mkw in amplitude ($U_{res.}$) with general level of interference 30-40 mkw. The phase variations are upto $7-10^\circ$; the peaks of this variation are displaced in relation to the amplitude peaks on the modulus curve. The survey route, shown in Fig.47-b, runs accross the strike of the ore zoneo but even in this case it is marked by amplitude (upto 50-70 mkw).

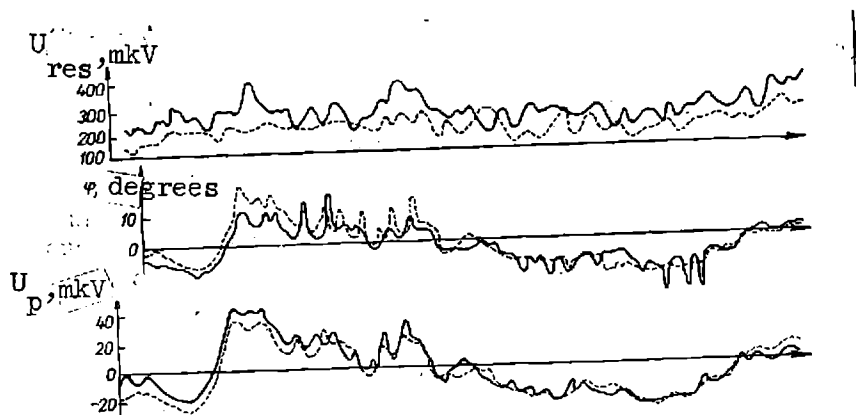


Fig.46

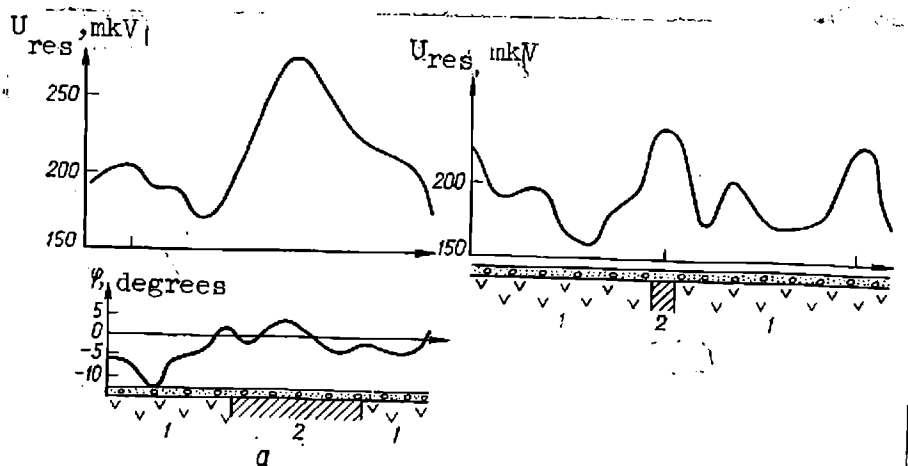


Fig.47

Method-testing in Kol'sky Peninsula (1962). The geoelectrical environment in sections of this area favors aerial electric prospecting. The overburden has resistivity 100-200 ohm/m, and the thickness is not over 10-20 m. The resistivity of bedrock is several thousands ohm/meters and even higher. The graphitized and chloritized shales and sulphidized rocks have resistivity about 10-30 ohm/m.

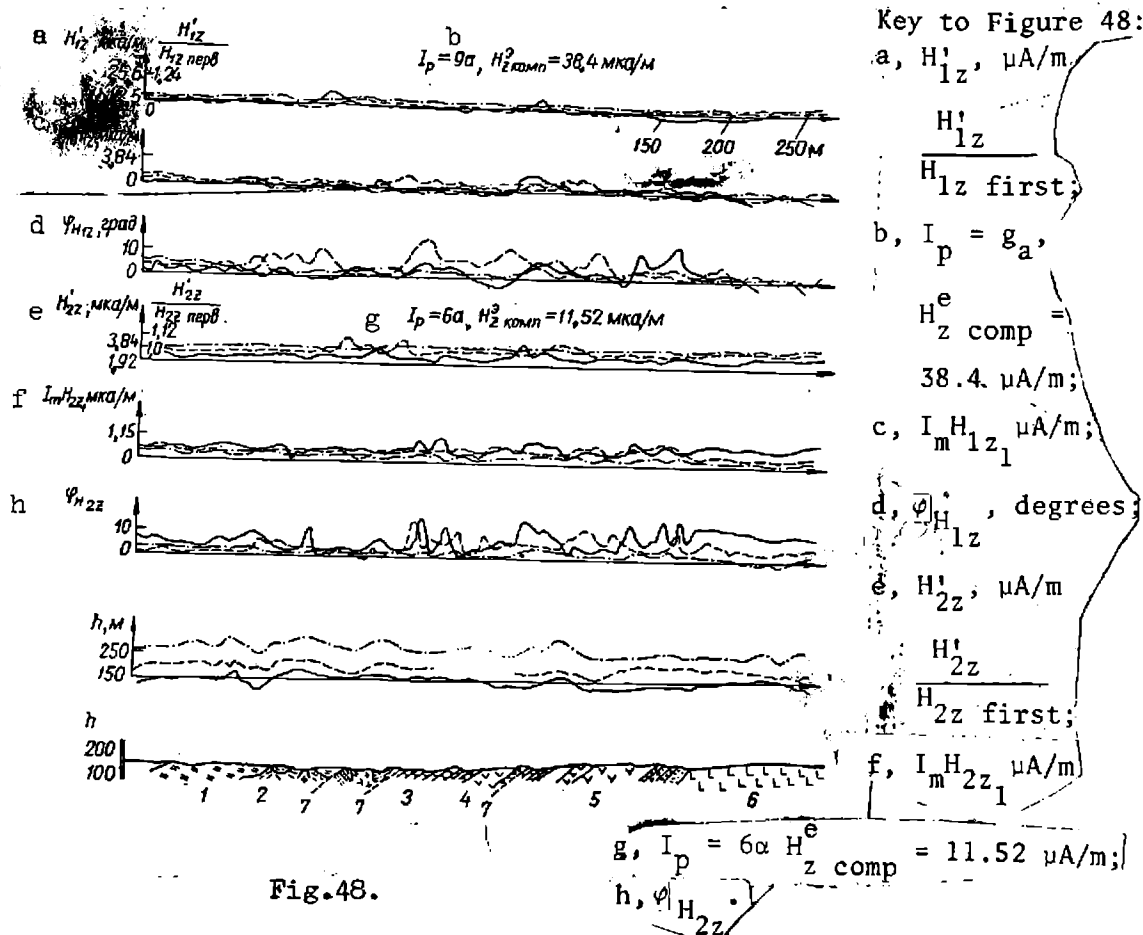


Fig.48.

Fig.48 shows result curves of the geophysical survey on two frequencies ($f_1 = 578$ cps and $f_2 = 1949$ cps), implemented by the geophysical party of the Western geophysical combine (33) with the AERI-2 devices (with compensation), and the geological section of the investigation area (1 - binary mica-schist; 2 - shaly amphibolite; 3 - dolomitized limestones; 4 - undisturbed covers; 5 - basis and volcanic plastic rocks; 6 - basic effusives; 7 - assumed faults): H'_{1zpr} , H'_{2zpr} - vertical component of

primary field on frequencies f_1 and f_2 respectively; H_z^e comp - equivalent intensity of the magnetic field, corresponding to compensating voltage input into compensating circuit; \bar{H}_z - geometrical difference between the resultant field and the field equivalent to compensating voltage, $\bar{H}_z = \bar{H}_z - \bar{H}_z^e$ kohmm' where \bar{H}_z - vertical component of the resulting field without compensation.

According to these curves, the anomalous zones are defined most clearly on phase (φH_z), a little less so from the reactive component and negligibly in modulus. Moreover, in contrast to the modulus and reactive component the phase parameter depends less on the altitude of flight - the phase is well marked at the altitude of survey 150 and 200 m.

Analysing the results of the survey in other sections of this area, it is easy to see that, on frequency 243 cps, the anomalous variations are marked only on phase and reactive component curves. On modulus curves, on higher frequencies (487 and 1949 cps), the fixed anomalies are connected with low resistivity rocks and have amplitudes 50-70 mkw. On the phase and reactive component curves, on frequencies 487 cps and higher, a great number of anomalies are defined, a portion of which conforms quite well with decreased values ρ_k with symmetric profiling and low-ohmic rocks. The anomalies of surface objects are the most clearly defined on the phase curve on frequency 3898 cps.

Thus the conclusion which may be drawn is that the aerial induction method makes it possible to separate within high-ohmic bedrock conductive beds with $\rho = 1-10$ ohm.m, i.e., sections with the possible presence of sulphide mineralization, and position mapping of graphitized gneiss, shales and other low-ohmic intrusions.

Field Operations with Apparature of VMP Devised by VITR (234). Method

testing and production operations with these devices were conducted in a number of the country's areas. For instance, in Turkmenia, the operations were conducted to clarify the possibility of finding fresh water lens. The instruments were set up on planes LI-2 (operating frequencies 1225 cps and 2450 cps, spread of planes 300-320 m, altitude of survey 150-180 m). The general survey results were positive - anomaly on frequency 1225 cps comprised 3-4% of the primary field with interference upto 1%, on frequency 2450 cps - 6-7% with interference not over 2%.

Field work with VMP devices was carried out also in Karelia. The object of the investigation were the zones of graphitized shales with pyrite-pyrrhotite mineralization. Anomalous sections in the survey area were clearly defined; they were several times the level of interference.

Good results were obtained in Karelia also with instruments set up on planes AN-2. Although the change in the type of plane caused a rise in the level of interference, the reduced altitude of the survey compensated for this rise. The results were checked by repeated flights along the same profiles. They were satisfactory with low anomalies and quite good with high (about 40-50% in amplitude and 30-40° in phase). It was noted that the intensity of anomalies increased with the run of profiles not perpendicular to the trend of the major geological structures, but at an angle of about 45°.

Field Operations by Induction Method in Other Countries:

N.P. Peterson in his work (66) throws some light on the results of theoretical, modelling and field (production) work, carried out by the aerial induction method with devices constructed in 1947-1953 in Finland and tested in 1954 in Canada by "Hanting". The apparatus is set up on a

twin-engine plane, the field detector - in outboard gondola. Operating frequencies comprise 400 and 2300 cps. The recording is of phase variation of the resultant field signal in relation to supporting voltage, taken off the oscillating frame. Normal altitude of flight 140-150 m with the length of wire-cable 130 m.

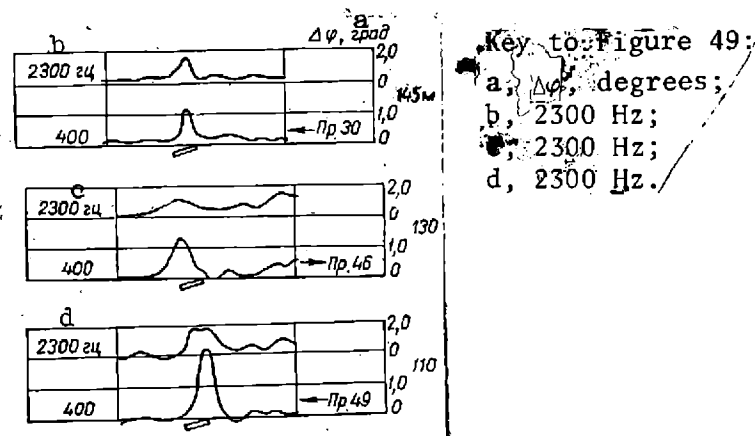


Fig.49

In Canada more than 5,00,000 km has been profiled by means of these devices. With only one set, 50 million tons of commercial ore has been found at the cost of survey 5 cents per ton of ore.

Fig.49 shows curves of phase angle step-out $\Delta\varphi$ above the clayotter deposit in New-Brunswick at different flight altitude (145, 130 and 110 m). The deposit is composed of massive sulphide ores (75% sulphide and 25% quartz), vertical thickness of which is 24 m. On profile 30, the magnitude of anomaly, reduced to altitude 120 m, comprises, with thickness of surface layer 8 m, 2.6° . On profile 46 and 49 the results obtained were similar (the anomalous body dips in the direction of the plane's flight).

The material of aerial survey is usually checked by aerial geophysical methods before it is finally processed by ground methods. For instance, the survey was conducted in an area of 440 sq.km and approximately one anomaly was defined per 1 sq.km. Interpretation of details decreased the number of possible anomalies to 250. Then these anomalies were classified according to aeromagnetic data with the object of sulphide ore exploration. 120 anomalies were investigated by ground methods, out of which 87 were interpreted as metal conductors, which was confirmed in 80% of cases. The gravity survey separated 22 of the most promising anomalies; all wells intersected metal conductors and in 20 of them compact sulphide ores were found.

The work (211) gives the results of aerial electric prospecting (coverage 10 thousand km of profiling) with the VMP apparatus in Sweden, obtained in 1956 by ABEM firm. The ore anomalies are upto 6-8% in amplitude and 3° in phase (resistivity of overburden comprises not less than 100 ohm.m).

5. Results of Survey by BDK Method:

Experimental, method-testing and production operations with devices of aerial electroprospecting by the BDK method have begun since 1957 in various geological areas of the Soviet Union: Ukraine, Urals, Kol'sky Peninsula, Khazakhstan, etc.. Considerable work is being done by geophysical combines Western (Leningrad) Khazakh (Alma Ata) and Novosibirsky (Novosibirsk). Information is available about similar operations in Sweden, Canada, USA, etc..

Flights with instruments of the mobile group are implemented along previously selected profiles with notable landmarks. The recommended scale of survey 1:25000 - 1:100,000. Measuring on operating topomap is usually carried out on two frequencies. The operating frequencies are determined,

as a rule, during experimental flights above the investigation area. The altitude of the magnetic field detector is maintained within 35-100 m.

The apparatus devised in USSR is set up on helicopter; the instruments permit to measure and record amplitude, phase and component of e.m.f., induced in the field detector of horizontal component in the magnetic field of cable H_x . The indicated parameters in the analogue form are recorded most frequently in pairs by two independent recorders (in the VITR construction the use is made of one diagram tape for two individual recording circuits).

Operations carried out in the Ukraine, particularly in the Maidan-Villa section of graphitised gneiss (see chapt.IV), have shown good possibilities of aerial electroprospecting by the BDK method. Fig.50 shows curves of measuring phase φH_x on four operating profiles. Zones with different resistivities $\rho_k^{(*)}$ are marked by considerable phase anomalies; the amplitude anomalies in phase are upto 30° .

By means of aerial electroprospecting it was possible to differentiate zones of graphitized gneiss ($\rho_k < 10 \text{ ohm.m}$), plotted in Fig.50 from the data of ground electric prospecting. The φH_x curves are clearly divided into two parts, characterised by two troughs, between which is a minor local peak. Similar operations have shown that in geological conditions with even highly conductive overburden, shielding the bottom bedrock, aerial electric prospecting by the BDK method gives better results than the induction method.

(*) Zones k were separated from material of V.I. Klushin (216).

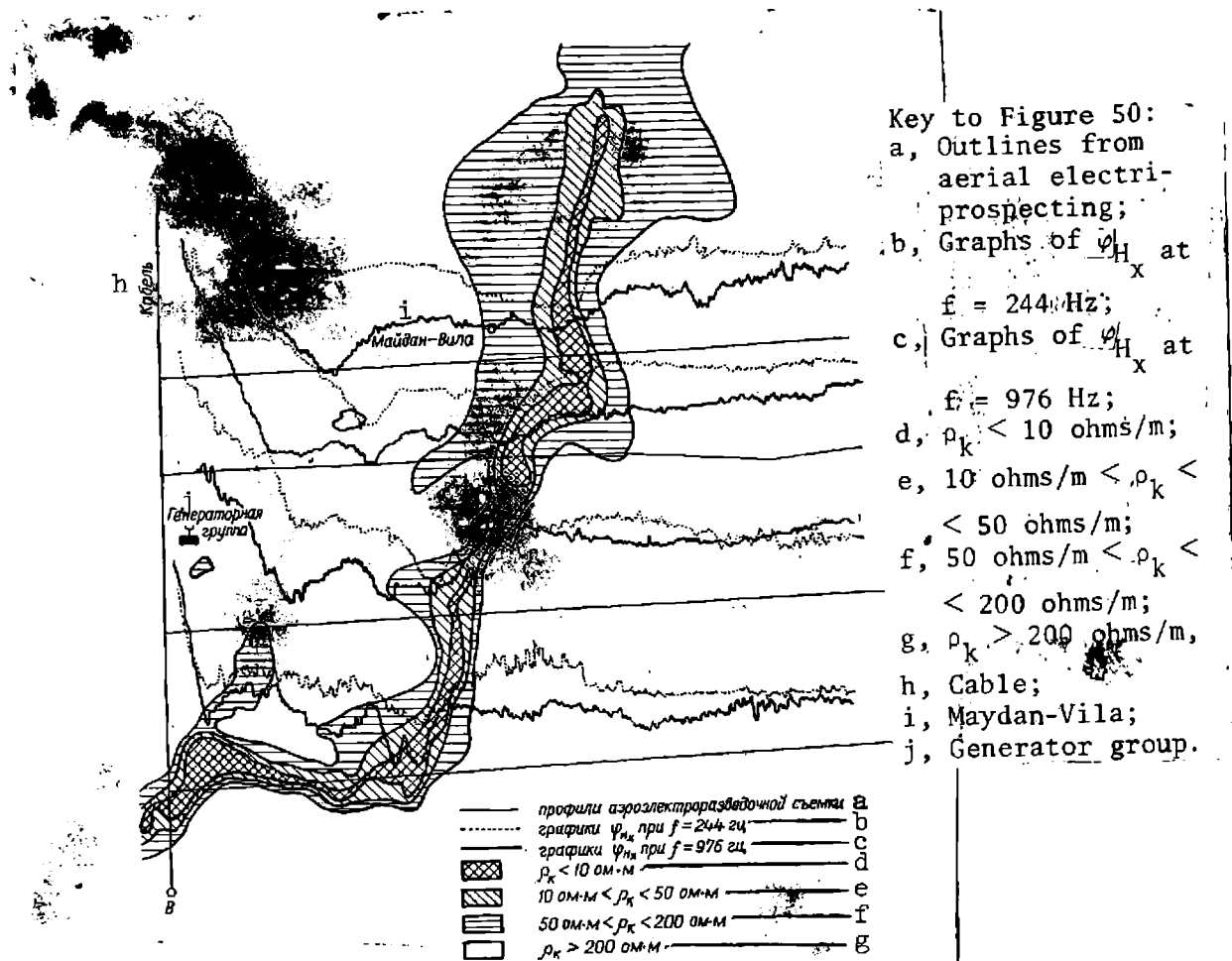


Fig.50

A sufficiently full concept of the possibilities of aerial electroprospection by the BDK method can be obtained from works (213, 215-218, 242, 243).

An example of the method's application may serve survey, conducted by aerial electroprospection party ZGT with participation of the VITR associates on Kol'sky peninsula with the object of ore bodies exploration (190). The joint operations of these organisation with the apparatus AERA-58 were begun in 1959 in an area of largely undulating landscape with vast boggy depressions and abundance of small and large lakes of the Kol'sky peninsula.

The object of the survey was to determine the geological effectivity of the BDK method in exploration of the copper-nickel sulphidised ore,

development of methods for aerial electroprospecting and investigation of the section promising in respect of the above ore. Moreover, the BDK method was compared with one of the ground methods of electroprospecting, e.g. shooting method.

The deposit, where the method and apparatus was checked, is shown in Fig.51, by ore body, confined to the intrusion of metaperidotites. The surrounding rocks - alternating biotite and amphibole-biotite gneiss and amphibolites.

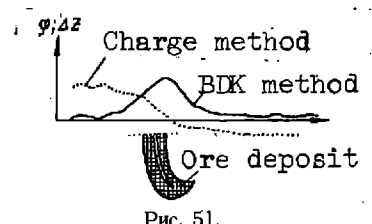


Рис. 51.
Fig.51.

Thickness of body at the top 12-15 m; with depth the body gradually pinches out, its depth down dip is upto 90 m. The deposit itself is overlaid by Quarternary deposits - glacial moraine - with thickness 10-20 m.

The resistivity of the Quarternary deposits varies from 100 to 1000 ohm.m, of the surrounding rocks - from 1000 to 5000 ohm.m, sometimes upto 10,000 ohm.m; resistivity of the ore body - from 0.1 to 1 ohm.m.

The survey was conducted with laying down of cable with $l_{cab.}=10.5$ km of single wire PSM. Current power in cable $I_{cab.}$ on frequency $f = 976$ cps comprised 3.6 , on frequency 244 cps - 3.2 . The cable was laid out parallel to the strike of the ore body at a distance of 3 km. The laying of cable 10.5 km and the rigging up of the ground oscillating group in conditions of arctic winter has taken two and a half days.

Used for survey was the helicopter MI-4 type, the speed of which on parallel profiles was upto 80 km/hr (one of the profiles passed above the center of the ore body). The operating length of the profile both sides of

the cable was 15 km. Satisfactory results were obtained with a gusty side wind with velocity 6 m/sec with the placing of the AkRA-58 devices on the tail beam of the helicopter.

No other aerial geophysical method is applied in these conditions. This indicates high possibilities of aerial electroprospecting by the BDK method.

Fig.52 shows φH_x curves, taken at $f = 976$ cps ($I_{cab.} = 3$, $l_{cab.} = 10.5$ km, $v = 80$ km/hr) at altitude of gondola $h = 35; 100; 200$ and 300 m.

On this profile, the ore body was at a distance 3.2 km from the cable. The peak anomaly of phase is evident at the minimum altitude of gondola - 35 m (the bottom curve). The phase anomaly is well traceable even at altitudes of over 100 m the width of phase anomaly comprises 300 m. The increment of flight altitude to 300 m sharply reduces the effect of non-uniformities in the overburden layer. Therefore measuring at this altitude permits to obtain by the BDK method characteristics of the normal cable field free of the effect of non-uniformities.

Curves $Re U_c$ of H_x field, taken at $f = 244$ cps (constant of field detector $C_d = 3.75 \frac{v}{m}$, $I_{cab.} = 3$, $l_{cab.} = 10.5$ km) at altitude 300; 200; 100 and 35 m with the speed of helicopter 60 km/hr, are shown in Fig.53. The position of the ore body corresponds to that analysed in the foregoing. As shown by the given curves, normal fields in altitude interval 35-300 m persist with accuracy upto 10%. The peak of the active component anomaly in amplitude is at low altitude (35 m) and is practically untraceable on an altitude of 300 m. The width of the anomaly increases with the increment of altitude. The increasing altitude of gondola flight also reduces the effect of non-uniformities.

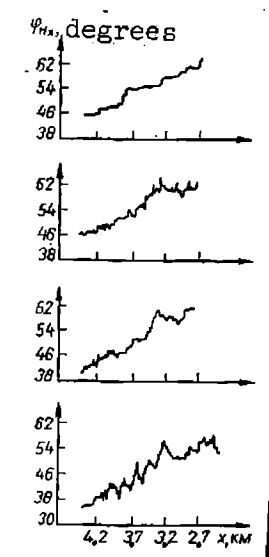


Fig.52

The results of recording of U_c parameters on the central profile were confirmed with repeated flights, as well as by the aerial survey in the section of deposit.

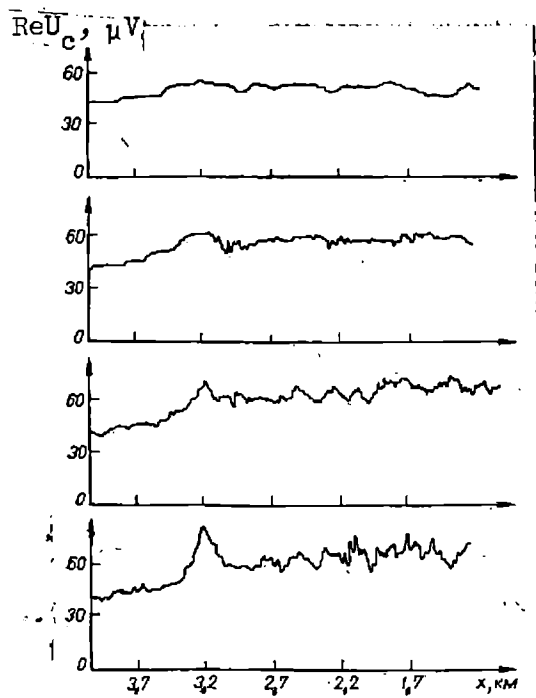


Fig.53

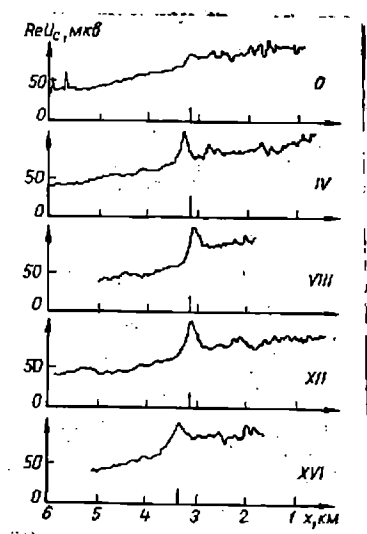


Fig.54

Fig.54 shows curves $\text{Re } U_c$ ($f = 976$ cps, $C_d = 15 \frac{v}{m}$; $h = 35$ m, $l_{\text{cab.}} = 10.5$ km, $I_{\text{cab.}} = 3$, $v = 80$ km/hr), obtained on various profiles, run in the immediate vicinity of the ore body. According to these curves, the ore body is outlined by clearly defined anomalies on profiles 0, IV, VIII, XII, XVI. The maximum width of the anomaly is evident on the central profiles. On end profiles, the anomaly decreases in magnitude and narrows down in width.

On the grounds of implemented experimental and productive operations, a conclusion was drawn regarding the possibilities of aerial electroprospecting by the BDK method in the search for sulphide deposits of Kol'sky peninsula. Some of the anomalies defined during the productive survey were checked by ground electric prospecting. Drilling has been conducted in areas of more promising anomalies and has confirmed their connection with mineralization (190).

It has been established that, by means of the BDK method, it is possible to define with assurance highly conductive zones of considerable

dimensions (faults and graphitization zones), highly conductive ore bodies, as well as to carry out geological mapping, etc. Aerial electroprospecting by the BDK method makes it possible to cover quickly considerable territory to define and trace tectonic faults. The gravity and aeromagnetic survey data are used with this method as auxiliary.

Thus, the results of operations carried out in the Soviet Union have shown that the BDK method has proved itself to be one of the most effective and major methods of aerial electroprospecting.

CHAPTER - V

QUANTITIES MEASURABLE BY AERIAL
ELECTRIC PROSPECTING.

1. Quantities Measurable by Aerial Method of the Near Zone:

The direct carrier of information regarding the magnetic field of the near zone is the e.m.f., induced in the detector by the resultant magnetic field. The latter may be taken conventionally as the sum of the primary and secondary fields. Naturally, the most useful signals, which in aerial electroprospecting characterise the investigation object (geoelectric irregularity), are the e.m.f. components, generated only by the secondary field. Other components are of relatively small interest.

The ways for defining electric parameters, closely connected with the e.m.f. components, which are mainly dependent on the anomalies sought, present a no less important problem than the choice of the pattern's geometry of frequency band of one or the other aerial method.

Let us take parameters, which are measured and recorded by devices of the near zone method.

1. The amplitude of one of the dimensional components of intensity of the primary and anomalous magnetic fields, determinable from the active modulus of the non-compensated part of e.m.f., induced in the field detector by these fields and amplified in the measuring unit of the apparatus.

2. One of the quadrature components of the non-compensated part of e.m.f., which, in relation to supporting voltage, is in phase (active component) or in quadrature (reactive component). In this case the phase of the supporting voltage may be closely connected with the current phase, e.g., in the generator frame.

3. Virtual value of the difference in e.m.f., induced in two receiving coils, or of the difference between e.m.f., in one of the coils and some auxiliary, compensating voltage, connected with e.m.f., of the second coil or with the current in the oscillating frame.
4. Phase shifts of e.m.f., or the differences of e.m.f. in respect of the key signal (or the current in the generating frame).
5. The ratio of virtual values of e.m.f., induced in two receiving coils.

Moreover, in the two-frequency survey, conducted for the separation of anomalies caused by bedrocks from anomalies, connected with surface overburden and topography, the measurable quantity could be the difference of two quadrature components in signals of two essentially different frequencies.

The listed parameters contain a certain amount of information regarding the geoelectrical conditions in the area of survey. Therefore, it would seem that the choice of one of the other parameter is of no significance. But actually the usefulness of any one of these quantities for the near zone methods is determined mainly by its shielding from the technical interference caused by the primary field. In the use of aerial methods it is necessary to know how much the useful signal differs from e.m.f., induced exclusively by the primary field or its variation during the flight caused by the instability of the circuit source-field detector. For instance, the first parameter is more exposed to the influence of this mechanical interference than the second (reactive component) (132). However, not all the measurable parameters are equally dependent on the altitude of flight, e.g., the first and second parameters depend on altitude variation to a greater extent than the fourth, and so on.

In the selection of measurable parameter it is necessary to estimate the initial geometry of the system and its possible application during the survey (see Chapter IX), the adopted method of electric compensation (see Chapter XI), and the topography of the areas where it is prepared to conduct aerial electric prospecting, as well as the bedding of the objects sought within the enclosing rocks.

The construction of some of the devices provides for the measuring of many parameters of e.m.f., of one or two field detectors (166, 263). However, devices of this type are bulky, less mobile and are meant mainly for survey review of the chosen area. A detailed survey is carried out by means of a more mobile set up and more exact measuring instruments, which, as a rule, provide for the recording of one-two parameters of the unbalance signal. (166, 263).

The apparatus of the aerial induction method, with rotating magnetic field and elliptically polarized field, measures the amplitude (modulus) and phase of unbalanced signal $\Delta \dot{U}$ or its active and reactive components. Besides, it is possible to compare signals \dot{U}_x and \dot{U}_z by measuring the deviation from normal of the amplitudes congruence (signal ratio measuring) and of phase shift 90° from normal. Also amplitude parameter A, which is a difference between the modulus ratio of measurable signals and the mean level of primary field (234), i.e.

$$A = \frac{|\dot{U}_x| - |\dot{U}_z|}{U_0}$$

where

$$U_0 = \frac{1}{2} (|\dot{U}_x| + |\dot{U}_z|).$$

When using aerial electric prospecting with elliptically polarized magnetic field (EPP), it would be expedient to measure the following quantities (153, 186): invariants of the polarization ellipse itself (major and minor semiaxes) from the signals; proportional to them; parameters characterising the orientation of polarization ellipse in space (for instance, the angle of major semiaxis) one of the time factors of the field (for instance, phase shift^{of}/field's intensity towards the major semiaxis relative to current in the field exciter).

In the set up with EPP it would be expedient, as in other patterns of the induction aeromethod, to apply simultaneous measuring on two frequencies, for unambiguous determination of the nature of conductive object.

Thus, in the near zone method the measurable could be various parameters of signals, induced in the magnetic field detectors.

2. REGARDING EFFECTIVITY OF MEASURING SIGNAL PHASE OF SECONDARY FIELD:

It is well known that in many geophysical investigations, carried out by electric prospecting, it is most important to know phase shift of the measurable signal in respect of another, the phase of which is conventionally taken as the starting point of reading. In contrast to amplitude measuring, when similar intensity anomalies may be caused by good but too deep-seated conductors or shallow-bedded but poor conductors, phase measuring provides information, from which in simple geological conditions it is possible to divide the defined anomalies into ore and rock product type (185, 251).

With the availability of preliminary data (e.g., obtained in ground conditions) regarding conductivity^{of} of ore bodies or other conductive

objects in the area of survey and, also, with the availability of the enclosing medium characteristics, it is possible to determine in the first approximation the dimensions of this body or object.

However, realisation of the hookup of instruments (for instance, in the induction method) to measure phase angles of the secondary field signal \dot{U}_2 in relation to phase of the primary field signal \dot{U}_1 or to supporting voltage \dot{U}_s , coinciding in phase with signal \dot{U}_1 , is rather difficult because of the accuracy required in measuring phase shift. This accuracy is stipulated by the choice of the pattern's geometry, electrical compensation of the primary field signal, peak operating frequency etc. In this connection, the question arises whether it is appropriate to measure phases of the secondary field in the near zone method at all.

In order to estimate the effectivity of measuring phases of the secondary field signal it is necessary to analyse the behavior of the amplitude and phase characteristics of the secondary field, formed by the presence in the primary field of conductive body. With this aim analysis of the secondary magnetic field, caused by the presence of conductive body in harmonic field of vertical magnetic dipole, should be conducted, as well as to show how the initial phase of the secondary field ϕ_{sec} depends on frequency f of the primary dimensions of conductive body and its conductivity γ . The analysis will be of the simplest case of conductive body in the shape of a sphere, since for a body of this type of isometric form it is most easy to implement excitation by a uniform primary field (133, 185, 250).

Let us place the origin of spherical coordinates in the centre of a sphere with radius Q (Fig.55). The line OZ is directed parallel to

moment \bar{m}_z of dipole. The dipole we place at point A, lying on plane YOZ; and we assume that the medium surrounding the sphere is homogeneous and non-conductive. Coordinates of the arbitrary point P, at which the secondary field is being determined, will be Φ , Θ_2 and $\bar{\Phi}$. Distance from the center of sphere to the center of dipole is b, distance from the center of dipole to recording point is R, and the angle between the line OZ and direction to dipole is Θ_1 .

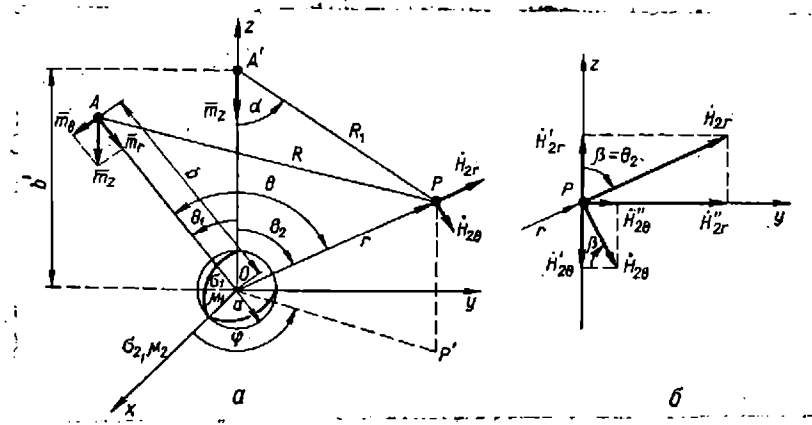


Fig.55.

The magnetic dipole with vertical magnetic moment \bar{m}_z may be shown as two dipoles - tangential, with moment \bar{m}_0 , directed perpendicularly to line OA, and radial, with moment \bar{m}_r , directed along this line. Each of the dipoles generates at the recording point P its own components of the secondary field - radial (H_{2r}^p , $H_{2\theta}^p$) and tangential (H_{2r}^r , $H_{2\theta}^r$) (38, 63, 261).

The complex coefficient D is a function, determinable at $\mu_1 = \mu_2$ by relationship [98, 251],

$$D = \frac{3vI_{-\frac{1}{2}}(v) + (3 + v^2)I_{\frac{1}{2}}(v)}{v^2I_{\frac{1}{2}}(v)} \quad (V.1)$$

where $I_{-\frac{1}{2}}(v)$, $I_{\frac{1}{2}}(v)$ - Bessel's functions of half-integral order from the complex argument (36); $v = \sqrt{j\gamma\mu\omega}\alpha^2$. Having denoted $\gamma\mu\omega$ by p , we obtain $v = \sqrt{jp}^2$. For an ideal conductive sphere $\gamma = \infty$, $D = 1$.

Since the reception and measuring instruments in the neighboring zone method usually pick up either the vertical or horizontal component of the anomalous field, it is necessary to change over from radial and tangential field components of the vertical dipole in question to vertical and horizontal components of the secondary field. The calculated relations we write in their complex form.

The moment of tangential dipole

$$\dot{m}_\theta = m_z \sin \theta_1. \quad (V.2)$$

The amount of radial dipole

$$\dot{m}_r = m_z \cos \theta_1. \quad (V.2a).$$

The radial and tangential components of the secondary field at the recording point are equivalent to the sum of field components in tangential and radial dipoles:

$$H_{2r} = \dot{H}_{2r}^T + H_{2r}^P; \quad H_{2\theta} = \dot{H}_{2\theta}^T + H_{2\theta}^P \quad (V.3)$$

In a majority of cases in aerial electric prospecting the radius of sphere α is invariably lower than b and r , and the conductive deposits create an additional error; therefore, for the secondary field components the terms could be written, with allowance for a negligible error, as

$$\begin{aligned}\dot{H}_{2r} &= -\dot{m}_z D \frac{a^3}{4\pi b^3 r^3} (\sin \theta_1 \sinh \theta + 2 \cos \theta_1 \cosh \theta); \\ H_{2\theta} &= m_z D \frac{a^3}{4 b^3 r^3} \left(\frac{1}{2} \sin \theta_1 \cos \theta - \cos \theta_1 \sin \theta \right).\end{aligned}\quad (V.4)$$

As shown in (63), the error in the determination of amplitude of the secondary field from formulas (V.4) in aerial electric prospecting does not exceed a few percents. This error in magnitude is known to be less than the error caused by the presence of the conductive surface deposits; therefore, it may be ignored.

In a particular case, when dipole m_z is located on line OZ at point A', i.e., at $\theta_1 = 0$ and $b' = b$ (above the epicenter of ore body), we have:

$$\begin{aligned}\dot{H}_{2r} &= -\dot{m}_z D \frac{2 a^3}{4 \pi b^3 r^3} \cos \theta_2; \\ H_{2\theta} &= -m_z D \frac{a^3}{4 \pi b^3 r^3} \sin \theta_2.\end{aligned}\quad (V.5)$$

For this case in spherical coordinates the primary field of dipole \bar{m}_z at recording point P is determined as :

$$H_{1r} = \frac{2\dot{m}_z}{4\pi R_1^3} \cos \alpha; \quad H_{1\theta} = \frac{m_z}{4\pi R_1^3} \sin \alpha \quad (V.6)$$

where $R_1 = (b^2 + r^2 - 2br \cos \theta_2)^{\frac{1}{2}}$

According to Fig.55-b, we find the terms for components H_{2z} and H_{2y} at point P:

$$\dot{H}_{2z} = \dot{H}'_{2r} - \dot{H}'_{2\theta}; \quad H_{2y} = \dot{H}''_{2r} + \dot{H}''_{2\theta} \quad (V.7)$$

where:

$$\begin{aligned}\dot{H}'_{2r} &= \dot{H}_{2r} \cos \beta; \quad \dot{H}'_{2\theta} = \dot{H}_{2\theta} \sin \beta; \\ \dot{H}''_{2r} &= \dot{H}_{2r} \sin \beta; \quad \dot{H}''_{2\theta} = \dot{H}_{2\theta} \cos \beta; \quad \beta = \theta_2.\end{aligned}$$

Hence,

$$\dot{H}_{2z} = \dot{H}_{2r} \cos \beta - \dot{H}_{2\theta}'' \sin \beta ; \quad \dot{H}_{2y} = \dot{H}_{2r} \sin \beta + \dot{H}_{2\theta} \cos \beta . \quad (V.8)$$

Having substituted \dot{H}_{2r} and $\dot{H}_{2\theta}$ from equation (V.5) into formula (V.8) and taken into account, that

$$\sin^2 \theta_2 - 2 \cos^2 \theta_2 = -\frac{1}{2} (1 + 3 \cos 2\theta_2),$$

after insignificant conversions we get

$$\dot{H}_{2z} = -\dot{m}_2 D \frac{a^3}{8\pi b^3 r^3} (1 + 3 \cos 2\theta_2); \quad (V.9)$$

$$\dot{H}_{2y} = -\dot{m}_2 D \frac{3}{8 b^3 r^3} \sin 2\theta_2. \quad (V.10)$$

The sum of components of the primary and secondary fields at point P determines the magnetic field actually existing at the moment with components \dot{H}_{zr} and \dot{H}_{yr} :

$$\dot{H}_{zp} = \dot{H}_{B_{pe3}} = \dot{H}_{1z} + \dot{H}_{2z}; \quad \dot{H}_{yp} = \dot{H}_{\Gamma_{pe3}} = \dot{H}_{1y} + \dot{H}_{2y} \quad (V.11)$$

The magnitude of components of the primary field, according to agreement, is determinable by relationships (III.15a).

From the terms (V.9) and V.10) it follows that characteristic phase of the secondary field is determined by the parameters of complex coefficient D, calculable from formula (V.1). To obtain this characteristic, coefficient D should be shown in terms of real and imaginary parts:

$$D = R_e D + j \operatorname{Im} D.$$

As shown in [133], in the region $|\mathcal{V}| > \pi$ the complex coefficient D could be given in the following terms:

$$D = \frac{-3(A - jB)}{\sqrt{}} + \frac{3}{\sqrt{}} + 1 = \frac{2x^2 - 3x(A-B)}{2x^2} + j \frac{3x(A+B) - 3}{2x^2}, \quad (V.12)$$

where

$$A = \frac{\operatorname{sh} x \operatorname{ch} x}{\operatorname{sh}^2 x + \sin^2 x}; \quad B = \frac{\sin x \cos x}{\operatorname{sh}^2 x + \sin^2 x}; \quad (V.13)$$

$$\operatorname{Re} D = \frac{2x^2 - 3x(A-B)}{2x^2}; \quad \operatorname{Im} D = \frac{3x(A+B) - 3}{2x^2}$$

$$x = \sqrt{\frac{Pa^2}{2}}. \quad (V.14)$$

Therefore,

$$\varphi_c = \operatorname{arctg} \frac{\operatorname{Im} D}{\operatorname{Re} D} = \operatorname{arctg} \frac{3x(A+B) - 3}{2x^2 - 3x(A-B)}. \quad (V.15)$$

In this case the terms for the components of the secondary field will be written as:

$$\dot{H}_{2z} = \dot{m}_z \left| D \right| \frac{a^3}{8\pi b^3 r^3} (1 + 3 \cos 2\theta_2) e^{j\varphi_c}; \quad (V.16)$$

$$\dot{H}_{2y} = \dot{m}_z \left| D \right| \frac{3a^3}{8\pi b^3 r^3} \sin 2\theta_2 e^{j\varphi_c}. \quad (V.16a)$$

It is difficult to use the terms (V.15) for φ_c determination in explicit form; therefore, relationship curves $\varphi_c = F_c(\gamma\alpha^2)$ are often plotted for the operating frequencies of instruments in aerial electric prospecting. As an example, Fig.56 shows relationship curve $\varphi_c = F_c(\gamma\alpha^2)$ for fixed frequencies 125; 250; 500; 1000; 1500 and 2000 cps. Moreover, it was assumed that for ore bodies the most probable conductivities comprise $\gamma = 0.05-50$ 1/ohm.m, and the dimensions of sphere could be within the range $\alpha = 1 \div 50$ m. Since

$$\gamma^2 = \frac{p \alpha^2}{\mu \omega} = \frac{p \alpha^2}{4 \pi 10^{-7} 2 \pi f} = \frac{p \alpha^2}{78,88 f},$$

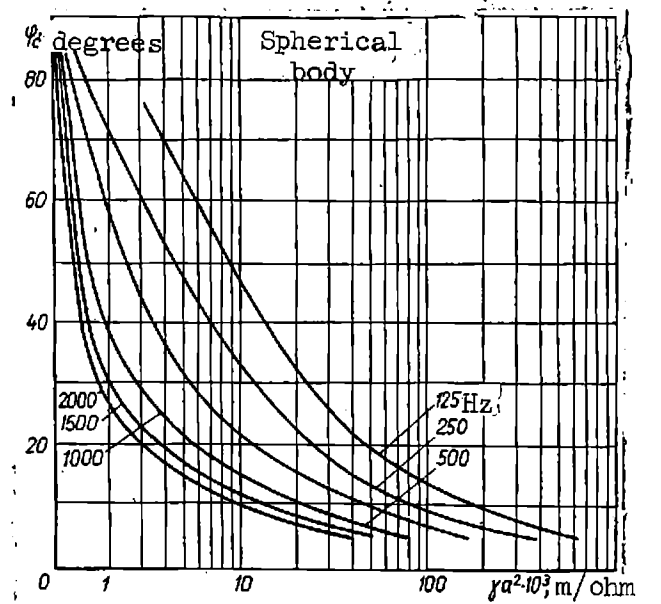


Fig.56

then with an estimate of the adopted values f , γ and α it is possible to assume that this relationship extends also to spherical conductors with parameter $p^2 = 500 - 600$, i.e., to actually existing conductive objects of spherical form (75, 98, 251).

From Fig.56 it can be seen that with sufficiently high conductivity of ore body, i.e., with high value of parameter $\gamma \alpha^2$, phase shift of this field in respect of the primary will be negligible (in this figure parameter $\gamma \alpha^2$ is in logarithmic scale). In this case, it is sometimes said that the secondary field has an active nature. On the contrary, with low conductivity, when parameter $\gamma \alpha^2$ is insignificant, which is characteristic of non-metallic bodies and bodies of composite structure, the phase of the secondary field in respect of the primary approaches $\frac{\pi}{2}$, and the secondary field is assigned ^{to} a reactive nature.

Analyzing the phase shift Φ_c vs. parameter $\gamma \alpha^2$ at various operating frequencies, it is possible to draw conclusion that frequencies below 500 cps make it possible to assure a higher resolving power of the method than higher frequencies both with active and reactive secondary field. With low $\gamma \alpha^2$ of conductive body, i.e., with predominance of reactive nature of the secondary field, slight variations of this parameter on high frequencies cause an appreciable phase shift of the given field. This leads to increased errors of measuring at high frequencies with the presence in the area of irregularities - deposits, surrounding rocks, etc.. Therefore, in aerial electro-prospecting, measuring of parameter Φ_s is effective in the interpretation of survey results.

According to Fig.56, it is possible to conclude that the phase shift Φ_s with excitation of spherical anomalous body by the uniform field throughout its dimension does not depend on the altitude of the aircraft. However, in actual geological conditions, conductive bodies of spherical form are encountered very seldom. A majority of them have the shape of cylinder, inclined bed, etc.. With aerial electric prospecting in the near zone for conductive bodies with the shape of a round cylindrical conductor of radius α of infinite extension, inclined bed, etc., it is impossible to assure uniformity of the exciting field through the whole dimension of the body; therefore, the field anomalies of a body of this type will be affected by the altitude of flight. In phase measuring, the altitude of survey has considerably less effect than in the measuring of other parameters (amplitude, components). In such cases, determination of phase parameter, as in the case of spherical conductor, will be justified and effective.

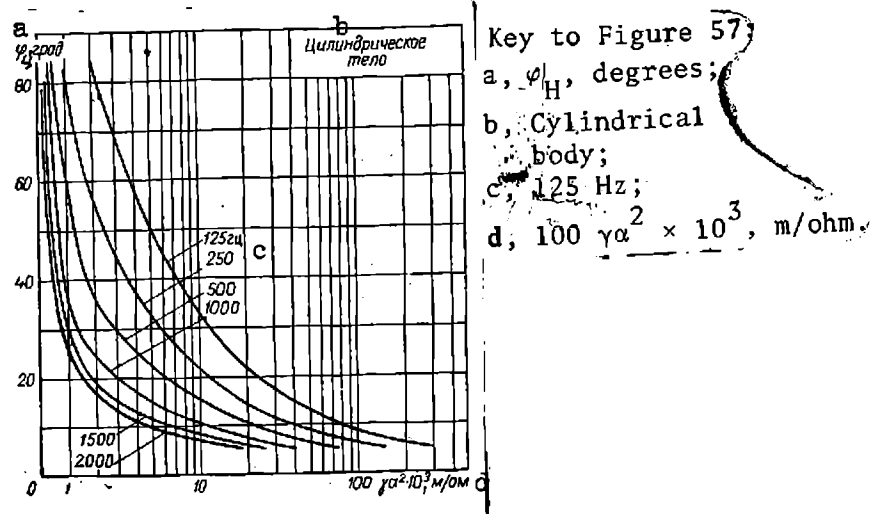


Fig.57

Indeed, ignoring the end effects for cylindrical body of finite extent being present in the exciter field of the oscillating dipole, which moves on the aircraft at altitude h , it is possible to determine approximately on the basis of relationships given in (172), the value also of phase parameter φ_c (133).

$$\varphi = \arctg \frac{1.414 - \frac{1}{\sqrt{\rho a^2}}}{1.414 - \sqrt{\rho a^2}}. \quad (V.17)$$

Fig.57 shows curve $\varphi_c = F_c(\gamma \alpha^2)$, similar to the curve in Fig.56 for the same operating frequencies and radii of cylinder. The conductivity is so taken that parameter $\rho \alpha^2$ would correspond to the actually existing conductive objects of cylindrical shape, i.e., $\rho \alpha^2 \leq 200-300$ (251). From Fig.57, according to operating frequency and the obtained phase shift of secondary field φ_c it is possible to determine the factor $\gamma \alpha^2$. It case also be shown that in aerial electric prospecting by the neighboring zone method it would be highly beneficial to use patterns, the apparatus of which permits the phase of secondary field being measured as the most effective parameter, depending very little on the altitude of survey.

3. Difference and Sum of Reactive Signal Components of Double-Frequency Fields:

The intrinsic shortcoming of the induction method with outboard gondola is the variability of reciprocal position of the source and field detector due to inevitable bumping of gondola, in which the field detectors are placed. As a result the recordable parameters are highly distorted. However, as has been pointed out, not all the parameters of usable signal, induced in the field detector, have similar perception of bumping.

Let us take the example as shown in Fig.58 and consider the vector diagrams of the field intensities, produced in the detector by the resultant (primary and secondary) field attached with the measurements with compensation of the primary field signal.

If the signal of the primary field U_1 is compensated in a way that the residual intensity ΔU coincides with it is phase (Fig.58a), while the angle between it and supporting voltage U_{sup} is φ (in this case the phase of supporting voltage is combined with the phase of current I_f in the generating frame), the motion of gondola should cause variation only of ΔU .

This is true only for the linearly polarised field of low frequencies in the quasi-stationary zone, when the field phase φ remains invariable with transition from one recording point to another.

The emergence of the secondary field generates in the detector of the magnetic field signal \dot{U}_2 , the phase of which is generally distinct from the phase of the signal generated by the primary field. The resulting signal \dot{U}_{res} is an addition of vectors $\Delta \dot{U}$ and \dot{U}_2 (Fig.58-b), and the phase shift between it and the key signal is equivalent to φ' . Measuring of amplitude (modulus) \dot{U}_{res} and phase shift φ' of resultant signal is made possible by amplitude voltmeter and phase indicator. It is easy to

see that with bumping of gondola the modulus and phase of the resulting signal will vary.

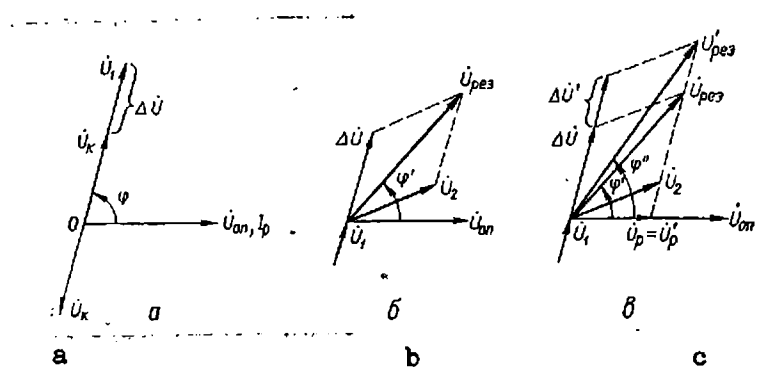


Fig.58

With the transition to measuring reactive component U_{rc} of the resulting signal U_{res} by phase-sensitive voltmeter, it is easy to see that the bumping of gondola does not result in the variation of reactive component value. In this case the stop-out of residual intensity to the extent of $\Delta U'$ will cause variation only of the resultant signal (U'_{res}) and its phase shift (φ'') in relation to key signal (U_k), whereas the equivalent to reactive component quantity U_r will not change its value ($U_r = U'_r$) (Fig.58-c). Thus, the reactive component of the signal is a parameter, theoretically independent of the bumping of gondola. In the actual conditions of using instruments of the aerial induction method, the considerable metal mass of the aircraft directly at the source of the primary field (generating frame), causes, as we know, non-linear, i.e., elliptical, polarisation of the primary field (6). This polarisation is due to the effect of currents, induced in the metal mass of the aircraft by the primary field. Bumping of gondola causes variation not only of the residual intensity modulus, but also of its phase, which affects indications of phase-response voltmeter, and thereby the advantages of measuring the

reactive component in the case of linearly polarised primary field are lost.

In confirmation of what is stated above we show curves of modulus U_{res} , phase and reactive component U_r of the resulting signal recorded by apparatus AERI-2 in various meteorological conditions (Fig.59-a - results of survey in relatively calm weather, Fig.59-b - in extremely windy weather). As follows from these curves, all the measurable parameters depend on the bumping of gondola.

If instruments of the induction method with outboard gondola permit simultaneous survey on two frequencies (on different operating frequencies), there is actual possibility of reducing the effect of gondola's bumping even in the case of polarised primary field (103).

For this, it would be expedient, besides the individual measuring of reactive components on both the frequencies, to measure directly the difference or the sum of output voltage in phase-response voltmeters, proportional to the reactive components of signals on two operating frequencies, i.e., to apply the differential method of measuring reactive components of two operating frequencies.

If the output voltages of phase-response voltmeters are equalized at a certain position of the source and field detector and similar polarization of these two-frequencies field, variation of their reciprocal position should not, in principle, disrupt the balance of the differential circuit. With dissimilar polarization on different frequencies, it is not possible to exclude the effect of gondola's bumping; but even in this case, with the correct choice of working frequencies, it would be useful to measure the difference of reactive components (103). In practice, the difference

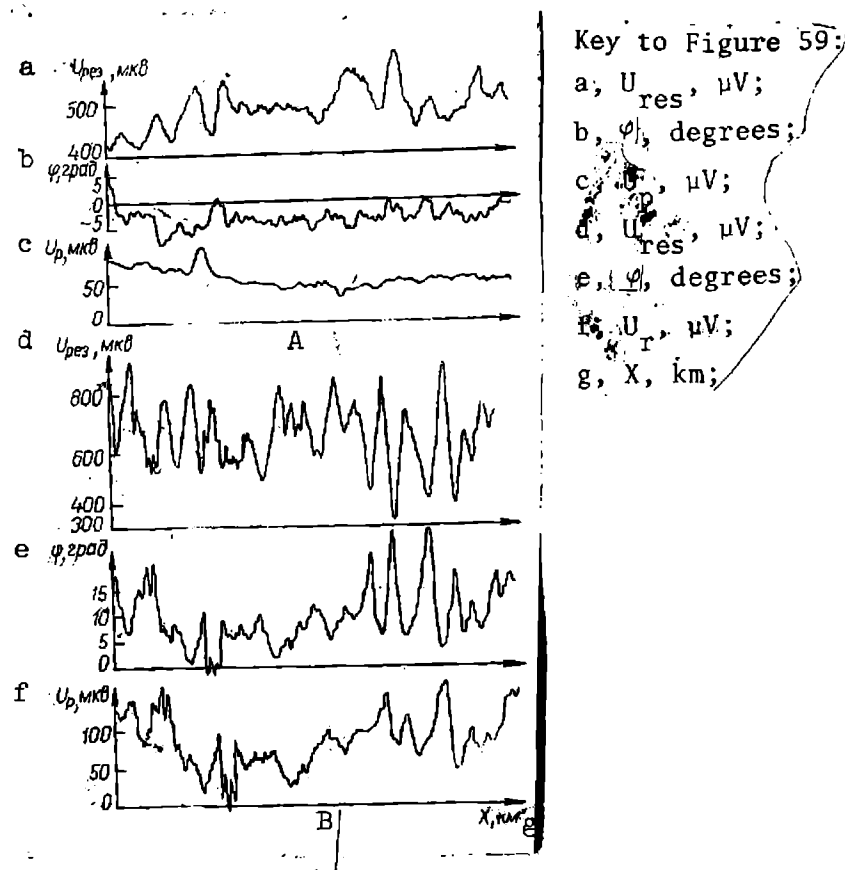


Fig.59

between operating frequencies with the induction method on two frequencies is usually not very high, for instance 244 and 1953 cps; therefore the polarization of the fields on these frequencies will be about the same.

The application of differential method for measuring the difference of reactive components of two signals of operating frequencies makes it possible, besides reducing the effect of gondola's bumping, to eliminate the effect of altitude variations and deposits. This is due to the fact that the field of both the operating frequencies depends practically to the same extent on altitude variations and on deposits; the field of low operating frequency depends mainly on conductive bodies bedded at certain depth. In the measuring of components and their differences, the signal should conform exactly either to the current phase in the oscillating frame, or to the phase of the normal field should be correctly compensated -

the phase of key signal should conform exactly either to the current phase in the oscillating frame, or to the phase of the normal field signal (in relative measuring), i.e., it is necessary that the phase of the residual signal be zero.

4. Quantities Measurable by Aerial Method of Combined Zone:

Of all the quantities, subject to measuring and recording in aerial electric prospecting by the combined zone method, the most significant are those which are directly connected with the object of investigation, i.e., with the normal and anomalous electromagnetic fields of field sources. Since the BDK method is the main method of the combined zone, we shall analyse the indicated quantities as applicable to this method.

The main aspects, discussed in Chapt.III and IV, which characterise the behavior of the normal and anomalous fields of cable, indicate primarily that the horizontal component H_x of the normal field dampens slower with removal from the cable, than the horizontal H_z components. In the case of the infinite cable, the component H_y is equivalent to zero, and in the case of the finite - it is very negligible in quantity. This circumstance is very significant in the choice of measurable quantities in the BDK method. Quick attenuation of the component H_z , smallness of H_y with comparatively high noise level on the aircraft, scanty competence of the generating ground apparatus hamper the construction of measuring devices of the required selectivity and quick action during the flight. At the same time, the convenience of flights across the cable, the possibility of taking off away from the cable with the same response of instruments to a considerable distance and other factors (216) confirm the expediency of investigating the component H_x instead of H_z (90, 103, 118). The investigation of other field components or parameters of the polarization ellipse

(185, 186), is apparently difficult.

The measurable parameters could be amplitude, phase and e.m.f. components of the signal induced by the component H_x in the magnetic field detector. In accuracy, appreciation of measuring and recording of these parameters, the two following features must be taken into consideration.

The first feature is due to the interpretation of anomalies from resistivity values (41), which are calculated on profile from the values of the resultant (normal and anomalous) field. This requires a comparatively high accuracy of measuring (the altitude of survey and the flight course should also be precisely maintained). With this type of interpretation, the phase characteristic of the field ϕ_H is practically of no significance; hence it is suggested that no time be wasted on its study (41). Actually, in this case, there is no need also to record the components.

The second peculiarity is connected only with the fact of the anomaly detection. In this case, the accuracy of measuring could not be high as compared to the first case. The interpretation technique of survey results, suggested by the authors of (216), is calculated for measuring the amplitude and phase, the components or one of the components (active or reactive) and of the phase in relation to geological conditions of the survey area. The permissible errors in measuring and recording - 2-3% in the amplitude or component and 1-2° in the phase. These requirements of instruments are quite sufficient for detecting the major, as well as very minor, field anomalies. Since from the results of the aerial survey there is bound to be a detailed ground survey, subsequently topped off, if required, by drilling, the absolute and exact measuring of anomalies in the air has only an auxiliary value. Moreover, in this case, the use is of a more complete information regarding anomalies, as the amplitude and

phase characteristics of the cable's field are measured on different frequencies (98).

Instruments which take into account the above peculiarities, are very much distinct. The first peculiarity is taken into account by the ground apparatus, as well as the airborne (mobile) one, having a precise recording voltmeter. It also requires a highly qualified crew for the aircraft, capable of maintaining at a given altitude, the set course; or the apparatus should be provided with devices for correcting the navigational errors.

In the estimate of the second peculiarity, the ground group is also required, but with transmitter of the principal phase signal. The measuring instruments need not be of very high accuracy for amplitude and phase measuring. The aircraft crew could be medium qualified. Thus, the second way is simpler and makes it possible to obtain a more comprehensive information regarding anomalies; therefore it is widely applied in practice (87, 89, 103, 216).

The minimum values of the amplitude of horizontal component H_x determine the required response of the measuring instruments. If the nominal current in the cable, the operating frequency and approximate correct geological conditions of the investigation area are known, then, from formula (IV.31), it is possible to determine the H_x field at such a distance from the cable as is required for ensuring a considerable flight around the survey area. The geological conditions of the chosen area are usually judged from the geological data and results of various geophysical investigations on land.

In the determination of the required quick action (legging in recording) of measuring instruments in the BDK method, it is important to know the nature of field variation at each point of the operation profile and the average speed of the aircraft. Investigations have shown (89, 216), that the field gradient near the cable has very high values and, at a distance from it, the gradient values decrease by two-three orders. Thus, with $I = 1$ near the cable the field gradient attains $10^{-2} - 10^{-3}$ a/m, and at a distance - only 10^{-4} to 10^{-5} a/m². The speed of the aircraft, which is determined by its type, is usually known.

Key to Figure 60
a, φ_{Mx} ;
b, $f = 244$ Hz;
c, Non-working zone.

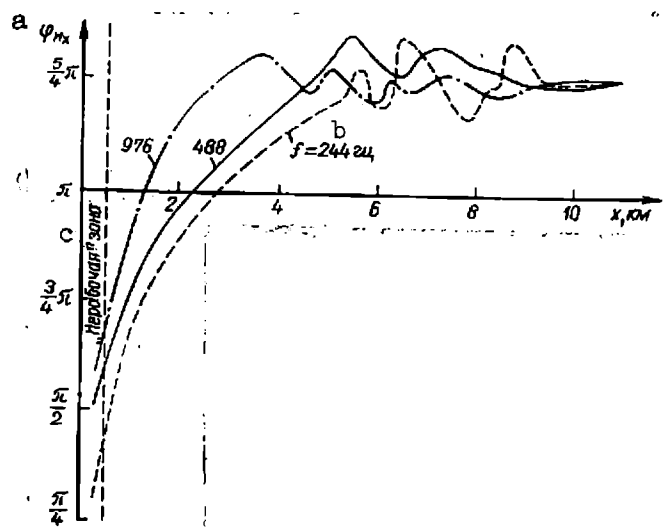


Fig.60

The indicated nature of variation of cable field H_x causes certain difficulties in devising measuring instruments. Indeed, the measuring time in aerial electric prospecting is limited; all recording devices, specially those with moveable mechanical details, have a limited quick action. The area of the survey map, with one laying of cable of 10-30 km, should be as large as possible (about 200 sq. km²). The nature of the H_x field is such that, to ensure the required accuracy of measurements throughout the whole operating profile, the apparatus should be provided with multi-

range measuring of amplitudes, i.e., the measuring range should be divided into a number of sub-ranges or measuring limits. This means that, during the flight, the operator has to commutate the range of measuring (and the nearer to the cable, the more often), or, in the selection of the operating range, it is necessary to cut in the device for automatic search and commutation. Experience shows that neither the one nor the other assures a normal operation of instruments near the cable; therefore, in aerial prospecting by the BDK method, the zone 0.5-1 km from the cable is assumed to be the non-operative zone. The application of digital recording, which in principle could resolve this problem, has not so far been practised.

The behavior of the amplitude characteristic of the field is similar to that of the phase characteristic φH_x , which with removal from the cable changes its value from zero above the cable to $\frac{5}{4} \pi$ in the furthest from its zone. For then normal field above a uniform half-space in the same zone, the φH_x characteristic theoretically does not depend on the parameters of medium (30, 68, 69). The variation velocity of the phase angle - phase gradient - is 50-90 degr./km near the cable, decreasing to a few electric degrees per 1 km at a distance from it.

In the event of non-uniform half-space, this relationship invariably has a composite nature. This is confirmed also by the test data obtained in various geological conditions. For instance, Fig.60 shows the actual phase characteristics φH_x , recorded in Maidan-Vila section (see para 5 Chapt. IV) in relation to the cable distance x on three frequencies: 244, 488, 976 cps (profile No.1, course 200° , $v = 100$ km/hr, $l_{cabl.} = 11$ km. altitude of gondola 35 m).

From Fig.60, it follows that, at various frequencies, in the same geological area with all other conditions equal, the behavior of ϕH_x varies. This is specially noticeable in the zone close to the cable. The highest phase gradient in this example is evident on frequency 976 cps. At a distance of 1.5 - 0.5 km from the cable, this phase gradient is 55 degr/km.

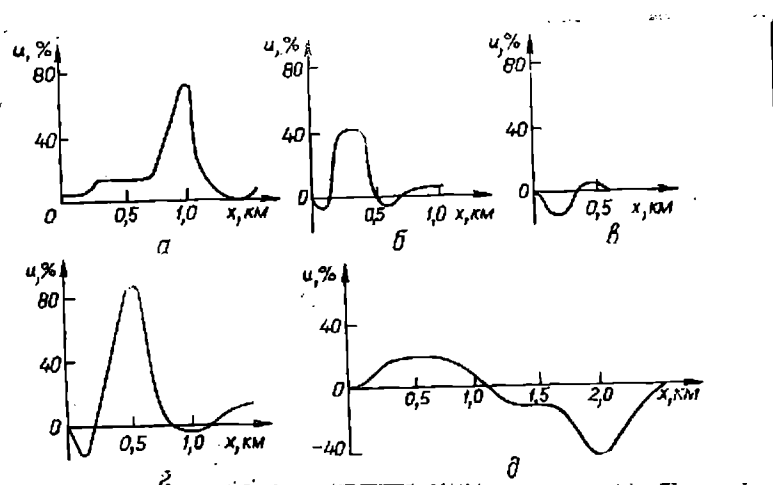


Fig.61

The methods of aerial electric prospecting are invariably based on the multifrequency principle of investigations. This principle is also applied in the BDK method. However, in this method the range of applicable frequencies is limited, on the one hand, by the fact that the measuring time on the aircraft is limited by its comparatively high speed and, on the other, by the fact that on higher frequencies the cable on the ground often conforms poorly to the oscillator and behaves as a line with distributed parameters, which also limits the operating voltages in the line. According to safety regulations, voltages on the cable should not exceed the disruptive voltage of its insulation (the current in the cable on higher operating frequencies should not increase considerably). It has been found (89, 102), that in laying out of the cable upto 30 km in the majority of

geological areas, the upper operating frequency of the generating unit should never be taken above 3-4 k-cps, and the lower below 60-80 cps.

Aerial electric prospecting by the BDK method is characterised by a comparatively high ratio of the field anomaly to the normal cable field on operating profile. The altitude effect on the magnitude of the anomaly is insignificant (see para 3 chapt.IV). The given method permits to anomalies directly on the background of the normal field being measured and does not impose any critical limitations on the accuracy of the apparatus set up.

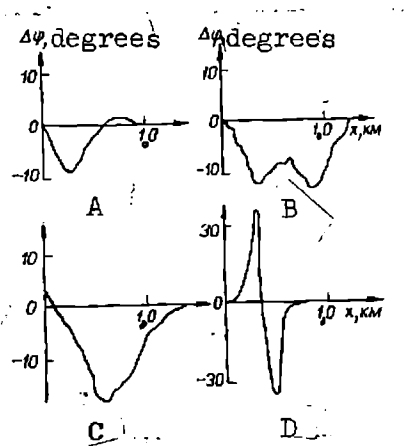


Fig.62

Fig.61 shows the behavior curves of anomalies' amplitudes (a - c) and of component (d, e), and Fig.62 - phase curves, obtained in various geological conditions by the BDK method. These curves show typical field anomalies. On the abscissae the width of anomalies is plotted and on the ordinates - either the ratio of the magnitude of the anomaly to the magnitude of the normal field at reception points (Fig.61) or phase variation at the same points. The operative altitude of survey 85 m. As follows from these curves, the behaviors of the typical amplitude of anomalies, the components

and phases are quite diverse. Nevertheless, on the basis of these curves, it is possible to determine the variation range of measurable quantities.

It is assumed that the amplitude and component anomalies are on an average 20-25%, and of phases - 10-15°. The width of the anomaly on an average is 2 km for the amplitude and components and a little less for the phase. With the altitude of the survey reduced to about 30-50 m, the width of the anomaly decreases proportionately whereas the variation range of the amplitude, components and phases increases.

PART II
PRINCIPLES OF PLANNING UNITS AND THE ELEMENTS OF
APPARATUS IN AERIAL ELECTRIC PROSPECTING

CHAPTER - VI
GENERATING UNITS.

1. General Requirements Imposed Upon Generating Units.

In conducting aerial electro prospecting by various methods, the excitation of the harmonic electromagnetic field requires a special low-frequency generating unit. At present, the generating units applied in BDK, induction and VMP methods have, as a rule, harmonic current at the output.

To increase the exploratory efficiency of the apparatus (depth, survey area, etc.), it is expedient to have as high as possible ratio $\frac{U_s}{U_n}$ (signal-noise), which, with the attainable minimum level of noise U_n , wholly depends on the magnitude of usable signal U_s . The magnitude of the usable signal is in its turn affected by the efficiency of the electromagnetic field exciter (oscillating frame in the induction method, grounded cable in BDK, etc.), and the competence of the generating unit.

Thus, with the same construction specifications of the primary field exciter, one of the ways of increasing the signal-noise ratio is to raise the competence of the generating unit. The power output of the generating unit is invariably limited. In the induction method, this limitation is the power supply for a given type of plane and the maximum allowed voltage at the terminals of oscillating frame ($U_{fr} < 500v$). For instance, in the apparatus fitted on planes IL-12 or IL-14, the allowed maximum power per

one operating frequency does not exceed 500 and 1000 watts. In the apparatus of the BDK method, considering its overall size and weight and also the safe voltage on cable, the maximum power at the output of the generating unit should not be over 2-3 k-watts.

It should be mentioned that the requirements imposed on the generating sets are also high with respect to the frequency stability and the time constant of the radiator's phase characteristics. This is explainable by the fact that, due to high noise level in the field detector the measuring devices are provided with special selective systems with narrow transmission band. This narrow-band characteristic imposes in its turn high demands for the accuracy of the set up and the time stability of current frequency in the exciter of the electromagnetic field.

Indeed, analysing the known terms (56)

$$n \approx - \frac{1}{\sqrt{1 + \left(\frac{2\Delta F}{F_p} Q \right)^2}}, \quad (\text{VI.1})$$

$$\varphi \approx \text{arctg} \left(\frac{2\Delta F}{F_p} Q \right). \quad (\text{VI.2})$$

it is not difficult to note that the instability of frequency F_p is reflected both in the amplitude and phase characteristics of the measuring set up. Due to steep phase characteristic, within the range of resonance frequency F_p negligible changes of the generator's current frequency cause considerable phase errors with relatively insignificant variations of amplitude characteristics. Therefore, the determination of the allowed frequency instability should be based on the allowed phase error.

Estimates show that with the tolerance error in phase of 2° and the general quality coefficient of the selective system $Q = 50-100$, the frequency stability of the oscillator should not be less than 0.05-0.1%. If it is taken into account that phase error is caused not only by the instability of the oscillator frequency but also by the parameter variability of selective systems, phase-shifting and phase-controlling circuits, etc., the requirements imposed on the stability of oscillator frequency should be higher. The optimum frequency stability of the oscillator is the quantity $(1-3)10^{-4}$.

At present the most popular are the electron tube and semiconductor oscillator. The most popular among the wide-range audio-frequency oscillators are those based on pulses and resistance-capacitance coupling. Of the narrow-band oscillators and those on fixed audio-frequencies, those widely known are the RC and LC-oscillators, magnetostrictive, piezoelectric, etc..

The application of wide-band oscillators is inexpedient, since these, besides the frequency instability under the effect of external coefficients (temperature, humidity, potential, tube seasoning, etc.), have initial error of frequency (graduation error). The popular factory-made audio-frequency oscillator GZ-33 has the graduation error $\delta F_{rp} = \pm (0.02F + 1)$. In the beat oscillators, the graduation error is also considerable. If we take into account also the frequency instability, caused by the effect of external and internal coefficients, it becomes clear that oscillators with wide-range even variation are not fit for the devices of aerial electric prospecting.

In oscillators on fixed audio-frequencies, there is no graduation error and, moreover, in this type of oscillators it is possible to attenuate the effect of external and internal coefficients on the frequency stability, which, therefore, comprises 1.10^{-3} (141). In rheostat-volumetric oscillators, the frequency stability depends mostly on the constancy of R and C quantities.

Investigations, which have been conducted (58), make it possible to assume that RC-oscillator with stability upto 0.1-0.2% in temperature range 20-70° can be constructed. However, in this case resistances should be made of manganese wire, and the capacitors should have low temperature coefficient (TKE). The manufacturing of this type of oscillator involves considerable difficulties, as the ~~manganin~~ resistances have parasitic reactance, which causes additional phase shifts, resulting in unstable operation of the RC-oscillator.

The frequency stability of LC-oscillators is determined mainly by the parameter stability of inductance L and capacitance C. For the audio-frequencies, the inductance is achieved by a core with a large coefficient of magnetic permeability μ . With the surrounding temperature varies the coefficient μ and hence the inductance L.

The maximum frequency stability, as shown in (174), depends on the quality coefficient of the circuit, which is determined by the quality coefficient of inductance $Q = \frac{\omega L}{R}$ at the lowest L/C ratio. On audio-frequencies, due to high L and C values, it is rather difficult to implement reciprocal compensation of inductance and

temperature coefficient (TKC) of the capacitance, in the audio-frequency range of LC-oscillators it is difficult to attain frequency stability higher than 1.10^{-3} . The magnetostrictive oscilla-

tors assure high stability of frequency (upto 1.10^{-5}) with temperature-controlled magnetostrictive rods or with those made of two metals of opposite temperature coefficients. Oscillators of this type could be used in aerial electric prospecting.

Very simple in construction are the oscillators with the quartz crystal control of frequency. They assure high stability of frequency ($10^{-5} - 10^{-6}$) even without the temperature control of quartz. The

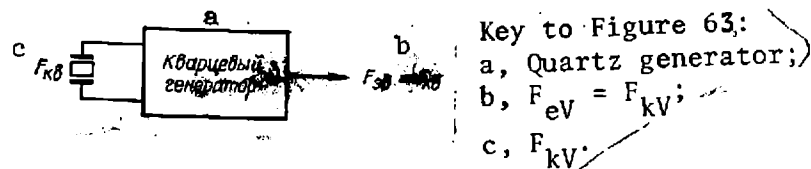


Fig.63.

audio-frequency oscillators, with the quartz crystal control, can be made from diagrams with quartz for operating frequency (Fig.63), with quartz for higher frequency, with subsequent frequency division (Fig.64) and on scheme for pulses (Fig.65).

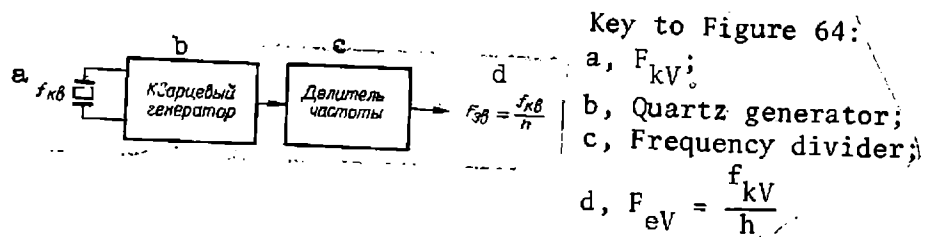


Fig.64.

In the quartz oscillators, for pulses, the use is made of quartz plates on radio-frequency ($f > 100$ kcs). The natural frequencies of oscillators are chosen in such a way that the difference would be equal to the required audio-frequency, t.e.

$$(f_{KB} \pm \Delta f_1) - (f_{KB_2} \pm \Delta f_2) = F_{3B} \pm \Delta f_2 \quad (VI.3)$$

where f_{KB_1} and f_{KB_2} - are the frequencies, respectively, of the first and second quartz oscillators; Δf_1 and Δf_2 - absolute values of frequency instability in both the oscillators; F_{3B} - resultant audio-frequency.

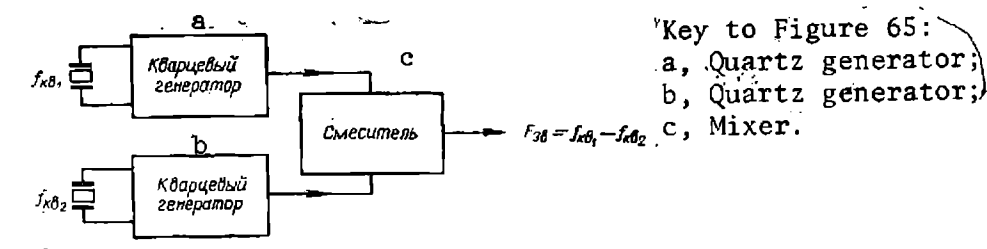


Fig.65

If the quartz plates have frequencies in the order of 100 kilocps, the absolute value of the oscillator frequency instability could be upto 1 cps. Thus, regardless of the resultant audio-frequency, its absolute instability in the oscillators for pulses may attain cps units.

Quartz oscillators of two other types have considerably lower instability. Thus, for the oscillator with quartz set directly for operating frequency (see Fig.63) we have

$$F_{3B} = F_{KB} \pm \Delta F,$$

where

$$\Delta F = F_{KB} (10^{-5} \div 10^{-6}).$$

In the apparatus of aerial electric prospecting, the most frequently applied is the audio-frequency master oscillator with subsequent division of quartz frequency. The frequency instability of oscillator of this type as in the preceding case, is in the order $10^{-5} - 10^{-6}$, since

$$F_{3B} = \frac{f_{KB} + \Delta f}{n},$$

where n - frequency division coefficient.

Besides the high frequency stability, the generating unit should have the non-linear distortion coefficient not over 5-10%, and its output should be consistent with the load resistance of the electromagnetic field exciter.

2. Master Oscillators.

To eliminate, in the receiving unit, noises, equivalent to the frequency of industrial power supply system and its harmonics (50; 100; 150 cps, etc.), at the initial development stage of aerial electric prospecting in USSR the following frequencies were selected for the BDK and induction methods: 81, 38; 244; 28; 976; 56; 1953; 13 and 3906,25 cps. These frequencies were obtained by the division of quartz frequency of 125 kilo cps 768-, 256-, 128-, 64-, 32-, and 16-times. In the first versions of the BDK and induction apparatus, the frequencies applied were 81,38; 244,14; 488,28; 976,56; 3906,25 and 7812,5 cps.

The construction principle of master oscillators becomes clear on examining their circuits in the apparatus of the BDK and induction methods (both were developed by Physico-Mechanical Institute of AN Ukraininan SSR).

Master Oscillator in the Apparatus of BDK Method: The functional circuit of the master oscillator in the AERA-58 set is shown in Fig.66.

The controlling harmonic current with frequency $F_q = 125$ kcps is fed from quartz oscillator 1 to multivibrator (frequency divider) 2. The rectangular impulses of voltage with frequency $f : 16 = 78125$, cps are fed to selective amplifier 3, the output voltage of which is harmonic.

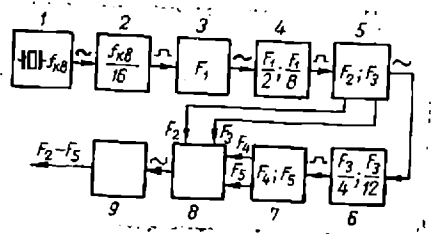


Fig. 66

The second multivibrator 4 is provided with a switch, which permits the time constant of RC-circuits being varied and thereby the oscillation frequency. This multivibrator is synchronised by frequency $F_1 = 7812.5$ cps and allows the obtaining of two frequencies $F_2 = \frac{F_1}{2}$ and $F_3 = \frac{F_1}{8}$, 3906.25 and 976.56 cps respectively. One of the frequencies F_2 or F_3 is fed into the selective amplifier 5, at the output of which the voltages with frequencies 3906.25 and 976.56 cps have harmonic form. The third multivibrator 6, synchronised by frequency F_3 , divides $F_4 = \frac{F_3}{4} \approx 244.14$ cps and $F_5 = \frac{F_3}{12} \approx 81.38$ cps. Beyond this multivibrator the signal centers then selective amplifier 7.

The output part of the oscillator is a phase inverter 8 and two-cycle amplifier of power 9 (A class) with a matched transformer at the output. The master oscillator, assembled according to the analysed block diagram, can assure at the output harmonic current of one of the fixed frequencies: 3906.25; 976.56; 244.14 and 81.38 cps.

In the airborne setup of the BDK method AERA-2 and AERA-3 (1961) and of the induction method AERI-2 (1962), the master oscillators were made with quartz for operating frequency 3900 cps.

Master Oscillator in AERI-2 Apparatus for Induction Method: Fig. 67 shows functional circuit of master oscillator with two-channel output on double frequency.

The alternate current with quartz frequency 3900 cps from quartz oscillator is fed into selective amplifier 2. From the output of the amplifier, the harmonic current with frequency $F_1 \approx 3900$ cps arrives at switches 11 and 15 of the amplifying output channels, hence as synchronizing current - to the first multivibratory frequency divider 3, with index factor $n = 2$. The rectangular current impulses at $F_2 = \frac{F_1}{2} = 1950$ cps enter selective amplifier 4 and hence to switches 11 and 15. In the same way operate dividers 5, 7, 9 and selective amplifiers 6, 8, 10, at the outputs of which harmonic currents with frequencies 975; 487.5 and 243.75 cps respectively are obtained. Thus, all the working frequencies are available at switches 11 and 15 of the amplifying channels.

With two-channel operations on two frequencies the current of the required frequency is fed from switch 11 of channel 1 through switch Bk_1 (position 1) to phase inverter 13, from which the working frequency current enters amplifier 14 of channel 1; through cathode follower 19 the reference potential of the working frequency is selected for the same channel of the measuring group.

From the change-over switch of frequency 15 of channel II the current of the second working frequency arrives at the input of phase inverter 16, hence, to amplifier 17. The reference potential is taken off through cathode follower 18.

With single channel operations on two frequencies, possible only on channel I, two currents of different frequencies from change-over switches 11 and 15 enter mixer 12 through switch Bk_2 (position 2) and hence enter amplifier 14 through switch Bk_1 (position 2) and phase inverter 13. The circuit is energized by its own unstabilized rectifier 20 and stabilized rectifier 21 of alternate current electromechanical

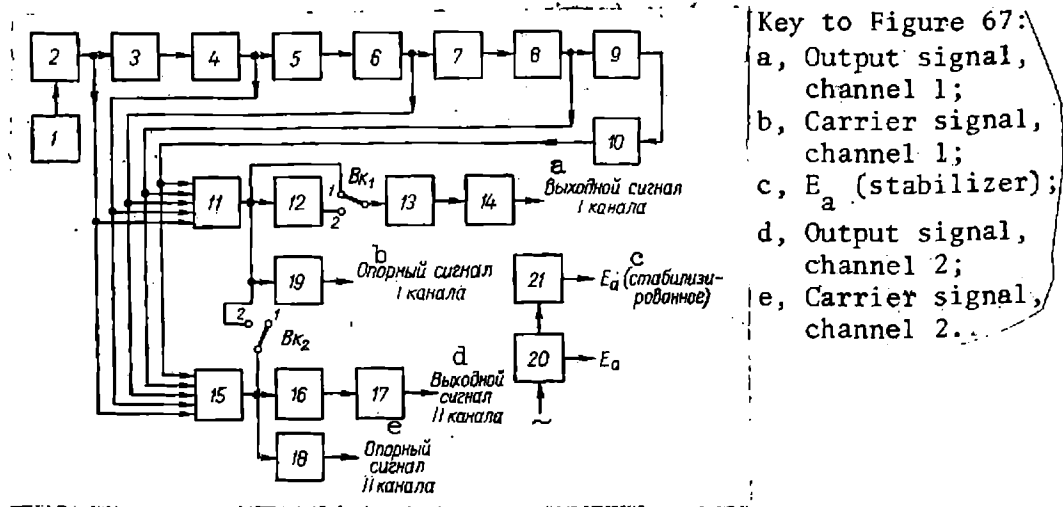


Fig. 67.

transducer (frequency 400 cps, voltage 115 v) of the aircraft power network.

The line diagram of the AERI-2 master oscillator is shown in Fig. 68. The quartz oscillator is assembled on left triode L_1 (6N1P) according to a three-point diagram with capacitive feed back and direct cut-in of quartz resonator with natural frequency $F = 3900$ cps. Used as a resonator is a quartz crystal plate with MT type shear. The feedback capacitances are those of the quartz-holder itself. Resistances R_1 and R_2 are the anode load of the oscillator and also the divider in the feedback circuit, voltage from which is fed to the resonator through capacitance C_1 . Current with frequency $F_1 = 3900$ cps from the quartz oscillator anode is fed through capacitor C_2 and quenching resistance R_4 to the grid of the first selective amplifier, on the right triode L_1 .

The selective amplifier is a current amplifier with transforming output with double T-like RC-filter in the backfeed circuit. Current with frequency $F_1 = 3900$ cps from the anode of right triode L_1 is fed through dividing capacitor C_6 to load resistance R_9 , hence to filter, consisting of two RC T-circuits: R_5, R_6, C_5, R_7 and C_3, R_8, C_4 . From

the output of the filter, the current of the negative feedback is delivered to the grid of the right-hand triode L_1 . By means of resistance R_7 the quasiresonance of the filter is tuned exactly. Resistance R_{10} implements the automatic shifting to the tube grid and additional feedback in the current.

Anode load of the selective amplifier cascade is the primary coil of transformer T_{p4} , from the secondary coil of which harmonic current with frequency $F_1 = 3900$ cps is fed to contact one of changeover switches P_1 and P_2 of the channel frequencies. Moreover, from the anode of right-hand triode L_1 through capacitance C_7 and quenching resistance R_{11} voltage is taken off for the synchronization of the first frequency divider L_2 .

The frequency divider is made up from the diagram of multivibrator. Time constant of the auto-oscillations is determined by the capacity of coupling C_8 and C_9 and resistances of grid leak R_{14} and R_{15} . The tuning of frequency and, thus, selection of the present index factor is implemented by means of variable resistance R_{14} . Index coefficient of the first multivibrator frequency $n = 2$; its output produces current impulses with frequency $F_2 = 1950$ cps. Resistance R_{12} and R_{13} - anode loads of the first multivibrator cascades.

From the anode of right-hand triode L_2 , the rectangular current with frequency F_2 is being fed, through dividing capacitor C_{10} and quenching resistance R_{16} , onto the controlling grid of the second selective amplifier L_3 . The quasi-resonance frequency of the selective amplifier 1950 cps is determinable by quantities R_{18} , R_{21} , C_{11} - C_{13} . The filter frequency is tuned by varying intensity of the variable resistance R_{20} .

From the secondary coil of transformer T_{p5} , harmonic current

with frequency $F_2 = 1950$ cps arrives at channel change over switches P_1 and P_2 . Circuits of the following three frequency dividers, operating on tubes L_4 , L_6 and L_8 , are similar to the circuit of the first multivibrator. The L_4 output produces rectangular impulses of current with frequency $F_3 = 975$ cps; at L_6 output we have $F_4 = 487.5$ cps and at $L_8 = F_5 = 243.75$ cps.

Beyond each frequency divider is cascade of selective amplifier (L_5 , L_7 and L_9). Harmonic currents of all operating frequencies (975; 487.5 and 243.75 cps) are lead-in to the corresponding contacts of channel frequencies change-over switches P_1 and P_2 . The current of one of the five operating frequencies taken-off switch P_1 , is fed to potentiometer R_{103} at the input of the signal mixing cathode follower, assembled on the left-hand triode L_{16} . In operations without mixing, resistance R_{103} gets cut off by switch Bk_3 . Moreover, from the change-over switch P_1 , the current of the operating frequency enters through dividing capacitance C_{52} into the input of cathode follower of channel I bearing pressure (left-hand triode L_{17}).

The current of the second operating frequency, taken off the change-over switch P_2 , is fed through switch Bk_2 to potentiometer R_{94} of the input adjustment of the mixing cathode follower (right-hand triode L_{16}) of the second operating frequency. Through dividing capacitance C_{51} , the current of the second frequency arrives at the cathode follower input of the channel II reference potential (right-hand triode L_{17}). The mixing circuit of frequencies is implemented on two cathode followers of tube L_{16} . The output voltage is taken off from the middle of resistances R_{98} , R_{99} and through dividing capacitor C_{48} fed to potentiometer R_{99} for adjusting amplifier of the mixed frequencies channel.

With two channel operations on two frequencies the switches Bk_2 and Bk_3 are disconnected and the current from change-over switch P_1 arrives through capacitor C_{50} onto the grid of left triode L_{16} . In this case, the grid of the right triode connects through R_{94} with the body. From the load of cathode follower R_{100} , R_{101} through R_{99} current with frequency, corresponding to the operating frequency of channel I, through capacitor C_{48} and adjustment potentiometer of output signal R_{59} is being fed to the grid of the phase-inverter left triod L_{10} .

The second operating frequency is taken off the change-over switch P_2 and through capacitor C_{47} ; resistance R_{93} and potentiometer R_{92} energizes the grid of the phase inverter's left triod L_{15} in the amplifying track of channel II.

With one-channel operations on two frequencies (the use is made only of the channel I amplifying track) the switches Bk_2 and Bk_3 are locked, frequency mixer correction. From resistances R_{98} , R_{99} the mixed currents of two frequencies are taken off and fed into the phase inverter of channel I. The phase inverters and power amplifiers of both the channels are implemented similarly.

Let us analyse the circuit of channel I. The phase inverter is made on autobalance circuit with a common grid on double triode L_{10} . From anode loads of triodes R_{63} and R_{64} currents, shifted in phase at 180° through intermediate capacitances C_{40} and C_{41} , energize the controlling grids of tubes L_{11} and L_{12} two-cycle outgoing power amplifier. The output cascade is executed on the circuit of ultra-linear amplifier with low coefficient of non-linear distortions (139). Both the cascades of the amplifier are covered by negative feedback via voltage. The output transformer Tp_2 has a special coil to obtain

the voltage, of the negative feedback, which energizes the grid of left triode L_{10} ; by means of resistance R_{72} it is possible to select the required intensity of this voltage.

The reference potentials are removed from the cathode resistances R_{105} , R_{106} and R_{108} , R_{109} of double triode L_{17} and enter, through capacitances C_{53} and C_{54} into change-over switch P_3 . By means of this switch, channels I and II of the measuring apparatus could supply the potential of the operating frequency or cut-in to external oscillators.

3. Power Amplifiers:

In the apparatus of aerial electric prospecting any amplifiers can be used as power amplifiers, provided they satisfy the requirements of output power, load resistance, nonlinear distortion coefficient, etc. For instance, in the apparatus of the BDK method it is possible to use amplifier TY-600 with some alterations and additions in the circuit. However, considering the specific operating conditions of the generating unit in aerial prospecting apparatus, power amplifiers should be planned after considering these conditions.

Besides, the general requirements, the power amplifier has to satisfy the following:-

1. Power amplifier for the BDK method should be made of separate blocks convenient for transportation by any means. At the output of the amplifier there should be a transformer, which would provide coordination with load (grounded cable). The operating frequency range of the amplifier should be 200-2000 cps. The voltage and current in the cable should be controlled by special measuring devices. The output of the amplifier must have an

arrangement for the removal of reference potential, which is in phase with the load current. The amplifier is energized from a portable power-plant of three phase alternate current with frequency 50 cps and 220/380v.

2. Power amplifier for induction and VMP method should have a minimum overall size and weight. It is meant for a 6-hour continuous operation. It can be cooled by rushing air current through it. The amplifier should have a system protecting it from vibrations during the flight, landing and takeoff. It should have a two-channel construction. The coordinating transformer should assure coordination of the amplifier with load (oscillating frame) in frequency range 200-4000 cps. Energizing of the amplifier should be from the power supply network of the aircraft through one-phase mechanical converter 115v and frequency 400 cps (for example, MA-2500, etc.).

4. Generating Unit in BDK Method:

The components of the generating unit, meant for aerial electric prospecting by the BDK method includes, besides the master oscillator and power amplifier of audio-frequency: a radio set for transmitting key signal to the measuring device; a device for the control and phase-adjustment of key signal emitted into the air; UKV-radio station for communication with the pilot and operator of measuring instruments; antenna, etc.

Fig.69 shows time-base functional diagram of the generating unit. From the output of master oscillator 1, the current of one of the fixed frequencies (243.75; 487.5; 975 or 1950 cps) is fed to subterminal amplifier 2, from which the sound current of excitation is fed to two-

cycle power amplifier 3. The output device 5 is meant for coordinating the output resistance of amplifier with load (grounded cable 6), current take-off onto measuring block and compensation of reactive component of load by means of capacitances and inductances. Device 4 is meant for automatic cut-off load from power amplifier with the break of connecting line A - B. The capacity of the output amplifier is about 2.5 kilo-watts.

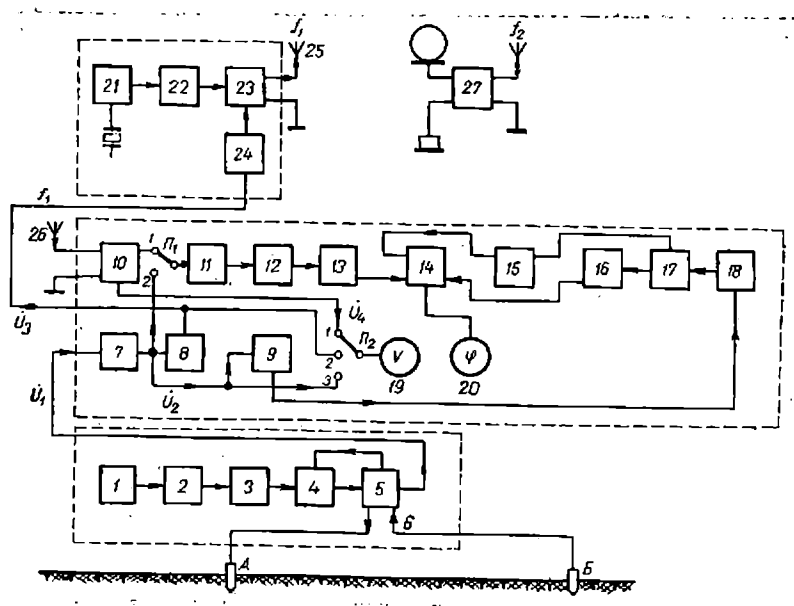


Fig. 69

For phase control of the key signal, emitted into the air, in relation to the current phase in cable, there is a special measuring instrument. Reference potential U_1 in phase with current in the cable is fed from output 5 to cathode follower 7 and hence to phase inverters 8 and 9. For compensation of phase shifts in the measuring circuit itself, the voltage, after the cathode follower, is fed through change over switch P_1 (position 2) to zero-indicator 20 through amplifier 11, limiter 12, cathode follower 13 and differential detector 14. The same detector is fed ^{to} two quadrature currents from cathode followers 15 and 16.

At phase inverter 17 the signal, amplified by amplifier 18, arrives from additional phase inverter 9. This phase inverter compensates phase shifts in the measuring circuit.

Voltmeter 19 controls the current of measuring circuit U_2 , which modulates voltage U_3 and reference potential U_4 , fed from control receiver 10, cut-in to antenna 26. Phase inverter 8 compensates phase shifts of the key signal radio-transmitter. For this, the change-over switch P_1 is fixed in position 1.

The radio-transmitter of the key signal consists of a master, oscillator with quartz crystal control 21, intermediate amplifier - frequency doubler 22, power amplifier 23 and modulator 24. The signals are emitted by antenna 25 with vertical polarization. The carrier frequencies of the signal, emitted into the air f_1 , are 2.3 or 3.2 megacycles per second.

The UKV-radio station operates on four fixed frequencies within the range 100-150 Mcps and is meant for command radio-communication with the plane.

5. Power Amplifier of the Induction Method Apparatus:

The power amplifier of the generating unit in apparatus AERI-2 consists, as does the master oscillator, of two channels - lower (243.75; 487.5, 975 cps) and higher (975; 1950; 3900 cps) frequencies. Each channel has its own amplifier. The load of the final stage in each amplifier is the corresponding section of oscillating frame, tuned to the working frequency of its channel.

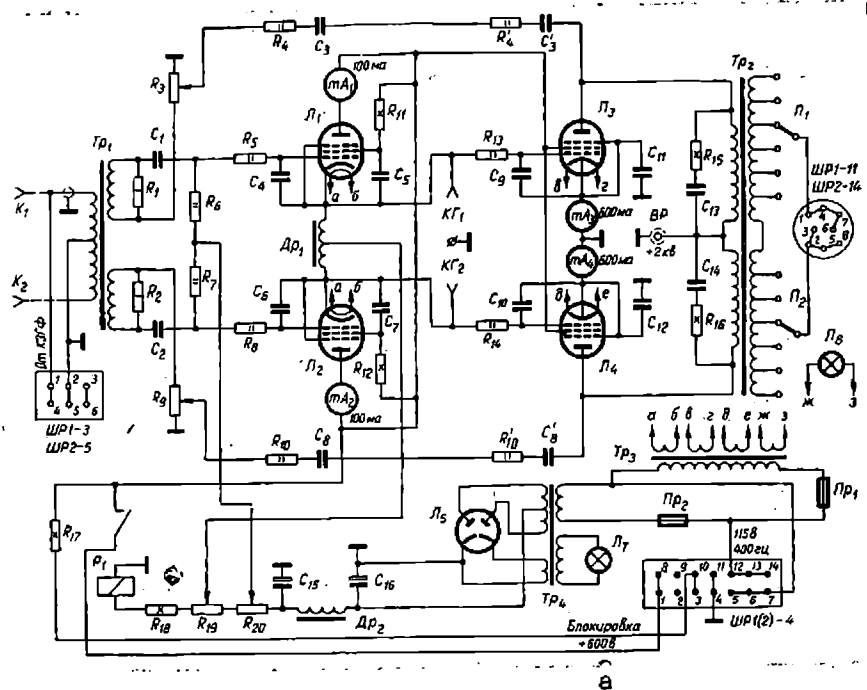


Fig.70

Competent amplifiers assure at the input approximately 100 v-a in the channel of lower frequencies and 600-v-a in the channel of the higher. The line diagrams of amplifiers of both the channels are identical.

Let us examine the diagram of the lower frequencies channel (Fig.70). The primary coil of the input transformer T_{p1} is energized by the excitation voltage from the output of master oscillator channel I (through contacts 1-4 and 2-5 of the plug and jack 1-3). The primary coil of transformer T_{p1} could be cut in to any other external master oscillator through terminals K_1 and K_2 .

From the secondary coils, of the output transformer T_{p1} the signal of the operating frequency (or mixed signals of two frequencies) proceeds in opposite phase to the controlling grids of L_1 and L_2 tubes of subterminal stage, implemented on a two-cycle circuit of cathode

followers with choke load in cathode circuits. Cathode followers assure low output resistance on alternate current and have a deep negative feedback, which is important for reducing the nonlinear coefficient distortion. Millimeters mA_1 and mA_2 control the anode currents of tubes and their symmetry. The screen grids of tubes are energized from a common source through filters R_5C_4 and R_8C_6 to prevent self-excitation of cascade on higher frequencies. Bias voltage on controlling grids of L_1 and L_2 tubes is taken off the potentiometer R_{20} of divider $R_{18} - R_{20}$. Resistance R_1 and R_2 , which shunt the secondary coils of transformer Tp_1 , are meant for rectifying the frequency response of the input transformer.

From the cathodes of L_1 and L_2 tubes, antiphase voltages arrive at the controlling grids of L_3 and L_4 tubes of the terminal stage. This stage operates in conditions B_2 with transformer Tp_2 serving as load. Fixed bias on controlling grids of L_3 and L_4 is put in from potentiometer R_{19} of divider $R_{18} - R_{20}$ on the middle point of choke Dp_1 and hence through antiparasitic filters $R_{13}C_9$ and $R_{14}C_{10}$ onto the tube grids.

On test jacks KG_1 and KG_2 it is possible to measure the amplitude and investigate the voltage shape of the subterminal stage, and also the intensity of bias voltage.

Cut in to cathode circuits of output tubes are the millimeters mA_3 and mA_4 for measuring the total anode and the screened current of tubes. The tubes L_3 and L_4 are energized from the individual coils of incandescent transformer Tp_3 .

To prevent self-excitation of the cascade on higher frequencies, both halves of the primary coil in output transformer Tp_2 are shunted by RC-circuits ($R_{15}C_{13}$ and $R_{16}C_{14}$).

The secondary coil of transformer Tp_2 is charged onto the oscillating frame. Input resistance of the oscillating frame section at various frequencies differs; therefore for load coordination this coil is sectioned. Outlets from sections of the secondary coil are cut in to change-over switches P_1 and P_2 , by means of which it is possible to attain optimum coordination of the power amplifier output stage with the load.

Application is made in the amplifier of successive in-current negative feedback, which encompasses the terminal and subterminal stages. Voltage of the negative feedback is taken off the anodes of the terminal stage tubes and, through dividing capacitances C_3C_3 and C_8C_8 , supplied to dividers $R_3R_4R'_4$ and $R_9R_{10}R'_{10}$ from which it is led into the secondary coils of transformer Tp_1 . The power magnifier is energized from the power-supply network of the plane through mechanical transducer MA-2500 with output voltage 115 v with frequency 400 cps.

The high tension rectifier for energizing anodes of L_3 , L_4 tubes and rectifier for energizing anode-screen circuits L_1 , L_2 , and also of screen-grid circuits L_3 , L_4 , are in a separate block and connect to the power amplifier block by special plug connectors (SHP1-4, BP). Bias rectifier, operating on kenotron L_5 , is mounted in power amplifier block.

For energizing the bias circuit of L_1 , L_2 tubes, the coil of relay P_1 is cut in ^{the} series with divider $R_{18} - R_{20}$. ⁱⁿ With normal operation of bias rectifier contacts 1 and 2 of this relay are closed and voltage + 600v is supplied to anodes and screen grids L_1 , L_2 , L_3 and L_4 . From resistance R_{17} , cut in to circuit 600v, voltage is taken off for circuit blocking of high tension transformers, energizing

anodes of L_3 and L_4 tubes. In the absence of bias voltage and tension +600v the high tension transformers are automatically cut off.

6. Transistor Generating Unit in the apparatus of Induction Method.

The above described generating units on electronic tubes were devised in 1958-61 for science research and production tests to determine the efficiency and potentialities of aerial electric prospecting.

Devices, meant for production work, should be distinguished by high reliability, low cost, overall size and weight. In this respect, preference should be given to transistor systems, which permit the build-up of generating units of high stability and required competence. Minor overall size and weight, low cost of energy make it possible to install this type of apparatus on light type planes (AN-2, etc.) and helicopters (MI-4, etc.). This provides an opportunity to carry out investigations at low altitude and speed of flight.

As an example of transistor oscillating apparatus, let us take the master oscillator^(*) (Fig.71), applicable in various methods of aerial electric prospecting, and power amplifier^(**) at 100 wt (Fig.72).

In the master oscillator, the quartz oscillator operates on transistor T_1 of P15A type on inductive three-point circuit with direct cut-in of the quartz resonator of natural frequency 7812 cps. The quartz plate, with shear NT type, operates in conditions of bending

(*) The system of the generator is devised and implemented in the Physico-Mechanical Institute of AN Ukrainian SSR by A.S. Lutsyshin and L.Y. Misiuk.

(**) Amplifier circuit is devised and implemented in the Physico-Mechanical Institute of AN Ukrainian SSR by E.I. Kurilov jointly with the authors.

oscillations. The load in the collector circuit is the parallel resonance circuit, tuned to quartz frequency and consisting of capacitance C_1 , inductance L_1 and primary coil of impulse transformer 1. From the secondary coil of impulse transformer the synchronization voltage is fed to the blocking-generator of timing impulses. Moreover, the collector of T_1 transistor is loaded through capacitance C_3 onto divider R_4R_5 , from which harmonic current of 7812 cps frequency is supplied through the changeover switch of operating frequencies P_{16} onto emitting repeater T_4 . The divider R_1R_2 assures initial bias voltage on T_1 base. By means of resistance R_3 , blocked by capacitor C_2 , some temperature stabilization is attained for the operation of the transistor.

The changeover of shift registers on ferrite cores required current impulses with amplitude upto 0.5 - 0.7 a. Obtaining of these impulses by amplification is irrational; therefore, in the circuit of the described oscillator the use is made of retarded blocking-generator on transistor T_2 with external start-up. The starting impulses taken off the secondary coil of transformer 1, are conveyed to base T_2 through starting circuit - resistance R_6 , diode D_1 and primary coil of impulse transformer Tp_1 . The source of blocking voltage is the divider R_7R_7' . The resistance R_7 is blocked by capacitances C_4 and C_5 .

The coils of impulse transformer Tp_1 are cut in so that increment of the collector current produces a rise in the trigger voltage on triode T_2 . The secondary coil of transformer Tp_1 , shunted by diode D_2 , is switched into collector circuit T_2 ; in series with it, through trigger bead Kn , is cut in the circuit of timing coils of shift registers and resistance R_8 . From this

resistance, positive voltage pulses are taken off for blocking the transistor key circuit on triode T_3 . The key controls the discharge circuit of the capacitances shift register.

The trigger voltage, taken off divider R_9R_{10} , connected parallel to the energy source, is conveyed through limiting resistance R_{11} to the base of triode T_3 . The blocking impulses from resistance R_8 arrive, through dividing capacitance C_6 , at the middle point of divider R_9R_{10} . The discharge circuit of the memory capacity of the two registers is connected to the circuit of collector T_3 .

To first register, consisting of eight ferrite-diode cells (cores 2-9, diodes $D_{11} - D_{26}$), is meant for the frequency division of timing impulses with division coefficient equal to two, four and eight. The link circuits of registers, with congruence circuit of "I" type, are used at the output as frequency dividers; they are distinguished by the high stability of the coefficient of frequency division within a wide range of frequencies and temperatures. The second register, consisting of three ferrite-diode cells (cores 10-12, diodes $D_{27} - D_{32}$), has the constant division coefficient three. The timing coils of both the shift registers are connected in series and cut in into the collector circuit of the blocking-generator.

The trigger bead K_n is used for changeover of the ends of timing coils in ferrite ring transformers 2 and 10; with the pressing of the bead the direction of the current in coils changes.

The pulses with a preset coefficient of frequency division are taken off various points of the ferrite-diode frequency divider. The beginning of core 2 primary coil connects thru diode D_{11} with collecting contact of P_{1a} plate of changeover switch P_1 operating

frequencies. Contacts 2-5 of this plate are connected with capacitances C_{25} , C_{27} and C_{31} of the first register; contacts 4 and 5 are cut in parallel. Thus, on contact 2 of plate P_{1a} the frequency of the impulse sequence is 3906 cps, on contact 3 - 1953 cps and on contacts 4,5 - 976.4 cps.

Impulses from the output of the first shift register arrive through divider $R_{48}R_{46}$ at the base of transistor T_{13} of the congruence circuit (circuit "I"). The output impulses of the second shift register with frequency sequence 2604 cps, taken off capacitance C_{34} , arrive through divider $R_{44}R_{45}$ at the base of the congruence circuit on second triode T_{12} .

The congruence circuit consists of two triodes - T_{12} and T_{13} , connected in series. The emitter of triode T_{12} is grounded, the collector is connected with emitter of T_{13} , into the collector circuit of which the load resistance R_{47} for both the transistors is cut in. The output impulses of positive polarity are taken off this resistance. Collector T_{12} (emitter T_{13}) connects to contacts 1-4 on plate P_{1v} of the frequency changeover switch; the collecting contact of this plate is grounded. Thus, in positions 1-4 triod T_{12} is shunted, and the congruence circuit becomes a key, operating as a phase inverter; in position 5 of the frequency changeover switch cuts in logical circuit, which assures obtaining, at the output, of impulses with frequency sequence 7812: $(8 \times 3) = 325.5$ cps. From the output of the congruence circuit, the signal arrives at the parallel connected contacts 2-5 of plate P_{16} . From the collector contact of plate P_{16} through capacitor C_7 voltage pulses with frequencies 7812; 3906; 1953; 976.4

and 325.5 cps are fed into the input of emitter follower T_4 . From emitter load R_{14} through dividing capacitor C_8 pulse voltage enters into the input of amplifier-limiter T_5 .

The output of rectangular impulses of negative polarity, taken off collector load R_{16} of amplifier-limiter, are converted by means of differentiating circuit $C_9 R_{17}$ into bipolar acute impulses. The negative impulses are shunted by diode D_4 , and the positive, taken off ^Cpotentiometer R_{17} , are fed to the first trigger through dividing capacitor C_{10} .

The first trigger is made up according to push-pull circuit on transistors T_6 and T_7 with simultaneous triggering to both the bases. Output tensions of rectangular shape are taken off resistances of collector loads R_{19} and R_{24} with a reciprocal shift in phase at 180° . The trigger operates in the method of frequency division with division coefficient $n = 2$, and, in this way, antiphase impulses are obtained at the output with frequencies 3906; 1953; 488.2 and 162.25 cps.

Cut in parallel to loads R_{19} and R_{24} are differentiating circuits $C_{11} R_{18}$ and $C_{16} R_{27}$ from which acute triggering impulses are taken off to the second and third triggers for obtaining quadrature voltage. Impulses of both polarities, taken off the differentiating circuit $C_{16} R_{27}$, are fed to the second trigger (T_8 and T_9) through capacitor C_{17} . Diodes D_7 and D_8 , implementing the functions of transitory capacitances, transmit only positive triggering impulses to bases of triodes T_8 and T_9 . From the collector load R_{28} the take off is of rectangular impulses with a frequency half that of the triggering impulses.

The third trigger operates in the same way, but its triggering impulses are shifted in phase in relation to triggering impulses of the second trigger at 180° . The output of rectangular impulses of the third trigger is shifted in relation to the corresponding output impulses at 90° due to division of frequency by coefficient two. In this way the quadrature of the output tensions is assured. From the output of the second trigger, tensions of working frequencies 1953; 976.5; 244.1 and 81.13 cps are conveyed to emitter follower T_{14} , and from the output of the third trigger - to emitter follower T_{15} . Both the emitter repeaters are assembled in circuit with transformer output. The secondary coils of transformers are grounded at one end, the other ends are cut in to output terminals U_1 and U_2 . The intensity of the output voltage is controlled by voltmeter, executed according to a bridge circuit; its dial scale is graduated in amplitudes of rectangular voltage.

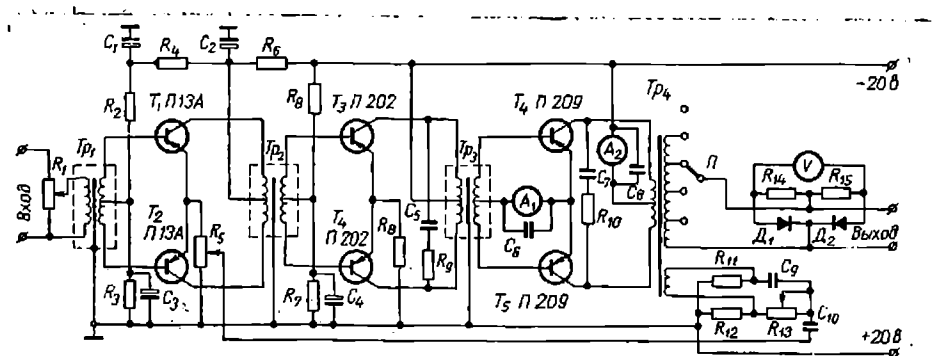


Fig.72

The master oscillator is energized from stabilized transistor rectifier. The alternate current from the secondary coil (3-4) of the power transformer Tp_3 is rectified by a bridge circuit $D_{36} - D_{39}$ and arrives at the input of the stabilizer. The intensity of rectified current composes 24 v. The stabilizer consists of adjustable

triode T_{19} , adjusting triode T_{16} and composite emitter follower T_{17} , T_{18} . The current obtained at the output of the stabilizer is 18 v. By means of tumbler Bk_3 the oscillator's circuit could be cut off from the rectifier; the oscillator could be energized from the external source of direct current (battery of plane energy supply network, etc.).

The transistor power amplifier (Fig.72) is a three-stage transforming two-cycle amplifier, estimated to operate from the power supply network of helicopter of plane, or from an individual battery.

The input signal of any shape, harmonic or rectangular, is initially supplied to the adjustment potentiometer of amplification coefficient R_1 , and then to the primary coil of input transformer Tp_1 . The inverted signal from the secondary coil is fed to bases of the first two-cycle amplifier (T_1 , T_2). To attenuate coupling on the supply circuit, the bias circuit to bases T_1 and T_2 has a filter R_4C_1 , and the collector circuit - filter R_6C_2 . The second amplification stage, made on transistors T_3T_4 of P202 type, assures the obtaining of power, required for the excitation of output power amplifier on triodes T_4, T_5 of P209 type.

The total base and collector currents of the output stage are controlled by ammeters A_1 (dial scale 0-1 a) and A_2 (dial scale 0-20 a). The filters in collector circuits R_9C_5 (subterminal stage) and $R_{10}C_7$ (terminal stage) are meant for protecting the stages from self-excitation on high frequencies.

The secondary coil of output transformer Tp_4 is sectioned and has outlets. By means of changeover switch P, the load is coordinated

with the output stage. Alternate current voltmeter V permits controlling the output voltage of the amplifier. The voltage of negative feedback is taken off from a separate coil of output transformer Tp_4 and, through bridge phase inverter $R_{11}C_9R_{12}$ ^{R_{13}} is fed into emitter circuit of the first stage. The current phase of feedback is varied by alternate resistance R_{13} , and its intensity lead into the first stage - by potentiometer R_5 .

7. Magnetic field Exciter in AERI-2 Apparatus.

In the AERI-2 apparatus, the primary magnetic field on two frequencies is built up by the oscillating frame tuned in resonance to the operating frequencies. The oscillating frame, in its turn, is energized by audio-frequency currents, generated by a two-channel generating unit, which, as has been mentioned, consists of a two-channel master oscillator and two separate power amplifiers.

The oscillating frame, with the elements of its tuning into resonance and dividing filters for simultaneous operation on two different operating frequencies, is one of those main part elements of the apparatus which determine the efficiency of geophysical survey on two frequencies (22). Let us take the elements of the primary magnetic field exciter.

Oscillating Frame: At any combination of operating frequencies the oscillating frame must provide maximum possible magnetic moment $m_f = IwS$, where I - current within the frame, a ; ω - number of turns in the frame; S - frame area, m^2 .

In view of the necessity to ensure normal production and safe flight of the IL-14 plane, the ~~perimeter~~ dimensions and diameter of the oscillating frame band were determined unambiguously. Therefore, with the chosen type of cable and its cross-section the number of turns in the frame will also be definite. Actually, the frame area consists of 88 m^2 ; with the use, for instance, of MCSL or BPVL cable with section 4 mm^2 the frame may consist of 20 turns.

Thus, the obtaining of maximum possible moment of frame at the preset power of the generating unit is practically reduced to assuring maximum possible current in its turns. This could be obtained by tuning the frame into resonance on each operating frequency and optimum congruence between the output of the power amplifier and the frame's input resistance.

For the simultaneous operation of the apparatus on two frequencies, the frame should be energised by two frequency currents. Simultaneous power amplification of two operating frequencies in one power amplifier is not feasible due to low efficiency of such an arrangement and the impossibility of tuning the frame into resonance on both the frequencies simultaneously. Energizing of the frame by two power amplifiers with different operating frequencies, without special dividing filters, is also unacceptable due to the impossibility of tuning the frame into resonance on these frequencies. In this connection, due to insufficient value of the frame's magnetic moment, when the sections of oscillating frame are united into one band, the coupling coefficient between them rises practically to one. Moreover, there is a possibility of overvoltage in the output stages of the power amplifiers, which will affect the reliable operation of the

apparatus. In these conditions, it would be more expedient to apply dividing filters, cut in to the outputs of power amplifiers and tunable to the working frequencies of adjacent channel. There are two possible ways of connecting the oscillating frame with dividing filters to the outputs of power amplifiers. To reduce the power loss, dividing filters should have the least possible number of reactive elements and maximum possible quality.

Fig.73 shows the circuit of oscillating frame with all its turns used for both the power amplifiers; in Fig.74 the oscillating frame is divided into two sections, each of which is cut in to its own amplifiers.

Key to Figure 73
a, Filter f_1 ;
b, Filter f_2 .

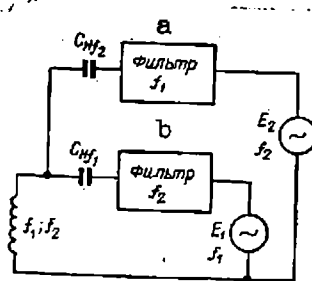


Fig.73

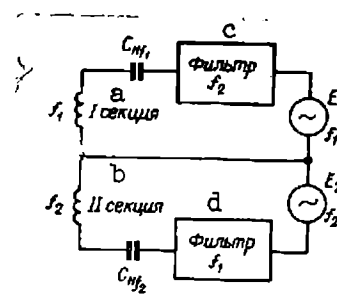


Fig.74

Key to Figure 74:
a, Section I;
b, Section II;
c, Filter f_2 ;
d, Filter f_1 .

In the AERI-2 apparatus, due to purely practical reasons, the application is of the second connecting circuit of the oscillating frame. It is desirable for the apparatus to have on every operating frequency similar equivalent response, determinable (on a given frequency) by the product of the oscillating frame magnetic moment by field detector response. Therefore, when choosing the number of turns in sections, it was taken into account that the lowfrequency channel of the generating unit assures the highest value of magnetic moment, since

the field detectors at these frequencies have the least response.

The following is the optimum number of turns determined by tests:
section I (low frequency channel) -11, section II (high frequency channel)
- 9 turns.

TABLE - 3

Sect.	Frequency cps	Current a	Moment a - t·m ²
I	243	19	18000
	487	16	15000
	974	12	11600
	974	15	11800
II	1949	9	7000
	3898	6	4500

Magnetic moment values obtainable in sections, tuned to resonance, of the oscillating frame at certain competence of output amplifiers and quite safe in respect of the dielectric strength of the cable's insulation currents on its sections (300-350v), are shown in Table-3.

Assuming that the section of the frame is a flat reel of rectangular section, the cross-section dimensions of which are negligible in comparison to the side of its middle turn, inductance of each section could be determined from the following terms (83, 84).

$$L = \frac{\mu_0}{4\pi} \omega^2 (b+c) \left[\ln \frac{2bc}{a+r} - \frac{c}{b+c} \ln (c + \sqrt{b^2 + c^2}) - \frac{b}{b+c} \ln (b + \sqrt{b^2 + c^2}) + \frac{2\sqrt{b^2 + c^2}}{b+c} - \frac{1}{2} + 0.447 \frac{a+r}{b+c} \right], \quad (VI.4)$$

where a and r - cross-section dimensions of the section, $a = r \approx 20$ mm;

b and c - dimensions of the middle turn sides, b = 8 m, c = 11 m;

w - number of turns in the section.

Thus, for the section composed of 11 turns, we get $L_{11} \approx 5.7$ millihenry, and for section composed of 9 turns, $L_9 \approx 3.8$ millihenry.

This estimate holds good for a case, when the frame is removed from the vicinity of considerable metal masses. Inductance of a frame, set up on a plane, is somewhat lower, due to the effect of the plane's metal mass, and is determinable by tests. The dependence of natural inductance on frequency in this case is hardly perceptible, as the difference in the ratio of high and low frequencies is insignificant.

Length of frame section's wire

$$l_{11} = (2a + 2b) w_1 \approx 420 \text{ M}; \quad l_9 = (2a + 2b) w_2 \approx 345 \text{ M}.$$

Ohmic resistances of each section will be respectively

$$r_{ak_{11}} = \frac{l_{11}}{s \gamma} \approx 1.85 \text{ OM}; \quad r_{ak_9} = \frac{l_9}{s \gamma} \approx 1.51 \text{ OM}.$$

where s - wire section, mm²; γ - sp. conductance of the wire's material, mho.

The total active resistance of each section of the frame is composed of ohmic resistance of copper and the resistance of the metal mass of plane (the latter depends on frequency):

$$r_{tot_{11}} = r_{ac_{11}} + r_{in_{11}}; \quad r_{tot_9} = r_{ac_9} + r_{in_9}$$

Parameters characterising the oscillating frame, set up on the plane, are obtained experimentally (Table 4).

TABLE -4

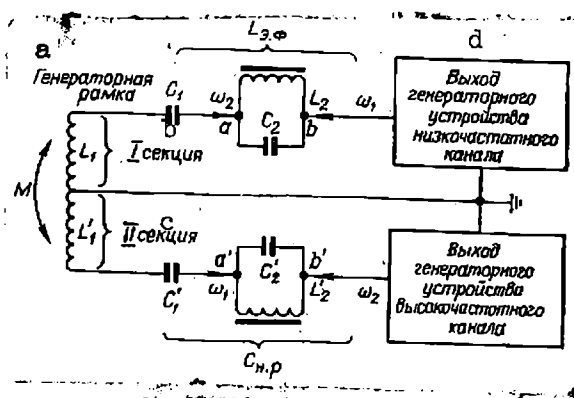
Section	Frequency * cps	r_{ac} ohm	* r_{in} ohm	r_{tot} ohm	L_1 m-h
I	243	1.8	1.3	3.1	4.85
	487	1.8	1.8	3.6	4.85
	974	1.8	3.0	4.8	4.80
II	974	1.4	2.4	3.8	3.15
	1949	1.4	5.7	7.1	3.10
	3898	1.4	33	34	3.05

Dividing filters and elements of the Oscillating Frame
Tuning into Resonance:

The dividing filter of one channel in the generating unit is a parallel LC-resonance circuit (filter-plug), tuned to the operating frequency of the adjacent channel and cut in series into the circuit between the output of the terminal amplifier and the section of the oscillating frame. A filter of this type has a considerable resistance for a resonance frequency of the adjacent channel and fairly low for a working frequency of the same channel, differing from the frequency of the adjacent channel not less than twice.

Key to Figure 75:

- a, Generator antenna;
- b, Section I;
- c, Section II;



- d, Output of generator device in low-frequency channel;
- e, Output of generator device in high-frequency channel.

Fig.75

Fig.75 shows a simplified diagram of the connection of oscillating frame sections to filters of the two-channel generating unit. In low frequency channel, the filter should provide a relatively high resistance between points a and b for the operating frequency of HF channel. The choice of optimum filter parameters was based on certain relationships in the parallel circuit (56, 83).

The equivalent resonance resistance of the filter could be shown by the following parameters of the circuit.

$$Z_{e.r} = Q\rho. \quad (VI.5)$$

Here $Q = \frac{\rho}{r}$ quality coefficient of the circuit, where r and ρ - active and characteristic resistances of circuit respectively, $\rho = \sqrt{\frac{L}{C}}$.

The best filtering property has a circuit with maximum possible Q-coefficient and characteristic resistivity.

For the operating frequency of its own channel, the equivalent resistivity of HF filter is inductive. In order to reduce active losses in copper, the equivalent inductivity of filter^(*) should be considerably lower than the self-inductance of the LF section of the oscillating frame, i.e. $L_{e.f.} \ll L_1$.

Ignoring the active losses in filter, we determine from known relations in parallel and series circuits the equivalent resistance of the filter, tuned to frequency of HF channel, for operating frequency of LF channel with an estimate, that $L_2 C_2 = \frac{1}{\omega^2}$:

(*) Equivalent inductance of filter is the inductance, which it has are resonance circuit for untuned frequency.

$$Z_{\phi} = j \frac{\omega_1 L_2}{1 - \frac{1}{\omega_2^2}} \quad (\text{VI.6})$$

The equivalent resistance of the separating filter, cut in into LF channel, has for frequency ω_1 inductive nature, i.e. $Z_{e.f.} \approx X_{L_{e.f.}}$.

Therefore, it is possible to assure that

$$j \frac{\omega_1 L_2}{1 - \frac{1}{\omega_2^2}} \approx j \omega_1 L_{\phi}$$

Then

$$L_{\phi} = \frac{L_2}{1 - \frac{1}{\omega_2^2}} \quad (\text{VI.7})$$

$$C_2 = \frac{1}{\omega_2^2 L_{\phi} \left(1 - \frac{\omega_1^2}{\omega_2^2} \right)} \quad (\text{VI.8})$$

(since $C_2 = \frac{1}{\omega_2^2 L_2}$);

$$C_1 = \frac{1}{\omega_1^2 (L_1 + L_{\phi})} \quad (\text{VI.9})$$

In HF channel resistivity of filter, tuned to frequency of LF channel, has the nature of capacitance for the operating frequency.

By similar reasoning and taking into account that for filter of HF channel, tuned to frequency of LF channel, $Z_{e.f.} \approx X_{C_{e.f.}}$, we find that

$$C_{\text{э. } \phi} = \frac{\omega_2^2 - \omega_1^2}{L_2' \omega_2^2 \omega_1^2} ; \quad (\text{VI.10})$$

$$C_2' = \frac{1}{\omega_1^2 L_2} ; \quad C_{\text{н.р.}} = \frac{1}{\omega_2^2 L_1} \quad (\text{VI.11})$$

when

$$C_{\text{н.р.}} = \frac{C_1 C_{\text{э. } \phi}}{C_1 + C_{\text{э. } \phi}} .$$

In the determination of the required capacitance of capacitor $C_{\text{тун}}$ there may be three cases: $C_{\text{е.ф}} < C_1$; $C_{\text{е.ф}} = C_1$; $C_{\text{е.ф}} > C_1$. When $C_{\text{е.ф}} < C_1$ and $C_{\text{е.ф}} = C_1$, it is impossible to assure the required capacitance of the condenser for tuning of HF section of the oscillating frame (one of the capacitance of condensers connected in series is less than that required for tuning of the frame's section). The condition is more acceptable, when $C_{\text{е.ф}} \gg C_1$. In this case the capacitance C_1 is close to $C_{\text{тун}}$ and will have a sufficiently high resistance for the frequency of the adjacent channel. At $C_{\text{тун.}} = C_{\text{е.ф}}$ the imposed conditions are not satisfied, since here the required inductance of choke is quite high and its active resistance may also be high.

Experiments on the determination of optimum values of choke inductance in filters L_2 and L_2 with the object of obtaining maximum possible Q-coefficients of filters on the preset operating frequencies with calculated currents in oscillating frame sections have shown that the most suitable chokes are those with inductance $L_2 \approx 1.1$ and $L_2 \approx 6.0$ millihenry. It is assumed that the inductance value of filter choke remains invariable on all the operating frequencies of the given channel, and the tuning of filter is implemented by connecting the

condenser of the required capacitance.

Due to specificity of the output arrangement in the AMRI-2 devices (considerable currents in sections of the oscillating frame, comparatively low operating frequencies, etc.) it was impossible to assure high Q-coefficient of filters in actual working conditions. The Q-coefficient of filters for high frequencies is not over 8-10, for low: 5-6. The active resistance of filters on resonance-frequency is slightly more than the active resistance of the whole track circuit.

Table - 5.

Parameter	Combination of frequencies, cps.					
	243-974	243-1949	243-3898	487-1949	487-3898	974-3898
L	1.17	1.12	1.1	1.17	1.12	1.17
	6.77	13.5	27.0	13.5	27.0	27.0
$C_1, \text{ M. F}$	62.5	62.5	62.5	15.5	15.5	3.9
$C_2, \text{ MF}$	24.3	6.06	1.52	6.06	1.52	1.52

Table 5 gives the results of calculations on deduced formulas of the main parameters of filter, capacitance of condensers for the tuning of filter and LF section of the frame.

According to the data of this table, it follows that the implementation of condition $L_{e.f} \ll L_1$ ($L_1 = 4.86$ millihenries) is practically impossible, specially on frequency 243 cps.

If it is assumed that on high resonance frequency (3898 cps) the Q-coefficient of filter = 10, its equivalent resonance resistance will

be 270 ohm and on frequency 974 cps ($Q \approx 8$) - 54 ohm. These values exceed several times the total resistances of the HF section of the oscillating frame (see Table 4), therefore the filter's action in the LF section of the oscillating frame may be taken as sufficiently effective.

TABLE - 6

Parameters	Combination of frequencies, cps.					
	974-243	1949-243	3898-243	1949-487	3898-487	3898-974
M_f						
$C_{e.f.}$	67	70.3	71.4	16.6	17.53	4.16
$C_2^{M_f}$	71	71	71	17.8	17.8	4.46
ρ , ohm	9.2	9.2	9.2	18.4	18.4	36.6
$C_1^{M_f}$	7.83	1.8	0.45	1.9	0.45	0.4
$C_{tun.}^{M_f}$	7.0	1.75	0.44	1.75	0.44	0.44

Table 6 gives the results of calculation of the main parameters of filter, capacitance value of capacitors for the tuning of filter and HF section of the oscillating frame into resonance.

According to the data of this table, the condition of tuning HF section of oscillating frame $C_{e.f.} \gg C_1$ is generally maintained.

The equivalent resonance resistance due to low Q -coefficient of filter in this channel is considerably lower than in LF channel (for frequency 243 cps at $Q=4$ it is 37 ohm, and the total resistance of LF section on this frequency - 3.1 ohm) and the efficiency of filter is slightly lower.

Due to the fact that the metal mass of plane changes the inductance of the oscillating frame sections, filter parameters and tuning capacitances of these sections may vary from the calculated ones in actual conditions, i.e., on the plane. Experience has shown that, in relation to operating frequencies, these variations comprise 10-15%, therefore, the final tuning of filters and matching of capacitances for the resonance tuning of the frame sections should be carried out directly on the plane during a flight with an operating generating unit.

Sections of the oscillating frame with separating filters have various input resistances in relation to operating frequencies. Coordination of outputs in terminal amplifiers with variable load is effected in these amplifiers by means of output transformers with sectional secondary coils. Depending on total resistances in sections of the oscillating frame, the sectional transformer should assure the possibility of varying output resistance from 5 to 60 ohm (within 5-10 ohm every 1 ohm, within 10-60 ohm - every 10 ohm).

The intensity of currents within the frame sections, during operation of the generating unit, are controlled by means of selective circuit, which eliminates the effect of the current of adjacent channel on the reading of measuring instruments in the operating channel, and also protects these instruments from outside noise and sighting.

The source of voltage for the current measuring set is the voltage drop on resistance, connected in series into the general circuit of the oscillating frame. The choice of the value of this resistance is determinable by minimum power loss on it, and with low currents - such drop in voltage intensity, which is several times the level of noises and sightings, affect the oscillating frame.

In the AERI-2 apparatus, it is assumed that resistance is 0.05 ohm. The nominal competence of resistance, determinable by the maximum current in the L^F section, should be not less than 20 watts. Comparing power, dispersable by this resistance and the output power of amplifier on low-frequency, it is possible to conclude that the loss on resistance is about 2% (this holds good for all the other operating frequencies also). From this resistance, currents of two operating frequencies are fed to the input of the selective circuit, where filtering and distribution of operating signals of frequencies on measuring channels and bringing up of their level to values adequate for normal operation of direct reading devices (current measuring set) are affected. Besides, compensation voltage, required for the set of measuring apparatus, is taken off the resistance. This voltage reflects the current phase in the oscillating frame.

Fig.76 shows line diagram of the coordinating block in the generating set of the AERI-2, containing control nodes of current in sections of the oscillating frame, separating filters and elements of tuning frame sections into resonance.

From resistance R_1 , cut in to the middle wire of the oscillating frame, voltages, proportional to currents in the sections, are fed to inputs of channels I and II of selective amplifiers, implemented on circuit of cathode follower (the right hand half of tube L_3 for channel I, left half of tube L_4 - for channel II). The connection between the input stage and the stage of amplification is through general cathode resistance R_{14} (R_{20}). The selective properties of amplifiers are assured by the cut in into circuit of the negative feedback of double

T-shaped RC-filters for each operating frequency of the channels (25, 229). Stage amplification on operating frequency is 20. Band width is controlled by variable resistance $R_{10}(R_{25})$. RC-filters for operating frequencies are cut in by means of relay P_1-P_3 (LF channel) or $P_4 - P_6$ (HF channel).

To eliminate shunting of RC-filters by load, outputs of selective amplifiers of channels I and II are cut in to the current measuring set through cathode followers L_5 . The current measuring set is assembled on bridge circuit on diodes D2B. Applied as current indicators are magnet-electric devices M-24 with dial scales 15 and 25 a.

The selective amplifiers are energized from the full-wave rectifier ($Tp_1, Dp_3, C_{29}, C_{30}$). It is also possible to take off compensation voltage for the measuring set from the outputs of selective amplifiers. Potentiometers R_5 and R_6 control the intensity of this voltage. By means of switch Bk_6 , compensation voltage for the measuring set could be taken either from resistance R_{17} (signals of two operating frequencies), or from the outputs of selective amplifiers (signals directly of each of the working frequencies). By means of switch Bk_5 , compensation voltage of the operating frequency could be fed into any channel of the measuring set.

Fig.76 shows elements of the separating filters in sections of the oscillating frame (choke Dp_1 , capacitors $C_1 - C_2$ of channel I; choke Dp_2 , capacitors $C_{21} - C_{23}$ of channel II), commutators P_{1v} and P_{2v} , and also capacitors of the frame section tuning into resonance ($C_5 - C_7$ of channel I and $C_{24} - C_{26}$ of channel II) with commutators F_{1b} and P_{2b} . Voltmeter V for 500v controls the voltage in sections of the oscillating frame.

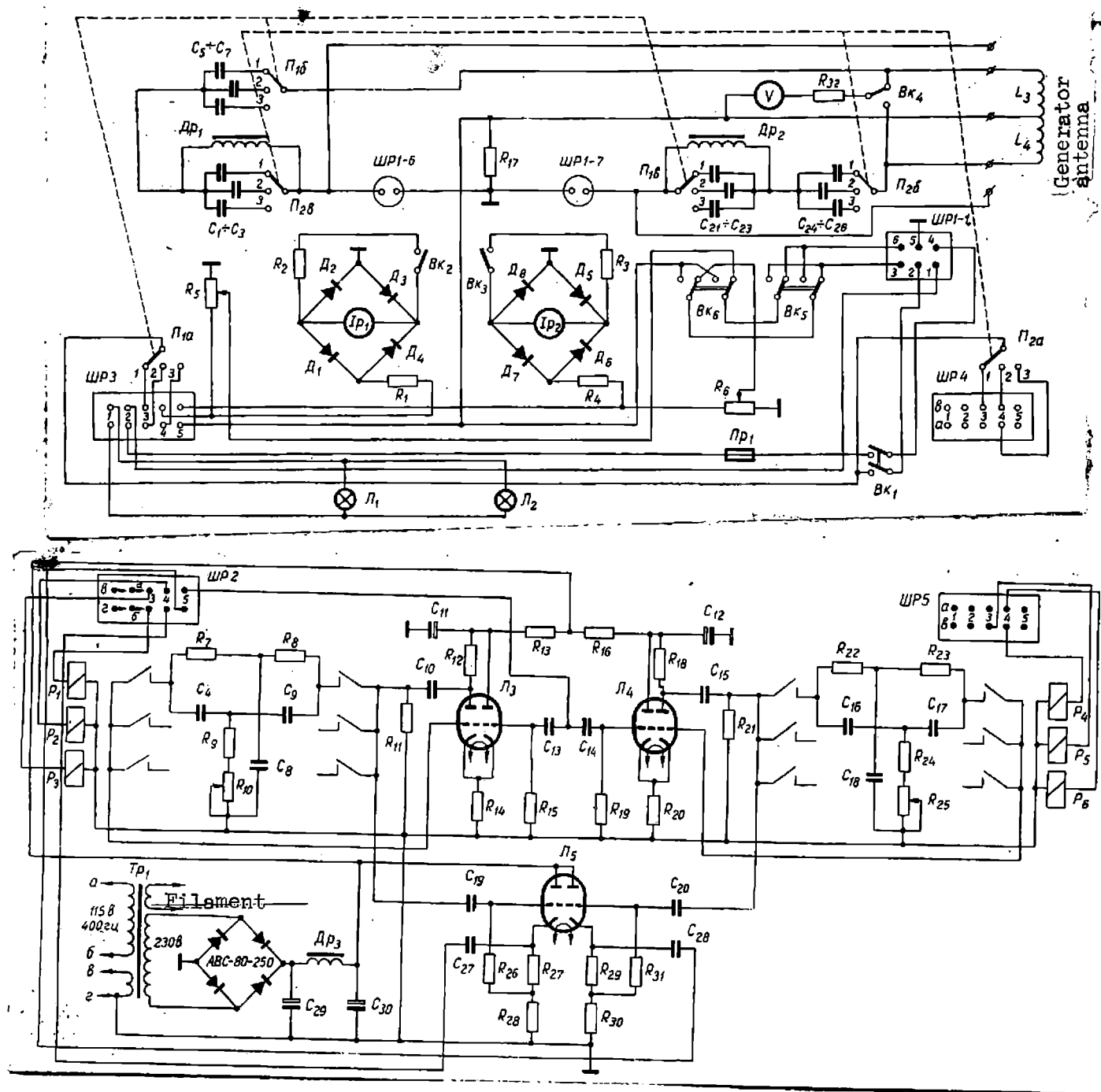


Fig. 76

CHAPTER - VII

CONSTRUCTION PRINCIPLES OF MAGNETIC FIELD
DETECTORS.

1. Brief Information Regarding Demands made on Magnetic
Field Detectors.

As the magnetic field detectors in aerial electric prospecting, the application of multiturn inductance coils (frames), operating on the principle of electromagnetic induction (103, 154) is widespread. The output e.m.f. of detectors of this type is determined by the variation velocity of magnetic field H , i.e., it is proportional to the field's frequency.

With reduced frequency, the sensitivity of the magnetic field detector decreases. To increase the sensitivity, it is necessary to increase dimensions and the number of turns in the inductance coil. However, in the apparatus of aerial electric prospecting the overall size and weight of the field detectors is restricted, which hampers measuring of the fields on low frequencies. In such frequency bands the magnetic modulation transducers (16) are more applicable.

To obtain the preset response, specially on low frequencies, the inductance coil of field detectors in airborne electric prospecting apparatus are made with ferrite cores, and tuned into the operating frequency (123, 125).

To overall size of the field detectors is restricted, primarily by the dimension of the outboard gondola, in which they are set up, and also by the dimensions of vibroprotective system. If the field detector is placed on the external part of air-craft, for instance, on the tail beam of a helicopter, the restrictions are even more rigid, since in this the weight of the field detector plays a big part (when detectors are placed in the middle part of the tail beam, its weight should not be over 15 kg (89). With simultaneous survey on two frequencies, the necessity of spreading out the two detectors arises so as to exclude their reciprocal effect.

At the same time, the amplitude and phase-frequency characteristics of field coefficients, measured in a wide range of external conditions, should vary insignificantly. Thus, phase errors with changes in the temperature of the surrounding medium by 10 degr. (within temperature range - 20 - + 40°C) should not exceed 1 degr. (electrical) for most methods, and the amplitude error (%) for the same temperature range should not exceed the given error in the measuring range of the amplitude or component register.

It should be mentioned that the external operating conditions of magnetic field detectors are also unfavorable and differ appreciably from the operating conditions of other units of the apparatus, placed invariably within the cabin of the aircraft. Usually the field detectors are either in the outboard gondola, or on the external parts of the aircraft, i.e., where the air humidity is upto 98%, and with the landing and take-off the gondola is subject to considerable vibrations, shock loads, etc.

Besides, the requirements of the overall size of magnetic field detectors, there are also demands for their shielding. In the field detector the e.m.f. could be induced by the magnetic as well as electric field. Since in aerial electric prospecting the field detector is meant for transforming into e.m.f. the tensions of the magnetic field, only it must be protected, specially in the case of a highly sensitive apparatus, from the effect of interferences in the electric field by means of electrostatic shield. The latter is so made that the eddy currents emerging in it, under the effect of the measurable magnetic field, would be minimum. Therefore, the shield should be made of open narrow metallic strips or wire (either copper or aluminium).

With the presence, on the clamps of the frame, of unbalanced tensions of insignificant level, special significance is acquired by the method of connecting the electrostatic shield with the rest of the shielding system, presence of uncovered, i.e. unshielded, sections in the input circuit, asymmetry of input circuit, etc. Each factor individually may not have an appreciable significance, but, taken as a whole, they may build up capacitive tracks for the penetration of noise and operating signal, which is undesirable due to increasing error in measuring, specially on the most sensitive limit of measuring. Also essential is the balancing of the input circuit. In this case, as we know, the electrical fields build up on the input terminals of the preliminary symmetric amplifier, cophasal potential, which are subtracted in its input stages.

Thus, the general system of shielding should be such that the currents in the screen, built up by the electric fields, will not affect, while flowing along it, circuit sections of the measuring unit, and specially the input currents of the measuring amplifier, or such as would provide

electric balancing.

It is this combination of factors that determines the unique approach to the planning of magnetic field detectors in conditions of aerial electric prospecting.

2. Electric Parameters of Magnetic Field Induction Detectors.

For the multiturn inductance coil, the input intensity is the current of vector $\vec{\Phi}$ electromagnetic induction \vec{B} , passing thru its turns w (Fig.77):

$$E = -w \frac{d\Phi}{dt} \quad (\text{VII-1}).$$

where E - electromotive force.

It is denoted in Fig.77: d - core diameter; l - core length; D_{cp} - diameter of the middle turn of coil; l_w - width of winding; m - thickness of winding.

Usually the coils are wound on the core symmetrically. Assuming that the axis of the core coincides with the direction of vector \vec{B} and taking into account that

$$\vec{\Phi} = BS = \mu_c S_e H,$$

from the term (VII-1) we get

$$E_m = j\omega \mu_c w S_e H_m e^{-j\omega t}. \quad (\text{VII-2})$$

where μ_c - magnetic permeability of the body of cores; S_e - equivalent area of the coil's cross-section; ω - circular frequency; H_m - tension amplitude of magnetic field.

Thus the amplitude of e.m.f., excited in the multiturn inductance coil by harmonic magnetic field, will be

$$E_m = \omega \mu_c w S_e H_m \quad (\text{VII-3}).$$

Constant $C_p = \mu_c \omega S_e$ determines the main constructive and electrical parameters of this field detector. However, to use directly (VII.3) is practically impossible, since the parameters of coil and core are shown in it in concealed form. In this connection, when constructing magnetic field detectors, the electrical and constructive parameters of inductance coils should be determined by calculations in accordance with the recommendations for planning coils with core (154, 155, 288,), taking into account the above requirements.

The permeability of core μ_c depends on the properties of material and the ratio of core's length to the area of its cross-section. The constant of magnetic field detector C_p is affected by μ_c . In the multilayer inductance coils, it depends to a considerable extent on the area ratio of coil and core. For magnetic field detectors with OD of the inductance coil similar to the diameter of core, it may be assumed that the magnetic flux, which pierces them, is equal to the flux in the core, due to which the section area of the coil should be approximately equal to the section area of the core (154, 155). But if the diameter of the coil is more than many times that of the core, it is necessary while calculating to take into account the magnetic flux adjacent to the core. For multilayer inductance coils, placed in the center of the core, variation of the active area of the coil is estimated by factor K_{cp} .

On the output side, the inductance coil is the source of e.m.f., the load of which in aerial electric prospecting is usually the input resistance of the preliminary amplifier. In coordinating the e.m.f. source with the load, it is necessary to know its inner resistance. Therefore, in determining the sensitivity of the magnetic field detector,

estimation should be made first of inductance L_k , active resistance r and fundamental capacitance C_0 of the inductance coil with core.

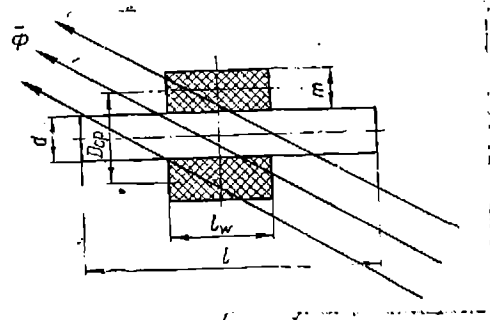


Fig.77

The inductance of multiturn inductance coil with core is proportional to the square of the number of turns:

$$L_k = K_L w^2. \quad (\text{VII-4}).$$

where K_L - factor related to geometrical dimensions of the coil, type of winding, parameters of core and coil position on the core.

The inductance of field detector of this type could also be determined from the inductance of coil without the core L_0 and the effective permeability of the coil's core μ_k . In this case the inductance L_0 is calculated formula (228).

$$L_0 = w^2 d_k \Phi \cdot 10^{-9}, \quad \text{H} \quad (\text{VII.5})$$

where d_k - diameter of coil, cm; Φ - constant, the value of which depends on the ratio of the coil's diameter to its length.

Therefore,

$$L_k = w^2 d_k \Phi / \mu_k \cdot 10^{-9}, \quad \text{H}. \quad (\text{VII-6}).$$

Inductance L_0 of the multi layer coil is shown, in its turn, with high accuracy in terms of relationship (84):

$$L_0 = F \omega^2 \quad (\text{VII.7})$$

where the coefficient F is determined from the ratio (39)

$$F = d^2 \frac{1}{l_w^2} \cdot \frac{1}{m^2} K_{xy},$$

in which m - thickness of coil;

$$K_{xy} = \frac{\pi^2(1+y)^2 x^2 y^2}{x + 1.45y + 0.45 + \frac{2}{3} \cdot \frac{1 + \frac{x}{1+y}}{2 + \frac{x}{1+y}} \cdot \frac{xy}{1+y}}$$

In this case

$$x = \frac{l_w}{d}; \quad y = \frac{m}{d}.$$

More approximate formulas for calculating L_0 are given in the literature (49, 116, 154, 182, 194).

The active resistance of coil with core includes the sum of resistances:

$$r = r_M = r_D + r_c. \quad (\text{VII.8})$$

where r_M - resistance of the coil's copper; r_D - resistance equivalent to dielectric loss in the coil; r_c - resistance equivalent to magnetic loss in the core.

The resistance of copper is determined in this way:

$$r_M = 4\rho w \frac{D_{cp}}{d_M^2} \quad (\text{VII.9})$$

where ρ - resistivity, ohm.m; d_M - diameter of wire, m; D_{cp} - average diameter of coil, m.

The quantity r_D is calculated on the basis of the following condition. Dielectric losses have effect equivalent to the addition in series with coil inductance of some resistance, determinable by the following formula (194):

$$r_D = \tau_c \omega^3 L^2 C, \text{ OM.} \quad (\text{VII.10})$$

Here ω - angular frequency, sec^{-1} ; L - true inductance of coil, H; C - distributed capacitance, Φ ; $\tau_c = \text{tg} \delta$, where δ - angle of loss.

Thus, loss resistance r_D depends on the construction of coil, signal frequency and the quality of insulation material. In calculations of resistance r introduction is frequently made of the correction coefficient K_D . For a multilayer coil without core, it is possible to apply with frequencies

of aerial electric prospecting $r_D \approx (1.2 \div 1.3) r_M$.

Magnetic losses r_c of inductance coil with ferrite core could be estimated in relation to frequency according to the recommendations and methods given in work (228). However, an estimate of this type is considerably complicated and, in practice, usually the test data are used. Therefore, the quantity r is also most frequently determined by experiments. For instance, active resistance r could be determined experimentally from the reading of tube voltmeter with high input resistance, considerably exceeding the equivalent resistance of the circuit, which, in its turn, is primarily tuned to operating frequency ω_0 of apparatus.

By measuring in band $2\Delta f$ (at level 0.707) the signal value in the circuit, the Q-coefficient of the circuit is determined from formula

$$Q = \frac{f_0}{2 \Delta f} \quad (\text{VII.11})$$

With the known inductance of coil L_k (or resonance capacity C_0), calculations of the active resistance of the coil are made:

$$r = r_M + r_D + r_c = \frac{1}{2\pi Q f_0 C_0} = \frac{2\pi f_0 L_k}{Q} \quad (\text{VII.12})$$

In the estimation of the magnetic field detector, made in the form of a multiturn coil with core, it is important to know the capacity of the winding distributed between turns, as otherwise it is impossible to resolve the question regarding the frequency range of the detector and to determine at what conditions it operates at the input of the measuring devices.

The capacity of the winding distributed between the turns of the winding is usually replaced by the equivalent concentrated capacity C_k , connected parallel to the coil. This capacity is often called

capacitance of the coil. It should always be less than the resonance capacitance on high operating frequency of the field detector. In this case, the tuning of the detector is assured to the given operating frequencies by the commutation of external additional capacitances.

The intensity of the capacitance C_k depends mainly on the length of the winding, the pitch ratio of the winding to the diameter of the wire, the composition of boucherizing, the diameter of the coil and the material of its frame.

In many layered coils, the distributed capacity, which is built up mainly due to capacitances between the layers of the winding, could be determined approximately by the following technique. If the coil is so wound in the usual way, i.e., that the voltage at one edge of the adjacent layers is equal to the doubled voltage of one layer, and the potential between the same layers on the other end of the coil is zero, the equivalent distributed capacitance could be taken as connected parallel to leads of the winding. Its value would be determined from the ratio (194).

$$C_{k.p} = \frac{0.118Pl\epsilon}{dT}, \quad n\phi \quad (\text{VII.13})$$

where P - circumference length of the middle turn, cm; l - axial length of the coil, cm; d - distance between the copper of adjacent layers, cm; T - number of layers; ϵ - mean dielectric constant of insulation between layers.

The distributed capacitance of the coil decreases with division of the winding into two and more sections. Each section should have as many layers as the whole coil, but the number of turns in the section layer should be less. In this case, the capacitance of each section is

determined from the indicated formula, and the capacitances of different sections are taken as connected in series. In the sum total, the general distributed capacitance of the coil is considerably lower than the capacitances of individual sections. For instance, with two sections, the aggregate distributed capacitance of the coil decreases four times. However, in this case, the capacitance of the winding increases to infinite value, which to a certain extent detracts from the coil's quality.

The composite relationship of the coil's natural capacitance C_k , specially of the multilayer one, does not always permit the determining of its value unambiguously. Therefore, in the construction of magnetic field detectors, the quantity C_k in the majority of cases has to be determined experimentally. As the experiments show, for multi-layer coils with a great number of turns-with close winding, this capacitance varies from a few tens to hundreds of micro-microfarads. If the core's material has low conductance, say, for instance, like ferrite, the natural capacitance of the coil is practically independent of the presence of the core (155).

The calculation of capacitance C_k on the basis of experimental data is derived from Tompson's formula (194):

$$\frac{1}{f^2} = 4 \pi^2 L_k (C_{BH} - C_k). \quad (VII.14)$$

where C_{BH} - external supplementary capacitance.

The resonance frequencies of the coil are determined in practice with several values of external supplementary capacitances C_{BH} . Measurements of this kind are usually carried out within the field of Helmholtz rings on frequencies somewhat lower than the natural resonance frequency of the

coil. If it is assumed that two measurements were carried out on two frequencies - f_1 and f_2 , when $f_2 = 2f_1$, the natural capacity C_k could also be determined from the following formula:

$$C_k = \frac{C'_{BH} - 4C''_{BH}}{3} \quad (\text{VII.15})$$

where C'_{BH} - external supplementary capacitance at f_1 ; C''_{BH} - external supplementary capacitance at f_2 .

3. Inductance of Multiturn Coil with Core;

The inductance of a coil with the core, as pointed out, could be found from the virtual magnetic permeability of coil with core (having previously determined from formula (VII.5) or in any other way the inductance of the same coil without the core L_0):

$$L_k = \frac{\mu_k}{\mu_0} L_0 \quad (\text{VII.16})$$

where μ_0 - magnetic permeability of air, equal to $4\pi \cdot 10^{-7}$ henry/m.

Permeability μ_k , in its turn, depends on the permeability of core μ_c , ratio of the length of winding l_w and diameter of coil D to the length l and diameter of core d .

For a multiturn coil, provided $\frac{l_w}{l} > 0.2$ (in aerial electric prospecting this condition is usually observed), value μ_k is given in terms of the following relationship (154):

$$\mu_k = \mu_c \frac{2(0,25 + 0,623 \frac{l_w}{l})}{\frac{D}{d} + \sqrt{\frac{D}{d}}} \quad (\text{VII.17})$$

The magnetic permeability of core μ_c in section l_w can be determined, if the initial magnetic permeability of the core's substance μ , ratio

$\frac{1}{d}$ and the length of the winding l_w are known. In multilayer coils the term for μ_c with cylindrical core could be written as :

$$\mu_c = \mu_{cu} \left[1 - 0,255 \left(\frac{l_w}{l} \right)^2 \right] \quad (\text{VII.18})$$

where μ_{cu} - magnetic permeability of the core's body in the central section.

For cylindrical cores, if $\frac{l}{d} \gg 10$,

$$\mu_{cu} = \frac{\mu}{1 + 0,765 \frac{\ln 2 \frac{l}{d} - 1}{\left(\frac{l}{d} \right)^2} \left(\frac{\mu}{\mu_0} - 1 \right)} \quad (\text{VII.19})$$

4. Quality and Sensitivity of Induction Magnetic Field Detectors.

It is a known fact that e.m.f., excited in receiving antenna, meant for receiving the electrical component of variable magnetic field, is proportional to the virtual height of this antenna h_d and the tension of electric field E in the direction of peak reception, i.e.

$$E_{A.e} = h_d E \quad (\text{VII.20})$$

For antenna made in the form of inductance coil,

$$h_d = \frac{2\pi \omega S_k}{\lambda}, \text{ M.} \quad (\text{VII.21})$$

where S_k - area of middle section of coil, m; λ - wave length, m.

If the receiving antenna has a ferrite core, its virtual height $h_{d.c}$ increases as much as the increment of efficient magnetic permeability μ_k :

$$h_{d.c} = \mu_k h_d = \mu_k \frac{2\pi \omega S_k}{\lambda}, \text{ M.} \quad (\text{VII.22})$$

where Z_c - wave impedance of medium $\left(\frac{E}{H} = Z_c \right)$. For the void (dielectric

and air) $\frac{E}{H} = \sqrt{\frac{\mu}{\epsilon}} = 120\pi = 377 \text{ ohm (18, 83)}.$

Due to rather small dimensions of the ferrite antenna , the sensitivity is inadequate; therefore, the antenna is tuned to the working frequency. In this case, its pick-up increases in accordance with the increased quality Q_{k_0} of the resonance circuit.

Having determined the active resistance of the coil with core r from the term (VII.12) and inductance L_k according to equation (VII.16), the quality of the magnetic field detector is calculated from formula

$$Q_k = \frac{\omega L_k}{r} \quad (\text{VII.24}).$$

In the case of idle running, the sensitivity of coil with core to the magnetic field is determined according to terms (VII.3) from formula

$$S_{\pi}^0 = \frac{\partial \bar{E}}{\partial H} \frac{A \cdot M}{\nu} \quad (\text{VII.25})$$

If the field detector (ferrite antenna) is tuned into resonance and is not loaded by the output resistance of the amplifying stage (or if this resistance exceeds considerably the resonance resistance of the tuned circuit), its sensitivity to the tension of magnetic field H will be determined from relationship

$$S_{\pi} = h_{d.c} Z_c Q_{k_0} \quad (\text{VII.26})$$

Substituting in equation (VII.26a) instead of $h_{d.c}$ and Q_{k_0} their values from formulas (VII.22) and (VII.24), and also taking into account that $Z_c = 120\pi$, we obtain (125).

$$S_{\pi} = \frac{240 \pi^2 w S_k \mu_k Q_{k_0}}{\lambda} \cdot \frac{\nu}{a/M} \quad (\text{VII.26-b})$$

In this case the μ_k value is determined from formula (VII.17).

Due to the fact that on the output side, the inductance coil with core is loaded into the input resistance of amplifier R, which for the frequency range of aerial electric prospecting may be taken as purely active (sometimes not even very high), the sensitivity of coil S_p should estimate its shunting action. For inductance coil, tuned into parallel resonance, the sensitivity is given in terms of relationship (154).

$$S_p' = \frac{\mu_c \omega_o^2 S_e^2 R L_k}{rR + \omega_o^2 L_k^2} . \quad (\text{VII.26-c}).$$

where ω_o - angular resonance frequency; R - resistivity of load (input resistance of amplifier).

5. Stability of Transmission Ratio in Magnetic Field Detectors.

For error determination of apparatus near the coil with core tuned into resonance the interest is only for the lower nonturning region, where the transmission ratio of the magnetic field detector and its phase characteristic is affected to a considerable extent by the variation of external conditions, specially by the temperature of the surrounding medium. But when ^{we} stipulate the use of ~~the~~ elements of the oscillating input circuit in the planned apparatus the basis should be the admissible phase and amplitude errors of the magnetic field detector.

The following could be referred to ^{as} the main factors determining the stability of the pick-up in the field detector in the form of coil with core tuned into resonance:

1) The temperature coefficient of magnetic permeability TK / μ_o of the core's material; 2) the temperature coefficient of concentrated capacitance, by means of which the detector is tuned into the operating frequency; 3) the input resistance of the amplifying stage, having shunting effect on the output resistance of the magnetic field detector;

4) parasitic capacitances of the coil's winding and connecting wires; 5) resistance of the winding and connecting wires insulation.

Experience has shown that parameter stability of the magnetic field detector is also affected by the change in humidity. Therefore, in aerial electro-prospecting it is necessary to apply air-tight high-quality condensers. To protect the inductance coils and other details of the detector from the effect of moisture it is expedient to apply various tars and compounds.

Amplitude relations of the magnetic field detector are highly affected by the non-stability in resistance of load R and loss resistance r . On the other hand, phase relations are affected by the non-stability of inductance L_k , resonance capacitance $C_{p,k}$, operating frequency ω_0 . It is mainly the non-stability of ω_0 that forces the application of quartz crystal control of frequency f_0 in oscillators, exciting the electromagnetic field. In this case, as we know, the phase instability of the magnetic field detector becomes to a great extent dependent only on the instability of capacitance $C_{p,k}$, on which more rigid demands are, therefore, imposed; than on inductance L_k .

For the magnetic field detector, assembled in the form of multiturn coil with core, the known formulas of amplitude and phase instability for coils without the cores (154) hold good on the whole. However, in determining inductance L_k vs. the magnetic permeability of the core μ_c , it is necessary to take into account the effect of the variation of its parameters on the detector's characteristics. The instability itself of inductance L_k in coils with core is shown by relationship

$$\frac{\Delta L_k}{L_k} = \alpha_M \frac{1}{1 + \frac{\mu}{\mu_0} N} \Delta \theta, \quad (\text{VII.27})$$

where N - coefficient of demagnetization; α_M - coefficient accounting for relative variation of quantity μ per 1°C ; $\Delta \theta$ - temperature gradient, $^\circ\text{C}$.

Coefficient of demagnetization N could be determined, according to the recommendations given in (155), from the core replaced by an equivalent ellipse of rotation, the demagnetization coefficient of which has analytical expression.^(*)

The relative instability of the core's magnetic permeability could, for practical purposes, be determined with sufficient accuracy from the relation.

$$\frac{\Delta \mu_c}{\mu_c} = \alpha_\mu \theta \frac{1}{1 + \frac{\mu}{\mu_0} N} \quad (\text{VII.28})$$

As follows from the equation (VII.28), the greater the N , the higher is the parameter stability of the magnetic field detector. This actually means that the core should not be too long and too thin, since the shorter it is and the greater its diameter, the higher will be the value of N .

At the frequencies of aerial electro-prospecting the instability of the core's material permeability is estimated mainly by coefficient α_μ , which determines the relative variation of μ per 1°C . For ferrite cores, which have found application in magnetic field detectors in aerial electroprospecting apparatus, this factor usually is $3.5 \cdot 10^{-3}$

(*) Moreover, for cylindrical and prismatic cores with rectangular section tables were given (97,178), in which the test values of N are given in function $\frac{1}{d}$, $\frac{1}{\sqrt{S}}$, where S - area of the core's cross-section.

The phase instability of the magnetic field detector, assembled as inductance coil with core tuned into resonance, is determined at low detuning from equation (154)

$$\Delta \varphi \approx - Q_k \left(\frac{\Delta C}{C} + \frac{\Delta L_k}{L_k} + 2 \frac{\Delta \omega}{\omega} \right), \text{ рад.} \quad (\text{VII.29})$$

Substituting in equation (VII.29) known or found values Q_k , $\frac{\Delta C}{C}$, $\frac{\Delta L_k}{L_k}$, $2 \frac{\Delta \omega}{\omega}$ is determined to a sufficient accuracy of the quantity $\Delta \varphi$.

6. Design and Construction of Magnetic Field Detectors.

Magnetic field detectors without core:- Receiving coils without core could, in principle, have different shape. Most frequently applied are the coils of rectangular and cylindrical shape. In the estimation of these coils, besides the general aspects stated above, their natural resonance frequency F_{pc} should be taken as higher than their highest operating frequency, i.e., for striving and reducing as far as possible, the natural capacitance of the coils. At the same time, the f_{pc} should be such that the transmission coefficient K would have a low dependence on the frequency within the range of operating frequencies of the field detector. Its admissible variations, as a rule, should not exceed 10%. To assure the highest possible sensitivity and quality, the number of turns and the wire diameter of the receiving coil should be selected the condition that the maximum possible section area at the preset overall size is obtained.

The natural resonance frequency f_{pc} of the receiving coil is determined by the value of its natural distributed capacity. Therefore, to assure condition $f_{pc} > f_{o2}$, where f_{o2} - highest operating frequency of

the field detector, the natural capacitance of the inductance coil should be negligible. With low value of this capacitance, the stability of the parameter of the field detector also increases.

The distributed capacitance between the turns of the coil's winding could be shown as concentrated and connected parallel to the winding. In this case, the equivalent diagram of the coil's winding will correspond to the one in Fig.78, where E - e.m.f., induced in the coil; L_o - natural inductance of the coil; C_o - distributed (interloop) capacitance; R_L - active resistance of the coil; U_c - tension on terminals.

According to the equivalent diagram

$$\frac{U_c}{E} = \frac{\frac{1}{j\omega C_o}}{R_L + j\omega L_o + \frac{1}{j\omega C_o}} = \frac{1}{(1 - \omega^2 L_o C_o) + j\omega R_L C_o}$$

Getting rid of the imaginary number in the denominator, we get

$$\frac{U_c}{E} = \frac{(1 - \omega^2 L_o C_o) - j\omega R_L C_o}{(1 - \omega^2 L_o C_o)^2 + (\omega R_L C_o)^2}$$

Modulus of this ratio

$$\left| \frac{U_c}{E} \right| \approx \sqrt{\frac{1}{(1 - \omega^2 L_o C_o)^2}} \approx \frac{1 + \omega^2 L_o C_o}{1 - (\omega^2 L_o C_o)^2} \quad (\text{VII.30})$$

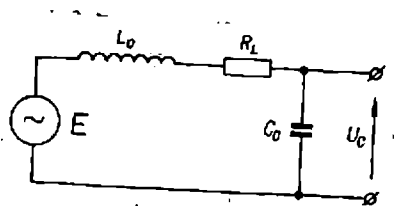


Fig.78.

since the condition $\omega^2 R_L^2 C_o^2 \ll 1$ is always observed for the receiving coils in the apparatus of aerial electric prospecting. The value $(\omega^2 L_o C_o)^2$ in the denominator of formula (VII.30) could also be ignored, since in practice $(\omega^2 L_o C_o)^2 \ll 1$.

Therefore,

$$\left| \frac{U_c}{E} \right| \approx 1 + \omega^2 L_o C_o \quad (\text{VII.31})$$

Value $\omega^2 L_o C_o$ determines the e.m.f. loss in the coil. Denoting it as q , we get

$$q = \left| \frac{\delta U_c}{E} \right| = \omega^2 L_o C_o \quad (\text{VII.32})$$

If it is assumed that the voltage at the terminals of the receiving coil could differ from the e.m.f., induced in it by not more than 1% in amplitude and 5° in phase, then in thick case $q = 0.01$ and the admissible distributed capacitance

$$C_o \leq \frac{10^{-2}}{\omega^2 L_o} \quad (\text{VII.33})$$

The phase shift in the receiving coil is determinable from formula

$$\varphi = - \operatorname{arctg} \frac{\omega R_L C_o}{1 - \omega^2 L_o C_o} \approx \operatorname{arctg} \omega R_L C_o (1 + \omega^2 L_o C_o). \quad (\text{VII.34})$$

The constructional data of the round coil are determinable from relation

$$C_o = \frac{3(n-1)}{4n^2 G} C_{c\pi} \quad (\text{VII.35})$$

In formula (VII.35) n - number of layers in winding; G - number of sections $C_{L\pi}$ - natural capacitance of layer,

$$C_{c\pi} = \frac{0.0885 \varepsilon D l_k}{\Delta} \quad (\text{VII.36}).$$

Here ε - dielectric constant of the winding wire insulation; l_k - the length of the circumference of the coil's loop, $l_k = 2\pi R = \pi D_k$; D - width of the winding, $D = \frac{w}{n}$ $t = \frac{w}{n} \Delta$, where n - the number of turns in the section; t - pitch of the winding; Δ - distance between the layers of the winding.

Let us take an example of calculating the receiving coil of the round section on the basis of ensuring its minimum distributed capacitance.

Preset: diameter of coil upto 50 cm; operating frequencies 75; 185; 475 and 925 cps; number of loops - not over 10 thous. with taps for operating frequencies from $4.0 \cdot 10^3$; $1.5 \cdot 10^3$; $6 \cdot 10^2$ of loop; wire PEV 0.2 mm in dia.; winding pitch and distance between layers $t = \Delta = 0.4$ mm. The winding should be so constructed that the voltage, measurable at its terminals, would be distinct from the e.m.f. induced in it by not more than 1%. We take $\varepsilon = 5$. $G = 1$.

The maximum allowed capacitance of the winding

$$C_o = \frac{3 (n - 1) 0.0885 \cdot 5 \cdot \pi \cdot 50 \frac{w}{n}}{4 n^2 \cdot 1}$$

i.e. $C_o = 100 \frac{w}{n^2}$. At $f = 925$ cps; $w = 600$ loops; $L_o = 0.75$ henry;

$\omega^2 = 3.4 \cdot 10^7$ 1/sec² we have

$$C_o \leq \frac{10^{-2}}{\omega^2 L_o} = \frac{10^{-2}}{3.4 \cdot 10^7 \cdot 0.75} \approx 400 \text{ n}\phi$$

This distributed capacitance corresponds to the coil, in which the number of layers is

$$n = \sqrt{\frac{100\omega}{c_0}} = \sqrt{\frac{100 \cdot 600}{400}} \approx 12$$

Therefore, the first section should have not less than 12 layers with $50 \left(\frac{600}{12} \right)$ loops in a layer.

If $f = 475$ cps; $\omega = 1500$ loops; $L_0 = 4.5$ henry; $\omega^2 = 9 \cdot 10^6$ 1/sec²,

$$c_0 \leq \frac{10^{-2}}{9 \cdot 10^6 \cdot 4.5} \approx 250 \text{ n}\phi$$

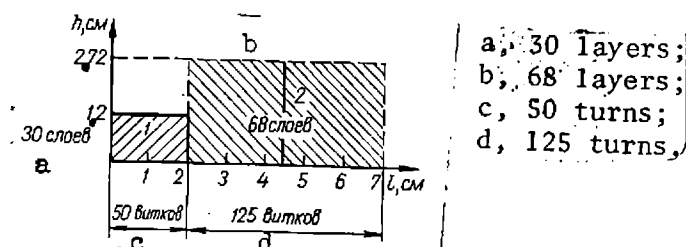


Fig.79

This distributed capacitance corresponds to the coil, in which the number of layers is

$$n = \sqrt{\frac{100 \cdot 1500}{25}} \approx 25.$$

Therefore, the second section should have not less than 25 layers with $60 \left(\frac{1500}{25} \right)$ loops in a layer. Since the second section includes also the first, to simplify construction the 1500 loops could be arranged in 30 layers, each layer having 50 loops, with unsoldering from the 12th layer, which corresponds to 600 loops.

When $f = 185$ cps; $\omega = 4000$ loops; $L_0 = 32$ henry; $\omega^2 = 13.5 \cdot 10^5$ 1/sec²,

$$c_0 \leq \frac{10^{-2}}{13.5 \cdot 10^5 \cdot 32} = 230 \text{ n}\phi; n = \sqrt{\frac{100 \cdot 4000}{230}} = 31.$$

i.e., a layer has $\frac{4000}{31} = 129$ loops.

This section should include 1500 loops of the preceding sections; the remaining 2500 loops could be arranged in 20 layers with 125 loops in a layer.

At $f = 75$ cps; $\omega = 10,000$ loops; $L_0 = 200$ henry, $\omega^2 = 2.2 \cdot 10^6$ 1/sec², we have

$$C_0 \leq \frac{10^{-2}}{2.2 \cdot 10^6 \cdot 200} = 230 \text{ n}\phi ; n = \sqrt{\frac{100 \cdot 10^4}{230}} = 66$$

The number of loops in a layer is 150 $\left(\frac{10^4}{66}\right)$. This winding includes the preceding sections, in which the number of loops in a layer for 1500 loops should not exceed 50, for 2500 - 129 and for the remaining 6000 - 150. Therefore, 8500 loops can be arranged by having 125 in a layer, with unsoldering on the 20th layer for 2500 loops. Thus, we get a two-section winding (Fig.79). To reduce the intraloop capacitance of the coil, the second section can be divided into two or three parts, i.e., to make the coil multisectional.

In the apparatus of aerial electro prospecting, the application is sometimes of field detectors in the form of rectangular "air" frames. However, detectors of this kind have considerable overall size and it is difficult to make them shock-absorbent. For instance, in apparatus AERIS, the use was made initially of receiving frames, calculated for assuring minimum natural capacitance. The irregularity of the transmission coefficient of such a frame (untuned and having $f_{pc} \approx 12$ k-cps) in the frequency range 400 - 4000 cps, was less than 10%. The receiving frame consisted of four sections, each 1000 x 200 x 77 mm in size (Fig.80). The arrangement of the receiving frame in the outboard gondola is shown in Fig.81. The main parameters of the frame, assembled

of wire PEL 0.27 mm in diameter at $f = 488$ cps, are as follows: number of loops in the section 200, active resistance of wire 350 ohm, inductance 0.78 henry, quality 6.33, sensitivity $0.63 \frac{V}{A/m}$, virtual height $1.64 \cdot 10^{-3} m$.

In tuning the frame to high frequencies the use was not of four sections, but of two or three depending on the operating frequency.

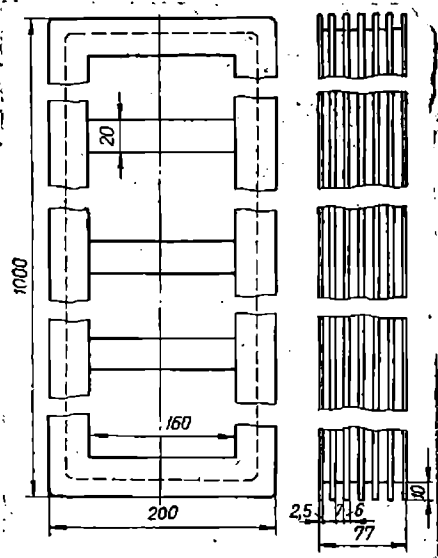


Fig.80

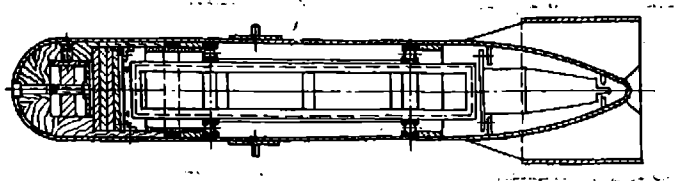


Fig.81

Field Detector in the Form of Coil with Ferrite Core. Multiturn coils with ferrite cores have a big advantage over the usual "air" coils (frames): small overall size and weight, insignificant sensitivity to electric fields and comparatively high sensitivity to the magnetic ones, possibility of constructing simple but reliable protection against vibration.

We assume that the field detector has to operate in a two-frequency apparatus of induction method, within a certain frequency range, at preset

magnetic moment of oscillating frame \bar{m} . As usual in aerial induction method, the product of moment (\bar{m}) by sensitivity S_p in preset frequency range should be a constant quantity (125). Therefore, the e.m.f., induced in field detector by primary field at reception point (i.e. with lowering of gondola to the whole operating length of wire-cable) should be the same on all operating frequencies of the apparatus ($mS_p = \text{const}$).

We assume that $mS_k = 2.25 \cdot 10^5$, but for assuring simultaneous two-frequency operation magnetic field detectors should have two coils: one, operating on frequencies 244; 487 and 974 cps, and the other - on frequencies 974; 1949 and 3898 cps. The magnetic moment of oscillating frame on frequencies 244, 487, 974, 1949 and 3898 cps respectively will have the following values (av.m^2): $m_1 = 18 \cdot 10^3$; $m_2 = 15 \cdot 10^3$; $m_3 = 9 \cdot 10^3$; $m_4 = 4.5 \cdot 10^3$; $m_5 = 3.6 \cdot 10^3$. The initial magnetic permeability of the core type^(*) MT-4000 (MC-2000), $\mu_c = 4000$; the constructive $\mu_k \approx 11$; the shape of the rectangular core dimensions 12 x 24 x 140 mm. The magnetic field detectors are set up inside the outboard gondola.

The required sensitivity of magnetic field detectors is determined on the basis of ratio $mS_p = 2.25 \cdot 10^5$. On working frequencies of the apparatus the sensitivity should correspondingly be ($\frac{V}{A/\bar{m}}$):

$$S_{p1} = \frac{2.25 \cdot 10^5}{18 \cdot 10^3} = 12.5; \quad S_{p2} = 15; \quad S_{p3} = 25;$$

$$S_{p4} = 50; \quad S_{p5} = 62.5.$$

Using formulas (VII.3) - (VII.6), and also recommendations of paragraph 1, we choose, according the required sensitivity, the type of

(*) Oxyfer MT-4000 (MC-2000) has very low temperature coefficient of permeability, which assures sufficiently high temperature stability of induction coil.

ferrite core and the construction of magnetic field detector for low frequencies and the systems of its protection against vibrations.

In the given example the construction of the coil was selected same as the one in Fig.82. The first coil for operating on low frequencies 9 consisted of six sections of 800 loops each. The frame of the coil 8 was made of high quality laminated bakelite. The winding was of wire PEV-2, 0.51 mm in dia. On frequencies 974; 1949 and 3898 only four sections were cut in, and on remaining frequencies - the whole winding. With switch-over of loops on two separate coils it was possible to obtain two magnetic field detectors for operations on two frequencies.

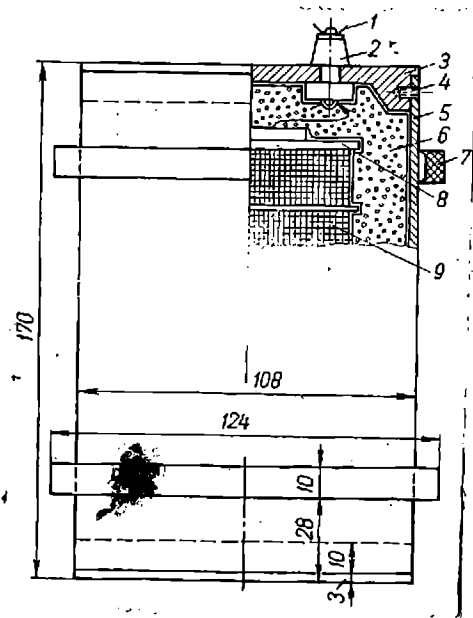


Fig.82

The splitting of the coil into six sections was done with the aim of reducing the natural parasitic capacitance of the coil. To decrease the humidity effect of the surrounding medium the coil was placed into cylinder 5 of plastic glass, the bottom and cover 3 of which were made of high quality textolite. Thickness of cylinder walls was 4 mm. The

covers were tightly fitted to the inner surface of cylinder. When the covers were placed the contact surface was smeared with bakelite varnish, with which the internal and external surface of cylinder was also saturated. Supplementary tightening of the bottom and lid to cylinder was implemented by textolite screws 4, which, before the screwing on, were also smeared with bakelite varnish. By these means a sufficiently high sealing of the coil was attained.

The space between the coil and inner surface of cylinder was filled with synthetic porous material - paralon 6, which was the first stage of shock-absorption. In order to raise the resistivity of insulation, the taps 1 of the coil were made inside the ceramic insulators 2, set in bakelite on the lid of cylinder. Due to low thermal conductance of paralon, air in the cylinder and the material of which the cylinder was made, the receiving coils were of high temperature inertia.

The cylinder was fitted with two textolite rings 7 with chamfers, by means of which the cylinders were suspended on rubber tape inside the gondola. This assured the second stage of shock-absorbing.

Given below are the experimental data, characterising the field detectors:

	<u>LF Coil</u>			<u>HF Coil</u>		
Frequency, cps.....	243	487	974	974	1949	3898
Sensitivity, $\frac{V}{a/m}$	6.25	21.5	68.0	59.4	85.3	106

According to these data, the required value of mS_p is not assured only in frequency 243 cps due to low S_p . Thus, the coil in principle could be reconstructed and the sensitivity of field detector obtained upto

about $S_{p1} = 12.5 \frac{V}{a/m}$. However, in some cases anomalous relations at low frequencies are considerably in excess of similar relations on high frequencies, as a result of which the above requirement for low operating frequency is not always observed. So it was with the apparatus had sensitivity on frequency 243 cps at which the product mS_p was almost half of the adopted value.

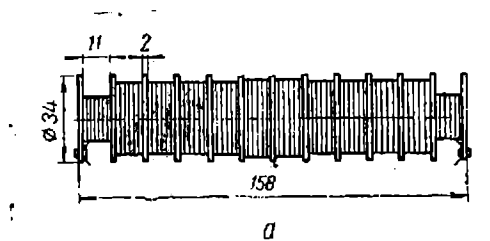


Fig.83

If on other operating frequencies sensitivity of coil is found to be higher than required for obtaining the specified mS_p , it should be reduced to the required one. This is resolved most simply and reliably by introducing into oscillating circuit (tuned to operating frequency) a supplementary active resistance, which reduces its Q-coefficient (125). Thus it was possible to assure the sensitivity of field detectors; required for AERI-2 apparatus basic parameters of which are shown in Table 7.

TABLE - 7

Parameter	LF Coil			HF Coil		
Frequency, cps	243	487	974	974	1949	3898
Sensitivity, $\frac{V}{a/m}$	5	15	25	25	50	62.5
Q-coefficient (at level 0.707).	35	66	56	56	74	35
Equivalent sensitivity according to field $mS_p \cdot 10^5$	1	2.25	2.25	2.25	2.25	2.25

In designing and planning of coils with core it is necessary to take into account the external conditions of the operating apparatus (specially temperature and humidity of the surrounding air). Experiments have shown, that in temperature range from -15 to $+50^{\circ}\text{C}$ at various humidity the magnetic field detectors had for 50 hrs almost invariable sensitivity and the frequency of tuning was maintained within them with high accuracy. Therefore, the coil with core meets the working conditions of apparatus in aerial electro-prospecting. The efficiency of measures adopted for the protection of apparatus from vibration should be tested additionally during the flight of aircraft.

The receiving coils with core for AERA-2 apparatus in BDK method are of the same type and almost the same specifications.

An example of receiving coils with cylindrical ferrite cores F-2000 (red dia. 10mm, height 215 mm) are the coils of AERIS apparatus. These coils are sectional and have a stepwise winding. Fig. 83-a, shows a diagram of this type of coil for frequencies 500-4000 cps, and in Fig.83-b, for frequencies 1000-8000 cps. Basic parameters of coils are shown in Table-8.

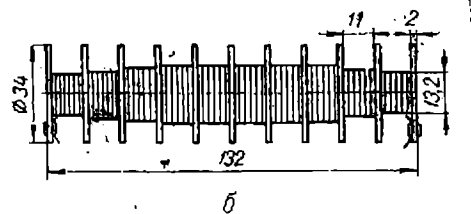


Fig.83

Table-8.

Parameter	LF Coil	HF Coil
Frequency range, cps	500-4000	1000-8000
Number of loops	5534	1617
Type of wire	PEV-0,38	PEB-0,35
Resistivity to direct current, ohm	67	13,7
Constructive magnetic permeability, μ_k	33	35
Inductance, millihenry:		
without core	65	6.5
with core	2150	237
Sensitivity, $\frac{V}{a/m}$:		
f = 488 cps	5	-
f = 976 "	30	-
f = 1953 "	50	-
f = 3906 "	72	40
f = 7812 "	-	74
Q-Coefficient:		
f = 488 cps	55,5	-
f = 976 "	61	-
f = 1953 "	67	-
f = 3906 "	40	78
f = 7812 "	-	66,5

7. Practical Determination of Main Parameters in Magnetic Field Detector.

To increase the reliability of apparatus in aerial electro-prospecting all its main units, including the magnetic field detectors, should be carefully checked even during its construction. Sensitivity and Q-coefficient determination of receiving coils is one of the main checks of the receiving-measuring group of the apparatus (91).

To build up a uniform magnetic field the application is of Helmholtz coils with known geometrical dimensions and number of turns on each coil. The magnetic field detector, which is being investigated, is set up within the coils. Sensitivity of field detector is determined from the intensity of magnetid field tension H_k within the coils (111):

$$H_k = 7,14 \cdot 10^2 \frac{w/k}{R_k^0} \cdot a/M. \quad (\text{VII.37}).$$

where w - number of turns in one coil; I_k - current passing through the coil, a ; R_k^0 - average radius of coils, m.

Usually the current intensity I_k , is passed through the coils, and from the known values w and R_k^0 determination is made of the field intensity H_k inside the coils. If $I_k = 1$ A, the ring constant is represented as:

$$C_k = \frac{1}{H_k} , \frac{a}{a/M} . \quad (\text{VII.38})$$

With a known constant of coils C_k (on Helmholtz coils the value of this constant is usually marked) field intensity inside them is determined from the relation:

$$H_k = \frac{10^3/k}{4\pi C_k} \approx 80 \frac{I_k}{C_k} , \quad a/M. \quad (\text{VII.39})$$

When the constant C_k , potential field induced in the detector U_p and the current of coils I_k are known, sensitivity of magnetic field detector is determined from formula

$$S_p = \frac{U_p C_k}{80/k} , \quad \frac{v}{a/M} \quad (\text{VII.40})$$

Fig.84 shows a diagram of a test unit for determination of values S_p and Q_k , where 3Γ - audio-frequency oscillator, $K3\Gamma\Phi$ - quartz master

oscillator of fixed frequencies; O - oscillograph; K - Helmholtz coils;
 ΠK - receiving coil (L_k and C - respectively inductance and capacitance of coil); LB - tube voltmeter; R_k - resistance, cut in series with Helmholtz coils (B-B terminals on resistance R_k) Πy - preliminary (gondola) amplifier of aerial electro-prospecting apparatus (A-A terminals at its input $\tilde{B}-\tilde{B}$ - terminals at the output).

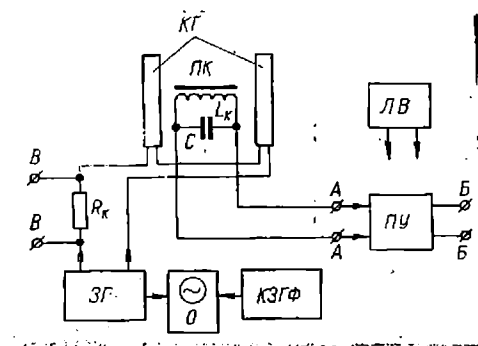


Fig.84

Current in Helmholtz coils is measured indirectly from the drop of the potential field U_R on resistance R_k (terminals B-B). The extent of resistance is taken such, as to prevent additional errors during the measuring, for instance, of errors due to outside induction, induction from power line, etc.

The sensitivity and Q-coefficient of magnetic field detector (L_k, C) is determined as follows. Primarily from voltmeter by means of audio-frequency oscillator the current is set in Helmholtz coils I_k of a chosen intensity and preset operating frequency. Then the tension is measured on terminals A-A or $\tilde{B}-\tilde{B}$. With known tension on the terminals A-A, current I_k and constant C_k , determination is made of detector's sensitivity from formula (VII.40). Or, with known tension U output on terminals tension U_R , resistance R_k and amplification coefficient of amplifier K,

sensitivity is determined of the magnetic field detector:

$$S_p = \frac{U_{out} C_k R_k}{80 k U_R}, \quad \frac{\sqrt{a/M}}{a/M} \quad (VII.41)$$

Tuning and resonance frequency of the receiving coil circuit are checked by varying frequency of the audio-frequency oscillator while measuring potential field U_{out} by tube voltmeter. The constancy of the moment of operating frequency f_p and resonance frequency f_o of the $L_k C$ circuit are checked by Lissajous figures by means of oscillograph. For this, signal from the $L_k C$ circuit is fed to one pair of terminals, and to the other - signal from the master quartz oscillator of the experiment apparatus. At the constant moment of frequencies, oscillograph screen shows an immobile image in the form of periphery (ellipse).

The Q-coefficient of magnetic field detector is determined from the deviation of frequency from f_o of receiving coil to the extent $2 \Delta f$ at level 0.707 of the maximum U_p (U_{out}) from formula (VII.11), i.e. $Q = \frac{f_o}{2 \Delta f}$.

The amplification coefficient of amplifier Πy is usually known on each operating frequency of the apparatus and is measured as ratio $\frac{U_{out}}{U_p}$. During the measuring it is necessary to make sure, that the voltmeter does not cause any appreciable distortions in electric parameters of the receiving circuit (its input resistance should be sufficiently high, and the input capacitance negligible).

--- --

CHAPTER - VIII

TRANSMISSION OF SIGNAL OF THE MAIN PHASE TO
THE MEASURING APPARATUS OF THE BDK METHOD.

1. Propagation Specifics of Key Signal Radio-Waves and
the Selection of Carrier Frequency.

In recording magnitude φ_x , U_x , U_{xp} and modulus U_x of the cable field signal in the measuring apparatus, set up on a mobile object (plane or helicopter), the key signal should be transmitted through a special radio-channel. This signal must reflect the current phase in the cable. To ensure reliability of the measuring apparatus, the key signal at the reception point should considerably increase interference in the air, and its phase should not depend on the position of the helicopter. In connection with this, let us consider the specificity in propagation of the key signal as applicable to radio-waves its transmission from the ground power unit to the mobile measuring group.

B.A. Vedensky (37) has shown that the electric field of radio-waves at the point of reception may be taken as a result of interference of surface rays, direct and those reflected from the ground which are picked up by the receiving antenna. This question is discussed in detail in (72), where the formulas for estimating the field density, the attenuation

coefficient has been introduced.

$$F = \sqrt{1 + 2R \cos \left(\theta + \frac{4\pi h_1 h_2}{\lambda r} \right) + R^2} \quad (\text{VIII.1})$$

Here R - modulus of reflection coefficient from the ground; θ - angle of phase loss with reflection; r - distance between reception and transmission points; h_1 and h_2 - respective height of transmitting and receiving antennas.

The field density at the reception point could be given in terms of the following formula:

$$E = \frac{173 \sqrt{P_1 D_1}}{r} F, \text{ M } \mu/\text{M}. \quad (\text{VIII.2})$$

where D_1 - directive gain of the transmitting antenna; P_1 - transmitter power kwt; r - distance of the transmitter, km.

According to formula (VIII.1) the attenuation coefficient F varies its magnitude in relation to distance r (Fig.85). For instance, with the reflection coefficient $R = 1$ it may vary from zero to two.

In our case, when the reception of the key radio-signal is on the helicopter, the role of the ground as a reflecting surface is performed by the body of the helicopter and the equivalent surface, formed by the fast-rotating screw (diameter of screw is about 22 m). These surfaces for radio-frequencies 38-40 m-cps, used for the transmission of the key signal in apparatus AERA-58, considerably exceed the operating wave length ($\lambda = 7.5$ m) and are quite satisfactory reflecting surfaces. However, in this case, the reflection coefficient cannot attain value equivalent

to one. Therefore, the variation range of the attenuation coefficient decreases considerably and the general variation of magnitude E will be lower. Density variations in the field of key signal E have the same recurrence vs. distance, as the AGC circuit of the receiver with amplitude modulation manages to operate at the speed of the helicopter's flight upto 120-140 km/hr.

This type of key signal variation takes place, when the helicopter flies along a straight line at one altitude. In turning around, descending and ascending, there may be considerable variations of E , caused by the additional screening of the receiving antenna by the rotating screw and the body of the helicopter.

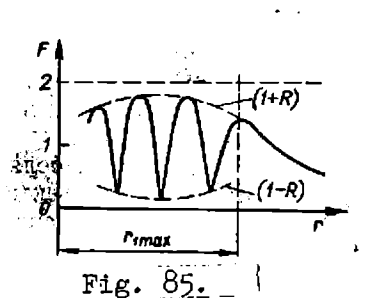


Fig. 85.

Electric prospecting by the BDK method is invariably carried out with the helicopter flying at an altitude of 30-50 m above the ground surface.

The maximum possible distance of the key signal transmission can be determined from the following formula (143).

$$r_{\max} \approx 4.12 (\sqrt{h_1} + \sqrt{h_2}). \quad (\text{VIII.3})$$

In accordance with this formula, which estimates the refraction of radio-waves in atmosphere, the distance of radio-communication is greater than the optical visibility. For instance,

for our case, when $h_2 = 30-50$ m and the height of the transmitting antenna of the generating ground unit of the apparatus $h_1 = 10$ m, the maximum distance of radio-communication by ground ray r does not exceed 35-42 km. With the setting up of the ground apparatus in the middle of the survey topomap, the obtained r values are quite acceptable.

However, in the practical implementation of the BDK method, the survey is frequently conducted in extremely rough locality (on hillocks, in mountains, etc.). In this case, there may be screening obstacles on the path of radio-waves propagation. If the dimensions of the obstacle are not large, then due to diffraction and additional reflections the signal at the reception point could be of considerable magnitude. But if the screening obstacles are considerable and are close to the transmitter or receiver, there may be cases when the radio-signal will be completely absent. In the presence of the screening obstacles, there are points at which the radio-signal may have additional amplification of up to 26 db due to the signal reflected from this obstacle (72).

In practice, these events are manifested at the receiving device, which is set up on the helicopter, in the form of total disappearance of the main phase radio-signal or by its considerable increment at individual points of survey traverses in hilly areas. Obviously, at the moments of disappearance of the key signal the normal operation of the measuring instruments ceased.

As mentioned in the foregoing, in the first AERA-58 apparatus of the BDK method the key signal was transmitted on the frequency of ultra-short wave range 38-40 mcps. These frequencies were

selected because of the low level of atmospheric interferences and of interfering radio-stations, and because of the relative simplicity of the transmitting and receiving antennas. It was noted, however, that the radio-signal of the main phase was sometimes not transmitted through AERA-58 apparatus. In 1961, in manufacturing the modernized apparatus AERA-2 and AERA-3, the carrier frequency of the key signal was taken within the frequency range 2-3 megacycles per second. Considerable reduction of the carrier frequencies was justified by the fact that they possess much better diffraction properties of the ground wave and less absorption in the ground. Although on these frequencies the atmospheric interferences are of higher magnitude than on ultra-short wave frequencies, they are compensated by power increment of the ground radio-transmitter. And, finally, surveys by the BDK method on the helicopter are conducted only during the day when interferences from other radio-stations on these frequencies are negligible.

2. The choice of polarization for transmitting and receiving antennas.

In the BDK method the helicopter with measuring instruments may take up various positions in respect of the ground generating unit. Because of this it is necessary to use for the radio-transmitter of the key signal an antenna with a circular directional diagram in the horizontal plane or directional antenna with automatic orientation towards the helicopter. The second course is more difficult and its application in the BDK method is inexpedient.

Application of the antenna with a circular diagram presents no difficulties. Therefore, both in the AERA-58 apparatus and in

the subsequent devices AERA-2 and AERA-3, the antennas used for the radio-transmitter of the key signal and on the helicopter are of the circular directional diagram.

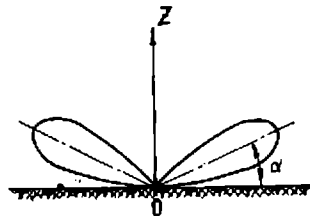


Рис. 86.

Fig.86

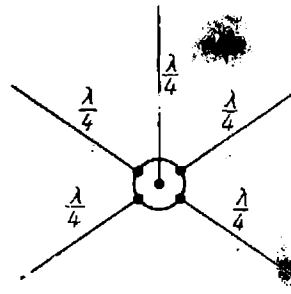


Рис. 87.

Fig.87

On the ground this type of antennae could be fitted for waves with horizontal and vertical polarization. It is very difficult to fit an antenna on a helicopter with horizontal polarization and circular directional diagram in the horizontal plane. Therefore, it would be expedient to use vertical polarization of the main phase signal.

For the ground radio-transmitter it is advisable to fit a vertical antenna with low angle of emission peak toward the horizon (Fig.86). Within the range of ultra-short wave, such an antenna could be a quarter-wave dowel with horizontal oscillators (Fig.87), half-wave dipole (Fig.88-a) and a system of half-wave dipoles (Fig.88-b). On the receiving side of the main phase radio-signal, a quarter-wave telescopic dowel antenna, can be used which moves out from the freight cabin vertically downward after the helicopter takes off.

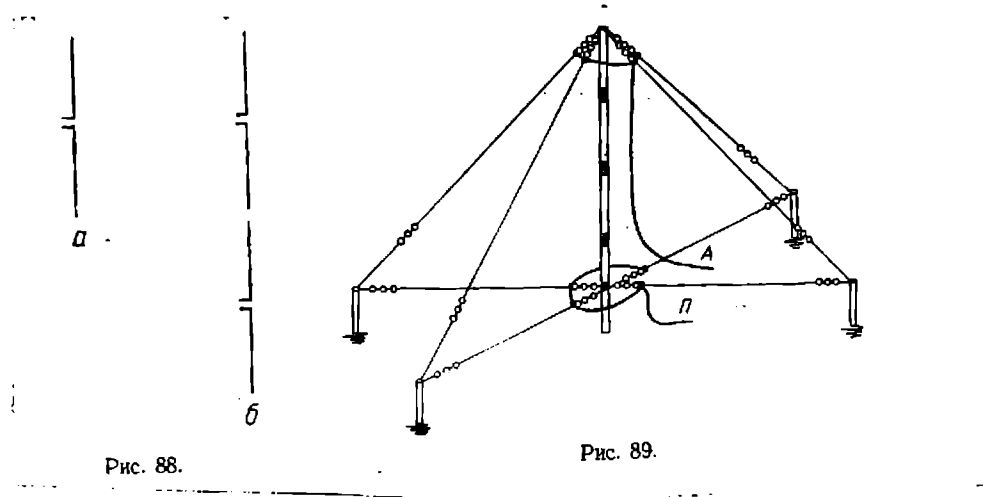


Fig.88

Fig.89

When using for the main phase radio-channel intermediate wave frequencies of 2-3 megacycles per second, the transmitting antenna could be made up in the form of vertical umbrella-like antenna (Fig.89, where A-antenna, П - counter-weight), and the receiving antenna, as in the case of frequencies 38-40 Mcsp, in the form of a telescopic dowel 2-3 m in length.

3. Modulation of the Main Phase Radio-Signal:

For electric prospecting by BDK method, the use could be made, in principle, of all the existing methods for the modulation of the main phase radio-signal. The expediency of transmitting the key signal on frequencies 2-3 Mcsp was pointed out in the foregoing. Hence, in selecting the type of modulation, it should be estimated whether it is applicable on these frequencies, and the specific operating conditions of the airborne apparatus should also be estimated.

It should be mentioned that, due to relatively low radio-frequencies, the radio-channel of the main phase should take up in the air a frequency band as narrow as possible. In this case, firstly, the radio-channel in question will be of minimum interference to the adjacent channels of radio-communication and, secondly, it will be possible to narrow down the transmission band of the receiving track, which assists in enhancing the protection of the channel against interference.

If frequency or phase modulation is applied, the width of the frequency band in the air will be determined by the following formula (206).

$$2 \Delta F = 2F (1 + m). \quad (\text{VIII.4})$$

where F - modulating frequency; m - modulation index.

With frequency modulation, when $m = m_{f-m}$, we have

$$m_{f, M} = \frac{k_f \cdot M \cdot U_{m\Omega}}{\Omega} = \frac{\Delta\omega}{\Omega} = \frac{\Delta f}{F} \quad (\text{VIII.5})$$

With phase modulation, when $m = m_{p-m}$, we get

$$m_{p, M} = \Delta\varphi k_p \cdot M \cdot U_{m\Omega} \quad (\text{VIII.6})$$

where $\Delta\varphi$ - maximum phase variation of oscillations during modulation; $U_{m\Omega}$ - amplitude of modulating tension; K_{f-m} , K_{p-m} proportionality coefficients, respectively, of frequency and phase modulation, which determine the steepness of the modulation characteristic.

The modulation index could be from $m \ll 1$ to $m \gg 1$. At $m \ll 1$ width of the frequency band, taken up by the radio-channel of

of the main phase, will strive toward two, i.e., toward the spectrum, taken up by the radio-signal with amplitude modulation.

However, with frequency or phase modulation with low deviation of frequency $\Delta\omega$ in the receiving track, the output voltage at the output of the detector will be low, since

$$U_{\text{er}} = S_{\text{er}} \frac{d\theta}{dt} = S_{\text{er}} \Delta\omega(t) \quad (\text{VIII.7})$$

In the actual circuits, the value m is taken within 0.5-20 and even higher. In this case, the band of frequencies taken up in the air even with one-frequency modulation, as in apparatuses AERA-58 and AERA-2, will according to formula (VIII.4), be very high, upto to some tens of kilocycles. Naturally, this type of radio-channel on frequencies 2-3 Mcps will be affected by the interference of other radio-stations.

On the basis of what is stated above, it may be reaffirmed that the application of frequency modulation for the transmission of the key signal in the BDK method is inexpedient.

Lately, the one-band radio-communication has become very widespread. Without discussing its advantages (4, 40, 245), let us analyse the possibility of its application in the apparatus of the BDK method.

It is well known that for the reception of one-band signal, the carrier frequency has to be restored in the detector. With thermostatic control of quartz resonator it would be very difficult to obtain in the movable apparatus frequency stability of the quartz oscillator above 10^{-7} - 10^{-8} . The variation of suppressed

carrier frequency in the transmitter or of that restored in the receiver due to external effect (temperature, pressure, humidity, etc.) results in displacing the side band spectrum to the same extent as in the case of variation of the carrier frequency. For instance, with the carrier frequency of the key radio-signal $F_c = 3$ Mcps, the absolute drift of frequency due to frequency instability of the quartz oscillator about $10^{-7} - 10^{-8}$ will be $0.3 - 0.03$ cps. Therefore, shifting of the key signal audio-frequency will be the same, as in phase measuring, which may cause an error of $10.8 - 1.08^\circ$. It is obvious that the use of some carrier frequency residue (pilot-signal) on the transmitting side with automatic tuning on receiving may reduce the phase errors of the radio-channel to permissible numbers.

With the transmission of the key signal by the method of one-band radio-communication, it is necessary also to estimate the Doppler effect which, in our case, is due to the shifting of the key signal detector in relation to the transmitter.

Distance variation between the stationary transmitter and the shifting receiver affects the absolute value of radio-signal frequency (140).

In the case of detector's removal

$$f'_H = f_H \left(1 - \frac{v}{c} \right); \quad (\text{VIII.8})$$

in the case of detector's approach

$$f'_H = f_H \left(1 + \frac{v}{c} \right) \quad (\text{VIII.9})$$

where f_c' , f_c'' - carrier frequencies of the key signal with an estimate of Doppler effect; f - absolute value of carrier frequency; v - velocity of detector's shifting; c - propagation velocity of radio-waves.

With the carrier frequency of the key signal $f_c = 3$ Mcps, its variation, due to Doppler effect, is 100 km/hr, ± 3 cps, at the flying speed of the helicopter which corresponds to the phase variation of the key signal over $\pm 1000^\circ$. The automatic control of frequency f_c is practically impossible due to difference in the relative velocities v of the receiver and the transmitter. Thus it is possible to come to the conclusion that the application of one-band radio-communication for transmission of the key signal in the BDK method without a complex diagram of automatic tuning of the frequency is excluded.

In apparatuses AERA-58 and AERA-2 the transmission of the key signal was implemented by amplitude modulation with quartz frequency stabilization of the master oscillator of the transmitter and the heterodyne of the receiver. Although from the energy point of view amplitude modulation takes the second place to frequency of receiver $2\Delta f_{rec} = 5-10$ kcps). The master oscillator and the heterodyne of the receiver may have stability upto 10^{-4} . It seems of interest to use the autoanode modulation of Kruglov, Dogherty diagram (206) and other methods of amplitude modulation, distinguished by higher efficiency.

During the development of the apparatus for the BDK method and in its later exploitation, the stability of phase response in the main phase-radio-channel was frequently investigated. In every

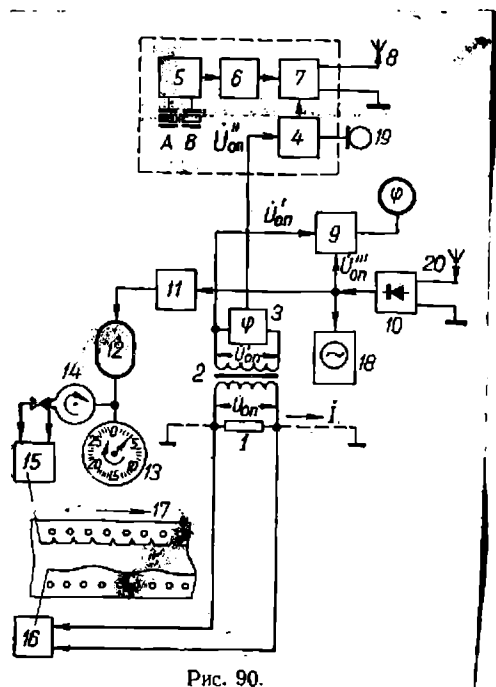
case the error did not exceed the allowed ($\pm 2^\circ$). It is obvious that amplitude modulation may be recommended for new sets of apparatus for the BDK method.

4. Apparatus of Key Signal Radio-Channel.

Fig.90 shows the functional diagram of radio-transmitting part of the radio-channel in apparatus AERA-58, which is on the ground generating unit (57).

The bearing voltage U_b , reflecting the current phase in cable I, is taken off the resistance 1. The transformer 2 ensures galvanic separation of voltage U_b and current I. The secondary circuit of the transformer is practically unloaded, therefore the introduced phase error does not exceed 10-20'. To compensate the phase shifts in subsequent track elements the modulator, the output stage of the transmitter, the transmitting antenna, etc.), the phase-inverter 3 connected at the output of the transformer 2. Bearing voltage U_2'' arrives after the phase-inverter to the modulator 4 of the transmitter.

Fig.90



Any types of commercial transmitters, which meet the demands of frequency range and stability, type of modulation and output power, may be used as radio-transmitters. Moreover, when the measuring and recording apparatus is set up on helicopter MI-4 the radio-transmitter of the key signal should permit continuous operation for 2.5-3 hrs. With the setting up of this apparatus on any other types of helicopters and planes the continuous operation period of the key signal radio-transmitter will depend on the duration of the flight with one full filling up of fuel. This specific requirement of the radio-transmitter has been noted in particular because many radio-transmitters, specially the ones in aviation, are, as a rule, estimated to operate for a short-period and when used for the transmission of the key signal during a prolonged period get overheated and go out of order.

The transmitter, included in the set of AERA-58 (Fig.90) consists of the master oscillator 5 with quartzes A and B, the multiplying stages of frequency 6, the output power amplifier 7 and the antenna 8. The modulator 4 modulates the output stage by anode and screen-grid. Through the same modulator, one-sided command radio-communication by means of the microphone 19 may also be executed.

The key-signal phase is controlled by means of a device 9, which is a ring phase-indicating detector, to one of the inputs of which is fed voltage U_b' , and to the other voltage U_b'' . From the indicator, the zero phase shift is fixed between U_b' and U_b'' . The U_b''' voltage is taken off the output of the special indicating

receiver 10, at the input of which the antenna 20 is cut in.

By adjustment of the phase inverter 3, the phase of the modulating voltage U_b'' is turned until the zero shift of phases is obtained between U_b' and U_b''' . In this way, the phase of the key signal, transmitted into the air is controlled. The oscillograph 18 controls the shape of the key signal.

On the transmitting and receiving side of the channel are the timers. The triggering of the timers is effected by the signal of the key signal radio-transmitter. With appearance of the key signal in the air, the low frequency synchronized oscillator 11 receives the triggering synchronizing voltage U_b'' , and the synchronous motor 12 power. The diagram of the oscillator 11 is constructed in such a way that, irrespective of the current frequency in cable I, voltage with frequency 40-65 cps is fed to the synchronous motor 12. Fixed on the motor axis is the needle of the seconds counter 13 and the contact system 14, which gives one impulse every 30 sec. Through the electromagnetic writing device 15 these impulses insert the time marks on the tape 17. Onto the same tape the galvanometer 16 records the current I in the cable. The command radio-communication with the measuring (mobile) devices is conducted through the helicopter radio-station.

In contrast to AERA-58, the AERA-2 apparatus does not have a device for current recording in the cable, nor a system for time marking on the tapes of pen-writers, connected with the frequency of the modulating key signal. However, the extensive productive tests of the BDK apparatus have shown, that there is continuous

current variation in cable I with non-stop operation of the generating unit (due to oxidation of grounding electrodes with the transmission of the alternating current). Moreover, there is evidence of short-period variations of voltage from the portable power plant, feeding the generating unit. Therefore, it becomes quite obvious that current recording in the cable and the timing would be expedient.

Fig.91 shows the functional diagram of the receiving arrangement of the key signal phase radio-channel in AERA-58. The modulated key radio-signal is picked up by the dowel antenna 1, pushed out of the helicopter cabin, and arrives at the amplifier of high frequency 2 of the radio receiver. Quartzes of channels A and B are cut in to the transformer 3. The fifth quartz harmonic and the receivable signal form the intermediate frequency, which is amplified by a two-stage amplifier of the intermediate frequency 4.

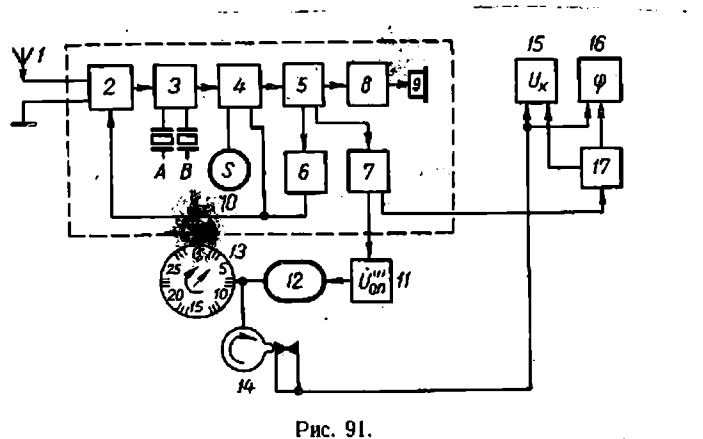


Рис. 91.

Fig.91

The transmission band $2 f_{tr} = 20$ kcps, intermediate frequency 3 Mcps. The wide transmission band on the amplifier of intermediate frequency has permitted reducing to 20-30, the phase errors of the radio-receiver, which emerge due to the withdrawal of the transmitter frequency, the heterodyne frequency, the variation of parameters of input circuits and the intermediate frequency transmitters. From the detector 5, the direct current voltage is fed to the circuit of the automatic sensitivity control 6. The automatic control is extended to the stages of HF and IF amplifiers. The indicator of the signal's magnitude 10 (S-meter) is cut in to the IF amplifier. The LF amplifier 8 and phones 9 are meant for audio-control of the key signal.

From the detector 5, the sound voltage (key signal) is fed into the input of the cathode follower 7 and, hence, to the measuring apparatus 17. The key signal also arrives at the input of LF synchroized oscillator 11. The circuits of synchroized timing oscillators in the ground and air-borne groups are identical; these are two-stage synchronized frequency dividers, controlled by modulating the voltage of the key signal. As the synchronic motors 12, energized from synchronized oscillators with frequency 40.65 cps, serve CD-2 motors with a supplementary reducer. On the shaft of the motor a needle is fixed and from the dial-face 13 it is possible to control the operation of the timer.

The pulses of direct current from the contact pair 14 are delivered to the recorders, where they are fixed as time breaks. The synchronous motor 12 begins rotating from the moment of emergence of the modulated key signal, which is cut in on the ground

generating unit at the command of the operator at the measuring instruments. In this way, synchronism is attained between the start of recording on the recording devices 15 and 16 and the ground recorder of the cable current and also the automatic printing of time breaks.

The radio-receiver of the key signal is AERA-3 is assembled on a similar circuit, but due to the lower carrier frequencies of the key signal (2.3-3.2 Mcps) the A and B quartz are used on the main frequencies without additional multiplication of frequency, and the intermediate frequency f_{tr} is assumed to be 465 kcps. The width of the transmission band on the intermediate frequency is 8-10 kcps.

The small size short-wave frequency radio-receiver with quartz control of the heterodyne frequency, devised for AERA-2 and AERA-3, could serve as prototype for the future development of similar devices. Therefore, we should analyse briefly its functional diagram, shown in Fig.92.

The HF signal of the main phase arrives from the antenna through the coupling condenser C_1 into the input circuit L_1, C_2, C_3 . Depending on the magnitude of the carrier frequency (channels A and B), a semivariable capacitor C_2 or C_3 is cut in to coil L_1 by means of change over switch Π_1 . From the input circuit through antiparasitic resistance R_1 the HF signal is delivered to the control grid of the HF resonance amplifier L_1 .

From the anode circuit L_2, C_7, C_8 the amplified HF signal is fed through separating capacitor C_9 to control the grid of the frequency

converter L_2 . Heterodyne signal L_3 with quartz crystal control is fed to the same grid.

The quartz heterodyne is assembled on the circuit of an autogenerator with electronic coupling, tuned by the circuit and quartz resonator, connected between the control grid and the cathode. This circuit is made distinct by its frequency stability of about $(1-10) \cdot 10^{-6}$ and has sufficient current amplitude of the operating frequency on one circuit. The coupled circuits L_6, C_{18}, C_{19} and L_5, C_{17}, C_{16} permit the attenuation of the high harmonics of the oscillator.

In the anode circuit of the frequency, the converter L_3, C_{13} emerges an intermediate frequency, which is further amplified by two amplification stages - L_4 and L_5 . From the last coupled circuit of the intermediate frequency $L_9, C_{34}, L_{10}, C_{36}$, the voltage arrives at the detector of the key signal - left-hand diode L_6 . The LF signal, taken off load resistances R_{33}, R_{34} , arrives at the supply circuit of the timer motor. The key signal is taken off resistance R_{34} .

For audio-control of the key signal and reception of one sided information from the generating (ground) unit, the receiver is provided with a special LF amplifier on pentode L_8 .

The right-hand diode L_6 is meant for operating within the circuit of automatic sensitivity control of the receiver. Onto its anode through the capacitor C_{39} is fed the voltage of intermediate frequency from the first circuit (L_9, C_{34}) of the

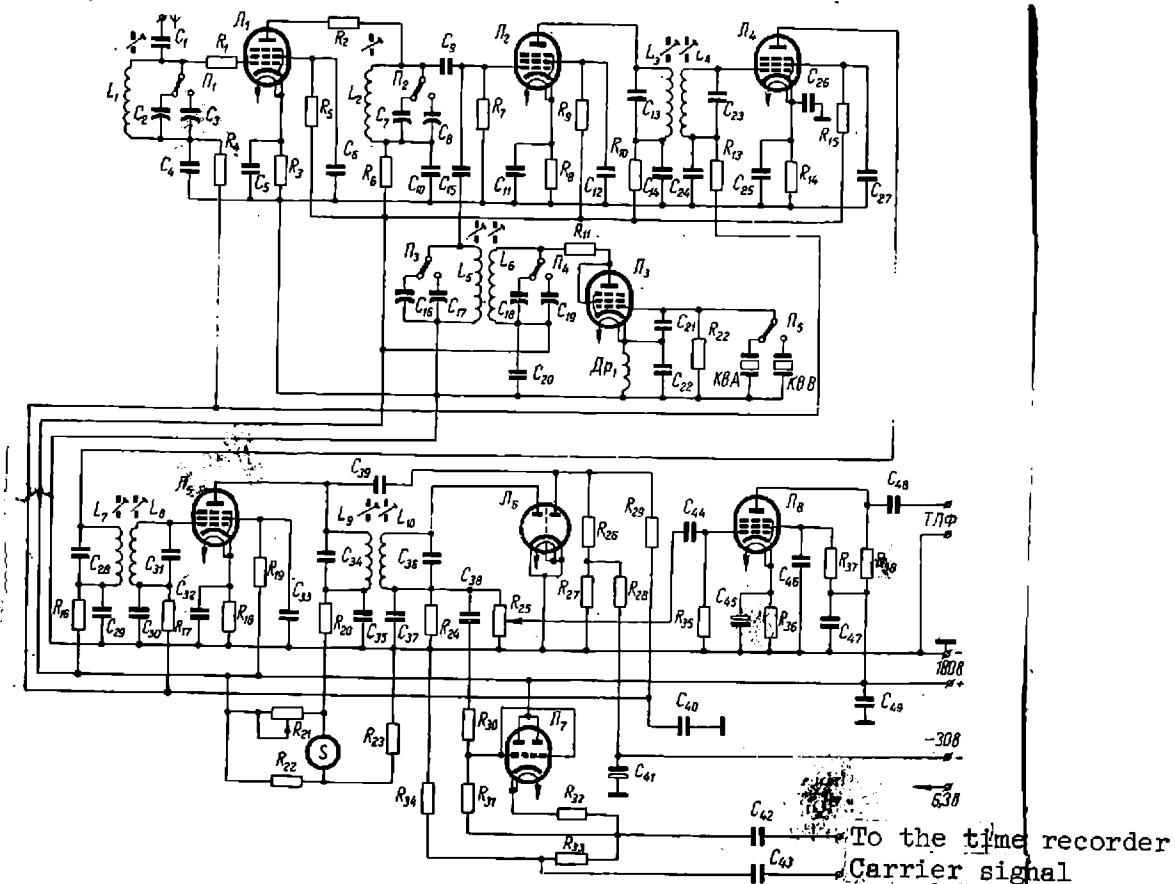


Fig. 92

last intermediate frequency transformer. The direct lag voltage is fed from the outside power source (-30V) onto dividers R_{26} , R_{27} through resistance R_{28} . The negative control voltage is taken off the anode of the right-hand diode L_6 and through resistance R_{29} and grid leak resistance R_4 , R_{13} and R_{17} is supplied to the controlling tube grids L_1 (HF amplifier), L_4 (I IF amplifier) and L_5 (II IF amplifier).

To control the magnitude of the main phase HF signal, the receiver has at the output a special device s , cut in on the bridge circuit into the anode circuit of the IF amplifier second stage. The receiver is mounted on a separate chassis and fitted into the measuring instruments block.

CHAPTER IX - INTERFERENCES IN AMPLITUDE AND PHASE MEASUREMENTS
AND THE METHODS FOR REDUCING THEIR EFFECT

1. General problems of improving protection against interference.

Distortion of the amplitude and phase of signals, received by the magnetic field detectors in the apparatus for aerial electric prospecting, besides those emerging due to changes in the geometry of the system in the near zone method, could be caused by vibrations and acoustic interferences; interference of industrial nature and from telephone and telegraph lines; interference of near-by operating radio-stations, atmospherics, the noises of magnetic field detectors, setting, or reciprocal effect, of channels (in two-frequency operations), noises of the first amplification stage, etc.

The listed interferences limit the lower threshold pickup of the measuring devices; therefore, there is the necessity for carrying out complex measures for protecting the apparatus from the effect of various types of interferences, and also the expediency of narrowing the transmission band within the region of operating frequencies in the amplifying track of the measurable signal. Therefore, limitations are imposed on the quick action and accuracy of the measuring and recording instruments as a whole and particularly in the dynamic method of operations.

The distortions are built up, as we know, by a combined action of all the listed interferences. However, the relative significance of each of these interferences in the sum total is not equal.

The possibilities of increasing the tangible sensitivity in the receiving and measuring devices depend primarily on the efficiency of the applied shockproof systems of the field detector and the choice of electric circuits for suppressing interference.

The execution of reliable mechanical shock-proofing of the field detector improves considerably the efficiency of the measuring instruments. Moreover, the application of special electric circuits for suppressing interference makes it possible to build up a highly sensitive apparatus for aerial electric prospecting, permitting the measuring of very low intensities of magnetic fields (in the order of 10^{-7} - 10^{-9} a/m).

In the resolving the problems of electric protection for measuring instruments from interference, it is necessary primarily to dampen (or exclude) interferences at their input to a level that would prevent in the amplifying track, during the amplification of the signal-noise mixing entry of the amplitude of this track's individual links into non-linear sections. If this condition is not observed, then with the high level of the signal-noise mixing, distortions of the useful signal in the amplifying track occur or even its complete loss takes place in the background of noise. In an ideal case it would be better to have a "clear" signal after passing through the magnetic field detector. However, the technical execution of this filter diagram for the various methods of aerial electric prospecting is,

unfortunately, not always possible and is, practically, unrealistic.

Digressing from the diverse specifics of these methods and taking into account the general aspects of the theory of communication (223, 225), it is possible to assume that the improvement of the electric interference-stability of the apparatus may be achieved by increasing the signal volume, characterised by its competence, width of spectrum and duration. The reserves for increasing the power of the signal in aerial electric prospecting are, as a rule, not high because of limitations of the power supply of the air-craft, the area of field emitters and the competence of the mobile ground power plants. The possibilities of expanding the signal's spectrum have so far been very little exploited, since the investigation is most often of the harmonic signals, the amplitude and phase of which vary with different rate at the moments of the appearance of anomalies. As a result, the stability of the measuring apparatus against interference may mainly be increased only on account of increase in the signal's duration. However, even this possibility is limited by the requirement of continuous recording of the signal variation during the flight of the aircraft along the profile.

The higher is the speed of the survey, the more precisely should be marked the variations of the signal receivable by the measuring and recording devices, which should be of the highest quick action and have the best quality of dynamics. With an

inadequately quick action of the apparatus in aerial electric prospecting, it is possible to miss local anomalies of short duration; the nature of the actual variations of the signal at the input of the amplifying track will be distorted and the result will be not only the difficulty of determining the location of the objects sought for but also of interpreting the obtained data. Therefore, the measuring time in aerial electric prospecting is always limited and is determined by the dynamic errors of the apparatus.

For increasing the stability of the measuring instruments against interference by increasing the duration of the harmonic signal, the filter is combined with synchronous correlational reception or with detection. In the latter case, the output of the detector is provided with LF filters (152).

The filtering method of the signal (frequency division) is usually applied directly at the input of the measuring unit and in the channel of the amplification track. This is explained, primarily, by the fact that at a low level of signals it is very difficult to build up multiplying circuits (commutation circuits), which are used in synchronous reception, whereas the resonance circuits, used in the filter method, are technically simple.

But as regards the optimum electric systems of protection against interference, with the preset dynamic characteristics of the apparatus all the electric methods of protection are equivalent. The difference between them lies in technical execution, when it is required to assure the stability of the amplitude and phase

characteristics of the amplifying track and the magnetic field detector or when it is necessary to have a bearing voltage (for instance, in synchronous reception).

In the amplification of low level signals, the filter method has undoubted advantages. However, in this case it would be impossible to obtain the simple circuits of high stability and the Q-factor. Therefore, in the apparatus for aerial electric prospecting, the potentialities of these circuits are not used fully (unless, of course, it is necessary to make them more composite, which involves an increase in the cost of the apparatus).

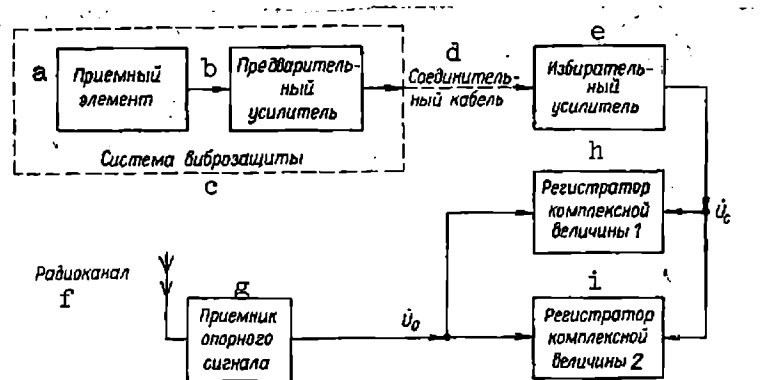
The introduction of the preliminary signal filter eliminates the effect of interference in the vicinity of frequency commutation harmonics in the circuits of synchronous reception, which has to be taken into account since the interference spectrum at the output of the magnetic field detector is sufficiently wide. On the other hand, the synchronous reception has advantages in the vicinity of the operating frequencies of the apparatus, where practically the whole selectivity of the amplifying track circuits is concentrated. The instability in the circuit of synchronous reception affects mainly the dynamic errors of the measuring and recording devices.

The theoretical analysis and practical results (89, 93, 103, 132, 152) show that effective stability of the apparatus against interference could be assured by the simultaneous application of mechanical vibration-proof systems of the magnetic field detectors and of methods free from electric interference. In the case of reception of harmonic signals, it would be more rational to assure

protection against interference by combining the electric circuits of the filter method and of synchronous reception and detection. It is expedient to cut in at the input of the measuring unit, filters with transmission band, providing for a reliable suppression of interference at medium and long distances, and having characteristics, at which instability of the parameter is of no significance. All this will eliminate distortion of the amplitude and phase characteristics of the signal in the amplifying track, or, at least, will not increase the present magnitude.

Key to Figure 93

- a, Receiving element;
- b, Preamplifier;
- c, Vibrational insulation system;
- d, Connecting cable;
- e, Selective amplifier;



- f, Radio channel;
- g, Carrier signal receiver;
- h, Receiver of complex value 1;
- i, Receiver of complex value 2.

Fig. 93

After the preliminary filtering, the measurable signal should be amplified to a level considerably higher than the zero drift of the circuits of synchronous reception or the initial non-linear sections of detecting circuits. In this case a more efficient application of synchronous reception or LF filters, connectable at the output of the detectors (including recorders which according to their dynamic characteristics, are LF filters (65, 88, 89)) is

possible. Therefore, the majority of circuits in the measuring unit are assembled according to the structural diagram shown in Fig. 93.

In this diagram the mechanical vibration-proof system is applied to the input assemblies - the receiving element and the preliminary amplifier, whereas the electrical methods of noise-proofing are all concentrated in the measuring units - the selective amplifier and the recorder of composite quantities 1 and 2. These units could be assembled for operating in the filter method as well as in the method of synchronous reception and detecting.

2. Vibratory interference.

Since the apparatus for aerial electric prospecting is set up on a mobile object, in specific conditions of application it is subject to the vibrations of high intensity of different frequencies and amplitudes and also to shock loads of different duration and intensity. The vibrations are most critical for the receiving and measuring units and specially, for those details which pick up the very low levels of the useful signal.

To free these details of interference is a complex technical problem. The main unit of the apparatus most sensitive to vibrations is the magnetic field detector. Therefore, by the vibratory interference in aerial electric prospecting is meant interference emerging in the field detector due to its vibration in the magnetic field of Earth (this type of interference is transmitted later on into the measuring track). The capacity of the magnetic field detector to withstand the vibrations, i.e., to carry out fault-free

and normal functions, is determined by its stability against vibrations.

It is well known that the pattern of the origin and transmission of vibrations is most complex (79-81); therefore, the theoretical determination of even such characteristics as frequency and amplitude of vibrations is extremely difficult. These characteristics are usually determined by tests. During the flight of the plane or helicopter usually there are vibrations, caused by the combined action of various factors, such as, for instance, the irregularity of the piston engine torque, the imbalance of the screw, the aerodynamic forces of its rotation, etc.

Investigations show (79, 81) that vibrations are characterised by value distribution and the composite nature of the amplitude spectrum. During the flight of the plane, the operating conditions of the apparatus change. The presence of transitional processes causes variation of the amplitude of vibrations within a wide range of frequency variations. According to test data, the apparatus of planes with piston engines is subject to vibrations with frequencies 10-500 cps and amplitude upto 1 mm(3). The limits of amplitude values A of the "chief" components of plane vibrations at $f=10-50$ cps, obtained by the processing of the statistical test data (113) are: in the central part of the plane $A = 0.5-2.10\text{mm}$, in the nose and tail parts: $A = 0.25-0.50$ mm the maximum vibration values correspond to the minimum frequencies of vibratory interferences).

On the helicopter the intensity of vibratory interference within the low frequency range of electric prospecting is even higher, but

its characteristics have not so far been fully investigated.

Thus, the determination of the effect of vibration on the field detector and its stability against vibrations during the flight of the aircraft is an extremely complex problem, aggravated also by the fact that the frequency spectrum of vibrations encompasses the main frequencies used in aerial electric prospecting. Moreover, it is necessary to take into account that the metal parts of the aircraft and its equipment being sources of interferences, different in amplitude and spectrum, distort the pattern of the constant magnetic field of Earth at the point of reception.

Undoubtedly, carrying of the field detector into the outboard gondola is a positive factor, since in this case the vibration effect of the aircraft itself is reduced and the effect of its metallic mass on the field structure at the point of the field detector is considerably damped. Nevertheless, even in this case vibrations of the field detector in the magnetic field of Earth cause the appearance of the interference signal on the operating frequency of the apparatus.

Let us determine which vibrations of the field detector result in the highest magnitude of interference. In the high grade field detector, we introduce the multiturn coil in the plane of the loop S. The e.m.f. of induction in the receiving coil (18) will be

$$e = - w \frac{d\Phi}{dt} , \quad (\text{IX. } 1)$$

where w - the number of loops; Φ - the flux of vector \vec{B} of inductance through the plane of turns in coil S (the geometrical dimensions of the coil are not estimated for the sake of simplicity).

We know that the flux of the vector of inductance through area S (Fig. 94) will be

$$\Phi = \int_S \vec{B} d\vec{S} = BS \cos (\vec{B}, \vec{n}^0),$$

where \vec{n}^0 - cross drift of the positive perpendicular to the plane of the coil turn.

The derivative of flux

$$\frac{d\Phi}{dt} = BS \frac{d}{dt} \cos (\vec{B}, \vec{n}^0). \quad (\text{IX. 2})$$

In Fig. 94 we have $\psi = 90^\circ$; $\alpha = \alpha_0 + d\alpha$; $\omega_\alpha = \frac{d\alpha}{dt}$; $\theta = 90^\circ - \varphi$; $\beta = \beta_0 + d\beta$; $\omega_\beta = \frac{d\beta}{dt}$; $\gamma = \gamma_0 + d\gamma$; $\omega_\gamma = \frac{d\gamma}{dt}$.

In accordance with these definitions, the angle between \vec{B} and \vec{n}^0 is determined as $\cos (\vec{B}, \vec{n}^0) = \cos \varphi \cos \alpha + \cos \varphi \cos \beta + \cos \theta \cos \gamma$ or

$$\frac{d}{dt} \cos (\vec{B}, \vec{n}^0) = - \cos \varphi \sin \alpha \omega_\alpha - \sin \varphi \sin \gamma \omega_\gamma. \quad (\text{IX. 3})$$

Considering formula (IX. 3), and also equations (IX. 1) and (IX. 2), we get for e.m.f. of the coil

$$e = w BS (\cos \varphi \sin \alpha \omega_\alpha + \sin \varphi \sin \gamma \omega_\gamma). \quad (\text{IX. 4})$$

Let us analyze formula (IX. 4). If we take $\omega_\alpha = \omega_\gamma$, $k_k =$

wBS and estimate that angle φ in northern latitudes is approximately $73^{\circ}10'$ (119), we get

$$e = k_k \omega_{\alpha} (0,29 \sin \alpha + 0,957 \sin \gamma). \quad (\text{IX. 5})$$

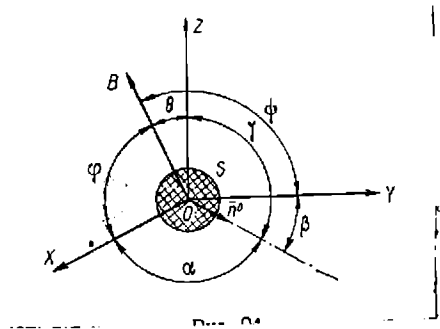


Fig. 94

This formula at $\alpha = \gamma = 90^{\circ}$ has the maximum value and, at $\alpha \rightarrow 0$ and $\gamma \rightarrow 0$ - , the minimum. If perpendicular $\overline{n^0}$ lies in the horizontal plane (for instance, horizontal projection of the vector of strength of the cable's magnetic field in the apparatus of the BDK method of the "Canadian" version of the induction method), then, at $\gamma \rightarrow 90^{\circ}$, noises in the coil are directed by both the projections of the \overline{B} vector of induction onto axes OX and OZ. When $\omega_{\alpha} = \omega_{\gamma}$, the noise form projection \overline{B} onto line OZ is three times that of the noise on line OX. The effect of the horizontal component of vector \overline{B} should be characterised by the variation of the noise level with the change in the direction of the aircraft's flight in the horizontal plane XOY.

The range of variation of the noise level depends on the ratio between ω_α and ω_γ and on values $d\alpha$, $d\gamma$ in actual application to the aircraft. Thus, with $\omega_\alpha = \omega_\gamma$, the maximum level of variation of the signal in the receiving coil, due to change in the direction of the flight, does not exceed 23%. Investigations, carried out during the flight of the aircraft in four directions of the compass along a magnetic course, have shown (89) that the noise level, induced in the receiving coil, actually changes close to the calculated level in the north and south, the noise magnitude was 10 mkw and in the east and west, 13 mkw.

In the application of certain methods, it is expedient to set up field detectors directly on the body of the aircraft. In this connection, it becomes important to determine the sections of the body of the aircraft with a minimum level of vibratory interference for the setting up of the field detector. Investigations of this type when applied to aerial electric prospecting have, unfortunately, been very few. Therefore, if the field detector has to be fixed on the body of the aircraft, instead of in the outboard gondola, the investigations are, usually, carried out in the actual conditions in the range of operating frequencies of the method applied.

For example, we shall describe the investigation technique of vibratory noise on helicopter MI-4, when the problem was to determine the location on the field detector on the tail beam of

the helicopter. Originally, it was decided that the most acceptable part of the helicopter with the least noise from vibration and electric equipment was the tail beam. Then by means of vibre-transmitters the vibration was investigated at various points of the tail beam. Mainly two types of transducers were applied bi-component piezoelectric transducer and the induction vibro-transducer (80, 81).

The measurements were mostly of the horizontal component of the vibration rate in cross-section planes parallel to the tail beam axis of the helicopter and perpendicular to this axis. The amplitude of vibration shifting was determined as the ratio of vibration velocity v to vibration frequency.

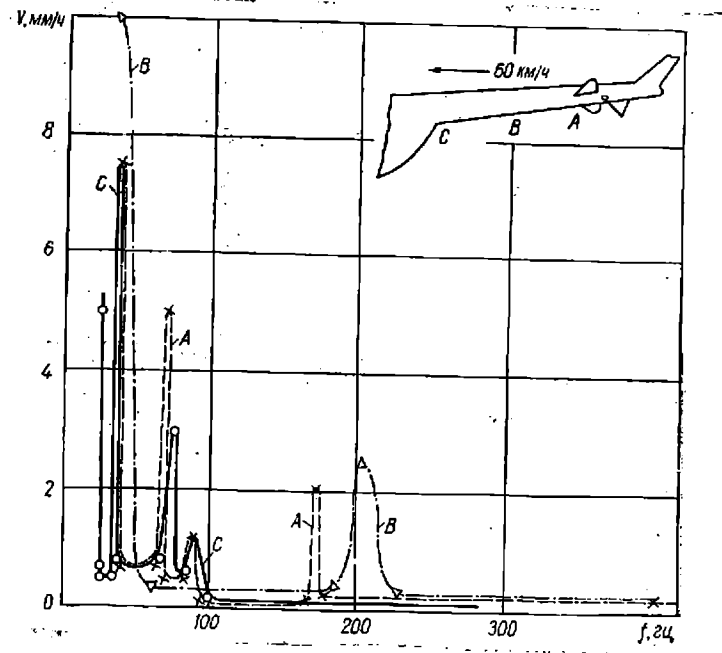


Fig. 95

On the basis of the test data the frequency distribution of

vibrations was determined on the tail beam of the helicopter (Fig. 95). This distribution is such that, on frequencies over 230 cps, the velocities of vibrations decrease almost uniformly at all the investigation points. At the lower frequencies, there is evidence of overshooting of the vibration velocity. In this way, the conclusion was drawn that on operating frequencies of the apparatus below 230 cps the protection of the receiving unit, set up on the tail beam, from vibrations should be more rigid than on frequencies 230 cps and higher.

Fig. 95

The investigations of vibratory noise, when the receiving device is set up in the outboard gondola, have shown that these noises are quite similar to the noises arising in the disposition of the receiving unit with a similar protecting system on the

tail beam, although the noise level in the first case is slightly lower and, with the increment of frequency the amplitude of noise decreases faster. It is quite possible that with the placing of the receiving unit in the outboard gondola, the noise level is affected less by the vibrating mass of the helicopter, which distorts the magnetic field of Earth at the point of reception.

In both these cases, the relationship between the noise level and the speed of the helicopter's flight is similar, with increasing speed the noise level gets higher.

Fig. 96 and Table 9 give the data of measuring, by means of the harmonics analyzer, the level of noise, equivalent to the magnetic field density H in the receiving coil on the tail beam of the helicopter at the flying speeds 60 and 120 km/hr. It was noted that in this case the noises increased at a high rate on lower frequencies (below 200 cps), on higher frequencies their increment was considerably less.

Speed of flight, km/hr.	Level of noises, equivalent to density of the field, $a/m \cdot 10^{-5}$, on different frequencies, cps										
	100	200	250	300	400	500	700	1000	1500	2000	4000
60	3,1	2,8	2,0	1,4	0,84	0,6	0,35	0,26	0,23	0,23	0,23
120	28	6	4,8	4,0	2,2	0,8	0,6	0,38	0,32	0,33	0,33

Thus to obtain the required resistance to the vibration of the receiving unit (field detector, preliminary amplifier) on low frequencies, it is necessary to provide a more efficient system of protection against vibration than on higher frequencies. It is also

necessary to try and obtain the natural frequency of the protection system below the lowest operating frequency of the apparatus, and the system itself should be fixed on a field detector close to its gravity centre.

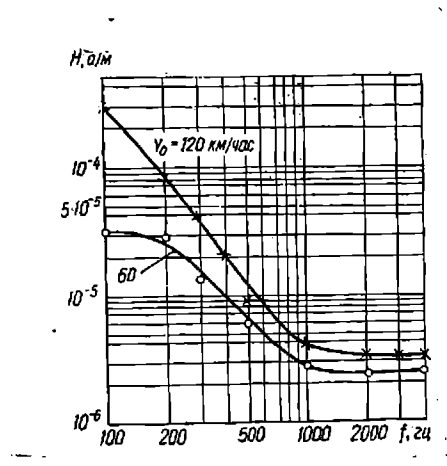


Fig. 96

The speed of the aircraft's flight always affects the magnitude of vibratory noises. Therefore, in striving to reduce these noises, the magnetic field detector is brought out from the aircraft cabin into the outboard gondola (for instance, in the apparatus of the BDK method). Sometimes, when using various modifications of the induction method, it is absolutely essential to place the magnetic field detector in the outboard gondola. In these cases it is necessary to know the behavior of vibratory noises with the let-down of the gondola from the aircraft at different lengths of the wire-cable and with changes in the flight speed.

Experiments show that, until a certain moment, the vibratory

noise initially drops sharply with the increasing length of the cable, then remains invariable or even increases, if the cable is extra long. Increased speed of the aircraft invariably increases the vibratory noise.

Table 10 shows the measuring results of the total level of the vibration and outside noises, affecting the magnetic field detector in AERI-2 apparatus of the induction method at various flight speeds when the drift angle of the gondola α varied from $60-70^\circ$ and the length of the wire-cable was 100 and 150 m (the measurements were carried out in windy weather at an altitude 900 m above the sea level).

From Table 10 it follows that with the indicated variations of flight speed the level of noises due to vibration increases on an average five-six times. On frequency 243 cps, the noise level is considerable even at the optimum flight of IL-14 plane of 250-260 km/hr. Moreover, on frequencies 243 and 487 cps with cable length 100 m, the level of noise is lower than with the length of 150 m. This is, apparently due to the fact that the natural frequency of the cable of the mechanical system given out by the gondola approaches, the natural frequency of vibrations in the mechanical system of the field detector with the increasing length of the cable. Other causes, unrelated to vibrations, were excluded in these experiments. Subsequently, a more perfect system than the one applied in these tests, has been devised and tested for the protection of the magnetic field detector from vibrations, as a result of which the level of vibration noises on all the operating frequencies

Table 10

Speed of flight km/hr.	Wire-cable length m	Operating frequency, cps				
		243	487	974	1949	3898
220	100	$\frac{8 \div 10}{16 \div 20}$	$\frac{5 \div 7}{3,3 \div 4,7}$	$\frac{1 \div 2}{0,4 \div 0,8}$	$\frac{1 \div 2}{0,2 \div 0,4}$	$\frac{3 \div 4}{0,48 \div 0,64}$
	150	$\frac{20 \div 30}{40 \div 60}$	$\frac{3 \div 5}{2 \div 2,3}$	$\frac{3 \div 4}{1,2 \div 1,6}$	$\frac{2 \div 3}{0,4 \div 0,6}$	$\frac{2 \div 3}{0,32 \div 0,48}$
240	100	$\frac{20 \div 25}{40 \div 50}$	$\frac{7 \div 10}{4,7 \div 6,7}$	$\frac{2 \div 3}{0,8 \div 1,2}$	$\frac{1 \div 2}{0,2 \div 0,4}$	$\frac{3 \div 4}{0,48 \div 0,64}$
	150	$\frac{35 \div 40}{70 \div 80}$	$\frac{6 \div 7}{4 \div 4,7}$	$\frac{3 \div 4}{1,2 \div 1,6}$	$\frac{3 \div 4}{0,6 \div 0,8}$	$\frac{2 \div 3}{0,32 \div 0,48}$
260	100	$\frac{28 \div 30}{56 \div 60}$	$\frac{3 \div 5}{2 \div 3,3}$	$\frac{5 \div 6}{2 \div 2,4}$	$\frac{1 \div 2}{0,2 \div 0,4}$	$\frac{5 \div 6}{0,8 \div 0,96}$
	150	$\frac{40 \div 45}{80 \div 90}$	$\frac{8 \div 10}{5,3 \div 6,7}$	$\frac{5 \div 6}{2 \div 2,4}$	$\frac{4 \div 5}{0,8 \div 1}$	$\frac{2 \div 3}{0,32 \div 0,48}$
280	100	$\frac{32 \div 35}{64 \div 70}$	$\frac{5 \div 8}{3,3 \div 5,3}$	$\frac{6 \div 8}{2,4 \div 3,2}$	$\frac{1,5 \div 2}{0,3 \div 0,4}$	$\frac{5 \div 6}{0,8 \div 0,96}$
	150	$\frac{45 \div 55}{90 \div 110}$	$\frac{8 \div 10}{5,3 \div 6,7}$	$\frac{6 \div 8}{2,4 \div 3,2}$	$\frac{5 \div 6}{1 \div 1,2}$	$\frac{4 \div 5}{0,68 \div 0,8}$
300	100	$\frac{35 \div 40}{70 \div 80}$	$\frac{7 \div 10}{4,7 \div 6,7}$	$\frac{5 \div 8}{2 \div 3,2}$	$\frac{2 \div 3}{0,4 \div 0,6}$	$\frac{5 \div 6}{0,8 \div 0,96}$
	150	$\frac{55 \div 66}{110 \div 120}$	$\frac{8 \div 10}{5,3 \div 6,7}$	$\frac{5 \div 6}{2 \div 2,4}$	$\frac{5 \div 6}{1 \div 1,2}$	$\frac{5 \div 8}{0,8 \div 1,3}$

N.B: (at the bottom of the table). Numerator indicates noise level (mkw), denominator - the same level, converted into equivalent density of the magnetic field.

was reduced by about half, but the nature of the relations described above remained unchanged (76).

It should be mentioned that if the field detector in the presence of harmonically varying primary field ($H = H_m \sin(\omega t)$) vibrates near its position of balance with angular frequency ω , the excitation within it is of a noise signal with a composite spectrum. With decreasing frequency of the primary field, the e.m.f. magnitude of vibration noises induced in the detector by this field also decreases. The resultant field density at the point of the field detector is invariably much less than the intensity of the constant magnetic field of Earth. Therefore, in spite of the fact that the individual harmonics vibration noises of this type are included in the frequency range of the apparatus, the vibration noises have practically no perceptible effect on the measuring apparatus, if it is of high selectivity. This is explained by the fact that the spectral power of these vibration noises, which falls to the narrow band of transmission in the vicinity of the operating frequencies, is comparatively low.

3. Outside interference.

The outside interferences, which affect the receiving - measuring apparatus, are those not directly connected with the aircraft, but caused by atmospherics and the effect of broadcasting and special radio-station fields.

Let us analyze more fully of interferences of this type.

Atmospheric noise. The noises caused by atmospheric discharges or electrification of air masses or aqueous vapours of atmosphere, are always present and affect the field detector with some medium

level, depending on meteorological conditions. Therefore, these are referred to the constantly active interferences.

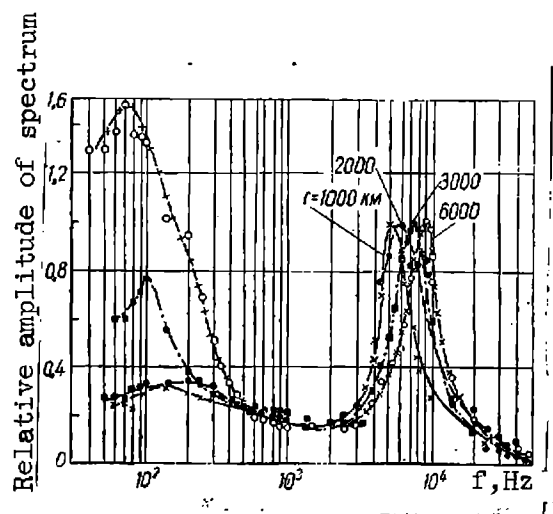


Fig. 97

Statistical data show that on an average about a 100 lightnings per second are observed on the Earth. Lightning interferences have impulsive nature and the frequency spectrum, in which the major part of the energy is concentrated, is 0.05-30 kcps (109, 156, 173). The intensity of the electric portion of the interference field caused by lightning is considerable even at a distance from the storm source of upto several thousands of kilometers, as the peak current within these surges is very high - in the order of tens of thousands of amperes; the lightning power is immeasurably greater than the power of major radio-stations. With propagation, lightning interferences become partially dampened, and yet the total field of interferences from individual sources or lightning discharge could be quite considerable in magnitude at the recording point.

The lightning noise level - a time variable quantity - varies considerably in relation to the geographical latitude (in southern latitudes the noise is considerably higher than in northern), the

frequency, at which the noise level is being determined (it may roughly be assumed that the intensity of atmospherics is inversely proportional to frequency) and time of the day and the year.

The qualitative evaluation of atmospherics could be implemented on the basis of the data in (173), which establishes that their amplitude spectrum in the low frequency range 0.05-10 kcps has two clearly defined peaks: one within the range 0.05-0.1 kcps, the other within that of 6-8 kcps. The interference trough is on frequencies 1-2 kcps.

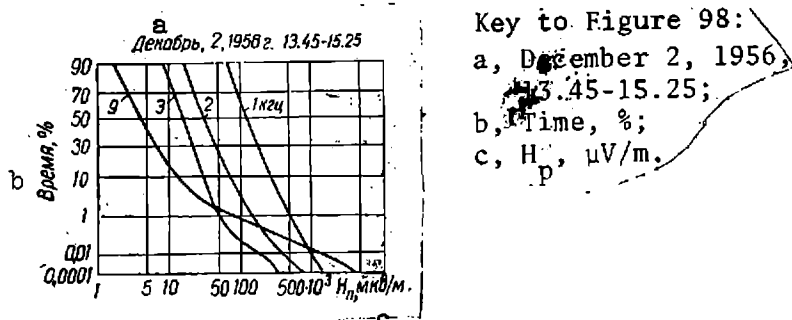


Fig. 98

The typical specifics of atmospherics are marked in Fig. 97, which gives the test data of "medium" spectra, obtained in work (156) for distance r from the storm centre of 1000; 2000; 3000 and 6000 km. The figure shows that with increasing distance from the source of noise the high-frequency peak is shifted into the region of higher frequencies (5-10 kcps) and the so-called tail peak shifts, on the contrary, into the region of lower frequencies (200 - 70 cps). Moreover, the peak ratio of the low-frequency portion of the spectrum becomes five times higher: from 0.3 at

$r = 1000$ km to 1.5 at $r = 6000$ km.

Thus at comparatively small distances (1000-2000 km) from the storm centre, the predominant signals in the atmospheric spectrum are of higher frequencies (4-10 kcps). With increasing distance, these signals attenuate much more intensely than those of low frequency, therefore at $r = 6000$ km the predominance in the interference spectrum is of signals with frequencies 60-100 cps. The work (156) shows that during a diurnal period there is a comparatively high and stable noise level and the high-frequency parts of the spectrum during a period of 24 hrs., as well as at different times of the year are subject to more perceptible variations.

The variation curves of relative duration of atmospheric noises H_n on frequencies 1; 2; 3 and 9 kcps vs. intensity of their field (173) are shown in Fig. 98. From this figure it is clear that on frequency, for instance 2kcps; in 70% of the recording time the field's intensity remains not more than 25 mkv/m and only $10^{-3}\%$ - 500 mkw/m. The transmission band of the measuring unit, read at level 0.5 has 140 cps, recording time on each frequency - about 3 min.

Fig. 99 shows the frequency characteristics (spectra) of the atmospheric field for time intervals of relative duration 70; 0.1 and $10^{-4}\%$ (curves I, II, III).

The recording time in the range 1-100 kcps was 1.5-2 hrs; the transmission band of the receiving frame - 140 cps (173). The curves in Fig. 99 show that the rare major impulses are minimal on

frequencies 2-3 kc. The "constantly active" component of noise increases with reduced frequency. For comparison with the data (173) the dotted line shows curve IV of field density of interference according to the data of measurements conducted by the Physico-Mechanical Institute AN Ukraininan SSR, in the area of L'vov on June 19, 1958, in cloudless weather. The indicated noises correspond to the arithmetical average of maximum noises. AN Ukrainian SSR and AN USSR have carried out observations, which have shown that the highest atmospherics are evident in the frequency range 40-100 cps. The conclusion was drawn that only in the comparatively low frequency spectrum can the atmospherics affect perceptibly the measuring apparatus with a threshold pickup of about 10^{-7} a/m (at these frequencies the noise levels are commensurable with useful signals); on other frequencies there was no evidence of appreciable noises.

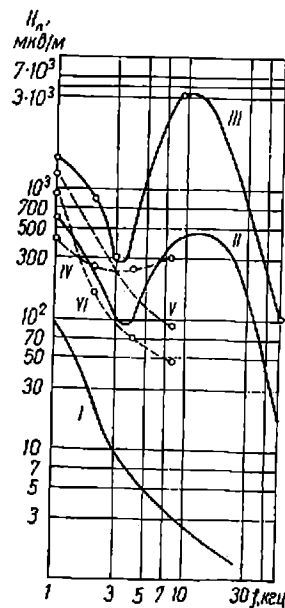


Fig. 99

Table 11

Frequency cps	Noise intensity, mkw					
	U_1	U_{II}	U_{III}	U_{IV}	U_V	U_{VI}
487	-	-	-	2,5	7,0	7,0
974	0,5	2,9	8,7	2,0	4,0	5,4
1959	0,25	1,9	7,7	3,0	1,1	3,4
3898	0,11	1,9	9,5	5,0	1,1	2,6

Remarks: (At the bottom of the Table) Legend: U_1 - voltage induced by "even" noise; U_{II} - voltage build up by impulses, duration of which is 0.1% of the observation time; U_{III} - voltage build up by rare impulses of highest intensity; U_{IV} - average value of highest noise impulses, measured on the Earth surface in June, 1958; U_V - average value of highest noise impulses, recorded during flying tests in January, 1958, with gondola let down to 100m; U_{VI} - ditto, but with drawn up gondola.

Table 11 gives the values of the intensity of noises, induced in the field detector on operating frequencies of aerial electric prospecting by the electric portion of the noise field. These values are calculated from curves I-VI, shown in Fig. 99 (according to the data of FMI AH Ukrainian SSR).

The measurements were carried out by means of "aerial" frame, in which at frequency $f = 974$ cps and the density amplitude of magnetic field $H_m = 8 \cdot 10^{-6}$ a/m. The induction was of e.m.f. with virtual value 7.5 mkw. The intensity of noise caused by the lightning discharge in the receiving frame exceed this value at some operating frequencies.

The outside interferences, including atmospheric, measured mostly in suitable meteorological conditions by the AERIS apparatus in 1959 and by AERI-2 in 1961-1962 (Table 12), have shown that according to frequencies these noises, on an average may be taken as stable. However, in magnitude, specially on low operating frequencies, interferences exceed the threshold pickup of the apparatus. Inclusion as the main component in these measurements was made of vibration noises, particularly perceptible on low operating frequencies of the apparatus (243; 487 and 974 cps).

Table 12.

Type of apparatus	Place and time of measuring	Frequency, cps				
		243	487	974	1949	3898
AERIS	L'vov area 22-5-59	-	$\frac{6 \div 9}{5 \div 7,5}$	$\frac{20}{6,7}$	$\frac{12}{2,4}$	$\frac{9 \div 12}{1,3 \div 1,7}$
	L'vov area, 8-6-59	-	$\frac{5 \div 10}{4,2 \div 8,3}$	$\frac{9 \div 12}{3 \div 4}$	$\frac{13 \div 15}{2,6 \div 3}$	$\frac{6 \div 8}{0,8 \div 1,1}$
	L'vov area, 23-6-59	-	$\frac{6 \div 9}{5 \div 7,5}$	$\frac{15 \div 18}{5 \div 6}$	$\frac{6 \div 9}{1,2 \div 1,8}$	$\frac{4 \div 8}{0,6 \div 1,1}$
AERI-2	Karelia, summer 1962	$\frac{21 \div 30}{43 \div 60}$	$\frac{3,5 \div 6}{2,3 \div 4,0}$	$\frac{3,5 \div 5,5}{1,4 \div 2,2}$	$\frac{2 \div 5,2}{0,4 \div 1,04}$	$\frac{9,7 \div 11,5}{1,6 \div 1,8}$

N.B: 1. The numerator shows noise level (mkw), the denominator - the same level converted into equivalent field density (10^{-7} a/m). 2. Investigations, carried out with apparatus AERI-2 in Karelia during summer, 1962, have shown that the noise level was on an average 6-15 mkw, and in conversion to intensity - $(2.5-4.0)10^{-7}$ a/m.

In cloudy weather, specially on frequencies 243 and 487 cps, the noise level rises. It may be assumed that the cause of it is the number and intensity of lightningless discharges in the clouds. It should be kept in view that these discharges could be dangerous source of interference in the presence of capacitive routes for their penetration into the receiving-measuring unit. Therefore, the receiving frame and input circuits of preliminary amplification require careful screening. Interference is possible also from the electrization of the plane and gondola's body during the flight through atmosphere zones of different potential. However these noises are not stable nor constantly active. The route for their penetration into the receiving and measuring devices is also through capacitance couplings. These noises are dampened by careful screening of the input circuits.

Interference from broadcasting stations.

Signals of broadcasting and other radio-stations, including those set up on board the aircraft, which carries the apparatus of aerial electric prospecting, affect mostly the first stage tube of the preliminary amplifier. Within the tube, due to the inevitable non-linearity of its characteristics, their rectification occurs. But the direct effect of radio-station signals on the following stages is not particularly dangerous, since the level of operating frequencies of the useful signals is sufficiently high. At the same time, there is concentration of frequency selectivity in these circuits, which is an LF filter in relation to the noise

signal. It is obvious that the reduction in the apparatus of noises of this type should be effected in two ways: by a build-up of obstacles to their penetration into the input of the amplifier and the choice of linear operating conditions of the first tube in as great a dynamic range as possible.

Obviously with negligible distances from the broadcasting radio-station (tens of kilometres) and its sufficiently high power (hundreds of kilowatts) the field density is considerable. Due to this, it is difficult to assure an admissible level of outside noise at the input devices of the apparatus. In this case the aerial geophysical survey should be carried out during the non-working hours of the broadcasting radio-station.

It must be pointed out that the noises built up by any radio-stations of the aircraft, on which the apparatus of aerial electric prospecting is set up, considerably exceed the admissible level; therefore, simultaneous operation of the radio-stations and the measuring apparatus is impossible. To suppress the noises, build-up by radio-transmitters only is possible; the radio-channel has several fixed frequencies (87, 102), which makes it possible to select the frequency less subject to interference.

Let us determine the admissible value of radio-noise intensity on the grid of the first amplifying tube of the gondola amplifier due to the effect of amplitude modulated signals of radio-stations, at which the audio component of the anode current of the tube will correspond to the lower limit of the measurable field or the threshold pickup of the apparatus.

To determine the low-frequency (audio) component let us show the anode current of tube i_a vs. voltage on its first grid E_g and U_{in} by Taylor series:

$$i_a = f(E_g + U_{in}) = f(E_g) + f'(E_g) U_{in}' + \frac{1}{2} f''(E_g) U_{in}^2 + \dots, \quad (\text{IX. 6})$$

where $f'(E_g) = S$ - steepness at the operating point; $f''(E_g) = S'$ - derived steepness at the same point.

With the arrival at the grid of the amplitude-modulated signal, determinable by the term $U_{in} = U_{m_0}(1+m \cos \Omega t) \cos \omega t$, audio component will appear in the anode current of tube the amplitude of which component I_m could be found from the third term of the series:

$$\frac{1}{2} f''(E_g) U_{in}^2 = \frac{1}{2} S' U_{m_0}^2 (1 + m \cos \Omega t)^2 \cos^2 \omega t, \quad (\text{IX. 7})$$

where m - the modulation factor of radio-noise; U_{m_0} - the amplitude of the carrier frequency of the radio-signal; Ω - the modulation frequency.

Since

$$\cos^2 \omega t = \frac{1}{2} + \frac{1}{2} \cos 2 \omega t,$$

by opening the brackets and ignoring the low values, we find the amplitude of the anode current:

$$I_{m\Omega} = \frac{1}{2} m S' U_{m_0}^2. \quad (\text{IX. 8})$$

The intensity of noise on the tube grid, equivalent to audio intensity, is determinable from the equation

$$U_{a.noise} = \frac{I_m \Omega}{S} = \frac{1}{2} m \frac{S'}{S} U_{m_0}^2. \quad (IX. 9)$$

Hence the intensity of radio-noise, equivalent to the signal voltage of audio frequencies on the first tube grid, will be

$$U_n = \sqrt{\frac{2U_{a.noise} S}{m S'}} \quad (IX. 10)$$

This equation permits drawing a conclusion that the rectification effect of the tube depends on the ratio $\frac{S'}{S}$, which may also serve as a criterion for the selection of the tube for the first amplifying stage of the preliminary or gondola amplifier.

Example. We assume that the threshold pickup of the apparatus on frequency 974 cps is 10^{-7} a/m and that the admissible voltage $U_{a.noise}$ from the radio-noise should be five times less than the threshold value of the usable signal voltage E_c at the output of the magnetic field detector. Moreover, we have the following parameters of the field detector: $S_d = 10 \frac{V}{a/m}$ $Q_k \approx 20$.

According to data (132), taking into account the equation (VII. 3) for the signal, $E_s \approx 2.7$ mkw.

Considering that voltage $U_{a.noise} = \frac{E_s}{5}$ should not exceed 0.5 mkw, we determine from formula (IX. 10) the admissible voltage of radio-noise U_n , equivalent to the voltage of the audio-frequency signal of the first tube grid. For calculations from formula (IX. 10)

it is necessary to know m values (we take $m = 0.9$), S and S' . The derivative S' is easy to determine by tests from characteristics $i_a = f(U_a)$ at $E_g = \text{const}$, where U_a - the voltage on the tube anode. For operating the circuit by the tube 6Ж1П it is determined that $S = 0.8 \text{ ma/v}$, and $S' = 0.33 \text{ ma/cv}^2$. After substitutions in formula (IX. 10), we get $U_n = 1.6 \text{ mv}$.

If the frequency of radio-interference from the orbadcasting station $f_{b.s.}$ considerably exceeds the resonance frequency f_o of the magnetic field detector, the setting pattern at the input of the measuring apparatus changes to some extent. Indeed with $\omega_o LK = \frac{1}{\omega_o C_o}$, when $\omega_{b.s.} \gg \omega_o$, the principal energy of outside interference is sensed by the inductance of the field detector, since $\omega_{b.s.} LK \gg \frac{1}{\omega_{b.s.} C_o}$, and $\omega_{b.s.} LK \gg 4$. Therefore, it may be assumed that

$$U_n = E_n \frac{\frac{1}{\omega_{B.C} C_o}}{\omega_{B.C} L_k} = E_n \left(\frac{f_o}{f_{B.C}} \right)^2. \quad (\text{IX. 11})$$

where E_d - the voltage at the input of magnetic field detector, and

$$f_o = \frac{1}{6,28 \sqrt{L_k C_o}}$$

Let us determine the electrical constituent of the $E_{b.s.}$ field, affecting the magnetic field detector in these conditions and inducing on the first tube grid signal E_d . It is a known fact (165), that

$$E_{\pi} = h'_d E_{B.C}, \quad (IX. 12)$$

where h'_d - the virtual height of the magnetic field detector, equivalent to the receiving antenna, which is not tuned into resonance in respect of the radio-broadcasting station field. In this condition, for h'_d we will have

$$h'_d = \frac{2 \pi f_{B.C} C_{\pi} Q'}{3 \cdot 10^8}, \quad (IX. 13)$$

where the quality factor of the circuit on the frequency of the radio-station $Q' = \frac{\omega_{bs}^{LK}}{r}$.

Having substituted equation (IX. 13) into equation (IX. 11), we obtain

$$E_{B.C} = \frac{U_{\pi}}{\left(\frac{f_o}{f_{B.C}}\right)^2 h'_d} = U_{\pi} \frac{3 \cdot 10^8}{\omega_o C_{\pi} Q_k} \quad (IX. 14)$$

If $U_d = 1.6$ mv on frequency $f = 974$ cps and $Q_k = 20$, then with the frequency of the carrying radio-sation $f_{b.s.} = 1000$ kcps it will be

$$E_{b.s.} = 1.6 \cdot 10^{-3} \frac{3 \cdot 10^8}{6.28 \cdot 974 \cdot 780 \cdot 20} \approx 0.65 \text{ v/m.}$$

Assuming that the field density of radio-interference, considerably removed from powerful broadcasting stations, is 0.1-0.05 v/m, then according to the given estimate the

receiving frame is a sufficiently good filter of low frequencies and assures the normal operation of the receiving and measuring devices in these conditions. The short-wave interferences are suppressed by the receiving frame to an even greater extent.

More dangerous are interference impulses, for instance the interferences from radio-locating stations. Their magnitude could be so great that the normal operations of the apparatus could be disrupted. However, an interference of this type is invariably of short duration and, in some areas of aereoelectric prospecting, such interferences could generally be absent. Moreover, there are circuit which permit the interference impulses compensating almost fully.

In industrial areas and in electrified villages, interferences from high-power transmissions, telephone lines, etc. can create certain difficulties for the survey. It is particularly difficult to build-up protection against the comparatively high level of interference from telephone-telegraph lines and the lines of radio-broadcasting due to their wide band of frequencies, which encompasses practically the whole operating frequencies, range of the electroprospecting apparatus. In the actual conditions of survey, when the investigation areas are invariably selected far away from industrial objects and the indicated interferences are hardly expected, no special protection against these interferences has so far been provided in the prospecting apparatus.

4. Apparatus noise.

The apparatus noise in aerial electric prospecting is that

originating from the disturbing factors directly in the apparatus set, and possibly due to intrablock parasitic coupling. The latter could, in certain conditions, cause the appearance of so called parasitic inducting* on the receiving-measuring circuit, i.e., result in the emergence of specific interference.

Apparatus noises usually originate due to the following causes the presence of powerful generating units in the direct vicinity of the measuring and receiving instruments of the near zone methods and working, as a rule, on the same frequencies; the operation of various transformers (voltage, current or frequency) in the apparatus set, meant for energizing individual assemblies, blocks or units or for the control of their operation;

the recording of measurable quantities by recorders with motors and mechanisms for marking the limits of recording, guiding lines, etc. :

the action of parasitic couplings inside the apparatus (for instance, coupling through general resistances, capacitances or inductivity):

by the jumps of direct-current voltage with cut-in of various auxiliary devices:

the inducting caused by the presence of intra-apparatus electromagnetic field, etc.

Due to parasitic coupling between radio-electronic units and assemblies, pertaining to the supply system, specially with the use of the alternating current network (for instance, with frequency

*Parasitic inducting means transmission of voltage from one element (assembly) into another, not provided for by the diagram or design of the apparatus or arrangement.

400 cps), there is the possibility of appearance of a background with frequency equal to, or a multiple of, the supply frequency.

In considering parasitic induction, the matter is usually concerned with the source of the inducible voltage, the receiver of inducible voltage and parasitic coupling between them. To define them directly is the most difficult problem in the elimination of parasitic inductions.

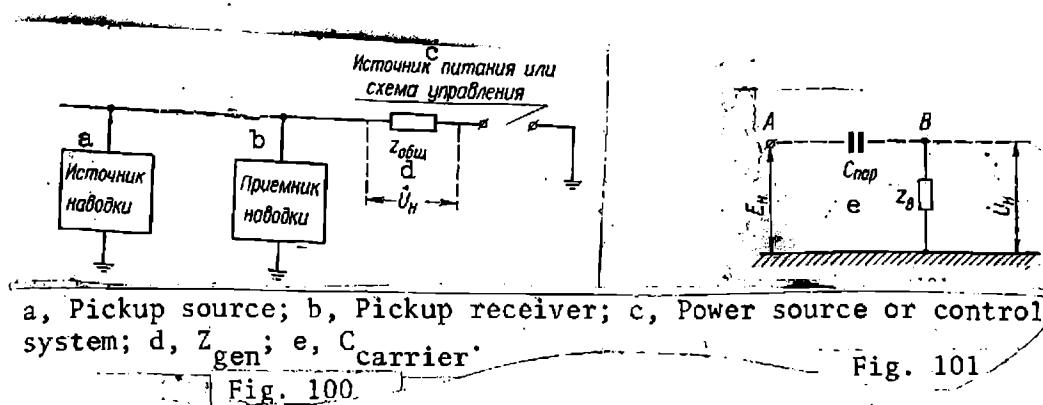
Various forms of parasitic couplings and inductions in radio-technical apparatus and possible measures for controlling them were analyzed in considerable details in a number of works (23, 45). Let us analyze briefly the main ones of these, namely, those which are in some measure characteristic of the apparatus of aerial electric prospecting.

Parasitic coupling through common resistance is effected most frequently through resistance consisting of the inner resistance of power supply sources, the control circuits of radio-unit operation and the resistance of connection wires.

In the parasitic coupling's circuit of this type (Fig. 100), the currents of all frequencies are transmitted through the circuit of the source of power supply, composing the signal spectrum of the inducting source. These currents cause voltage drop on all resistances cut into the power supply circuit. A part of the resistances composes the common resistance of coupling Z_{com} , cut into the circuit of the induction receiver, and the voltage U_n , taken off this resistance, is the main induced voltage. Generally, the resistance value of parasitic coupling depends on the frequency of the inducible voltage.

For low frequencies, this resistance is made up mainly of the direct current resistance of connecting wires and the capacity reactance of the output capacitor of the power supply filter. Therefore, at low operating frequencies and with low frequency source of induction due to insignificant Z_{comm} , the induction voltage U_i is also insignificant. On some high frequencies, where the inductance effect of connecting wires and distributed capacitance of cabling is quite appreciable, with an infelicitors combining of the value of these inductances and capacitances, the Z_{comm} may be considerable, which will result in increasing the U_i also.

Parasitic capacity coupling is caused by the presence of the common metal chassis, with which the connection of some points in the circuit of the measuring device is made. This coupling is dangerous on high frequencies, since with this connection, excuted directly or through the blocking capacitor, the appearance of high-frequency voltage between each point of the aircuit and the body of the device is possible.



The circuit diagram of the parasitic capacity coupling is shown in Fig. 101. The voltage divider consists of two resistances -

capacity reactance X_{par} and ballast resistance Z_B . If at some point A, the voltage in relation to the body is E_1 , then at point B, coupled with point A by parasitic capacitance C_{par} , induced voltage U_i , appears, the intensity of which is determinable by the ratio of capacity reactance

$$X_{\text{par}} = \frac{1}{j\omega C_{\text{par}}}$$

and total ballast resistance Z_b between point B and the body. The intensity of \dot{U}_i can be determined from formula

$$\dot{U}_h = E_h \frac{Z_b}{Z_b + X_{\text{nap}}} \quad (IX. 15)$$

Hence it follows that the voltage induced at point B will be all the higher at the least capacitance X_{par} and the highest resistance Z_b .

In some cases, resistance Z_h could be the resonance resistance of LC-circuit, tuned to frequency ω_0 of the induction source. If in this case $X_{\text{par}} \gg Z_b$, then from (IX. 15) we get

$$\dot{U}_h = E_h \frac{Z_b}{X_{\text{nap}}} = E_h \frac{j\omega_0 C_{\text{nap}}}{\omega_0 C d_e} = E_h \frac{jC_{\text{nap}}}{Cd_e}, \quad (IX. 16)$$

where C - the capacity of resonance circuit, and d_e - its equivalent attenuation.

Parasitic flux linkage. In conductors subject to the effect of the variable magnetic field, there is excitation of variable e.m.f., the intensity of which rises with increasing frequency. The equivalent

circuit of flux linkage is shown in Fig. 102.

In the presence of outside wire AB, both the elements of the circuit are flux-linked. The intensity of coupling is determinable as mutual inductance M_1 of AB wire in relation to the induction source or mutual inductance M_2 of the same wire in respect of the induction receiver, as well as by the total resistance Z_{AB} , which has an outside wire in relation to the body.

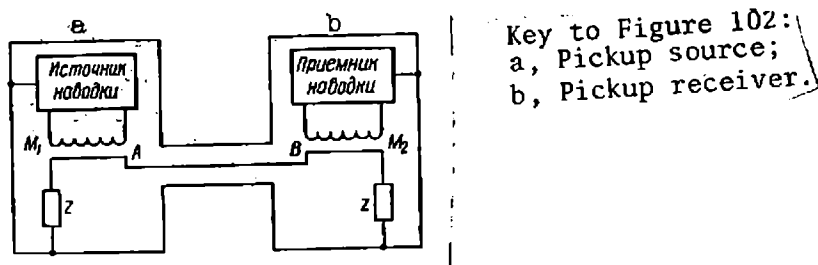


Fig. 102

Parasitic coupling through electromagnetic field leads to the appearance of methodical interferences, which are being analyzed below; this is characteristic of the induction methods in aerial electric prospecting, especially in the methods of the near zone.

Jump of direct-current voltage is the cause in many cases of high-frequency induction along the circuits of parasitic coupling in the elements of the apparatus containing resonance circuits (builds up impulse excitation or ringing). Each jump of voltage or current in the circuit corresponds to one high-frequency attenuating impulse (Fig. 103). Parasitic impulse excitation is possible with the cut-in of individual devices during the operating period of the measuring apparatus, for instance of recorders. In this case, there is an appearance of induction, the

intensity of which increases with the application of amplifying systems with high amplification factor, when the jump of the voltage is quite sufficient to bring up low power at the input to intensities, which may build up an appreciable interfering effect at the output of the measuring device.

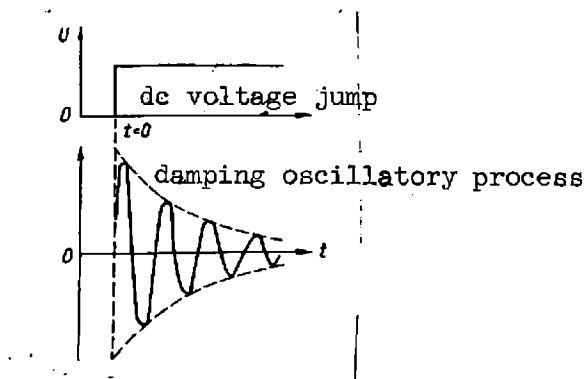


Fig. 103

The above indicated parasitic inductions are eliminated mainly by rational selection of block constructions, their careful electrostatic and magnetic screening, reasoned and well - executed arrangement according to the recommendations of a number of works (23, 49, 194).

Apparatus interferences also include the fluctuation noises of the field detector, the input circuits of measuring devices and the microphonic noise in these circuits. These interferences result in the increment of the basic error of measurements by measuring instruments, which is quantitatively estimated in Chapter XIII.

5. Interferences from the aircraft.

An aircraft, inasmuch as it includes a set of electro - and

radio-equipment, rotating elements building up sound oscillations, is a source of interference for the highly-sensitive measuring apparatus of aerial electric prospecting set up on it. These interferences are specially high in helicopters, heavy and medium planes. In the event of the field detector being located in the direct vicinity of an aircraft or at some of its parts (for instance, rigid and combined arrangement of the source and receiver of the field in the apparatus of the induction method) these interferences increase sharply.

Let us analyze the main types of interferences from the aircraft.

Acoustical interference. Noises of the working engine and rotating propeller blades of the plane or helicopter cause in the field detectors acoustical interference. The effect of sound wave may cause changes in the corresponding reciprocal position of the loop and the rod in the coil of field detectors, in the geometrical dimensions of core made of soft magnetic material, etc. As a result of this induction appears on the operating frequency.

The investigate acoustical interference, the following experiment was conducted during development and the tests of apparatus for the BDK method. The microphone and the ferrite receiving coil were placed on rubber, stretching inside a special sound-absorbing box (upholstered inside with felting and having a removable cover). The whole system was also shock-proofed and placed on the tail beam of the helicopter MI-4. During the flight, the interference was measured, first with closed cover and then with an

open one, in the receiving coil and in the sound pressure in the microphone. In the second case, the intensity of interference in the receiving coil was reduced to some extent, whereas the sound pressure decreased ten times. This indicates that although the level of acoustical interference is negligible as compared to vibration interference, it has nevertheless to be taken into account.

The tests carried out afterward on the ground have shown that the acoustical interference is approximately equal to the atmospheric. Thus, on frequency 1000 cps, some increment of acoustical interference in respect of the atmospheric level (from $8 \cdot 10^{-8}$ to $6.4 \cdot 10^{-7}$ a/m) was evident with the operating engine of the helicopter. The same results were obtained on frequencies 80-4000 cps.

Therefore, the field detectors, located in the vicinity of acoustic noise source, should be, sound-proof. Consequently it would be expedient to use a frame filled with sound-proof material, such as felting, foamrubber, cotton-wool, etc.

Interference from electric and radio equipment. The main sources of these interferences are the ignition system of motors and electric generators of the power supply network of planes or helicopters.

The measuring of levels of these interferences and determination of their frequency range, for instance, in IL-14 plane, have shown that with insignificant removal from the aircraft the interference level considerably decreases and, beginning from approximately 20-25 m, is practically unchangeable, remaining equal to the general level of interferences, sensed by field detectors with non-active electric

equipment.

Similar investigations were carried out on MI-4 helicopter. it was established that bringing out the field detectors into the outboard gondola at a distance of over 20 m for the plane and 10 m for the helicopter reduces interferences to the level of atmospherics. Therefore, with the removal of field detectors to the specified distance, interferences from electric equipment need not be taken into account. As regards the frequency spectrum, the tests have shown that it completely encompasses the operating frequency range of the apparatus in aerial electric prospecting (70-10,000 cps). The interference peaks are evident in the range of 100-500 cps and on frequencies in the order of the first tens of megacycles.

With the disposition of the receiving elements in the direct vicinity of the motors the level of interferences of this type considerably increases and may exceed tolerance limit. Instead of the usual "smooth" interferences, in this case there is the emergence of impulse interferences of various level and recurrence frequency. Therefore, in this case, there should be careful screening of field detectors and protection against the sparks of ignition circuits and power sources of board-network and board-apparatus.

The radio-equipment of the aircraft and instruments of navigation are also interference sources for the apparatus of aerial electric prospecting. Specially interference from the aircraft radio-station. Therefore, as pointed out, simultaneous operation

of the radio-station and the prospecting apparatus is impossible.

Radio-compass and radio-altimeter are practically non-interfering or their effect is negligible with proper screening of the input circuit of the amplifying channel. More likely, the prospecting apparatus interferes with their precise operation. Therefore, these instruments require correction in their indications in flights with the apparatus.

It would be relevant to mention here that there is unfortunately, no complete information available regarding interferences during the flight of any one aircraft, which interfere with the operation of the set up electroprospecting apparatus. This should be kept in view when working out the method for aerial electric prospecting.

Here is a method for investigating interferences on board the aircraft. On the MI-4 helicopter, the investigation, first of all, is of the effect of electric and radio equipment on the magnetic field detectors, set up at various points in the cabin and outside it. This is necessary to define the possibility of setting up multiturn coils with or without cores directly within the cabin of the helicopter, and also for obtaining the alignments of the helicopter in flight with the set up of all measuring and recording apparatus inside the cabin (the apparatus would then be in the center of gravity of the helicopter). Moreover, it is also necessary to determine the possibility of reducing the effect, on receiving elements, of interferences from the electric and radio equipment of the helicopter and of the measuring apparatus itself, set up on

board, by scattering in space the source and receiver of interferences.

The effect of interference by the electric and radio equipment of the helicopter on the receiving elements was determined according to the diagram shown in Fig. 104. During the tests, the ring-shaped coils 1 were in the shaft cut in the floor according to the center gravity of the helicopter. To the left of the receiving coils block was the measuring apparatus 2, to the right - power supply sources 3. Next to the coils were the batteries of the helicopter 4. The receiving unit with ferrite receiving antennas 5 was placed on the tail of the helicopter.

The ring-shaped receiving coils were meant not only for measuring and the study of interferences within the cabin of the helicopter, but also for investigating the behavior of the spatial horizontal and vertical components of the cable's field during the flight of the helicopter at various altitudes, etc. At other points, interferences were measured by a portable ferrite receiving coil and by a unit, the diagram of which is shown in Fig. 105. As analyzer of harmonics, the analyzer of infra low frequencies, devised by L'vov polytechnical institute, was used. Frequency range 20-8000 cps, Q-factor of selective amplifier in operations within narrow band - 25.

To separate the interferences of electromagnetic origin, inducible in receiving elements, built-up by the electric equipment of the helicopter and the measuring apparatus itself, from those caused by vibrations, the mechanical, coupling was preliminarily

dislocated between these devices and the helicopter's body (the use was of a special system for protection against vibration).

The first experiments with the apparatus, set up in the helicopter, have shown that the integral level of interferences in the range 40-8000 cps, which takes place in the cabin during the flight of the helicopter and equivalent field density $2.4 \cdot 10^{-3}$ a/m, is reduced by five-ten times on the ground; other interferences inside the cabin were considerably less than those indicated. Interferences during the flight increased with the cut-in for charging from the board generators of direct-current batteries by means of board automatics.

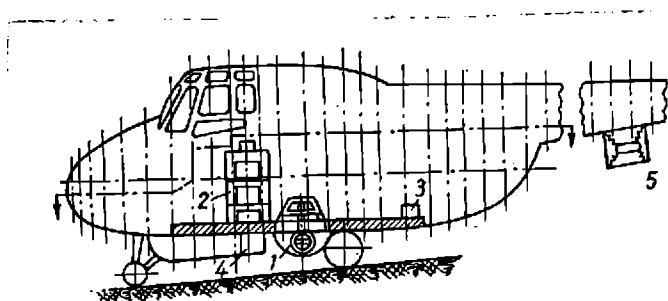


Fig. 104

Key to Figure 105:
a, Power block (dc sources); b, Receiver coil; c, Wideband amplifier; d, Harmonic analyzer.

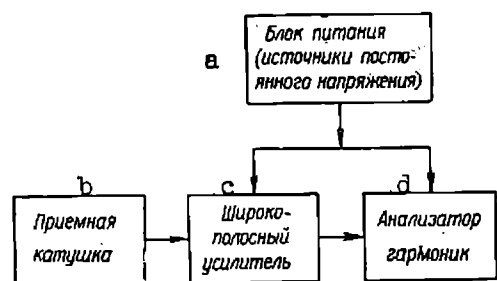


Fig. 105

Undoubtedly, the obtained level of interference is too high. This is easy to ascertain by comparing it with the level of the useful signal in the zone farthest from the cable in the range of the operating frequencies for this method for any resistivity with nominal current in the cable. For instance, for frequency $f = 200$ cps with resistance $= 10^2$ ohm, m, $I = 1$ a at distance $x = 10$ km we get $(H_x) = 0.8 \cdot 10^{-6}$ a/m. Thus, the integral interference may exceed the useful signal by a factor of 10^2 or 10^3 .

The characteristics of the level of interferences, measured by means of harmonics analyzer on fixed operating frequencies vs. the operation of one or the other unit of the helicopter and the apparatus inside its cabin, are shown in Table 13.

Table 13

Operating sequence of apparatus in measuring interferences	Operating frequency, cps	Interferences equivalent to tension of horizontal component of the field, 10^{-6} a/m	Interference equivalent to tension of vert. component of field, 10^{-6} a/m
Cut-in of apparatus			
Cut-in of transformer	976	0,1	0,1
MA-500 (115v, 400 cps)	976	3,6	3,2
Cut-in of transformer PO-45(18v, 110-125 cps)	976	0,3	0,3
Cut in of transformer PO-45 and according circuit	976	6,4	3,5
Cut-in of helicopter motor (screw not rotating).	976	3,8	2,5
Disconnection of batteries and measuring apparatus (helicopter in the air).	81 244 976	120 - 260 39 - 90 8 - 25	120 - 240 80 - 120 8 - 16

N.B: The result of measuring interferences from the electric equipment of the helicopter and of the measuring apparatus are given mainly for frequency 976 cps.

According to Table 13, the lowest level of interferences is evident on the ground, when the practically possible are only atmospherics, apparatus noise, etc. With the out in individual blocks, interferences increase and specially sharply during the flight. Interferences from individual consumers of energy from the network of the helicopter are, on the whole, not very high, except for these from the recording circuit. Hence it follows that interferences, equivalent to the intensity of the field's vertical component, correspond approximately to these equivalent to the intensity of the horizontal component.

Experiments were also carried out with the aim of elucidating the distribution of interferences within the cabin of the helicopter, their directional characteristics, where they are minimum, etc. It has been established that interferences inside the helicopter cabin actually change very little even with changes in the orientation of the field detector in space. Investigations to define the points of low level of interferences from the electric equipment inside the cabin made it possible to determine that they are low at the initial point of the tail beam and decrease towards its end. The same interferences sharply decrease with carrying out of the field detector into the outboard gondola at a distance of 5 m and over:

Distance from helicopter, m	0	3	5	10	15	20
Interference level, mv.....	12.5	5.0-5.6	3.0	2.2	2.2	2.2

Thus, on the basis of these experiments, it was defined that the lowest level of interferences of electrical origin is at the tail

beam and in the outboard gondola and, moreover, that their level inside the helicopter cabin exceeds all other interferences, except radio interference.

Simultaneously, determinations were made of the effect of operating radio-stations and radio-altimeter, as well as of navigational and other instruments on board the helicopter on the receiving unit, placed on the tail beam and in the outboard gondola. The receiving unit consisted of the receiving coil and the preliminary wide-band amplifier with negligible amplification factor ($K = 10$).

The action of the radio-altimeter did not change appreciably the level of interference in the field detector, placed in the helicopter cabin, or in the outboard gondola. Only when the field detector was placed on the tail beam close to the radio-altimeter antenna itself, was its effect perceptible.

For the frequency of radio-channel (main phase) interferences from the electric equipment of the helicopter (chiefly from the ignition system) on frequencies 20-40 mega-cycles with rod aerial $\lambda/4$ have magnitude 10-20 mv (sensitivity threshold of receiver 5 mv). One of the ways to reduce this interference is to shorten the coaxial cable, connecting the input of the receiver with the antenna and pushing it out from the helicopter cabin through a hole in the floor, made approximately in the center of helicopter's gravity. In this case, with the length of the connecting coaxial cable 2.5 m it was possible to reduce interference to 2-3 mv.

Other interferences. Other "inconstant" interferences are also evident in the helicopter and affect, to a certain extent, the measuring channel of the useful signal as well as the channel of the main phase.

The interference most difficult to remove is the one in the radio-channel from the rotation of the big screw. With the turning of the helicopter, and sometimes with flights over broken ground, amplitude variation of carrier frequency of the type of "beat" was evident. The beat amplitude varied in a wide range, and its frequency - from zero to tens of cps. The origin of this event is of a highly composite nature and is, apparently, connected with signal reflection from the rotating big screw, the equivalent "area" of which with rotation of four blades is about 350 m^2 . The variation of the reflection phase and other manifestations build up conditions, at which the "beats" of the main signal begin. As a result, distortions appear, which lead to the spread of indications in recording (86). This effect could be attenuated by applying in automatic gain control and limiters in the measuring apparatus.

6. Methodical interferences.

Methodical error in aerial electric prospecting means the varying signal, induced by the primary field source in the magnetic field detector due to unstable geometry of the system of the oscillating frame - field detector. To methodical interferences may also be referred the interfering signals, caused by the incorrect set-up of the field detector in relation to the oscillating frame or the variation of its orientation during the survey. However, for convenience in reciprocal

comparison of the different versions of the aerial induction method, these interferences are analysed separately from the methodical ones (117, 128, 132).

Methodical interferences are inherent to the apparatus of all versions of the aerial induction method. In the apparatus of other methods, their role is insignificant (63, 132, 148, 208, 263). They emerge mainly due to "bumping" of the gondola during flight, when the field detectors are in the outboard gondola, and the oscillating frame - on the aircraft itself. These interferences also arise in the event of using two aircrafts, since it is practically impossible to assure reciprocal stability of their flight. Even insignificant changes in the position of the magnetic field detector in relation to the oscillating frame result in the appearance of a signal of such a type which is the predominant total interference and finally determines the efficiency and practical value of one or the other version of the aerial induction method.

Quantitative and qualitative analysis of methodical interferences makes it possible to choose a well-founded version of the induction method for resolving concrete geophysical problems. Therefore, the study of the nature of these interferences should be in great detail.

We shall analyze methodical interferences with the use of the calculated ratios obtained in Chapt. III and with consideration of works (35, 63, 69, 128, 132, 208).

Let us take first the versions of the induction method with one aircraft, when the field detector could be placed at points P_1 , P_2 , P_3

and P_4 (see Fig: 29), angle comprises respectively 0; 45; 65 and 90°. We analyze the variations of vertical and horizontal components of the primary field in the general case, i.e., within the variations of angle θ from 0 to 90°. The initial formulas for calculating these components are the following:

$$H_B = \frac{m_z}{8\pi r^3} (1 + 3 \cos 2\theta) = \frac{1}{2} A (1 + 3 \cos 2\theta); \quad (\text{IX.17})$$

$$H_r = \frac{3m_z}{8\pi r^3} \sin 2\theta = \frac{3}{2} A \sin 2\theta, \quad (\text{IX.18})$$

where A - constant (parameter) of the method's version,

$$A = \frac{m_z}{4\pi r^3}.$$

From formula (IX.17) it follows that if $\theta = 54^\circ 45'$, the vertical component won't be present, If $\theta = 0$, $H_v = H_{v.\max}$, and if $\theta = 90^\circ$,

$$H_v = \frac{1}{2} H_{v.\max}.$$

The horizontal component, as follows from formula (IX.18), is not present, if $\theta = 0$ and $\theta = 90^\circ$, and has the maximum value at $\theta = 45^\circ$.

Variation of geometry of the system (i.e. variation of angle θ) results in the appearance of methodical interference, the intensity of which is determined by the location point of the field detector, the value of the measurable component of the field at this point and the variation range of angle θ (magnitude of $\Delta \theta$).

Let us determine the value of increments ΔH_v for the vertical and ΔH_h for the horizontal components of the primary field with variation of angle θ to the extent of $\Delta \theta$.

Expanding functions $H_v = F_1(\theta)$ and $H_h = F_2(\theta)$ into Taylor's series and taking into account only the terms of the first order of smallness, we get

$$\Delta H_B = \frac{\partial H_v}{\partial \theta} \Delta \theta = -3A \sin 2\theta \Delta \theta; \quad (\text{IX.19})$$

$$\Delta H_r = \frac{\partial H_r}{\partial \theta} \Delta \theta = 3A \cos 2\theta \Delta \theta. \quad (\text{IX.20})$$

From ratios (IX.17) - (IX.20) it is possible to determine the absolute dimensionless values of the vertical and horizontal components (i.e., the intensity of interference)

$$x_B = \frac{H_B}{A}; \quad x_r = \frac{H_r}{A}$$

for any location point of the field detector within the range $0-90^\circ$.

For the vertical component

$$x_B = \frac{H_B}{A} = \frac{I}{2} (1 + 3 \cos 2\theta). \quad (\text{IX.21})$$

Similarly, for the horizontal component we get

$$x_r = \frac{H_r}{A} = \frac{3}{2} \sin 2\theta. \quad (\text{IX.22})$$

From the given ratios it follows that the absolute magnitude of interference X_v for the vertical component will be maximum at $\theta = 0$ and $\theta = 90^\circ$, and interference X_h for the horizontal component - at $\theta = 45^\circ$.

It should be mentioned that not every position of the magnetic field detector (at points $P_1 - P_4$), and all the greater variations of angle θ within a wide range can meet the requirements of the safety technique for piloting the aircraft; therefore in calculations we take the variations of angle θ within $\pm 5^\circ$, permissible from the standpoint of safe piloting.

Let us analyze variations of the vertical component at points $P_1 - P_4$ and of the horizontal component at points P_2, P_3 of the practical location of the magnetic field detectors. For this we determine the maximum relative variations of the primary field components, termed in percentage of their values at the above points of observations ($\Delta = \frac{\Delta H}{H} \cdot 100, \%$), for several increments of $\Delta \theta$ within $\pm 5^\circ$.

To raise the accuracy of ΔH determination for low increments ($\Delta \theta \leq 2^\circ$) we will use formulas (IX. 19) and (IX. 20) with the estimate of terms of the second order of smallness, and for high increments ($\Delta \theta \geq 2.5^\circ$) we use formula

$$\Delta = \left| \frac{\Delta H}{H} \right| \cdot 100 = \left| \frac{F(\theta + \Delta \theta) - F(\theta)}{F(\theta)} \right| \cdot 100, \% \quad (\text{IX. 23})$$

Thus, in the first case

$$\Delta H_B = - 3A \sin 2\theta \Delta \theta - 3A \cos 2\theta (\Delta \theta)^2, \quad (\text{IX.23a})$$

$$\Delta H_r = 3A \cos 2\theta \Delta \theta + 3A \sin 2\theta (\Delta \theta)^2.$$

For point P_1 , at which $\theta = 0^\circ$, we have

$$\Delta H_B = - 3A (\Delta \theta)^2. \quad (\text{IX.24})$$

For point P_2 , at which $\theta = 45^\circ$, we will have

$$\Delta H_B = - 3A \Delta \theta; \quad \Delta H_r = 3A (\Delta \theta)^2. \quad (\text{IX.24a})$$

For point P_3 , at which $\theta = 65^\circ$, we obtain

$$\begin{aligned} \Delta H_B = - 2,3A \Delta \theta + 1,93A (\Delta \theta)^2; \quad \Delta H_r = - \\ 1,93A \Delta \theta + 2,3A (\Delta \theta)^2. \end{aligned} \quad (\text{IX.24b})$$

For point P_4 , in which $\theta = 90^\circ$, it will be

$$\Delta H_B = 3A (\Delta \theta)^2. \quad (\text{IX.24c})$$

TABLE - 14.

Observation point and components value at these points.	Variation of angle θ ($\pm \Delta \theta$)								
	$0^\circ 12'$	$0^\circ 30'$	1°	$1^\circ 30'$	2°	$2^\circ 30'$	3°	4°	5°
$P_1 (\theta = 0^\circ);$ $H_B = 2A$	0	0.01	0.05	0.11	0.18	0.29	0.43	0.73	1.14
$P_2 (\theta = 45^\circ);$ $H_B = 0.5A;$ $H_r = 1.5A$	$\frac{2.14}{0}$	$\frac{5.28}{0.02}$	$\frac{10.5}{0.06}$	$\frac{15.7}{0.14}$	$\frac{21.0}{0.24}$	$\frac{28.2}{0.38}$	$\frac{31.4}{0.55}$	$\frac{41.7}{0.97}$	$\frac{52.4}{1.52}$
$P_3 (\theta = 65^\circ);$ $H_B = -0.46A,$ $H_r = 1.15A$	$\frac{0.85}{0.45}$	$\frac{3.48}{1.40}$	$\frac{7.96}{2.87}$	$\frac{12.5}{4.27}$	$\frac{17.3}{6.1}$	$\frac{22.4}{7.82}$	$\frac{26.8}{8.7}$	$\frac{36.5}{12.6}$	$\frac{46.2}{16.0}$
$P_4 (\theta = 90^\circ);$ $H_B = -1A$	0	0.03	0.09	0.21	0.36	0.58	0.85	1.46	2.28

B.B:- The numerator shows the relative variation of the vertical, denominator - of the horizontal, components of the primary field.

With known constant A, it is possible to calculate the value of the component at a given observation point and its relative and absolute changes with variations of angle θ in the limits shown above. This makes it possible to determine the magnitude of the signal, induced in the field detector (assuming, that the constant of the field

detector C_d is known) by the constituent of the primary field and its variation, for comparing this signal (interference) with the useful signal from the sought for anomaly.

The data of Table 14 permit drawing the conclusion that the least methodical interference is typical of the induction method versions, in which the field detector is placed at points P_1 or P_4 during the measuring of the vertical component and at point P_2 , when measuring the horizontal component. It should be mentioned that for these versions of the induction method additional electric compensation of the direct signal is required in measuring part of the apparatus, since here $H_B \neq 0$ and $H_r \neq 0$.

Analysis shows that for the induction method version with $\theta = 65^\circ$ (apparatus AERI-2) methodical interferences are quite high; therefore, this version is optimum as regards stability against interference (21, 128, 132).

It is definitely of interest to know the nature of variation of the angle of inclination of the intensity vector \vec{H} of the primary magnetic field to axis OZ for points P_1 and P_4 with the variation of angle θ within the indicated limits.

$$\beta = \operatorname{arctg} \frac{H_r}{H_B} = \operatorname{arctg} \frac{3 \sin 2\theta}{1 + 3 \cos 2\theta}$$

This is necessary for estimating the methodical interference of two-plane version with linear polarisation of the field. The corresponding calculations are given in Table 15.

TABLE-15.

Observation points	Variation of angle $\theta (\pm \Delta \theta)$								
	$0^{\circ} 30'$	1°	$1^{\circ} 30'$	2°	$2^{\circ} 30'$	3°	4°	5°	
$P_1 (\theta = 0)$	$0^{\circ} 38'$	$1^{\circ} 30'$	$2^{\circ} 15'$	$2^{\circ} 59'$	$3^{\circ} 46'$	$4^{\circ} 30'$	$5^{\circ} 58'$	$7^{\circ} 31'$	
$P_4 (\theta = 90^{\circ})$	$1^{\circ} 18'$	$3^{\circ} 00'$	$4^{\circ} 30'$	$5^{\circ} 58'$	$7^{\circ} 28'$	$8^{\circ} 58'$	$11^{\circ} 56'$	$14^{\circ} 52'$	

N.B: At point P_1 at $(\theta + \Delta \theta)$ the value should be taken with plus sign, at $(\theta - \Delta \theta)$ - with minus sign, and at point P_4 at $(\theta \pm \Delta \theta)$ - with plus sign.

The apparatus of the induction method with oscillating and receiving frames rigidly interconnected and placed at distance one from the other requires an intense and stable geometrical or electrical compensation of the direct signal. Geometrical compensation is obtained by a corresponding disposition and cut in of the receiving frames (see Fig. 31, 106). Here, depending on the set-up of receiving frames, it is possible to measure both the vertical and horizontal components of the field. However, as shown by the data of Table 14, preference should be given to a diagram, meant for measuring the vertical component.

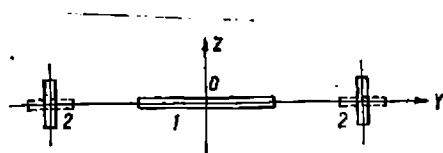


Рис. 106.

Fig: 106.

The relative increment of the field in this diagram with uniform and simultaneous displacement of the field detectors in relation to the preset position (most unpleasant case) should be doubled.

Let us consider the induction method with the receiving frame at center O' , as shown in Fig: 32 ($Z_0 = 0$, $Y = 0$). In the determination of methodical interference for this version, it is necessary to vary not the drift angle of the gondola, as in other versions, but the shifting of the magnetic field detector relatively to the center of the receiving frame, termed, for instance, in percentage to the radius of the oscillating frame. This variation of the geometry of the system is brought into formulas (III.32) for determination of the increment of components H_y and H_z .

Let us take three practical cases of varying the geometry of the system.

1. The shifting of the field detector occurs only along the line $O'Z'$, to an extent of Δz_0 , determinable in fractions of radius R ($\Delta z_0 = 0.0005; 0.001; 0.005; 0.01; 0.015$ and $0.02 R$).
2. The shifting of the field detector occurs only on line $O'Y'$, i.e., along the radius R of circular circuit, to an extent Δy , determinable in fractions of radius R ($\Delta y = 0.0005; 0.001; 0.005; 0.01; 0.015$ and $0.02 R$).
3. There is spontaneous shifting of the field detector in plane $Y'C'Z'$, and $\Delta y = \Delta z_0$.

Here are the initial formulas for calculating the components H_y and H_z :

$$\dot{H}_y = 0.75 \dot{I}_m w \frac{R^2 y z_0}{\rho_0^5} \left[I - \frac{5}{8} \cdot \frac{y^2}{\rho_0^4} (3R^2 - 4z_0^2) \right] ;$$

$$\dot{H}_z = 0.5 \dot{I}_m w \frac{R^2}{\rho_0^3} \left[I + \frac{3}{4} \cdot \frac{y^2}{\rho_0^4} (R^2 - 4z_0^2) \right] .$$

Assuming that $0.75 \dot{I}_m w = \dot{A} = \text{const}$ and $0.5 \dot{I}_m w = \dot{A}_1 = \text{const}$, these formulas may be written as:

$$\dot{H}_y = \dot{A} \frac{R^2 y z_0}{\rho_0^5} \left[I - \frac{5}{8} \cdot \frac{y^2}{\rho_0^4} (3R^2 - 4z_0^2) \right] ;$$

(IX.25)

$$\dot{H}_z = \dot{A}_1 \frac{R^2}{\rho_0^3} \left[I + \frac{3}{4} \cdot \frac{y^2}{\rho_0^4} (R^2 - 4z_0^2) \right] .$$

Determining, generally, the increment of components with variation of the initial geometry of the system, with the use of expansion of Taylor series. In this, it should be kept in view that

$$\rho_0^2 = (R - y)^2 + z_0^2 .$$

The increment of component H_y with the change only of coordinate z_0 ($y \approx 0$) will be

$$\Delta \dot{H}_y^{(z_0)} = \left(\frac{\partial \dot{H}_y}{\partial z_0} \right)_{z_0=0} \Delta z_0 + \frac{1}{2} \left(\frac{\partial^2 \dot{H}_y}{\partial z_0^2} \right)_{z_0=0} (\Delta z_0)^2 = 0; \quad (\text{IX.26})$$

with the change only of coordinate y ($z_0 = 0$) we have

$$\Delta \dot{H}_y^{(y)} = \left(\frac{\partial \dot{H}_y}{\partial y} \right)_{y=0} \Delta y + \frac{1}{2} \left(\frac{\partial^2 \dot{H}_y}{\partial y^2} \right)_{y=0} (\Delta y)^2 = 0. \quad (\text{IX.27})$$

The increment of component H_z with the change of only the coordinate z_0 ($y = 0$) will be

$$\Delta \dot{H}_z^{(z_0)} = \left(\frac{\partial \dot{H}_z}{\partial z_0} \right)_{z_0=0} \Delta z_0 + \frac{1}{2} \left(\frac{\partial^2 \dot{H}_z}{\partial z_0^2} \right)_{z_0=0} (\Delta z_0)^2, \quad (\text{IX.28})$$

with the variation only of coordinate y ($z_0 = 0$) -

$$\Delta \dot{H}_z^{(y)} = \left(\frac{\partial \dot{H}_z}{\partial y} \right)_{y=0} \Delta y + \frac{1}{2} \left(\frac{\partial^2 \dot{H}_z}{\partial y^2} \right)_{y=0} (\Delta y)^2. \quad (\text{IX.28a})$$

The increment of component \dot{H}_y with the variation of both the coordinates y and z_o will be

$$\Delta \dot{H}_y^{(y, z_o)} = \frac{\partial \dot{H}_y}{\partial y} \Delta y + \frac{\partial \dot{H}_y}{\partial z_o} \Delta z_o \Big|_{\substack{y=0 \\ z_o=0}} +$$

$$+ \frac{1}{2} \left[\frac{\partial^2 \dot{H}_y}{\partial y^2} (\Delta y)^2 + 2 \frac{\partial^2 \dot{H}_y}{\partial y \partial z_o} \Delta y \Delta z_o + \frac{\partial^2 \dot{H}_y}{\partial z_o^2} (\Delta z_o)^2 \right] \Big|_{\substack{y=0 \\ z_o=0}} \quad (\text{IX.29})$$

and for component \dot{H}_z in the same conditions

$$\Delta \dot{H}_z^{(y, z_o)} = \left(\frac{\partial \dot{H}_z}{\partial y} \Delta y + \frac{\partial \dot{H}_z}{\partial z_o} \Delta z_o \right) \Big|_{\substack{y=0 \\ z_o=0}} +$$

$$+ \frac{1}{2} \left[\frac{\partial^2 \dot{H}_z}{\partial y^2} (\Delta y)^2 + 2 \frac{\partial^2 \dot{H}_z}{\partial y \partial z_o} \Delta y \Delta z_o + \frac{\partial^2 \dot{H}_z}{\partial z_o^2} (\Delta z_o)^2 \right] \Big|_{\substack{y=0 \\ z_o=0}} \quad (\text{IX.30})$$

For the first case of changes in the geometry of a system, when $y = 0$ and $\rho_o^2 = R^2 + z_o^2$, we find from formulas (IX.25); (IX.26) and (IX.28) that

$$\Delta \dot{H}_y^{(z_o)} = 0; \Delta \dot{H}_z^{(z_o)} = \frac{1}{2} \left(\frac{\partial^2 H_z}{\partial z_o^2} \right)_{z_o=0} (\Delta z_o)^2 = \frac{1,5A_1}{R^3} (\Delta z_o)^2 \quad (\text{IX.31})$$

(for $\dot{H}_z^{(z_o)}$ the term of the first order of smallness, i.e., the first derivative at point z_o , converts into zero, therefore, the sought for increment determines the term of the second order of smallness, which at $z_o = 0$ has a finite value). Therefore, the given variation of the geometry system of the affects the field detector, which perceives only component H_z .

For the second case of variation of the geometry of the system when $z_o = 0$ and $\rho = R - y$, we find from formulas (IX.25), (IX.27) and (IX.28a) that

$$\Delta \dot{H}_y^{(y)} = 0; \Delta \dot{H}_z^{(y)} = \left(\frac{\partial \dot{H}_z}{\partial y} \right)_{y=0} \Delta y = \frac{3A_1}{R^2} \Delta y \quad (\text{IX.32})$$

(here at $z_0 = 0$ the term of the second order of smallness is equal to zero; therefore, for determination of $\Delta \dot{H}_z^{(y)}$, we shall use the term of the first order of smallness, which at $z_0 = 0$ has finite value).

Thus, in the first, as well as in the second, case the variation of the geometry of the system affects only the field detector, which perceives the vertical component H_z of the primary field. In both the analyzed cases

$$\dot{H}_y(0) = 0; \quad H_z(0) = \frac{A_1}{R} = \frac{0.5 j_m}{R} \quad (\text{IX.33})$$

For the third (general) case of variation in the geometry of the system, when $\rho^2 = (R - y)^2 + z_0^2$, and $z_0 = \Delta z_0 = y = \Delta y$, we get from formulas (IX.25), (IX.29) and (IX.30)

$$\Delta \dot{H}_y^{(y, z_0)} = \left(\frac{\partial^2 \dot{H}_y}{\partial y \partial z_0} \right)_{\substack{y=0 \\ z_0=0}} \Delta y \Delta z_0 = \frac{A}{R^3} \Delta y \Delta z_0; \quad (\text{IX.34})$$

$$\Delta \dot{H}_z^{(y, z_0)} = \left(\frac{\partial \dot{H}_z}{\partial y} \right)_{\substack{y=0 \\ z_0=0}} \Delta y = \frac{3A_1}{R^2} \Delta y. \quad (\text{IX.35})$$

as the remaining terms in expansion of (IX.29) and (IX.30) convert into zero at $y = z_0 = 0$. In this case, the variation of the geometry of the system will affect both the receiving frames.

On the basis of the given ratios, similar to the preceding, we calculate the relative variation of the field's intensity (Δ , %) at the adopted displacement of the field detector, i.e. determine the methodical interference. For $0.015 R$ and $0.02R$ the intensity of Δ we calculate from formula (IX.23) (Table 16).

The resolution of the equation (IX.25) in relation to its maximum in the near zone by the approximation method, required in the third case for calculating the relative variation of H_y component of the field's density H , gives $y = z_0 = R$ and $H_{y \max} = 0.204 \frac{A}{R}$.

TABLE-16.

Direction of displacement	Components	Displacement					
		0,0005R	0,001R	0,005R	0.01R	0.015R	0.02R
Along the line O'Z'	$H_z = \frac{A_1}{R}$						
	$H_y = 0$	0	0,00025	0,00375	0,015	0,035	0.06
Along the line O'Y'	$H_z = \frac{A_1}{R}$	0.15	0.30	1.5	3.0	4,7	6,3
	$H_y = 0$						
In plane Y'O'Z' }	$H_y = 0$ $H_{y \max} = 0,204 \frac{A}{R}$	0,00013	0,005	0,013	0,052	0,12	0,22
	$H_z = \frac{A_1}{R}$	0.15	0.30	1.5	3.1	4,7	6,3

The data of Table 16 make it possible to assume that the highest methodical interference is built up during the measuring of component \dot{H}_z from displacement of the receiving element along the axis O'Y', and also from its displacement in the plane Y'O'Z. During the measuring of \dot{H}_y , the methodical interference is considerably less in both the cases. However, it should be kept in view that the nearness of the field source to the detector in these versions of the induction method may give rise, in the field detector, to a signal considerable in absolute intensity, although the relative variation of its intensity may be negligible. Therefore, at first, calculations of the density of the field affecting the pertinent field detector (specially in respect of the component H_z), should be made, then the intensity of the direct signal, induced by the primary field in the field detector (taking interference into account), should be compared with the assumed intensity of the useful secondary signal.

Let us carry out a comparative estimation of methodical interferences in the two-plane version of the induction method. For this estimation with the use of the circular rotating magnetic field, it is necessary to calculate the difference in amplitude of components for the allowed deviations of angles θ and φ with changes in the geometry of the system.

As follows from Fig: 16 and 33, the components of the vector of intensity of the resultant field \vec{H}^P will be H_x^r and H_z^r , the values of which are determinable from formulas (III.34). The receiving frames, placed at point P, are meant for receiving the indicated components.

For the determination of methodical interference, caused by changes in the geometry of the system, we deduce ratios, which totally reflect variations of c.m.f., induced in the receivers, through the corresponding variations of the field's components H_x^r and H_z^r , affecting these receivers.

Since in the receiving multi-turn frame $e = -\omega \frac{dF}{dt}$, in this case it may be assumed that e.m.f., excited in the field detectors by components H_x^r and H_z^r , are determinable from relations

$$E_x^p = -k_x \frac{dH_x^p}{dt}; \quad E_z^p = -k_z \frac{dH_z^p}{dt},$$

where k - the proportionality factor, which takes into account the parameters of the receiving frames.

The resultant output voltage of the receiving-measuring channel, recorded in the composite form, will be

$$\dot{U}_{BbIX} = \Delta \dot{U} = \dot{U}_x^p - j \dot{U}_z^p \quad (IX.36)$$

Here

$$\dot{U}_x^p = j \omega K_x \dot{H}_x^p; \quad \dot{U}_z^p = j \omega K_z \dot{H}_z^p, \quad (IX.37)$$

where K_x and K_z - the proportionality factors taking into account the parameters, both of the receiving frames and of the wholereceiving-measuring channel. Usually $K_x = K_z = K$.

Substituting in equation (IX.36) the values U_x^r and U_z^r from the equation (IX.37), we get

$$\Delta \dot{U} = j \omega K \left(\dot{H}_x^p - j \dot{H}_z^p \right) \quad (\text{IX.38})$$

The implication here is that

$$\dot{H}_x^p - \dot{H}_z^p = a_x \cos \omega t - b_x \sin \omega t; \quad (\text{IX.39})$$

$$j \dot{H}_z^p \rightarrow H_{zp} = a_z \cos \left(\omega t + \frac{\pi}{2} \right) - b_z \sin \left(\omega t + \frac{\pi}{2} \right) = -a_z \sin \omega t - b_z \cos \omega t$$

where H_{zp} - component H_z^r , shifted in the phase by $\frac{\pi}{2}$.

The difference of components $H_z^r - j \dot{H}_z^r$ will be

$$\Delta = a_x \cos \omega t - b_x \sin \omega t + a_z \sin \omega t + b_z \cos \omega t =$$

$$= (a_x + b_z) \cos \omega t + (a_z - b_x) \sin \omega t.$$

Thus

$$\Delta = (a_z - b_x) \sin \omega t + (a_x + b_z) \cos \omega t = \Delta_m \sin (\omega t + \psi_\Delta), \quad (\text{IX.40})$$

where factors $a_x, b_x; a_z$ and b_z are determinable from formulas (III.37) and (III.37a).

According to formula (IX.38), the output voltage of the receiving-measuring channel is determined by the difference $\ddot{H}_x^r - \dot{j}\ddot{H}_z^r$, therefore, the analysis may be confined to this difference vs. changes in the geometry of the system.

The difference amplitude of components

$$\Delta_m = \sqrt{(a_z - b_x)^2 + (a_x + b_z)^2}, \quad (\text{IX.41})$$

and the initial phase

$$\psi_{\Delta} = \text{arctg} \frac{a_x + b_z}{a_z - b_x} \quad (\text{IX.41a})$$

Substituting in formulas (IX.41) and (IX.41a) factors $a_x, b_x; a_z$ and b_z from equations (III.37) and (III.37a), we obtain

$$\Delta_m = \frac{3m_0}{4\pi r^3} (\cos^2 \theta - \sin^2 \theta \cos^2 \varphi); \quad (\text{IX.42})$$

$$\psi_{\Delta} = \text{arctg} \frac{2 \sin \theta \cos \theta \cos \varphi}{\cos^2 \theta - \sin^2 \theta \cos^2 \varphi}. \quad (\text{IX.42a})$$

The circular polarization of the field corresponds to the normal reciprocal position of the oscillating and receiving frames at $\theta = \varphi = 90^\circ$ and $\Delta_m = 0$. But if angles θ and φ differ from 90° , the $\Delta_m \neq 0$, and there is elliptical polarization of the field, resulting in the appearance of methodical interference. Let us analyze three cases of this appearance of interference.

1. With the variation only of angle θ , i.e., $\theta' = 90^\circ \pm \Delta\theta$, $\varphi = 90^\circ = \text{const}$ - there is displacement of the field detectors in plane YOZ.
2. The variation is only of angle φ , i.e. $\varphi = 90^\circ \pm \Delta\varphi$, $\theta = 90^\circ = \text{const}$ - the displacement of the field detectors occurs in plane ZOY.
3. Simultaneous variation of both the angles, i.e., $\theta' (\varphi') = 90^\circ \pm \Delta\theta (\Delta\varphi)$ - there is displacement of the field detectors in space.

The data of calculations of methodical interference are shown in Table 17, where it is given in percentage of the intensity of one of the components with normal position of the frames ($\Delta = \left| \frac{\Delta_m}{A} \right| \cdot 100\%$). For this component, it is assumed in all cases that $\Delta = \frac{m_0}{4\pi r^3} = \text{const}$.

Table 17

Condition	Variation of angles θ, φ ($\pm \Delta \theta \varphi$)								
	$0^{\circ}12'$	$0^{\circ}30'$	1°	$1^{\circ}30'$	2°	$2^{\circ}30'$	3°	4°	5°
$\varphi = 90^{\circ} = \text{const}$	0,004	0,023	0,09	0,21	0,36	0,57	0,82	1,46	2,28
$\theta = 90^{\circ} = \text{const}$	0,004	0,023	0,09	0,21	0,36	0,57	0,82	1,46	2,28
$\pm \Delta \theta = \pm \Delta \varphi$	0,008	0,046	0,18	0,42	0,72	1,14	1,64	2,92	4,56

From Table 17 it follows that both the cases of change in the geometry of the system produce similar methodical interference, which is in accordance with the symmetry of the field of two reciprocally perpendicular frames. With simultaneous variations of angles θ and φ to the same extent, which often happens in practice, it is possible to assume that the maximum total interference is twice that of interference with the variations of only one angle.

But if we compare the one - and two-plane versions of the induction aeromethod with the rotating magnetic field, then, as follows from formulas (III.38) and (III.40), in the first case, the methodical interference is greater and depends mainly on the location point of the field detector, i.e., on angle θ . This may be explained by the fact that the primary field at a point, for which angle θ is neither 0 nor 90° , should be elliptically polarized, whereas with negligible variations of angle θ the elliptical polarization of the field sharply increases, although at the initial point of location of the receiving frames the primary field is made into a circular rotating field by means of special

measures (see chapt.II).

In conclusion, let us determine methodical interference for the induction method with linear polarization of the field. This field, as well known (236, 237), is excited by the horizontal oscillating frame (by vertical magnetic dipole) and induces in the two receiving frames e.m.f. similar in intensity, with no phase shift between them. Taking into account formulas (III.15a), it may be assumed that in measuring the ratio of the output voltage of the receiving device we will get

$$\dot{A} = \frac{U_{IBbIX}}{U_{2BbIX}} \frac{H_B \cos 45^\circ}{H_B \cos 45^\circ} = 1, \quad \psi = 0 \quad (\text{IX.43})$$

With the appearance of the secondary field, the primary field acquires an elliptical polarization, therefore, the ratio balance is disturbed and the phase shift between signals changes, which is what the apparatus records. This invariant system relates to the primary field, when the possible shifting of the receiving frames occurs along axis $O_1 Y_1$ or with the turning of frames around axis $O_1 Z_1$, as shown by arrows in Fig: 18. But if the shifting of the receiving frames occurs in the direction of axis $O_1 Z_1$ (the center of the frames shifts from point O_1 to point O'_1) or they are turning at some angle around axis $O_1 X_1$, methodical interference appears from the changing geometry of the system. In the first case, it is caused by the changing inclination of the intensity vector of the primary field, and in the second, by changing

the orientation of the receiving frames in relation to axis $O_1 Z_1$; moreover, the projection of vector \vec{H} on the perpendicular of the first and second frames varies. The highest methodical interference arises with the shifting of the frames towards axis $O_1 Z_1$ (for point P_4).

As follows from formula (III.17) and Table 15, for point P_4 inclination of vector \vec{H} of the density of the primary field in respect of the vertical line (axis $O_1 Z_1$) varies considerably (by an angle β). Therefore, the angles between vector \vec{H} and its projections on the perpendicular of the first and second receiving frames will differ, respectively, by $45^\circ + \beta$ and $-45^\circ + \beta$ (angle β could be either positive or negative). The modulus of vector \vec{H} , determinable from formula (III.14), also varies with the variations of angle O . Therefore, in this case, changes in the geometry of the system cause variation also of e.m.f., induced in the receiving frames by the primary field.

Thus

$$H_1 = H \cos 45^\circ; H_2 = H \cos (-45^\circ); H_1' = H' \cos (45^\circ + \beta);$$

$$H_2' = H' \cos (-45^\circ + \beta) = H' \cos (45^\circ - \beta)$$

In measuring the ratio of e.m.f., excited in the receiving frames, in the case of changing geometry of the system, it is possible to write that

$$\frac{E_1}{E_2} = \frac{H_1'}{H_2'} = \frac{H' \cos (45^\circ + \beta)}{H' \cos (45^\circ - \beta)} = \frac{\cos (45^\circ + \beta)}{\cos (45^\circ - \beta)}, \quad (\text{IX.44})$$

where H' is determined from formula (III.14).

The signal ratio in respect of the normal, i.e., initial, position of the frames varies equal to the variation of the primary field

$$\Delta = \frac{\frac{H_1}{H_2} - \frac{H'_1}{H_2}}{\frac{H_1}{H_2}} 100 = 1 - \frac{H'_1}{H_2} 100, \% \quad (\text{IX.45})$$

since $H_1 = H_2$.

In measuring the difference of signals for the equivalent methodical interference of field density ΔH , we get from the analogy with the VMP version

$$\begin{aligned} \Delta &= \frac{\Delta H}{H_1} 100 = \frac{H'_1 - H'_2}{H_1} = 100 = \\ &= \frac{H' [\cos (45^\circ + \beta) - \cos (45^\circ - \beta)]}{H_1} 100, \% \quad (\text{IX.46}) \end{aligned}$$

Formulas (IX.45) and (IX.46), and also (III.14) and Table 14, enable determining for the given version of the induction aeromethod the methodical interference with the variation of angle θ . With this we take into account both the possible positions of the oscillating frame: horizontal and vertical. In accordance with the latter, selection

from Table 15 of angle is made for point P_4 or point P_1 . Calculation is carried out for the most probable and worst case, from the stand point of the magnitude of methodical interference, of change in the geometry of the system - when the shifting of the receiving frames occurs in the direction of axis $O_1 Z_1$ (i.e. with the variations of angle θ within $\pm 5^\circ$).

Table 18

Oscillating frame	Variations of angle θ (+ $\Delta \theta$)							
	$0^\circ 30'$	1°	$1^\circ 30'$	2°	$2^\circ 30'$	3°	4°	5°
Horizontal	$\frac{4,4}{3,2}$	$\frac{10,0}{7,4}$	$\frac{14,6}{11,1}$	$\frac{19,0}{14,7}$	$\frac{23,2}{18,4}$	$\frac{27,3}{22,1}$	$\frac{34,9}{29,5}$	$\frac{42,0}{36,7}$
Vertical	$\frac{2,2}{1,6}$	$\frac{5,1}{3,7}$	$\frac{7,6}{5,5}$	$\frac{9,9}{7,3}$	$\frac{12,4}{9,3}$	$\frac{14,6}{11,1}$	$\frac{19,0}{14,7}$	$\frac{23,3}{18,5}$

N.B: The numerator shows value Δ (%) in measuring the signal ratio, the denominator - in measuring the difference of signals.

From Table 18 it follows that the magnitude of methodical interference with the vertical oscillating frame is practically half of that with the horizontal one. This is also confirmed by curves $F_1(\theta)$ for the vertical (see Fig.26) and $F_2(\theta)$ for the horizontal(see Fig: 27) components of the primary field. The big and small petals of directional characteristics of $F_1(\theta)$ are different two times in their relative size. Since the variation of curve $F_2(\theta)$ in both the positions of the oscillating frame is similar, it follows that the variation rate of

of the magnitude and inclination of the primary field vector \vec{H} is half that of the second in the first position of the oscillating frame.

By similar methods, it is possible to calculate all versions of the induction aeromethod and to determine methodical interferences for other methods of aerial electric prospecting.

7. Vibration-free fitting of field detectors:

Vibrational interference is one of the main interferences affecting the receiving-measuring apparatus in the methods of aerial electric prospecting. The real threshold of sensitivity in the apparatus of any method of aerial electric prospecting depends on the extent to which the level of vibrational noises in the field detector could be reduced. At present the problem of protecting high-sensitivity magnetic field detectors is only slightly developed theoretically and, practically, hardly at all.

A number of organisations, dealing with the devising of the geophysical apparatus for aerial electric prospecting, both in the USSR and abroad, have carried out an enormous amount of work to devise an effective protection against vibration of the magnetic field detectors in the constant magnetic field of Earth. Vibre-proof fitting was worked out of the field detector, set up directly on the aircraft or in the out-board gondola. All these efforts attained some success. However, the application in this direction was not very advisable. Thus, it was not possible to bring up the sensitivity threshold of the apparatus at low frequencies to $10^{-8} - 10^{-9}$ a/m. In order to get an understanding of the work carried out, let us consider some of results obtained.

Protection against vibration of magnetic field detectors set up directly on the aircraft. The most unfavorable conditions for operating airborne electric prospecting apparatus are on the helicopter. Vibration noises on the helicopter are considerably higher than similar ones on the piston-engine plane. Therefore, let us analyze vibro-protection of the field detectors after the example of helicopter MI-4 type.

The vibro-protection systems of the field detectors, set up on helicopter MI-4, should meet the following requirements (89).

1. Maximum suppression in the range of operating frequencies of the harmonic components of vibro-oscillations.
2. It should not allow angular low-frequency vibration of the field detector, exceeding ψ_{\max} (see para 2, chapt.IX).
3. Linear shifting of the receiving element should be negligible and the overall size of the vibro-protection system constructionally convenient.
4. The weight of the vibro-protection system should not be excessive; for maintaining central balance, it should be not be over 15 kg, when the system is located in the middle of the helicopter's tail beam.
5. The natural frequency of the field detector's mechanical system should be considerably lower than the working frequency of the apparatus.

The first requirement should determine the required factor of vibro-protection (the amplitude ratio of shifting the vibration of the coil's suspension point to the amplitude of shifting of the coil itself). However, it is known (102, 123%), that the vibro-protection factor on helicopter MI-4 has not as yet been established due to the non-availability of the required calculation data regarding the volume distribution of vibrations. This, by the way, predetermines at present the experimental way for building the required vibro-protection systems.

The requirement that the angular vibrations of the coil should not exceed ψ_{\max} is connected with the amplitude modulation of the receivable signal, taking place in the coil due to these vibrations. For instance, in the BDE method, ^{with} the error allowed in measuring the amplitude of signal $\delta_M = 2\%$ we get $\cos \psi_{\max} = 0.98$, or $\psi_{\max} = 10^\circ$. The obtained angle of the coil's vibrations is valid only within the limits of the frequency transmission band of the recording apparatus. Outside the transmission band, the recording system will not respond to this signal modulation due to inertia.

Due to constructional reasons it was assumed that the linear shiftings of the field detector in any direction should not exceed 6-7 cm. In different constructions the shifting may have other values.

The fourth requirement ensues from the safety technique of the helicopter - the weight of an object suspended on the tail beam is limited to 15 kg. Similar requirements are imposed, apparently, on the field detectors, suspended at the ends of wings in light or average type of planes with piston engines, used in aero-geophysical methods.

And, finally, the fifth requirement is due to the condition that if the mechanical system of the field detector has very low (a few cps) natural frequency of mechanical resonance, such a system, vibrating under the effect of disturbing factors, will produce interferences with frequencies below the lowest operating frequency of the apparatus and the interference amplitude will quickly attenuate with decreasing frequency. This requirement is usually satisfied by heavier magnetic field detectors.

One of the first versions of the vibro-protection system of the field detector placed on the tail beam of the helicopter is shown in Fig: 107. The receiving coil 1 with rings of spongy rubber 2 is placed inside a housing 3, which is fixed, by means of spongy rubber cushions 4, to auxiliary ebonite rings 5. The whole system jointly with the cover 6 is set up on the tail beam of the helicopter.

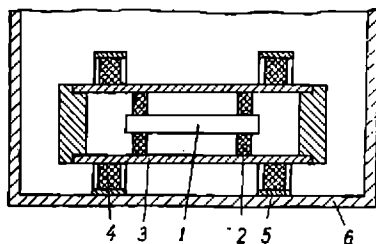


Рис. 107.

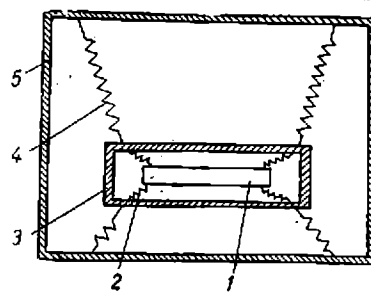


Рис. 108.

Fig: 107.

Fig: 108.

Since the system is meant for operations on a frequency of about 1000 cps, the natural frequencies of seismic masses were taken comparatively high: coil 1 - "spring" 2 - system 30 cps; corpus 3-"spring" 4

system - 40 cps. Damping of the system was attained mainly due to resistance of the air, passing through the pores in spongy rubber. This system assured the protection required in this case from vibration interference. For instance, on the frequency 976 cps the vibration interference was about $4 \cdot 10^{-6}$ a/m.

Another version of vibro-protection is shown in Fig: 108. The receiving coil 1 is stretched inside the body 3 by means of soft tape rubber 2. The body of the coil is fixed by similar rubbers 4 to the case 5, which is rigidly fixed on the tail boom of the helicopter.

The natural frequency of the coil's vibrations in relation to case 3 were taken 5-7 cps, and of the case 3 in relation to body - about 2-3 cps. The damping of the system was obtained by air resistance and internal friction in the stretched rubbers. The angle of the coil's vibrations $\psi_{\max} = \pm (2-3^\circ)$. In this way the natural frequency of vibrations in this system was considerably lower than in the preceding one. The interference, induced of frequency 976 cps, now was $6 \cdot 10^{-7}$ a/m, which could be accepted as satisfactory. On frequencies below 900 cps a construction of this type did not provide reliable protection from vibrations.

The most successful version of the vibro-protection system is shown in Fig: 109. Coil 1 by means of spongy rubber rings 2 is placed inside a cylinder 3, which, stretched on rubbers 4, is fixed on the streamlined case 5, is fitted by means of similarly stretched rubber 6 to the Duralumin frame 7. The whole construction is rigidly joined with the sheathing of the helicopter's tail beam 8. From Fig: 109 it follows that this is a three-stage system of vibro-protection. The natural

vibration frequency of coil 1 - cylinder 3 is 30 cps, cylinder 3 - case 5 - 5 - 6 cps, case 5 - helicopter body - 3-4 cps. Vibration angle $\psi_{\max} \pm (3 \div 5^\circ)$.

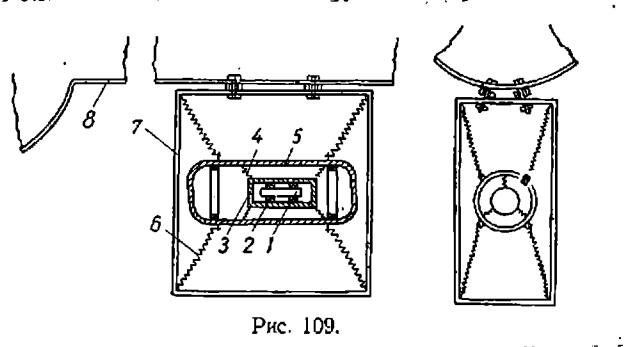


Fig: 109.

Fig: 110 shows the curve of the level of vibration interference (in unit of magnetic field density) vs. The frequency of the given vibro-protection system. The dotted line shows the variation of this level without the vibro-protection system (see Fig:96).

According to this figure, for frequencies above 200 cps, the application of the vibro-protection system has a comparatively good effect, whereas on lower frequencies this effect is negligible.

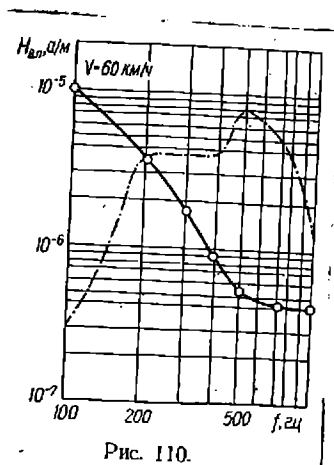


Fig: 110.

On the basis of the given data, it is possible to conclude that by reducing the frequency of natural vibrations of the intermediate masses of the vibro-protection system it is possible to reduce considerably the level of interference in the magnetic field detector. Special devices should be provided for protecting the system from impact loads, built up during the landing of the aircraft, specially of helicopters. In the case of a plane, it is necessary to provide a special streamlined unit, in which the vibro-protection system of the field detector should be placed. The unit itself should be rigidly fixed for carrying construction -s of the plane.

Vibro-protection of field detector in outboard gondola: The location of field detectors in the outboard gondola makes it possible to raise the efficiency of investigations by the methods of vibration noises of aerial electro-prospecting specially with change-over to low frequency, when it is difficult to devise a system of vibro-protection for the above given location of the field detectors. In this version the protection of the receiving element from vibrations is considerably simpler.

For the helicopter and plane versions, for instance, not bad results were obtained with the use as the first, main, stage of shock-proofing an eight-tape rubber stretches, on which the receiving coil was suspended inside the gondola. A suspension of this type is shown in Fig: 111 (1-receiving coil; 2-tape rubber; 3 lock of tape rubber). The natural frequency of the coil's vibrations in relation to the gondola itself was about 5 cps.

Measuring of noises in the coil, when the gondola is let out of the helicopter 7-10 and even more, has shown that their level is quite close to the level of noises with a three-stage vibro-protection system, placed at the tail beam of the helicopter (see Fig: 109).

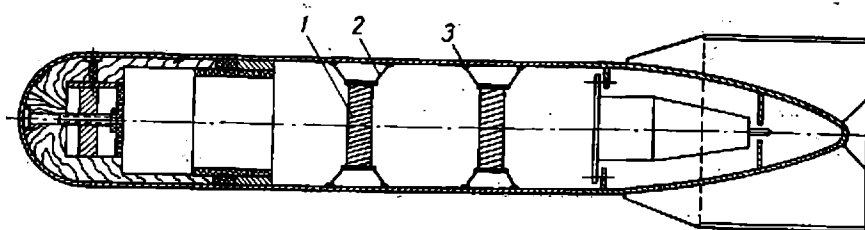


Fig: 111.

Later on, the level of noises was reduced by means of additional rubber cord-shock-absorber, fitted between the fixing point of the cable to the gondola and the cable itself at a distance of some tens of centimetres (Fig: 112, 1-wire-cable, 2 shock-absorber). The rigidity of the shock-absorber was selected with an estimate of the gondola's weight, so that the natural frequency of the system gondola-shock-absorber would be 2-2.5 cps. Checking the vibro-protection of this version has shown that the level of noises in the coil were reduced mainly in the range of lower frequencies. The results of these investigations at the speed of the helicopter $v_0 = 60$ km/hr are as follows:

Frequency, cps.	100	200	250	300	400	500	700	1000
Noise, equivalent to the magnetic field density, 10^{-6} a/m	8.6	2.8	0.8	0.6	0.56	0.45	0.4	0.33

From the given data and Fig: 111 it follows that the general level of noises in the gondola is lower, than on the tail beam of the helicopter, moreover, it is lower in a rather wide range of frequencies. Similar investigations were conducted on planes LI-2, IL-12 and AN-2.

A similar system of suspending the field detector, devised for the outboard gondola of a plane, was the second stage of shock-proofing. The first stage was executed with the use of porous material (paralon) directly within the cylinder of the magnetic antenna (see para 6, chapt. VII). The rigidity of rubbers was selected with an estimate of natural frequency of the system to comprise 1.5-3 cps. The suspension points of tape rubbers of one of the coils appear as though they are at the apex of a cube; therefore, the rigidity of the system in the direction of three coordinate axes is similar.

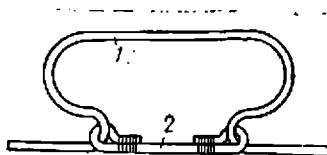


Рис. 112.

Fig: 112.

Experimental investigations of this system of vibro-protection have shown that on high operating frequencies the level of vibration noises was very low (10^{-7} a/m) and approximately equivalent to the sensitivity threshold of AERI-2 apparatus. On low operation frequency (243 cps) the vibration noises exceed to some extent the indicated sensitivity threshold. Experiments with outside shock-absorber have

shown that it will not assure any appreciable damping of noises, therefore it was not applied in the planes.

Thus, constructions of vibro-protection systems could be diverse. For instance, the vibro-protection of receiving coils in the VOP apparatus developed by VITR(234) has a different system from the systems described above. The receiving coils are placed into individual covers of spongy rubber 5mm in thickness and are fixed perpendicularly to each other on a suspended plate, which is fitted on the rubber shock-absorbers inside a special frame. The latter is screwed on to the housing of preamplifiers, due to which the frames and amplifiers constitute a single block, easily set up in gondola (234).

In the BDK apparatus of IAE SO AN USSR (118) the vibro-protection of the receiving coil is similar to the vibro-protection of the BDK and induction apparatus, devised by FMI AN Ukr. SSR. In this case, the coils are suspended on tape rubber stretches, so that the lines, provisionally drawn along these stretches, would intersect in the gravity center of the coil.

CHAPTER X

CONSTRUCTION PRINCIPLES OF THE MEASURING APPARATUS.

1. Classification of measuring circuits.

An important factor, largely determining the efficiency of geophysical investigations by various methods of aerial electric prospecting, is the operating sensitivity threshold of the measuring apparatus. With the artificial excitation of the field (see para 4, Chapt. IV) the minimum strength of the magnetic field in the range of operating frequencies of aerial electric prospecting is $(1-5) \times 10^{-7}$ a/m. Therefore, the measuring apparatus should have a sensitivity threshold at which this strength could be measured in this range. Moreover, the measuring apparatus should assure the required accuracy in measuring. For practical purposes the acceptable error in measuring the amplitude and components should be within the limits 1-3%, and the error in the measuring phase within the limits $0.5-1^{\circ}$. In some cases, for instance with the use of the rotating magnetic field, it would be expedient to have higher accuracy in measuring the indicated parameters(234).

The diversity of the measuring apparatus in aerial electric prospecting calls for the necessity of its classification. This would, in some measure, eliminate the difficulties in the analysis of the measuring circuits and would assist in a more rational selection of the optimum measuring circuits in the development of new apparatus.

K.B. Karandeyev, associate of AN USSR, and G.A. Shtamberger, a candidate of Technical Science, and others have suggested classification of the measuring circuits, applicable to electric prospecting, by the methods of alternate current (107). This classification is sufficiently well-founded, estimates most fully the applicable methods of electro and radio-measurements and could be used in the development of apparatus for aerial electric prospecting.

The analysis of the apparatus for aerial electric prospecting with harmonic field shows that it is based on particular cases of two main classic methods of measuring - direct measuring and compensation. Therefore, the measuring method and its modification are set as the main classification indices of the measuring circuits.

First of all, it is necessary to define the general elements of the measuring apparatus in aerial electric prospecting. Some of these elements, although indispensable in the said apparatus, could be of subordinate significance but for the resolution of the given problem.

The general links and elements of the apparatus, as shown in Table 19*, include: the magnetic field detectors P_r , transforming the tension of the electromagnetic field into e.m.f.(voltage); the auxiliary elements VE - amplifiers, adaption systems, voltage dividers (attenuators) phase-shifting circuits, etc.; the selective systems IS for separating the useful signal and indicators of measurable parameters $I(U)$.

* Some assumption are adopted in this Table: e.g. in the compensation method of measuring the compensation is not directly of the electromagnetic field strength, but of the output voltage of the selective system, fed from the magnetic field detector, as this with a certain error, reflects the nature of the measurable field at one or other time.

All these links and elements are present in any measuring apparatus, however, the demands imposed on some of them, the combination and relation between them vs. the resolvable problem could vary. Structure diagrams, shown in Table 19, are common, determining, but not the only ones possible. The simplest system of the direct measuring apparatus is the selective amplitude voltmeter, the structural diagram of which 1 is not complex and includes, besides the common elements, the amplitude detector AD (146, 177).

A more composite system (diagram 2), containing almost double the quantity of elements, as compared to diagram 1, is a differential selective voltmeter, for measuring the amplitude difference of two signals of one or two different frequencies. The difference is obtained and measured by the differential detector DD. This type of voltmeter is used in the apparatus IAE SO AN USSR for a two-frequency aerial electric prospecting (105).

For the determination of components of the measurable signal in Cartesian coordinates, the phase-sensing-selective voltmeter, is used block diagram 3 of which is distinct from diagram 1 by virtue of the presence of phase-sensing detector FD and the channel of key signal KOS. Indications of the measuring device are proportional to the projection of the measurable signal vector x_1 into vector x_0 of the comparative voltage. The channel of the key signal is meant for receiving, amplifying and transforming the comparative voltage, which controls the operation of the phase detector. In the phase, the comparative voltage matches most often the vector direction of the exciting field, But if there is simultaneous control of two phase detectors, shifted at 90° by comparative

voltages, it is possible to determine both the quadrature projections of the measurable signal x_1 in rectangular coordinates, preset by the direction of vector x_0 . This type of diagram is applied actually in a number of developed apparatuses (21, 90, 102).

The differential phase-detecting selective voltmeter serves to measure the difference in the components of input signals with two different operating frequencies (diagram 4), which are the projections of input signals onto the direction of vector x_0 . By means of this diagram, depending on the problem assigned, the measuring done is of the difference of the active and reactive components of signals x_1 and x_2 . If the subtracting diagram VS is replaced by the summation diagram SS, it will also be possible to measure the sum of the components. The example of this diagram's realization is the differential phase-detecting voltmeter of AERI-2 apparatus (127).

Measuring of the amplitude ratio of two signals could be effected by diagram 5, where the received signals are detected by amplitude detectors AD and then fed to ratio circuit SO. Quotient meters, compensation and special electronic arrangements may be used as this circuit (104, 232, 234).

But if the requirement is to measure the component ratio of two signals in coordinates preset by the direction of vector x_0 , the measuring apparatus may be designed in accordance with block diagram 5,b, which includes the channel of the key signal and phase detectors, instead of amplitude detectors.

The second group of this classification includes systems based on the compensation method of parameter measuring by means of the compensating device (KY). The compensator is controlled through the channel of the compensating voltage (KKH). If the measuring and generating units of the apparatus are placed on one aircraft, i.e., in direct vicinity to each other, the compensating voltage is usually taken off the generating unit. In the presence of two aircrafts or with the positioning of the generating unit on the ground, the compensating signal is transmitted by radio-channel.

The measuring unit with balanced compensator (diagram 6) makes it possible to obtain readings in the polar or Cartesian coordinates. To determine the compensation moment, the use is made of zero amplitude indicator AY, cut in at the KY input. The parameter values are determined by a reading device OY. This diagram has the distinctive feature that the reading may be obtained only at the moment of complete compensation of the measurable signal. This diagram was used, for example, to construct the ground apparatus AFI-2 (11,115).

The measuring unit, based on the principle of quasi-balanced compensation (diagram 7), is characterised by the presence of two compensating units, enabling the compensation and separately measuring of the required parameters. Since in this case the measuring is scalar, the moment of quasi-balance is marked by means of phase or differential indicators.

When applying the principle of non-balanced compensation (diagram 8), the compensation is of the basic value of the measurable composite quantity. The indirect measuring is only of the increment components of the measured vector. Hence in this diagram, besides the compensating device, it is necessary to have two phase-detecting voltmeters. This principle of measuring is applied in the apparatus of aerial electric prospecting by the VMP (rotating magnetic field) method (234).

Diagram 9 is based on the autocompensation principle of measuring. Autocompensation means a static type system with reverse feedback - the autocompensator is most often of electronic type with adjustable current. The main elements of the autocompensator - a deducting circuit, an amplifier with sufficiently high amplification factor, two component gauges KI, a summation circuit and a feedback circuit from the output of the summation circuit to the VS circuit. Although these diagrams are most popular in ground electric prospecting, in future, apparently, they will find application also in the aerial electric prospecting apparatus.

2. Pre-amplification of the measurable signal.

Pre-amplification of the working signal is a necessary operation for practically all known units of aerial electric prospecting. It is required with the setting up of field detectors in the outboard gondolas, as well as with their placing directly on the aircraft.

Pre-amplification is necessitated by the following.

The field detector is usually tuned into resonance oscillating LC-circuit. Its resonance resistance, being output resistance in the

given link of the receiving measuring apparatus, is usually quite high. The field detector is often placed outside the main set of the aerial electro-prospecting apparatus, i.e. it is brought out from the aircraft, sometimes to a considerable distance. In this case, the transmission channel of the signal from the field detector to the measuring apparatus, made in the form of connecting cables (shielded, unshielded, steel line, etc), is affected by noises from the aircraft.

To reduce the effect of noises, specially on the joining cables, it would be expedient to decrease the internal resistance of the whole section of the circuits, "field detector output - connecting cable - measuring apparatus input". This is achieved in the simplest way by pre-amplifying the received signal (the amplifier is set directly after the field detector) and by the adaptation of high-ohmic resonance resistance to comparatively low-ohmic resistance of the electric supply channel of the field detector with measuring instruments by means of cathode (emitter) repeaters at the output of the pre-amplifier.

Since the aircraft causes noises, the level of which is not high, the noises in the transmission channel of the working signal from the field detector to the measuring instruments may sometimes distort the received useful signal, specially if it is of low intensity, or extinguish it. In this case there should be a considerable rise (approximately by a factor of 10) in the useful signal level over the level of noise in the given channel. Hence, pre-amplification is necessary also for increasing the signal/noise ratio in the transmission circuit of the useable signal from the field detector to the measuring unit.

The transmission channel of the signal from the field detector to the measuring unit has a certain stray capacity and the latter, due to its instability, may affect the tuning of the field detectors, specially on high operating frequencies. In using steel line (gondola version), the stray capacity may reach upto 100 Mmf and even more per 1 m length of this cable. Therefore, the capacity has an appreciable effect, on high operating frequencies of the apparatus. Thus, preamplification is required for eliminating the capacity effect of the signal transmitting circuit on the field detector tuned into resonance, which may also be achieved by the setting up the preamplifier directly after the field detector.

The field detector and preamplifier form a receiving section of the measuring apparatus and play a considerable role in the general complex of reception, pre-processing and amplification of the useful signal and in the measuring of its parameters. They are usually placed directly next to each other. The preamplifier set up in the outboard gondola is often called the gondola preamplifier.

The unique operating conditions of the preamplifier on a mobile object determine the following technical requirements.

1. The preamplifier should have high (not less than 1-1.5 Mohm) input resistance to avoid shunting of the field detector, whereas its input resistance should be low (less than 200-300 ohm) for matching the subsequent input resistance.

2. The preamplifier should be vibration-proof; microphonic noise should be absolutely absent in it.
3. The level of the amplifier set noise, specially of its first amplifying stage, should be very low, considerably less than that of the signal, induced in the field detector at the required sensitivity threshold of the apparatus.
4. In service conditions, the preamplifier should have high stability in its characteristics, as its assignment includes amplification of low intensity signals. Instability of the amplification factor or variation of its phase response may result in emergence of pseudoanomalies or in systematic drifting of zero.
5. In many cases for realizing simultaneous operations on two frequencies, the input of the preamplifier should provide for connection without reciprocal effect of the two field detectors and the mixing of signals of two different operating frequencies. Hence the frequency characteristic of the amplifier should be uniform within the frequency band, determinable by the lowest and highest operating frequencies of the apparatus, i.e., the amplifier should be aperiodic.
6. The rectilinear section of the amplifier's amplitude characteristic in the apparatus of some methods of aerial electric prospecting should be widened as far as possible, since the levels of measurable signals may vary in comparative-ly wide range.

The energizing of the preamplifier, the switch-over of the field detector to the required operating frequencies, as well as the efficiency checking of efficiency of the whole receiving unit is done usually by remote control.

Construction of amplifiers with the requirements specified above is a rather difficult problem. However, its implementation is simplified by the fact that, in many cases, in practice, it is not necessary to reduce the power consumed from the power network of the aircraft in order to obtain high stability, good quality, of frequency characteristics, etc. of this unit.

Let us consider briefly the circuits of the main types of preamplifiers, used in some methods of aerial electric prospecting.

Gondola preamplifier for AERA-2 apparatus of the BDK method
(Fig. 113). This is an aperiodic amplifier, assembled on three tubes 6 117 (should be of vibration-stable series), and estimated for a single-channel operation. To reduce the noises, brought in by the first stage, a triode cut-in of the first tube is used in the amplifier. At the second stage, the use of a pentode cut-in is made. The output stage of the amplifier is assembled on a circuit of cathode repeater. The general amplification factor without backfeed is approximately 1000. The reverse feedback was so chosen that the general amplification factor would be 100. The cut-in at the input of the amplifier is a special change-over circuit with step relay SHI-11, which carries out change-over according to the operation of elements, brought out into the outboard gondola, and is controlled by one common starting push button.

Double damping has been applied for protection against microphonic noise: the whole amplifier is suspended on rubber shock-absorbers and moreover, the tube panels are fixed on paralon cover plates. The input resistance of the amplifier is not less than 1.5 Mohm, and the output - approximately 150 ohm. This permits matching the amplifier with the field detector and eliminating the noises from the helicopter equipment in the transmission channel of the signal as well as the noise from electric discharges caused by electrifying the insulation dielectric of the cable with its deformation under the effect of vibrations and oscillations during the flight of the helicopter.

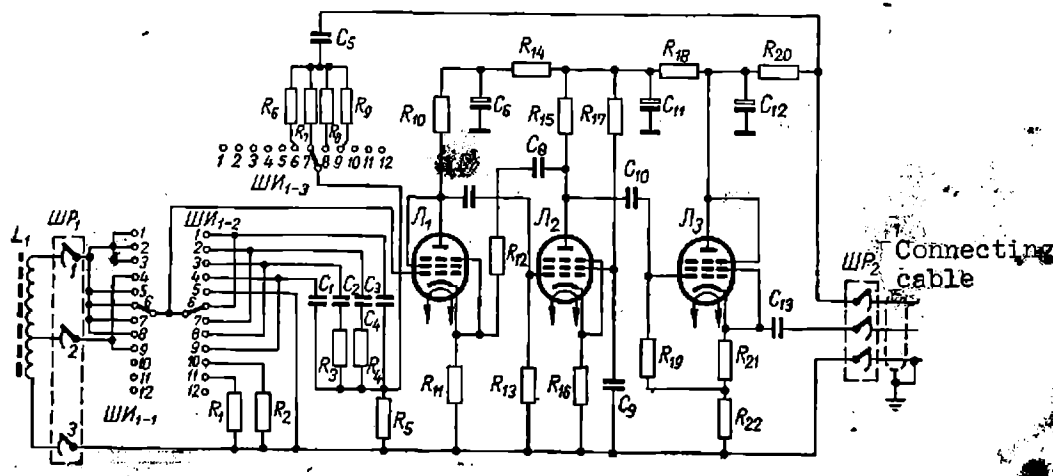


Fig: 113

The amplifier details are selected with high electric characteristics and the fitting is carried out with great care. The anode voltage is 100v. Incandescence filaments of the tubes are connected in series and cut in through the attenuator (not shown in the diagram) to

the circuit of anode supply. The control of the step-by-step switch is effected through the circuit of the output signal.

TABLE - 19

Diagram No.	Measuring device	Block diagram
<u>Direct measuring method.</u>		
1.	Selective voltmeter	
2.	Differential selective voltmeter	
3.	Phase-detecting selective voltmeter	
4.	Differential phase-detecting selective voltmeter	
5.	Quotient meter:	
	a) for measuring modulus ratio	
	b) for measuring component ratio	
<u>Compensation method of measuring</u>		
6.	Balanced compensator	
7.	Quasibalanced compensator	
8.	Unbalanced compensator	
9.	Autobalanced compensator	

Preamplifier of the BDK apparatus developed by IAE SO USSR(118)

(Fig. 14): is also of a single channel and meets all the requirements listed above. It is assembled on vibration-stable tubes of low-voltage series X-6 with anode supply voltage 24v, which makes it possible to use as the source of this supply, the helicopter power network directly. The incandescent filaments of tubes, connected in series, are energized from the board-network. To eliminate the effect of the varying loads(working conditions of helicopter, switching on and off of electric equipment,etc.) on the preamplifier the voltage of the board-network is pre-filtered and stabilized by means of the semi-conductive stabilizer, located in the automatics block of the measuring unit. The amplifier is encompassed by reverse feedback, which helps assure its low output resistance. Variation of the reverse feedback makes it possible to change the factor of amplification from 30 to 1500 smoothly.

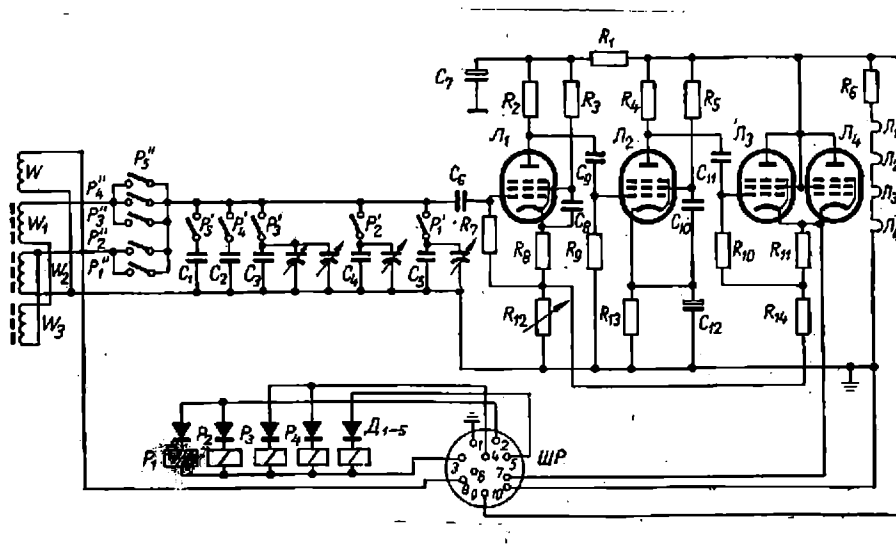


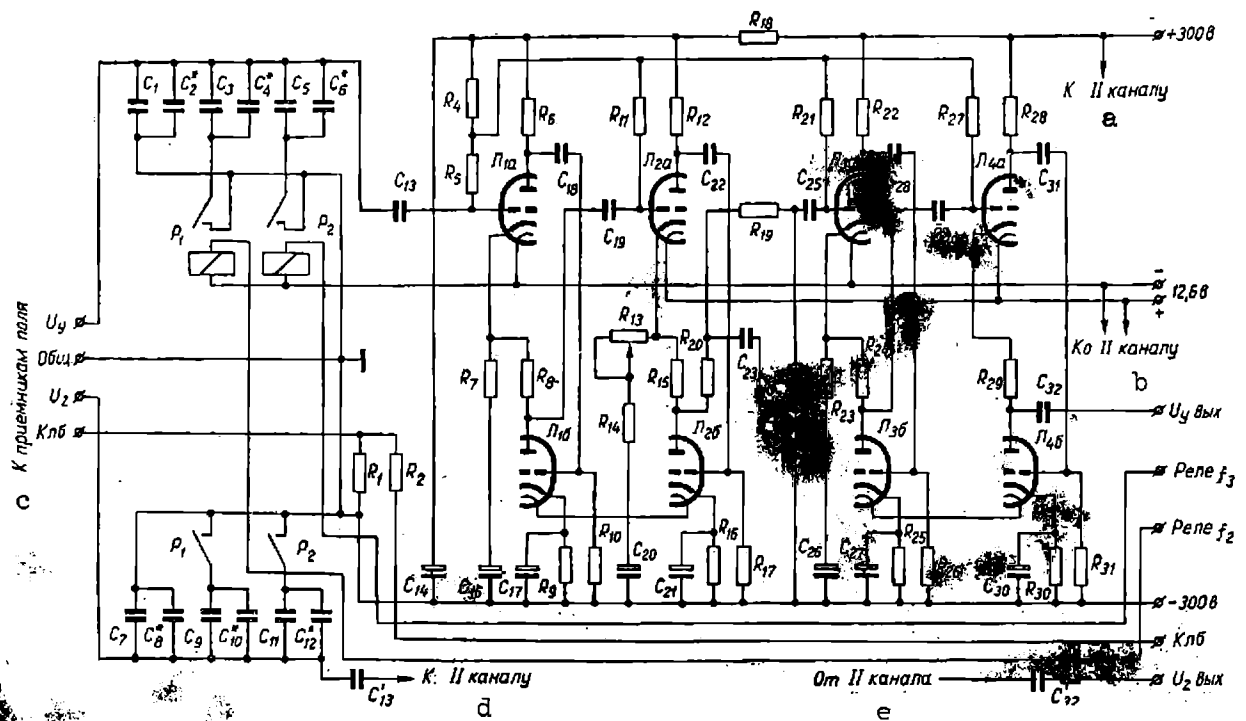
Fig: 114.

The last (output) stage is assembled on the circuit of the cathode repeater on two parallel connected tubes in the triode method of operation which assures low output resistance with maximum amplification factor. The noise level at the output of the amplifier, reduced to its input, in frequency band 20 kcps - is not over 3 mv, input resistance - not below 3 Mohm. Effective elimination of microphonic noises is achieved by suspending of the amplifier in the gondola on rubber guys. The change-over of field detectors to operating frequencies is done by remote control, with the help of relay circuit (relay of RSM-1 type).

Pre-amplifier of VMP apparatus, developed by VITR(234) (Fig.115) - is a two-channel one. Its construction is meant for installation in the outboard gondola. The amplifier has three amplifying stages and one matching (output amplifier).

The distinctive feature of the amplifier is the use in it of cascade connection of tubes, i.e., connection in series of two tubes in each stage. The tubes of the cascade circuit are a part of anode or cathode lead, each for the other, which makes it possible to assure high stability and the least dependence of the common amplification factor on the unstable parameters of tubes, supply voltage, etc.

The relay system at the input of the gondola amplifier helps implement remote tuning of both the operating field detectors to the operating frequencies of the apparatus.



Key to Figure 115:
 a, To channel II; b, To channel II; c, To the field receivers; d, To channel II;
 e, From channel II.

Fig: 115.

Each half of the tube 6H2II (the small panel for the tube L_1 is mounted on rubber shock-absorber) builds up amplification of about 30. Generally, with the use of the cascade circuit, it is possible to obtain amplification of one stage in the order of 1000. However, the intense reverse feedback in the stage reduces its general amplification to 10, which provides sufficiently high stability of the amplifying stage.

The second stage (tube L_2) is similar to the first, but has a higher common factor of amplification (20). At the output of this stage, filter R_{19} , R_{20} , C_{23} , C_{24} is cut in to serve for suppressing frequencies, lying above the maximum operating frequencies of the apparatus (2450 cps). Adjustment of the amplification factor from 10 to 30 (during tuning) could be implemented by potentiometer R_{13} .

The third stage is similar to the second (its amplification factor is 20). Thus, the resultant amplification factor of the gondola amplifier is 4000. The fourth stage is matching, it has low output resistance. The frequency characteristic of the amplifier is uniform in frequency band 600-2500 cps.

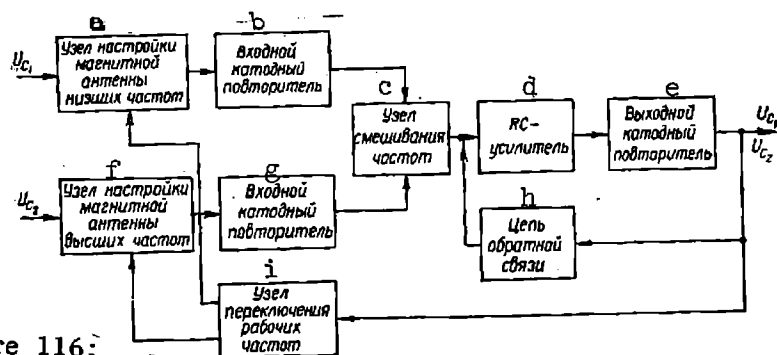
The incandescent filaments of each pair of amplifier tubes are connected in series and are energized from the board network by filtered direct current 12.6v. Filament current of one amplifier - 0.7 a. Anode voltage of 300v is fed from the ordinary unstabilized rectifier, located in the block of the measuring apparatus. The second amplifier is similar to the first.

Preamplifier of AERI-2 apparatus for aerial induction method

(Fig. 16). This amplifier carries out simultaneous operation of the receiving channel on two frequencies. The reconstruction of field detectors from one operating frequency to another is effected by the tuning nodes for low and high operating frequencies. Cathode repeaters, cut in at the output of the tuning nodes, match the output resistance of the receiving antennas (on high working frequencies it is about 10^6 ohm) with the other element of the circuit. Since the possibility of separate transmission, i.e., along separate cores of the cable, of a two-frequency signal from the gondola preamplifier into the measuring apparatus with remote supply and control of this amplifier is rather restricted (by the three-core cable), the signals of two operating frequencies received in the gondola amplifier are mixed and then simultaneously amplified in the intermediate aperiodic RC-amplifier. The output cathode repeater reduces the output resistance of the RC-amplifier and matches it with the low-ohmic channel of signal transmission. To ensure high stability of the amplifier parameters and the additional reduction of its output resistance, a reverse feedback circuit has been provided, which encompasses the output cathode repeater and the RC-amplifier.

The change-over node permits remote retuning of the receiving antennas to different combinations of operating frequencies, as well as the carrying out of the required commutations of the gondola amplifier input with control measurements (calibration, short-circuiting of the input for checking the natural noises of receiving channel, etc.). The line diagram of the gondola amplifier is shown in Fig: 117. Resistances

marked with an asterisk (see example, R_1^*), are selected during the tuning. Tubes cut in of the input cathode repeaters and of the node of frequency mixing by triodes, application of low load resistances ($R_{19}=R_{23}=13 \text{ kohm}$), and also the absence of shunting capacitances in the tube cathode circuit, assure a low level of natural noises in these stages. Elements of summation circuit R_{21} and R_{24} of the frequency mixing node are chosen in such a way as to prevent them from appreciable shunting of the anode loads of tubes L_3 and L_4 . The amplification factor from the grid of tube L_1 and L_2 to the middle point of circuit R_{21} , R_{24} is 2.5. The pentode cut in of resistive amplifier tube L_5 , high resistance of anode lead and blocking capacitance in cathode circuit make it possible to obtain the amplification factor of stage K of high value (upto 40).



Key to Figure 116:

a, Unit for adjusting ground antenna for low frequencies; b, Input cabinet repeater; c, Frequency mixing unit; d, RC-amplifier; e, Output cabinet repeater; f, Unit for adjusting magnetic antenna for high frequencies; g, Input cabinet repeater; h, Feedback circuit; i, Unit for changing working frequencies.

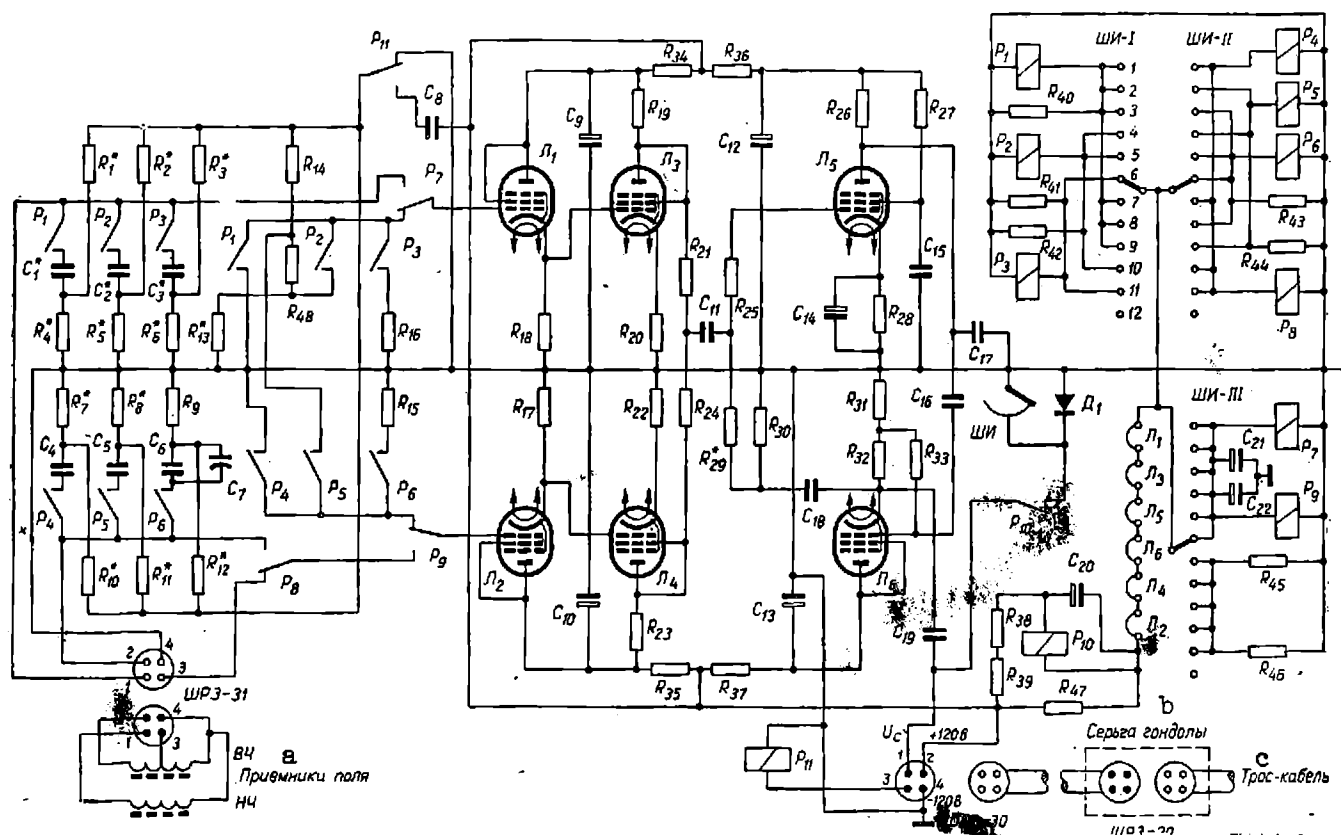
Fig. 116

Experimental investigations have shown that the voltage of fluctuating noises on all operating frequencies does not exceed 0.5 mv, and the voltage of noises and inductions in the transmission channel of the signal received on the measuring apparatus 40-50 mv; the required amplification factor $K = 100$ has been determined on this basis.

The last two stages are encompassed by reverse feedback. The voltage of reverse feedback is supplied from the cathode of tube L_6 through circuit $C_{18}R_{29}$ onto the grid of tube L_5 . In this case, the output resistance is reduced to 55 ohm(44, 249). The voltage of the anode supply is limited by the working allowed voltage for the cable cores; it is taken as 120 v. Incandescent filaments of the tubes are energized from the source of anode supply with their subsequent connection. Excess voltage is dampened on additional resistance R_{47} .

As change-over devices for the cutting-in of condensers tuning the field detectors the use is made of relays RSM-1 and RCM-2, which are cut in turn by the contacts of the step-by-step switch SHI-II in 12 positions. Of these 12 positions, 11 are used for the control of the gondola amplifier, and one, the 12th, is applied for checking the operation timing of the finder in the gondola amplifier and of the double-finder in the block of stabilized rectifier of this amplifier, located in the measuring unit of the apparatus, from which the remote control of the gondola amplifier is effected. In this position of the finder, the supply circuit breaks, which is marked by the position of the double finder and controlled by the measuring device.

Connected parallel to resistance R_{47} (circuit + 120v) is the relay coil R_{10} , connected in series with which are the damping resistances R_{38} and R_{39} . With a nominal supply current (working conditions), the drop in voltage on resistance R_{47} feeds this relay coil and this, while operating, unlocks its contacts. This results in the cutout of the finder's coil from the output of the gondola amplifier, thereby removing the possibility of parasitic magnetic intercoupling between the coil of



Key to Figure 117:

a, Field receivers; b, Gondola connector; c, Connecting cable.

Fig: 117.

the finder and the receiving antennas. For protection against extra current the relay coil R_{10} is blocked by electrolytic condenser C_{20} .

The coil of the finder is cut in to the output of the amplifier only during the feed of change-over impulses (at this time the supply voltage is taken off the amplifier), Diode D_1 , which shunts the coil of the finder, serves for damping the extra currents. In series with resistance R_{47} and incandescent filaments of radio-tubes the connection is made through contact groups of finder SHI-I-SHI-III of the relay group RCM coils. The resistances, which shunt the coils, are so matched that the group of relays RCM would operate reliably at a nominal working supply current and the common current transmitted through the relay coils and resistances would be similar in all positions of the finder.

The rectilinear section of the amplifier's amplitude characteristics is permissibly widened, so that at the extreme operating frequencies $M_{low} \leq 1.005$ and $M_{high} \leq 1.005$, and $k_f = 0.01$.

Unified transistorized preamplifier OKB MG USSR (Fig.118), where 1-10 are the points of the electric circuit, soldered to the branches of the plug connector. This amplifier was developed in 1965. It consists of unified nodes. An amplifier of this type could form the basis for systems for preamplifying signals received by the field detector in many methods of aerial electric prospecting.

It is known that, in amplifiers of low frequency, the amplifying properties of transistors are most fully utilized by direct coupling between stages. Besides improving the condition of matching and frequency characteristics in the zone of low frequencies coupling of this type makes

it possible to simplify considerably the diagram of the amplifier and to reduce its overall size. The characteristic feature of the diagram is the presence of transistors, operating in the input stages in conditions of low currents and voltages, which improve to a considerable extent the energy and noise indices of the diagram. To ensure these conditions, it is necessary for transistors to have sufficient amplification factor on current α at low intensity (about 0.2-0.4 ma) of the collector current. These properties are possessed by a majority of silicon transistors, specially transistors MP101-MP103 (in the present diagram $T_3 - T_6$ are transistors MP102). As shown by measurements, the value of factor α in these transistors with collector current 0.3-0.4 ma is half the α values, measured in nominal test conditions.

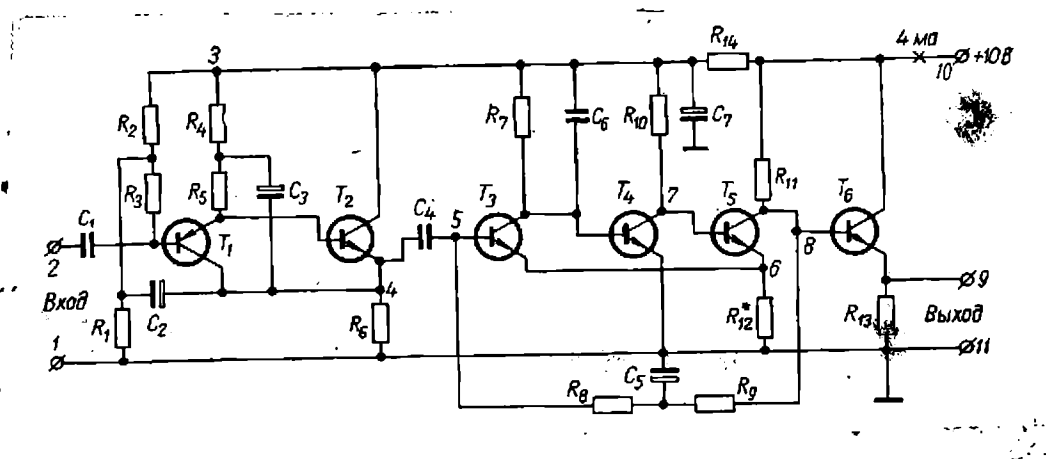


Fig: 118.

The input portion of the amplifier is assembled on a circuit of doubled emitter(54). This circuit has a sufficiently high input resistance (upto 2.5-3 Mohm) with transmission factor close to one.

Transistors T_1 (P28) and T_2 (MP103A) operate in "lownoise" conditions: the voltage between the collector and emitter of transistor T_1 is almost equal to that between the base and emitter of transistor T_2 and is only 0.1-2v. The collector current, transmitted through the first transistor, is also very low (0.1-0.15ma). Moreover, in the first stage of the circuit low-noise transistor P28 with noise factor not over 5 db is used.

From the collector of transistor T_5 to the base of transistor T_3 is fed voltage of reverse feedback on direct current. Feedback on alternate current is eliminated by the cut-in of condenser C_5 between resistances $R_8 - R_9$ and the common busbar of the amplifier. The increase the input resistance on the side of transistor T_3 input, and also for raising the stability of the amplification factor, resistance R_{12} has been cut-in into the emitter circuit of transistors T_3 and T_5 , due to which resistance there is additional circuit of reverse feedback in series on direct and alternate current. The intensity of resistance R_{12} does not exceed 30-40 ohm, therefore, its cut-in does not affect the estimated circuit on direct current. To reduce the output resistance, the last stage (T_6) is cut-in on circuit with a common collector. The range of the amplifier's frequencies is within 10-30 kcps. Frequency characteristics of the amplifier in the region of low frequencies depend mainly on the value of capacitors C_4, C_5 . Capacitor C_6 is cut in to prevent parasitic excitation on high (30-60 kcps) frequencies. The tuning of the amplifier

means correcting resistances $R_8 - R_9$ from 47 to 100 kohm. Consumption of power by the circuit from the supply source is not over 40-50 mkwt.

3. Selective amplification.

The increase in efficiency of the measuring unit in aerial electric prospecting with harmonic field (see para 3 chapt.IX) may be obtained with additional selective amplifying of the receivable signal. In this case, it would also be possible to increase signal to noise ratio at the output of the selective amplifier as compared to the ratio at its input. Simultaneously, the effect of natural noises of field detectors and preamplification nodes of the received signal is reduced, as of vibration noises and possible inductions on the measuring instruments from some nearby generating units, specially with the simultaneous operation of the apparatus on two frequencies.

Selection amplification in aerial electric prospecting is usually achieved by the application of selective LC - and RC-amplifiers. In this case, the anti-resonance circuit is very seldom used in the amplifying channel.

The main requirements of the selective amplification could be stated as follows:

1. The selective circuit should ensure suppression (upto 50 db) of side-band frequencies.
2. Frequency characteristics of the selective circuit within the limits of negligible detuning due to operating resonance frequency should have "flat" top.

3. Phase characteristics on the operating frequency and with negligible detuning should be almost linear.
4. Parameter instability of the selective circuit and amplifying channel should not cause additional error exceeding the basic error of the apparatus.

Calculations and practical work with the apparatus of aerial electric prospecting have shown that for the implementation of the first requirement the use could be made of selective circuits with suppression of side-band frequencies by tens and even hundreds of times (20-50 db). For the single-frequency apparatus these requirements naturally, are lower, for double-frequency one - higher. The constructive assembly of circuits is rendered difficult mainly in the building of the two-frequency apparatus, where it is necessary to reduce the inter-effect of the channels. The main attention in this should be paid to shielding, correct and rational disposition of the input and output circuits of individual nodes, connections between separate blocks, constructive arrangement of the measuring and generating units both in separate blocks and in the common body, etc.

The shape of frequency characteristic in the selective circuit near the operating frequency, applied in the apparatus of aerial electro-prospecting, is shown in Fig: 119. Here on axis of abscissae is plotted detuning $\frac{\Delta f}{f_0}$, and on axis of ordinates - output voltage ratio $\frac{U_{out}}{U_{out.max}}$, where U_{out} - voltage with detuning Δf , and $U_{out.max}$ - voltage on resonant frequency f_0 .

Within the limits of the flat frequency characteristics the amplification factor of the selective circuit remains invariable or varies insignificantly. As a result, it is possible to reduce the stability demands of frequency f_0 in the oscillating apparatus (since negligible detuning from the field detector's resonance is allowed); also, a somewhat higher instability of the selective circuit, than with sharp frequency characteristics. In the practical implementation of this circuit, the effort is usually to obtain the selectivity curve symmetrical in respect of the ordinates axis.

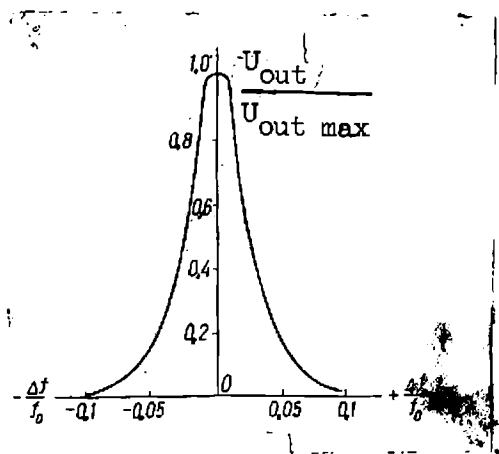


Fig: 119.

The requirement of linear phase characteristics in the selective circuit ensues from the necessity of studying the phase characteristics of the field with a certain error in the phase. Minimum additional error in the measuring channel of the phase will

be when with a negligible deviation of resonance frequency f_0 , the phase characteristics of selective circuit will hardly change. To obtain this type of characteristic is very difficult; therefore, the effort is to assure its linear relationship within the transmission band of frequencies $2\Delta f$ (at a level 0.707). This permits preventing to some extent the appearance of pseudoanomalies in the phase due to possible jumps of phase characteristics in the selective circuit (e.g., variation of external conditions during the flight: temperature, humidity, etc.).

The measuring apparatus should be vibration-stable, and the first amplifying stages should be protected to an extent that the level of vibrational noises in the selective circuit itself would be low.

LC-selective amplifiers, widely adopted in low and high-frequency apparatus of aerial electro-prospecting, usually consist of one or several LC-circuits. In the concentrated inductances of the circuit the use is most often of inductance coils with Alsifer cores. At low frequencies the inductance value of the circuit is limited by the size of the standard core and practically does not exceed 1 henry. In the same conditions the inductance of coil on ferrite core increases upto 1.5-2 henries. The application of LC-selective circuits on low frequencies is somewhat difficult due to the presence of amplitude characteristic in inductance value of LC-circuit, assembled on ferrite core, and also low Q-factor of inductance itself, assembled on Alsifer core. According to the test data, inductance ferrite core of toroidal shape 200 NN ($\mu_H = 250$) with variation of signal amplitude from 0.1 to 10v varies its value to such an extent that the resonance frequency of the circuit changes within the limits of 5 to 10%. Circuits of these types are not used for measuring purposes.

The low Q-factor of toroids with Alsifer cores, and also increment in the capacitance value of the circuit's tuning into resonance at reduced resonance frequency, make whose application on low frequencies difficult. Thus, on frequency $f = 244$ cps at $L = 0.7$ henry capacitance of C circuits comes upto 0.6 mF. This means that the capacitance of condensers, which could have been applied in the circuit, will be too low, as a result of which the temperature stability of the circuit will also be low, and the application of such a circuit in the amplification channel is inexpedient. The advantages of LC-circuits on high frequencies are more apparent (116).

To reduce the overall size of the measuring circuits, to increase their stability, Q-factor and other characteristics the application is often made of selective RC-amplifiers of blocking type with double T-shaped RC-bridge in the reverse feedback circuit, assembled usually according to two- and three-stage circuits with high amplification for the working signal. Due to sufficiently low capacitance values required in this bridge, application is possible of small size stable tuning condensers.

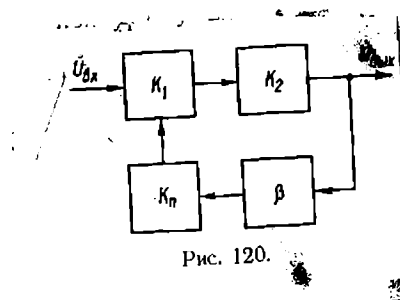


Fig: 120.

The two-channel RC-amplifiers are usually assembled according to the diagram shown in Fig. 120, where U_{in} and U_{out} - are the input and output voltage respectively; K_1 and K_2 - amplification factors of the first and second stages respectively; β - the transmission factor of anti-resonant circuit; K_{π} - the transmission factor of the cathode repeater. To obtain high Q-factor of RC-amplifiers it is necessary to apply stages with high amplification factor. However, in this case the selective amplifiers have one substantial short-coming-tendency to singing (14, 15, 176, 249). It is known that the cause of singing in the amplifier with closed feedback is the phase shift $\varphi = 360^\circ$ or $\varphi_c = 30^\circ$ whereas the amplification factor K on any frequency outside the pass-band of the amplifier should be considerably greater than one.

In the selective RC-amplifier, assembled according to the diagram in Fig. 120, on distant side-band frequencies, where the transmission factor of anti-resonant circuit $\beta \approx 1$, the amplification factor is given by formula

$$K_{обл} = \frac{K_o}{1 + K_o} \approx 1, \quad (X.I)$$

where K_o - the amplification factor of two stages on resonance frequency.

With the high amplification factor K_o , the presence of the parasitic capacitance in the amplifier will cause general phase shift, at which there is positive feedback, resulting in unstable operation of the amplifier or its singing. Due to insufficient stability, inherent

in high quality low-frequency RC-amplifiers with double RC-bridges in feedback circuit, these amplifiers are not widely used in the apparatus of aerial electro-prospecting. But in the practical diagrams for amplification stabilizing of selective RC-amplifier combination of active and frequency-dependent feedback is very widespread. Selective amplifiers with the so called intensified reverse feedback with improved productive characteristics even on very low frequencies, may also become popular (13, 14).

The diagram of a one-circuit selective RC-amplifier, operating on this principle, is shown in Fig. 121 (denotations are the same as in Fig. 120, moreover, $U_{e.c}$, $U_{e.c}$ - feedback voltages; K_2 - the amplification factor of additional amplifier of feedback voltage). In this diagram, the signal is amplified only by one stage, and the general amplification factor on tuning frequency is equivalent to the amplification factor of the first stage.

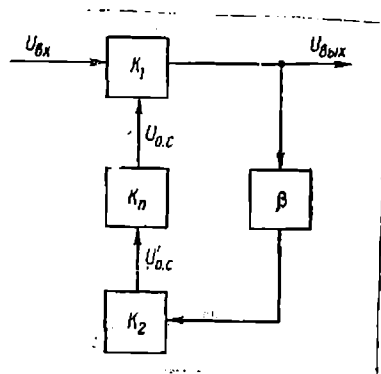


Fig: 121.

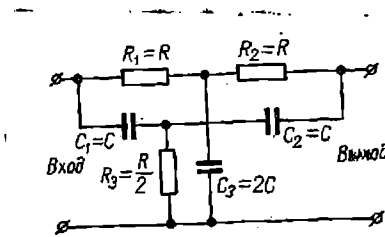


Fig: 122.

On side-band frequencies, the amplification factor is determinable from formula

$$K_{\omega} = \frac{K_1}{1 + \beta K_1 K_2 K_n}, \quad (X.2)$$

In this case, Q-factor of the selective stage could be determined from ratio

$$Q = \frac{K_1 K_2 K_n + 1}{4}, \quad (X.3)$$

In the capacity of frequency-dependent feedback, the use is made of symmetric double T-shaped RC-bridge (Fig. 22). Elements of the bridge are calculated from the known ratio

$$f_0 = \frac{1}{2 \pi K C} \quad (X.4)$$

Selectivity increase in the amplifying channel in the apparatus of aerial electric prospecting could be obtained either by the application of several selective RC-amplifiers, or of LC-circuits with cut-in into discrete amplifying stages in the build-up of band-pass filter or into one amplifying stage. In the latter case, besides the selectivity increment, there is improvement in the rectangular factor of the selectivity system, and the phase characteristic becomes almost linear.

It is a known fact that the three-circuit band-pass filter is an optimum version of selective circuits (116). Input diagram of the selective LC-amplifier with three-circuit band-pass filter is shown in Fig: 123. Stabilization of the amplification factor of the amplifier and value increment of R_1 tube can be implemented by reverse feedback in the current. Inductances of circuits are selected similarly.

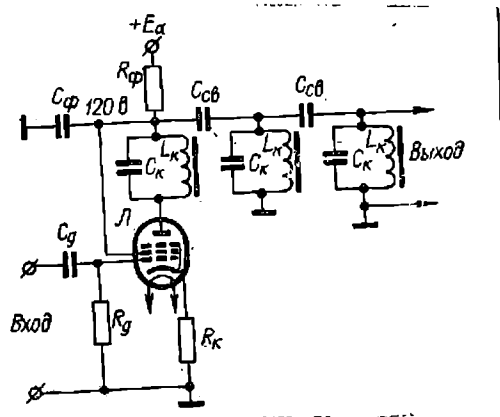


Fig: 123.

Between the separate circuits of the band-pass filter is a capacitance coupling through condensers C_B . The capacitance of the coupling condenser is taken as critical and is calculated from formula

$$C = \frac{C_{\text{KOHT}}}{Q} \quad (\text{X.5})$$

where C_{cent} - circuit capacitance.

The selectivity of the diagram at low detuning (less than 10% f_0) is determinable from formula

$$s_1 = \frac{a^6 - a^4 + 8a^2 + 9}{3} \quad (X.6)$$

where

$$a = \frac{2 \Delta f}{f_0}, \quad Q$$

At distant detuning selectivity of the diagram may be determined from the term

$$S = \frac{Q^3}{3X^4} \quad (X.7)$$

where

c

$$x = \frac{f}{f_0}$$

To reduce the possibility of amplitude-phase distortions, the band-pass filter should be cut in in the first stage of the amplifier. This diagram, successfully applied in the selective measuring amplifier of AERIS apparatus, could be recommended for practical application. Given ahead are the specifics of such a band-pass filter:

	Frequency, cps				
	500	1000	2000	4000	8000
Circuit inductance, henry	0.5	0.25	0.125	0.0625	0.03125
Circuit capacitance, mF	0.2	0.1	0.05	0.025	0.0125
Noise damping with					
frequency 50 cps	$21 \cdot 10^7$	-	-	-	-
Noise damping with fre-					
quency 400 cps	$5 \cdot 10^3$	$3 \cdot 10^4$	$1.3 \cdot 10^6$	$21 \cdot 10^7$	-

N.B: On the indicated frequencies, the following parameters remain invariable: Q-factor of circuit - 40; amplification factor - 46; selectivity with 10% detuning - 170 (over 40 db); amplitude variation in the range of 1% detuning - 1.26.

It has been established by experiments that the phase error with variation of input voltage in the working portion of the phase recorder scale does not exceed 2° for each frequency.

In building selective diagrams of the measuring apparatus, the importance is that of their temperature stability, moisture resistance and being vibration-proof. It is a known fact that the stability of the selective RC-amplifier, including that with the amplified reverse feedback, is determined mainly by the stability of condensers and resistances of the double T-shaped RC-bridge. By introducing active feedback, the instability of the amplifying stages could be reduced to negligible as compared to bridge stability.

In the case of applying two selective amplifiers connected in series with bridges detuned in respect of each other, the highest effect on the amplification factor is caused by the asymmetric instability of the transmission factor. Temperature asymmetry of the bridge is caused by dissimilar temperature factors of condensers and resistances.

The highest temperature stability of amplifiers is provided by mica condensers SGM and KSG type with temperature stability $\pm 0.005\%$ per 1°C . The resistances of VS type have negative temperature factor (45) (thus, for power 0.5-2 wt it is 0.1% per 1°C with temperature range -60 to $+20^{\circ}\text{C}$), whereas resistances MLT have the temperature factor $\pm 0.12\%$ per 1°C . The most stable in temperature factor are the resistances of BLP type (upto 100kohm). Temperature factor of the resistances of A type is 0.01% per 1°C within the temperature interval $+20 - +60^{\circ}\text{C}$ and 0.0125% per 1°C in interval $+20 - +60^{\circ}\text{C}$.

If for the resistances with temperature fluctuations from -10 to $+40^{\circ}\text{C}$ variation of their values is about 5% then for the BLP in the same temperature limits it is about 0.5% . This value is close to the temperature factor of mica condensers capacitances.

To avoid high asymmetric instability it would be expedient to use, as adjusting resistances of the bridge, wire adjustable resistances (manganin, PPZ-12 with temperature factor 0.003% per 1°C).

The instability of LC-circuits is determined in the same way as of the inductive magnetic field detectors (see para 5 chapt.VII and (154)).

4. Application of phase-detecting principle:

During the last few years, phase-serving detectors (FHD) have been widely applied in serial electric prospecting.

The operating principle of PHD has been sufficiently described in literature (100, 101, 224, 259); therefore, here we discuss its main properties in application to the diagrams of measuring and recording apparatus in aerial electric prospecting. It is known that FHD have rather high selectivity, high input resistance, wide range of operating frequencies, comparatively high zero stability, etc. (101, 151, 179).

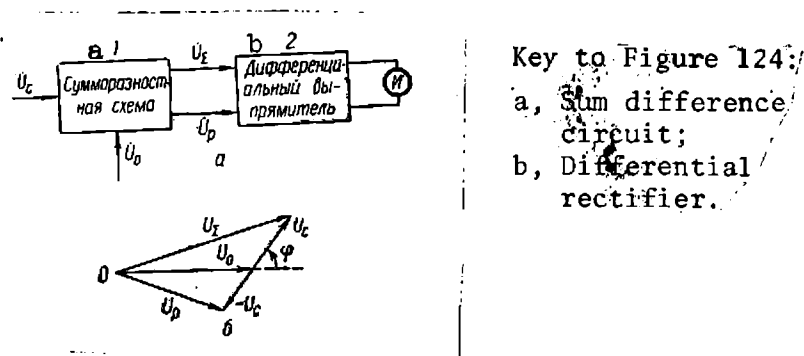


Fig: 124

There are two operating methods of PHD: detecting and keying. The detecting method is characterised by comparative voltage having sinusoidal shape; the detecting could be diode, anode or cathode type. The detecting circuit of FHD includes, as a rule, a differential detector with a circuit of geometrical adding and subtraction. A block diagram

of this type of FHD is shown in Fig. 124,a. The measurable signal \vec{U}_c and comparative voltage \vec{U}_o are lead in to sum-differential circuit, providing for the phase-inversion of one of the voltages and obtaining of their vector sum \vec{U}_Σ and difference \vec{U}_p . The vector diagram, explaining the operation of this circuit, is shown in Fig.124,b. Voltages \vec{U}_Σ and \vec{U}_p are then fed into the input of the differential detector, the output terminals of which are so connected so that the cut-in electromagnetic device I shows the difference of these two voltages as average. The indication of device is determined from the following relation (101):

$$\sqrt{\alpha} = C \sqrt{U_c^2 + U_o^2 + 2U_o U_c \cos \varphi} - \sqrt{U_c^2 + U_o^2 - 2U_o U_c \cos \varphi} \quad (X.8)$$

where C - factor dependent on the circuit parameters; φ -angle of the phase shift between \vec{U}_c and \vec{U}_o .

With fulfilment of condition $U_o \gg U_c$ formula (X.8) simplifies, indications of device I become proportional to the active component of signal

$$\alpha = CU_c \cos \varphi \quad (X.9)$$

If to FHD, assembled according to the block diagram in Fig. 124,a, comparative voltage of rectangular shape is applied, its operating method will be the method. Indications of device at $U_o \gg U_c$ are also determinable by formula (X.9).

The key method is characterised by lower dependence of voltage at the output of the FHD on the level of comparative voltage with the shape of rectangular pulses ("quadratrix" of sinusoid), which periodically open and close the circuit. This method resembles the operation of the phase-detecting circuit with mechanical rectifiers. To obtain a "quadratrix" the sinusoids use the usual circuits of limiters.

Depending on the method of supply and adjustment of comparative voltage phase, indications of device I could be proportional to the active and reactive components, the amplitude or phase of the measurable signal (Fig. 125).

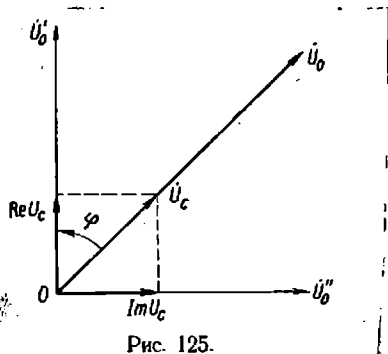


Fig: 125.

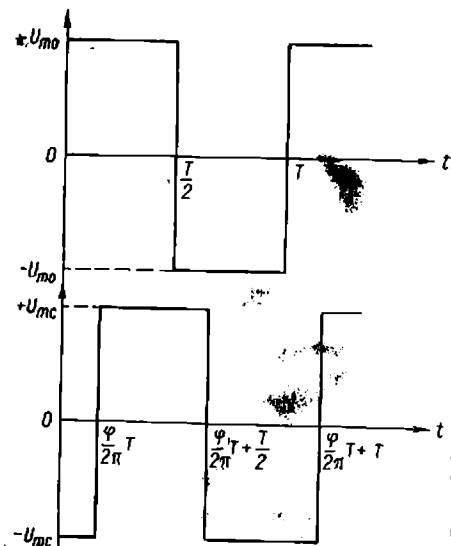


Fig: 126.

If the vector of comparative voltage U_0 coincides in direction with vector U_c , the voltage at the FHD output is proportional to the amplitude of the measurable signal U_c . When the vector of comparative voltage U_0 makes with vector U_c angle φ , its projection onto direction U_0 will be $\text{Re}U_c$. The voltage at the FHD output, proportional to $\text{Re}U_c$, is denoted as the active component of the measurable signal. But if vector U_0'' makes with U_c angle $90^\circ - \varphi$, then at the output of the FHD the voltage is proportional to $\text{Im}U_c$, or to the reactive component of the measurable signal.

The turn of the phase at the required angle may be provided by means of various types of phase-invertors*, providing, as a rule, the turn of the phase in the channel of the key signal at any required electric angle.

From formula (X.9) it is seen that for measuring the phase angle it is necessary to ensure either constant amplitude of the measurable signal, more precise product CU_c , or to use the property of the FHD as zero indicator of transition over the phase shift $\varphi = \pm 90^\circ$ (in this case voltage at the output of FHD is equal to zero). This requires operating by graduated phase-invertor of phase shift to indicated moment. In this case, the reading of the phase is taken from the graduated phase-invertor.

Indications of the phase meter, constructed by the first method, vary in accordance with the cosine curve, which is not always profitable and acceptable. Therefore, it is expedient to have indications of the phase meter proportional to the phase shift. It can be shown that the

* Direction of vector U_c may or may not coincide with direction of vector U_0 ; therefore, the sign of active & reactive components could generally be either positive or negative.

FHD has this possibility. Indeed, if the FHD is imagined as multiplication circuit (56, 64), at the outputs of which arrive two signals (U_c and U_o), having between them the phase shift of rectangular shape, it may be assumed that

$$\alpha = C \int_0^T U_{mc} U_{mo} dt. \quad (X.9a)$$

Thus, both the signals could be written as follows (Fig. 126)

$$U_o = \begin{cases} + U_{mo} & 0 < t < \frac{T}{2} \\ - U_{mo} & \frac{T}{2} < t < T \end{cases}$$

$$U_c = \begin{cases} - U_{mc} & 0 < t < \frac{\varphi}{2\pi} T \\ + U_{mc} & \frac{\varphi}{2\pi} T < t < \frac{\varphi}{2\pi} T + \frac{T}{2} \\ - U_{mc} & \frac{\varphi}{2\pi} T + \frac{T}{2} < t < T \end{cases}$$

Substituting the obtained U_c and U_o values into formula (X.9a), we obtain

$$\alpha = c' U_{mc} U_{mo} \left(\frac{\pi}{2} - \varphi \right) \quad (X.10)$$

At a moment, when $\varphi = \frac{\pi}{2}$, we have $\alpha = 0$.

Therefore, the FHD circuits are universal. Their diversity is clearly shown by the block diagrams shown in Fig. 127.

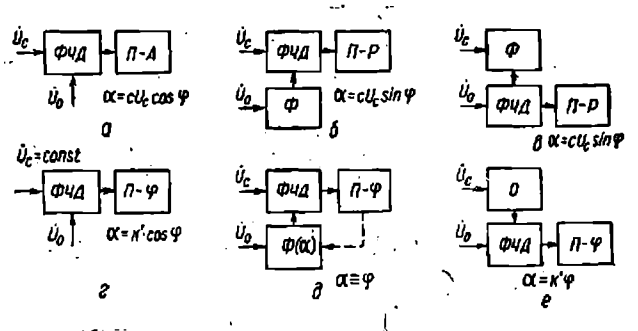


Fig: 127.

where ϕ - the phase-invertor; $\Pi - A$, $\Pi - P$, $\Pi - \varphi$ - recorders respectively of the active, reactive components and of the phase; O - the level arrester. Other FHD diagrams are given in chapt.XII.

Let us consider the selective properties of the FHD, which are so important in aerial electric prospecting. The high selectivity of FHD is explained primarily by the fact that, due to the effect of comparative voltage, the conductivity of detector time varies with certain recurrence and, therefore, from the average value of the rectified current, exclusion of components from the input signal of non-synchronous commutation frequency is made to some extent. If we compare the selective properties of the detector insensitive to the phase (for instance, of rectifying system voltmeter) with phase-sensitive detector on the action of sinusoidal voltage of noise, it would not be difficult to become convinced of the advantages of the latter.

With the action of noise U_{π} voltage at the output U_{α} of the

phase-insensitive detector in the case of $\frac{U_n}{U_c} \ll 1$ is expressed by the following relationship (101):

$$\frac{U}{\alpha} = aU_c \left[1 + \left(\frac{U_n}{U_c} \right)^2 \right], \quad (X.11)$$

where a - the conversion factor of the detector, equal to the ratio of average rectified voltage to the virtual sinusoidal voltage.

Relative error due to noise effect is given in the following terms

$$\delta_{\alpha} = \frac{1}{4} \left(\frac{U_n}{U_c} \right)^2 \quad (X.12)$$

The significance of the given relation lies in that the value of error increases slower than the noise-to-signal ratio $\frac{U_n}{U_s}$, i.e., in this case, there is an event, which is characterised as suppression of noise by the signal. Thus, with noise of 30% of measurable voltage, the error comes to only 2.3%.

In the determination of error due to noise action, in a case where the FHD is applied it should be assumed that there is a differential detector in its composition, which in turn should be considered as two linear detectors, to the input of which in the absence of noise are fed two voltages (see Fig. 124,a):

$$U \quad U_c$$

$$\begin{aligned} U_{\Sigma} &= \sqrt{U_c^2 + U_o^2 + 2U_c U_o \cos \varphi}; \\ U_p &= \sqrt{U_c^2 + U_o^2 - 2U_c U_o \cos \varphi}. \end{aligned} \quad (X.13)$$

Indications of device, cut in at the output of the differential detector, are proportional to the difference of voltage amplitudes $a(U_{\Sigma} - U_p)$. The presence of noise with amplitude U_n causes the increment of voltage at the output of both halves of the detector, and for one half it may be determined in accordance with relation (X.11) from the terms

$$aU_{\Sigma} \left(1 + \frac{1}{4} \cdot \frac{U_n^2}{U_{\Sigma}^2} \right)$$

and for the other - from formula

$$aU_p \left(1 + \frac{1}{4} \cdot \frac{U_n^2}{U_p^2} \right)$$

Voltage at the input of the differential detector is proportional to

$$U \approx a \left[U_{\Sigma} \left(1 + \frac{1}{4} \cdot \frac{U_n^2}{U_{\Sigma}^2} \right) - U_p \left(1 + \frac{1}{4} \cdot \frac{U_n^2}{U_p^2} \right) \right]$$

After conversion of this equation, we obtain the term for relative error of the FHD, caused by the noise effect:

$$\delta = - \frac{1}{4} \frac{U_n^2}{U_{\Sigma} U_p}$$

or with $U_s \ll U_d$ and $\sum U_d \approx U_c^2$ we get

$$\delta = - \frac{1}{4} \left(\frac{U_n}{U_c} \right)^2 \quad (X.14)$$

In the first approximation the error of the FHD, caused by the action of noise, does not depend on quantities U_s and φ , but is determinable only by ratio $\frac{U_n}{U_c}$. In spite of the fact that the structure of formulas (X.12) and (X.14) is similar, the error of the FHD from the noise action is found to be much lower than the error of the ordinary detector, since U_c is considerably higher than U_s (usually $U_s < 0.1 U_c$).

The selectivity of the FHD could be considerably increased, if instead of detecting the application is of key method of operation, i.e., change-over to comparative pressure of rectangular shape. If commutation error is known (Fig. 128), it is easy to find the amplitude, equivalent to the detecting method of comparative voltage:

$$U_{mT} = \frac{U_T}{\sin} \quad \frac{U_T}{Y}, \quad (X.15)$$

since value is low.

Substituting into formula (X.14) instead of U_c the value of U_{mT} , we determine the relative error of the FHD, operating in key conditions:

$$\delta_K = - \frac{1}{4} \gamma^2 \frac{U_n}{U_r}^2, \quad (X.16)$$

where U_t - the intensity of comparative trapezoidal voltage (see Fig.128)

Thus in key conditions, the FHD has considerably higher selectivity than with detecting. For instance with $\gamma = 0.1$ and $U_c = U_t$ the error in keying is 100 times less than in detecting.

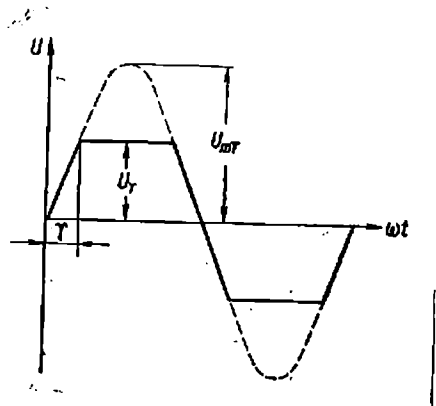


Fig: 128.

However, selectivity of odd harmonics of U_s signal in the FHD is not high. Thus, for n -th harmonic of signal current at the output of the FHD is given by relation (137).

$$I_{cp} = \frac{c U_k}{k} \cos \varphi_k, \quad (X.17)$$

where φ_n - the angle of phase shift of n -th harmonic.

Therefore, the FHD error from the signal harmonics should be equal to the harmonic divided by its number. To avoid this short-coming, the high signal harmonics, where possible, are filtered by means of selective circuits, cut in at the input of the FHD.

Moreover, the comparatively high selectivity of the FHD in the key method makes possible substantial suppression of all noises, incoherent to the key signal but similar in frequency, even if they are of considerably higher intensity than the signal. In this case, it is important for the intensity of comparative voltage to remain higher than the intensity of noise. This makes it possible to use the FHD for measuring low alternative voltage and as the node for the comparison of follow-up systems in automatic recorders of modulus, components and phases in aerial electric prospecting.

5. Measuring of amplitude (modulus):

In the majority of the measuring apparatuses for aerial electric prospecting, the possibility of measuring and continuous recording, with the required precision, of the sinusoidal signal level has been provided.

From the classification table of measuring circuits (see para 1, chapt.X) it follows that in accordance with the problems of aerial electric prospecting, it is possible to make a choice of methods for measuring the level of the anomalous field signal. Thus, in the methods of near and combined zones the direct measuring of the signal level by means of phase-detecting and amplitude voltmeters has become very popular.

In the apparatus of radio control and measuring, the "direct" measurements are carried out after frequency conversions (222). However, in the choice of the measuring method, the consideration should be not only of merits, short-comings and potentialities of each of the indicated methods, but also of the difficulty of constructing the measuring devices.

The direct measuring of the signal level is most simple by means of electronic voltmeter of any type (175, 193, 207). The operating principle of electronic voltmeters is based on the detection of the measurable sinusoidal voltage by means of electronic tube, and of the rectified current by electro-magnetic measuring devices, the scale of which is graduated directly in units of the measurable voltage. Depending on the principle of detecting, there are electronic voltmeters with anode, grid, cathode and diode detection. In comparison with voltmeters of other systems, electronic voltmeters have some advantages, the main ones of which are the high input resistance and the wide range of operating frequencies. In aerial electric prospecting the most popular are voltmeters with cathode and diode detecting.

The main difficulty in measuring with electronic detecting voltmeters is in providing effective prefiltering of the usable signal from outside noises and those arising in the preamplification channel. Therefore, besides the introduction of selective elements in the input circuits of electronic voltmeters, it is also necessary to choose the most noise-proof operation conditions.

There are three main methods for operating the electronic detecting voltmeters (175, 207) Class A, in which the virtual (effective) value of voltage is measured by the voltmeter; Class B, in which the voltmeter is used for measuring the average voltage intensity in the case of linearly-broken characteristic of detector; and class C, in which measuring by the voltmeter is of the peak intensity of voltage. When measuring sinusoidal voltages without noise, all the three methods of operating the detector are in principle equivalent.

The extent to which voltmeters are noise-proof and which determines the virtual, average and amplitude (peak) intensities of voltages is not identical; this is described in detail in (192) (see also para 4, chapt.X). The voltmeter for measuring the peak intensity of voltage is the least noise-proof; the most noise-proof is the voltmeter for determining the mean voltage intensity. The latter is most simply and conveniently measured by the cathode detector of Class B. The tube voltmeter with cathode detector Class B has high input and low output resistances; it is characterised by absolute accuracy of measuring.

The shape of the detector characteristic varies with the change of detecting tube or with the change of resistance of detector's load. The most subject to variations is the initial section of the characteristic, which is usually not used in measuring instruments. The error in the last two-thirds of the measuring instrument scale, i.e., in the section, where the detection characteristic is almost linear, does not exceed 1%, which is quite permissible for the general purpose of aerial electric prospecting.

As an example of electronic voltmeter with detector system, let us take the tube voltmeter, meant for measuring the average intensity of voltages with cathode detecting, which has been applied in AERIS and AERI-2 apparatus. The diagram of the tube voltmeter is shown in Fig. 129. The control grid of the tube is fed direct bias voltage, independent of anode current intensity. This is done by means of the external source of bias voltage $E_c = 150v$. To obtain half-wave detecting the bias voltage should be slightly lower than the blocking

voltage of the tube. In this type of detecting the anode current of the tube is practically proportional to the effective intensity of the applied voltage. The measure of the U_{in} voltage applied to the grid is the increment of the constant component of the tube's anode current. The intensity of anode current is measured by milliammeter or microammeter of direct current, cut in into the cathode circuit of the tube. To separate the variable component, the measuring device is shunted by condenser C_{71} . The voltmeter circuit is so constructed that in the absence of the measurable signal, the direct anode current, transmitted through the measuring device, is compensated by the lead-in into the circuit of additional compensating voltage source E_k , which is at the same time bias voltage source. In this case, the whole of the measuring device is used for measuring the current induced by the applied signal U_{in} .

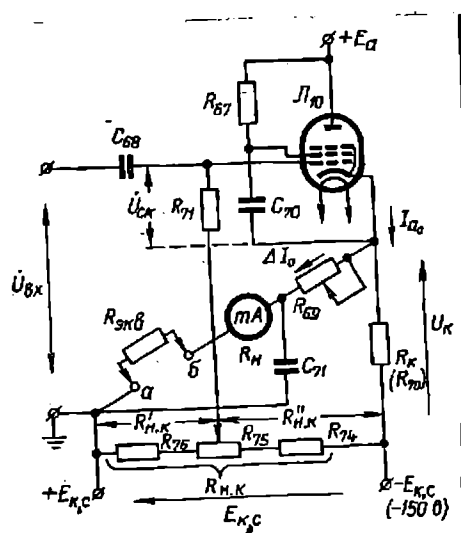


Fig: 129.

Load resistance R_k in the tube's cathode determines the characteristics curve of the tube voltmeter. In the absence of the signal the spacing current of tube I_a completely passes through resistance R_k . The higher is the value of this resistance, the less the spacing current depends on the tube parameters and, apparently, all the higher will be, all other conditions being equal, the sensitivity of the circuit. The compensating voltage $E_{k.c}$ is so cut in that it is directed towards the U_k voltage, operating between the cathode of the tube and general minus, and with compensation $U_k = E_{k.c}$.

Connected in series with the measuring device is the recorder with equivalent inner resistance R_{eq} (terminals a and b). Part of the fixed component of the anode current, transmitted through the measuring device and the recorder, can be determined, in the presence of alternate voltage at the input of the voltmeter, from the following ratio

$$I_H = \frac{U_{mc}}{\pi(R_{69} + R_L + R_{9KB})} \quad (X.18)$$

where U_{mc} - the amplitude of input voltage U_{in} ; R_L - the active resistance in the frame of the measuring device with direct reading.

The given diagram assures practically undistorted measuring of the input signals with intensity upto 55-60v (with tube 6Ж1П in pentode connection) at the maximum current of the recorder upto 5 ma.

In the apparatus of aerial electric prospecting, application is made sometimes of the logarithmic vacuum-tube voltmeter(for instance,

in the apparatus of the BDK method, where the measurable signal varies in a wide range (118). The simplified diagram of this amplifier is shown in Fig: 130 (193). The measurable voltage arrives at the input of a two-stage amplifier on tubes with variable steepness, becomes rectified by one half of the diode and read off the scale of the electromagnetic microammeter, connected in series into its cathode (loading) circuit. The amplified alternate voltage arrives at the second half of the diode, where it is rectified and defined as direct current voltage on load resistance R_2 . This voltage in the shape of negative bias is supplied to the grid of amplifying tubes. With the rise of input voltage, the negative bias increases, while the amplification factor decreases, which result in reduced relative increment of the output voltage in relation to that of input. Due to this, measuring device, graduated in units of output voltage, has a scale similar to the logarithmic*.

An example of the diagram for measuring the modulus with linear detector on transistor is the diagram in Fig: 131, where 1 - the phase-inverter; 2 - the cathode (emitting) repeater (147). This diagram is calculated for connecting with its input of recorder in the form of automatic potentiometer. Detector T_1 , assembled on transistor П 16, has practically a linear characteristic curve; the most sensitive scale of this type of voltmeter - 10 mv.

* In the BDK apparatus developed by IAE SO AN USSR part of detected voltage, proportional to the modulus of the amplifiable signal, is supplied to antidynatron grids of tubes in the two tube circuit of the logarithmic amplifier on pentodes (6* 217). The variation in controlling voltage level by means of resistances, cut in into antidynatron grids, makes it possible to approximate sufficiently accurately the preset logarithmic curve.

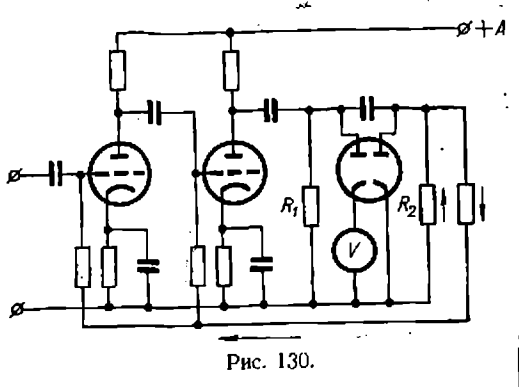


Fig: 130

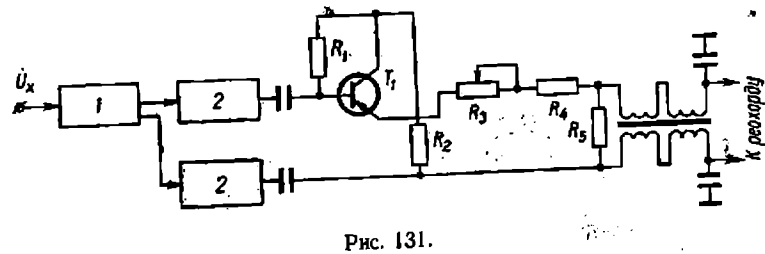


Fig: 131.

In the compensation method of measuring on alternate current a considerable advantage over other known methods of signal level (modulus) measuring is that the instability of the amplification factor in the intermediate (linear) amplifier practically does not affect the measuring results. In this case, the serious difficulties encountered are to construct a recorder - automatic potentiometer of alternate current, which should have two regulating members and, therefore, two servomotors. The main virtue of this method of measuring is the envelopment by feedback of the whole system. However, to ensure the stability and quick action of recorders in the presence of two interconnected regulating members in the system is very difficult (246). Moreover, for the automatic compensation of alternate current, it is necessary to obtain the stable value of the key signal both in the modulus and the phase, which is unobtainable in the apparatus of some of the methods in aerial electric prospecting.

6. Measuring of phase shifts:

The specifics of measuring phase shifts in the apparatus of aerial electric prospecting is the variation, within a wide range, of one out of two or, simultaneously, of both voltages, between which the phase shift is being measured. One of these - the voltage of the useable signal received by the field detector, is amplified and filtered from noises in the measuring channel. The second voltage, in relation to which the phase shift is being measured, is the comparative pressure, little varying in intensity in the apparatus of the near zone method and of considerable variation in the apparatus of the combined and distant zone methods.

This voltage in the apparatus of the near and combined zone methods is generated by the master oscillator and is supplied to the measuring unit directly from the master oscillator, or from the oscillating frame with disposition of oscillating and measuring units on one aircraft, or from the receiving frame, when the generating unit is on one and the measuring unit on the other aircraft. If the field emitter is on the ground (e.g. in the apparatus of the BDK method), the key signal is sent to the measuring apparatus on board through radio-channel. In this case, the comparative voltage phase should repeat the current phase of the primary field source.

This specific behavior of the signals largely determines the choice of the principle for measuring phase shifts, block and line diagrams of the electronic phasometer in the apparatus of aerial electric prospecting. Considerable amplitude variations of the measurable and key signals can result in increasing the error of the phasometer, since in

phase reading on the recorder, graduated in degrees, random increment of its indications will be recorded as actual phase variation.

The most widely adopted circuits of electronic phasometers are those with everlapping arrangement (congruence circuit, summation circuit); with triggers (single-cycle, and push-pull circuits); with linearly changing voltages; with frequency transformation; with phase-detectors (FHD). The construction principle of the first four phasometers is described in detail in (43).

Phasometers with triggers and phase-detectors have become very become very popular in the apparatus of aerial electric prospecting. Phasometers of this type are very accurate and not too complex. Therefore, it seems expedient to discuss the principles of measuring of phase shifts with these phasometers and to give brief descriptions of the diagrams of some of them, assembled for the apparatus of earial prospecting.

The phase shift between two sinusoidal signals is measured as follows. First, in order to obtain, at the output of the circuit, oscillations similar to symmetric rectangular impulses, the signals are amplified and limited. Then these oscillations are fed to the circuit, sensitive to phase shift between the input pulses (time shift). The phase-detecting circuit generatess the current (voltage), linearly coupled with the phase shift. Amplitude errors in these circuits are not high, as the levels of limited signals are kept 'constant with sufficient accuracy.

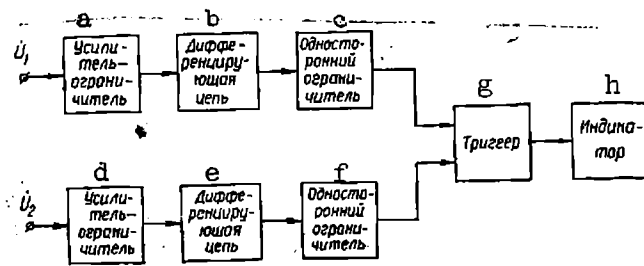
The main error in phasemeters is the one arising from the level variation of the input signals, causing changes in their duration in limited circuits. Therefore, the main requirement of the phase-detecting circuit is to provide reading of instruments free from the effect of possible negligible variation in the duration of input pulses.

Trigger circuit: Phasemeters, the circuits of which are based on triggers with two stable positions, are widely applied in the measuring technique. The simplest of these phasemeters is the two-channel one with one trigger, providing unambiguous reading within one period.

The simplified block diagram of the phasemeter with one trigger is shown in Fig: 132. Rectangular voltages, obtained as a result of preamplification and limitation of input voltages U_1 and U_2 , differentiate into short triggering impulses, delivered hence to the trigger's input. The operating polarity of the differentiated impulses may usually serve one polarity, and the other is either sheared off by means of one-sided limiter or enters the trigger's input, without affecting its operation. The indicator is cut in between the anodes of the trigger's tubes or into the cathode circuit of one of the tube.

Key to Figure 132:

- a, Amplifier limiter;
- b, Differential circuit;
- c, Unilateral limiter;
- d, Amplifier limiter;



- e, Differential circuit;
- f, Unilateral limiter;
- g, Trigger;
- h, Indicator.

Fig: 132.

Fig: 133 shows the impulse diagram of triggering device for controlling positive half-waves of rectangular voltages. In one condition the trigger sends into indicator current I_m (other versions of the trigger's operation are also possible, e.g. in one condition current sent into the indicator is of positive direction, and in another-negative). The average current of the indicator is preportional to the phase shift. With phase variation from 0 to 360° , the average current varies from 0 to I_m . The short-coming of this phasemeter is the error from zero shift in limiters and low frequency range (upto a few tens of kilocycles) and also the error from hysteresis, specific for all trigger devices.

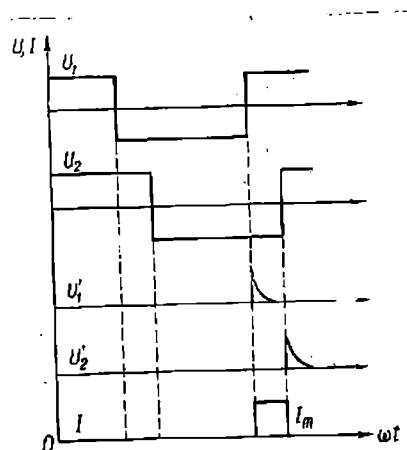


Fig: 133.

Two-cycle trigger circuit: Unambiguous reading of this circuit is possible from -180 to 0° and from 0 to $+180^\circ$. It is possible to

avoid in the circuit the effect of level variations of both the signals on the accuracy of reading in the output devices.

In as much as the two-cycle trigger circuit has higher Q-factors (adequate range of angle measuring, lowest response to level variations of input signals, unambiguity of reading, etc.) it has found a widespread application in the measuring technique, including that in the apparatus of aerial electric prospecting.

The simplified block diagram of phasemeter with two-cycle trigger is shown in Fig: 134. Here from the input of limiters-amplifiers, the rectangular oscillations are delivered to the commutating circuit, where the pulses are differentiated and acquire the shape of peaks. The starting positive pulses of channel I and negative pulses from channel II are delivered from the output of the commutating circuit to the input of trigger I, and the starting negative pulses of channel I and the positive pulses of channel II - to the input of trigger II. As a result, the output voltages of the triggers acquire the shape of rectangular pulses, the duration of which is linearly bound with the phase shifts of signals at the inputs of channels I and II.

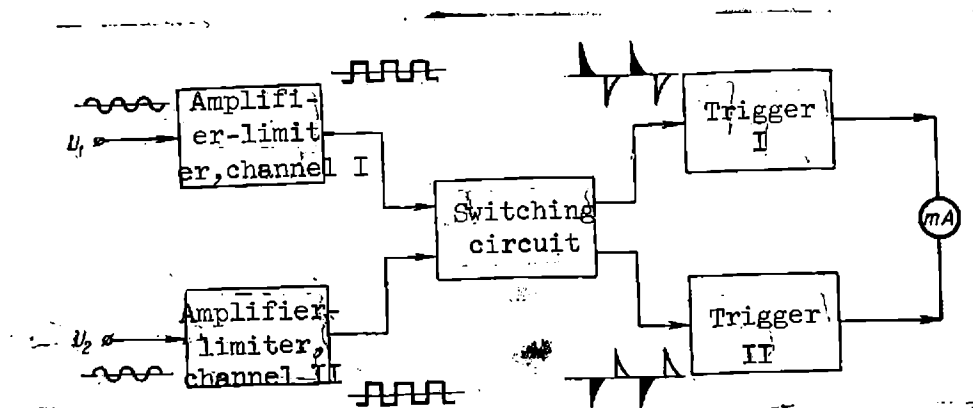
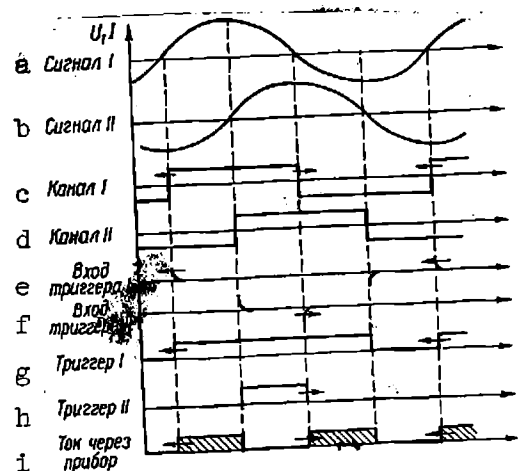


Fig: 134.

The diagrams of voltages and currents for various sections of the block diagram shown in Fig: 134, which illustrate the operating principle of this phasemeter, are shown in Fig: 135. The output voltages of the triggers are subtracted and added to the output device. The current transmitted through the device is proportional to the phase shift between signals and could be positive, as well as negative, when showing the sign of the measurable phase shift. The two-cycle trigger circuit is insensitive to level variations of the input signals, which could be explained in the following way. If the level variation of the signal in channel I causes expansion of positive half-waves of output oscillations, the pulses of both the triggers elongate. With sinusoidal shape of the signal, displacement of zero line leads to zero shifts similar in extent, therefore, the trigger pulses elongate uniformly. Hence, their difference remains practically invariable, therefore, the reading of the recorder does not vary either. Thus, in this circuit, phase shifts are measured with the transition of both sinusoidal voltages through zero. Let us analyze in more detail the two main elements of the two-cycle trigger circuit - the commutating circuit and the trigger itself.

Key to Figure 135

- a, Signal I;
- b, Signal II;
- c, Channel I;
- d, Channel II;
- e, Input, trigger I;
- f, Input, trigger II;



- g, Trigger I;
- h, Trigger II;
- i, Current through device.

Fig: 135.

The commutating circuit: is meant for an appropriate selection of starting pulses, formed out of rectangular by means of differentiating chain. In low-frequency phasemeters, the differentiating chain usually consists of resistance R and capacitance C, connected in series, to which the differentiated voltage, e.g. U_{in} , is being delivered.

With certain R and C values, the output voltage, taken off the resistance (Fig: 136), will be determined by the derivative of the input voltage

$$U_{BbIX} = RC \frac{dU_{BX}}{dt} \quad (X.19)$$

$$i = C \frac{dU_c}{dt} \quad (X.20)$$

If the resistance does not affect the intensity of the current, it may be assumed, that $i \approx C \frac{dU_{BX}}{dt}$.

With the input of the rectangular signal with certain finite continuation of the front at the moment of voltage appearance, the current attains by a jump intensity $\frac{U_{in}}{R}$ and the condenser begins to charge. In measure with the charging of the condenser the current and output voltage begin to decrease according to the exponent.

$$U_{BbIX} = U_{BX} e^{-\frac{1}{RC}} \quad (X.21)$$

The rate at which voltage U_{out} decreases is determined by the time constant of circuit $\tau = RC$.

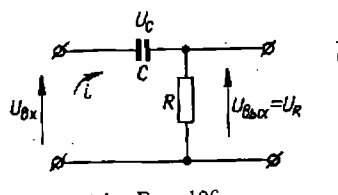


Fig: 136.

The differentiating chain builds two pointed pulses of positive and negative polarity, which in their time position correspond to the forward and rear fronts of the input rectangular voltage. Since considerable decrease of pulse amplitude at the output of the differentiating chain is undesirable, its resistance R is taken in the order of several tens of kilo-ohms, or so, that $R \gg R_{in}$, where R_{in} - the internal resistance of pulse source (in a special case $R_{in} = R_a$, where R_a - the load resistance of the output stage tube in limiter-amplifier).

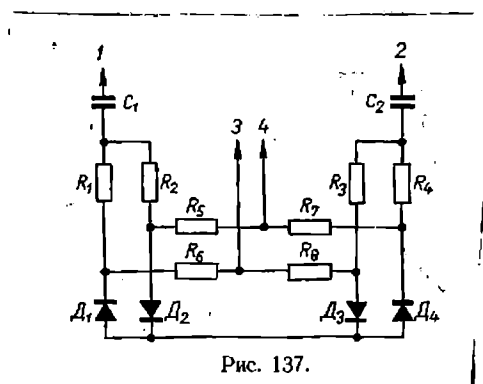


Fig: 137.

Fig: 137 shows the diagram of differentiating and selection of output pulses in two limiter-amplifiers, i.e. the diagram of the commutating circuit. Let us trace the positive and negative steepness fronts of pulse in one channel of phasemeter through the commutating circuit. The positive front at input I unlocks diodes D_2 and D_3 and locks diodes D_1 and D_4 . Elements of the differentiating chain include capacitance C_1 and resistance R_2 . The differentiated pulse passes through divider R_1 , R_6 , R_8 and starts the first trigger, cut in to point 3. The front of the negative steepness at input 1 locks diodes D_2 and D_3 and unlocks diodes D_1 and D_4 ; differentiation takes place on resistance R_1 and capacitance C_1 . The pulse passes through divider R_2 , R_5 and R_7 and disrupts the second trigger, cut in to point 4.

The second half of the circuit (from limiter-amplifier of channel II) is activated in the same way. The positive front at input 2 also unlocks diodes D_2 and D_3 (C_2R_3 - differentiating chain), and the differentiated pulse passes through divider R_4 , R_7 , R_5 and starts D_3 and unlocks diodes D_1 and D_4 (C_2R_4 - differentiating chain). The pulse passes through divider R_3 , R_8 , R_6 and disrupts the first trigger (point 3). Thus, the first trigger starts by the positive starting pulse of phasemeter channel I and disrupts by the negative pulse of channel II, the second trigger starts by the positive impulse of channel II and disrupts by the negative pulse of channel I. Therefore, the given diagram assures the required selectivity of the starting pulse in matched activity of the two-cycle trigger circuit.

Since the calculated differentiating capacities are usually of low value, to reduce the effect of parasitic capacitances of the pulse selecting circuit, it is expedient to use point diodes D2-E.

Triggers: belong to the category of change-over devices. They generate steep jumps of U_{out} voltages at any preset moments of time t_1, t_2, \dots , fixed by the control voltage, which actuates their input (Fig: 138). Triggers are often denoted as starters with two stable positions of symmetry, and sometimes also with "electronic relays" (82).

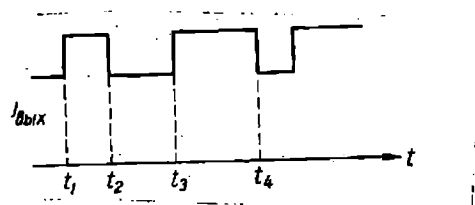


Fig: 138.

The trigger is capable of changing-over by jumps from one position of balance into another every time, when the control voltage at its input passes over some fixed levels - the operation thresholds of trigger U_{tr} . The controlling voltage, called the starting voltage is most often a pulse or voltage jump.

Assuming at moment $t = 0$ the state of the trigger was determined by symmetry point 1' ($U_{out} = U_1$). With the action of starting voltage (Fig: 139) of any shape, as long as the input voltage $U_{in} = U_s \leq U_{tr.1}$, the point, showing the state of trigger shifts along the bottom branch

of the characteristic curve and of $U_{out} \approx U_1$ (Fig: 139,c).

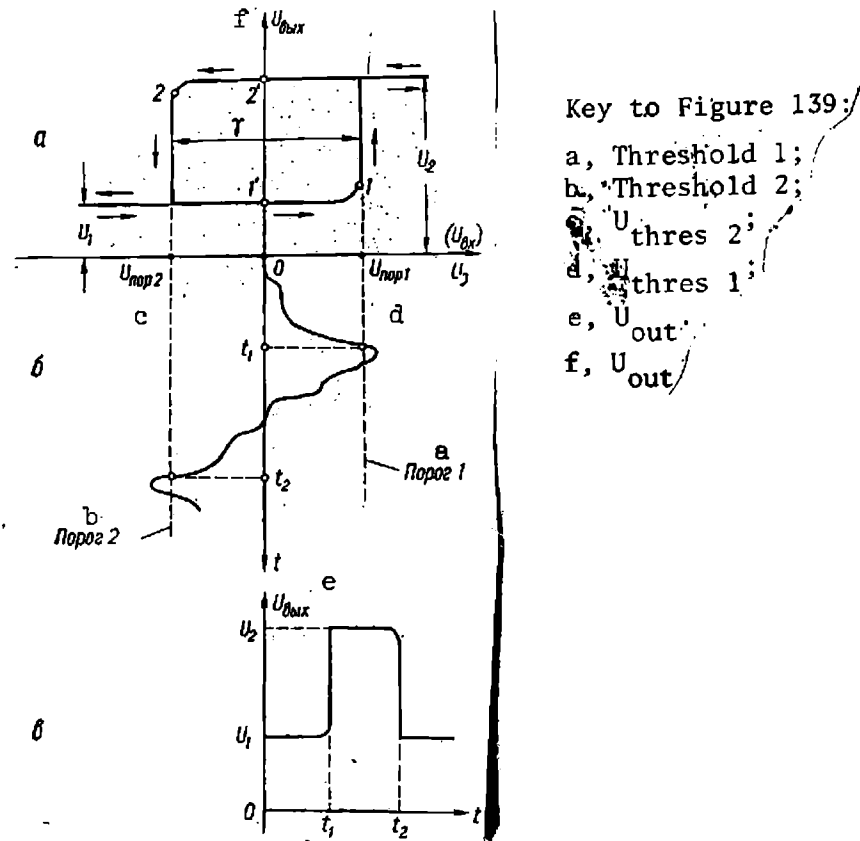


Fig: 139.

At moment t_1 , when $U_s = U_{tr.1}$, the point by a jump passes onto the top branch of the curve. With this, the input voltage increases by a jump to intensity U_2 ($U_{out} = U_2$) and remains almost invariable during the whole period of $U_s > U_{tr.2}$.

At moment t_2 , when $U_s = U_{tr.2}$, the depicting point returns by a jump from position 2 onto the bottom branch of the curve and U_{out} decreases to intensity U_1 .

Thus, U_{out} , independently of the shape of the starting voltage, has the appearance of voltage jumps (Fig. 139,c). The shape and the intensity of U_s establish only the emergence moments of voltage jumps.

The typical ideal starting (dynamic) curve of the trigger shows output voltage U_{out} vs. starting voltage $U_s = U_{in}$, which activates its input (Fig. 139,a). The top and bottom branches of the curve correspond to the two possible states of stable balance. Points 1 and 2 determine the limits of the stable conditions, i.e. threshold voltages $U_{tr.1}$ and $U_{tr.2}$. The points of the curve's intersection with the axis of ordinates (1" and 2") determine the symmetry state of the trigger, in which it stays in the absence of the starting signal ($U_s = 0$).

The starting curve of the trigger has hysteresis properties. This means that two alternating operations of the trigger occur at various intensities of the starting voltage. The area of the curve, confined between its lateral branches, is called the hysteresis area. The width of the hysteresis region determines hysteresis voltage $U_h = (U_{tr.1} - U_{tr.2})$.

The quick action of the trigger is determined by the highest number of change-over (operations), which it is capable of executing in 1 sec at constant interval between the pulses. The minimum interval of time between two impulses of start, activating the trigger (without a break), is called the resolving time of trigger T_{res} . The limitation of the trigger's quick action, connected with finite duration of its change-over from one state into another, is due to the finite steepness

of the starting pulse front, the inertia of some of the non-linear devices used in the circuit, and also the effect of parasitic capacitances of the circuit.

The indicated factors determine, on the one hand, the finite duration of the change-over of the trigger T_{c-o} , resulting in changes of its qualitative state; on the other hand, due to the effect of some of the indicated factors, the trigger, after a routine change-over, loses, for some time, controllability (sensitivity to the effect of subsequent starting pulses). The repeat change-over may be effected only after some time required for the restoration of the trigger's properties. Taking all this into account, the whole process of the trigger's change-over from one state of symmetry into another can be divided into three stages: start (T_s), tilting (T_t) and restoration (T_r).

The starting stage - initial part of the process, during which the trigger, being in the symmetry state (point 1"), under the effect of starting impulse is lead up to the threshold of operation (to point 1). The procedures in this "passive" stage are unconnected (or very slightly so) with the "internal" mechanism of the trigger's operation.

The duration of the starting stage is determined mainly by the steepness of the starting impulse front and the time constants of the starting circuit and the input circuit of the trigger.

The tilting stage - active part of the dynamic process, developing after the attainment of the trigger's operating threshold, which results in the change-over of the trigger. On the starting curve,

this stage corresponds to the transition of depicting point from one branch of the curve to another.

The term tilting shows the unstable state of the trigger at this stage, as well as the transience of the process development in the trigger, which occurs with progressively increasing speed.

The duration of this stage depends mainly on the inertia in the non-linear elements of the trigger, on the time constants of reactive elements, participating in the process of tilting, and on parameters of the starting signal. In certain conditions, the process of tilting may continue, terminating only with the cessation of the starting signal action.

The total duration of the starting and tilting stages determines the duration of the trigger-change-over from the position of symmetry in one qualitative state into another qualitative state (which may or may not be a symmetry state), $T_{c-o} = T_s + T_t$.

The restoration stage (includes also transitory stage) contains the terminating part of the operating process, as a result of which the trigger, being in the new qualitative state, attains the corresponding state of symmetry (or a very similar state). The restoration stage usually takes place in the absence of the starting pulse. The duration of this stage is determined, as a rule, by the time constants of the trigger's reactive elements, and in some cases - even by the inertia of the circuit's non-linear element.

In phasemeters of the aerial electro-prospecting apparatus the most widely adopted are the triggers, the action principle of which is based on the use of properties in amplifiers with positive feedback (82, 150). It is well known that in these systems it is possible to build up suitable conditions for the formation of voltage jumps. For the triggers, the application is most often of two-tube push-pull circuits in the form of two identical amplifiers on resistances interlocked by a loop of positive feedback. The circuit of this type of trigger is very similar to that of symmetrical multivibrator with grid-anode coupling (32, 82, 120, 150). To obtain two states of symmetry, the negative bias (twice braked multivibrator) is lead into the grid circuit of both the tubes. Application can also be made of two-tube systems with cathode coupling and others. For instance, the principle of measuring the phase shift with the use of push-pull trigger circuit is used in the apparatus of induction method AERIS and AERI-2. Practical application of this apparatus has confirmed the positive qualities of these phasemeters.

Key to Figure 140: a, Measured signal; b, Input switch; c, Amplifier-limiters; d, Differential circuits; e, Trigger I; f, Switching circuit; g, Switch for measurement limits; h, Carrier signal; i, Square phase converter 0-360°

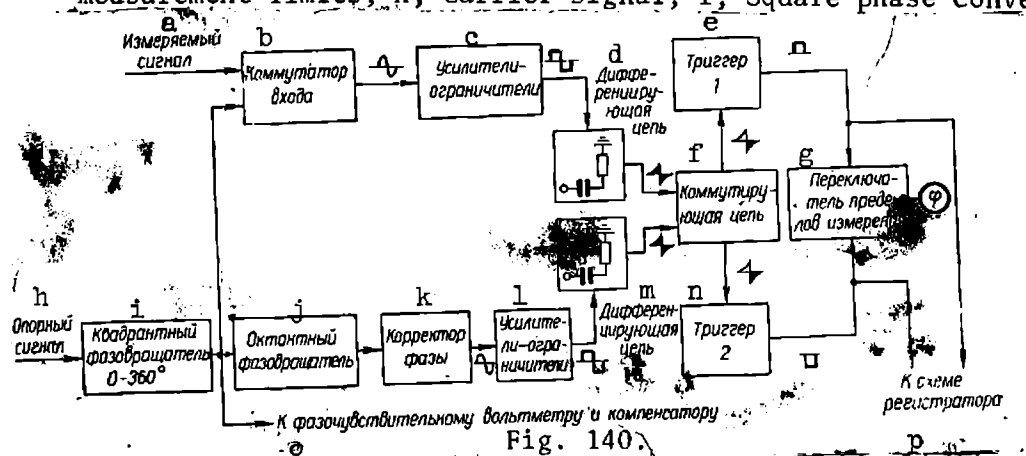


Fig. 140

j, Octant phase converter; k, Phase corrector; l, Amplifiers-limiters; m, Differential circuit; n, Trigger II; o, To the phase-sensitive voltmeter and compensator; p, To the recording circuit.

The block diagram of AERI-2 phasemeter is shown in Fig: 140. Sinusoidal voltages (measurable U_x and comparative U_{com}), the phase shift between which has to be measured, are delivered to limiting-amplifying stages, in which they are amplified and transformed into rectangular pulses of a certain amplitude. If the limiter-amplifiers are sufficiently effective, the signals at their output should have the shape of symmetrical rectangular pulses. Differentiating chains convert rectangular pulses of each channel into two pointed pulses (of positive and negative polarity), which according to their temporary position correspond to the forward and rear fronts of the rectangular input impulses (i.e., to moments of transition through zero of sinusoidal voltages U_x and U_{com} at the inputs). The commutating circuit, where the pointed pulses arrive, distributes them according to sequence and polarity and delivers them as starting pulses to the push-pull trigger circuit (triggers 1 and 2). The starting positive pulses of the measurable signal channel and the locking negative pulses of the key signal channel are fed to the input of trigger 1, and the negative pulses of the measurable signal channel and positive pulses of these key signal channel - to the input of trigger 2.

The output voltages of triggers are applied through the change-over switch of the measuring limits to the direct phase reading device. By means of the change-over switch, the shunt of the appropriate value is cut in to this device. This ensures obtaining of the preset limits of phase shift measuring ($\pm 45^\circ$, $\pm 90^\circ$ and $\pm 180^\circ$).

The voltage arrives to the recording circuit directly from the outputs of the limiter-amplifier of the key signal channel, phase corrector with adjustment limits $25-30^\circ$, for rectifying the phase characteristics of the channels (zero adjustment of phasemeter), and octant phase-invertor with the measuring limits of phase $\pm 180^\circ$ at 45° (through octant), for expanding the recording limits of the phase shifts are set up. The commutator at the input of the measurable signal channel permits with zero adjustment of the phasemeter the delivery, at both the inputs of the circuit, of the same signal (either the measurable or the comparative). In this case, the octant phase-invertor should be in zero position, and the zero adjustment of the phasemeter is executed by the phase corrector.

The quadrant phase-converter in the key signal channel with adjustment limits $0-360^\circ$ - discretely at each quadrant (90°) and continuously within each quadrant - is required for the compensation of the phase shifts, generated in the circuits of the measuring unit.

The line diagram of the phasemeter is shown in Fig: 141. The measurable signal, arriving on contact 6 of the plug commutator (position 2-4) and transitional capacity C_{41} to the input of the first limiter-amplifier L_4 . In position 2 of the switch P_3 , the measuring limit of the phasemeter is $\pm 45^\circ$, in position 3 and 4 - respectively it is $\pm 90^\circ$, $\pm 180^\circ$. The first limiter-amplifier is assembled on double triode on a circuit with cathode coupling and cathode load devided by direct current.

The direct current positive bias voltages are delivered from divider R_{71} , R_{72} , R_{73} . To obtain steeper fronts in the limiter-amplifier, low intensity positive feedback (R_{50} , C_{43}) is applied. The second stage of amplification and limitation L_5 is assembled according to the usual circuit of the limiter-amplifier with cathode coupling. Finally, the signal is limited in the third limiter-amplifier L_6 . The limiter-amplifiers of the key signal channel $L_8 - L_{10}$ are similar to those of the measured signal channel.

Condensers C_{91} and C_{92} , cut in to the anode circuits and control grids of terminal limiters-amplifiers, make additional improvement in the shape of limited signals on high operating frequency. From the outputs of the terminal amplifiers-limiters the limited signals are fed to the differentiating chain and the commutator circuit (C_{53} , C_{68} , $R_{74} - R_{81}$, diodes $D_1 - D_4$).

The triggers are assembled on double triodes L_7 and L_{11} on the circuit with cathode coupling and fixed positive bias for the left half of the tube (dividers $R_{82} - R_{85}$ and $R_{122} - R_{125}$) and automatic - for the right half. By means of potentiometer R_{83} (R_{123}) the bias level, at which the trigger is tilted is adjusted. The level of the reverse tilting is determined by the value of resistance R_{93} (R_{132}).

The output voltage of the triggers is fed to the direct reading device of the phase shift. Resistances R_{134} , R_{94} and R_{95} determine the working current of this device at the first measuring limit of phase angles ($\pm 45^\circ$).

Page intentionally left blank

Page intentionally left blank

From the anode loads of triggers R_{90} and R_{130} the voltage is taken off for its subsequent delivery to the recording system of the phase shifts. The input part of the recording circuit consists of a divider ($R_{135} - R_{137}$, $C_{73} - C_{74}$), symmetric in relation to the ground with high-ohmic input, a three-section RC-filter ($C_{75} - C_{77}$, $R_{138} - R_{145}$) for adjustment of the time constant and a transformer of direct current input voltage into alternate (relay P_{11} type RP-4 and transformer Tr_2).

The wire rheostat of the recorder is energized from the full-wave rectifier activated by voltage 6.3v and assembled on transformer Tr_1 and diodes $D_{5.6}$ with RC-filter (C_{78} , R_{147} , C_{79}) at the input. The stabilization of the wire rheostat of voltage is effected by stabilivolt D_7 . Resistance R_{146} is stabilizing, R_{148} - serves to adjust the current supply voltage.

The ends of the wire rheostat through contacts 3 and 6 of the socket SHR3(4)-6 are cut in to the source of its supply and to divider $R_{149} - R_{150}$, through which the output signal of the phasemeter is connected by one pole with the finishing system (wire rheostat), and by the other to the transformer armature. The middle point of the wire rheostat (contact 5 of the same socket) is connected with the middle point of transformer Tr_2 . The transformer (relay P_{11}) is energized by voltage 10v with frequency 100 cps. L_{12} , L_{13} , L_{14} and L_{15} - the electronic amplifier of recording with reversible divider RD-09.

The key signal through contact 12 of the plug socket SHR3(4)-5 is delivered to the input of quadrant phase-invertor L_1 , and hence - to octant phase-invertor L_2 , the commutator of the input and on contact 4 of the same socket for further delivery to the phase-detecting voltmeter.

In position 1 of change-over switch P_3 the key signal is delivered to both the channels of the phasemeter, and with "zero" position of the octant phase-invertor the phase curve of the channels is rectified by the phase corrector ($C_{36} - C_{40}$, R_{36}). $P_1 - P_{10}$ - the change-over relay of phasemeter frequency. Resistance R_{45} is shunted by big capacitance C_{90} and does not participate in the phase-shifting RC chain, but jointly with resistance R_{46} forms resistance to the grid leak of the left half of tube L_8 . The octant and quadrant phase-invertors are both potentiometric; the principle of their action has been discussed in para 9 of the present chapter. The cathode repeater on the right half of tube L_3 works for the interstage separation of the octant phase-invertor and phase corrector.

In zero adjustment of the phasemeter proper (first position of switch P_3) the indicator is cut in only by shunt R_{94} and its pickup, in this case, increases. This provides for a more exact correction of the phasemeter's channels.

Diagrams of phasemeters with phase-detector: In a number of apparatuses for aerial electric prospecting, the application was of phasemeter, constructed on the principle of phase-detecting. Let us analyze the diagrams of phasemeters, developed by FMI AN Ukr. SSR and IRE SO AN USSR.

The phasemeter of AERA-2 apparatus (FMI AN Ukr.SSR) is meant for measuring and recording the phase-shift between the measurable and key signals within the range $0-360^{\circ}$. The diagram of the phasemeter is constructed on the principle of follow-up system, that comparison unit of which is the FHD.

The simplified block diagram of the phasemeter is shown in Fig: 142. The voltage of the comparative signal U_{comp} arrives at the amplifier with amplification factor $K = 100$, hence to the limiter, the output voltage of which remains invariable with the variation of the signal at the input from 4 to 50v. The limited comparative voltage, being commutating, is delivered through the matching cathode repeater KP_1 to the middle connecting point of capacitors C_1 and C_2 of the circular balance detector.

The voltage of the measurable signal U_x is delivered to the phase-invertor, after which two equal in intensity voltages U_x , shifted in relation to each other at 180° , are fed through cathode repeaters KP_2 and KP_3 also to the circular detector.

If phase shift φ , exists between the voltage U_x and U_{comp} , then at the output of the FHD direct current voltage $U_{\text{=}}$, separates proportional to product $U_x \cos \varphi$. This voltage passes through filter F with variable transmission band (adjustment τ) and in the shape of voltage U_{out} arrives at the recording circuit.

The line diagram of the phasemeter, included in the set of AERA-2, is shown in Fig. 143. In accordance with the action principle of the phasemeter, its line diagram may be divided into three parts: the channel of measurable signal U_x , the channel of comparative signal U_{comp} and the channel of controlling signal in the follow-up system $U_{\text{=}} \rightarrow U_{out}$.

Measurable signal channel: From the output of the selective amplifier block the measurable signal is delivered to phase-inverter L_9 . Uniform antiphase voltages U_x are delivered through matching cathode repeaters L_7 and L_8 to the ring circuit of the FHD. From the output of the measuring amplifier block, the measurable signal is also delivered through matching cathode repeater L_{105} into level control circuit of signals U_x and U_{comp} .

Comparative signal channel: From the output of the selective amplifier in the receiver block, the comparative signal is fed to the matching cathode repeater L_{1a} , hence it consecutively passes through four phase-invertors. The operation of the phase-invertor is based on the known RC-circuit of the phase-invertor, assembled on phase-reversal stage (see para 9 of the present chapter).

The first (continuous) phase-invertor L_{1b} allows adjustment of the phase shift between the input and output voltages at an angle $\pm 20^\circ$ and serves for the primary setting of the phasemeter in the middle of scale (zero). This is done by means of adjusting resistance R_9 . Resistance R_8 limits the measuring range of the phase shift. Capacitances C_3-C_6 (commutated by plate SHI 3-1 of the step-by-step switch) serve for

for the tuning of the phaseinverter to one of the fixed frequencies of the apparatus.

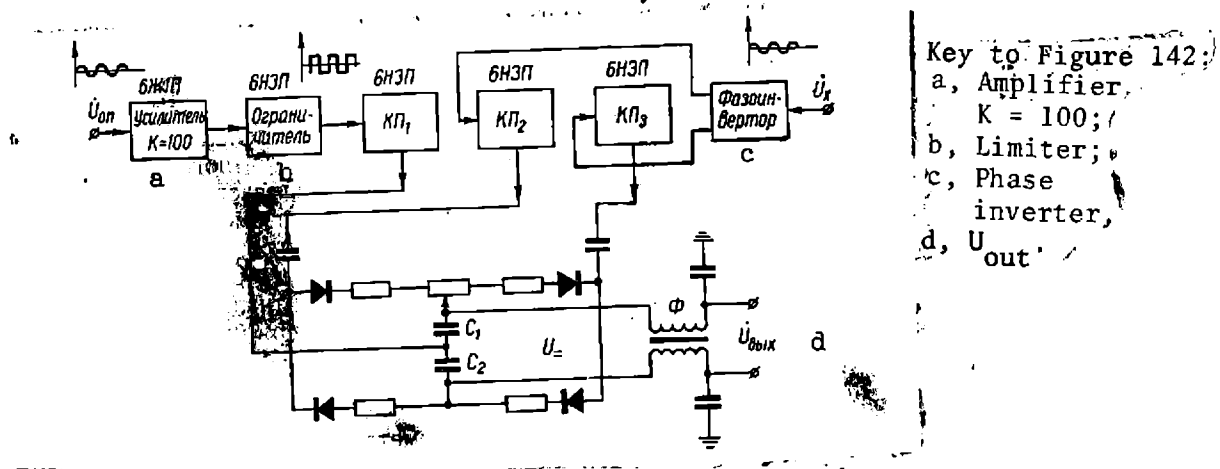


Fig: 142.

Phase-inverter L_{2a} , which provides for adjustment of the phase shift between the input and output voltages within $0-36^\circ$ by jumps at every 30° , serves for changing-over the measuring range of the phasemeter (the commutation is carried out by means of relay P_1-P_8 and the plate of step-by-step switch SHI 3-2). Phase-inverter L_{2b} produces constant phase shift of 90° between the input and output voltages and, jointly with matching cathode repeaters L_{3a} and L_{3b} , serves to energize the wire rheostat R_r . The wire rheostat with limiting resistances R_0 forms the circuit of continuous graduated phase-inverter to an angle of $\varphi = 60^\circ$.

Voltage U_{01} , taken off the rheochord arm, is fed to limiter-amplifier L_4, L_5 . Amplifier L_4 of this unit has the amplification factor $K = 100$. The frequency characteristic of the amplifier is linear within frequency range 200-2000 cps. At the output of L_5 limiter a rectangular signal (pulse) with amplitude of about 30v is emitted and, practically independent of voltage U_0 , fed to the input of the comparative channel input. Through the matching cathode repeater L_6 the output voltage of the limiter, now as commutating, is delivered to the ring circuit of the FHD, to assure its operation in the key method.

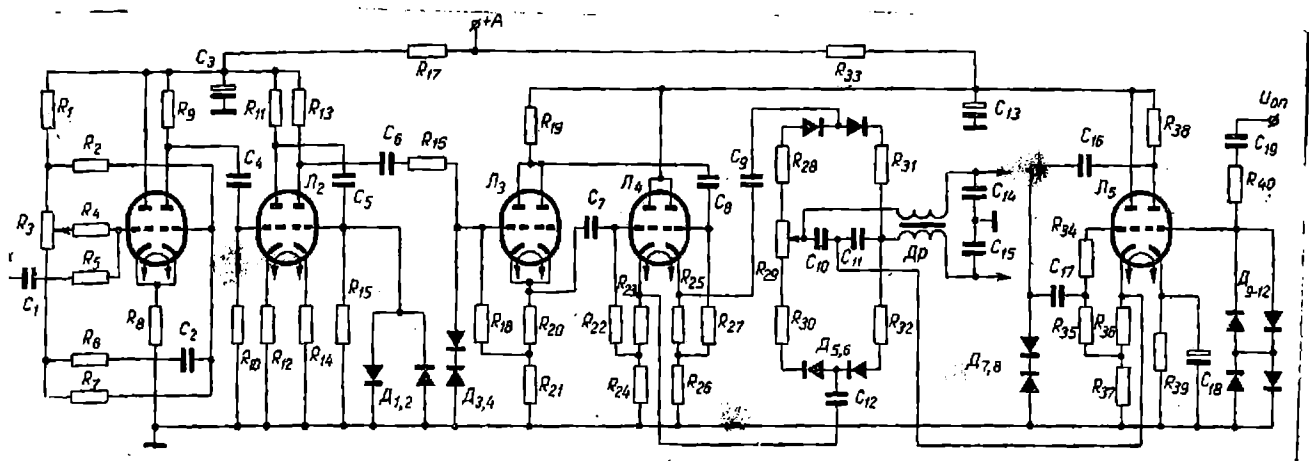


Fig: 144.

Control signal channel: At the moment of the follow-up system, discrepancy at the output of the FHD appears direct current voltage U_- , which is filtered by low frequency filter (Dr. C_{39}, C_{40}) and

delivered to the two-component - shaped filter ($R_{65}, R_{72}, C_{41}-C_{43}$) with variable transmission band for the control of the time constant in recording. The filtered voltage $U_{\text{—}}$ is fed to vibrotransformer VP, which, jointly with the input transformer Tr_1 of the phase recorder amplifier, serves to transform voltage $U_{\text{—}}$ into proportional alternate current voltage U . The excitation winding of the vibrotransformer and the reversible motor of the follow-up system of the phasemeter are energized from transformer with frequency $f = 125$ cps.

The composition of the phasemeter in the BDK apparatus developed by IAE SO AN USSR (Fig: 144) includes a circular balance detector, assembled on semi-conductive diodes (D101), limiters of comparative and measurable signals, a low-frequency filter and recording circuit (not shown in the figure).

The comparative signal, arriving from the multivibrator, is limited by means of basic silicon diodes (D809), amplified by the right half of tube L_5 to 30v and to the FHD through the cathode repeater left half of tube L_5 .

For efficient limiting of the measurable signal, three limiting stages are applied. The first stage - limiter with cathode coupling L_1 with limit threshold 5v - protects subsequent stages from overload and related distortions. The second and third stages are assembled on tube L_2 with diodes cut in to its anode circuits. The output signal of limiters is fed to phase-inverting circuit L_3 , and then through the matching cathode repeaters L_4 - to the symmetrical input of the ring detector. The direct current output voltage from the FHD output arrives, after filtering, at the input of the recording circuit.

With the perfection of methods and apparatus of aerial electric prospecting the need for raising the accuracy of measuring and recording the phase is felt. One of the comparatively easy methods for reducing the error of reading and expanding the measuring range of the phase is the application of subtraction circuit SV at the FHD input. Fig: 145 shows the block diagram (a) and vector diagram (b), explaining the operating principle of this phasemeter-recorder.

The subtractor circuit receives two signals - \dot{U}_c and \dot{U}_o (after the phase-inverter F); to ensure normal stable operation of the follow-up system one signal should be slightly high or than the other. For instance, signal \dot{U}_c is taken higher than \dot{U}_o , at the moment when the phase shift $\varphi = 0$, we will have at the SV output signal $\Delta \dot{U}$, which is in phase with signal \dot{U}_o . With the appearance of a slight phase shift there is generation of voltage $\Delta \dot{U}'$, the projection of which $\Delta \dot{U}_r$ is the signal controlling the action of the follow-up system UP and RD. By means of this system, the turn of vector \dot{U}_c is carried on until the projection $\Delta \dot{U}_r$ becomes zero, i.e., until at the SV input voltage ΔU becomes fixed or there is no $\varphi = 0$. The phase is read off the graduated phase-inverter F.

The advantage of this phasemeter is that besides the expansion of the measuring range by selection of ratio $\left| \frac{\dot{U}_c}{\dot{U}_o} \right|$ independence of phasemeter reading from the instability of the FHD circuit is also achieved, zero drift of which circuit has practically no effect on the operation of the follow-up system. Experiments have shown that with this circuit of the phase recorder it is easy to obtain error in phase reading 3-5' (on fixed frequency), whereas in other systems of phase reading the errors are about 1-2° (89, 94).

In the USSR apparatus for aerial electric prospecting, the phase-meter recorders are similar to those described above; no information is available about the phasemeters used in the apparatus of foreign firms.

7. Measuring of components, their sum and difference:

Orthogonal components of the signal received by the field detector (active and reactive components) could be measured comparatively simply by the phase-detecting voltmeter(FHD), based on the phase-detecting circuit.

The simplicity of the FHD circuit, specially of ring-shaped on semi-conductive diodes, and their high metrological qualities are the reasons for their widespread application in measuring instruments of electric prospecting apparatus, including the circuits of phase-detecting voltmeters.

The standard block diagram of the phase-sensitive voltmeter, included in the set of aerial electro-prospecting apparatuses, is shown in Fig: 146. The FSV consists of the channel of measurable signal U_c , the channel of the comparative voltage U_{comp} , the phase-sensitive detector and the recording circuit of component CPK (I - indicator).

The measurable signal U_c arrives at the cathode repeater KP_1 , which matches the input resistance of attenuater A with the output resistance of the proceeding stage. Hence the signal is delivered to amplifier YC_1 for raising the level of the measurable signal and the amplification factor could be controlled within certain limits. To

current voltage is delivered through the time constant switch P to recording circuit CPK.

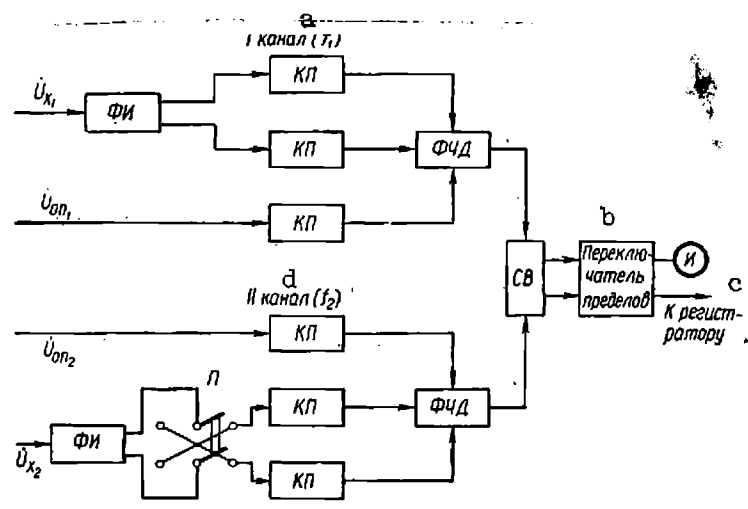
The rectangular voltage is required for FHD operation in the key method, which assures the best stability against noise and linearity of the circuit's reading (101). For the limiter-amplifier, it would be expedient to use cathode-anode limiting; to obtain symmetrical to zero line limited signal and improve the stability of the circuit in the amplifier-limiter the reverse feedback should be on direct current (43).

The sum or difference of the reactive components of signals with two different operating frequencies (see para 3 of chapt.V) may be measured by the differential phase-sensing voltmeter (DFHV). The voltmeter is a two-channel one, the circuits of channels are similar to the circuit of the ordinary FHD. In construction, the DFHV should have a minimum number of elements, i.e., if the apparatus contains FHD for the separate measuring of components in the signals of two different frequencies, the DFHV should have only those nodes of phase-sensing voltmeters as functional, which assure obtaining output voltages proportional to the corresponding components of the measurable signals, addition or subtraction of which is effected in DFHV.

It should be mentioned that to remove the interaction of channels with simultaneous measuring of the difference (sum) of components by means of two FHD, the DFHV circuit is sometimes made more convenient without galvanic coupling with the FHD detectors of individual channels. In this case, DFHV has a separate circuit of differential detectors, operating continuously on one common load.

The block diagram of DFHV, shown in Fig: 147 may serve as an example of this.

The diagram has two channels. Channel I is fed sinusoidal voltage U_{x1} of f_1 frequency, channel II - U_{x2} of f_2 frequency. The U_{x1} voltage arrives at phase-inverter FI, by means of which two voltages of equal amplitude are obtained, but shifted at 180° as required for the FHD operation. These voltages are fed to the FHD through cathode repeaters KP. The U_{x2} voltage arrives at phase-inverter FI, by means of which two voltages of equal amplitude are obtained, but shifted at 180° as required for the FHD operation. These voltages are fed to the FHD through cathode repeaters KP.



Key to Figure 147: a, Channel I (f_1); b, Limit switch; c, To recorder; d, Channel II (f_2).

Fig: 147.

To comparative voltage U_{comp} of f_1 frequency is taken off the limiter of the FHD block channel I and is supplied through the cathode repeater to the phase-sensing detector of the first DFHV channel. The U_{x2} and $U_{comp.2}$ are delivered in the same way to channel II.

The FHD outputs are put in to subtracting circuit CB. Addition or subtraction of signals in the measuring of the sum or difference of components is effected by changing the phase of FI phase-inverter output signals in the second channel of DFHV by 180° (by means of the change-over switch P). The same thing may be obtained by changing, for instance, polarity of one of the signals of opposite to the FHD. The sum or difference of components is controlled visually by the direct reading device I, put in at the output of the subtraction circuit and is recorded by the recorder.

By means of the phase-detector, the component may be measured in volts. With the use of the FHD it would be expedient to measure the sum or difference of components in relative units and, during the interpretation of results, to convert the obtained values into absolute. As in the measuring of components separately, so in the measuring of their sums or differences there may be positive and negative values. Therefore, the direct reading device and DFHV recorder must have the zero in the middle of the scale.

In measuring the sum of components, the input voltages of signals with frequencies f_1 and f_2 , measurable by separate FHD, should be such that their sum would not exceed the extreme digit of the DFHV scale. However, an excess during measuring is quite possible. Therefore, to avoid the off-scale reading of instruments, the DFHV should be provided with several measuring limits or with changing scale dial divisions. On the contrary, measuring the difference of components, more sensitive limits are required than for each FHD individually. With

this object, the DFHV is provided with several limits of measuring and recording, less and more sensitive than for the individual FHD (e.g., 0.5; 1; 2 and 4 times). And if the scales of DFHV and FHV are identical in dial divisions, then for the convenience of the mark on the diagram tape of DFHV recorder, the measuring limit is denoted as "1:1". But if the scale of dial divisions of DFHV is half that of FHV, the first scale is denoted as "1:2" and so on. This type of DFHV circuit has been applied in AERI-2 apparatus (127) (Fig: 148). Since both the channels of DFHV are practically identical, let us take the work of only channel I.

The measurable voltage, preamplified in FHV block, arrives through contact 12 of the plug socket SHR 1 on the grid of tube L_1 of the phase-invertor, assembled on the circuit with separated load. The voltage from the anode R_2 and cathode R_5 resistances of the phase-invertor is delivered through separating capacitors C_3 and C_4 onto the control grids of cathode repeaters L_3 and L_5 , meant for matching the phase-invertor with the ring-shaped detector, and hence, through separating capacitors C_7 and C_{11} , is fed to the phase-detector.

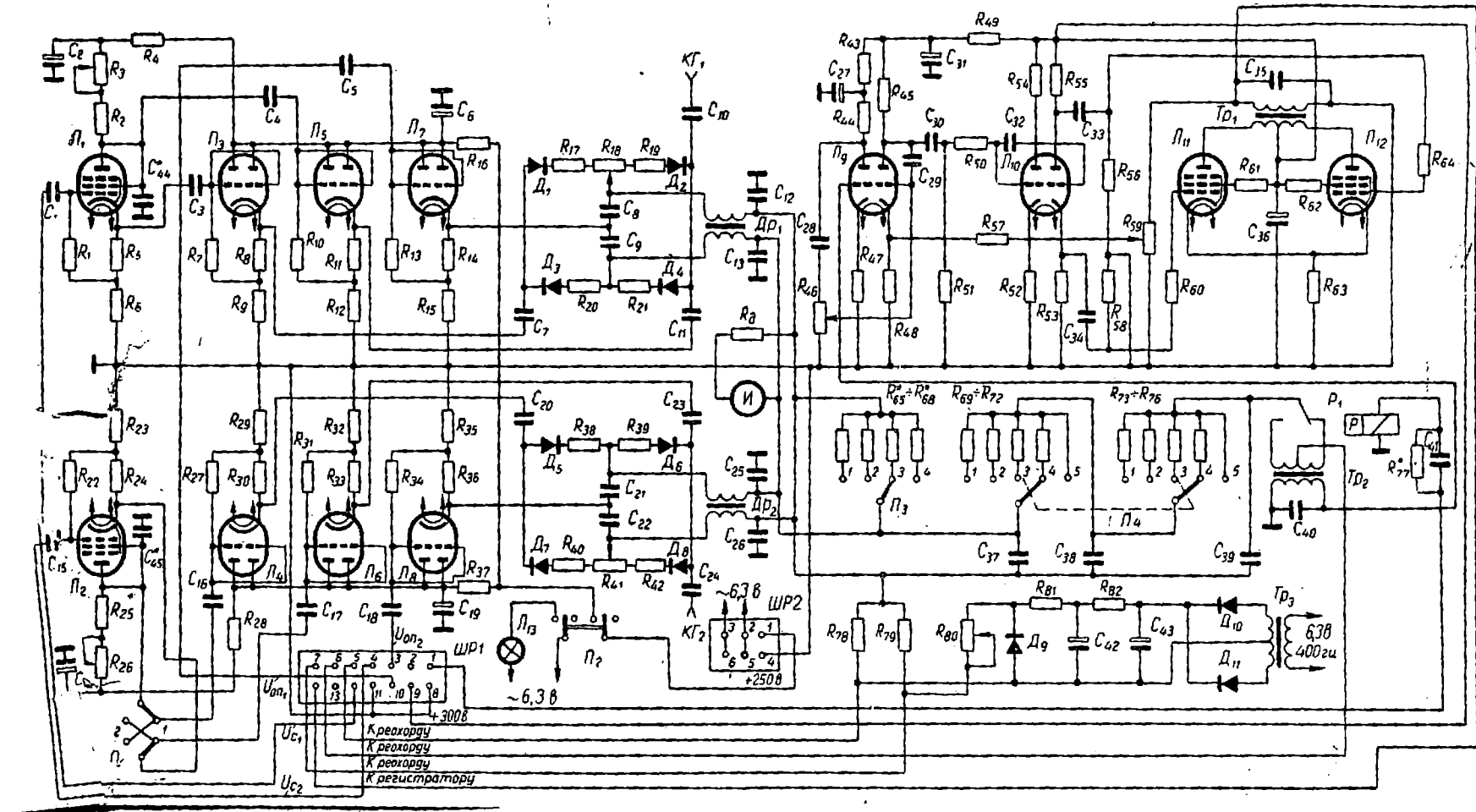
The comparative voltage is delivered through contact 10 of the plug socket SHR1 to the grid of cathode repeater L_7 and hence - the middle connection point of capacitances C_8 and C_9 of the FHD. For the filtering of comparative voltage, the output portion of the detector is connected with the filter, consisting of bifilar throttle valve Dp_1 and two condensers - C_{12} and C_{13} .

Channel II operates in the same way. However, here the outputs of phase-invertor L_2 are cut in to switch P_1 , by means of which the output voltages may change their phase by 180° .

The outputs of ring-shaped detectors of both the channels are connected parallel on direct current. The direct reading device of the measured quantity, cut in to the output, will show the sum or the difference of the components, depending on the position of switch P_1 . In the position "components sum" the polarity of the output voltages in ring-shaped detectors is similar and they are added; in the position "difference of components", the polarity of the output voltages is different and they are subtracted.

By means of switch P_3 , at the output of DFHV, connection is made of one of the four resistances $R_{65} - R_{68}$, which serves as a shunt for the direct reading device and the recording circuit. This provides variation of limits of measuring and recording.

In position 1 of switch P_3 , the DFHV scale corresponds to FHV scale (1:1); in position 2 - twice less sensitive than the FHV scale (2:1); in position 3 - has double sensitivity of FHV scale (1:2); in position 4 - four times more sensitive in comparison with the FHV scale (1:4). As mentioned, scales 2:1 and 1:1 are used in sum measuring, and 1:1; 1:2 and 1:4 in measuring the difference of the components. In range 1:1, the scale of direct reading device and of the recorder has divisions 100-0-100. Hence it follows that in range 2:1 it will have as though 200-0-200 divisions and in the range 1:4, respectively, 25-0-25 divisions.



The recording circuit of DFHV is similar to the FHV circuit. At the input of the recording circuit is cut in a two-sectional Π shaped RC filter $R_{69} - R_{72}$, C_{37} - and $R_{73} - R_{76}$, C_{38} for varying the width of the recorder's transmission band, the resistance change-over of which is carried out by switch P_4 .

The rheochord is cut in to block through contacts 5, 6 and 7 of the plug socket SHR1. The voltage on the winding of relay RP-4 arrives through contacts 1 and 8 of the same socket. Energizing of the rheochord is form a full-wave rectifier with valves DGG-27, the filtering of rectified voltage by Π -shaped RC-filter C_{42} , R_{82} , C_{43} , and stabilization by silicon stabilitron D808.

Resistances R_{78} and R_{79} form the middle point of the rheochord connection (on direct current) to one output pole of the ring-phase detectors. The second pole is connected with the middle point of the rheochord through the resistance of RC-filter and the mobile contact of relay RP-4.

For rectifying the intensity of the input voltages U_{x1} and U_{x2} provision has been made for rheostats R_3 and R_{26} in the anodes of phase-invertors. Balancing of detectors is implemented by resistances R_{18} and R_{41} .

8. Measuring amplitude ratio of two voltages:

In aerial electric prospecting, as a rule, relative measuring of two signals is carried out, received either by two field detectors with a simultaneous two-frequency survey, or by two reciprocally oriented field detectors in one-frequency survey (in the apparatus of induction

method, VMP and linearly polarised field in the investigation of natural fields, etc). In these cases, it would be expedient to measure the amplitude ratio of the received signals, which permits interpreting sufficiently logarithmic the results of geophysical investigations. For this purpose, it is possible to use quick-acting logometric compensation systems and special electronic devices (171, 188, 196).

The (104) describes the method which permits measuring the ratio of various combinations of two voltages. The principle of the method lies in converting two direct current voltages (or two previously rectified alternate current voltages) into alternate current voltages and their quadrature adding with subsequent measuring of phase angle between the total vector and the vector of voltage, executing the transformation. Let us analyse this method in more detail.

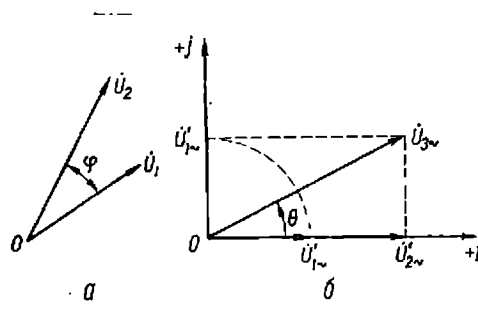


Fig: 149.

Two vectors are present of voltages: $U_1 = U_{1m} \sin \omega t$ and $U_2 = U_{2m} \sin (\omega t + \varphi)$, lying at random angle φ to each other (Fig: 149,a). After the rectification of each voltage separately, we obtain two direct current voltages: $U_{1-} = k_1 (U_1)$ and $U_{2-} = k_1 (U_2)$.

proportional to moduli of voltages U_1 and U_2 . Subsequently, direct current voltages convert into alternate on frequency ω_0 with simultaneous turn of one of them at 90° angle (Fig: 149,b). At the output of the modulator there will be again two alternate voltages, generally of different frequency shifted at 90° , i.e.

$$\ddot{U}_{1\sim} = k_1 k_2 U_1 \sin \left(\omega_0 t + \frac{\pi}{2} \right) = k_1 k_2 \cos \omega_0 t; \quad (X.22)$$

$$\ddot{U}_{2\sim} = k_1 k_2 U_2 \sin \omega_0 t,$$

where k_2 - the transmission factor of modulators.

As a result of adding two quadrature voltages $U_{1\sim}$ and $U_{2\sim}$, we get resultant (third) voltage

$$\begin{aligned} U_{3\sim} &= k_1 k_2 k_3 U_1 \cos \omega_0 t + U_2 \sin \omega_0 t = \\ &= k_1 k_2 k_3 \sqrt{U_1^2 + U_2^2} \sin \left(\omega_0 t + \arctg \frac{U_1}{U_2} \right) \end{aligned} \quad (X.23)$$

where k_3 - the transmission factor of summator circuit.

Voltage $\dot{U}_{3\sim}$ is shifted at angle $\theta = \arctg \frac{U_1}{U_2}$ in relation to $\ddot{U}_{2\sim}$, or, which is the same thing, in relation to the vector of voltage, controlled by modulators.

Measuring by any phasometric system the phase shift between the ultimate voltage and of the then converted one, it is possible to determine the amplitude ratio of these signals. Since the indications of phasometers are independent of the amplitudes input signals, the scale of the phasometer could be graduated directly in moduli ratio of two voltages.

A block diagram, serving to measure the moduli ratio of two voltages of one frequency, as well as of two frequencies, is shown in Fig: 150. It includes two amplitude detectors AD_1 and AD_2 , two modulators M_1 and M_2 , controlled by auxiliary voltages U_0 and jU_0 with frequency, generated by the commutating voltage generator GKN, summation S and phasometric FM circuits. The modulators are controlled by voltages in quadrature; therefore, the voltages at their outputs will also be in quadrature. Addition circuit could be the tube cascade or (in simplest case) active resistance, through which currents are transmitted shifted at 90° . The modulators could be energized by one and the same voltage with subsequent turn in phase at 90° of one of the transformed voltages. In the ratio determination of two direct current voltages there will be no amplitude detectors.

An important condition for the normal operation of the system is the high accuracy of quadrature between the voltages controlling modulators, and also the application of phasometers of higher accuracy the measuring error should not exceed $0.5-1.0^\circ$ (24, 43, 114).

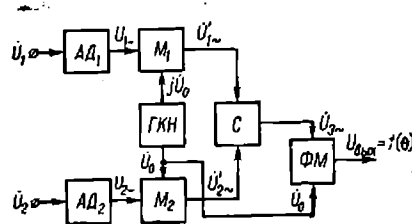


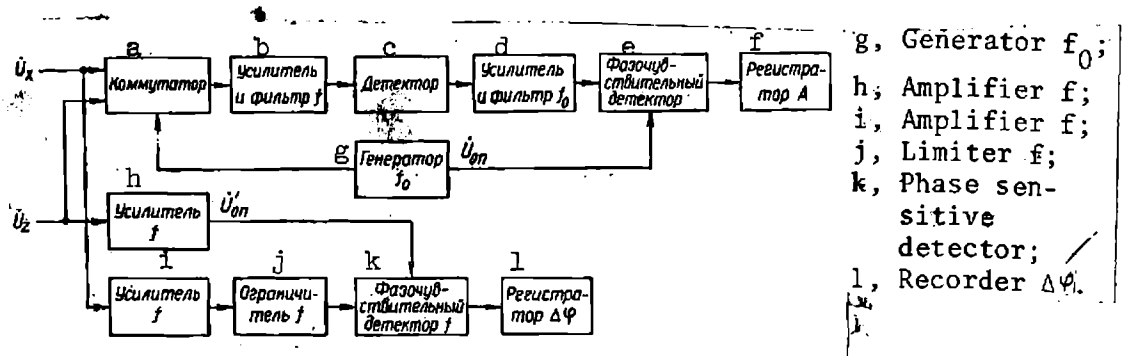
Fig: 150.

Since ordinarily the pickup of phasemeters is close to zero with measurable angle $\theta \rightarrow 0$ or $\theta \rightarrow 180^\circ$, it is expedient, in presetting possible values of the measurable ratio, also to choose the phase of the comparative voltage of the phasemeter. For instance, the diagram shown in Fig: 150 is convenient for measuring on the condition that

$\frac{U_1}{U_2} > 1$. But $\frac{U_1}{U_2} < 1$, then for the control of the phasemeter it would be more convenient to feed the comparative signal jU_0 .

Key to Figure 151:

- a, Switch;
- b, Amplifier and filter f ;
- c, Detector;
- d, Amplifier and filter f_0 ;
- e, Phase sensitive detector;
- f, Recorder A;



- g, Generator f_0 ;
- h, Amplifier f ;
- i, Amplifier f ;
- j, Limiter f ;
- k, Phase sensitive detector;
- l, Recorder $\Delta\varphi$.

Fig: 151.

Measuring of the amplitude ratio with higher accuracy could be carried out by means of a circuit, operating on the commutation principle (232, 234) (Fig: 151). The distinctive feature of this circuit is that the measurable voltages U_x and U_z are not compensating each other. With the help of the commutation method, the difference is measured of moduli $\Delta U = (U_x) - (U_z)$ of signals U_x and U_z and phase shift $\Delta \varphi = \varphi_{ux} - \varphi_{uz}$ between them. In this case, the measurable difference of moduli ΔU is equivalent to their ratio, i.e., quantity $A = \frac{U_x}{U_z}$.

Difference ΔU is produced by means of the electronic commutator, which connects to the input of the amplifier with filter f voltages U_x and U_z alternately. The change-over frequency f_0 of the commutator is preset from the individual generator. The detected signal arrives at the input of the amplifier with filter, tuned to commutation frequency f_0 , and from its output in the form of an envelope with frequency f_0 arrives at the phase-detector, which also operates on frequency f_0 (the generator supplies comparative voltage U_{comp}). At the FHD output, amplitude recorder A is cut in a device with zero in the middle of the scale. The increment sign of ΔU is determined by the FHD circuit.

The phase shift between the voltages of U_x and U_z signals is measured in the second channel. The amplifier and limiter impart to U_x signal an almost rectangular shape. This signal arrives at the circuit of the second FHD, which receives on signal frequency f comparative voltage U_{comp} from the amplifier of U_z signal. From the output of FHD voltage, proportional to phase shift $\Delta \varphi$, is supplied for recording to phase recording circuit.

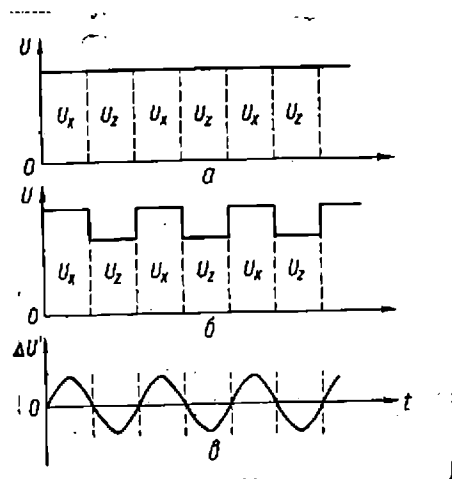


Fig: 152.

The commutator voltage curves are shown in Fig: 152. When amplitudes of comparative signals U_x and U_z are equal, the envelope of voltage U at the output of the detector will be almost a straight line (Fig: 152,a). If $U_x = U_z$ the U voltage is step-shaped, as shown in Fig: 152,b, and, by means of the selective amplifier, it is possible to separate from it the first harmonic of commutating voltage with frequency f_0 , i.e., signal $\Delta U'$, the intensity of which is proportional to difference $(U_x) - (U_z)$ or ratio $\frac{|U_x|}{|U_z|}$ (Fig. 152,c).

9. Phase-shifting circuits and phase-inverters:

In phase measuring and in measuring by means of the FHD, the important elements of units in the apparatus of aerial electric prospecting, besides the phase-shifting and phase-inverting chains, are the phase-inverters with the measuring range of phase shift from 0 to 360° .

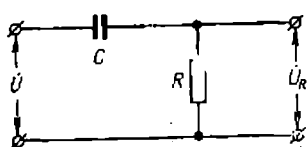


Рис. 153.

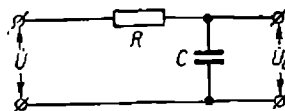


Рис. 154.

Fig: 153.

Fig: 154.

The most popular and convenient for obtaining and controlling the phase shift within a small range is the circuit, which is a combination of active R and reactive x resistances, connected in series. The latter is usually the condenser of constant or variable capacitance C . For instance, the elementary chain, shown in Fig: 153, is the simplest circuit for obtaining phase shift upto 90° . Analysis of the given chain shows that by varying the ratio of its elements within limits from $x = R$ to $x \ll R$ ($x \frac{1}{\omega C}$) it is possible to vary the phase shift between voltages at input (U) and output (U_R) of the circuit from 45 to 0° .

If the RC-chain is cut in according to the diagram shown in Fig. 154, then with variation of ratio between resistances R and x in the same limits, the phase shift between voltages at the input and output of the circuit varies in the interval 45 - 90° .

By conforming to condition $x = R$ the phase shifting chains (see Fig: 153 and 154) make it possible to obtain additional phase shift $\pm 45^\circ$ without an appreciable reduction of the output voltage. But if $R \gg x$ (see Fig: 154), the phase shift between voltages at the output and input of the circuit will be close to 90° , but then the voltage at the output will be considerably lower than the voltage at the input and will vary during the adjustment of R . Moreover, the circuits, similar to those shown in Fig: 153, 154, do not have sufficient linearity and it is difficult to use them as graduated linear phase-invertors. Nevertheless, the chains are widely applied in composite phase-invertors, meant for changing the phase shift within a wider range (e.g. upto 180°). Combination of chains with phase-invertors, providing phase shift at 180° and assembled on electronic tubes or semi-conductive triodes, enables the shifting of phases in an easy way by 360° (10).

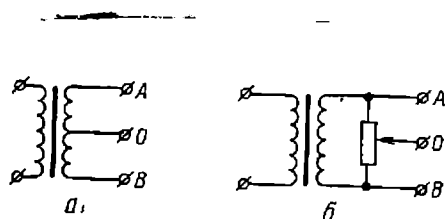


Рис. 155.

Fig: 155.

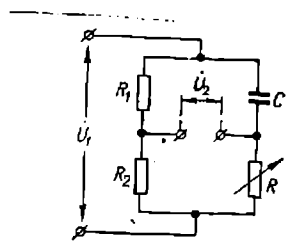


Рис. 156.

Fig: 156.

To obtain a phase shift of 180° , the use is often made, besides the phase-invertor, of the transformer, the secondary winding of which has either a middle branch (Fig: 155,a), or an artificial middle point (Fig: 155,b).

Phase-invertors, which permit changing smoothly the phase of being lead-in voltage within a range of upto 180° , usually consist of adjustable and constant active and reactive resistances, cut in on the bridge circuit (Fig: 156). Investigations show that the nature of voltage variation at the output of this phase-invertor, with the adjustment of phase shift, is determined by the ratio of resistances R_1 and R_2 . At $\frac{R_2}{R_1} = 1$ voltage amplitude at the output of phase-invertor U_2 with adjustment of phase by variation of resistance R remains constant and equal to half the amplitude of input voltage U_1 . In this case, the phase angle φ is determined from formula

$$\varphi = \text{arctg} \frac{2n}{1 - n^2} \quad (\text{X.24})$$

where

$$n = \frac{1}{\omega CR}$$

From formula (X.24) it follows that at $n = 1$ the phase shift, generated by the phase-invertor, is 90° , and the extreme n values (zero and infinity) correspond to phase angles 180° and 0 . Phase shift over 180° is most simply obtained theoretically with step-wise connection of phase-invertors, as a result of which to phase shift φ_1 of the first phase-invertor is added phase shift φ_2 of the second and so on. However, it is difficult to carry this out in practice, since it is necessary to take into account the interference of individual phase-invertors.

Potentiometer phase-invertors should be considered the most acceptable for operation on frequencies of aerial electric prospecting with adjustment of phase shift within the range $0-360^\circ$. Their main advantage is that they are free from transitional processes and are easily shielded. The disadvantage is the difficulty of assembling phase-invertors with low error of phase angle reading.

The base of the potentiometric phase-invertor contains a closed circular potentiometer with linear winding, at four points of which voltages are supplied from individual phase-invertors shifted in phase with respect to each other at 90° (Fig: 157,a). By moving the side along the potentiometer it is possible to change smoothly the phase shift of the output voltage within limits $0-360^\circ$ (10). The equivalent circuit of one quadrant $\frac{\pi}{2}$ of potentiometric phase-invertor is shown in Fig: 157,b.

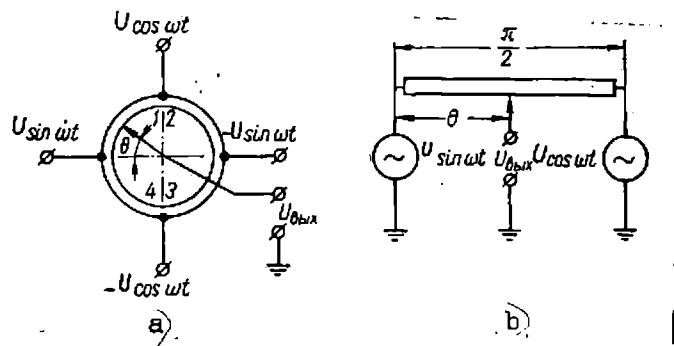


Fig: 157.

Applying the principle of superimposition, output voltage is determined from this formula (220)

$$U_{BbIX} = \frac{\frac{\pi}{2} - \theta}{\frac{\pi}{2}} \sin(\omega t) + \frac{\theta}{\frac{\pi}{2}} \cos(\omega t) \quad (X.25)$$

Denoting

$$\frac{\theta}{\frac{\pi}{2}} = A \sin \varphi, \quad \frac{\frac{\pi}{2} - \theta}{\frac{\pi}{2}} = A \cos \varphi,$$

we obtain

$$U_{BbIX} = A \sin(\omega t + \varphi). \quad (X.26)$$

The modulus of this formula

$$A = \sqrt{\left(\frac{\frac{\pi}{2} - \theta}{\frac{\pi}{2}}\right)^2 + \left(\frac{\theta}{\frac{\pi}{2}}\right)^2} \quad (X.27)$$

and phase

$$\varphi = \operatorname{arctg} \frac{\theta}{\frac{\pi}{2} - \theta} \quad (X.28)$$

Analysing formulas (X.27) and (X.28), we will find that within one quadrant the phase angle varies from 0 to 90°, and the output voltage (modulus), varying slightly, passes through its minimum value, corresponding to the position of the slide in the middle of the potentiometer (0=45°):

$$A = U_{BbIX.MNH} = \frac{U_{BX}}{\sqrt{2}} \quad (X.29)$$

Parameters of other quadrants of the potentiometric phase-invertor are determined in the same way.

Potentiometric phase-invertor could be made not only in the shape of circular locked potentiometer with four feeding points, but also in the form of four resistances equal in value (three constant, and one adjustable), connected in series. The constant resistances form three discrete phase quadrants, and the adjustable - an even phase quadrant (Fig: 158a).

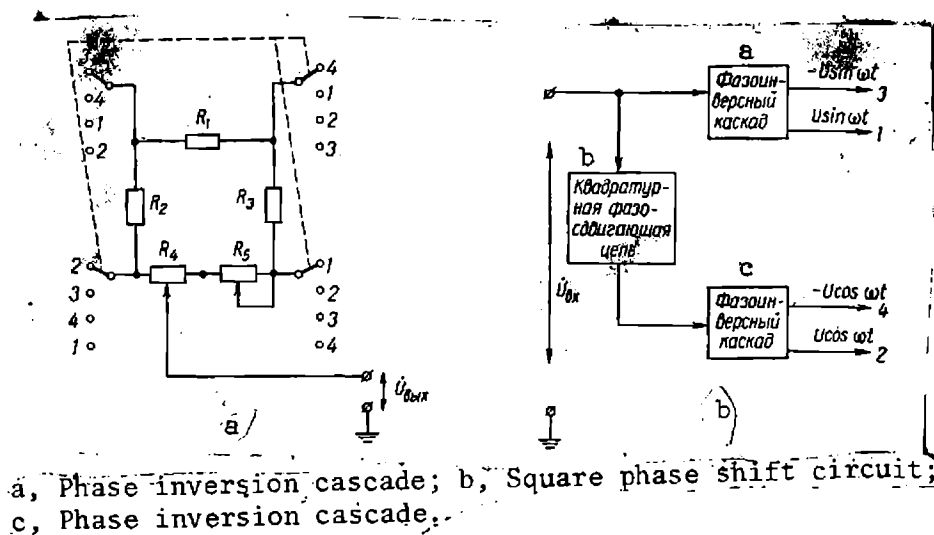


Fig: 158.

In order to obtain with one adjustable resistance the control of the phase shift within the limits $0 - 360^{\circ}$, phases of voltages feeding the rheostat phase-invertor should alternate. Provided for this is a special phase-invertor circuit (Fig: 158,b) and four-arm change-over switch for positions (Fig: 158,a). In this way, the output of the circuit has phase shift within $0 - 360^{\circ}$ by jumps over each quadrant ($0; 90; 180$ and 270°) and evenly ($0-90^{\circ}$) within each quadrant.

For a more even and exact setting of the phase shift in series with the main adjustable resistance, an additional one is switched on, the value of which is usually $0,1 R$. However, it should be kept in view that the cut in of this resistance increases the intensity of the output voltage, as compared to that obtained from formula (X.27), since the electric symmetry of quadrants changes.

Apparently, the greater the length of the active part of adjustable resistance, the more convenient and accurate will be the adjustment of the required phase shift. The choice of high-value resistances of the potentiometric phase-invertor (several tens of kilo-ohms) is useful for low shunting of load in the phase-invertor or transformer, and also for reducing power consumption by the phase-invertor.

Step-wise variation of the phase shift, at every 45° (octants) within $0-360^{\circ}$, may be effected also by means of quadrant potentiometric phase-invertors. This is done by dividing each of the four resistances, forming the locked potentiometer, into two equal parts. A block diagram of such an octant phase-invertor is shown in Fig: 159.

With an appropriate commutation, the voltage at the output of the phase-inverter (between the ground and points 1; 2; 3; 4; ...) will vary in the phase by jumps at 45° . At point 8 the phase shift will attain 315° .

The error of the potentiometric phase-inverter is determined mainly by the accuracy in selecting arms resistances of locked potentiometer and may be not ever 1% for the octant or quadrant.

Another type of low-frequency phase-inverter, enabling us to obtain even the phase shift of signals within 2π , is the phase-inverter with rotating transformer (for example, VTM type). In this phase-inverter the phase shift depends on the angle of rotation of the revolving transformer rotor.

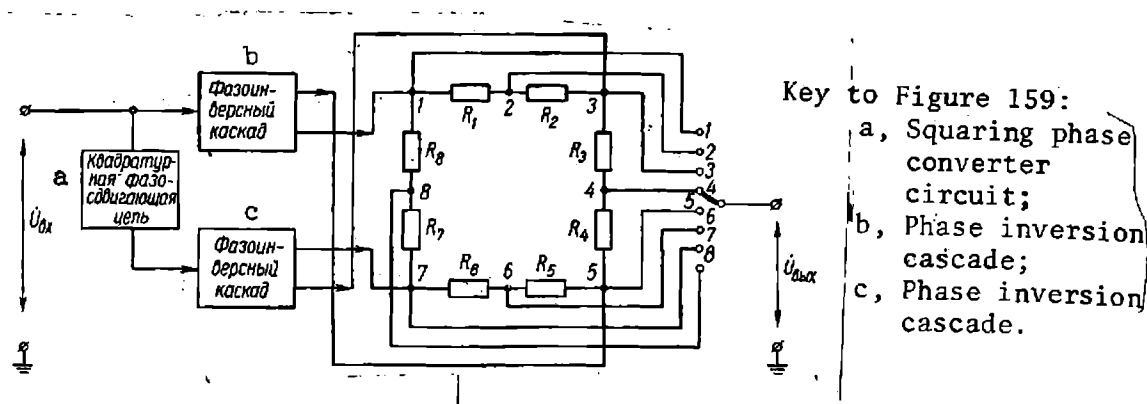


Fig: 159.

One of the diagrams of phase-inverter with VTM is shown in Fig: 160 (160, 161). Here the input signal \bar{U}_{in} is fed to the rotary winding. Voltages on reciprecallyperpendicular stator windings are written as

$$e_1 = U_1 \cos \theta_e j \omega t,$$

$$e_2 = U_2 \sin \theta_e j \omega t,$$

where θ - the angle of rotation of VTM rotor; ω - the angular frequency of the input signal.

If $R_1 = R_2 = R$, $C_1 = C_2 = C$ and for a certain part of signal we have $R = \frac{1}{\omega_0 C}$, with amplitude partly of voltages on stator windings ($U_1 = U_2 = U_m$) and when $\omega R_1 C_1 = \omega R_2 C_2 = 1$, then for the output signal we get

$$\begin{aligned} U_{BbIX} &= \frac{U_m}{\sqrt{2}} e^{j \omega_0 t} \left[\cos \left(\theta - \frac{\pi}{4} + j \sin \theta - \frac{\pi}{4} \right) \right] = \\ &= \frac{U_m}{\sqrt{2}} e^{j \left(\omega_0 t + \theta - \frac{\pi}{4} \right)} \end{aligned} \quad (X.30)$$

From formula (X.30) it follows that the vector of the output voltage is shifted in the phase relating to the vector of the input voltage by an angle $\theta - \frac{\pi}{4}$, i.e., the phase shift of the output voltage, with appropriate selection of phase-inverter parameters and a certain initial setting of its scale, is proportional to the angle of rotation of the VTM rotor, and the amplitude of this voltage does not depend on the rotor's rotation. However, if $\omega \neq \omega_0$ or phase-inverter

The presence in the phase-invertor with VTM of two RC-chains complicates the diagram and its tuning, however, this phase-invertor is simpler to make, more reliable in operation than the potentiometric. Moreover, it has the advantage of unvarying amplitude of the output voltage U_{out} with variations of the phase-shift at fixed operating frequencies.

When the use of standard automatic potentiometer is made as phase recorder then the adjustable element of the phase-invertor should be its rheochord. In this case, the most convenient the diagram are those in which the rheochord is grounded and has low resistance (upto 1 - 2 kohm). A diagram of such a phase-invertor, plotted on RC-chain and phase-invertor on semi-conductive triode T_1 , is shown in Fig: 162. The adjustable element is the rheostat R_e , the voltage amplitude at which (at point F) may vary from 0 to (U_0) .

The vector diagram, explaining the operating principle of this phase-invertor, is shown in Fig: 163. To obtain linear relation of the phase to the arm of resistance R_e the output voltage U_{out} is taken off not from point B, as usual (90), but from point E. With total change in the position of arm F from O to D angle α varies from the position of vector $\overline{E_4 F_4}$ to the vector position $\overline{EF_4}$, or by angle 2α . The magnitude of the angle depends on the chosen ratio $\frac{R_2 + R_3}{\omega C}$ and R_2/R_3 .

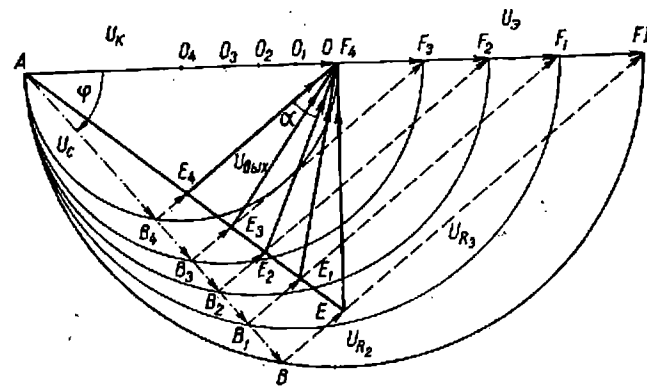


Рис. 163.

Fig: 163.

Resistance values, with adopted value of capacitance, known frequency and preset variation of 2α could be determined from formulas

$$R_2 = \frac{1}{\omega C} \operatorname{tg} \alpha; \quad R_3 = \frac{1}{\omega C} \cdot \frac{1}{\sin 2\alpha}. \quad (\text{X.31})$$

The maximum error of deviation from linear scale ΔK is determined from ratio

$$\Delta K_{\text{MaKc}} = \pm 0.56 \pm \frac{\operatorname{tg} 0.56 \alpha}{\operatorname{tg} \alpha} \quad (\text{X.32})$$

and

$$K = \frac{OF}{OD} = \frac{\Delta R_e}{R_g} \quad (0 \leq \Delta R_e \leq R_g).$$

R_k value in the diagram, shown in Fig: 162, is determined by parameters of rheochord R_e ($R_k \approx R_e$). This rheochord is usually brought out into the phase-recorder block.

A diagram of phase-invertor at four fixed frequencies, assembled on electronic tube, is shown in Fig: 164. The selection of one of the four frequencies is made by the connection of appropriate capacitance ($C_1 - C_4$).

10. Remote control of field detector and preamplifier:

In the apparatus of aerial electric prospecting, field detectors and preamplifiers are either brought out into the outboard gondola, or placed directly outside the aircraft at some distance from the aircraft's personnel. Therefore, the control of the operating frequencies of the receiving channel (of field detectors and preamplifiers) and the checking of its efficiency are carried out at a distance, which, of course, considerably reduces the non-productive consumption of flying time and simplifies the work of the operators.

If multicore cables are used for electric coupling of the receiving channel with the measuring unit, the scheme of remote control is not complex and, hence, is of no interest for an analysis. With the letting out of the gondola on wire, cable with a limited number of current-carrying cores (e.g. three cores and casing) the diagram of remote control becomes much more complex. This kind of diagram has been used in the apparatus of the induction method (AERI-2) and the BDK method (AERA-2). Let us analyze in more detail the operation control diagram of the receiving channel in AERI-2 (127).

The retuning of field detectors from one frequency to another, as well as control operations, connected with the commutation of the gondola amplifier input, are executed remotely from the block of stabilized rectifier of the gondola amplifier, which, jointly with other units of apparatus, is set up in the plane cabin. The line diagram of the gondola amplifier (see Fig: 117) shows the circuits and their elements, participating in the above operations.

Remote control and the required commutation of elements in the input circuit are effected by means of the usual step-by-step switches SHI-11 for 12 positions and small-scale relays type PCM. A description of the operations, which are executed the step-by-step switch of the gondola amplifier in AERI-2, is given in Table 20.

TABLE - 20

Position of Switch	Channel I	Channel II	Decoding of Operations.
1	243 cps	974 cps	Reception of signal or calibration of field detectors on the indicated frequencies.
2	243 cps	1949 cps	
3	243 cps	3898 cps	
4	487 cps	1949 cps	
5	487 cps	3898 cps	
6	974 cps	3898 cps	
7	K.z.	k.z.	k.z. - input short-circuited (at common minus).
8	K.z.	e.c.	e.c. - input short-circuited per alent of field detector.
9	k.z.	k.l.b.	k.l.b. - calibration of amplifier.
10	k.l.b.	k.z.	

N.B: 12th position is used for checking synchronism of the step-by-step switch in the gondola amplifier and indicator operations of the stabilized rectifier block.

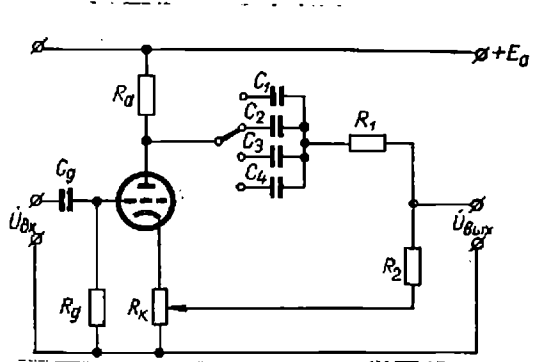


Fig: 164.

The explain the interaction of elements in the remote control system, Fig: 165 shows the diagram of change-over and delivery of pulses, feeding the winding of the step-by-step switch in the gondola amplifier.

The voltage of received signals of operating frequencies is fed to the separating filters of compensators in both the channels through condenser C_{19} , cable core, contacts 2 and 3 of Kn button controlling step-by-step switch and fitted in the stabilized rectifier block of the gondola amplifier. The winding of finder SHI_2 of the gondola amplifier is not connected with the amplifier input in its operating conditions, since relay P_{10} is energized from the anode circuit of the gondola amplifier and its contacts are unlocked.

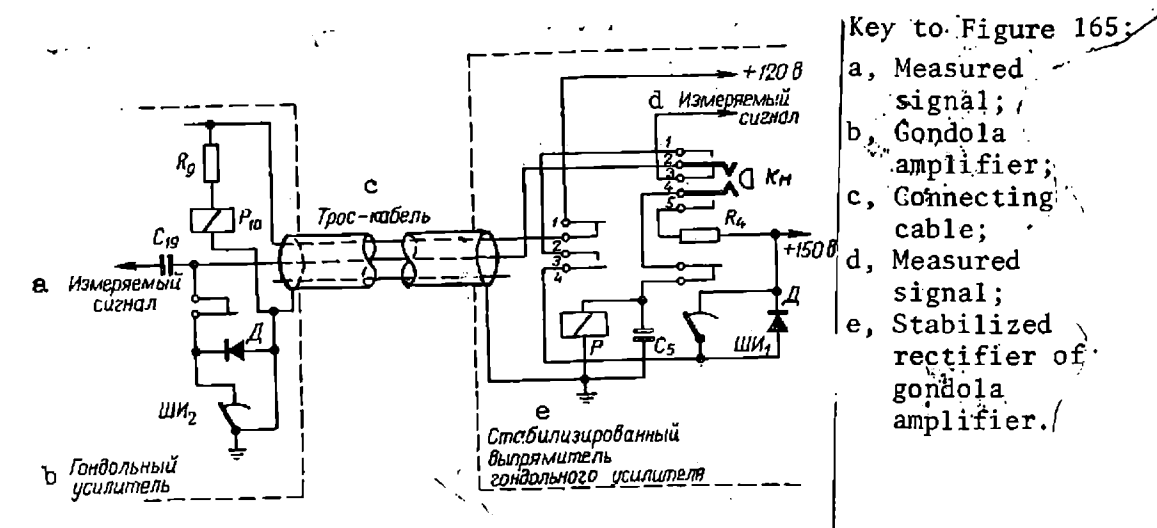


Fig: 165.

With the pressing of Kn button, contacts 2 and 3 unlock and the inputs of the separating filters are cut out. The power supply voltage of the amplifier (+ 120v) is fed through the contacts of double-finder SHI₁ (indicator of synchronous operation of finder SHI₂) to the winding of relay P₁ which, by operating, breaks the supply circuit of voltage into the gondola amplifier. Relay P₁₀ of this amplifier becomes de-energized and connects by its contacts finder SHI₂ with the signal core of the cable, to which, through the winding of finder SHI₁, contacts 4 and 5 of Kn button and resistance R₄ (damping), voltage is fed + 150v. In this case, both the finders operate simultaneously, shifting their brushes by one step.

If the button is released, the finders fix their new position and the original circuit is restored. When the button remains pressed, onto the winding of the finders a routine feed pulse arrives, after they move by one step, after which the finders move another step and so on.

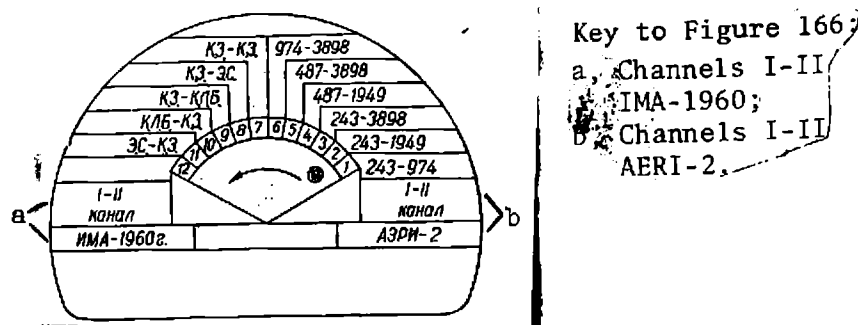
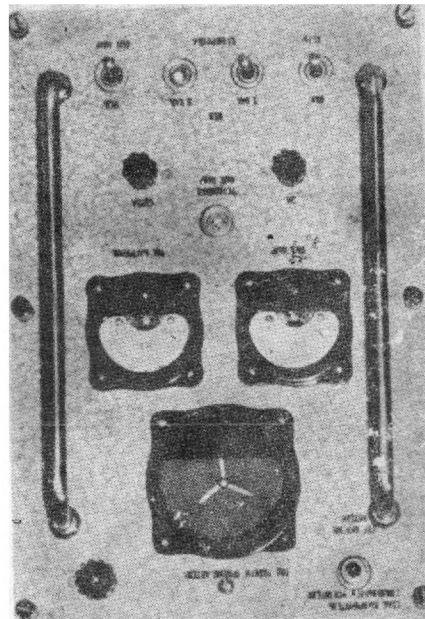


Fig: 166.

Since the shifting of brushes is only possible in one direction, with continuous pressure of the button through twelve steps of the finder, the cycle is repeated. Connection in series of finders SHI_1 and SHI_2 provides for a reliable synchronism of their operation. The position of brushes of both the finders is controlled visually. Brushes of SHI_1 finder have an arrow attached, which shows on a dial (Fig: 166), fitted on the front panel of stabilized rectifier block (Fig: 167), the position of the finder's brushes.

Let us analyse the operation of remote control elements in the change-over of operating frequencies and other control operations for positions of finder brushes 1-12 (see Fig 117). Positions 1-6 provide for the tuning of magnetic field detectors to the operating frequency and amplification of the received signals. Positions 7-12 are for control and calibration. The third field of finder SHI -III connects balast resistances R_{43} and R_{46} , required for providing



. Fig: 167.

continuous resistance of relays group connection.

Position 1: Along channel I - on frequency 243 cps, on channel II frequency 974 cps. Operate relays P_1 , P_4 , P_7 , P_8 and P_9 . Relays P_1 and P_4 connect capacitances C_1 and C_4 of tuning, relay P_7 - the field receiver of low, and relay P_8 and P_9 - the field receiver of high frequencies with the control grids of the corresponding cathode repeater tubes (L_1 and L_2).

Position 2: On channel I - on frequency 243 cps, on channel II - on frequency 1949 cps. Operate relays P_1 , P_5 , P_7 and P_9 . Relay cuts in capacitance C_5 for tuning the section of coil of the field receiver of high frequencies to frequency 1949 cps. The functions of the other relays are described above.

Position 3: On channel I - on frequency 243 cps, on channel II - on frequency 3898 cps. Operate relays P_1 , P_6 , P_7 and P_9 . Relay P_6 cuts in capacitance C_6 for tuning the coils section of HF field receiver to frequency 3898 cps. The functions of the other relays are the same as above.

Position 4: On channel I - on frequency 487 cps, on channel II - on frequency 1949 cps. Operate relays P_2 , P_5 , P_7 and P_9 . Relay P_2 cuts in capacitance C_2 for tuning the coil of LF field receiver. The functions of the other relays as above.

Position 5: On channel I - on frequency 487 cps, on channel II - on frequency 3898 cps. Operate relays P_2 , P_6 , P_7 and P_9 , carrying out the same functions as above.

Position 6: On channel I - on frequency 974 cps, on channel II - on frequency 3898 cps. Operate relays P_3 , P_6 , P_7 and P_9 . Relay P_3 cuts in capacitance C_3 for tuning the coil of LF field receiver. Functions of the other relays as above.

Position 7: The input of the gondola amplifier on both the channels is locked to common minus.- the measuring is of internal noises and inductions. Operate relays P_1 , P_4 and P_8 . Relays P_1 and P_4 cut in by the second group of contacts controlling the grids of tubes L_1 and L_2

Position 8:

Input of gondola amplifier on LF channel is locked on the common minus, and on HF channel - on the equivalent to field receiver resistance (on the average frequency for the given field receiver). The operation is of relay P_1 and P_6 . Relay P_6 cuts in by the second group of contacts resistance R_{15} .

Position 9:

Input of gondola amplifier on the LF channel is locked on the common minus, and on HF channel calibration circuit is being prepared of the gondola amplifier. The operation is of relay P_1 and P_5 . The P_5 relay cuts in by the second group of contacts control grid of tube L_2 to divider R_{14} , R_{48} , R_{13} , to which the calibrating voltage is being input.

Position 10:

The input of the gondola amplifier on HF channel is locked on common minus, and on LF channel preparation is being made of the calibration circuit for the gondola amplifier. Operate relays P_2 , P_4 and P_8 . Relay P_2 cuts in the control grid of tube L_1 to divider R_{13} , R_{48} , R_{14} , to which the calibrating voltage is being fed. Relay P_8 remains idle.

Position 11:

The input of the gondola amplifier on LF channel is locked on resistance R_{16} , equivalent to the resistance of field receiver on its medium operating frequency, and on HF channel - on common minus. Operate relays P_3 , P_4 and P_8 . Relay P_3 cuts in by the second group of contacts resistance R_{16} . Relay P_8 remains idle.

Position 12: The cophasal operation of the gondola amplifier finder and of doubler-finder of the measuring group is checked. In this case, the circuit is broken of the filament-anode supply of the gondola amplifier, which is fixed by control device as consumption by the gondola amplifier of rectified current.

A slightly different system of remote control has been used in the BDK apparatus (90). Let us examine the diagram for the choice of operating frequencies of AERA-2 apparatus, shown in Fig: 168, which is also semi-automatic and enables, by pressing button K_1 "Type of work", the switch over of pertinent circuits in all the blocks of the apparatus during transition from one frequency to another. Signalling regarding the type of work is carried out by means of light dial.

In the initial position of K_1 button capacity C_1 is charged upto the voltage of the power network of helicopter + 26v. At the moment of pressing the button, the capacity discharges through the winding of relay P_1 . The relay operates and by means of contacts Kp_1 cuts in the circuit of contact-relay P_2 , and through its contacts Kp_2 , the supply circuits of all step-by-step switches SHI of the measuring unit. Step-by-step switches operate, and their brushes pass on to the next contact. During this time the discharge current of capacitance C_1 reaches the intensity of relay P_1 release current, as a result of which contacts Kp_1 become unlocked; this is followed by the unlocking of condenser-relay contacts Kp_2 , and the supply circuits of the step-by-step switches de-energize. Duration of the discharge time is easily adjusted, since it is determined by C_1 value and the release current of relay P_1 , i.e.,

by parameters of the discharge circuit.

One of the plates (SHI_{1-4}) of the step-by-step finder SHI_1 in the block of selective amplifier, is used for the commutation of power supply circuits of signal bulbs $L_1 - L_{12}$, which are located on the light dial. The remaining plates (SHI_{1-1} and SHI_{1-3}) are used for the commutation of appropriate circuits of the selective amplifier.

The winding of the step-by-step finder SHI_2 in the phasemeter block is connected with the power supply circuit of step-by-step finders through contacts of button K_2 "Synchronization of SHI". In the operating position, the button is released and the control of the step-by-step finder is executed by button $K_1 - K_2$ button serves to set the step-by-step finder SHI_2 in the initial position. With the pressing of button K_2 the winding of the step-by-step finder is cut in to the board network, which causes it to operate. In position 12 ("Control SHI") plate SHI_{2-4} switches on signal bulb L_{13} . The remaining plates of this finder ($SHI_{2-1} - SHI_{2-3}$) are used for the commutation of phase-shifting circuits of phase-inverters in the phasemeter block.

The control circuit of the step-by-step finder SHI_3 in the receiver block is similar to the control circuit of the step-by-step finder in the phasemeter block described above. The supply and control circuit of the step-by-step finder's position in the outboard gondola is comparatively complex, since for the coupling with the gondola the use can be made only of two cables - signal and minus.

The command relay P_3 in the receiver block has control circuit, similar to the one described above. This relay can be cut in by means of Button K_1 in the selection of the type of work, as well as by means of button K_3 in position control of the step-by-step finder in the gondola.

With the winding connection of relay P_3 , the signal cable through contact group Kp_3 gets connected with filter output (+ 240v) of the stabilizer rectifier of voltage for the supply of the gondola amplifier. The neon tube L_{16} lights up, and the step-by-step finder SHI_4 in the gondola amplifier operates. Capacitance C_7 prevents the falling of high voltage on the cathode of tube L_3 (output stage of the gondola amplifier). With the release of button K_3 , tube L_{13} goes out, removing the shunting effect of the step-by-step finder on the output of the gondola amplifier, and the circuit returns the initial position.

The synchronization of the step-by-step finder SHI_4 in the gondola is controlled in the following way. In position 12 ("Control SHI ") through plate SHI_{3-4} the winding of relay P_4 gets energized, and the signal cable gets connected through contacts KP_4 with the special rectifier (-27v), serving to feed signal bulb L_{15} , which indicates synchronization of the step-by-step finder of the gondola amplifier. If, at this moment, the contacts of the gondola finder SHI_4 are also in position 12, the supply circuit of bulb L_{15} (through contacts Kp_3 , Kp_4 and conformably connected to voltage -27v diodes D_1 , D_2) will be locked. The supply of the next change-over positive pulse (+240v) with the changing of the circuit to the next operating position will not cause its

shunting due to the opposing connection of diodes D_1 and D_2 . The remaining plates SHI_{4-1} - SHI_{4-3} of the step-by-step finder SHI_4 are used for switching over the corresponding input circuits of the gondola system, etc.

However, the circuits of remote control, constructed on step-by-step finders, contacts of which were used directly for the transmission of minor signals, were found to be unreliable and required careful maintenance (regular washing by alcohol, insulation against dust, etc.). Therefore, preference should be given to circuits, in which for this purpose, small-scale and reliable relays are applied, while the finders themselves serve as controlling elements.

Chapt. XI - COMPENSATION OF THE PRIMARY FIELD SIGNAL IN THE METHOD OF INDUCTION

1. Methods of signal compensation.

Effectiveness and practical value of any version of the aerial induction method depends entirely on the high protection of its apparatus from various noises, including those caused by the primary field itself, which may be perceived by the receiving portion of the apparatus equally with the useable signal from the secondary field. When the primary field induces time-continuous interference, it is comparatively easy to compensate this interference, for example, by electrical methods. But if due to a slight unavoidable variation in the reciprocal position of the source and the field detector caused by disruption during the flight of the geometry of the system, the time interference varies at random (even if only in intensity), it is practically impossible to eliminate it, since it is of the same frequency as the useable signal. Therefore, the variable signal of the primary field, perceived by the field detector, is an undesirable background, on which the useable signal is easily lost, specially its comparatively negligible variations, connected with conductivity variation of various layers of the earth crust. Hence a confident measuring of the anomalous signal in the aerial induction method is only possible with efficient suppression of the direct signal, induced in the primary field detector.

Suppression of the primary field signal in the aerial induction method could be achieved in at least four ways.

The first way consists in slackening the bond between the source and the field detector by removing the latter from the aircraft and letting it approach the ground. This is done by placing the field detector in the outboard gondola. This way has some positive sides. For instance, with increasing spread (distance between the source and the field detector) there

is some increase in the sensitivity of the induction method to anomalous objects, since in this case there is a higher ratio of the secondary field density to the primary and the signal to the noise ratio improves (whether the noise is external, vibrational, from electric equipment of the aircraft, etc.).

It is well known that with the increasing altitude of flight/density^h of the secondary field reduce in the proportion of h^6 . However, with the spread of about 100 m and over and the approximation of the field source to ground density, the reduction of the secondary field at the point of the field detector will be approximately determined by relation $h^{4,5-5}$, which is an appreciable gain in the level increase of the secondary field (103). But even in these conditions, the primary signal invariably remains considerably higher than the secondary. This way of suppressing the primary signal has the following negative sides: reduction in the method's sensitivity with increasing altitude of flight, and to supplement the loss of sensitivity requires raising the power of the primary field source (to increase the torque of the oscillating frame); the piloting conditions become more difficult; variations of the selected geometry of the system of source field detector, due to random shifting of the outboard gondola (its bumping) with sufficiently long and soft suspension, are more likely. Bumping of the gondola frequently results in the appearance of quite considerable methodical interference.

Thus, increased distance between the source and the receiver of the field and the flight of the aircraft at a minimum altitude is incompatible. The possibility of reducing the effect of the primary signal on the measuring results by this way is limited on account of the required safety of piloting. Therefore, there is usually some compromise.

The second way envisages placing of the field detector at those points in the zones of the space surrounding the field source, at which the primary signal is either a zero (in particular, one of the primary field components is equal to zero), or is generally insignificant, and its unavoidable variations with the disruption of the geometry of the system are negligible.

The third way assumes the application of electric compensation, i.e., decrement in the measuring apparatus of the intensity of the direct (primary or resultant) signal received by the field detector due to subtraction from it, by special circuit, of auxiliary (coherent) compensating voltage with a certain amplitude and initial phase.

The fourth way is implemented by the use, for instance, of the rotating magnetic field and the placing of field detectors in those zones where the primary field has circular polarization. Signals, excited in receivers by the corresponding components of the primary field, are transformed into electric circuits in such a way that, in the absence of a disturbing object, the modulus difference of transformed signals and the phase shift between them are maintained equal to zero.

The first two ways for the suppression of the primary signal, based on a selection of the position and orientation of the field receiver in relation to the source, determine the so called geometric compensation.

The third way, i.e., electric compensation, has its own varieties, distinguished both by the choice of the initial phase of the compensating voltage and by the nature of the fixing modulus of this voltage during compensation and its behavior in the process of changing. The source of the compensating voltage could be directly the master oscillator or the ohmic resistance, connected into the circuit of the oscillating frame, as well as additional receiver (one or several) of the primary field, excited by the

main or the auxiliary source, etc.

The fourth way for suppressing the primary field signal is a combination, as in this case there are elements both of the geometrical compensation (selection of location zone by the field receiver), and of electric compensation (the signals excited by the primary field and transformed in electric circuits are so subtracted one from the other that their difference is zero).

A practical example of applying purely the geometrical compensation are the systems, combined and rigidly fixed together by frames (Fig. 169) (63, 117). These systems are used in the units of the induction method.

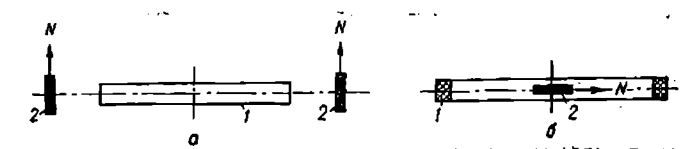


Fig. 169.

Fig. 169-a shows the diagram of an arrangement in which the oscillating frame 1 is placed in a horizontal plane and the two vertical receiving frames (coils) 2, connected in series, are placed on both sides of the oscillating frame and are oriented in such a way that the direct signal at their outputs is equal to zero.

In the horizontal receiving frame 2 is set in the centre of a circular oscillating frame 1 (Fig. 169-b), then, as follows from the analysis data of the primary field, there is no horizontal component of the field in the centre of this frame. Therefore, in the horizontally oriented field receiver the direct signal is practically non-existent.

In the first case, even with very rigid geometry of the system, it is possible to achieve suppression of the primary signal not over 10^3 - 10^4 times. But in the second case, since a point field receiver can not be made, the signal of the primary field is also present; it is caused by the vertical

component of this field, which corresponds in intensity to the residual signal in practical suppression of the primary signal by 10^3 - 10^4 times.

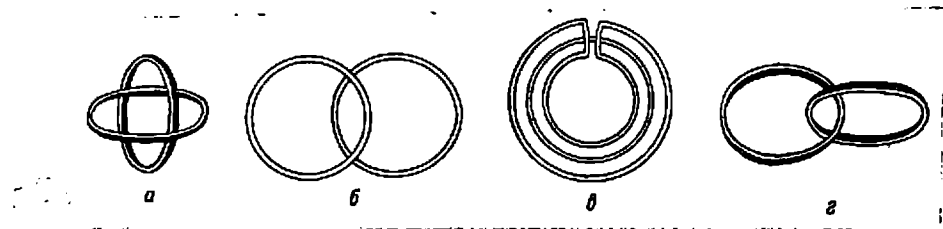


Fig. 170

Description of other methods for eliminating the effect of the primary field on the receiver by geometrical compensation is given in the work (157). The obvious sign of excluding the primary field \bar{H}_0 may be the parity to zero of flux \bar{F} through the field receiver:

$$\bar{F} = \mu_0 \int_S (\bar{H}_0, d\bar{S}) = 0, \quad (XI.1)$$

where S - the active area of the field receiver.

Fig. 170-a shows the oscillating and receiving frames, made in the form of a circular loop of radius a . In this case, the planes of both the frames are perpendicular, their centres combined and parity (XI.1) is automatically effected, as the integrand is equal to zero. If the shape and area of the oscillating and receiving frames are similar, the maximum size of the setting will be $2a$.

Let us take two more methods for excluding the effect of the primary field, based on the fact that the magnetic field of the loop inside and outside of it is in opposite direction (Fig. 170, b and c). The receiving frame could be so placed that one of its portions would be above the inner and the other above the outer sides of the oscillating frame (Fig. 170, b). In this case the condition should be met.

$$\bar{F} = \mu_0 \int_{S_1} (\bar{H}_{01}, d\bar{S}_1) + \mu_0 \int_{S_2} (\bar{H}_{02}, d\bar{S}_2) = 0, \quad (XI.2)$$

where \bar{H}_{01} and \bar{H}_{02} - the primary field inside and outside of the oscillating frame respectively; S_1 and S_2 - the part of the receiving frame area, located respectively above the inside and outer side of the oscillating frame;

$S_1 + S_2 = S$ - the area of the receiving frame.

With similar dimensions of the oscillating and receiving frames of round shape, condition (XI.2), as shown by theoretic calculations, will be met, when the receiving frame intersects horizontal frame at a distance $r = 0.48a$ from the centre (see Fig. 170, b). Therefore, the maximum size of the setup is approximately $3.5a$, i.e., considerably greater than in the first case.

When the receiving frame is made in the shape of a flat ring (see Fig. 170, c), the size of the setup with equal areas of both the frames will be $2.6a$. This system is less sensitive to reciprocal transpositions. The double compensation method is implemented in accordance with the diagram shown in Fig. 170, d).

In the apparatus of the aerial induction method, the application is of multiturn oscillating and receiving frames. Therefore, practical implementation of a high-degree compensation of the primary signal by the above means with high response of the apparatus is hardly possible (even with their very rigid fixing). It may be assumed that, in this case, additional electric compensation would be required in measuring the portion of the apparatus with a high stability of parameters both of the source and the field receiver, and of the electric compensation circuit itself. In practical work, the application is mainly of the combined compensation, i.e., combination of geometrical and electrical.

2. Main data of electric compensation.

Analysis of the main versions of the aerial induction method has shown

that, in some of them, the field receivers, due to specially selected geometry of the system, do not receive the primary field signal, i.e., there is purely geometrical compensation (e.g., the version with combined oscillating and receiving frames). In other versions due to the specific structure of the primary field and certain geometry of the system the signals of the primary field, received by the field detectors, are automatically subtracted in the receiving system, as a result of which in the non-presence of the secondary field the measuring system reacts only to external and internal interferences, unconnected with the primary field. Hence, the geometric and electric compensations here are implemented simultaneously (e.g. both versions of VMP). In other versions (helicopter, when the source and receiver of the field are on one vertical line, "Canadian", plane version with outboard gondola at $\theta \approx 65^\circ$, etc.), the signal of the primary field, perceived by the receiving frame, is an interference and, moreover, quite considerable as compared to the intensity of the useable signal. To increase the susceptibility of the method, it would be necessary, besides geometrical compensation, i.e., spreading and corresponding orientation of the frames, to implement additional electric compensation of the primary field signal, so that the useable signal would be higher than that of the primary field or at least would be absolutely distinct in the background of the latter.

The quantitative measure of compensation will take its depth n , determinable from formula

$$n = \left(1 - \frac{U_c^* - U_k^*}{U_c^*} \right) \cdot 100, \% \quad (XI.3)$$

where U_c - the composite value of the normal field resultant signal (taking into account the effect of uniform ground surface with finite conductivity);
 U_k - the composite intensity of the compensation voltage.

The lower is the residual voltage ($\dot{U}_c - \dot{U}_k$), the greater will be the degree of compensation n , i.e. the more this voltage approaches the actual intensity of the sought-for anomalous signal. With the residual voltage close to zero, the anomalous effect is shown in its entirety. However, the main difficulty in implementing a sufficiently high degree of electric compensation is the random variations of geometry in the system source-field receiver, which may considerably increase the error in measuring.

In view of the special importance of this question for estimating the efficiency of the apparatus in aerial electric prospecting, the main methods for electric compensation of the primary field signal, their potentialities and recommendations for the selection of measurable parameters are given ahead. The methods of electric compensation and the systems applied are analysed on the basis of the induction method with one place and spread out oscillating and receiving frames. However, in certain conditions the analysis data may be applied to some other versions of the induction method.

The signal, induced in the receiving frame and which we shall denote as \dot{U}_p , generally represents the vector sum of the primary field signal (the so called direct signal) \dot{U}_1 and of the secondary field \dot{U}_2 , determined by eddy

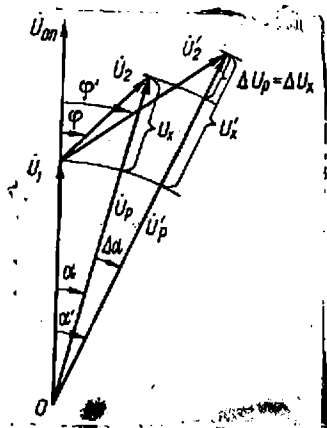


Fig. 171

currents in conducting bodies of upper layers of the earth crust (Fig. 171).

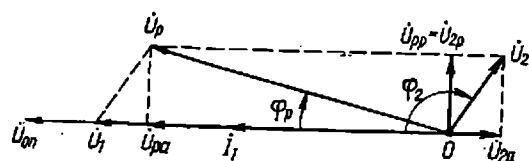


Fig. 172.

We know that for the apparatus of the induction method with spread-out oscillating and receiving frames $\{\dot{U}_2\} \ll \{\dot{U}_1\}$, and the phase angle φ of signal \dot{U}_2 in relation to signal \dot{U}_1 may vary the nature of the conducting body (parameter $pa^2(98)$) in a very wide range- from units to some tens of degrees. With high conductivity of the anomalous body, with predominance of the active component, this angle is negligible, but with comparatively high resistance and composite structure of this body, when the predominant is the reactive component, angle $\varphi \rightarrow \frac{\pi}{2}$.

If the measurements are conducted without electric compensation, then with variation of the secondary field signal from \dot{U}_2 to \ddot{U}_2 increment of the resulting signal $\Delta U_p = U'_p - U_p$ in the measuring unit is several percent of the virtual value of the total signal, and the increment of the phase angles $\Delta \alpha = \alpha' - \alpha$ -units of degrees. Therefore, in this case, in the background of considerable interferences of various origins it is practically impossible to measure these increments.

In ALRI-2, VMP and other apparatuses of the aerial induction method, there is a possibility of recording the virtual value (modulus) of the resultant field signal U_p and of the phase angle φ_p of this signal vs., a certain voltage, taken as comparative U_{comp} as well as of quadrature components U_{pa} , U_{pp} , which are the projections of the resultant signal vector in the direction of vector U_{comp} in perpendicular direction respectively (Fig. 172).

The active component of the useable signal \dot{U}_{2a} is the projection of the useable signal \dot{U}_2 onto the vector direction of comparative voltage \dot{U}_{comp} coinciding with the vector direction of current \dot{I}_1 . The reactive component \dot{U}_{2p} is the projection of the useable signal \dot{U}_2 onto the direction perpendicular to the vector of current \dot{I}_1 . However, as can be seen from Fig. 172, the active component \dot{U}_{pa} of the resultant signal is quite different from the active component \dot{U}_{2a} of the useable signal; therefore, it would be inexpedient to measure it without the preliminary electric compensation of the primary field signal.

Electric compensation in the ideal case, i.e., in the absence of different voltage caused by the primary signal, makes it possible to measure the voltage amplitude of the secondary field signal \dot{U}_2 and its phase angle φ_2 vs. current in the oscillating frame \dot{I}_1 or the comparative voltage \dot{U}_{comp} coinciding with this current in the phase. In this case, there is a full possibility of measuring both the components (\dot{U}_{2a} and \dot{U}_{2p}) of the useable signal. Obviously, the compensating signal should be coherent with the current frequency in the oscillating frame.

In the build-up of the apparatus it makes no difference as to which of the parameters, characterizing the useable signal, will be measured—the amplitude and phase or its active (reactive) component. However, to reduce the error, caused by the random variation of the initial geometry of the system and resulting in disrupting compensation of the direct signal, the selection of measurable parameter is not so indifferent. As we will see further on, the phase ratio between the compensation of measurable and comparative signals depends on the mode of compensation and the selection of the measurable quantity. On the mode of compensation, also depends the error in the measuring of parameters with variation in the geometry of the system.

Depending on the structure of the system of electric compensation, the number of field receivers and the circuit of connections and the interaction of the measurable and compensating signals in these systems, the mode of electric compensation may be divided into two groups: the simple and composite.

The distinctive feature of the simple means of electric compensation is the presence of only one field receiver and, therefore, of one receivable signal. The block diagrams of compensation here are simple and there is no considerable transformation of the measurable or compensating signal in them. There are two versions of these methods of compensation and two diagrams for their practical implementation (20). For systems of the first version, the initial phase of the compensating voltage, combining with the initial phase of the direct signal, remains invariable during the measurements; for systems of the second version, the compensating voltage always coincides in the phase with the resultant signal. On the basis of the first and second systems, it is possible to build a third, which makes it possible to measure the components approximately, without applying the phase-sensitive voltmeters.

The problem of the composite methods of compensation is to assure measuring with the acceptable error of one or several parameters, characterising the useable signal, with admissible variations of the geometry of the system. The composite methods of compensation are invariably connected with certain transformation of the signal, and the output voltage of the compensation circuit is determined by the interaction of measurable and compensating voltages. Generally, the output voltage of the compensating circuit may noticeably differ in the amplitude and the phase from the interacting voltages, but it reflects, more or less, the variation nature of the secondary signal. For relative measurements, which are conducted in the aerial induction method, this circumstance has no substantial significance. However, when necessary, knowing

parameters of the compensating circuit, it is possible to obtain by the date of calculations the characterising signal of the secondary field.

Several modifications of systems for the composite methods of electric compensation for the apparatus of the induction method with spread out source and receiver of the field have been devised and patented in the USA (18). These systems are meant mainly for reducing the magnitude of methodical interference and the error in measurements, determined by it, with some variations in distance between the source and receiver of the field or with minor angular transpositions of the field receiver vs. the source. The systems are based on the use of additional receivers and, sometimes, also of auxiliary field source.

FTI AN Ukr. SSR developed four systems of the composite methods of electric compensation, fundamentally different from those developed in the USA: total compensation system of resultant field signal, system with auxiliary receiver of horizontal component of the field, and two versions of systems with the use of automatic gain control (AGC).

3. System with invariable initial phase of the compensating voltage, matched with initial phase of the primary signal.

The block diagram, assuring the indicated compensation, is shown in Fig. 173. The resultant field signal \dot{U}'_{po} (in flight at operating speed and comparatively high altitude), induced in the receiving frame 1, tuned in resonance, after amplification by the gondola amplifier 2, arrives in the

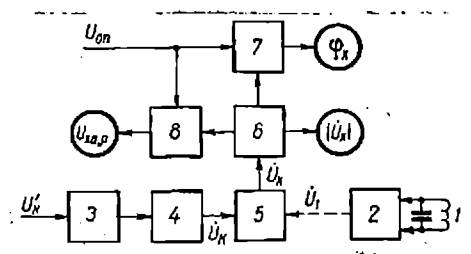


Fig. 173.

form of voltage $\dot{U}_1 = \dot{U}_{pc} = k U_{pc}^*$ (where k - the transformation factor of the preamplifier) at one of the inputs of the subtraction system 5. Fed to the second input of this system is the compensating signal \dot{U}_k , obtained by the conversion of signal U_k^1 in the phase-inverter 3, where this signal is matched in the phase with comparative signal U_{comp} and in attenuator 4, by means of which the desired modulus ratio of signals U_k and $U_1 = U_{pc}$, i.e., the depth of compensation, is set.

The selective measuring amplifier 6, the phasemeter 7 and the phase-detecting voltmeter 8 make it possible to measure at the output of the subtraction system modulus U_x of residual voltage \dot{U}_x , phase shift φ_x vs. comparative signal U_{comp} , and also the active (cosine) or reactive (sine) components of signal \dot{U}_x . The phase of comparative voltage could be previously matched with the current phase in oscillating frame \dot{I}_1 (in absolute measurements) or with the phase of resulting signal U_{po} , which during flight at high altitude corresponds to the phase of the primary field signal (in relative measurements, which are the most usual).

The relationship between quantities U_p , U_1 , U_2 and U_k in this system of compensation is shown by the vector diagram, plotted for the case of incomplete compensation (Fig. 174, a), when $\{U_k\} < \{U_1\}$, and the voltage U_{comp} coincides in the phase with \dot{U}_1 . In the case of total compensation, when $\dot{U}_k = \dot{U}_1$, all quantities, measurable by instruments, determine directly the useable signal \dot{U}_2 . The less is the depth of the compensation, the more will be the difference between the reading of instruments and the actual parameter values of the useable signal. The exception is only the reactive component \dot{U}_{xp} , which with any depth of the compensation remains equal to the reactive component \dot{U}_{2p} of the useful signal.

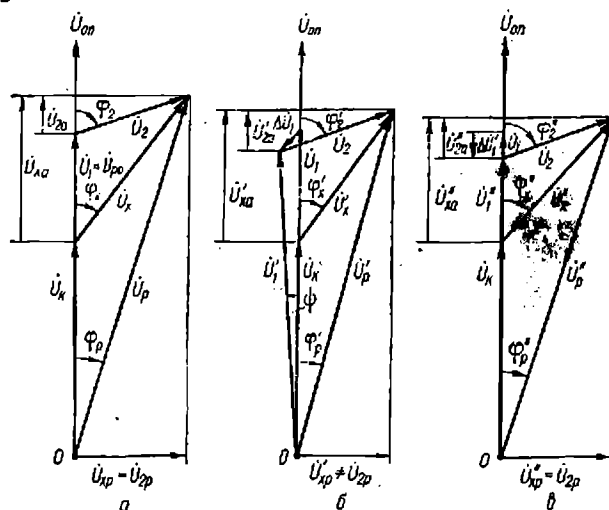


Fig. 174

Increasing depth of electric compensation provides a more accurate reproduction of the useful signal and measurement of its parameters. However, in the actual conditions of geophysical survey some changes are evident in the disposition of the receiving element in relation to the oscillating frame due to the disruption of the initial geometry of the system (for example, bumping of the gondola). If polarization of the primary field is non-linear, which is caused by the effect of currents, induced in the metal body of the aircraft, the primary signal changes not only in intensity ΔU_1 , but also in the phase (ψ). Some variation of this signal in relation to comparative voltage (Fig. 174 b) with invariable useful signal \dot{U}_2 results in the appearance of the residual signal U'_x different in intensity and the phase (φ'_x) from signal U_x .

Thus, it may be assumed that the variation of the primary signal \dot{U}_1 to a certain extent of ΔU_1 , in this case, is approximate to the appearance of the additional secondary signal of the same intensity, and the measuring portion of the apparatus will be measuring the new signal $\dot{U}'_x = \dot{U}_x + \Delta \dot{U}_1$. In this case, the active \dot{U}'_{xa} and the reactive \dot{U}'_{xp} components of the residual

*Hence under the signal of resulting field U_p will be assumed signal, input directly into subtraction system from the side of field receiver, i.e. signal at the output of preamplifier.

signal may considerably differ from the preceding values of components $U_{x\alpha}$ and $U_{xp} = U_2 \rho$. Only in the case of the linearly polarized primary field, when this signal varies only in the modulus retaining its phase as invariable (Fig.174-c), its increment $\Delta U_1'$ does not affect the reactive component magnitude of the residual signal ($U_{xp}'' - U_2 \rho$).

In view of the fact that the secondary signal is approximately in quadrature with the primary signal, comparatively insignificant increment of the primary signal without change in its phase will have a negligible effect on the results of measuring U_x .

If it is assumed that there is a possibility of achieving total compensation, then, as can be seen from the vector diagram in Fig.175-a, even in the case of the linearly polarized primary field with negligible variation of the geometry of the system, instead of the secondary field signal U_2 and its phase angle φ_2 in relation to comparative voltage, the measuring apparatus will be recording the modulus of a new vector, equal to the vector sum of signals $U_2 + \Delta U_1 = U_x'$ and phase angle φ_x ($\varphi_x = \varphi_2$) between the new vector and the comparative voltage U . In this case, the reactive component U_2' remains invariable, the active $U_2' = U'$ varies substantially.

Therefore, with linear polarization of the primary field and possible minor disruption of the geometry of the system it would be expedient to measure the reactive component with total (ideal) compensation, as well as with partial compensation of the primary signal. Appearance of the reactive component will indicate the presence of an anomalous object in the flight expedient to measure the active component of the resultant or the secondary field signal.

Thus, it is possible to assert that a high degree of compensation can be taken as ideal with negligible variation of the geometry of the system in the apparatus of aerial induction method, when the receiving frame is rigidly fixed on one mobile object at a comparatively long distance from the oscillating frame. For other versions of the induction method, it is necessary to depend on partial compensation only.

4. System with a follow-up phase.

In the system with a follow-up phase, the amplitude of the compensating voltage is determined by the set degree of compensation and, during the measurements, remains invariable; the phase of the comparative signal continuously combines with the phase of the resultant field signal \dot{U}_p . The given compensation is explained by the vector diagram in Fig. 177, which takes into account variation in the phase and the amplitude of the resultant signal \dot{U}_p , which assumes various values (U_p^1 and U_p^2). The block diagram of the compensator, implementing the said compensation, is shown in Fig. 178.

Received by the field detector 1 the signal of the operating frequency, after an appropriate amplification in the (gondola) preamplifier 2 in the form of voltage \dot{U}_p is delivered at the compensation block 7, where at the input a of the compensator's subtracting system it is fed directly, and at the input b through the amplification circuit with automatic control of the constant output level, consisting of the amplifier-limiter 3, the phase-inverter 4, the phase corrector 5 and the attenuator 6.

The received signal is preamplified in the amplifier-limiter by about a factor of 10, and then limited from the top and bottom to a level exceeding not more than one and a half or two times the level of the signal at the input of the amplifier-limiter, and is maintained constant

with the variation of the input signal within 1:20. The phase-inverter and the phase corrector provide the exact setting for the phase-shift of the compensating signal in relation to the measurable, fed to input^a of the subtracting circuit. The attenuator presets the amplitude required to obtain the preset degree of compensation of the compensating voltage.

The differential voltage between the sinusoidal voltage of the input a and the first harmonic of rectangular voltage of the operating frequency of input b of the subtracting circuit is fed to the measuring amplifier, which carries out selective amplification only of the operating frequency signal, and suppresses all the side-band frequencies of the rectangular signal spectrum.

R

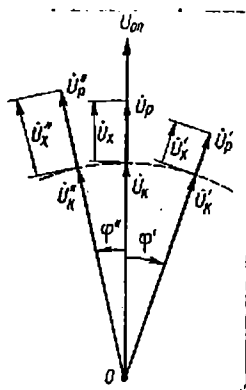
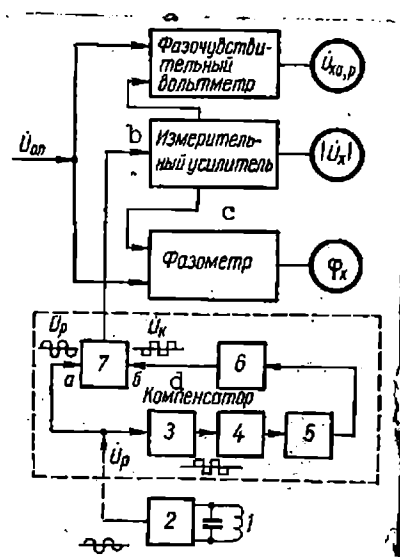


Fig. 177

The relation between quantities \hat{U}_p , \hat{U}_1 , \hat{U}_2 and \hat{U}_k for this method of compensation is shown by the vector diagram in Fig. 179, Fig. 179-a and 179-c show the relationship of measured parameters with the variation of the primary field signal \hat{U}_1 only in its own magnitude, i.e., in the case of the primary field's linear polarization and some changes in the geometry of the system. Fig. 179-b shows the same relations in the case of non-linear polarization, when due to change in the geometry of the system there is

variation of the amplitude and the phase ^{ψ} of the primary field. In accordance with Fig. 179, in this method of compensation, even with its total degree, not one of the quantities measurable by the instruments $(|\dot{U}_x|, \dot{U}_{xa}, \dot{U}_{xp}, \varphi_x)$, corresponds exactly to the parameters of the useable signal. Only with low angle $\varphi_p = \varphi_x$ and total compensation $|\dot{U}| \approx U_{xa} \approx U_{2a}$.

Therefore, the given system of compensation may assure the required accuracy of measuring some of the parameters of useful signal only with low phase shifts between the primary and the resultant signals. Since it may be assumed that the secondary signal is approximately in quadrature with the primary, with total compensation the increment of the primary signal without changing its phase will be reproduced in its entirety by variation of (\dot{U}_x) , without however affecting the magnitude of the secondary signal reactive component $(\dot{U}_{2p} = \dot{U}'_{2p})$. Therewith, the measurable values \dot{U}_{xp} and \dot{U}'_{xp} change very little, i.e., it may be assumed that $\dot{U}_{xp} \approx \dot{U}'_{xp}$. In view of the shortcomings pointed out the system of compensation with a follow-up phase has not found application.



Key to Figure 178:

- a, Phase-sensitive voltmeter;
- b, Measurement amplifier;
- c, Phase meter;
- d, Compensator.

Fig. 178

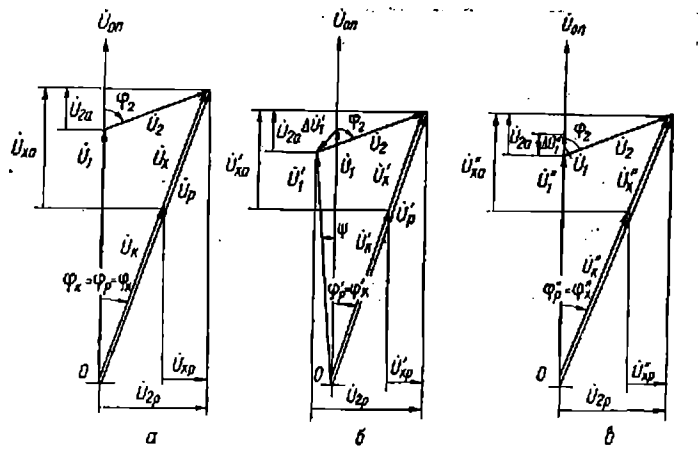


Fig. 179

5. System for the approximate measuring of components without the application of phase-sensing voltmeter (FHV).

The analysis of two main simple methods of compensation has shown that the first of these assures a more precise reproduction of the useful signal, while the second may provide the required accuracy in measuring increment $\Delta \dot{U}_{2a} \approx \Delta \dot{U}_x$ only with insignificant phase shift between the primary and the resultant signals. In these methods of compensation, phase-sensing voltmeters should be applied for measuring the active and reactive components.

By combining the first and second methods, it is possible to measure approximately the active and reactive components of the secondary signal without the application of phase-sensing systems. For this, at the input a of the subtracting circuit (see Fig. 178) instead of \dot{U}_p , it is sufficient to feed $\dot{U}_K = U_1$ provided angle φ_p is so low that $\sin \varphi_p \approx \varphi_p$. In this case, the compensation voltage is taken off from a separate source of the compensating signal according to the diagram shown in Fig. 173.

Thus, in the given method of compensation the intensity of the compensating voltage in the initial position is set equal to the intensity of the primary field signal and hence maintained invariable, i.e., $\dot{U}_K = \dot{U}_1 \text{ const}$,

6. Block diagram of the apparatus for simple electric compensation.

A simplified block diagram of the apparatus for aerial electric prospecting by the induction method, which permits implementing all the three methods of electric compensation, is shown in Fig. 181. Here 1-7 are the nodes (see Fig. 178); 8- the smooth phase-inverter (from 0 to 360°); 9- the attenuator of the compensating signal; 10- the phase corrector of the comparative signal; 11- the fixed phase-inverter at 180° .

In position 2 for the switch P_2 and position 1 for switch P_3 implementation is of the first method of electric compensation; in positions 1 for P_2 and 2 for P_3 - of the second method and in positions 2 for P_2 and P_3 of the third method.

In the third method of compensation, the given system measures only the reactive component. For measuring the active component, it is necessary to lead in a second subtracting circuit, connected with points 1 of the switch P_2 and 2 of switch P_3 and of the additional selective amplifier. In this case, there will be simultaneous measuring and recording of the active and reactive components without the application of phase-sensing voltmeters.

In the first and third methods of compensation, the source of the compensating voltage could be the master oscillator or voltage drop on the active resistance r , connected at the output of the power amplifier in series with the oscillating frame (GR). The commutation is performed by switch P_1 . The same voltage is the comparative one for phase-sensing units of the measuring apparatus.

Take off of compensation voltage U_K and comparative voltage U_{Comp} from resistance r eliminates decompensation with the variation of the current

Page intentionally left blank

Page intentionally left blank

It should be mentioned that in the measuring apparatus itself there could be different phase shifts for the applied operating frequencies. If in measuring the phase and the components the phase is not corrected previously at each operating frequency, there may be a considerable additional error. Preliminary correction of phase shifts in the measuring channel on operating frequency may be carried out by means of the phase corrector 10 and switch P_1 in position 3, switches P_2 and P_3 in position 1 (see Fig. 181). The phase of one of the signals automatically turns by means of the phase-inverter 11 at 180° and the subtracting circuit of signal U_p converts into summing. This correction permits exclusion of the phase error of relative measurements, possible with the transition from one operating frequency to another, provided the preamplifier and wire-cable do not cause an appreciable phase shift throughout the whole spectrum of operating frequencies, i.e., they are aperiodic elements of the receiving-measuring system.

7. Compensation systems in AERIS and AERI-2 apparatus.

The compensating systems in AERIS and AERI-2 apparatus differ considerably in the method of electric compensation, parameters and diagrams.

AERIS apparatus. In this apparatus the electric compensation is carried out only by the simple method, with the application of the system in which the initial phase of the compensating voltage, matching the initial phase of the primary signal, remains invariable during the measuring. Since protection against interference of the receiving channel here is not very high, the interference pulses in the compensator are suppressed by the special system of limiting interference pulses (see para 11, chapt. XIII).

Fig. 182 shows the line diagram of the compensator in the AERIS apparatus.

The received signal is delivered through the contact 5 of plug socket SBR-70 to the separating cathode repeater L_{12} , protecting the channels of the

measuring group from possible reciprocal parasitic coupling. Voltage from its output, commutated by tumbler Bk_1 , may be fed to the input of the subtracting circuit L_{11} directly or through the limiter of interference pulses (OIP).

The compensating voltage through the contact 5 of the plug socket SHR-71 and the cathode repeater L_1 arrives at the potentiometric phase-inverter (see para 9, chapt. X), providing for phase adjustment of the compensating voltage by jumps over 90° from 0 to 360° , smoothly within one quadrant (by potentiometer R_{45} , connected with the arm of bridge, made up of resistances $R_{42}-R_{45}$) and very smoothly within a few degrees (by potentiometer R_{46} of the same arm). The adjustment of the phase by jump is carried out by switch P_3 , which commutates voltages, taken off the anodes and cathodes of tube L_2 .

The amplitude of the compensating voltage is controlled by ohmic divisor $R_{20}-R_{39}$, connected through the cathode repeater L_3 subsequently to the phase-inverter, with division in steps of 10 db. Smooth adjustment is implemented by potentiometer R_{40} , and very smooth - by potentiometer R_{41} . Hence the compensation voltage arrives at the second input of the subtracting circuit.

From the output of the subtracting circuit, the residual voltage is fed through the matching cathode repeater L_{10} and the contact 1 of the plug socket SHR-71 to the parameter meters of the decompensation signal. The adjustable resistance R_{117} in repeater cathode, required with the replacement of bulbs, serves to rectify the transmission factors of the compensators in channels I and II. Placed in the same block is the second phase-inverter (L_{14}, L_{15}, L_{16}), with a system similar to that described, cut in to the comparative signal circuit and meant for the compensation of phase shifts in the measuring track of the given channel. Switch P_5 in the voltage circuit

of the main phase permits commutating the measuring channels into divided (according to frequencies) operation and operation parallel on one frequency. The filament voltage of the tube in the subtracting stage is stabilized by barretter L_{13} .

The compensator was investigated in the laboratory and in flying conditions. In laboratory conditions, the investigations were of the quality of work and parameters of the limiter of interference pulses (its main elements - the input divider, the amplifier-limiter, the differentiating and integrating chains, etc.), the phase-inverter and the attenuator in the compensating signal circuit. The extent and stability of compensation were also determined under the effect of external noise.

Investigations of the limiter of interference pulses have established that with pulse frequency investigations similar to the frequency of the working signal, specially with coincidence of these frequencies, the operation stability of the node was disrupted, which indicated normal activity of the limiter of interference pulse. In these conditions, the latter does not affect the spectral components of interferences, frequencies of which are similar to operating frequency.

It should be kept in view that compensation does not require very high precision of the phase-inverter's graduation, as the phase-inverter is used, not for measuring but for turning the compensating voltage; phase the exact value of which is not required. The main problem in the investigations of this unit was checking the stability of the phase-inverter's operation and determination of the minimum phase shift, which could be set for the compensating signal by smooth phase adjustment. The investigation has shown

that the minimum adjustable angle is $0.3-0.5^{\circ}$ and the operation stability of the phase-inverter is quite satisfactory. The graduation of the divider in the compensating signal circuit was also implemented approximately. However, in this case, the possibility of providing even variation of the signal to a few microvolts, at any level within the preset range of compensation voltage adjustment was confirmed. Compensation had to provide for the subtraction factor of 10^{-3} .

During the flight in optimum conditions of survey (speed, elevation, weather) the primary signal was compensated upto different levels.

At each level the recording was made of instrument-reading during calm horizontal flight. Investigations have shown that the compensation is sufficiently stable if the minimum differential voltage exceeds the noise level not less than three-four times having on an average 50 mv.

To control the operation stability of the apparatus and to select the measuring technique all recordings were made twice. Fig. 183 shows an example of recording along profile No. 1 in the area of Maidan-Villa st. on frequency 488 cps with compensation. The mean arithmetic divergence between the primary and secondary readings of the vertical component were for the modulus - $\pm 4.6\%$, for the reactive component - $\pm 2\%$.

Higher divergence in second reading of the modulus, as compared to the reactive component, is explained by greater sensitivity of this parameter to changes in reciprocal orientation of the oscillating and receiving frames.

AERI-2 apparatus. This apparatus permits carrying out simple methods of electric compensation according to the system used in AERIS station and by a system in which the compensating voltage invariably coincided in phase with the resultant field signal. In AERI-2 apparatus sufficiently high preliminary selectivity has been achieved, due to which there was no need to use the limiter of interference pulse and it has been excluded from the

compensator. There are some differences also in the subtracting circuits.

The diagram of the compensator is shown in Fig. 184. The measured signal through the contact 1 of plug socket SHR3(4)-14 is fed initially into the input divider 10:1 (switch P_4 and resistances R_1 and R_2) for attenuating major signals, and hence to the selective amplifier of the compensator (L_6, L_7) with double symmetrical T-shaped RC-bridge, connected into reverse feedback circuit of tube L_7 . The elements of bridge for its tuning to the required operating frequency get connected by means of relay P_6 - P_{10} . The equivalent Q-factor of selective amplifier $Q_e \gg 5$.

Increased selectivity of the amplifier with remote detuning (for instance, on frequency of the adjacent channel) is obtained in the following way. Voltage from the anode load R_{70} of the tube L_{6a} through resistance R_{73} is delivered to potentiometer R_{74} , which is connected with the anode of tube L_7 . Due to the fact that voltages of the received signal on the anodes of tubes L_{6a} and L_7 are in phase opposition, it is possible to select on potentiometer R_{74} a point at which the resultant voltage is zero. Since, on the operating frequency, the intensity of the signal on the anode of tube L_{6a} (i.e. on resistance R_{74}) due to amplifying properties of the stage is considerably higher than the intensity of the signal arriving from the anode of tube L_{6a} to potentiometer R_{74} , the effect of the latter on the former may be ignored. Therefore, on the cursor of the potentiometer, the voltage of the operating frequency signal is practically equal to the voltage, amplified by the selective amplifier of the compensator. Signals of other frequencies (noise signals) are not amplified by the amplifier and their amplitudes are approximately equal. Moreover, these signals are in phase opposition, therefore, they are reciprocally subtracted. Thus the resultant voltage from

the interference signals on the cursor of potentiometer R_{74} is sufficiently low.

From cursor of potentiometer R_{74} the amplified signal of the operating frequency is transmitted through cathode repeater L_{6b} to switch P_{1c} of the input commutator, and hence - to active divider $R_{43} - R_{45}$, the ratio of division in which is equal to $\frac{1}{K_{v.s.}}$, where $K_{v.s.}$ - the amplification factor of the subtracting circuit. Division of the working signal is required, so that the transmission factor of the subtracting stage, through which the measuring amplifier with a certain amplification factor measures the normal field signal without compensation, and also the comparative, compensating, etc., would be one. Potentiometer R_{44} of the divider makes it possible to correct the division ratio by replacement of tube L_3 . The required bias intensity of this tube is set by potentiometer R_{49} .

From the anode load R_{48} of the right half of tube L_6 the residual voltage during compensation or total voltage of the working signal in auxiliary measurements is fed to the output cathode repeater L_4 and hence through the contact 7 of plug-jack SHR3(4)-13 - to the selective amplifier of the measuring voltmeter.

The compensating signal from the generating group (contact 5 of plug-jack SHR3(4)-14) arrives through switch P_{1a} of the input commutator to potentiometric phase-inverter L_1 , similar to the one in AERIS compensator. The operating frequencies of the phase-inverter are changed over by relay $P_1 - P_5$. To turn the phase of the compensating signal at 180° , the application is of phase-inverter, made up on the circuit with separated load on tube L_{2a} . Switching of the phase is effected by switch P_{1b} of the input commutator. After this, the compensating signal is fed through the cathode repeater L_{2b} to the attenuator. Switch P_5 carries out rough

adjustment (by steps of 10db) of the compensating signal, potentiometer R_{41} -. The compensating signal from the cursor of the potentiometer gets into the second input of the subtracting circuit.

The described part of the compensator provides compensation by a circuit in which the initial phase of the compensating signal matches the initial phase of the primary signal and remains invariable during the measurements.

In compensation on a circuit with a follow-up phase, the received signal after selective amplifier of the compensator arrives through the contacts of switch P_{10} (7th position) to the left half of the subtracting circuit tube L_3 , and through the amplifying circuit with automatic control of invariable output level, phase-inverter and attenuator to the right half. In this case the amplifier of the operating frequency signal is the stage with amplification factor $K \approx 10$, operating on the left half of tube L_{8a} .

The automatic adjustment circuit of the invariable output level is a two-sided limiter, by means of which the working signal is limited at the top and bottom to a level exceeding not more than twice its level at the input. The limiter is built on tubes L_9 and L_{10} on a circuit with cathode coupling providing for symmetric limiting with high input resistance. Tube grids of amplifier-limiters with common resistance in the cathode circuit are energized by direct positive bias voltage from divider R_{93} - R_{96} . The intensity of the bias on the left half of tube L_9 and the right half of tube L_{10} is fixed, and on the right half of tube L_9 and on the left half of tube L_{10} is adjustable (by means of potentiometers R_{92} and R_{97}). This controls the limiting threshold.

From the output of limiter R_{102} , the working signal voltage of

rectangular shape is initially supplied to the cathode repeater L_{8b} , hence through switch P_{1a} of the input commutator (6th and 7th positions) - phase-shifter, phase-inverter, switch P_{1b} of the input commutator, cathode repeater L_{2b} , attenuator of the compensating voltage - to the right half of the subtracting circuit tube. The phase-shifter and attenuator fix the initial phase and intensity of the compensating signal for obtaining the preset degree of compensation, after which any phase variation of the input signal will automatically change the phase of the compensating signal, which provides for autotracing by phase. At the same ^{time} the intensity variation of the measured signal will not affect the intensity of the compensating signal.

Through the cathode repeaters on tube L_5 the measured and compensating signals are fed into the block of oscillographic control for the visual observation of compensation. To increase working stability of the compensator, the anode supply is stabilized and the filament circuits of all the tubes are energized by direct current.

The following values are measurable by the input commutator:

	<u>Switch position</u>
Residual voltage after compensation by U_K voltage	1
U_K voltage after the adjustment of its modulus and phase	2
Input signal voltage U_c	3
U_{comp} voltage after adjustment of its modulus and phase	4
Residual voltage after compensation by U_{comp} voltage	5
U_K voltage after adjustment of its modulus and phase in circuit of follow-up phase	6
Residual voltage in circuit with follow-up phase	7
U_K voltage incoming from generating system	8
U_{comp} voltage incoming from generating system	9

The investigations in laboratory conditions were of the same common nodes as found in the compensator AERIS, as well as the amplifier-limiter of the compensation circuit with a follow-up phase and the selective amplifier of the compensation circuit. The common nodes of the compensating systems in AERIS and AERI-2 apparatus (phase-shifters, attenuators, etc.) are practically identical. The investigations of the amplifier-limiter have shown that the minimum level of the signal for its normal work is 30 mv, (millivolt) which corresponds to the intensity of the signal voltage of 30 microvolt at the input of the gondola amplifier.

Amplitude characteristics of the amplifier-limiter:

U_{in}, mv	8	10	20	30	60	120	240	480	960	2000
U_{out}, mv	930	950	970	980	990	990	995	995	995	960

From the above data it follows that with signal variation at the input of the amplifier-limiter from 20 mv to 0.9 v its output voltage (the first harmonic) is maintained constant with accuracy $\pm 2.5\%$. The useful signal at the input is practically never below 20 mcv (level below 10-15 mcv corresponds to noise level). The ultimate value of the stable subtraction factor for the first compensation circuit on all operating frequencies in laboratory conditions (with careful shielding of the compensator elements) was $0.5 \cdot 10^{-3}$; the level of compensator's set noise did not exceed 10 mcv when measured by the usual vacuum-tube voltmeter LV-9 or MLV-2M and 0.5 mcv - in individual measuring at each operating frequency by selective measuring amplifier of apparatus.

The linearity of the compensator's output voltage with variation of the input signal from zero to maximum value (0.8-0.9v) was checked in the following way. The input signal of certain intensity, e.g. 450 mv, was fed into the compensator, and compensation was effected upto the maximum

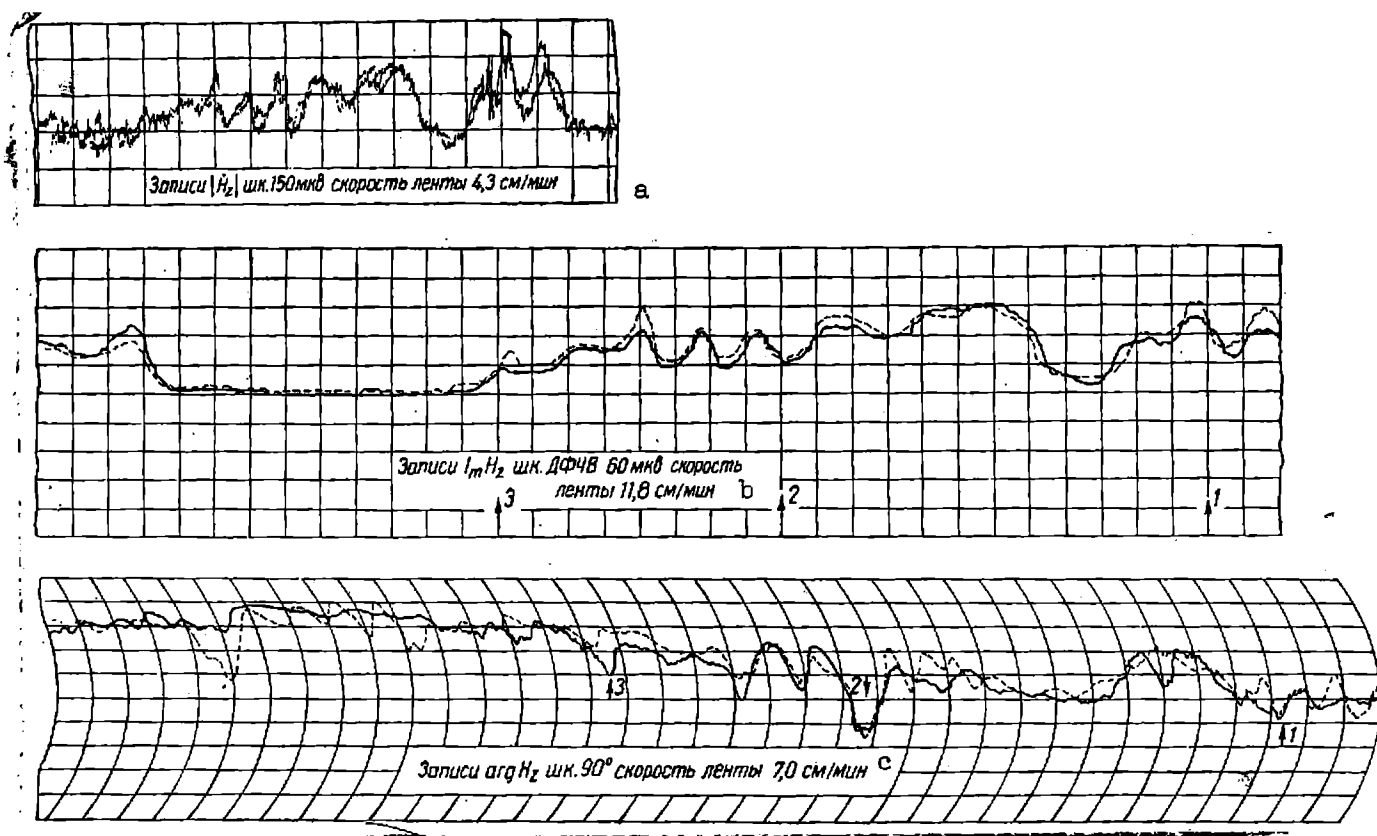


Fig. 183

a, Recording $|H_z|$ -- 150 mV at the rate of 4.3 cm/min tape speed; b, Recording $I_m H_z$, DFCHV, 60 mV, tape speed 11.8 cm/min; c, Recording of $\arg H_z$, 90° ; tape speed 7.0 cm/min.

possible degree. Then the input signal was reduced to zero or increased to the maximum and the output voltage of the compensator measured.

On the grounds of the obtained data, a curve was plotted $U_{out} = f(U_{in})$ at $U_k = \text{const}$ (Fig. 185), which shows, that at $U_{in} = 0$ the $U_{out} = 0$ (set noises of the compensation circuit are not taken into account). With negligible increment of U_{in} , U_{out} sharply increases until the amplifier-limiter begins to operate. Subsequent increment of U_{in} causes linear decreasing of U_{out} to a zero, which will take place at the moment $U_{in} = U_k$. If $U_{in} > U_k$, U_{out} begins increasing linearly to about 900 mv, but the sign of U_{out} will change as happens with the phase turn at 180° . At $U_{in} > 800-900$ mv, due to change in the working conditions of the subtracting stage tube, increments of U_{out} will not be linear, and will be even more defined with higher increment of U_{in} , but until the voltage is 2.5-3 v this deviation is not over 4-5%.

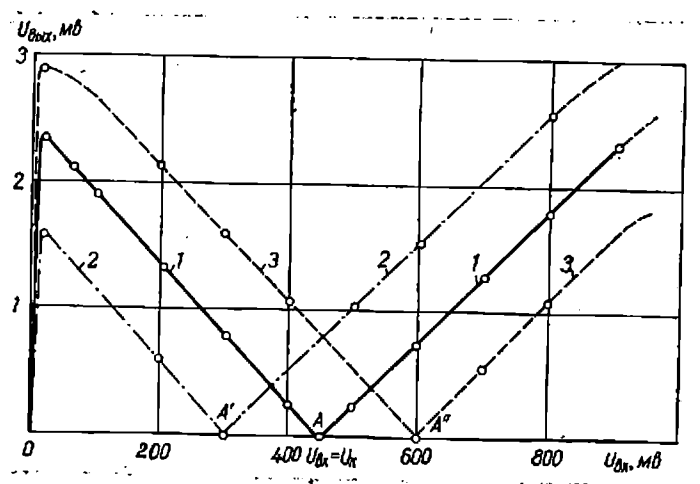


Fig. 185

Fig. 185 shows the experimental curves for three cases of penetrating compensation: $U_{in} = 450$ mv (point A), $U_{in} = 300$ mv (point A') and $U_{in} = 600$ mv (point A''). It is clear from the figure that curves 1-3 are sufficiently linear in the working interval of U_{in} and parallel to each other.

The transmission factor of variation of the input divider 10:1 is

maintained with precision upto + 2%. Selectivity of the selective preamplifier has Q-factor in the limits 5-7 (for all operating frequencies), which attenuates selectivity by not less than 3% with detuning $\pm 10\%$ of the operating frequency. The temperature stability of the amplifier was checked in conditions of positive temperature 20-40°C. In this case, the detuning of bridges at all frequencies was not higher than 2%.

In flying conditions the operation of the compensator was checked at various depths of compensation on the first and second circuits (the flights were along one and the same area).

8. Total compensation system of the resultant field signal.

This method of compensation assures invariability of the fixed degree of compensation and considerable reduction in the measuring error with variation of the primary field signal due to some irregularity in the reciprocal position of the source and receiver of the field (85, 96). The compensation system contains two opposing subtracting circuit with output voltages equal in amplitude. In one of these circuits, the phase of the output voltage matches the phase of the resulting field signal.

The block diagram of the compensator is shown in Fig. 186. The signal of the primary field $\dot{U}_1 = \dot{U}_{p0}$ admitted by the receiving frame 1 and amplified by the gondola pre-amplifier 2, comes in simultaneously into two subtracting circuits 3 and 4 and to the input of phase shifter 5 of the compensation channel, which we shall define as the second compensation channel.

The first compensation channel, with subtracting circuit 3, subtracts from signal \dot{U}_{p0} the compensating signal \dot{U}_{k1} , which could be voltage \dot{U}'_k of the master oscillator or voltage taken off from resistance, connected in series into the circuit of the oscillating frame (see Fig. 181). By means of phase-shifter 7 and phase-meter 6, connected to points a and b, matching in the phase of signal \dot{U}_1 and compensation signal \dot{U}_{k1} is obtained. Adjusting the

amplitude of the compensating voltage \dot{U}_{k1} by attenuator 8, we obtain at the output of subtracting circuit 3 of the first compensating channel the selected or admissible intensity of decompensation voltage \dot{U}_{x1} , which for the subtracting circuit 14 is the compensation.

Similarly, in the second compensation channel by means of phase-shifter 5 and phase-meter 6 (points a' and b') the required matching in the phase is obtained of the amplified admitted signal \dot{U}_1 and the compensation signal \dot{U}_{k2} , the source of which is the amplifier-limiter of the admitted signal. The amplification and limiting in peak of the measurable signal \dot{U}_1 is implemented by block 10. The compensation signal, almost rectangular in shape, amplified and limited by this block on a preset level, is fed to selective stage 11, as a result of which the first harmonic of compensation signal \dot{U}_{k2} with stable amplitude is formed at its output. Amplitude control of this signal is carried out by attenuator 9.

Connected with the output of compensation circuit 4 is a block of voltage measuring (selective vacuum-tube voltmeter) 12, indications of which are in proportion to the virtual value of decompensation voltage $\dot{U}_x = \dot{U}_{po} - \dot{U}_{k2}$ at the output of subtracting circuit 4 with the appearance of the useful signal.

From the outputs of the first (3) and second (4) channels of the subtraction circuit, the residual voltages \dot{U}_{x1} and \dot{U}_{x2} are fed into subtracting

circuit 14. Connected with the output of this circuit is block 13 (selective vacuum-tube voltmeter), serving for measuring the voltage, which, as will be shown, is proportional to this signal amplitude of the secondary field. The compensation is meant to achieve moduli parity of voltages \dot{U}_{x1} and \dot{U}_{x2} , which is controlled by the vacuum-tube voltmeter 13 (during the measuring the attempt is to obtain its zero or minimum reading). The phase of decompensation voltage $\Delta \dot{U}_x = \dot{U}_{x1} - \dot{U}_{x2}$ in relation to the comparative signal phase is measured by phasemeter 6 at the output of subtraction circuit 14.

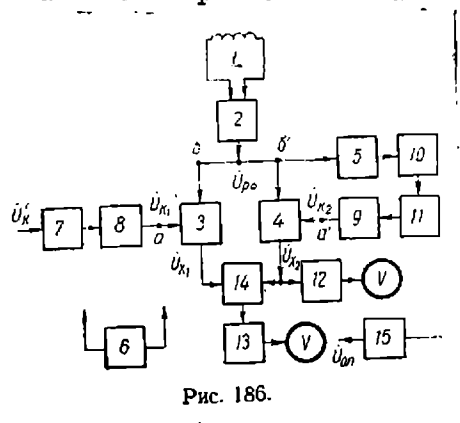


Fig. 186

A vector diagram, explaining the principle of the given method of compensation with variation of the primary field signal due to disruption of the geometry of the system, both in the absence and in the presence of the secondary field signal, is shown in Fig. 187.

Fig. 187-a shows the diagram of compensation to a certain degree, when only the primary field signal \dot{U}_1 is being received. At the output of compensation circuit 3 will be some residual voltage \dot{U}_{x10} , and at the output of compensation circuit 4 voltage \dot{U}_{x20} , which is measured by the vacuum-tube voltmeter 12. In this case, at the output of subtracting circuit 14, depending on the accuracy of obtaining parity in the intensity of compensating signals \dot{U}_{x10} and \dot{U}_{x20} and their stability a certain unbalance voltage $\Delta \dot{U}_{x0}$ measurable by vacuum-tube voltmeter 13 is obtained. The phase of the comparative voltage

\dot{U} is combined with the phase of unbalance voltage $\Delta \dot{U}_{x0}$ by means of
 Comp
 phase-shifter 15 and phasemeter 6.

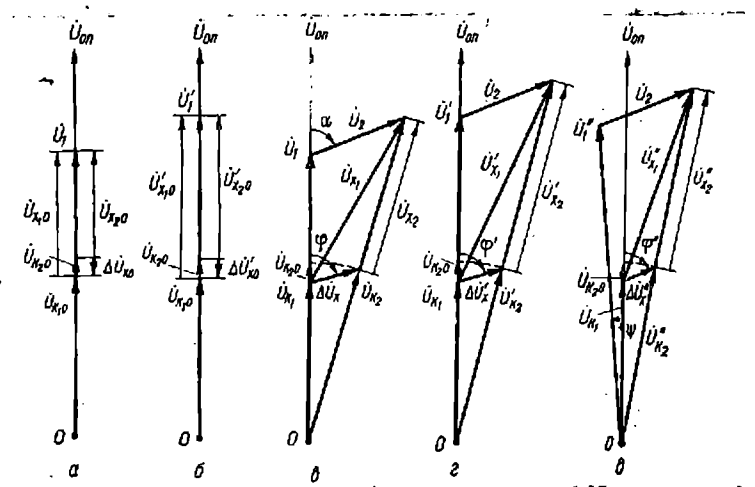


Fig. 187

If due to variation of the geometry of the system, the primary field signal increases (Fig. 187 b), signals \dot{U}_{x1} and \dot{U}_{x2} , which have increased simultaneously to the extent of primary signal increment, appear at the output of compensating circuits 3 & 4. However, the unbalance voltage in this case does not change its intensity, i.e., $\Delta \dot{U}_{x0} = \Delta \dot{U}_{x0}'$.

With the appearance of the secondary field signal U_2 (Fig. 187 c) the outputs of compensation circuits 3 and 4 will produce, respectively, residual signals \dot{U}_{x1} and \dot{U}_{x2} , differing in phase and intensity. At the output of compensation circuit 14 will appear unbalance voltage $\Delta \dot{U}_x$, the phase shift of which in relation to the comparative signal will differ considerably from the initial (zero) value. These variations are established by the vacuum-tube voltmeter 13 and phasemeter 6. The unbalance signal $\Delta \dot{U}_x$ does not correspond in intensity and phase to secondary field signal \dot{U}_2 , i.e. an absolutely new signal. However, with set values of \dot{U}_{k1} and \dot{U}_{k2} , it is unambiguously determined by signal \dot{U}_2 , wholly reflecting its variations.

If there is a useful signal \dot{U}_2 , and the primary field signal varies,

e.g., increases to \dot{U}_1' (Fig. 187-d) provided $\dot{U}_2 = \text{const}$, the residual signals \dot{U}_{x1} and \dot{U}_{x2} at the outputs of compensation circuits 3 and 4 respectively are subject to considerable changes. The unbalance signal $\Delta \dot{U}_x'$ at the output of compensating circuit 14, as shown by the diagram, does not change appreciably.

Thus, in the given method of compensation with linear polarization of the primary field variation of the geometry of the system has less effect on the measuring of intensity of unbalance signal $\Delta \dot{U}_x$, which characterises the useful signal \dot{U}_2 and its variations. With increasing degree of compensation $\Delta \dot{U}_x \approx \dot{U}_2$.

A vector diagram for non-linearly polarized field is shown in Fig. 187-e, from which it is evident that unbalance signal $\Delta \dot{U}_x''$ is quite distinct in intensity and phase from signals $\Delta \dot{U}_x$ and $\Delta \dot{U}_x'$. Therefore, this method of compensation is effective only in the case of linear polarization of the primary field.

The compensation of the resultant field signal \dot{U}_{p0} at the output of preamplifier 2 in this method (Fig. 186) is carried out in the following order.

1. By means of selective voltmeter 12 the amplitude of \dot{U}_{p0} is determined at point b. For this, the commutation of subtraction circuits 3 and 4 is such at which only signal \dot{U}_{p0} is transmitted through them.
2. By alternate variation of voltages at points a and a' by voltmeter 12, equal values of compensation voltages \dot{U}_{x1} and \dot{U}_{x2} are set with sufficient accuracy (commutation is only of the subtracting circuit 3).
3. By an alternate connection of phasemeter 6 at points a, b, a', b', zero phase shift is obtained by phase shifters 5 and 7 between voltages \dot{U}_{p0} and \dot{U}_{x1} .
4. By means of selective voltmeter 13, the intensity of unbalance signal is determined at the output of subtracting circuit 14 and brought down practically

to zero by the adjustment of even attenuator in block 9.

Bumping of the gondola is controlled by selective voltmeter 12.

9. Compensation system with the horizontal component of auxiliary receiver of the field.

This system for a composite compensation has been devised for AERI-2(122, 124) with the object of reducing the effect of changes in the geometry of the system on measuring results. With an appropriate selection of the system's parameters it may be used for compensating devices and some other versions of the aerial induction method.

In the apparatus of a single-plane version of the induction method, when the field receivers are located in the outboard gondola, the most frequent are the relative parameter measurements of the signal, induced in the vertical component of receivers of the resultant field. This is specified by the fact that in the case of the horizontally placed oscillating frame the anomalous effect is more clearly defined on the vertical component of the secondary field. For obtaining the maximum useful information the field detector is oriented in such a way as to react only to the vertical component of the resultant field.

In the analysis of the primary field in various versions of the aerial induction method, ratios were obtained for the determination of components H_v and H_h (III. 15a), and also function curves $F_1(\theta)$ (see Fig. 26) and $F_2(\theta)$ (see Fig. 27), characterising the directivity of field components in the oscillating frame, which may be taken as magnetic dipole, i.e. giving the pattern of the primary field in vertical plane with variation of the gondola's drift angle θ within the range $0-180^\circ$. According to Fig. 26 and 27, the magnitude of the vertical component close to direction OZ, typical for some versions of the aerial method with outboard gondola, exceeds practically more than twice the magnitude of the horizontal

component near the same direction. Therefore, the secondary field signal, dependent on the vertical component is not less than twice higher than the signal from the horizontal component. For AERI-2 apparatus of the induction method with the length of cable 150 m, the speed of flight 260 km/hr and calm weather, when the variations of the geometry of the system are negligible, $\theta = 64-65^\circ$. In this case, at the point of the field detector, as shown by calculations, the horizontal component of the primary field exceeds about two and a half times the vertical component (the signs of these components are conflicting).

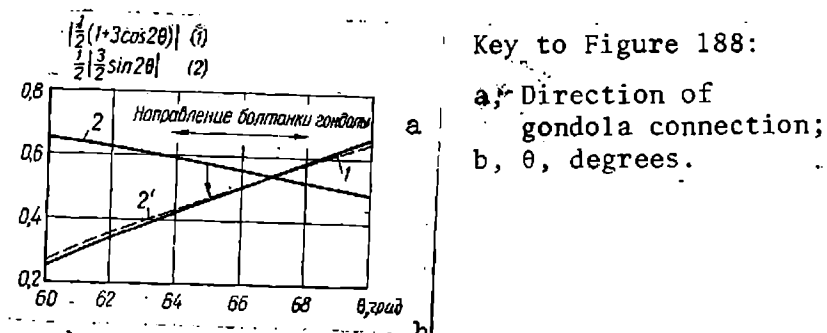


Fig. 188

The principle of this compensation method consists in the following. If both the components of the primary field are received simultaneously and the amplitudes of the corresponding signals are equalized after amplification and then these signals are added, the resultant signal will be zero with invariable geometry of the system. The appearance of the secondary field, the signal from which is better defined the vertical component, will disrupt the attained party. As a result, the signal of unbalance, which determines the effect of the secondary field, will appear at the output of the adding circuit.

To estimate the possibilities of this method of compensation with the variation of the geometry of the system, it is necessary to take into account

that the maximum allowed variations of the gondola's drift angle θ on survey route (from the point of view of safe piloting) do not exceed $\pm 5^\circ$. The drift of the gondola occurs mainly in the vertical plane, determinable by the direction of the flight. Moreover, assuming that the parameters m and $\frac{1}{r^2}$ are preset and constant, from formulas (III. 15a) we calculate angle θ functions, which determine components H_v and H_h within the variation range of this angle from 60° to 70° . The results of the calculations are shown in Fig. 188, where curve 1 shows relationship $\frac{1}{2}(1 + 3 \cos 2\theta)$, and curve 2 - relationship $\frac{1}{2} \left(\frac{3}{2} \sin 2\theta^* \right)$. In the assumed limits of angle θ variations flexure of curves 1 and 2 is insignificant, they are practically straight. With increasing angle, component H_v increases, and H_h decreases when the increment rate of component H_v is higher than the decrement rate of component H_h . Therefore, the variation of the geometry of the system affects mainly the magnitude of the vertical component.

Thus in the actual conditions of operation of the apparatus no stable compensation could be implemented by the above methods. However, if in the compensating system the subtracting signal is the voltage of signal U_h , generated in the auxiliary field detector by the horizontal component and before the addition to maintain automatically the level of this signal equal to the level of signal U_h , received by the main field detector, it is actually possible to obtain, even with considerable variation of the geometry of the system, compensation which is stable and insufficient degree.

If all these reasonings are applied directly to Fig. 188, there should be something like combining of curve 2 with curve 1 (to obtain curve 2'). When the bend of curves in the preset interval of variation of angle θ is negligible, they combine with an accuracy sufficient for practical purpose.

*For convenient comparison the relationship shown on the curve is $\frac{1}{2} \left| \frac{3}{2} \sin 2\theta \right|$

To produce this combination, it is expedient to apply the system of automatic level control according to the block diagram shown in Fig. 189. Here two reciprocally perpendicular field detectors (frames P_1 and P_2 for receiving, respectively, vertical and horizontal components of the field are tuned by condensers C_n and C'_n to the operating frequency and have similar sensitivity) jointly with preamplifiers YC and YC' are placed in the outboard gondola. Signals U_v and U_h of the two components of the field of the operating frequency are fed to amplifiers YC_1 and YC_2 of the compensating system, placed in the measuring part of the apparatus. The signal from component U_v arrives at the input of amplifier YC_1 directly, and the signal from component U_h - at the input of amplifier YC_2 through the modulus regulator (attenuator) PM . By means of the modulus regulator, the signal from the horizontal component $U_h = U_{h0}$ with the initial geometry of the system (e.g., with the drift of gondola angle $\theta = \theta_0 = 65^\circ$), is fixed equal to the signal from the vertical component $U_v = U_{v0}$, i.e. $U_{h0} = U_{v0}$. Let this initial level be "zero" level (of course, "zero" level may be chosen also with another initial drift angle of gondola θ).

Thus, the transmission factor of the section PM is determinable by ratio

$$K_{PM} = \frac{U_v(0)}{U_h(0)} \quad (XI.5)$$

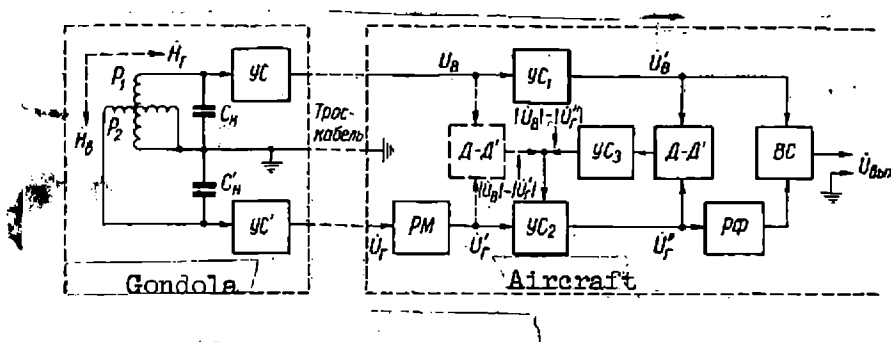


Fig. 189

The amplification factor of amplifier YC_1 is constant and of amplifier YC_2 variable. Amplifier YC_2 is controlled by converted input signals U_{ν} and U_{λ} from differential detector $D - D'$, which could be connected in this system in two ways: on the input side of amplifiers YC_1 and YC_2 (system "ACG-forward", denoted in Fig. 189 by dashes), or on the output side of these amplifiers (system "AGC-back", denoted in Fig. 189 by continuous line).

Since the system "AGC-back" is a system with backfeed, the effectivity of automatic gain control and stability of operation of the AGC system considerably increase (121). However, this system is more difficult to implement, as with rigid demands for the parity of output signals it is necessary to have an additional amplifier YC_3 in the control voltage circuit of automatic gain control. Being the amplifier of direct current, it should have a sufficiently high amplification factor and should be made up on a balance circuit, which produces output voltage of different polarity. In this case, the insignificant deviations of voltages from condition $U'_{\nu} - U''_{\lambda}$ at the outputs of amplifiers YC_1 and YC_2 should be quite sufficient for controlling the amplification factor of the adjustable amplifier YC_2 .

The problem of the differential detector includes generation of controlling direct current voltage, proportional to the difference $U_{\nu} - U_{\lambda}'$ for the first case and $U'_{\nu} - U''_{\lambda}$ for the second. At zero level the amplification factors of both the amplifiers should be similar and the control voltage, generated by the differential detector, should be zero. Therefore, when the output voltages U'_{ν} and U''_{λ} of amplifiers YC_1 and YC_2 , respectively, are equal and the phase shifts of these voltages are similar (combined on zero level by means of link RF), there is no unbalance voltage

at the output of subtracting circuit BC. Moreover, if after attaining compensation the ratio of the amplifier's output voltages changes, the link $D - D'$ should generate controlling voltage sufficient for changing the amplification factor of amplifier, YC_2 to a value, at which the output signal of this amplifier would strive to attain parity $U_k'' = U_v'$. To fulfil this condition, the differential detector $D - D'$, as well as the adjustable amplifier YC_2 , should meet certain requirements.

10. Construction principles of the main nodes in the compensation system with the horizontal component of auxiliary receiver of the field.

The theory and calculations of the AGC systems have been described in a number of works (121, 199, etc.). But since the application of the aerial induction method is dependent on certain limitations (measurable and controllable quantities, the range of their measuring, etc.), it is necessary to describe the main links of the AGC systems, applied in composite electric compensation.

The main requirement of the controllable amplifier YC_2 in both the cases of the differential detector's connection is that its amplification factor would vary within the required limits with difference of signals $U_v - U_k'$ ($U_v' - U_k''$) not exceeding the allowable, determinable by the measuring limits of angle θ . The dead zone of controlling the amplification factor of amplifier YC_2 with low intensity of controlling voltage, produced by link $D - D'$, is determined mainly by the intensity of this voltage and the dynamics of the AGC system. In the case under discussion it would be desirable to have the dead zone not over 0.5-1% of the maximum difference $(U_v) - (U_k')$. The variation steepness of the amplification factor in amplifier YC_2 should depend on the level of the controlling voltage and should be maximum at the low intensities of this voltage.

The achievement of ideal parity of voltages U'_v and U''_h at the outputs of amplifiers YC_1 and YC_2 is impossible due to the presence of some errors in the differential detector and the dead zone of the adjustable amplifier YC_2 , and also due to errors in other links of the AGC system. Therefore, the relative error of automatic follow-up will

$$\frac{(U'_v) - (U''_h)}{(U'_v)} 100 = \delta, \% \quad (\text{XI.6})$$

always be finite.

Value δ is taken in relation to the degree of compensation, necessary for practical purposes, and accuracy in parameter measuring of the decompensation signal.

Now let us analyse in more detail the individual links of the AGC system, applied in the method of compensation described above.

Differential detector D - D'. This detector could be made up, for instance, on the circuit shown in Fig.190-b. The circuit is based on a symmetrical amplitude discriminator on double triode, a block diagram of which is shown in Fig.190-a. Here $R_{a1} = R_{a2}$ - resistance of the tube's anode loads; R_b - the load resistance of the discriminator and balance resistance of the differential detector; D_1 and D_2 - the detectors (rectifiers) of signals, respectively, from vertical (δ_1, R_{11}) and horizontal (δ_2, R_{12}) components, induceable in the field receivers. The initial bias on the controlling grids is generated by stabilizer D, connected with the cathode circuit. The drift stabilization is implemented by stabilizing the stabilizing the resistance R_{st} in cathode, connected following stabilitron.

The output voltage of the amplitude discriminator (voltage on resistance R_b) is determinable by the relationship where K_{ap} - the

amplification factor of the discriminator, $K_{ap} = \frac{\mu R_a}{R_i + R_a}$. The time constants of detector circuit τ_d and of filter τ_f at the output of the discriminator should be less than the bumping period of the gondola

$$(T_{b.g} \gg \tau_d, T_{b.g} \gg \tau_f).$$

$$U_{out} = U_d = \frac{\mu R_a}{R_i + R_a} (U_1 - U_2) = K_{ap} (U_1 - U_2), \quad (XI. 7)$$

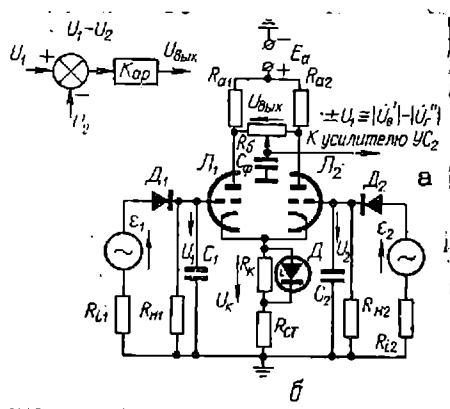


Fig. 190

When $U'_v > U''_k$, the D - D' link should generate controlling voltage of positive polarity for increasing the amplification of amplifier YC_2 upto the required magnitude, if $U'_v < U''_k$ - negative polarity for reducing the amplification of amplifier YC_2 . At $U'_v \rightarrow U''_k \rightarrow 0$ the control signal should also strive towards zero.

Linear amplifier YC_1 . The amplification factor of this amplifier is selected on the condition that the peak of its output voltage, which takes place at $\theta = 70^\circ$ (see Fig. 188), would not exceed that admissible for working in the linear section of the subtracting circuit BC (see Fig. 189) and the differential detector (these links should not be overloaded). The dynamic range of the amplifier should be higher than the dynamic variation range of the input signal (minimum intensity of the input signal is determined at $\theta = 60^\circ$). Naturally, the amplitude characteristic of the amplifier should be

linear in the given dynamic range. The zero level is taken approximately in the middle of the curve's linear section. In everything else, the estimate of the amplifier should be in accordance with the operation recommendations of (199, 249).

Adjustable amplifier YC_2 . The amplification factor of this amplifier at zero level K_{20} must be equal to the amplification factor K of amplifier YC_1 . In this case, the adjusting, i.e., controlling for amplifier YC_2 voltage $\Delta U = U_V - U'_K = 0$. The initial bias voltage is determined at the same level.

If the differential detector is out-in on the input side of amplifiers YC_1 and YC_2 (system "AGC-forward"), the required variation curve of the amplification factor in the adjustable amplifier should match the variation curves of voltages U_V and U'_K , which are shown in Fig. 188 by curves 1 and 2, respectively. This matching is attained by selecting the parameters of the amplifier's circuit, in particular its amplification curves $K_2 = f(E_g)$.

Curve $K_2 = f(E_g)$, matched with curves 1 - 2, can be plotted in the following way. On curve in Fig. 191-a, identical to that in Fig. 188, ordinates are drawn through the point of zero level and through a certain number of angle θ variation degrees (for instance, through two degrees) to the point of their intersection with curves 1 and 2. The obtained points of intersection which we denote as $A_n, \dots, A_2, A_1, A_0, A_1, A_2, \dots, A_n$ (on curve 2) and $B_n, \dots, B_2, B_1, B_0, B_1, B_2, \dots, B_n$ (on curve 1), will correspond to points $C_n, \dots, C_2, C_1, C_0, C_1, C_2, \dots, C_n$ on the axis of abscissae. Ordinate segments, confined between points A_n and B_n , i.e. $\frac{B_n C_n}{A_n C_n} = \frac{U_V - U'_K}{U_V - U'_K}$, are proportional to the difference between input voltages $\Delta U = U_V - U'_K = \frac{B_n C_n}{A_n C_n}$. For the given ΔU value, in accordance with the working principle of this method of compensation, there should be the following relationship.

$$K_1 U_v = K_2 U_h' \quad (\text{XI. 8})$$

Hence

$$\frac{K_2}{K_1} = \frac{U_v}{U_h'} = \frac{\overline{B_n C_n}}{\overline{A_n C_n}} \quad (\text{XI. 9})$$

Naturally, for the zero level, when $U_v = U_h'$, we have $\frac{K_2}{K_1} = 1$.
 At $\theta < \theta_0$, when $\overline{B_n C_n} < \overline{A_n C_n}$ and $\Delta U < 0$ we obtain $\frac{K_2}{K_1} < 1$ with
 $\theta > \theta_0$ and $\overline{B_n C_n} > \overline{A_n C_n}$, $\Delta U > 0$ we get $\frac{K_2}{K_1} > 1$.

Plotting of the adjustment curve of amplification factor YC_2 according to this reasoning given could be implemented as follows: for $\theta = \theta_0$ from Fig. 191-a we determine $\left(\frac{K_2}{K_1}\right)_n = \frac{\overline{B_n C_n}}{\overline{A_n C_n}}$. Simultaneously, taking into account the scale on the axis of ordinates, we find U_n , corresponding to the given θ . In this way, we determine abscissae ΔU_n and ordinates $\left(\frac{K_2}{K_1}\right)_n$ for the points of curve $\frac{K_2}{K_1} = f(\Delta U)$. From this curve, with the change of scale on the axis of ordinates, it is easy to pass on to curve and then, taking into account, that $E_g = E_{g0} + \Delta U$, - to curve $K_2 = f(E_g)$, which determines the sought for curve.

$$K_2 = \left(\frac{K_2}{K_1}\right) K_1 = f(\Delta U),$$

Having obtained the amplification curve $K_2 = f(E_g)$ and having selected the tube for the adjustable amplifier, we determine the resistance value of its anode load and the corresponding slope of the load line on the curve $i_a U_a$. In this we should strive to obtain the maximum possible coincidence within the preset variation range of control voltage U_g of the amplification characteristic in amplifier YC_2 with calculated characteristic K .

The achievement of the highest coincidence of calculated and actual curves of amplifiers YC_1 and YC_2 assures a more precise parity of output signals U_v' and U_v'' of these amplifiers. As a result the relative error of automatic follow-up becomes considerably reduced.

If the levels of both the signals at the input of the subtracting circuit are maintained practically equal, the subtracting circuit, also responsive to phase changes of the input signals, will react only to the variation of the phase ratio between signals from vertical and horizontal components, caused by the anomalous field. Thus, the unbalance signal U_{out} at the output of subtraction circuit BC, proportional to the phase shift between signals U_v' and U_v'' is the one sought for. When the compensation is almost of 100%, the total effect of the secondary field will be defined. The Phasemeter,

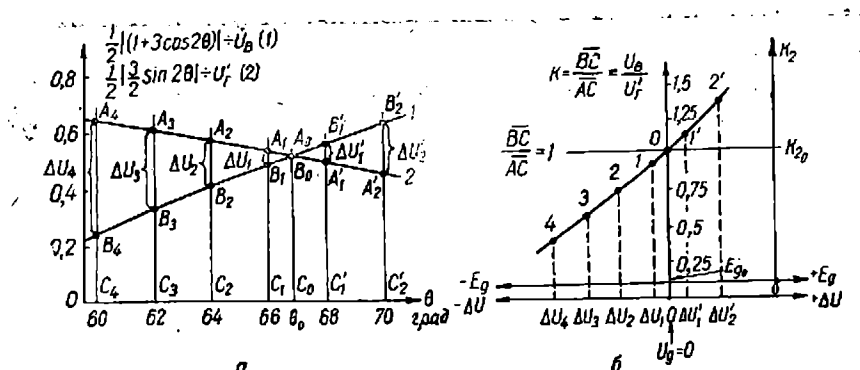


Fig. 191

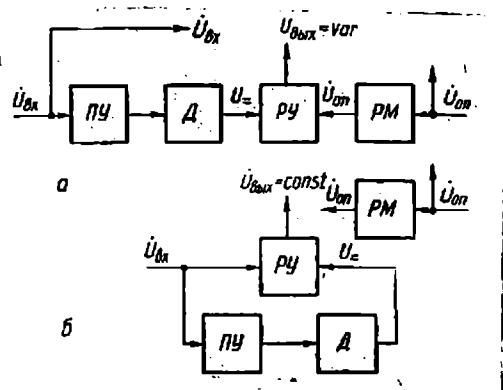


Fig. 192

connected at the output of the subtracting circuit (following the selective amplifier), will measure phase the shift between the comparative signal, taken, for instance, from the master oscillator, and the output signal of the compensator. The magnitude of the shift angle is determinable by characteristics of geoelectric irregularities in the upper layers of Earth in the survey area.

Since, usually, the vibration period of the gondola is comparatively high, it is not difficult to provide the quick-acting circuit of automatic maintenance of the compensating signal level at the outputs of the subtracting circuit equal to the level of the measurable signal.

The application of the given method of compensation, besides reducing the dependence of aerogeophysical survey on weather conditions provides other advantages also.

1. The effect of parameter variation of the primary field source and of the distance between the source and the receiver of the field on the stability of compensation is considerably reduced.
2. The effect of vibration noises in the receiving tract on the measuring results is reduced.
3. Cophasal inductions are reduced on the receiving channel.
4. The effect on the stability of compensation of the non-linear polarization of the primary field caused by the metal mass of plane (since it affects similarly both the components) is eliminated.
11. Compensation circuits with independent (inner) automatically controlled compensating signal (circuits with AGC).

The operation of the systems described below is based as in the preceding, on the principle of sustaining the compensating signal on the level of the measurable and on measuring anomalous variation of unbalance signal (its modulus and phase shift in relation to comparative signal). However, in contrast to the

preceding, the compensating signal in these systems is the comparative voltage, produced by the master oscillator. Therefore, a two-channel receiving system is not required (two field detectors and preamplifier) here per one operating frequency, nor of the composite compensating system. At the same time, these compensating systems permit substantial reduction of effect from the variation of the geometry of the system with negligible non-linear polarisation of the primary field.

For these compensation systems, it is possible to apply various systems of sustaining the compensating signal at the level of measurable (AGC systems). With this the use is mainly of phase anomalies (131).

Let us take the general aspects of some AGC systems, applicable in compensating systems of the induction method apparatus with combined or spread out source and receiver of the field.

Fig. 192 shows two possible versions of the systems, in which principle of automatic gain control "AGC-forward" is applied. In the system shown in Fig. 192- a, output voltage U_{out} of the controllable amplifier RY follows the variation only of input voltage U_{in} amplitude, remaining equal to this voltage within certain limits of its variation, i.e. $(U_{out}) = (U_{in}) = \text{var}$ and $f_{in} = \text{var}$, $f_{out} = \text{const}$. In the system in Fig. 192 - b output voltage U_{out} remaining invariable in the amplitude, with a certain variation of the input voltage, follows only variation of the input voltage phase, i.e. $(U_{out}) = \text{const}$ at $U_{in} = \text{var}$ and $f_{in} = f_{out} = \text{var}$.

In the system shown in Fig. 192 - a, the direct control voltage of positive or negative polarity at the output of detector D (PY-intermediate amplifier) is a function of the input signal, i.e. $U = f(U_{in})$. It controls the amplification factor K of the adjustable amplifier RY. With varying amplitude of input signal U_{in} , for instance with its increment, the control

voltage increases, increasing (or decreasing) amplification of the controlled amplifier. Since at the second input of amplifier through modulus regulator RM, the input is of comparative voltage U_{comp} the output signal U_{out} (transformed comparative) will either increase or decrease in relation to the amplification factor of the controlled amplifier. Therefore, the output signal is a function of two parameters: $U_{out} = F(U, U_{comp}) = F_1(K, U_{comp})$. In amplitude, this signal with a definite error should always be equal to the input signal with its variation within the preset limits, i.e. $U_{out} = U_{in}$. The subtracting circuit, at which voltages $U_{out} = U_{in}$ arrive equal in amplitude reacts only to the variation of phase ratio between these signals.

In the system in Fig. 192-b, voltage $U =$ at the output of detector D controls the amplification of adjustable amplifier PY in such a way that the amplitude of the output signal remains invariable and independent of the amplitude of input signal U_{in} ($U_{out} = \text{const}$). The initial phase of output voltage corresponds to the phase of the input voltage, i.e. $\varphi_{in} = \varphi_{out} = \text{var.}$ Thus, the subtracting circuit receives two signals: U_{out} with invariable amplitude and varying phase and invariable in intensity, and phase comparative voltage U_{comp} which in this case is compensating. Therefore, the subtracting circuit will react only to the variation of the input signal phase. A more complete block diagram of the compensating system is given in Fig. 193. Here IY - the selective amplifier; F (FHV) - the phase meter (phase-detecting voltmeter); I - the gauge of measurable parameter. However this system of compensation does not assure the required level of stability of the output voltage of the adjustable amplifier throughout the whole variation range of the amplitude of the input signal existing in practice (with variation of gondola drift angle θ within $\pm 5^\circ$). Hence the application of this system is limited.

Let us consider in more detail the first system of functional resolution of analyzed electric compensation to apparatus of induction aeromethod. The block diagram of the compensating system (for one operating frequency) is shown in Fig. 194. This system permits the measuring, with an error allowed in practice, of parameters of amplitude U_x and of phase φ_x , specified by the secondary field signals.

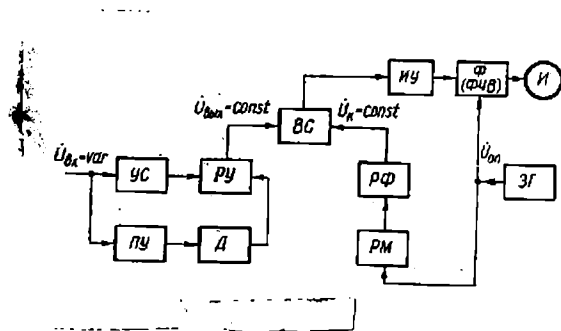


Fig. 193

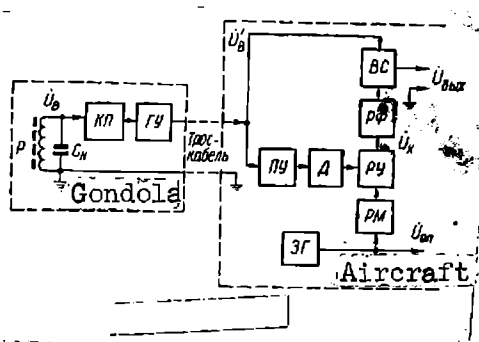


Fig. 194

The operating frequency signal $U_v = U_p$, received and amplified by the receiving system, consisting of receiving frame R, its tuning condenser C_m , matching cathode repeater KP and preamplifier GY, arrives at the compensating system: at one of the inputs of the subtracting circuit BC and at the intermediate amplifier PY. From the PY output the signal is delivered to rectifier D (detector) for obtaining the control voltage. This voltage controls the amplification of amplifier RY, to the input of which from master oscillator ZG through the regulator of modulus RM comparative voltage U_{comp} is fed. The output voltage of adjustable amplifier arrives through phase shifter RF at the second input of subtracting circuit BC. The required amplitude of compensating signal U_K is set by the modulus adjuster, and the required phase shift between the measurable and compensating signals in the initial conditions of the apparatus activity is set by the phase shifter.

The characteristics of elements PY, D and RY, which are being led into the compensating circuit, should be such that the amplitude of compensation voltage U_K at the output RY at any moment of time would be equal to the amplitude of the input voltage U_p (with the set error), i.e., the transmission factor of node PY-D-RY should at all times be one. The time constant of the detector's filter assures the required quick action of the AGC system with variations of the input signal, caused by the break in the geometry of the system. Experience of working with AERI-2 apparatus has shown that this constant should not exceed 0.15-0.8 sec. Pentod with elongated characteristic is used as the control tube.

In AERI-2 the power of the generating system and the torque of the radiating frame determine the density of the primary field, at which in normal flying conditions the signal, induced by the vertical component of this field in the tuned receiver, is 600-800 mv, at the input of the compensating system (after amplification by the gondola amplifier) - 0.6-0.8 v.

The variations of the amplitude of the signal with disruption of the geometry of the system in percentage of the intensity of the signal, specified by the primary field at the point of the field detector's initial position (angle $\theta = 64-65^\circ$), for point P_3 with the reception of the vertical component H_v are given in Table 14.

According to Fig. 195, the initial phase of the primary field signal on frequencies upto 1300-1500 cps varies actually very little, i.e., on these frequencies the primary field may be assumed to be linearly polarized. On frequency 1949 cps, the variations of the phase, specified by polarization of the primary field, are not over $3-3.5^\circ$. The curves in Fig. 195 were obtained in 1960 from the measuring data of AERI-2 apparatus, set up on the IL-14 plane. The measurements were taken at the speed of flight of 200-280 km/hr, which

is equivalent to the variation of the geometry of the system within $64 \pm 5^\circ$. With the variation of the geometry of the system, besides the reactive component, the parameter suitable for measuring, as follows from Fig. 195, is the signal phase, which with the increasing degree of compensation defines itself more clearly.

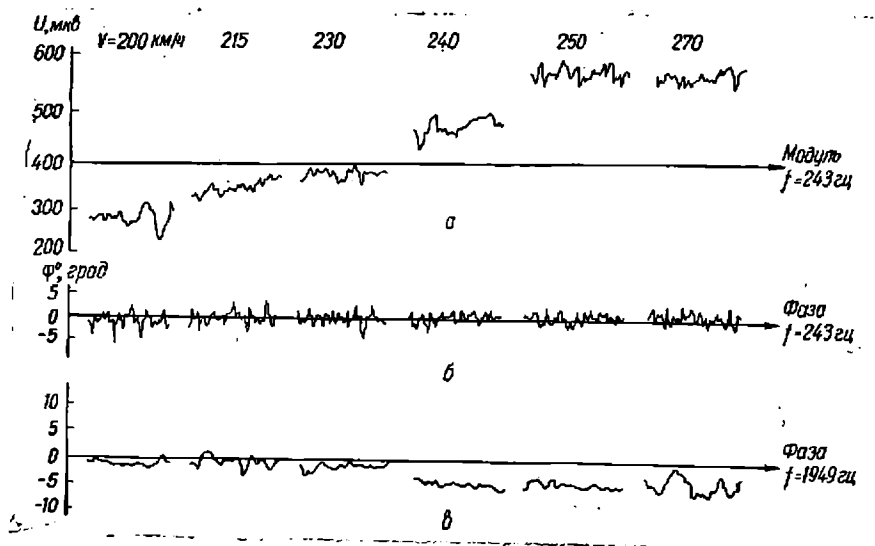


Fig. 195

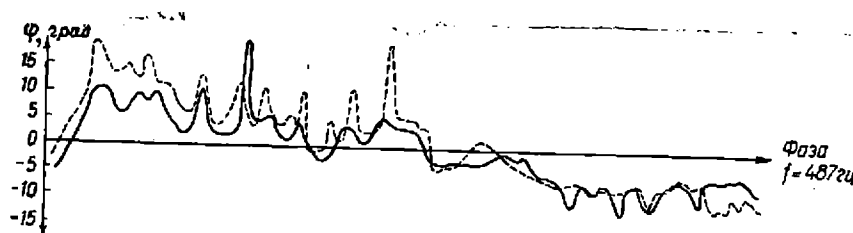


Fig. 196

The curve, shown in Fig. 196, of phase variation with compensation three times the signal of the primary field and with twice-repeated flight along the profile with geoelectric irregularities (speed of flight 260 km/hr, altitude above the ground about 200 m) confirms the stated assumption.

Calculations and practical work with AERI-2 apparatus provide grounds to assume that the usual intensity of the useful signal U_2 is 0.1-0.05 of the intensity of the primary field signal U_1 . Taking $U_1 = 600$ mv, we get

$$U_2 = \frac{600}{10 - 20} = 30 - 60 \text{ mv.}$$

If the variations of the gondola's drift angle θ do not exceed $\pm 3^\circ$, the primary field signal varies practically within $\pm 25\%$. Thus, with the initial mean value of signal $U_1 = 600$ mv its variations comprise 300 mv (± 150 mv). In the background of these variations of the received resultant field signal \dot{U}_p it is practically impossible to define the useful signal.

The initial phase of signal \dot{U}_2 is determined by the nature of the conductive object, i.e., by parameter pa^2 (98); it may vary from a single to several tens of degrees. However, in the absence of electric compensation, the apparatus, according to Fig. 171, should measure values $\ddot{U}_x (\Delta \dot{U}_x)$ and $\alpha (\Delta \alpha)$, containing respectively a few per cents of the total signal and degree unit. Measurements of this type are rather difficult.

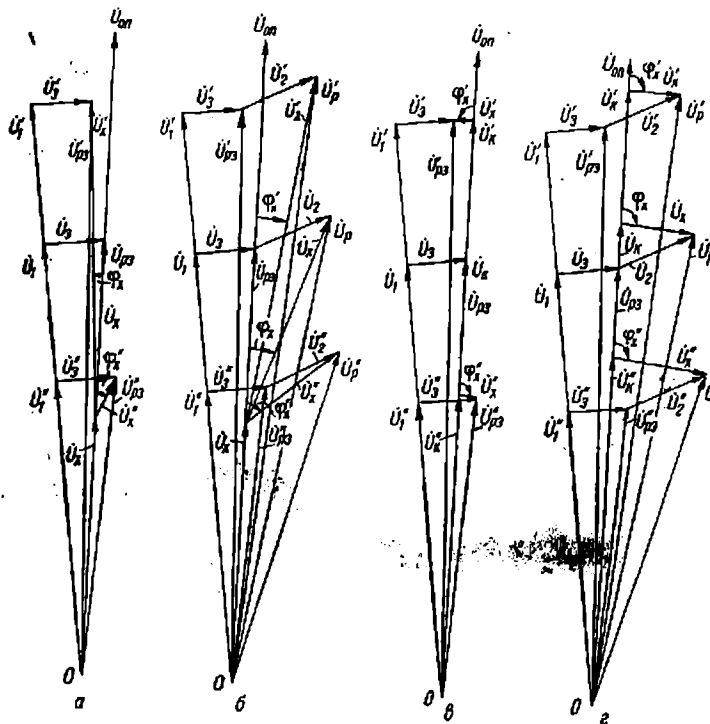


Рис. 197.

Let us evaluate the efficiency of this method of compensation by the application of the AGC system by comparing vector diagrams, showing the simple (see para 3, chapt. XI) and composite methods of compensation (134). With this we shall take into account the values of parameters, measurable by AERI-2 apparatus, and also the effect of the ground surface with finite resistivity.

Assuming approximately that the ground effect gives the interference signal U_3 , the amplitude of which is about $1/30$, the amplitude of the primary field signal U_1 , i.e. $U_3 \ll 20$ mv. Assuming that the amplitude of the interference signal U_3 does not vary in either case, and the phase shift of signal U_3 in relation to U_1 is 90° (the worst possible condition from the point of view of interference intensity).

Simple method compensation with invariable initial phase of the compensating voltage, matched with the initial phase of the primary signal.

A vector diagram, which accounts only for the ground effect, is shown in Fig. 197a^(*). The amplitude variation of signal U_1 , due to disruption of the geometry of the system is ± 150 mv ($\pm 25\% U_1$). The compensation voltage here is taken less than $U_{P2} = U_{P2}''$. We assume that $U_K = 400$ mv. The measuring apparatus measures the unbalance voltage $U_x (U_x', U_x'')$ and the phase angle $\varphi_x (\varphi_x, \varphi_x')$. The diagram shows that, in this case, the variation of the unbalance voltage is rather high and that of the phase angle not very high. According to calculations, $U_x = 200$ mv, $U_x' = 300$ mv, $U_x'' = 50$ mv; $\varphi_x = 0$, $\varphi_x = 0^\circ 40'$, $\varphi_x' = 2^\circ 30'$. Further, we assume that signal $\bar{U}_2 = 40$ mv, which has appeared from the anomalous object, does not vary with changes in the geometry of the system, either in intensity or in phase (Fig. 197 b). Therefore, the measuring is of unbalance signal

*For descriptiveness the scale of values in the drawing is not fully adhered to.

$U_x(U'_x, U''_x)$ and its phase shift $\varphi_x(\varphi'_x, \varphi''_x)$ in relation to the comparative voltage. The unbalance voltage and its phase shift are subject, with the variations of primary signal \dot{U}_1 due to bumping of the gondola, to considerable changes. It is easy to become convinced from Fig. 197 b, that the amplitude variations of unbalance voltage $\dot{U}_x(\dot{U}'_x, \dot{U}''_x)$ are considerably greater than those of the useful signal \dot{U}_2 . The results of calculations of U_x and $\varphi_x(U_2 = 40\text{mv}, U_3 = 20\text{mv}$ and also assuming that with $U_1 = 600\text{mv}$ the angle between \dot{U}_2 and U is of 60°) are as follows:

Comp

U_1, mv	750	600	450
U_x, mv	371	223	80
φ_x	$3^\circ 42'$	$9^\circ 26'$	$29^\circ 40'$

Composite compensation method with the AGC system. A vector diagram,

which takes into account only the ground effect, is shown in Fig. 197 c, where $(U_k) = (U_{pz})$. According to this figure, the amplitude of the unbalance voltage at $U_1 = 600\text{mv}$ is equal to zero ($U_x = 0$), $U'_1 = 750\text{mv} - U'_x, U''_1 = 450\text{mv} - U''_x$, in which case \dot{U}'_x and \dot{U}''_x are considerably lower than \dot{U}_3 . Simple calculations show that $U'_x = 4.8\text{mv}$, and $U''_x = 5.1\text{mv}$. But the phase shifts of unbalance voltage U_x vs. comparative voltage vary considerably. It may be assumed that the obtained intensities of unbalance voltage almost correspond to the sensitivity threshold of AERI-2 apparatus and are practically the same as the noise level. Therefore, even considerable increments of angles and changing the geometry of the system will not affect the measuring results, since in this case the phasemeter will not operate.

With the appearance of useful signal \dot{U}_2 (Fig. 197-d) the receiving frame perceives signal \dot{U}_p , and the apparatus measures the amplitude of unbalance voltage $\dot{U}_x(\dot{U}'_x, \dot{U}''_x)$ and the phase shift $\varphi_x(\varphi'_x, \varphi''_x)$. The amplitude variation of voltage \dot{U}_1 has very little effect on the variation of the unbalance signal and its phase and this is important - signal \dot{U}_x differs

little in amplitude from the useful signal \tilde{U}_2 .

The intensity of signal \dot{U}_x is determined from relationship

$$U_x = K_{s.c} \sqrt{U_p^2 + U_k^2 - 2U_p U_k \cos \alpha}, \quad (XI. 10)$$

where $K_{s.c}$ - the amplification factor of the subtracting circuit; α - the phase shift of U_p signal vs. U_k signal.

It is easy to note that the phase shifts of the unbalance signal are considerable, which permits their fixing with more assurance. With the variation of the phase shift α between signals U_p and U_k , due to the appearance of useful signal U_2 , the measurable angle φ_x between comparative U_{comp} (or compensating U_k) and the measured \dot{U}_x signals is determined from the equation obtained by resolving the oblique-angled triangle, formed by vectors \dot{U}_k , \dot{U}_p and \dot{U}_x (Fig. 197-d) vs. angle φ_x (74):

$$\varphi_x = \arctg \frac{a \sin \alpha}{1 - a \cos \alpha}, \quad (XI. 11)$$

where a - the modulus ration of the resultant \dot{U}_p and compensating \dot{U}_k signals, $a = \frac{(\dot{U}_p)}{(\dot{U}_k)}$, i.e., factor a characterises the degree of difference between these signals in amplitude.

From formula (XI. 11) it follows that angle φ_x is greater than angle α and increases if $a \rightarrow 1$, i.e., when $(\dot{U}_k) \rightarrow (\dot{U}_p)$. The last condition is provided with the increment of sensitivity of the compensation system and the decrement of error in the automating control of the AGC system.

Given below are the results of calculating values U_x and φ_x at $U_2 = 40$ mv, $U_3 = 20$ mv:

U_1 , mv	750	600	450
U_x , mv	34	35	41
φ_x	91°16'	91°38'	92°30'

Comparing the diagrams shown in Fig. 197 and the calculation data

of values U_x and φ_x for both the discussed methods of compensation, it is possible to be convinced that compensation with the AGC system has certain advantages in measuring the amplitude of the unbalance signal (amplitude parameter). Moreover, in this case, it is possible to give an approximate quantitative evaluation of the secondary field signal also, since the amplitude of unbalance signal \dot{U}_x does not differ very much from the amplitude of useful signal \dot{U}_2 . But the amplitude variations of the unbalance signal with disruption of the geometry of the system are not very high, being on an average 17-20% (in the first of the simple compensation methods with similar conditions for the geometry of the system the amplitude of the unbalance signal varies 4.5 times).

The given estimates correspond also to other values of \dot{U}_x signal, and with the lower interference signal \dot{U}_3 , which may often have place even with a smaller variation range of the geometry of the system, the variations of \dot{U}_x signal will also be less. Analyzing the calculation results of \dot{U}_x and φ_x in the composite method of compensation, we come to the conclusion that the variation of the unbalance voltage phase shift φ_x with bumping of the gondola is on an average 37'. Actually, this is a very low variation in comparison with seven to eight times greater variation of the phase shift in the first simple method of compensation. However, if angle α between signals \dot{U}_p and \dot{U}_k is high (several degrees), and its relative variations with variations of useful signal \dot{U}_2 are low, there will be no gain in measuring the phase parameter, and the "amplification of the phase shift", determinable as ratio $\frac{\varphi}{\alpha}$ (74), is not a decisive factor in this case. The main criterion for the expediency of measuring the phase parameter for the compensation system discussed is the quantity $\frac{d\varphi}{d\alpha}$. However, in the given case this quantity remains very low.

12. Principles of building up main nodes in compensators with the AGC system.

Compensation systems, in which the AGC principle is used on condition that $U_{\kappa} = U_{\gamma} = \text{var}$, could be implemented in the apparatus of various methods of aerial electric prospecting. The selection of the system is necessitated mainly by the method of controlling the adjustable amplifier and the type of radiotubes applied in this amplifier.

The block diagram of the compensator, in which the adjustable amplifier is made up on tube 6K3 with third grid control (131), is shown in Fig. 198, where the only nodes shown in detail are those not present in AERI-2 apparatus. The initial negative voltage on the third grid of 35 (248), is generated on resistance R_{14} of divider $R_{11}-R_{14}$, which at the same time serves as divider for the second grid voltage. The initial method of operation is made more precise by adjusting resistances (R_{12} for voltage adjustment on the second grid and R_{14} - on the right grid). Working conditions of tube 6K3: $E_a = 240$ v; $R_a = 27$ k-ohm; $U_{g2} = 120$ v; $I_{a.c} \approx 9$ ma; $E_{g3} = -35$ v; $E_{g1} = -5.5$ v. Used as detector (rectifier) of the control signal is diode D2E, cut in through the cathode repeater at the output of the intermediate repeater with amplification factor $K \approx 25$. The operating conditions of the rectifier ($C_3, R_6 - R_8, C_4$) are so taken that the average value of the output voltage would be equal to the virtual value of the initial alternating voltage within the range of the latter's variation 5 - 40 v. The output voltage of the adjustable amplifier could either be taken off either the whole anode load R_{15} , or its portion depending on the ratio taken between the intensities of the comparative signal and the input voltage $U_{in} = U_{\gamma}$.

Investigation of control voltage detector consisted in more precise determination and matching in its circuit of parameters which were meant to assure the maximum possible linear section of the detector curve and

also that in the same scale on the coordinate axes of voltages $U_{in}(af)$ and $U_{out}(z)$ the slope of this curve in relation to the indicated axes would be 45° .

In the investigation of the detector, a diagram of which is shown in Fig. 198, a detector curve was obtained (Fig. 199), which meets the above requirements. Since the detector in question gets cut in at the output of the intermediate (linear) repeater through a matching cathode repeater, the latter must assure practically without distortions the transmission of the whole variation range of the intermediate repeater output voltage (from 0 to 40 v) at the peak value of the transmission factor. To meet this condition, the bias voltage to the controlling grid of the cathode repeater is fed from the divider cut-in to the circuit of anode supply source. Experiments have shown that the transmission factor of the cathode repeater at high signals (20-40 v) is 0.97.

The diagram investigation of the controlled amplifier included the determination and matching of parameters, which would assure obtaining the amplitude curve of this stage, satisfactory for the problem of the controlled amplifier in maintaining the level of its output voltage at the level of input voltage (with a minimum error) with variations of the input and comparative voltages within the preset limits.

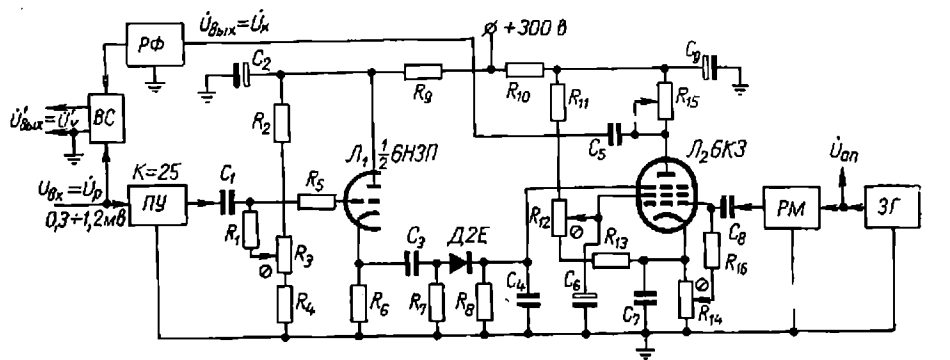


Fig. 198

Fig. 200 shows the experimental amplitude curves of an adjustable stage worked out on a model at various intensities of input $\dot{U}_{in} = \dot{U}_r$ and comparative \dot{U}_{Comp} voltages. The curves show that the adjustable stage assures a sufficiently linear maintenance of the output voltage level at the level of the input voltage with the latter's variations from 0.3-1.2 volt and with $(\dot{U}_{Comp}) = 0.4 - 1.0$ v. Quantities U_{Comp} , U_{out} and U_{D_3} , which determine the curve, are interconnected by relationship $U_{Comp} U_{D_3} = k U_{out}$, where k - the proportionality factor for the given circuit, equal to two.

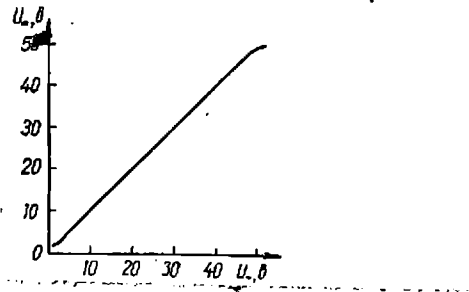


Fig. 199

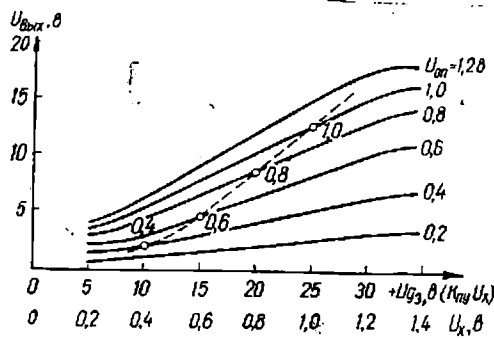


Рис. 200.

Fig. 200

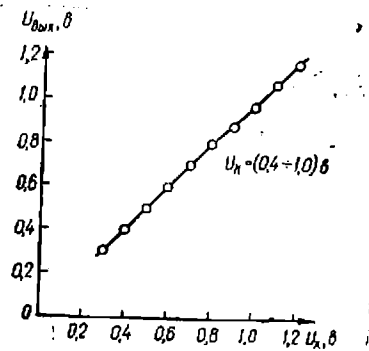


Рис. 201.

Fig. 201

The amplitude curve of the whole AGC system, encompassing the intermediate repeater PU, the detector and adjustable cascade on tube 6K3, is shown in Fig. 201. It makes it possible to assume that the error of sustaining the level of the output voltage at the level of the input voltage does not exceed 5% with the variation of the comparative signal

within limits 0.4-1.0 v, which, in the given systems, carries out the role of compensating voltage U_k .

Thus, the discussed AGC system permits the assurance, with an error upto 5%, of automatic maintenance of the output voltage $\dot{U}_{out} = \dot{U}_x$ at the level of the input voltage $\dot{U}_{in} = \dot{U}_r$ with the latter's variations within the operating range 0.3-1.2 v and with $U_{comp} = 0.4-1.0$ v. The output voltage of the subtracting system $\dot{U}'_{out} = \dot{U}'_x$ of this level arrives at the amplitude and phase gauge.

Fig.202 shows the block diagram of another version of the compensating system, which assures compensation by amplitude in a range of signal variation wider than the above system (129).

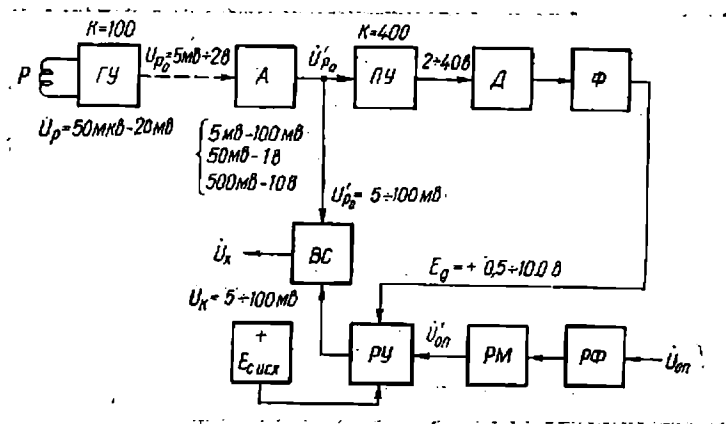


Fig.202

Assuming that the amplitude variation range of the resultant field signal at the input of the gondola amplifier $U_r = 50$ microvolt-20 millivolt. In this case at the input of the measuring unit with the amplification factor of the gondola amplifier $G_{MK} = 100$ the measured signal \dot{U}_{ro} will vary within the limits 5 mv-2v, i.e., its dynamic range equals 400. It is obvious that to provide the required depth by simple methods and systems, the stability and precision of compensation with such a high variation range of the input signal does not seem to be

possible. Therefore, at the input of the compensation system an attenuator A has been provided with ratio of division 1 ; 10 and 100 with the following variation ranges of amplitudes of the input signal 5-100 mv; 50 mv-1 v; 500 mv - 10 v. Automatic compensation is provided for within the variation range of input signal equal to 20 (about 26 db).

From the output of attenuator A signal $\dot{U}_{ro} = 5 - 100$ mv is fed to one of the inputs of the subtracting system BC and to the intermediate repeater PU, the amplification factor of which $K = 400$. At the input of detector D, the signal varies from 2 to 40 v, thereby assuring linear section of detector curve for the adopted variation range of the input signal. In this diagram detector D and filter F are identical to those in the diagram in Fig. 198. At the output of the filter is a constant divider (not shown in the diagram), assuring the reduction of the control voltage to 0.5-10 v (ratio of division 4). This voltage is required for the control of the adjustable amplifier RU.

The adjustable amplifier also receives comparative voltage \dot{U}'_{comp} , the amplitude and phase of which are controlled by the governors of modulus RM and phase RF. Moreover, the adjustable amplifier receives initial bias voltage $E_{c.in}$ of positive polarity. The adjustable amplifier is made up on the double triode 6N1P with sufficiently high resistances of anode loads. According to the data of (248), this assures good linearity of the amplitude curve with variation of negative bias voltage from 0.5 to 10v.

It can be asserted that it is possible to obtain the amplification factor of the adjustable amplifier, linearly increasing with increment of the input signal in the range of 26 db, with variation of bias voltage on the control grid from -1 to -10.5 v. To make sure that the indicated condition is obtained the control of the RU amplification factor is effected by the control voltage $E_g = +(0.5-10)v$, delivered to the control grid of the tube

in the presence of initial bias voltage $E_{c.in}$ of positive polarity, with 11 v for the given system and fed into the cathode circuit of tube 6N1P. The resultant negative control voltage $-E'_g$, active between the cathode and the triode grid, is generated by the difference of the following voltages: invariable initial bias voltage $E_{c.in}$ of positive polarity and varying control voltage E_g , also of positive polarity.

A diagram of the adjustable amplifier is shown in Fig. 203. The elements of the system, for instance, resistances R_1 and R_3 of the anode load, and the mode of the amplifier's operation are so matched that with the variation of control voltage, which fully reflects the amplitude variation of the input signal \dot{U}'_{ro} , and with $U'_{comp} = 5$ mv, there is the required intensity of compensation voltage (5-100 mv) with accuracy of the automatic follow-up, acceptable for practical purpose.

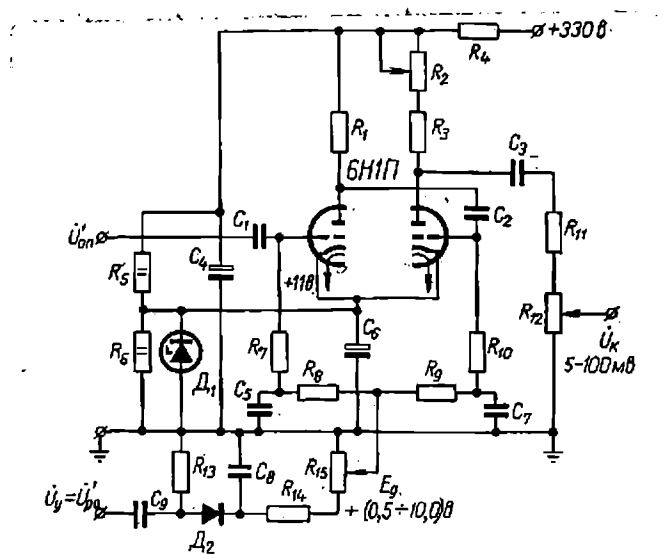


Fig. 203

The source of anode and filament supply for the RU system correspond to the input of voltages to compensator AERI-2 apparatus (330 v stabilized anode voltage, 6.3 v of direct current). The source

of the direct bias voltage is stabilatron D_1 type D-811, connected with the lower arm of the anode supply circuit divider R_5-R_6 . The use of stabilatron as the bias source and its setting in the cathode circuit make it possible actually to exclude reverse feedback on direct current. This makes the amplification factor of the adjustable amplifier independent of the active inner resistance of the bias voltage source, cut in to the cathode circuit. Non-presence of the reverse feedback on alternate current is specified by the connection into the cathode circuit of by-phase capacitor C_6 of sufficiently high capacitance.

The analysed control system permits practically total exclusion of the reciprocal effect of two individual sources of voltages, applied for the control of the AGC system.

At the RU output is a divider $R_{11} - R_{12}$ of the output signal, by means of which the required amplitude of the compensating voltage \dot{U}_K is set (the amplification factor of a two-stage adjustable amplifier with optimum anode loads, at which the linearity of the amplification curve is assured, considerably exceeds that required). By means of variable resistors R_2 , R_{12} and R_{15} the initial adjustment of the RU system is attained and also its tuning during the changing of the tube.

To investigate the RU system with a high dynamic range of adjustable quantity, the choice was of the anode load of the amplifying tube, its mode of operation, also the method for controlling the amplification factor. In the final estimate of the RU system, determination was made of its $\dot{U}_{out} = F(E_g)$ curve at $\dot{U}_{in} = \text{const}$, its non-linearity and the effect of tube changing was defined more accurately.

To carry out automatic gain control of the compensating signal within limits 5-100 mv with accuracy not below 5%, the anode load of each triode

in tube 6N1P was taken as 91 k-ohm with controlling voltage 0.5-10 v, supplied to the tube's cathode circuit. According to the dynamic grid-plate characteristics of the triodes in tube 6N1P, the amplitude curve of RU on resistors is sufficiently linear within the measuring range of the input signal (hence, the bias voltage also). It should be mentioned that the dynamic range and linearity of the RU curve depend on the intensity of voltage of the anode supply source. Satisfactory automatic control may be obtained with anode voltage 330 v.

Resistors $R_5 - R_6$ of the divider for the source of direct bias voltage of positive polarity were taken so as to obtain the working current of stabilatron not less than twice the minimum stabilization current of 5 ma and the voltage drop on resistor R_6 about 15-20 v. In this case, stabilatron D-811 provided sufficiently high stability of the initial bias voltage $E_{c.m.} = 11$ v with the anode current variation of each triode in tube 6N1P from its minimum at the highest negative resultant bias voltage of 10.5 v to 2-2.5 mv at -1v. The divider resistors $R_{14} - R_{15}$ were taken with the object of obtaining the required ratio of division (1:4) and of possible adjustment of the control voltage within negligible limits. The latter is provided by variable resistance R_{15} .

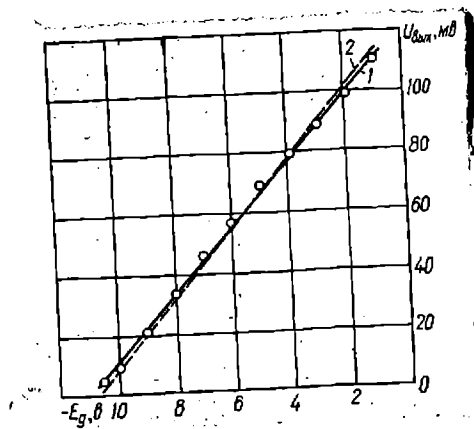


Fig. 204

The source connection of the initial bias voltage into the cathode circuit of the tube provides an ideal galvanic separation of this source from that of the control voltage. Therefore, parameter variation of one of them does not affect the second source of voltage.

Fig. 204 shows how the experimental curve of the adjustable amplifier $\dot{U}_{out} = F(E_g)$ combines with calculated for a case, when $U_{comp} = 5 \text{ mv} = \text{const}$ and $E_a = 330 \text{ v}$ (continuous line 1). According to calculations, non-linearity does not exceed $\pm 3\%$. The change of the RU tube slightly increases this divergence (dash line 2 - average RU curve with the change of tubes). By an appropriate adjustment of the system, curve 2 could be combined with curve 1.

The subtracting system, the phase shifter, the attenuators, the aperiodic amplifiers and other nodes and elements of the analyzed compensation system, which are common for the simple and the composite methods of electric compensation, were not investigated in addition.

13. Reduction of effect of the variation of geometry on the stability of compensation by means of additional field sources and detectors.

In USA, several modifications were worked out for the apparatus of the induction aeromethod of Schemes for composite electric compensation, based on the use of additional receivers or auxiliary sources of the field. By means of these elements it is possible to obtain a compensating signal equal in magnitude to the increment of the primary field signal from variations of the initial geometry of the set-up. In the compensation schemes, this signal is subtracted from the main signal, thereby making the measuring results independent of the slight variations of the geometry of the system and subsequent deep and stable electric compensation of the primary field signal (181).

Let us analyze in more detail some of the compensation methods, which,

as a rule, reduce or eliminate the disturbing effects, emerging with the slightest variations of distance between the field's source and receiver, and also with their reciprocal slight angular shifts.

Fig. 205 shows schematically plane 1 with the outboard gondola 2, towed by cable 3. The line of motion of the gondola coincides with the flight line of the plane. Set up inside the plane is the oscillator 4, the energizing oscillating frame 5, placed on special brackets in the nose part of the plane and having a horizontal magnetic moment. The primary magnetic field is excited by the ore body 10. The receiving frame 6 is set up in the gondola. The second oscillating frame 7 is placed in the tail part of the plane and gets the energy from oscillator 4. Axes of frames 5-7 lie on one straight line. The oscillating frame 7 generates compensating voltage on the receiving frame and excites the ore body. Thus in the receiving frame is induced a signal, specified by the primary field of the main supply frame, compensating field of the oscillating frame 7 and the secondary field from the ore body. The resultant signal of these three separate fields is amplified by amplifier 8 and delivered along a cable from the gondola to measuring unit 9. A diagram of frame arrangement in the given set-up is shown in Fig. 206.

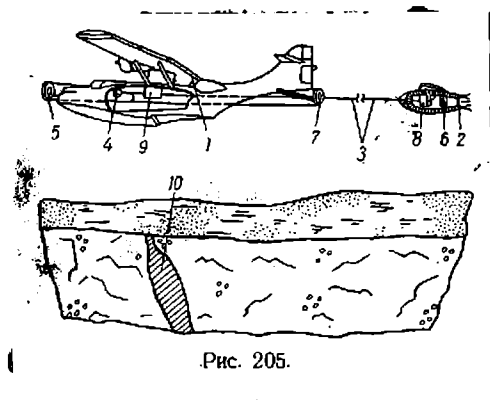


Fig. 205

The following definitions are being adopted: M_1 - the magnetic moment of frame 5; M_2 - the magnetic moment of frame 7; r_1 - the distance between frames 5 and 6; r_2 - the distance between frames 7 and 6; H_1 - the primary field intensity on frame 6, specified by frame 5; H_2 - the compensating field intensity on frame 6, specified by frame 7; N - the number of turns in frame ; U_1 and U_2 - voltage, induced in frame 6 by H_1 and H_2 fields respectively.

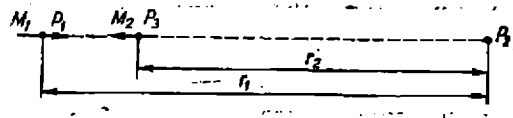


Fig. 206

We then get

$$\begin{aligned} H_1 &= C_1 M_1 r_1^{-3}, \\ H_2 &= C_2 M_2 r_2^{-3}, \end{aligned} \quad (\text{XI. 12})$$

$$\begin{aligned} U_1 &= KNH_1; \\ U_2 &= KNH_2, \end{aligned} \quad (\text{XI. 13})$$

where C_1 , C_2 , K - constant.

Magnetic dipoles M_1 and M_2 are opposing and directed along the axes of frames 5 and 7 (see Fig. 206). If centre P_2 of frame 6 is at considerable distance from centres P_1 of frame 5 and P_3 of frame 7 and $C_1 = C_2$, the fields H_1 and H_2 are opposing in direction.

Voltage U_1 is proportional to H_1 , therefore, a slight variation of r_1 distance due to stretching or bending of the cable, the temperature effect on carrying construction vary the H_1 and U_1 intensities (there are either pseudoanomalies or distortions of true anomalies). However, if H_2

and H_1 are opposing, and U_2 and U_1 are in phase opposition and vary to the same extent with r_1 variations, errors of this type could be eliminated.

If r_1 and r_2 values are high in comparison with the difference between them, r_1 variation is associated with equal variation of r_2 . If r_1 variation is caused exclusively by the elongation of the cable, the r_1 and r_2 values vary practically similarly.

In order that the U_1 and U_2 values would vary similarly, the following condition should be satisfied.

$$\frac{dH_1}{dr_1} = - \frac{dH_2}{dr_2} , \quad (\text{XI. 14})$$

i.e.

$$-3C_1 M_1 r_1^{-4} = 3C_2 M_2 r_2^{-4} . \quad (\text{XI. 15})$$

Substituting in equation (XI. 15) the H_1 and H_2 values according to formula (XI.12), we get

$$-H_1 r_1^{-1} = H_2 r_2^{-1} .$$

Therefore,

$$\frac{H_2}{H_1} = \frac{r_2}{r_1} ; \quad (\text{XI. 16})$$

$$\frac{U_2}{U_1} = \frac{r_2}{r_1} . \quad (\text{XI. 17})$$

Thus, from equation (XI. 15) it follows that the magnetic moment of compensating frame 7 will be

$$M_2 \frac{C_1 r_2^4}{C_2 r_1^4} = M_1 ,$$

and since $C_1 = C_2$,

$$M_2 = - \frac{r_2^4}{r_1^4} M_1 . \quad (\text{XI. 18})$$

The field of compensating frame 7 reduces the effective intensity of the primary field from the energizing frame 5, but the higher accuracy in measuring of the anomalous field warrants this loss. For instance, if $r_2 = 0.8 r_1$, $H_2 = -0.8H_1$, the primary field H_1 and the compensating field H_2 generate in the receiving frame the resultant field signal, the intensity of which $H_1 + H_2 = 0.2H_1$.

In the ore body, which is practically at the same distance from the energizing frame 5 and compensating frame 7, occurs generation of the magnetic field, the intensity of which

$$M_1 + M_2 = M_1 - \left(\frac{0.8r_1}{r_1} \right)^4 M_1 = 0.5904 M_1 . \quad (\text{XI. } 19)$$

The subsequent electric compensation of the primary signal in the measuring unit considerably increases the sensitivity of the set-up to field anomalies.

A diagram of another set-up, for which the above terms and deductions hold true, is shown in Fig. 207. The receiving frame with a vertical axis is placed at point P_2 . If the frame is in the gondola, it may shift in relation to the energizing frame (dipole), located at point P_1 , i.e., approach point P'_2 . This angular shifting is less reflected in measuring results in the presence of the compensating frame, located at point P_3 . If the field density at point P'_2 increases the increment of the signal in the receiving frame, generated by the primary field, gets compensated by the increment of the signal, generated by the compensating field of frame 7. The effect of angular shifting is more noticeable when the M moments of the energizing and compensating frames are not opposing and are not directed along a line joining points P_1 and P_2 (see Fig. 206)

or if they are neither opposing nor perpendicular to this line (see Fig. 207).

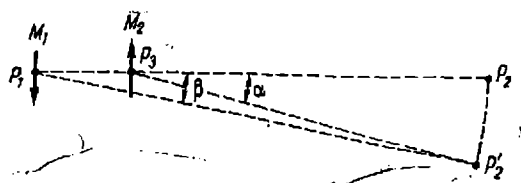


Fig. 207

If the gondola cable is fixed on the plane closer to oscillating frame 7 than to frame 5, the downward movement of the gondola reduces to some extent distance r_1 , whereas distance r_2 remains almost unchanged. This should cause the effect of the primary field H_1 to be higher than the effect of the compensating field H_2 . However, in the same conditions angle α (see Fig. 207) increases faster than angle β , as a result of which the effect of the compensating field is higher than that of the main primary field.

Similar reasoning holds good also for the case in which the gondola cable is fixed on the plane closer to frame 5 than to frame 7.

The closer is point P_2 to points P_1 and P_3 , the greater is the probability of angular shifting and appearance of pseudosignals due to the variation of distances r_1 and r_2 and of the angle α and β . Therefore, it is desirable that the distance between the main energizing frame and compensating frame should be small in comparison to distance r_1 (for instance, 15 and 90 - 120 m).

It would be possible to reduce the effect of angular shifting of frame 6 vs. The oscillating and compensating frames by the application of three receiving frames with reciprocally perpendicular axes. In this case, each receiving frame is sensitive only to one of the fields components, moreover, the main receiving frame 6 is meant to receive the highest intensity

component of the primary field, which most often corresponds to the highest intensity component of the secondary field. Signals from the three receiving frames get transmitted into the measuring unit through the quadratic addition system, by means of which the square root is extracted from the sum of signal squares of each frame. In practice, when the angular shiftings of the receiving frame are not high ($\alpha < 10^\circ$) and when, for example, component H_x of summarized field H is high in comparison with components H_y and H_z , it is possible to assume

$$H = H_x + \frac{H_y^2}{2} + \frac{H_z^2}{2} .$$

By applying compensation frame 7 the effect of induction currents in the metal parts of the plane also is considerably dampened since the field of the compensation frame strives to destroy the primary field (in particular between frames 5 and 7). Therefore, it would be expedient to set up frames 5 and 7 in the nose and tail parts of the plane.

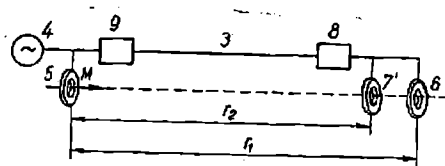


Fig. 208

A diagram of the set-up, which is not affected by distance variation between the source and receiver of the field, is shown in Fig. 208. Here 4 - oscillator, 5 oscillating frame, 6 - main receiving frame; 7' - compensating receiving frame. The signals from frames 6 and 7', cut in opposition, are delivered through amplifier 8 along the cable 3 into the measuring unit 9. Frames 5-7' are set up on one horizontal axis. Here, as was the case in the first scheme, variations of voltage U_1 , caused by variation of r_1 , get compensated by equal variations of voltage U_2 in frame 7', if $\frac{dU_1}{dr_1} = \frac{dU_2}{dr_2}$, i.e. $\frac{U_2}{U_1} = - \frac{r_2}{r_1}$.

To obtain the best results, each receiving frame should be replaced by three frames with reciprocally perpendicular axes. It is desirable that with this scheme of compensation the measuring unit would permit recording separately the active and reactive components of the residual signal.

It should be mentioned that the motion of gondola up and down vs. the plane is less probable, if the gondola is at the same elevation as the plane and has wings, which are set up so as to obtain variable and adjustable angle of attack. But if the gondola flies at an altitude different to the plane, the frames 5-7 (5-7') should be so set up that their axes would be in vertical plane and, moreover, they should be colinear or perpendicular to the line passing through their centres (points P_1 - P_3 in Fig. 206).

14. The main conclusions and recommendations for the compensation of primary fields and signals.

The analysis of the simple methods of electric compensation of the primary field signal shows that in the real conditions of geophysical survey not one of them is capable of excluding completely the effect of variation of the geometry of the system. Only in the case of non-polarised primary field, regardless of the system adopted, increments of the primary signal from disrupted geometry of the system have no effect on the reactive component of the measured signal. The more composite schematic resolution in the first simple method of compensation (application of phase-sensitive voltmeter) says for itself by the increased stability of the components measuring channel against noise: .

Therefore, when using the simple methods of electric compensation the most acceptable measurable parameter, reflecting in its entirety the variations of the useful signal, is the reactive component of the decompensation signal. This component should be recorded in the apparatus

of the induction aeromethod, meant for geophysical mapping. With the measuring of the reactive component, the stability of the measuring unit against noise increases. In the search for purely ore objects, the active component should also be measured.

The composite methods of electric compensation, like the induction aeromethods of the second class, are applicable in relative geophysical determinations. The second of these methods eliminates the effect of the variation of the geometry of the system and may be applied in elliptical polarization of the primary field (caused by the metal mass of the plane). The first and third methods considerably reduce the effect of variations of the geometry of the system only with the linear polarization of the primary field. The third method, as the simplest and most rational, may be recommended for practical application.

Appropriate parameters of the AGC system and its components, in particular the adjustable amplifier, are selected in relation to the magnitude of the input signal and its variations. Therefore, the functional system of the third method could be applied for the compensating systems of the apparatus in various versions of the induction aeromethod, where the oscillating and receiving frame are combined, i.e., when the variations of the geometry of the system are negligible. In this case, a deep and stable compensation of the direct signal is quite assured.

Every system of the composite method of compensation permit recording (the intensity and phase variations of unbalance signal, caused by the varying signal of the resultant field due to variations of the secondary field signal). However, in the third system of the composite compensation method, the amplitude of unbalance voltage even with comparatively high variation of the primary signal differs relatively little (by about 20%) from the amplitude of the secondary field signal. Therefore, the

determination of the amplitude parameter, i.e., the amplitude of the unbalance signal, substantially increases the resolving power of the induction aero method with the bumping of the gondola; while the determination of the unbalance signal phase shift in this system is inexpedient.

If the set-up of the induction aeromethod provides for the use of the outboard gondola, which moves along the same flight line as the plane, geometry application of compensating sources and receivers of the field should be made for the exclusion of the effect caused by the variation of the initial set-up. The additional electric compensation of the primary signal in this set-up should be carried out by the first simple or the third composite method.

---.---.---.---.---

CHAPT. XII - RECORDING OF MEASURABLE PARAMETERS

1. Methods and systems of parameter recording.

Uptil now the output quantity to be recorded in the apparatus of aerial electric prospecting is invariably the voltage (current) at the output of the measuring system. Therefore, the most popular recording devices are the recording galvanometers of various types and the systems of follow-up contact transformation - automatic potentiometers (in USSR - galvanometers SG-17, SK-100, potentiometers EPP-01, EPP-09, PS-1-01, etc., in other countries - devices "Brash", "Sunborn", "Gulf").

The output quantities of recorders are usually marked as a segment of a straight line or a section of the arc of a circumference. For the determination of numerical values of the measured parameters it is naturally necessary to read off or to process the obtained results. More convenient in form are the results of recording in the shape of curves on the diagram tapes*. The diagram is a document, on the basis of which it is possible to judge the correctness of the operator's actions and also of the good working order of the apparatus itself.

The recorder consists of two main parts - the recording element and the carrier. The recording element activates the carrier, leaving on it signs (symbols) of recording, showing the measured quantity. The methods of activation of the carrier by the recording element could vary and they are frequently defined as recording methods. The following three methods of recording are used in aerial electric prospecting.

The first method - the recording is by pencil, ink or printing. The most popular is ink; the carrier is the paper.

Second method (less popular) - electric sparking, electrochemical method, magnetic recording, electronic rays, etc. are applied.

*Similar recorders are denoted in literature as the analogue type. Another type of recorders widely applied in technique are digital recording devices (50, 164, 205).

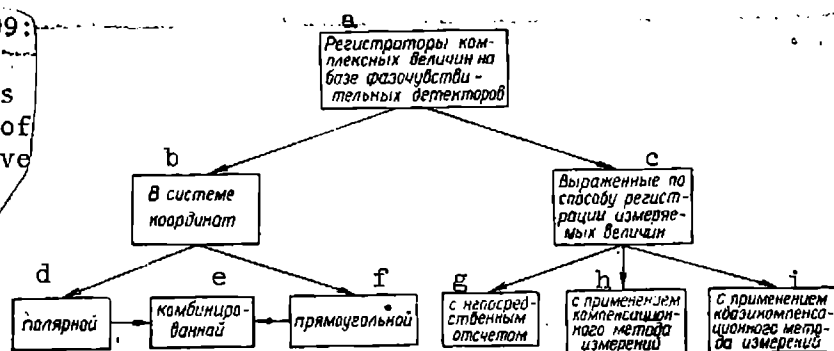
In the third method recording is on paper, covered by a layer of wax, soot, etc. This method is also applied in aerial electric prospecting in other countries.

The recording is either single-channel or multichannel. The natural result of the non-availability of standard special multi-channel recorders is that the apparatus of almost all methods of aerial electric prospecting has its own specific multichannel* recorders or single-channel recorders, converted into several channels**. The principles of their operation and construction characteristics are described in (5, 263) and in other works.

The most popular in aerial electric prospecting are the recorders of complex quantities (RCQ), erected on the basis of phase discriminating detection (FHD) (94).

Key to Figure 209:

- a, Recorders of complex values on the basis of phase-sensitive detectors;
- b, In system of coordinates;
- c, Expressed by means of recording the measured values;
- d, Polar;



- e, Combined;
- f, Rectangular;
- g, With direct recording;
- h, Using compensating method of measurement;
- i, Using quasicompensatory method of measurement.

Fig. 209

If all the RCQ executed on the FHD phase and applied in electric prospecting were classified (94) according to their coordinates or the recording method of measurable quantity (Fig. 209), operation of the analysis of RCQ systems would be considerably simplified. In the present case, the method of direct estimation assumes direct measuring and recording

*In standard recorders of the follower type the reconstruction is usually of direct current amplifiers with mixers, slid resistance are rewound, imprinting mechanisms of the measuring range, time breaks, bench marks on profiles, etc. are added.

**For instance by combining two or three recorders of SG-17 type (234).

***Compensation measurements, which are the measuring principles of the recorders themselves, are not taken into account.

at the FHD output***; compensation method - compensation of the measurable quantity at the FHD input; quasicompensation - compensation of one of the quantities upto a certain constant value, for instance, compensation of the phase at the FHD input $\varphi_0 \pm 90^\circ$ by means of the follower phase shifter (88, 94). The systems of FHD, the properties of which were discussed in detail in para 4 of chapt. X, make it possible to measure and record investigation parameters in the rectangular and polar coordinates. The systems of recorders, executed on the FHD base permit the carrying out of recording in combined system of coordinates (rectangular and polar, simultaneously) (89).

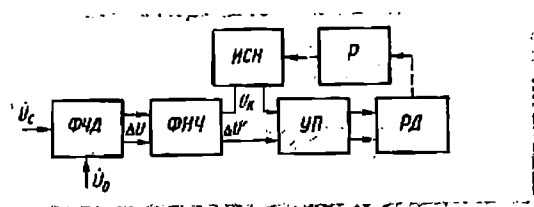


Fig. 210

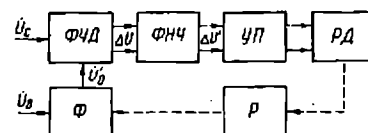


Fig. 211

The RCQ systems are composed of the following nodes: the phase-discriminating detector, LF filters, the source of stabilized voltage (ISN), the amplifier with mixing (UP), the reversive motor (RM) with reducer (R). The operating principle of the RCQ systems can be illustrated by two examples. Fig. 210 shows the block diagram of the recorder, meant for the recording of components by direct reading at the FHD output. Voltage ΔU at the output of FHD gets recorded by means of the follow-up system in the automatic compensator of the direct current. For this, the voltage ΔU is prefiltered in FHD and fed as voltage $\Delta U'$ to the circuit of the amplifier with mixing UP, at the input of which the compensating voltage U_k from the ISN arrives simultaneously. Difference $\Delta U'_k - U$, transformed into variable voltage, gets amplified in UP and controls the rotation of the reversive motor until the difference is reduced to almost zero level. In this way the recording itself of ΔU voltage

is carried out by the compensation method.

The phase recorder operates in the following way by the quasicompensation method (Fig. 211). ΔU voltage, appearing due to the phase shift between signals U_c and U'_0 , passes through FHD, gets transformed into variable voltage and, amplifying in the UP block, rotates the reversible motor. The slid resistance in the system of even phase shifter F rotates until the phase shift of \dot{U}_c and \dot{U}'_0 voltages at the input will be 90° ($\Delta U=0$).

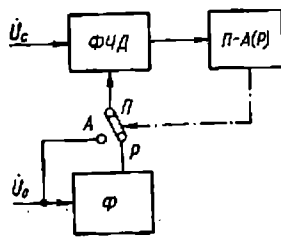


Fig. 212

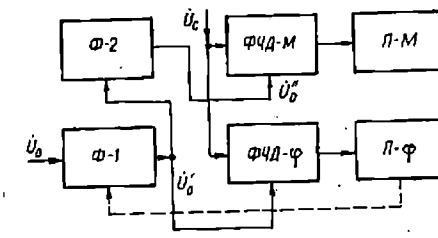


Fig. 213

Thus, it may be assumed that the main problem of the follow-up system of the recorder is the reduction of vectors at the FHD input to a phase shift of 90° by means of the even graduated phase shifter.

Recorders in rectangular coordinates. Fig. 212 shows the block diagram of RCQ of the active and reactive components by the direct estimation method. The recorder P-A (R) records, respectively, either the active or reactive components. The phase shift at 90° is carried out by means of phase inverter F.

Recorders in polar coordinates. The quasicompensation method of recording in polar coordinates is illustrated by the block diagram shown in Fig. 213. The task of the follow-up system of the phasemeter P- φ is to provide at any moment at the FHD- φ phase shift between U_c and U'_0 voltages of 90° . The necessary condition for normal operation of the amplitude recorder P-M is to provide at any moment by means of additional 90° phase shifter, F-2 zero phase shift between vectors of the measured U_c and the comparative U_0 , signals at the FHD-M input. This is almost always assured during the

operation of the follow-up system of the phase recorder $P-\varphi$ except at moments of very quick time variations of the phase, which are too fast for the follow up system of the phase recorder.

Recorders in combined system of coordinates. The block diagram of RCQ by direct estimation is shown in Fig. 214. The active component of U signal is measured and recorded at the out-put of FHD-A by means of recorder $P-A(U)$ in position A of switch $P-1$. The reactive component of U_c signal is measured and recorded at the output of FHD-R by means of recorder $P-R(\varphi)$ in position R of switch $P-2$. The phase shift of 90° at FHD-R is provided by the phase shifter $F-1$. Simultaneously signals at the output of FHD-A and FHD-R are transformed by two transformers $Pr-1$ and $Pr-2$, on frequency F of generator M of rectangular pulses. Signals, obtained as a result of this transformation, arrive at the circuit of quadratic summation SS (55), at the output of which is the cut-in amplifier, selective on frequency F (IU).

In work (53) it is shown that in this circuit the signal at the output of detector D , connected after IU, is directly proportional to the amplitude of measured signal U_c . Therefore, in the position M of switch $P-1$, recorder $P-A(U)$ can record the amplitude. The phase is recorded by phase recorder $P-R(\varphi)$, constructed on FHD- φ base with both the signals being limited by means of limiters O type at its inputs. In the position φ of switch $P-2$, the recording is of phase angle φ .

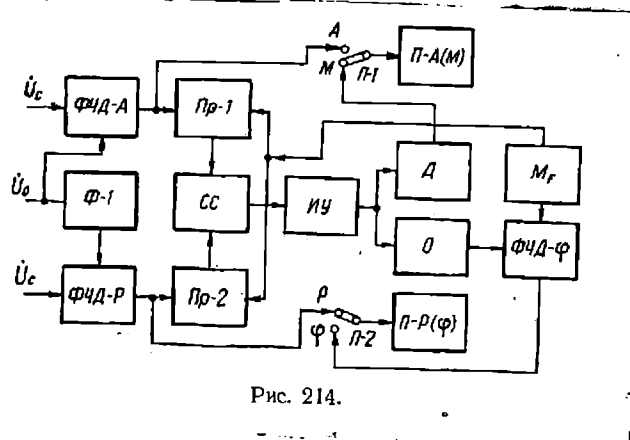


Рис. 214.

Fig. 214

2. Properties of RCQ of quasicompensation method of measuring.

The block diagram of the phase recorder by the quasicompensation method of measuring is shown in Fig. 215. The quality of the recorder is clearly defined in the analysis of its follow-up system with the actual curves on linear model (88, 89)*. Here are equations of individual units of the system:

$$U = CU_c \varphi; \quad (\text{XII. 1})$$

$$(T_2 P^2 + T_1 P + 1) U \phi = U; \quad (\text{XII. 1a})$$

$$U_y = K_y U \phi; \quad (\text{XII. 1b})$$

$$P(T_m P + 1) Q_{in} = K_4 U_y; \quad (\text{XII. 1c})$$

$$Q_{out} = \frac{Q_{in}}{i}; \quad (\text{XII. 1d})$$

$$\varphi_{out} = \frac{Q_{out}}{K \phi}, \quad (\text{XII. 1e})$$

where U - the voltage at the FHD output; C - the factor of FHD parameters;

$\varphi = \varphi_{in} - \varphi_{out}$, with low displacement angles $\varphi_{in} - \varphi_{out} = \frac{\pi}{2} + \varphi \mp \varphi$; T_1 (also T_4) - the time constants of transmitting function $A(r)$ of FHD,

determinable from filter parameters, sec; $T_2 = T_1 T_4$ - the product of time

constants, sec^2 ; U_f - the voltage at the output of LF filter; K_y , U_y - the

amplification factor and voltage, respectively at the output of the amplifier

with mixing; T_m - the electromechanical constant of motor; Q_{in} - the angular

shifting of motor; i - the reduction factor of the reducer; Q_{out} - the angular

shifting of the reducer's outlet axis; $K\phi$ - the proportionality factor of

phase inverter.

*In the deduction ^{for} the differential equation for reversible motor it is assumed that the system's moment of resistance reduced to the shaft is not present and that the value of the electromechanical time constant of motor T accounts for the moments of inertia of motor and pulley. In the deduction of LF filter equation it is assumed that the filter consists of two π -shaped RC-chains which are used in the real systems of these phase recorders and has time constant $T_1 = R_1 C_1$, $T_4 = R_2 C_2$ (90, 93).

On the basis of the individual units equations (XII. 1 - XII. 1e)

we may write the typical equation of a closed system

$$T_M T_2 P^4 + (T_1 T_M + T_2) P^3 + (T_1 + T_M) P^2 + P + K_1 = 0. \quad (\text{XII. 2})$$

Here

$$K_1 = \frac{K_d K_Y C}{K_{\Phi i}} U_c = K_0 U_c, \quad (\text{XII. 3})$$

where

$$K_0 = \frac{K_d K_Y C}{K_{\Phi i}}. \quad (\text{XII. 3a})$$

From formula (XII.3) it follows that the behavior of the preceding system depends on the level of the measured signal U_c . With its values determined, the linearized system (see Fig. 215) could be stable, neutral or unstable. The stability limit of the system's parameters should be determined from Gurvitch criterium (135):

$$\Delta_3 = (T_1 T_2 + T_2)(T_1 + T_M) - T_2 T_M - K_1 (T_1 T_M + T_2)^2 > 0, \quad (\text{XII.4})$$

where Δ_3 - third determinant of the typical equation (XII.2).

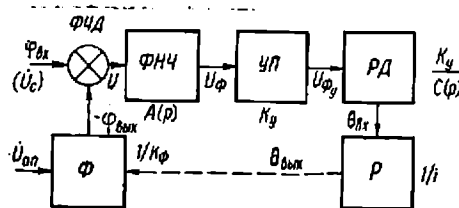


Fig. 215.

In accordance with formula (XII.4), the ultimate amplification factor of the system

$$K_{1ult} = K_0 U_{cult} \quad (\text{XII.5})$$

For the real system of the recorder, in which value K_0 is determined

from formula (XII.5), the ultimate value of factor K_{1ult} depends on the level of the measured signal \dot{U}_c . With a certain value of the signal ($U_c \gg U_{ult}$) the system is found to be unstable, as a result of which the normal operation of the phase recorder becomes disrupted.

It can also be shown that with the reduction of the signal U_c below a certain level, the errors of phase recording increase sharply within the system and its dynamic characteristics, on the whole, deteriorate. However, having compared the curves K_{1ult} obtained in the phase recorder by the quasicompensation method with curves, the determining behavior of the follow-up system of the second order vs. the variation of its parameters, we note that the variation of the signal \dot{U}_c is equivalent to the variation of the relative damping coefficient ξ_n in this system (see para 6, chapter XIII).*

In these conditions, the relative damping coefficient becomes dependent on the signal U_c and may vary from very low (at $U_c \rightarrow U_{c.ult}$) to very high (at $U_c \rightarrow 0$). The feature of RCQ has a definite value in phase recording. In the usual two-channel phase recorders (43), in the absence of one of the signals (measured \dot{U}_c or comparative \dot{U}_{comp}), there is no stable indication of a device. In the present case, the system is neutral in the absence of the signal \dot{U}_c and is in stable condition.

Thus, in the planning of phase recorders by the quasicompensation method of measuring, the parameters of the recorder's system should be so selected that the RCQ error, with the measuring of the phase within the amplitude variation range of the signal U_c , would be reduced to the permissible quantity.

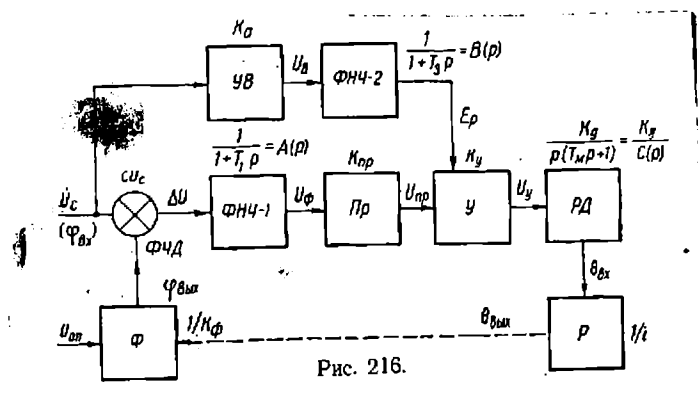


Fig.216

* The relative coefficient of damping $\xi_n = \frac{n}{\omega_0}$ depends on the damping coefficient n of the system and on the natural frequency ω_0 of undamped oscillations of this system ω_0 ; the latter is directly related to U_c variations.

If the characteristic of the damping factor vs. \dot{U}_c level does not for some reason meet the requirements of imposed problems and has to be reduced to the minimum, method described in (86,88) is sometimes applied. In this method, the use is made of the automatic gain control system "AGC-advance", which varies the amplification factor K_y of the amplifier in accordance with the level of variations of the signal \dot{U}_c ; and, as a result, the common amplification factor of the system varies very little. The diagram of the phase recorder in the quasicompensation method is shown in Fig. 216. The operation of the recorder itself is very little different from that of the system in Fig. 215.

The "AGC-advance" system consisting of the amplifier-rectifier UV and LF filter FNH-2, controls the first tube on the amplifier U by means of rectified and filtered voltage E_p . The necessary filtering of the high harmonics of signals after rectification is executed by the single-section RC-filter of low frequencies FNH-2. The intensity of voltage E_p is so estimated that with low values of the signal $U_c = U_{c_{min}}$ the total amplification factor of the amplifier would be the maximum, and with high values of the signal $U_{c_{max}}$ the minimum.

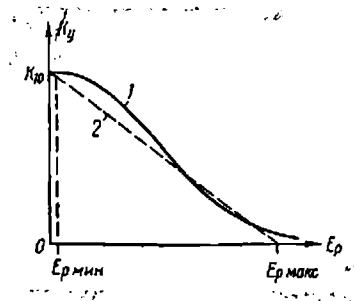


Fig. 217.

The variation curve of the amplification factor K_y , under the effect of signal E_p , proportional to U_c , is shown in Fig. 217. With variations of $U_{c_{min}}$ from $U_n(E_{p_{min}})$ to $U(E_{p_{max}})$, this recorder has a uniform sensitivity to the phase. The dynamic range of the signal \dot{U}_c depends on the type of applied AGC system and on the mode of operation of the LF filter

em (199).

Let us analyze the properties of RCQ with AGC system. We assume the main tolerance to be the same as in the system in Fig.215. But in deducting the equation of FNH-2, we assume that it consists of single-section π -shaped RC-filter:

$$\begin{aligned} (T_3 p + 1) E_p &= U_B; & U_B &= K_a U_c; \\ U_y &= K_y U_{np}; & U_{np} &= K_{np} U_{\phi}. \end{aligned} \quad (\text{XII.6})$$

The characteristics of K_y factor vs. voltage with the account of the curve in Fig.217 could be given as

$$K_y = \frac{K_{10}}{b_0 E_p}$$

where K_{10} - the maximum amplification factor of amplifier at $E_p \leq E_{p.\min}$;
 b_0 - the coefficient accounting for parameters of AGC system, v^{-1} .

By resolving the equation series (XII.6), we get typical equation of a closed system as

$$T_M T_3^2 p^4 + (T_1 T_M + T_2) p^3 + (T_1 + T_M) p^2 + (1 + K_2 T_3) p + K_2 = 0. \quad (\text{XII.6a})$$

where

$$K_2 = \frac{CK_{np} K_{10} K_y}{b_0 K_a K_{\phi i}}$$

From formula (XII.6a) it follows that the coefficient K_2 is theoretically independent of the \bar{U}_c level of the signal. Therefore, in the assumed variation range of \bar{U}_c , there is no relation between the recorder's sensitivity in the phase and the level of measurable signal.

Attention should also be paid to newly appearing characteristic of RCQ vs. time constant T_3 of the AGC circuit. In formula (XII.6a) coefficient $(1+K_2 T_3)$ at p , determines, as we know, damping of the system. Therefore, the presence of parameter T_3 , the value of which may be varied, permits adjusting within certain limits, the system's dynamics. This means that in a system with AGC stability, reserves could always be made higher than in a system without

However, in the presence of quick, sharp variations of \bar{U}_c voltage as a result of the action of interference on the preceding system of the phase recorder, the parameter characteristic of AGC circuit vs. T_3 leads to an

undesirable happening, called "distortion of the envelope", i.e., in the presence of a certain level of noise, similar in frequency to the signal \dot{U}_c at YB (AGC) input, or with quick amplitude variation of the signal itself the signals "envelope" appears at the AGC system, for instance, with the frequency beat of the signal due to noise, which has passed through the LF filter FWH-2. As a result the coefficient K_y of the amplifier Y varies under the effect of the "envelope" which in turn may distort the results of phase measuring and recording. In adverse conditions, this happening may completely disrupt the normal activity of the phase recorder.

3. Recording devices on galvanometer base.

The recorders made in the USSR SG-17, SK-100 and those made in other countries by "Brash" firm ABEM, etc. are devices which permit the recording in ink on paper tape the time variations of the electric current. The Soviet recorders (SG-17, SK-100) are single-track, those of foreign made are invariably multi-track. For instance, the recorder of ABEM firm has five recording channels (tracks) and one channel for making the position of the plane (Fig.218) (5). This galvanometric type of recorder writes with a heated rod on paper, covered with wax.

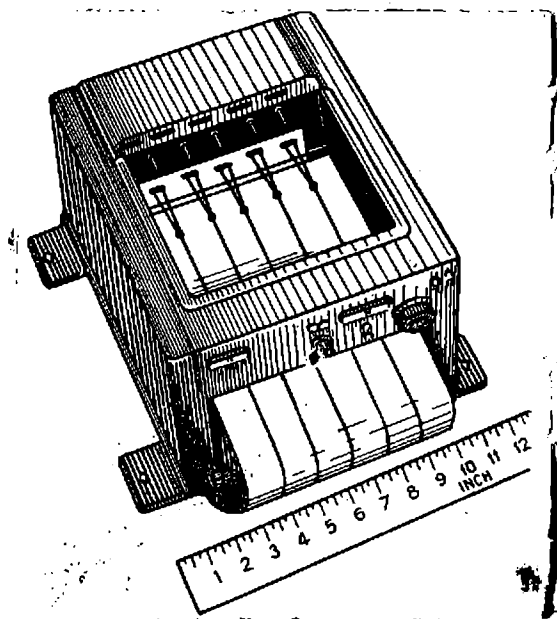


Fig.218

Let us analyse the recorders SG-17 and SK-100, used sometimes in the Soviet apparatus of aerial electric prospecting (123, 234). The recorder SG-17 consists of tape mechanism with table, an electric motor with reducer,

a galvanometer with a pen and ink pot, stamp mechanism and other fine details (Fig. 219). The record chart of this device is curvilinear. With denenergized galvanometer, the recorder pen is in the middle position. Complete deviation of the pen to the left or right takes place at current 0.5 ma. The resistance of the galvanometer frame 2800 ohm ($\pm 5\%$), critical resistance about 11 k-ohm.

The electric motor of tape mechanism is energized by direct current of about 100 ma at voltage 24 v, supplied directly by the network of the aircraft. By means of speed-switch, the reducer provides tape speed 1.8 or 5.4 m ($\pm 20\%$). The recorder is equipped with a printer, which permits plotting on paper tape digits from "00" to "99" at every digit with delivery of external control pulse of direct current 1.8 a with voltage of pulse source 24 v. The weight of the recorder is about 10 kg. The electric connection of the recorder with measuring unit and energizing device is through a common plug socket (SHP-50).

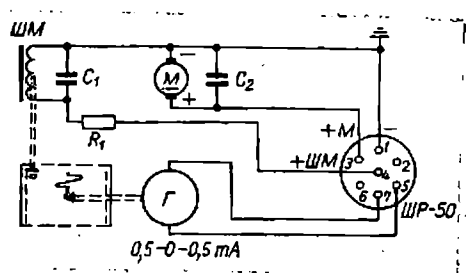


Fig. 219.

The recorder SK-100 (Fig. 220) has the same nodes as the recorder SG-17, but, in contrast to the latter, it has a mechanism which transforms the curvilinear motion of the pen into rectilinear. This permits recording the parameter in rectangular coordinates. Non-linearity of recording does not exceed $\pm 1\%$.

The reducer of tape mechanism is activated from the external mechanical drive or from its own electric motor of 5 watts, fed from the network of direct current 12 v. The width of recording is upto 100 mm. The needle of

the recording galvanometer in de-energized condition is in the extreme left-hand position. The total deviation current of the galvanometer is 5 ma, the frame resistance 3000 (± 100) ohm, the recording error 2.5%. The tape speed 1;2;5 and 20 mm during one revolution of the input shaft. The speed is changed over by a special switch of the reducer.

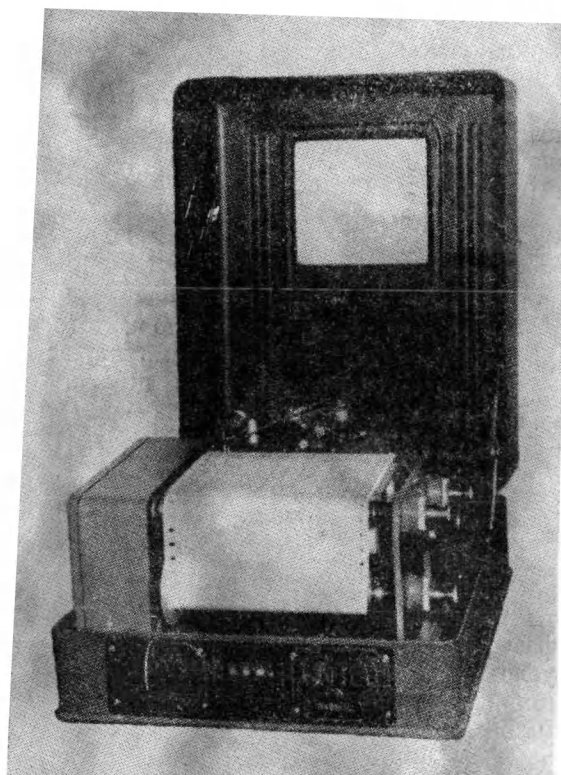


Fig. 220.

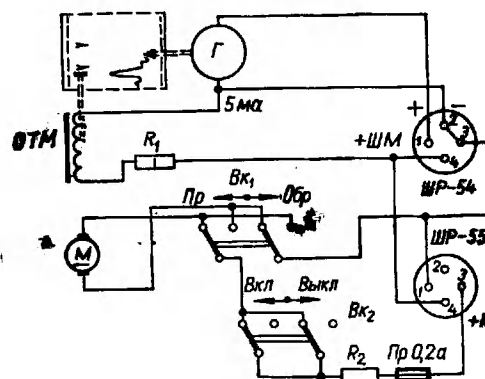


Fig. 221.

The recorder is provided with an electromagnetic marker, which makes it possible by means of a special pen to plot on the tape marks in the form of dashes (Fig. 221) with each individual pulse of direct current. The operating voltage of marker 12 v, the winding resistivity of electromagnet 250 (± 10) ohm. All the energizing voltages on the recorder are fed through two plug sockets (SHR-54, SHR-55); the energy supply to the electric motor could be taken directly from the energy network of the aircraft.

The use of the recorders SG-17 and SK-100 in flying conditions has shown insufficient stability of the writing device with open capillary recording with ink.

4. Recorders of compensation type.

Automatic bridges and potentiometers of direct current MS1-01, PS1-01 are frequently applied in the Soviet apparatus of aerial electric prospecting as direct recorders of the compensation type. The principle of the compensation method is that the measuring voltage is apposite to the voltage drop at a certain known resistance (slid resistance). The system of compensation type recorder consists of the follow-up system, which includes direct voltage changer (of discrepancy voltage) into variable, electronic amplifier, reversible motor, slid resistance and direct recording system.

In the apparatus of aerial electric prospecting, the measuring is generally of several parameters of the perceptible signal. Therefore, although the systems of recording are practically identical, their matching with the measuring systems is effected by different methods. And this demands unification of the multiple nodes of the follow-up system. But the measurable signal converting networks depend, as we know, on the type of outputs in devices for measuring the preset quantities. For instance, the output network of the device for measuring the amplitude (modulus) of the measurable signal (see Fig. 129) is asymmetric in relation to the ground, whereas the output networks of the phasemeter (see Fig. 140) and components meter (see Fig. 148) are symmetrical. Besides, some output networks (for instance, outputs of trigger phasemeters) are under high potential in relation to the ground, and others (for instance, the outputs of modulus and components meters) under low. Due to this, the networks, which convert direct voltage into variable voltage are planned for at least two types of outputs in the measuring systems

of recordable quantities - symmetric and asymmetric with an estimate of the specifics pointed out in the output potentials of the networks.

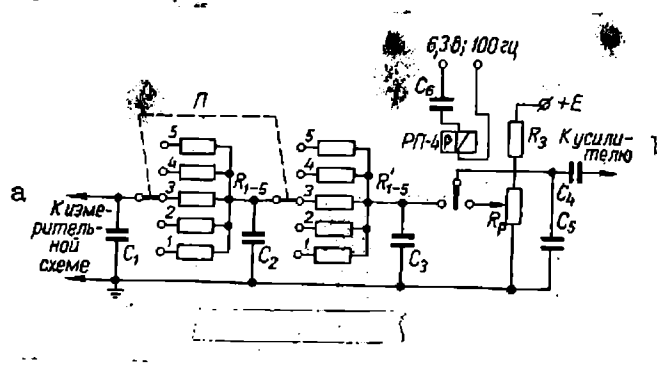
It is also necessary to take into account the requirements of providing control of the time constant (frequency transmission band) of the recording system, which determines the noise-proof quality of the measuring system as a whole and the speed of the pen from an extreme position to another. Adjustment of the time constant can be effected by the RC-filter through the variation of quantity of one of its elements (for instance, active resistance) and by other methods.

Let us analyze concrete networks for the conversion of direct voltage into variable, as applied in the recording systems.

Converting network for asymmetric output of measuring systems (for instance, module recording) is shown in Fig. 222. Connection of the network with the measuring circuit of the vacuum tube voltmeter does not affect indication by the device, since the network has sufficiently high input resistance. For the adjustment of the time constant, the network is provided with change-over switch P of R_{1-5} and R'_{1-5} resistances of the three-section RC-filter.

The capacitance of condensers C_1-C_3 is the same (4 mF). The values of filter resistances are selected keeping in view the possible variation of the time constant, for instance 1; 1.5; 2; 3 and 4 times in comparison with the natural time constant of the recorder.

After the filter, the recordable signal is compared in intensity with the voltage drop at the section of slid resistance R_p (by means of relay contact RP-4). The voltage unbalance through the condenser C_4 is fed to the electronic amplifier circuit of the recorder's follow-up system.

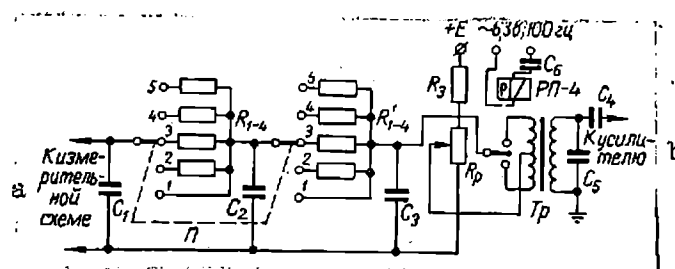


Key to Figure 222:

- a, To measurement circuit;
- b, To amplifier.

Fig. 222.

The condenser C_5 eliminates affecting the amplifier's operation of voltage overshoot during the change-over of the contact RP-4. Slid resistance R_p energizes from the source of stabilized voltage $+E$ through the damping resistance R_3 , made of manganin with error not over 0.5%.



Key to Figure 223:

- a, To measurement circuit;
- b, To amplifier.

Fig. 223.

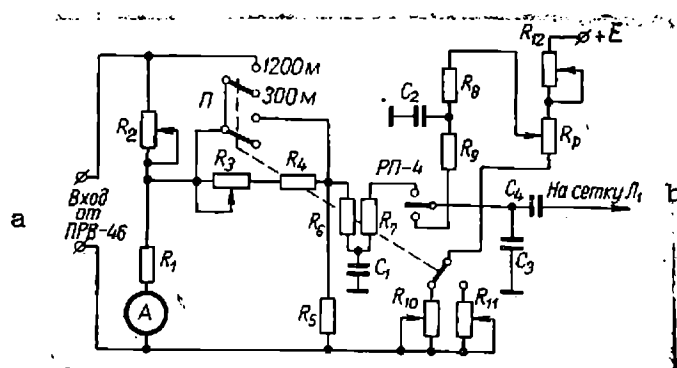
Converting circuit for symmetrical output of measuring systems. For recording the phase, the active or reactive components, their sum or difference on two frequencies (see paras 6,7 of chapter X) the network for converting direct voltage into variable (Fig. 223) is utilized.

The time constant is adjusted similarly with the above network. The condensers $C_1 - C_3$ of the RC-filter have capacitance 10 mF. With lower

capacitances, it is necessary to increase the resistance of the filter, which is undesirable due to higher pickup by them of external inductions in two-frequency operations.

To obtain an asymmetric transformer of converting network, in relation to the ground output, Tr is cut in at its output. The signal from the secondary winding of the transformer is delivered through condenser C_4 to the electronic amplifier of the recorder.

For recording the survey altitude, the application is of slightly modified converting network. Radio-altimeters applied for the determination of flight altitude, generally have relatively high-ohmic input with a high time constant. As a rule, at the output terminals of the altitude indicator there is a constant potential, differing generally for each individual device. The radio-altimeter RV-2 with indicator PRV-46 may serve as an example of this altimeter. Fig. 224 shows one of the possible converting networks, meant for connecting with indicator PRV-46. The input circuit of the converter consists of high-ohmic circuit of device A (set up directly in the apparatus of aerial electric prospecting) for visual control of the plane's flight altitude h and high-ohmic divider R_2 - R_5 . The input of the converter is connected with indicator PRV-46 of radio-altimeter RV-2.



Key to Figure 224:
a, Input from
PRV-46;
b, To grid of tube
 L_1 .

Fig. 224.

The control of the time constant in the altitude recorder is inexpedient due to the considerably natural time constant of RV-2; therefore, there is no input filter in the recording system. The range of recordable altitudes is changed by switch P. The signal to be recorded is compared, after the divider R_2 , R_3 , with the voltage drop on slid resistance R_p by means of relay contact RP-4. Voltage unbalance is fed through condenser C_4 to the recording amplifier for further processing by the follow-up system.

The needle of the indicator FRV-46 is adjusted at zero with initial current I_0 of the altimeter directly at the indicator. Resistance R_2 serves for the zero adjustment of indicator A in the altitude recording system and, for the compensating voltage, generated by the initial current, resistances R_{10} and R_{11} respectively are cut in to the system for each of the adopted ranges of the recordable altitudes. The slid resistance is energized by the stabilized direct voltage from source E.

To eliminate noises, which may appear during the change-over of the relay contact, and to distort considerably the useful signal, T-shaped RC-filters R_6 , C_1 , R_7 , and R_8 , C_2 , R_9 . Semi-conductive triods, instead of polarized relay, could be applied in this system a converter of direct voltage into variable voltage.

An important element of any follow-up system is the electronic amplifier. Amplification of the signal to be recorded is done in two stages: at first the voltage is amplified upto the intensity required for the controlling tubes of the power amplifier, then the signal power is brought up by output stage to intensity, sufficient for controlling reversible motor of recorder's follow-up system.

When working out recording systems for the unifying follow-up systems

of recorders it would be advantageous to use the same type of amplifier, which could be made up on electronic tubes, semi-conductive or magnetic elements. An example of this are the AERI-2, AERA-2, etc. In this apparatus the voltage amplifier is of three-stages (tubes 6N2P) with push-pull power amplifier (tubes 6P14P) (see Fig. 141, 143).

To generate the local reverse feedback on the current in the cathode circuit of tubes L_{12} and L_{13} connection of resistances R_{152} , R_{155} , R_{160} is made. Coupling between stages is effected through variable condensers C_{82} , C_{85} , C_{90} . The adjustable resistance R_{151} controls the amplification factor of the voltage amplifier. The second and subsequent stages are encompassed by a ring-shaped reverse feedback on voltage, which is taken off the adjustable resistance R_{167} and fed into the cathode circuit of the tube L_{12} second half. The same resistance controls the amount of the reverse feedback and the extent of stability of the system.

On the right half of tube L_{13} is assembled the phase-invertor for energizing the push-pull output stage (L_{14} , L_{15}) of power amplifier with output transformer Tp_3 , voltage from which is fed to the winding of the reversible motor. Condenser C_{89} tunes the secondary winding of Tp_3 to the main frequency of conversion, and the penetration of high harmonics current into the winding of the motor gets considerably dampened.

The output voltage of the amplifier, when there is unbalance, rotates reversible motor RD-09 of the recorder, which shifts on the slid resistance R_p to a position of matching, i.e., to the moment of parity between voltages arriving from the measuring system and taken off the slid resistance R_p . Thus, each value of the signal, taken off the output

of the measuring system, corresponds to a certain position of the slid resistance and mechanically coupled with it, carriage with indicator and writer.

Stable work of the operating system is assured by bringing in the feedback on the variation speed of mismatching. The speed of the carriage cannot change immediately after an instantaneous change of the torque (from action of mismatching signal) as due to inertia of movable parts it decreases gradually. At the time when the motor shifts the slid resistance to the position of matching, the speed may not be exactly zero. Then under the effect of inertial forces the mobile system will continue its motion and the cursor of slid resistance will pass the position of equilibrium. The unbalance voltage induced by this builds up a reverse torque of the motor, i.e., its reverse stroke. This oscillating motion will continue until kinetic energy, reserved in the mobile parts, is not totally consumed for overcoming the moments of friction and inertial forces.

To ensure quick damping of the mobile system on its approach to a position of equilibrium, there is feedback in the amplifier on the speed of mismatching variation, which could be implemented by feeding part of the reaction voltage of the motor's armature into one of the voltage amplifier stages (for instance, in a system with a separate tacheogenerator DID-0.5). In this case, when approaching the position of equilibrium, the reversible motor will slow down its movement.

5. Constructive design of the recorder of complex quantities of compensation type with follow-up system.

Automatic compensators (bridges) PS1-01, EPP-09, MS1-01, of serial production, have become increasingly popular during the last few years in the Soviet apparatus of aerial electric prospecting. For use in this type

of prospecting, certain reconstruction of the mechanical part of these devices has to be made.

The application of the conversion circuit with identical output makes it possible to unify the recording devices almost completely. Let us take, for example, the unified recorder of measurable parameters, used in AMRI-2 apparatus.

Recorders, set up in compartments of the measuring group cabinet (one with a closed front panel, the other with removed), are shown in Fig. 225. The general view of the recorder, removed from the compartment of the cabinet, is shown in Fig. 226, a (front with open tape mechanism), 226, b (the top), 226, c (back).

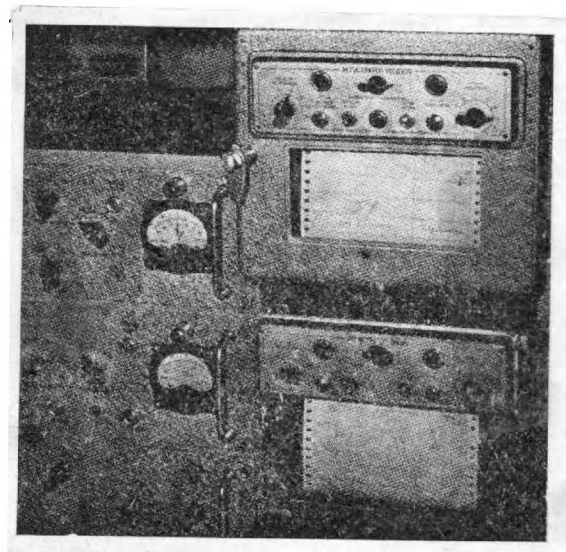


Fig. 225

The following are the main parts of the recorder: rotating cantilever, reversible motor with slid resistance, synchronous motor with reducer, tape mechanism, writer (carriage with automatic pen), printer, control board, cover with hinged glazed door.

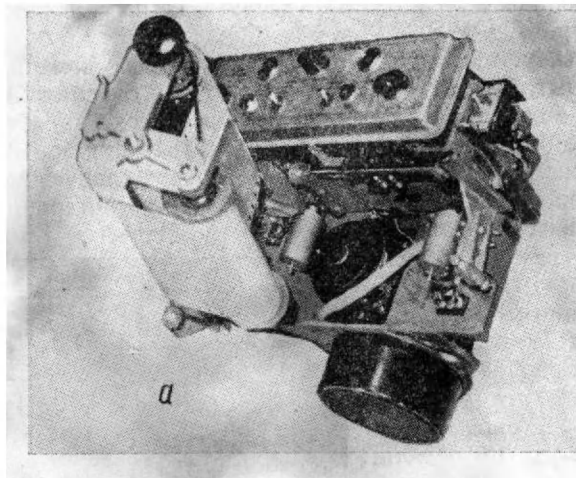


Fig. 226

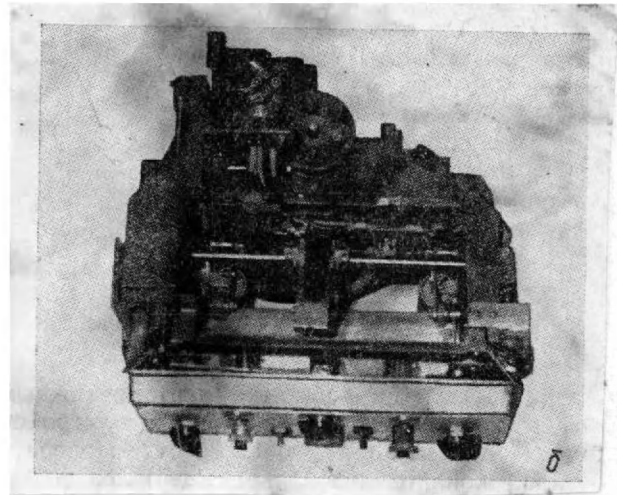
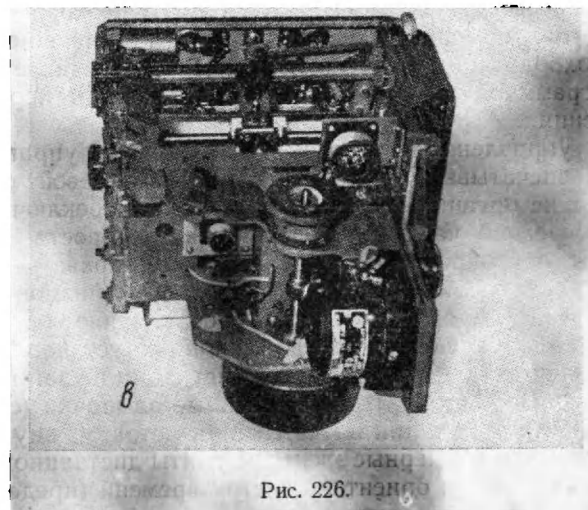


Fig. 226 b.



The rotating standard cantilever, on which all nodes and details are set up, is fixed in the cabinet's compartment by clasp joints. With removed cover, the recorder can be turned around the axle at an angle over 135° ; this makes it easy to check all the details set up on it. The recorder is fixed in the compartment by a catch with lever, fitted on the right hand side of the main cantilever. A second cantilever also standard, with tape mechanism is fixed on clasps to the front portion of the main

cantilever. At the top of the latter, the writer and electromagnets of the printer (see para 1 of chapter XIV) and details for transporting the transfer tape and control panel are arranged. Set up within the hollow space of cantilever are the synchronous motor with reducer, reversible motor RD-09, slid resistance and kinematic elements, by means of which the motion is transmitted from the motor to slid resistance curser and to the carriage. The reducer provides two tape speeds - 3 and 6 m/hr. The speed is changed over on the control panel.

The controls of the recorder and printers are set up on the control panel. The face of the panel contains the following controls: on the left- the change-over switch of recording limits in the middle - the change-over switch of tape speed; on the right- the change-over switch of indicator . numbers, tumbler for commutation of time markers (measuring limits) and guiding lines for their automatic remote printing or by hand with knobs set up on the same panel; tumbler for cut-in of the system for recording the measurable parameter. Fitted on the panel are signal bulbs (with glass light filters) to indicate the printing of marks. On the inside of the panel are the piston electromagnets for remote switch-over of mechanisms for marking guiding lines, time marks (limits). The composition of mechanisms includes printing wheels with numbers (indices) of limits and guides.

The recorder cover is removable and has a hinged glass door for continuous observing of recording and putting in, if necessary, remarks on the chart during the recording of operation. On the right-hand side of the cover is a handle with a built-in lock.

6. Marking circuit of time breaks, measuring limits and guide lines.

In multirange measuring in aerial electric prospecting, it is

sometimes convenient and more often necessary to mark on the charts the numbers of measuring ranges at their cypher. Due to the irregular speed of the tape it is very convenient to use a time marker. For tying the results of the survey to the locality on diagrams, prominent features should be marked on topography. There is quite a number of systems, which carry out these functions and their choice depends mostly on the constructor's whim. As an example, let us make the circuit marking guides, time breaks and measuring ranges, implemented in AERI-2 apparatus (Fig. 227).

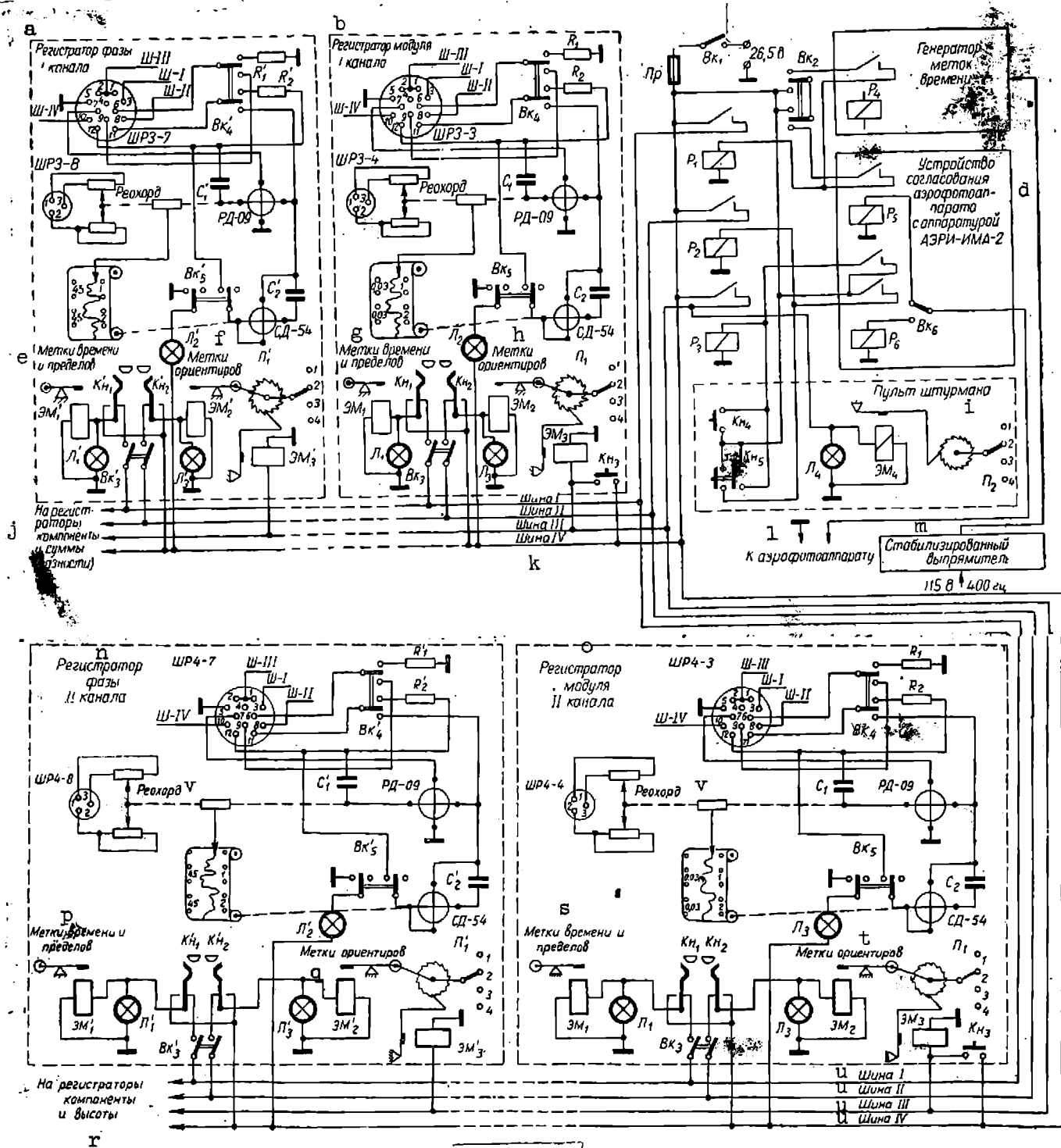
Time breaks could be fed to printers both from the inner mark generator and from the aerial photo-camera. Time breaks from the inner generator are fed in the following way. Relay P_4 closes the circuit of intermediate relay P_1 , which, while operating, cuts in by its contacts voltage of board power supply network + 26.5 v to busbar SH-1. Relay P_1 itself is energized from the same source. Voltage from busbar SH-1 through tumbler Bk_3 (Bk_3' , Bk_3''), which connects the time (range) marker of recorders, is delivered through normally closed contacts Kh_1 (Kh_1' , Kn_1'' , ...) to the windings of printers electromagnets. Connected parallel to the electromagnet windings are signal bulbs L_1 (L_1' , ...).

Voltage + 26.5v is put in from busbar SH-IV by means of knobs Kn (Kn_1 , Kn_2 , ...) to the windings of electromagnets EM (EM_1 , EM_2 , ...) in printers, which makes it possible for the operator to put marks by hand directly on the recorders.

Switch Bk_2 enables delivery to relay P_1 of control voltage into the circuit of time breaks (ranges) from the inner generator, as well as from the aerial photo-camera. The marking of guides is done either automatically from the camera (when photographing prominent features), or manually (by navigator) by means of knob Kn_5 from a special control board. Numbers of

Key to Figure 227:

a, Phase recorder, channel I; b, Module recorder, channel I; c, Generator; d, Device for matching aerial photography with apparatus AERI-IMA-2; e, Time marker and limits; f, Orientation markers; g, Time and limit markers; h, Orientation markers; i, To recorders of component and sum (difference); j, k, Track I, II, III, and IV; l, To camera; m, Stabilizing rectifier; n, Phase recorder, channel II; o, Module recorder, channel II; p, Time and limit markers;



q, Orientation markers; r, To recorders of component and altitude; s, Time and limit markers; t, Orientation markers; u, Tracks; v, Rheostat.

Fig. 227

guides (prominent local features) are switched-over by relay P_3 , which is controlled automatically by the camera or manually and also by knob Kn_4 - from navigator control or by knob Kn_3 -directly from the control panel of the modulus recorder. This automatically changes the number (index) of the guide.

Tumbler $BK_5(Bk'_5, \dots)$ cuts in the synchronous motor SD-54 of the tape mechanism; at the same time, it switches on indicator bulb $L(L_2, L'_2, \dots)$. Tumbler $Bk_4(Bk'_4, \dots)$ switches on the finishing circuit or ballast resistance $R_1(R'_1, \dots)$ with unoperating recording system to ensure constant load of the rectifier +300v of recording amplifier supply.

CHAPTER XIII - MEASURING ERRORS AND INCREASING ACCURACY OF MEASURING INSTRUMENTS

1. Classification of errors

One of the most important characteristics of the measuring and receiving apparatus in any method of aerial electric prospecting is its practical sensitivity, which determines the ability to detect and measure weak signals from the conductive objects sought for.

The actual sensitivity depends both on the level of noise, arising within the receiving system itself, and on the level of interferences, affecting it from outside. Therefore the real sensitivity of the receiving apparatus is the sensitivity at which the useful signal at its output could be reliably detected and measured on the background of another signal, caused by internal as well as external noises (20, 132).

Since the process of geophysical survey is confined to detecting and measuring of useful signals from geoelectric irregularities or the ore bodies, it has its own intrinsic errors just like any other process. The real sensitivity of the measuring-receiving apparatus may only be increased when the origin and the nature of these errors is known and everything is available for estimating their effect on measuring results and finding ways and means for their reduction. With the availability of all required data, a fundamental approach is possible for a rational resolution of the problem pertaining to increasing noise-stability and resolving power of the receiving systems, applied in aerial electric prospecting.

It is possible to point out three main groups of errors, characteristic of any apparatus used in aerial electric prospecting

(117): 1) instrument errors; 2) errors of vibration nature and those due to change in the preset orientation of field receiver, and also errors caused by the effect of the external sources of noise; 3) methodical and geological errors.

The resultant error γ_{res} is determined by geometrical summation of its components:

$$\gamma_{pe} \approx \sqrt{\gamma_1^2 + \gamma_2^2 + \gamma_3^2} \quad 100, \% \quad (\text{XIII. 1})$$

where $\gamma_1, \gamma_2, \gamma_3$ - errors of the first, second and third groups respectively.

Determination of measuring error in conditions of aerial electric prospecting is extremely difficult. Since the magnitude of γ_{res} is determined by many objective and subjective factors, estimation of its components would have been most correct by the use of methods of the probability theory (165). However, for practical purposes it would be sufficient to determine the resultant error of the method from formula (XIII. 1).

It may be assumed that the relative error of the first group γ_1 is inherent to all receiving electronic systems, used in the measuring apparatus of aerial electric prospecting, and for many versions of the induction method this error is of approximately the same magnitude. The second and third groups of errors are also characteristic of the majority of methods in aerial electric prospecting, though different in magnitude for various methods.

Each of the three main groups of errors could in turn be divided according to the type of their source, its characteristic and results of source effect on the measuring and receiving system.

The first group of errors is divisible into static and dynamic errors

which include the basic and supplementary errors of the apparatus, errors from the effect of noises, due to microphone sound of input circuits and fluctuation noises in receiving elements, as well as dynamic noises of complex quantity recorders (time constants of receiving and amplifying channel is usually less than the time constants of recorders).

The second group includes errors caused by the vibration of receiving elements or receiving systems in the magnetic field of the Earth, incidental changing by field receiver of the preset orientation, effect on receiving elements of atmospherics, signals of broadcasting and other radio-stations, effect on receiving elements, input circuits or measuring apparatus of sound from rotating screws (acoustic errors) and power equipment of the plane or helicopter.

The third group of errors is of specific nature. The emergence of these errors is due to the following: disruption of reciprocal position of the field's source and receiver by the random variation of the geometry of the system (this is peculiar to the induction method), effect of metal parts (body) of plane or helicopter, effect of irregularities of surface detritus and surrounding medium, topography of locality and the nature of the soil.

Each of the three main groups of errors is divided also into systematic and random errors. For instance, error from the interference of radio-stations is of random nature.

The total error of measuring apparatus γ_1 is composed of the total systematic $\theta_{\Sigma t}$ and random errors $\xi_{\Sigma t}$. The random errors are summed up geometrically, i.e., according to quadratic law (at various time instants they may have different values and signs and compensate each other

partially (193):

$$\varepsilon_{tot} = \sqrt{\sum \varepsilon_i^2} \quad (\text{XIII.2})$$

where ε_i - components of random error.

The systematic errors are summed up algebraically with an estimate of their highest possible values:

$$\theta_{tot} = \sum \theta_i, \quad (\text{XIII.3})$$

where θ_i - components of systematic error.

Thus, the total error of the apparatus γ_1 , denoting its accuracy, is determined by an algebraic sum, in which the total random error is taken with the same sign as the total systematic error (193):

$$\gamma_1 = \theta_{1 \text{ tot}} + \varepsilon_{1 \text{ tot}} \quad (\text{XIII.4})$$

The approach is similar to the determination of components γ_2 and γ_3 of resultant error of the method.

All the enumerated errors could be determined according to the recommendations given in (165, 193). However, the specific operation of the apparatus in aerial electric prospecting necessitates a special approach to determination of one or the other error. The estimation of errors accounting for specificity of aerial electric prospecting will show the virtual working condition of the measuring instruments.

One of the main characteristics of the receiving and measuring devices in aerial electric prospecting is their protection against interference. This determines to a considerable extent their meteorological qualities, in particular measuring the errors. To estimate the required protection against interference, it would be expedient to analyze those

main factors which determine the general level of interferences of various origin affecting the receiving and measuring devices and to specify their errors of measuring. Moreover, it is necessary to examine in more detail those errors, which have specific nature in aerial electric prospecting. It is also necessary to systematize, to estimate qualitatively and quantitatively individual components of the resultant error separately in the three groups and then, for comparison, to determine the resultant error of measuring, typical for one of the other method of aerial electric prospecting with harmonic field.

The analysis of circuits for electric compensation of the primary field signal in the apparatus of induction aeromethod and exposure of determining compensator errors makes it possible to select well-founded optimum measurable parameters of residual signal.

Thus, the presence of the above errors and the problem of measuring signals of very weak fields enables us to come to the conclusion that the relatively high demands of accuracy in measuring, imposed directly on the measuring instruments, are quite warranted.

In evaluating the resultant error of measuring it is possible to assert that although random errors are present, they are not so significant and are not so often encountered; therefore, it is not in every condition that they have to be accounted for, whereas analysis and estimate of systematic errors are of primary importance.

2. Instrumental errors

The receiving and measuring apparatus, applied in aeromethods of electric prospecting, is mostly a complex of electric and radio-measuring systems and devices, which operate in specific, unfavorable conditions due to their set-up on aircraft (considerable vibrations, wide range of

variation of surrounding temperature, considerable moisture of air, in some cases upto 100%, etc.). These conditions contribute to the increment of error in the apparatus for measuring.

In aerial electric prospecting, the instrumental error is compounded of the basic error in measuring blocks and nodes, including field receiver and input circuits, due to fluctuation noises, and also of additional errors, specified by the effect of external factors (temperature, pressure, etc.), detuning of frequency, instability of power supply sources, effect of microphonic noises on the input circuits of receiving and measuring systems.

At present it is quite possible to reduce the basic error of individual measuring systems of selective measuring amplifiers, phase-sensing voltmeters, phasemeters, etc.) to 1-1.5% of measurable quantity. However, such components of the basic instrumental error as incorrectness, admitted in determining parameters of field receiver, possible variation of these parameters during measurements, incorrect estimate of amplification factor of the whole set of measuring apparatus (receiving channel*, etc.) increase the basic error of the receiving channel.

In the apparatus of aerial electric prospecting, all nodes, except the field receiver and gondola preamplifier, operate at stable temperature within the cabin of the aircraft; therefore, the temperature error is practically constant. In field receivers, however, specially if they are made as coils with ferrite cores, temperature error in relation to weather conditions may considerably vary with time and become very high.

*The precise calibration of this channel and its periodic checking reduce the basic error of the receiving-amplifying apparatus to a magnitude not exceeding 1.5-2%.

Highly-sensitive magnetic field receivers (with the use of ferrite cores) are at present developed to operate in the frequency range from a few tens to several thousands cps, which practically show no instability in a temperature range $-15 - +45^{\circ}(125)$. These magnetic field receivers are successfully applied in the apparatus of many aerial methods of electric prospecting.

To stabilize the amplification factor of the preamplifier or gondola amplifier, the application is of a penetrating reverse feedback and highly-stabilized supply source, time and temperature, stable details etc.

Additional error in the remaining systems of the measuring apparatus, specified by frequency detuning, instability of supply source, etc., could be made quite negligible without any difficulty. By thermal compensation and thermal stabilization of individual nodes and elements of measuring circuits, quartz crystal control of operating frequency of master oscillator and, therefore, frequency of comparative, compensating and calibrating signals the additional error could be brought down to 0.5-1%.

The natural level of noises of the measuring system and of microphonic noise could be reduced with application of certain protective measures, to a magnitude, which has practically no affect on additional and summarized instrumental errors.

The results of tests, carried out with receiving and measuring apparatus of BDK and induction methods (AERI-2), have shown that the summarized additional error is actually not over 1%, and the summarized fundamental error - 4%.

Given further is a brief description of factors, specifying the appearance of fundamental and additional errors in the selective amplifier,

measurers of modulus, components and phase of the signal being measured and quantitative appraisal of these errors.

Selective amplifier. In para 3 of Chapter X it has been pointed out that, in selective amplifiers of the measuring apparatus in aerial electric prospecting, the application is of selective LC- or RC-filters. The fundamental error in these amplifiers is caused mainly by the incorrect matching of selective filter elements, and the additional - by their temperature instability. The fundamental error is reduced by the careful matching of filter elements and its precise tuning to the operating frequency. During application, the main role is of the additional error. Therefore, the selective amplifier circuit is chosen with an estimate of temperature instability of its amplification factor in the transmission band of frequencies.

It is well known that in selective LC-circuit, with parameter variation of L or C circuits due to temperature effect, the variation is only of the tuning frequency of this circuit, whereas the amplification factor of the stage (specially with the amplification circuit on electronic tubes) and the Q-factor remain practically unchanged, if the measured frequency remains similar to that of circuit tuning or coincides with it. In selective RC-circuits, temperature variation causes not only deviation of the resonance frequency, but also considerable variations of the amplification or transmission factor and of Q-factor. Therefore, it may be assumed that the main source of the summarized error in the selective amplifier is the temperature instability of elements in filter sections with the use of vacuum-tube amplifying circuits or the one mentioned and temperature instability of transistors in amplifying circuits with semi-conductors.

In selective LC-amplifiers of low frequency with parallel LC-circuit, there is amplitude instability with the use of ferrite toroidal cores due to amplitude variation of measurable signal. Moreover, temperature instability is also typical of these amplifiers. All this specifies possible deviation of the tuning frequency upto 5-10% and variation of the amplification factor, as a result of which there is a considerable additional error in measuring.

The temperature instability of highly selective LC- and RC-amplifiers of low frequency is analyzed in detail in (15). For the selective amplifier with a single LC-circuit the relative drift of tuning frequency with temperature variation can be determined from ratio

$$\frac{\Delta \omega_0}{\omega_0} = - \frac{1}{2} \left(\frac{\Delta L}{L} + \frac{\Delta C}{C} \right), \quad (\text{XIII. 5})$$

where ΔL and ΔC - variation respectively of inductance and capacitance of the circuit with temperature variation; ω_0 - angular frequency of tuning, $\omega_0 = \frac{1}{\sqrt{LC}}$.

In the case of using Alsifer cores and paper condensers of low stability $\frac{\Delta L}{L} \ll \frac{\Delta C}{C}$. Therefore, it may be assumed that

$$\frac{\Delta \omega_0}{\omega_0} \approx - \frac{1}{2} \cdot \frac{\Delta C}{C}. \quad (\text{XIII. 6})$$

Here

$$\frac{\Delta C}{C} = \alpha_c \Delta t, \quad (\text{XIII. 7})$$

where Δt - temperature drop; α_c - temperature coefficient of the condenser (TKE).

The dependence of the working amplification factor of the selective amplifier on required Q-factor at low TKE values is shown by formula

$$K_p = \frac{K_0}{\sqrt{1 + Q_2^2 \left(\frac{\Delta C}{C} \right)^2}} \quad (\text{XIII. 8})$$

Due to variation of the working amplification factor of the selective amplifier with temperature there is emergence of error, the relative magnitude of which may be up to several per cents even for high-quality selective systems.

In the usual selective RC-amplifiers, the fundamental error due to possible deviation filter elements, nominal values from the calculated could be appreciable and this must be taken into account. Formulas are given in (62, 238), which permit us to make a general determination of allowable transmission band of frequencies in accordance with the present general instability of amplifier's parameters. However, in literature, as a rule, no recommendations are given for the choice of the deviations allowed for individual RC-filters, which makes it rather difficult to determine the fundamental error of the selective amplifier as well as the instability of those elements of filter which specify the highest variation of amplitude-phase characteristics of this type of amplifier.

To prove the validity of demands imposed on details in RC-filters in respect of their stability and precise adjustment, let us take an RC-amplifier with filter in feedback circuit. Here is an example of theoretical estimate of parameters of the system, most popular in practice, of selective RC-amplifier (Fig. 228) and symmetrical double T-shaped RC-filter (Fig. 229) (62, 187).

Amplification factor of RC-selective amplifier

$$K = \frac{\dot{U}_{Bblx}}{\dot{U}_{BX}} = \frac{\dot{K}_0}{1 + \dot{\beta}_0 \dot{K}_1} \quad . \quad (\text{XIII. 9})$$

If the module coefficient of amplification in the feedback section $(K_1) < 1$, it is a most common case of filter being connected ^{with} the feedback circuit, but if $(K_1) \gg 1$, - it is a case of filter being connected circuit of amplified feedback.

It is known that the transmission ratio of double π shaped RC-filter, tuned to frequency ω_0 , at any other frequency ω will be

$$\dot{\beta} = - \frac{1}{1 - j \frac{\rho_0}{\rho_0^2 - 1} m} \quad , \quad (\text{XIII. 10})$$

where $\rho = \frac{\omega}{\omega_0}$; m - coefficient depending on the ratio of filter elements. In a particular case, when $R_1=R_2=2R_3$ and $C_1=C_2=\frac{C_3}{2}$, coefficient $m = 4$.

On frequency $\omega = \omega_0$ with the calculated values of filter elements the transmission ratio should be zero. However, due to unavoidable deviations of filter parameter from the calculated ^{β} values on frequency ω_0 we have $\dot{\beta} \neq 0$.

Denoting the real and imaginary parts of $\dot{\beta}_0$ by a and b respectively, then

$$\beta_0 = a + j b.$$

With a minor deviation of frequency ω from ω_0 it is possible to assume with sufficient accuracy that the transmission ratio of the real 2T-RC-filter composes

$$\dot{\beta} = - \left(\frac{1}{1 - j \frac{\rho_0}{\rho_0^2 - 1} m} + \dot{\beta}_0 \right) . \quad (\text{XIII. 11})$$

In this case the amplification factor of the amplifier is determinable from formula:

$$\dot{K} = \frac{\dot{K}_0}{1 + \dot{K}_0 \dot{K}_1 \left(\frac{1}{1 - j \frac{\rho_0}{\rho_0^2 - 1} m} + a + jb \right)} . \quad (\text{XIII. 12})$$

Coefficients K_0 and K_1 in the range of operating audio-frequencies could generally be taken as independent of frequency ω . It may also be assumed that phase-shifts of amplifiers on frequency ω_0 , prior to the connection of feedback, are zero, i.e. \dot{K}_0 and \dot{K}_1 are real on the frequency of quaresonance*.

It can be shown, that with low deviations of frequency the term $\frac{\rho_0}{\rho_0^2 - 1} m$ is considerably higher than one.

Denoting

$$\gamma = \frac{\rho_0}{\rho_0^2 - 1} m,$$

we get after transformations

$$\gamma = m \frac{\omega \omega_0}{(\omega + \omega_0)(\omega - \omega_0)} .$$

If it is taken that $\omega - \omega_0 \approx \Delta \omega$ and assumed $\omega_0 - \omega \approx \omega_0^2$, and $\omega + \omega_0 \approx 2 \omega_0$, then

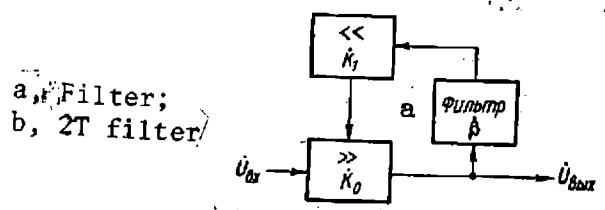


Fig. 228

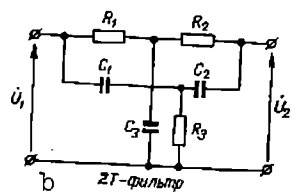


Fig. 229

$$\gamma = \frac{m}{2} \cdot \frac{\Delta \omega_0}{\Delta \omega} \quad (\text{XIII } 13)$$

The given formula proves that with low deviations from frequency ω_0 ratio $\frac{\Delta \omega}{\omega_0}$ is always considerably less than one. Since in 2T-RC-filter $m > 4$, then $\gamma \gg 1$. On this basis, after certain conversions, formula (XIII. 12) can be simplified in the following way:

$$1 + a + b\gamma \approx 1 + b\gamma; \quad \gamma(1 + aK_0K_1) - bK_0K_1 \approx \gamma(1 + aK_0K_1);$$

$$1 - j\gamma \approx -j\gamma; \quad 1 + K_0K_1 \approx K_0K_1.$$

After substitution of these terms into formula (XIII. 12) and slight conversions for the modulus of ratio $\frac{\dot{K}}{K_0}$ we get the following equation:

$$\frac{\dot{K}}{K_0} = \frac{\gamma}{\sqrt{K_0^2 K_1^2 \left(b + \frac{1}{\gamma}\right)^2 + (1 + aK_0K_1)^2}} \quad (\text{XIII. } 14)$$

From this equation it follows that ratio $\left| \frac{\dot{K}}{K_0} \right|$ attains maximum in condition

$$\frac{1}{\gamma} = -b \quad (\text{XIII. } 15)$$

*In actual systems, this condition is usually observed, specially when the amplifier with amplification factor K_0 has its own intrinsic active reverse feedback.

Hence it is easy to determine the variation of resonance frequency of the selective amplifier due to the imperfection of 2T-RC-filter. Substituting in equation (XIII. 15) γ values from formula (XIII. 13), we get

$$\frac{\Delta \omega}{\omega_0} = - \frac{m}{2} b. \quad (\text{XIII. 16})$$

Amplification on resonance frequency

$$\left| \frac{\dot{K}}{\dot{K}_0} \right| = \frac{1}{1 + a K_0 K_1}. \quad (\text{XIII. 17})$$

From the last two equations it follows that the variation of resonance frequency is due to imaginary, and the amplification factor - real component of $\dot{\beta}_0$. The variation of resonance frequency is determined only by the deviation of T-filter parameters and does not depend on the amplification factor \dot{K}_0 .

Equations (XIII. 16) and (XIII. 17) also permit the fixing of the limits of allowed variations in the value of resistances and condensers forming T-filter, so as to prevent deviations of $\Delta \omega$ and ΔK above the fixed value.

Table 21 gives values for coefficients a and b of symmetrical 2T-RC-filter ($R_1=R_2=2R_3$, $C_1=C_2=\frac{C_3}{2}$). According to the data of this table, increment of parameters R_1 , R_2 , C_1 and C_2 mainly affect the variation of resonance frequency and to a lesser extent variations of the amplification factor on resonance frequency as compared to the corresponding variations of parameters R_3 and C_3 . This permits the conclusion that it would be more expedient to tune the frequency of

of the resonant amplifier by varying resistances R_1 , R_2 or capacitances C_1 and C_2 and the coefficient of amplification on resonance frequency - resistance R_3 or capacitance C_3 .

Table 21.

Parameters	Substance part of transmission factor a	Imaginary part of transmission factor b
$R_1; R_2$	$-\frac{1}{16} \cdot \frac{\Delta R}{R}$	$+\frac{3}{16} \cdot \frac{\Delta R}{R}$
$C_1; C_2$	$+\frac{1}{16} \cdot \frac{\Delta C}{C}$	$+\frac{3}{16} \cdot \frac{\Delta C}{C}$
C_3	$-\frac{1}{8} \cdot \frac{\Delta C_3}{C_3}$	$+\frac{1}{8} \cdot \frac{\Delta C_3}{C_3}$
R_3	$+\frac{1}{8} \cdot \frac{\Delta R_3}{R_3}$	$+\frac{1}{8} \cdot \frac{\Delta R_3}{R_3}$

Let us determine the phase characteristic of selective RC-filter in the vicinity of resonance. From relations (XIII. 9) and (XIII. 10), after conversions and substitutions, we get

$$\frac{1}{\dot{K}} = \frac{1}{\dot{K}_0} + \frac{\dot{K}_1}{1 - j \frac{\dot{\rho}_0}{\rho_0^2 - 1} m} ;$$

$$\operatorname{tg} \alpha_0 = \frac{\gamma K_0 K_1}{1 + \gamma^2 + K_0 K_1} .$$

In the vicinity of resonance $\gamma \gg 1$, therefore it may be assumed that $\tan \alpha_0 \approx \frac{K_0 K_1}{\gamma}$, or more approximately, taking into account γ values,

With the knowledge that the variation of frequency ω_0 in the selective amplifier with RC-filter in feedback circuit affects only the imaginary part of the filter transmission coefficient (XIII. 9), it is possible to write for symmetric 2T-RC-filter

$$\alpha_0 = -bK_0K_1. \quad (\text{XIII. 19})$$

Therefore, the phase-shift depends to a considerable extent on the instability of amplification factors K_0 and K_1 and those parameters of the filter which affect to a greater extent, the variation of the imaginary portion of the filter's transmission coefficient β in the vicinity of the quaresonance frequency ω_0 .

Let us take, as an example the variations of frequency ω_0 and the phase characteristic of selective amplifier with symmetrical RC-filter at $K = 100$ and $K_1 = 1$, when resistances R_1 and R_2 are matched with precision $\pm 0.5\%$. From Table 21, we extract the formula for the imaginary part of transmission factor β , and determine from it $b = \pm \frac{3}{16} - \frac{\Delta R}{R} = \pm 0.001$. Then from formula (XIII. 16) we determine the frequency variation of the amplifier due to incorrect matching of two parameters R_1 and R_2 : $\frac{\Delta \omega}{\omega} = -mb = -0.004$. From formula (XIII.9) we have $\Delta \alpha_0 = -0.1$ rad. Thus, in the given case resonance frequency shifts by $\pm 0.4\%$, and phase shift α_0 - by $\pm 5^{\circ}50'$.

In this way, it is possible to fix the effect of all the filter parameters on the selective amplifier* and to determine the fundamental error of measuring with incorrect selection of filter elements. The

*In the same way, it is possible to determine the effect of elements, composing other varieties of filters cut in to the feedback of the selective amplifier.

relations and calculations shown permit to the conclusion that the most exact demands for stability and accuracy in the matching of filter elements should be imposed on parameters R_1, R_2, C_1 and C_2 .

The question of temperature stability of RC-amplifiers has been adequately dealt with in (15, 183). However, the investigations were conducted for low-quality amplifiers and without estimating the effect of asymmetric instability, which meant incomplete accounting for destabilizing factors.

Asymmetric instability of resistances and condensers is manifested due to dissimilar values of TKE and TKC and results in the non-presence of zero transmission factor on the frequency of bridge tuning, and also to phase distortion within angles exceeding $\pm 90^\circ$. In these conditions, with variation of temperature, the reverse feedback increases in the region of resonance frequency and the Q-factor of the amplifier decreases correspondingly. The appearance of positive coupling is also possible, resulting in increasing amplification factor and Q-factor.

Analysis of asymmetric instability effect is considerably complex and requires an estimate of probable TKE and TKC characteristics. An attempt to carry out such analysis was made in (138), but was not carried to engineering calculations. Therefore, the asymmetric instability is usually assessed by experiments.

Symmetrical temperature instability of RC-filter, with similar TKE for condensers and TKC for resistances, has been theoretically analysed in (15). The relative variation of angular frequency of the RC-filter, tuning with temperature variations, is determinable by formula

$$\frac{\Delta \omega_o}{\omega_o} = - \left(\frac{\Delta R}{R} + \frac{\Delta C}{C} \right) , \quad (\text{XIII. 20})$$

where quantity $\frac{\Delta R}{R}$ is determined by estimating the temperature factor of resistance α_R in ratio

$$\frac{\Delta R}{R} = \alpha_R \Delta t. \quad (\text{XIII. 21})$$

In the same conditions $\frac{\Delta C}{C}$ is expressed by formula (XIII. 7).

Therefore,

$$\frac{\Delta \omega_o}{\omega_o} = - (\alpha_R + \alpha_C) \Delta t. \quad (\text{XIII. 22})$$

The amplification factor of highly-selective RC-amplifier with consecutive amplified reverse feedback and symmetrical 2T-RC-filter is determined from relation

$$K = \frac{K_o \sqrt{\left(\frac{\Delta R}{R} + \frac{\Delta C}{C} \right)^2 + 1}}{4Q^2 \left(\frac{\Delta R}{R} + \frac{\Delta C}{C} \right)^2 + 1} \quad (\text{XIII. 23})$$

Thus, deviation of the amplification factor

$$\Delta K_o = K_o - K. \quad (\text{XIII. 24})$$

To eliminate symmetrical instability in RC-filters, use should be made of resistances with low values TKR (BLP, MGP and of manganine wire) (145).

Pick up moduli. The emergence of errors is specified by the

instability of the amplification factors of a periodic amplifier, sensitivity variation of vacuum-tube voltmeter or recorder, transmission coefficient of phase-inverter in the adjustment of measurable signal phase, change of tube, etc. The error should be eliminated by regular calibration of the module measuring channel. However, they may take place in those elements of the module measuring circuit, which are not enclosed by the calibration circuit. These errors are usually due to the instability of attenuator's resistances, shape variation of the detecting characteristic in the vacuum tube voltmeter and also incorrect reading during the calibration.

Error due to the instability of the amplification factor, with sufficiently extensive reverse feedback, stabilization of anode and filament voltages could be brought up to 0.5-1%. Error caused by sensitivity variation of the vacuum-tube voltmeter (during changing of tubes, semi-conductive triodes) or recorder, although it could be high, is easily detected in calibration, so that further on the changed value of the recording scale division is kept stable. This error, specified usually by the shape of the detecting characteristic, is most noticeable in its initial section. On the remaining portions of the scale, where the detecting characteristic is almost linear, the error, as a rule, does not go beyond 0.5-1%. Error of the standard recorder could be considerably less than 1%.

The transmission coefficient of the phase-inverter may vary during the phase adjustment of the signal by several per cents. For eliminating this error, the compensation of phase shift is implemented prior to calibration.

Error of matching divider's resistances could be $\pm 0.2\%$. The high temperature stability of dividers is attained either by the application of wire resistances or by the selection of special resistances, including mastic (e.g., BC), the temperature coefficient of which of about 10^{-3} has negative sign (145). As a result of the fact that the heating of all the divider's resistances is usually similar, the error of division ratio is maintained, as a rule, constant not exceeding 0.5-1%.

Error arising due to non-linear distortion with high noise level cannot be calculated, and it is impossible to eliminate it by calibration. If the noise level is commensurable with the signal level or exceeds it, the control grid tube gets overloaded and changes over into anode-grid detecting condition, with which the direct proportionality between the level of the amplifier's input voltage and the level of the signal at the output gets lost. Application of high preselectivity substantially reduces such additional error in measuring.

The error of calibration is determined by the fundamental error of the indicator or recorder, from the scale of which the required amplification factor is checked or calibrated and, besides, by the error admitted in determining the calibrating voltage intensity. With individual graduation of the indicator, for instance of M-24 or M-265 device, its fundamental error could be brought down to 1%. This permits determining with accuracy upto 1% both the intensity of the calibration voltage and the amplification factor of the module gauge. With calibration from the standard recorder the accuracy is higher. Therefore, the total systematic error in the measuring channel of the signal module with the presence of calibration circuit,

determinable from formula (XIII. 3), is 1.5-2%.

Phase-meter. The direct estimate of errors in electronic phase-meters is discussed in detail in (43). Therefore, here, in our opinion, it would be expedient to analyse the probable phase errors in application to the whole channel of phase-measuring.

Prior to measuring the phase-angle between the measured and comparative signals, there must be phase correction (i.e. compensation) of phase shifts, introduced by the measuring channel, in connection with which the general error of phase measuring should also be divided into individual errors. Some of the errors could be eliminated during correction, others cannot be eliminated and taken into account in measuring.

Phase shift in aperiodic circuits of the amplifier at various operating frequencies is similar neither in absolute magnitude, nor in instability. The least error is mainly evident on the middle operating frequencies. On high frequencies, phase shift is caused by the instability of interelectrode and equipment capacities, shunting anode load of tubes. For instance, each pentode stage shifts the phase at an angle $\psi = - \arctan \omega C_o R_a$, where C_o - total capacity, R_a -the load for shunting the anode.

In amplifier planning, it is necessary to obtain minimum angle ψ , therefore, the tangent of the angle could be replaced by the angle itself in radians. In this case, the variation of phase shift $\Delta \psi$ in one stage with the variation of C_o to the extent of ΔC_o is $\Delta \psi \approx - \omega R_a \frac{\Delta C_o}{C_o}$

For instance, at $f = 3898$ cps, $R_a = 50$ kohm, $C = 50$ pF we have

$$\frac{\Delta C_o}{C_o} = 2\% \text{ and } (\Delta \psi) = 6.28 \times 3898 \times 50 \times 10^{-12} \times 50 \times 10^3 \times 2 \times 10^{-2} \approx 1,2 \times 10^{-3} \text{ rad} \approx 4'.$$

In this case, maximum error in the presence of two-channel phase

measuring circuit could be about 10'. With implementation prior to measuring the compensation of phase shifts in the measuring channel the error could be reduced to an even greater extent.

Error due to reciprocal detuning of resonance circuits, if these are present in the measuring channel, is more considerable. It could be completely eliminated with maintenance of thermal compensation and periodical correction of phase shifts.

For instance, if under the effect of surrounding temperature variation the capacitance of the circuit has changed to the extent that the frequency has become detuned by 0.5%, then with quality of circuit $Q = 10$ phase error

$$\Delta\varphi \approx Q \frac{\omega}{\omega_0} - \frac{\omega_0}{\omega} = 10 (1.005 - 0.995) = 0.1 \text{ rad} \approx 6^\circ.$$

The most significant component in the fundamental error of electronic phase-meter with the use of amplifier-clippers is taken to be the error due to asymmetry of the output pulses of amplifier-clipper, caused by the fluctuations and drift of limitation levels. To reduce this type of error it is expedient to apply as amplifier-clippers circuits with anode-cathode limiting. The fineness of limiting and dynamic range of input signal in these circuits are considerably higher. Therefore, the phase-meter with this circuit will also have a smaller error from the asymmetry of pulses (43). For instance, if at the input of amplifier-clippers voltage is delivered with amplitude U_m , and both the limiting levels shifted to one side to the same extent ΔU_0 , as shown in Fig. 230, the periods of positive and negative impulses become unequal. Their ratio is determined in the following way:

$$C = \frac{\pi - 2 \arcsin \frac{\Delta U_o}{U_m}}{\pi + 2 \arcsin \frac{\Delta U_o}{U_m}} \approx \frac{1 - \frac{\Delta U_o}{1,57U_m}}{1 + \frac{\Delta U_o}{1,57U_m}} \quad (\text{XIII.25})$$

Usually, amplitude U_m of input signals in the electronic phase-meters reaches several tens of volts, and the shifting of ΔU_o levels with stabilized supply is in the order of a few tenths of a volt. In this connection, to avoid error periodic balancing of amplifiers-clippers is required, specially after the replacement of tubes. With a dipole congruence circuit or a dipole trigger circuit this error is practically non-present (43, 151).

Error caused by the change in steepness of the impulse front depends on type of the selected amplifier-clipper and their number in a single channel. If several amplifier-clippers are used with anode-cathode clipping, the error does not exceed $0.8-1.0^\circ$.

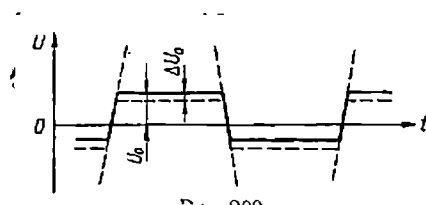


Fig. 230

Thus, it may be assumed that the basic error of the phase measuring channel in the apparatus of aerial electric prospecting with periodic checking and correction of phase shift in this channel and in phase-meter channels is not over $1-1.5^\circ$ ($2.5-3\%$ with 45° scale). Any further reduction of error is only possible by means of special measures or by applying

more composite circuits for phase measuring.

3. Error caused by fluctuation noises of field receiver and input circuit

In the apparatus of aerial electric prospecting, the low-frequency receivers of the magnetic field are usually multiturn inductance coils, either with core or without. On frequencies below 100 cps, it is also possible to use successfully the magnetic modulation transmitters (16, 19). The magnetic field receiver is tuned, as a rule, to preset the operating frequency, thereby attaining increase in its sensitivity and selectivity. The receiver is connected to the measuring unit through the preamplifier. Therefore, its intrinsic noises and the noises of the preamplifier's input circuits in measuring the low tensions of the magnetic field can be commensurable with the useful signal in the field receiver. The noises are amplified by the pre-amplifier on a par with the useful signal and delivered to the measuring circuits, thereby creating interference and causing a certain error in measurements, which is a part of the basic measuring error.

Investigations have shown that the noise level of multiturn coils of the frequency range in aerial electric prospecting are not above the atmospheric level (usually they are by one order lower). For extremely highly-sensitive apparatus, it may be assumed that this level is commensurable with the useful signal.

Given further is a brief analysis of the indicated interferences for the purpose of their quantitative appraisal and determination of the extent of their effect on the quality of operation of the receiving channel.

Fluctuation noises of field receiver. It is well known that the noise source in the oscillating circuit is only the loss resistance r , since the

inductance L and capacitance C of the circuit are practically noiseless.

The mean square value of fluctuation noises e.m.f. on the terminals of the complex circuit with resistance Z is determined from Naisquist formula (249):

$$\mathcal{E}_{\omega}^2 = \frac{4kT}{2\pi} \int_{\omega_1}^{\omega_2} r(\omega) d\omega, \quad (\text{XIII. 26})$$

where k - Boltmann constant, $k = 1.374 \cdot 10^{-23}$ joule/deg; T - absolute temperature, deg; $r(\omega)$ - active component of resistance Z, generally dependent on frequency ω_1 and ω_2 - frequency limit, for which determination is being made of fluctuation noises e.m.f.

At room temperature ($+20^\circ\text{C}$), assuming resistance r in the measured frequency range is constant and active, we obtain the following formula for the virtual value of fluctuation noises e.m.f. (136, 249):

$$\mathcal{E}_{\omega} = 0,127 \sqrt{r \Delta F} \approx \frac{1}{8} \sqrt{r \Delta F}, \quad (\text{XIII. 27})$$

where r - resistance, kohm; ΔF - transmission band, kcps; \mathcal{E}_{ω} - e.m.f., mv.

Passing on to the resonance oscillating circuit, the equivalent diagram of which is shown in Fig. 231, we determine the voltage of fluctuation noises on the terminals of the circuit caused by the presence within it of the noisy resistance r. E.m.f. of noises in the circuit of the receiving frame acts consecutively; therefore, with resonance the voltage on circuit

$$U_{\omega} = \mathcal{E}_{\omega} Q, \quad (\text{XIII. 28})$$

where Q - quality factor of circuit.

Since $Q = \frac{\rho}{r} = \frac{\omega_0 L}{r}$, then from formulas (XIII. 27) and (XIII. 28) we find:

$$U_{\omega}^2 = \xi_{\omega}^2 Q^2 = \frac{1}{64} \Delta F \frac{\rho^2}{r},$$

where $\frac{\rho^2}{r} = \rho Q = R_{\alpha}$ equivalent resonance resistance of the circuit.

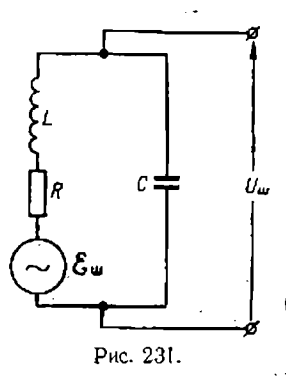


Fig. 231

Frequency band Π for single oscillating circuit, which is the tuned receiving frame, will in this case get determined from the following relation (116):

$$\Pi = \frac{\pi f_0}{2Q} \quad (\text{XIII. 29})$$

where f_0 is given in kilo-cycles.

Therefore, the fundamental noises

$$U_{\omega} \approx \frac{1}{8} \sqrt{R_{oe} \Pi}, \text{ MKB}, \quad (\text{XIII. 30})$$

where resistance R_{oe} is given in kilohms, and the frequency band Π - in kilocycles.

As an example, we take the magnetic field receivers in apparatus AERI-2 (see Chapter VII). The results of calculation of equivalent resonance resistance, frequency band Π and fundamental noises U_{ω} of

these receivers are as follows:

f, cps	243	487	974	974	1949	3898
R_{oe} , kohm	32.5	122.8	208.3	92.5	244.6	231.5
$\Pi \cdot 10^{-3}$, kcps	10.9	12.6	27.3	27.3	41.4	179
U_{Δ} , mcv	0.075	0.15	0.3	0.2	0.4	0.79

According to the data shown above, the voltage of fluctuation noises in the magnetic field receiver does not exceed 0.8 uv . If it is taken into account that the main selectivity is concentrated in the measuring part of the apparatus, the actual noise voltage, affecting the measuring inputs of pertinent parameters of the useful signal, will be reduced even to a greater extent, due to additional selectivity at the input of the receiving system.

The receiving apparatus of aerial electric prospecting is meant for measuring the tension of magnetic fields of about $10^{-4} - 10^{-7}$ a/m; it would be of interest to reduce the fluctuation noises in the receiving coil, expressed in micro-volts, to units of measuring magnetic field tension amper/meter (assuming, that $U_{n.e} = H_{n.e}$), and to compare them with the sensitivity threshold of the receiving-measuring apparatus. The sensitivity threshold of the apparatus in aerial electric prospecting is taken as 10^{-7} a/m.

Signal, induced in the field receiver without core, by external magnetic field will be, according to formula (VII. 3), $E = C_R H$, v.

For a coil with ferrite core tuned into resonance this signal could be determined from the following ratio (132, 165):

$$U \approx 8 \mu_k f_0 \omega_p^{SQH} \cdot 10^{-6}, \quad \text{v.} \quad (\text{XIII. 31})$$

For the equivalent tension of the noise field we have

$$H_{\text{u.e.}} = \frac{U_{\text{u.e.}} \cdot 10^6}{8 \mu_k f_0 \omega_p^{SQ}} \quad (\text{XIII. 32})$$

Substituting in equation (XIII. 32) $U_{\text{u.e.}}$ from formula (XIII. 30), expressed in volts, we find that the equivalent noise tension of the field

$$H_{\text{u.e.}} = \frac{\sqrt{R_{oe} \Pi}}{64 \mu_k f_0 \omega_p^{SQ}}, \quad \text{a/m.} \quad (\text{XIII. 33})$$

It would be of interest to analyse data, pertaining, for instance, to AERI-2 apparatus. It was fixed experimentally that the core permeability of multiturn coil in this apparatus $\mu_k \approx 11$. For the magnetic field receivers equivalent noise tension $H_{\text{u.e.}}$, calculated from formula (XIII. 33), has the following values:

f, cps	243	487	974	974	1949	3898
$H_{\text{u.e.}}, 10^{-8} \text{ a/m}$	1,8	0,95	1,12	0,75	0,84	1,78

According to the given data, the equivalent noise tension of the magnetic field receiver for almost all operating frequencies is considerably below the adopted sensitivity threshold of apparatus, 10^{-7} a/m . Thus, the interferences in the measuring apparatus of AERI-2, caused by the natural noises of the field receiver, are insignificant and practically do not affect the magnitude of the fundamental error in measuring. This

conclusion holds true for the majority of the apparatuses in aerial electro prospecting.

The noise levels of magnetomodulated transmitters not infrequently exceed the equivalent tension 10^{-6} a/m throughout the whole frequency range of aerial electro prospecting. Given below for comparison are the noise data of magnetomodulated transmitters, developed in FMI AN Ykr. SSR (16):

Frequency of measured field, cps	75		925	
Time constant, sec	0.3	2	0.3	2
Sensitivity threshold (with signal-noise ratio = 1), 10^{-6} a/m	1.6-2.4	1	0.8-1.6	2

The search for ways to reduce noise levels in magnetomodulation transmitters has begun only during the last few years (17). In future, apparently, characteristics of these transmitters will be improved.

Noises of input amplifier tubes. The current fluctuations of input amplifier tubes in pre-amplifiers cause an interference which, after amplification in subsequent circuits, affects the measuring systems of the apparatus.

Calculations show that the equivalent noise tension of the preamplifier the first tube is negligible and, in any case, less than the equivalent noise tension of the receiving multiturn coil tuned into resonance. For instance, for the preamplifier of AERI-2 apparatus, if it is assumed that $R_{oe} = r_{in.t}$, where $r_{in.t}$ - noise resistance of tube 6 1 (for triode cut in $r_{n.t} = 0.4$ kohm, for pentode - 1.9 kohm (249)), and the equivalent noise tension of the tube carried over to passband (for each operating frequency),

then, in accordance with formula (XIII. 33), we get for the first amplifier tube:

f, cps	243	487	974	974	1949	3898
$H_{n.t.} \cdot 10^{-9}$ a/m triode cut-						
in.	0.2	0.06	0.06	0.06	0.03	0.08
pentode cut-in	0.43	0.12	0.13	0.13	0.07	0.16

Experiments with short-circuited input of the gondola amplifier in AERI-2 apparatus have shown that on frequencies 243-1949 cps the noise level of the tube does not exceed centesimal fractions of microvolts, and on frequency 3898 cps is 0.5-1 microvolts, which is equivalent to field tension $(0.8-1.6)10^{-3}$ a/m. Identical results were obtained with the replacement of field receivers by active resistance, the selected value of which was the same as the resonance resistance of the field receiver on average operating frequencies. Therefore, the noises of the input tube are actually so insignificant that they need not be taken into account with sensitivity threshold 10^{-7} a/m.

With the use of special protective measures (23, 249), the microphonic noise of the tubes could be reduced to a volume, not affecting appreciably additional and fundamental error in the measuring apparatus of aerial electric prospecting.

4. Regarding errors in subtracting circuit of compensator

Electric compensation of the primary field signal is usually obtained by delivery to a special subtracting circuit of the indicated and compensating signals during the parity presetting of their volumes and

the fixing of appropriate phase shift between them. As a result, the output voltage of the subtracting circuit should be approximately zero.

The general analysis of subtracting circuits has been given in (144, 151, 191); therefore, here we shall only briefly examine the errors taking place in one of the subtracting circuits, which determine practically the total error of the compensator.

The main requirements of the compensator are: 1) maximum possible operating stability of the compensator, including that of the subtracting circuit; 2) maximum possible compensation, close to 100%; 3) invariability of the amplitude and phase of the compensating voltage.

The quality of compensation, i.e., its penetration and stability, are characterised by the working value of the subtraction factor K , which is the ratio of residual voltage modulus at the output of the subtracting circuit to the modulus of the compensated (input) signal, arriving at one of its inputs, i.e.

$$K_s = \frac{|\dot{U}_{out}|}{|\dot{U}_{in}|} = \frac{|\dot{U}_c - \dot{U}_k|}{|\dot{U}_c|} = \frac{|\dot{U}_2 - \dot{U}_1|}{|\dot{U}_2|}, \quad (\text{XIII. 34})$$

where $\dot{U}_c = \dot{U}_2$ - compensated, and $\dot{U}_k = \dot{U}_1$ - compensating signals.

The amount of compensation is determined from formula (XI. 3).

The most suitable for compensation in its simplicity, sensitivity and stability is the asymmetric subtracting tube circuit on resistances with symmetric inputs and asymmetric output, shown in Fig. 232, a (Fig. 232, b shows its equivalent diagram).

The subtraction proper in this system takes place in the grid circuit of tube L_2 . The L_1 tube, at the input of which arrives one of the voltages (\dot{U}_1), plays the part of cathode follower, the output voltages of which

is fed to control grid of L_2 tube, where simultaneously arrives the second voltage (\dot{U}_2). Therefore, the voltage virtually active on the grid of L_2 tube, is equal to the difference of voltages $\dot{U}_g = \dot{U}_2 - \dot{U}_1$, applied to the subtracting circuit, and the variation of this difference determines the variation of anode voltage (current) of L_2 tube. The higher adjustable bias, fed to controlling grid of L_2 tube, makes it possible to obtain $\mu_2 < \mu_1$ and thereby to balance the circuit. Other subtracting circuits, for one or the other reason, have worse metrological properties, lesser value of subtraction factor, etc. (144, 191).

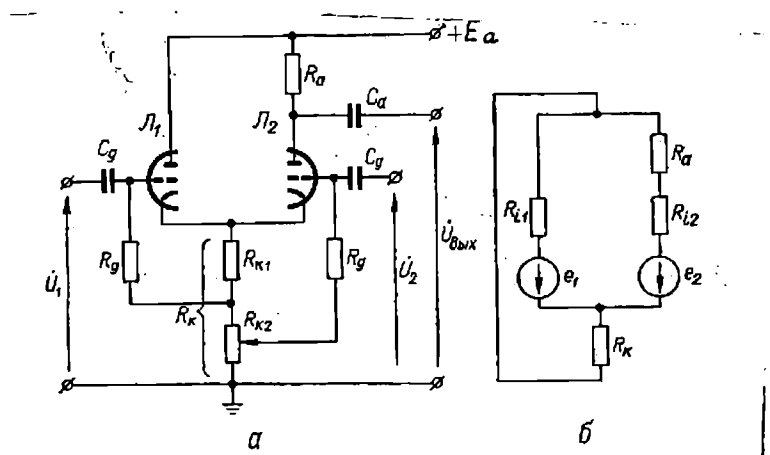


Fig. 232

The first and second of the above demands, imposed on the compensator in this system, are met mainly by the selection of the type of tubes in the subtracting circuit and its optimum parameters, and also stabilization of energizing voltages. The third demand is usually met by rigid coupling of the compensating voltage source to

current in oscillating frame or, with the use of comparative voltage from master oscillator, with the quartz crystal control. In both the cases, stabilization of parameters should be provided in the transmission circuit of the compensating signal from the generating unit into the compensator.

The balance of the subtracting circuit take place with fulfilment of condition

$$\mu_1 = \mu_2 \left(1 + \frac{R_{i1}}{R_k} \right) \quad . \quad (\text{XIII. 35})$$

The amplification factor of the subtracting circuit at

$\mu_1 \approx \mu_2 = \mu$ is determined from formula

$$K_{s.c} = \mu \frac{R_a R_k (1 + \mu)}{(1 + \mu) R_k (R_{i1} + R_{i2} + R_a) + R_{i1} (R_{i2} + R_a)} \quad . \quad (\text{XIII. 36})$$

Since usually $(1 + \mu) R_k > R_{i1}$, it may be assumed that

$$K_{s.c} = \mu \frac{R_a}{R_{i1} + R_{i2} + R_a} \quad . \quad (\text{XIII. 36a})$$

If $R_{i1} = R_{i2}$, then

$$K_{s.c} \approx \mu \frac{R_a}{2R_i + R_a} = \frac{\mu}{1 + \frac{2R_i}{R_a}} \quad . \quad (\text{XIII. 36b})$$

In this case output voltage

$$U_{out} = K_{s.c} (\dot{U}_2 - \dot{U}_1) \approx \frac{\mu}{1 + \frac{2R_i}{R_a}} (\dot{U}_2 - \dot{U}_1) \quad (\text{XIII. 37})$$

But actually even with parity $\dot{U}_1 = \dot{U}_2$, the output of the subtraction circuit has a residual signal $U_{out_{min}}$, the minimum volume of which is determined by the noise level of the tube and instability of its parameters and of the subtracting circuit elements. This minimum signal determines the fundamental error of subtraction, which could be expressed by ratio

$$\sigma = \frac{U_{out_{min}}}{K_{s.c} U_{in}} \quad (\text{XIII. 38})$$

where $U_{in} = (U_2 - U_1)_{nom.}$

The additional error of subtraction is determined from relation

$$\sigma = \frac{\Delta U_{out_{min}}}{K_{s.c} U_{in}} \quad (\text{XIII. 39})$$

where $U_{out_{min}}$ - increment of residual voltage, caused by the instability of the energizing voltages and the variation of external conditions.

In order to increase the amount of compensation, it is necessary to increase in the subtracting circuit signal/noise ratio at its inputs.

This is attained by the selection of a tube with higher and stable static

, and providing conditions of its operation, at which the transmission ratio would be higher than one. Stability and linearity of the given circuit are determined by the selection of a sufficiently high cathode resistance

R_k , and amplification factor - by high resistance value of anode load R_a , i.e., by the selection of $R_a > R_{i1} + R_{i2}$ (see formula (XIII. 36a)).

For the subtracting circuit, the most suitable are double triodes. In order to assure minimum frequency error, this triode should have a high static steepness and low input capacitance. On low frequencies, used in the induction method of aerial electric prospecting, frequency error is usually disregarded.

For an exact calculation of the fundamental subtraction error, it is necessary to determine analytically the intensity of $U_{out_{min}}$ provided, that $K_{s.c} = \text{const}$ and $U_{in} = U_{in. nom}$. However, this is rather a difficult problem, requiring cumbersome calculations, therefore, intensity of $U_{out_{min}}$ is usually determined by experiments. The determined value of $U_{out_{min}}$ gives only the first component part of the fundamental error. The second component part is determined by the instability of the subtracting circuit amplification factor, caused by the variation of all parameters in the subtracting circuit (see formula (XIII. 36)).

Let us determine the variation of the amplification factor due to instability of parameters of the tubes and the circuit. The total differential of relation (XIII. 36b) will be

$$dK_{s.c} = \frac{\partial K_{s.c}}{\partial \mu} d\mu + \frac{\partial K_{s.c}}{\partial R_i} dR_i + \frac{\partial K_{s.c}}{\partial R_a} dR_a .$$

(XIII. 40)

Partial derivatives, which compose this equation, will be written as

$$\frac{\partial K_{s.c.}}{\partial \mu} = \frac{R_a}{2R_i + R_a} ; \quad \frac{\partial K_{s.c.}}{\partial R_i} = - \frac{2\mu R_a}{(2R_i + R_a)^2} ;$$

$$\frac{\partial K_{s.c.}}{\partial R_a} = \frac{\mu(2R_i + R_a) - \mu R_a}{(2R_i + R_a)^2} .$$

Substituting into formula (XIII. 40) values of partial derivatives and simplifying, we find

$$dK_{s.c.} = K_{s.c.} \left\{ \left[\frac{1}{\mu} d\mu - \frac{2}{2R_i + R_a} dR_i + \frac{2R_i}{R_a(2R_i + R_a)} dR_a \right] \right\} . \quad (\text{XIII. 40a})$$

The relative variation of amplification factor of the subtracting circuit with variation of parameters μ , R_i and R_a we get from relation

$$\Delta K_{s.c.} = \frac{dK_{s.c.}}{K_{s.c.}} 100 = \left[\frac{1}{\mu} d\mu - \frac{2}{2R_i + R_a} dR_i + \frac{2R_i}{R_a(2R_i + R_a)} dR_a \right] 100, \% . \quad (\text{XIII. 41})$$

Knowing values μ , R_i and R_a and setting their increments, as observable in practice, it is easy to calculate the numerical value of percentage variation of the subtracting circuit amplification factor. It should be mentioned that the main unstable parameter of the subtracting circuit is the inner resistance of the tube. With invariable values of voltages \dot{U}_1 and \dot{U}_2 the variation of the amplification factor also causes corresponding variation of input voltage of the subtracting

circuit (see formula (XIII. 37)) which, in the final count, determines the fundamental error of subtraction.

As an example, let us take the subtracting circuits and their errors in two versions of apparatus + AERIS and AERI-2.

For the carrying out of experiments it was proposed to investigate the effect on the subtracting circuit of the type of tubes, and also the circuit's parameters, at which the required extent of subtraction would be assured, as well as the stability of its operation, time stability and sufficient value of transmission ratio ($K_{s.c} > 1$). The fundamental error should be reduced to a magnitude not exceeding 0.5-1%, whereas the additional, due to its insignificance, could be disregarded.

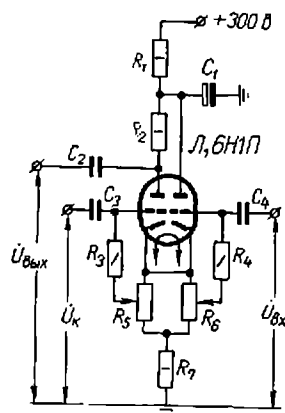


Fig. 233

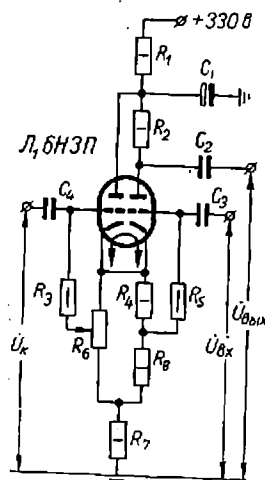


Fig. 234

For the subtracting circuit, the most suitable are double triodes 6H1P and 6H3P, which, as a rule, have identical characteristics for both its triodes, comparatively low inner resistance R_i (11 and 7.5 kohm), low fundamental noises and sufficiently high steepness of characteristic S (3.2 and 4.9 ma/v).

In the development of the compensating system in AERIS with the use of tube 6H1, investigations of the subtracting circuit, shown in Fig. 233, were confined to the resistivity selection of anode and cathode loads, assuring the required extent of compensation, high time stability of its work, and also to the determination of the optimum bias voltages on controlling grids for implementation of condition (XIII. 35), stable subtraction and linearity at high, as well as low signals.

Investigations, carried out at voltage of anode supply 300v, have shown that the optimum resistance values of anode and cathode loads are the following: $R_2 = 13 \text{ kohm}$; $R_7 = 13 \text{ kohm}$; $R_5 = R_6 = 10 \text{ kohm}$, and bias voltages - $E_{g1} = -3.5\text{v}$; $E_{g2} = -6\text{v}$. In this case, the subtracting circuit is linear with variation of input signal only from 50 mv to 5v or from 50 microvolt to 50 millivolt, i.e. subtraction factor with compensation of high signals comprises 10^{-2} , and with compensation of low signals - 10^{-3} . Additional error from the variation of supply voltages with the indicated parameters of the subtraction circuit is quite negligible. This error is shown in percentage in Table 22. By applying the stabilized supply sources, the additional error could be totally eliminated.

The fundamental error, determinable from formula (XIII. 38), comprises with compensation of signals upto 5 v 4%, and with signals upto 5 mv, 0.5%. Therefore, the amount of compensation and its linearity increase, whereas the fundamental error gets reduced with admission to the inputs of the subtracting circuit in relation to low signals not exceeding 0.1-0.5 v.

With the use in the subtracting circuit of double triode 6N3P

(compensator of AERI-2 apparatus) besides confirming the parameters of the circuit shown in Fig. 234 ($R_2 = 300 \text{ kohm}$; R_4 and $R_8 - 2.4 \text{ kohm}$ each; $R_6 = 10 \text{ kohm}$; $R_7 = 200 \text{ kohm}$), determination was made of the dependance of its basic characteristics on destabilizing factors.

Table 22

Parameters	U = 6,3 = const			E = 250 = const		
	225	250	275	5,7	6,3	5,9
$U_{in}=5v; E_{g1} = -3.5v;$ U_{out}, mv	4,6	5,0	6,0	1,6	5,0	5,5
$U_{out}=5mv; E_{g2} = -6v;$ $\Delta U_{out}, mv$	-0,4	0	+1,0	-3,4	0	+0,5
$K_{s.c} = 3.4; \sigma_{al}, \%$	-0,002	0	+0,006	-0,02	0	+0,003
$U_{in}=50mv; E_{g1} = -3.5v$ U_{out}, mcv	48	50	60	48	50	56
$U_{out}=50mcv; E_{g2} = -6v;$ $\Delta U_{out}, mcv$	-2	0	+10	-2	0	+6
$K_{s.c} = 1; \sigma_{al}, \%$	+0,004	0	+0,02	-0,004	0	+0,012

Dependence of subtraction coefficient upon variation of filament voltage
(the anode voltage is stabilized). Three tubes 6N3P, with small difference in parameters (Table 23), were taken for determination of the given relation, and then the necessary measurements were carried out with the change of tubes. The experiment was conducted in two versions and in both of them the same signal $U_{in} = 1$ was admitted at the input of the subtracting circuit.

Table 23

No. of tube	Left triode		Right triode	
	S, ma/v	I _a , ma	S, ma/v	I _a , ma
1	4,95	9	4,75	7,8
2	4,95	9	4,9	8,4
3	4,65	7,7	4,65	7,5

In the first version, by selecting bias voltage with invariable E_{g1} the decumensation voltage was set at $U_{out} = 17$ mv, which corresponded to the subtraction factor $K_s = 10^{-3}$. Then the filament voltage was varied by $\pm 10\%$. The characteristic curve of tube 1, obtained as a result of experiment, is shown in Fig. 235 (curve 1). Similarly, the curves were taken for tubes 2 and 3 (curves 2 and 3 respectively).

In the second version, the maximum possible compensation was attained by the selection of bias. With this amount of compensation, the subtraction factor was upto 10^{-3} (for any tube 6N3P the value of factor does not exceed 10^{-3}). With the variation of the filament voltage by $\pm 10\%$, it was possible to obtain the curves sought for shown in Fig. 236 for tubes 1-3 respectively. According to these curves, the highest stability with the variation of the filament voltage has the subtraction circuit, in which the tube applied is with low difference in parameters of triodes (tube 3).

Dependence of subtraction coefficient upon temperature was determined for tube 3 only at positive temperatures, since the compensator in this apparatus operates, as a rule, in conditions of stable positive temperatures approximately 35-40°C.

Curve 1 (Fig. 237) for the theoretically required subtraction coefficient

of about 10^{-3} , was taken at initial temperature $+20^{\circ}\text{C}$ with its subsequent rise to $+45^{\circ}$ (heating of the whole subtracting circuit in thermostat).

Curve 2 was taken in reverse order, i.e., at first, the maximum possible was obtained at $+45^{\circ}\text{C}$, then the circuit was gradually cooled to $+15^{\circ}\text{C}$.

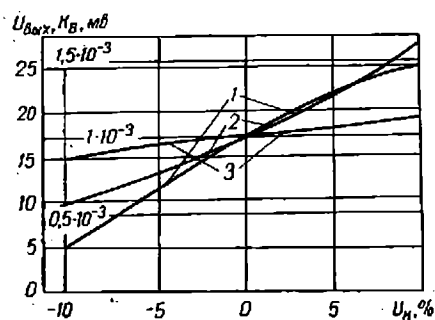


Fig. 235

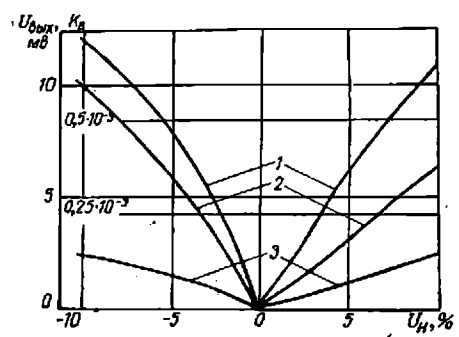


Fig. 236

The curves in Fig. 237 show that the subtraction factor in interval $20-40^{\circ}\text{C}$ in both the cases remains less than 10^{-3} , and its minimum variations correspond to the temperature range $20-35^{\circ}\text{C}$. The working temperature conditions of the compensation system require its additional cooling by means of a fan or outside stream of air. In this case, the stability of the compensator work is considerably increased and the subtraction coefficient could be brought up to 10^{-3} .

As regards the intensity of the admitted voltages for the given system, the same conditions prevail as for the subtraction circuit assembled on tube 6N3P. Therefore, if the input voltage of the useful signal exceeds 0.5v , it should be admitted into the subtracting circuit through ohmic divider with division ratio about $1:10$.

This investigation of the compensator's subtracting circuit in

AERI-2 apparatus, in which the main demands were met, has shown that its fundamental error does not exceed 0.5-1%. By stabilizing the supply voltages and applying thermostable details, the additional error in the working conditions of the apparatus could be brought down to 0.2-0.3% and need not be taken into account. The subtraction factor is up to $5 \cdot 10^{-2} - 10^{-3}$, and the amount of compensation, which is assured directly by the compensator, is quite sufficient for the purpose of aerial electric prospecting, i.e. almost 100%.

5. Vibration errors, caused by the variation of field receiver preset orientation

In flying conditions, the highest errors may emerge in the measuring unit due to vibrations and the preset orientation variation of the field receiver in space. To confirm this let us find the magnitude of linear displacement of axis in the plane of receiver's axis magnetic meridian of the vertical component of the resulting field with vibrations of the

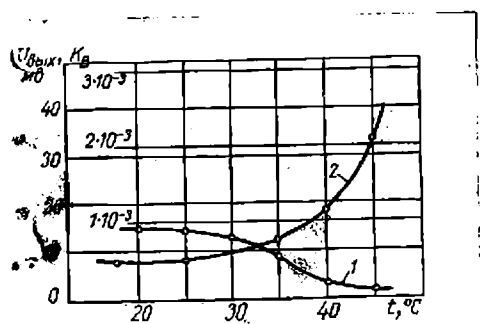


Fig. 237

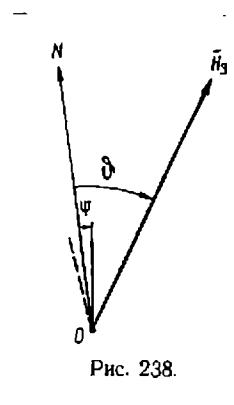


Fig. 238

receiver in the magnetic field of Earth for the case when the e.m.f. induced in the receiver, is of the same power as the taken sensitivity threshold of the measuring apparatus, for instance, 10^{-7} a/m. Assuming that the field receiver is swinging in relation to the vertical line

(direction N) and the deviation angle varies sinusoidally, i.e. $\psi = \psi_m \sin \omega_{vb} t$. Generally, the angle between the direction N of the field receiver and the vector of the magnetic field of Earth H_E equals ϑ (Fig. 238). Let us determine the e.m.f. induced in the field detector by the constant magnetic field of Earth.

For the field receiver, made up in the form of a multiturn inductance coil, the e.m.f., induced in it by the varying magnetic flux (see para 2, Chapter VII) will be

$$e = - \frac{C_{\Pi} d\Phi}{dt},$$

where $C_r = \mu_k S_p$ - constant of the field receiver.

In the case in question the time variable magnetic flux Φ could be replaced with vibrations as its simonilian to the variable field of Earth. Therefore, with accounting for the above conditions of vibration e.m.f. we get

$$e_{vb} = - \frac{C_{\Pi} d\Phi_3}{dt} = - \frac{d}{dt} C_{\Pi} H_3 \cos(\vartheta - \psi), \quad (\text{XIII. 42})$$

i.e.

$$\begin{aligned} e_{vb} &= - \frac{d}{dt} (C_{\Pi} H_3 \cos \vartheta \cos \psi + C_{\Pi} H_3 \sin \vartheta \sin \psi) = \\ &= C_{\Pi} H_3 \cos \vartheta \sin \psi \frac{d\psi}{dt} - C_{\Pi} H_3 \sin \vartheta \cos \psi \frac{d\psi}{dt} = \\ &= C_{\Pi} H_3 \omega_{vb} \psi_m \cos \vartheta \sin \psi \cos \omega_{vb} t - C_{\Pi} H_3 \omega_{vb} \psi_m \sin \vartheta \cos \psi \cos \omega_{vb} t. \end{aligned}$$

Since $H_e \cos \vartheta = H_{v.e}$ - vertical, and $H_e \sin \vartheta = H_{h.e}$ - horizontal components of the Earth's field, we may write

$$e_{vb} = C_{\Pi} H_{v.e} \omega_{vb} \psi_m \sin \psi \cos \omega_{vb} t - C_{\Pi} H_{r.3} \omega_{vb} \psi_m \cos \psi \cos \omega_{vb} t. \quad (\text{XIII. 43})$$

Angle ψ is negligible, therefore, it may be assumed, that $\sin \psi \approx \psi$, $\cos \psi \approx 1$. In this case

$$\begin{aligned} e_{vb} &\approx C_n H_{v.3} \omega_{vb} \psi_m \cos \omega_{vb} t - C_n H_{r.3} \omega_{vb} \psi_m \cos \omega_{vb} t = \\ &= C_n H_{v.3} \omega_{vb} \psi_m^2 \sin \omega_{vb} t \cos \omega_{vb} t - C_n H_{r.3} \omega_{vb} \psi_m \cos \omega_{vb} t = \\ &= \frac{1}{2} C_n H_{v.3} \omega_{vb} \psi_m^2 \sin 2 \omega_{vb} t - C_n H_{r.3} \omega_{vb} \psi_m \cos \omega_{vb} t. \end{aligned}$$

(XIII. 44)

Hence it follows that in this case the e.m.f., induced in the vertical field receiver, is determinable by the difference of two components, one of which is specified by vertical, and the other by horizontal components of the Earth's field, i.e.

$$e_{vb} = e_{vb}^{v.3} - e_{vb}^{r.3} \quad . \quad \text{(XIII. 45)}$$

In accordance with equation (XIII. 44), the vibration's e.m.f., specified by the vertical component of the Earth's field, varies with double angular frequency of vibrations $2 \omega_{vb}$, and is proportional to this component's value and the amplitude square of deviation angle ψ_m^2 . But the vibrations e.m.f., specified by the horizontal component of the Earth's field, varies only with angular frequency of vibrations ω_{vb} , and is proportional to this component's value and the linear amplitude of deviation angle ψ_m .

Therefore, it is possible to write $e_{vb}^{v.e} = E_m^{v.e} \sin 2 \omega_{vb} t$, where $E_m^{v.e} = \frac{1}{2} C_n \omega_{vb} \psi_m^2 H_{v.e}$; $e_{vb}^{h.e} = E_m^{h.e} \cos \omega_{vb} t$, where $E_m^{h.e} = C_n \omega_{vb} \psi_m H_{h.e}$.

The effective values of the shown e.m.f. are the following:

$$E_{e\phi}^{y.3} = \frac{E_m^{y.3}}{\sqrt{2}} = \frac{\sqrt{2}}{2} c_{\pi} \pi f_{yb} \psi_m^2 H_{y.3},$$

$$E_{e\phi}^{h.3} = \frac{E_m^{h.3}}{\sqrt{2}} = \sqrt{2} c_{\pi} \pi f_{yb} \psi_m^2 H_{h.3}. \quad (\text{XIII. 46})$$

The effective value of the e.m.f., actuated in the field receiver by sinusoidally varying magnetic flux H_m will be

$$E_{e\phi}^m = \frac{E_m^m}{\sqrt{2}} = 2c_{\pi} \pi f_{oH_m} H_m, \quad (\text{XIII. 47})$$

where f_o - operating (resonance) frequency of the field receiver.

The calculation of vibrations e.m.f. in the case of horizontal orientation of the field receiver are implemented in the same way.

In accordance with the previously assumed condition that $H_m = \sqrt{2} \cdot 10^{-7} \text{ a/m}$, (the effective value of sinusoidally varying magnetic flux = 10^{-7} a/m), and also

$$\frac{E_{e\phi}^m}{E_{e\phi}^{y.3}} = \frac{E_{e\phi}^m}{E_{e\phi}^{h.3}} = 1 \quad (\text{XIII. 48})$$

and taking into account formulas (XIII. 46) and (XIII. 47), from relation (XIII. 48) we get

$$\frac{E_{e\phi}^m}{E_{e\phi}^{y.3}} = \frac{\sqrt{2} c_{\pi} \pi f_{oH_m} H_m}{\frac{\sqrt{2}}{2} c_{\pi} \pi f_{yb} \psi_m^2 H_{y.3}} = \frac{2 f_{oH_m}}{f_{yb} \psi_m^2 H_{y.3}} = 1; \quad (\text{XIII. 48a})$$

$$\frac{E_{e\phi}^m}{E_{e\phi}^{h.3}} = \frac{\sqrt{2} c_{\pi} \pi f_{oH_m} H_m}{\sqrt{2} c_{\pi} \pi f_{yb} \psi_m^2 H_{h.3}} = \frac{f_{oH_m}}{f_{yb} \psi_m^2 H_{h.3}} = 1. \quad (\text{XIII. 48b})$$

From the formulas (XIII. 48a) and (XIII. 48b) the amplitude is determined for the operating frequency f_0 of deviation angle ψ_m .

For instance, for the operating frequency $f_0 = 244$ cps in an area with density of the Earth's field comprising on an average 34 a/m for the vertical component and 16 a/m for the horizontal, we find: for the vertical component

$$f_{vb} = \frac{f_0}{2} = \frac{244}{2} = 122, \\ \psi_m^{B.3} = \sqrt{\frac{2 f_{0m}^H}{f_{vb} H_{B.3}}} = \frac{2 f_0 \sqrt{2} \cdot 10^{-7}}{\frac{0}{2} 34} \approx 0,13 \cdot 10^{-3} \text{ rad} \approx 27'' ,$$

and for the horizontal

$$f_{vb} = f_0 = 244, \\ \psi_m^{r.3} = \frac{f_{0m}^H}{f_{vb} H_{r.3}} = \frac{244 \cdot \sqrt{2} \cdot 10^{-7}}{244 \cdot 16} = 0,09 \cdot 10^{-7} \text{ rad} \ll 1''.$$

The variation amplitude of the axis slope in the field receiver with vibrations corresponds to linear displacement (swaying) of one of its ends in relation to the other to an extent of Δx .

In the magnetic field receiver of AMRI-2 with its height 125 mm for $\psi_m^{v.e}$ we have $\Delta x_{v.e} = 125 \cdot 0,13 \cdot 10^{-3} \approx 16 \cdot 10^{-3} \text{ mm}$ and for $\psi_m^{h.e} - \Delta x_{h.e} = 125 \cdot 0,09 \cdot 10^{-7} \approx 1,13 \cdot 10^{-6} \text{ mm}$. These negligible displacements on the operating frequencies of the apparatus are quite likely with the suspension of the field receiver in the outboard gondola, even more so with its setting directly on the aircraft, specially on helicopter (154).

From the given calculation and formula (XIII.44) it follows that for the vertical field receiver the main (decisive) factor is the vibration interference, specified by the horizontal component of the Earth's field. For the horizontal field receiver, as shown by a similar calculation, the main factor is the vibration interference caused by the vertical

component of the Earth's field:

Let us take the errors emerging due to the incorrect initial setup of the field receiver or random static variations of its orientation in respect of the preset direction, very likely in conditions of flight (for instance, in the apparatus with the outboard gondola of induction aeromethod they are caused by the impact load on the gondola). This may cause a substantial error in measuring.

If the random variation of the vertical field receiver's orientation for instance, of aerial frame) is occurring in the flight plane (Fig. 239), the e.m.f., induced in the receiver by a harmonically varying primary field, will be

$$e = - C_{\Pi} \frac{d}{dt} H_m \cos (\vartheta + \beta) \sin \omega t =$$

$$= - \omega C_{\Pi} H_m (\cos \vartheta \cos \beta + \sin \vartheta \sin \beta) \cos \omega t. \quad (\text{XIII. 49})$$

Since the angle of deflection ϑ is usually negligible, the term $\sin \vartheta \sin \beta \cos \omega t$ of formula (XIII. 49) could be disregarded. As a result we will get

$$e \approx - \omega C_{\Pi} H_m \cos \vartheta \cos \beta \cos \omega t. \quad (\text{XIII. 50})$$

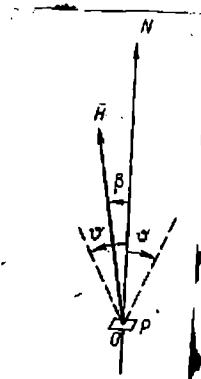


Fig. 239

Thus, in the given case the amplitude of the e.m.f. induced in the frame varies in proportion to the cosine of the deflection angle ϑ . For instance, with deflection of the frame by 10° the variation of the e.m.f., induced by the primary field, is only 1.5%. This is comparatively a low intensity. However, for the apparatus of some aerial induction methods, it may be commensurable with the useful signal. In two-plane and also in the helicopter versions of the near zone, when a second (compensation) frame is being used, interference of this type is very negligible, due to the subtraction of signals activated in the frames. The additional error, emerging in this case, has practically no effect on the total error of measuring.

If there is a spontaneous variation of the preset orientation N of the field receiver, and direction of the tension vector of the primary field \bar{H} coincides with this direction (Fig. 240,a), the e.m.f., activated in the field receiver, is determined from relation

$$e' = - \frac{d}{dt} C_{\Pi} \bar{H} \bar{n}_s \sin \omega t = - \omega C_{\Pi} \bar{H} \bar{n}_s \cos \omega t, \quad (\text{XIII. } 50a)$$

where \bar{n}_s - unit vector in a plane perpendicular to the plane S_p of the receiving frame; in Cartesian coordinates

$$\bar{n}_s = \bar{i} n_{sx} + \bar{j} n_{sy} + \bar{k} n_{sz} = \bar{i} \cos \alpha + \bar{j} \cos \beta + \bar{k} \cos \gamma.$$

In the present case

$$\bar{H} \bar{n}_s = H_z n_{sz} = H_z n_s \cos \gamma = H_z \cos \gamma$$

the mod. value of the unit vector is one, i.e. $(n_s) = 1$). Therefore,

$$e' = -\omega C_{\Pi} H_m \cos \gamma \cos \omega t. \quad (\text{XIII. 50b})$$

Generally, if the direction of the vector does not coincide with the preset orientation N (Fig. 240, b), then with spontaneous variation of the field receiver's orientation

$$e' = -\omega C_{\Pi} H_m \cos \varphi \cos \omega t, \quad (\text{XIII. 50c})$$

as the scalar product of vectors

$$H n_s = H_x n_{sx} + H_y n_{sy} + H_z n_{sz} = H \cos \varphi, \quad (\text{XIII. 51})$$

where

$$\cos \varphi = \frac{H_x n_{sx} + H_y n_{sy} + H_z n_{sz}}{|H|} = \frac{H_x \sin \gamma \sin \alpha + H_y \sin \gamma \cos \alpha + H_z \cos \gamma}{|H|}.$$

With normal orientation of the field receiver ($\gamma = 0$) we have

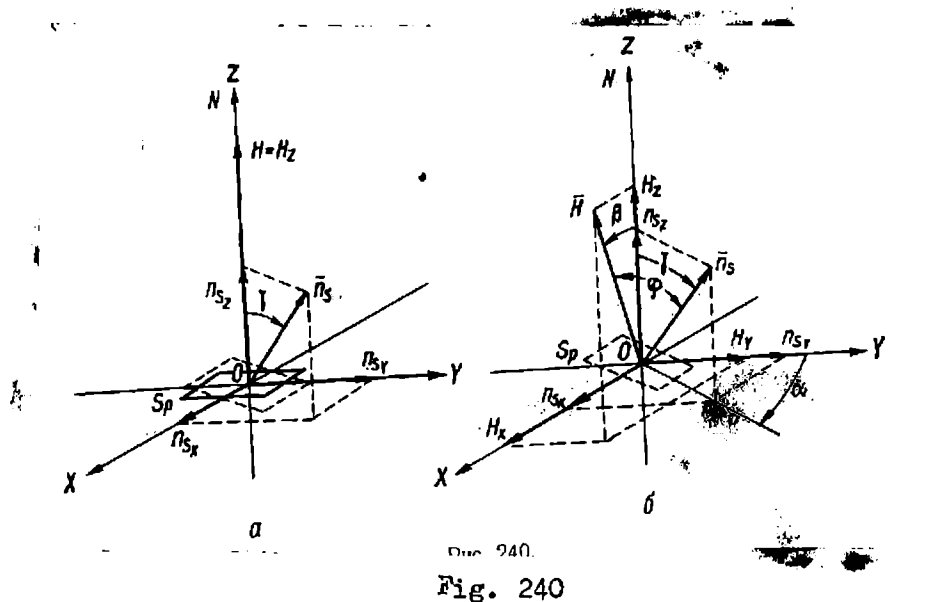
$$e_v = -\omega C_{\Pi} H_m \cos \beta \cos \omega t. \quad (\text{XIII. 52})$$

The virtual increment of the e.m.f., induced in the receiver by primary field \vec{H} , is proportional to difference $\Delta E = E' - E_v$, i.e.

$$\Delta E = C_{\Pi} H (\cos \varphi - \cos \beta). \quad (\text{XIII. 53})$$

Usually, the variation range of angle φ does not exceed a few degree; therefore, the variation of difference $\cos \varphi - \cos \beta$ is negligible. Consequently, the amount of the e.m.f. increment, i.e., the error, in this case, will be low (interference will constitute one per cents of the e.m.f. e_v , activated in the field receiver with its normal orientation). Naturally, all this holds true when there is no electric compensation of the primary field signal.

Considerable variations of orientation of the field receiver result in considerably greater error. However, these variations are purely incidental and of short duration; hence they need not be taken into account. But if the orientation change is static and takes place during the initial setting of the field receiver or during the flight, there is constant displacement of indications, which could be easily noted and compensated during the first calibration or checking of the receiving-measuring channel.



Thus, it may be assumed (and this is confirmed in practice) that the error from random changing by the field receiver of the preset orientation does not exceed 1 - 1.5%. It is substantially less in the apparatus of the aerial induction method, where the e.m.f., induced by the primary field in two receivers, are reciprocally subtracted.

6. Dynamic errors of RCQ (recorder of complex quantities).

The main selectivity of the measuring apparatus in the narrow band close to the operating frequency is concentrated, as a rule, in recorder

circuits. This means that the inertia of recorder circuits introduces substantial distortions into the recording of normal and anomalous signals, causing additional dynamic errors of apparatus.

Generally the analysis of dynamic properties of analogue type RCQ is carried out by the operative technique. According to (135, 164) the total error of RCQ $\Delta X(S)$ will be depicted as

$$\Delta X(S) = \frac{X(S)}{1+K(S) \beta(S)} \quad (\text{XIII. 54})$$

where $X(S)$, $K(S)$ and $\beta(S)$ - terms, showing, respectively the input signal X , the transmitting function of direct circuit of the system of feedback circuit.

Expanding function $\Delta X(S)$ into series according to ascending power S , we obtain a series, convergent with low S values:

$$\Delta X(S) = (A_0 + A_1 S + \frac{A_2}{2!} S^2 + \frac{A_3}{3!} S^3 + \dots) X(S). \quad (\text{XIII. 55})$$

To obtain the original $\Delta X(t)$ each term is inversely converted

$$\Delta X(t) = A_0 X + A_1 \frac{dX}{dt} + \frac{A_2}{2!} \frac{d^2 X}{dt^2} + \frac{A_3}{3!} \frac{d^3 X}{dt^3} + \dots \quad (\text{XII. 56})$$

These series converge with high times t (i.e. in stable working conditions).

Thus, the error $\Delta X(t)$ consists of static error $A_0(X)$ and of dynamic errors, proportional to derivatives of the measured time function $A_1 \frac{dx}{dt}$, $\frac{A_2}{2!} \cdot \frac{d^2 x}{dt^2}$ etc. Static error $A_0(X)$ takes place in RCQ of static type (89, 135); it is usually taken into account during calibration of the scale.

For determination of dynamic error $\Delta X_{\text{dyn}}(t)$, it is often quite sufficient to summarize two dynamic errors, proportional to the first

and second derivatives from signal, i.e. to assume that inequation (XIII. 56) initially $\frac{dX}{dt} = \text{const}$, and then $\frac{d^2X}{dt^2} = \text{const}$. Sometimes for determination of the dynamic error the application is of a more graphic method, applicable to a majority of the described RCQ systems, which permits judging from the ideal system, described by the linear differential equation of the secondary order, the behavior of real system, involving some equivalent parameters. The method is based on Ishlinsky's principle (95, 135) of reducing linear differential equation of a higher order to a differential equation of the secondary order. Resolutions of this equation are known for a whole series of external effects and could be reduced to general parameters and graphic curves. Therefore, the foremost requirement is to determine the nature of outside effects.

According to theoretical and experimental data of aerial electric prospecting, a considerable number of determinable anomalies could be described either by a sinusoidal wave with frequency Ω , or more approximately, by a single rectangular impulse with duration τ (we shall call them "typical" anomalies). This should be accounted for in the analysis of the secondary differential equation and it should also be kept in view that the interaction time of the anomaly of the measured parameter with the measuring apparatus τ is limited by the speed of survey v and the width of anomaly l :

$$\tau = \frac{l}{v} ; \quad \Omega = 2\pi \frac{v}{l} . \quad (\text{XIII. 57})$$

Thus, the RCQ equation in its complete form will be written as:

$$\left[p^2 + 2np + \omega_0^2 \right] \varphi_{out}(t) = \omega_0^2 \varphi_{in}(t), \quad (\text{XIII. 58})$$

where n - damping factor of system, ω_0 - fundamental frequency of

undamped system oscillations; value $\varphi_{in}(t)$ is determined by "typical" anomalies (any kind of effect could generally be estimated as calculated anomalies).

We resolve equation (XIII. 58) at the initial zero conditions for anomaly of the type of duration jump $\tau = \frac{1}{v}$:

$$\varphi_0(\theta_t) = \frac{\varphi_{out}(\theta_t)}{\omega_0^2} = \begin{cases} 1 + \frac{1}{\varepsilon_k} e^{-\varepsilon_n \theta_t} \sin(\varepsilon_k \theta_t - \psi) & \text{при } 0 < \theta_t \leq \theta_\tau \\ \frac{1}{\varepsilon_0} e^{-\varepsilon_n \theta_t} \{ \sin(\varepsilon_k \theta_t - \psi) - e^{\varepsilon_n \theta_t} \sin[\varepsilon_k(\theta_t - \theta_\tau) - \psi] \} & \text{при } \theta_t \geq \theta_\tau \end{cases} \quad (\text{XIII. 59})$$

Here

$$\theta_t = \omega_0 t; \quad \varepsilon_k = \frac{k}{\omega_0}; \quad k^2 = \omega_0^2 - n^2,$$

$$\theta_\tau = \omega_0 \tau = \omega_0 \frac{1}{v}; \quad \varepsilon_n = \frac{n}{\omega_0}; \quad \psi = \arctg \frac{\varepsilon_k}{\varepsilon_n}.$$

From equation (XIII. 59) we plot curves, which make it possible to judge the distortion of the "typical" anomaly. Fig. 241 shows curves $\varphi_0 = f(\theta_t)$ for various values θ_τ at $\varepsilon_n = 0.86$ ($\omega_0 = 41.3$ rad/sec, $n = 35.7$ rad/sec). These curves may also be used to determine τ values, at which considerable distortions of the measured signal anomaly are evident in the form of a jump, and from them to determine the required parameters of the RCQ system.

Similarly, equation (XIII. 58) is resolved for anomaly in the shape of sinusoidal wave with duration $\tau = \frac{2\pi}{\Omega}$ and the curves plotted in dimensionless coordinates (φ_0, θ_t). In this case for the initial

zero conditions we get

$$\varphi'_0(\theta_t) = \begin{cases} \frac{1}{\sqrt{(1 - \varepsilon_0^2)^2 + 4\varepsilon_n^2 \varepsilon_0^2}} \left[\sin(\varepsilon_0 \theta_t - \psi_1) - \frac{\varepsilon_0}{\varepsilon_k} e^{-\varepsilon_n \theta_t} \sin(\varepsilon_k \theta_t - \psi_2) \right] \\ 0 < \theta_t \leq \theta_\tau; \\ F(\theta_t) - F(\theta_t - \theta_\tau) \text{ при } \theta_t > \theta_\tau \end{cases} \quad (\text{XIII. 60})$$

where

$$\psi_1 = \text{arctg} \frac{2\varepsilon_n \varepsilon_0}{1 - \varepsilon_0^2}; \quad \varepsilon_0 = \frac{\Omega}{\omega_0}; \quad \varepsilon_k = \frac{k}{\omega_0};$$

$$\psi_2 = \text{arctg} \frac{-2\varepsilon_n \varepsilon_k}{2\varepsilon_n^2 + \varepsilon_0^2 - 1}; \quad \varepsilon_n = \frac{n}{\omega_0}; \quad \theta_\tau = 2\pi \frac{\omega_0}{\Omega}$$

$$F(\theta_t) = \frac{1}{\sqrt{(1 - \varepsilon_0^2)^2 + 4\varepsilon_n^2 \varepsilon_0^2}} \left[\sin(\varepsilon_0 \theta_t - \psi_1) - \frac{\varepsilon_0}{\varepsilon_k} e^{-\varepsilon_n \theta_t} \sin(\varepsilon_k \theta_t - \psi_2) \right];$$

$$F(\theta_t - \theta_\tau) = \frac{1}{(1 - \varepsilon_0^2)^2 + 4\varepsilon_n^2 \varepsilon_0^2} \left\{ \sin \varepsilon_0(\theta_t - \theta_\tau) - \psi_1 - \frac{\varepsilon_0}{\varepsilon_k} e^{-\varepsilon_n(\theta_t - \theta_\tau)} \sin \varepsilon_k(\theta_t - \theta_\tau) - \psi_2 \right\}.$$

Fig. 242 shows curves $\varphi_0 = f(\theta_t)$ for various values θ_τ , calculated with the above-taken ω_0 values ($\varepsilon_n = 0.86$). These curves clearly show distortions in the amplitude and shape of anomalies of the measured parameter. In the same way, curves may be plotted for any values of factor ε_n .

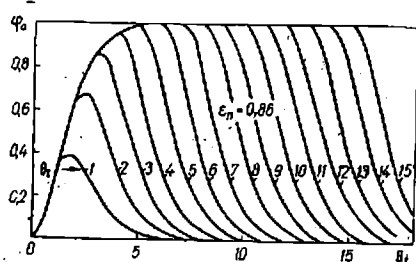


Fig. 241

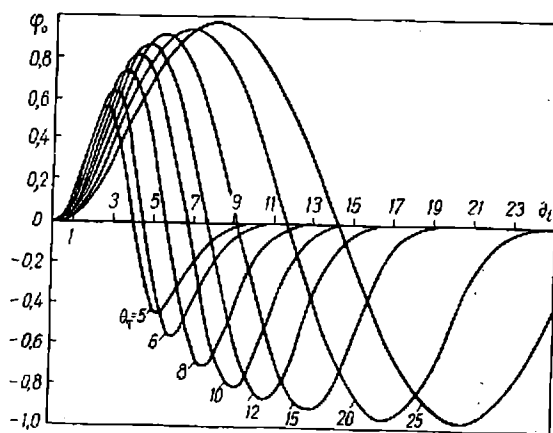


Fig. 242

7. Methodical and geological errors

In the analysis of methodical interferences (see para 6, Chapter IX), it was pointed out that they pertain mainly to the aerial induction method and dominate a number of other interferences. Therefore, these interferences determine the resulting error of measurements.

With the available calculated data regarding the magnitude of methodical interferences, it is easy to determine the methodical error caused by these interferences (in relative and absolute values).

For the aerial induction method, with a source spread out in space and receiver of the field, it is possible to determine from formulas (IX. 19) and (IX. 20) the relative ξ and absolute η measuring errors (dimensionless) during the reception of the vertical as well as horizontal components for any location point of the field receiver within the variation range of the gondola's drift angle $\theta = 0 \div 90^\circ$.

For the vertical component the absolute error value

$$\zeta_v = \frac{H_v}{A \Delta \theta} = -3 \sin 2 \theta, \quad (\text{XIII. 61})$$

relative value

$$\eta_v = \frac{H}{H_v \Delta \theta} = -6 \frac{\sin 2 \theta}{1 + 3 \cos 2 \theta}. \quad (\text{XIII. 62})$$

For the horizontal component the absolute error value

$$\zeta_h = \frac{H_h}{A \Delta \theta} = 3 \cos 2 \theta, \quad (\text{XIII. 63})$$

relative value

$$\eta_h = \frac{H_h}{H_h \Delta \theta} = 2 \frac{\cos 2 \theta}{\sin 2 \theta} = 2 \operatorname{ctg} 2 \theta. \quad (\text{XIII. 64})$$

Fig. 243 shows the curves of formulas (IX. 21), (XIII. 61) and (XIII. 62) for the vertical component and Fig. 244 - curves (IX. 22), (XIII. 63) and (XIII. 64) for the horizontal, calculated with variations of angle θ from 0 to 90° . The same figures show the variation curves of interference \mathcal{H}_r and \mathcal{H}_h (in dimensionless form) in relation to angle θ (see para 6, Chapter IX).

Analysing Fig. 243, it is possible to draw the conclusion that, in the region delimited by angles $\theta_1 \approx 45^\circ$ and $\theta_2 \approx 62^\circ$ (boundaries of the region are marked by hatching), the relative error is very high and that with a flexible geometry of system measuring the vertical component in this region is inexpedient and at $\theta \approx 54^\circ$ -, is generally pointless. As the points, at which $\theta \rightarrow 0^\circ$ and $\theta \rightarrow 90^\circ$, are approached, the relative

and absolute errors decrease, becoming zero at $\theta = 0$ and $\theta = 90^\circ$.

From Fig. 244 it follows that in the two regions, delimited by angles $0-10^\circ$ and $80-90^\circ$ (the region limits are marked by hatching), the relative error is very high and that to measure here the horizontal component with the flexible geometry of system is inexpedient and, at $\theta = 0$ and $\theta = 90^\circ$, it is pointless. As the point is approached, at which $\theta \approx 45^\circ$, the absolute and relative errors become considerably less, tending towards zero at $\theta = 45^\circ$.

With the available calculated formulas for determining the primary field tension or its components at the location point of the field receiver (see paras 2-4, Chapter IV), and also with data regarding the variation of the measured component with disruption of system's geometry (see para 6, Chapter IX), it is possible to determine the magnitude of methodical interference. Thereafter, it is easy to determine the real sensitivity of the apparatus and the magnitude of methodical error, for the adopted measuring range of signal in one or the other group in the aerial induction method.

For AEMI-2 apparatus, the intensity of the signal from the vertical component ($f_{op} = 488$ cps) $U_v \approx 0.6$ mv (see para 11, Chapter XI), and the variation of this signal with disruption of system's geometry in the range $\Delta \theta = \pm 2^\circ$ is $\frac{\Delta H_v}{H_v} \approx 17\%$ (see Table 14). Thus, the intensity of methodical interference $U_{m.i}^v \approx 200$ mcv, and methodical error $\gamma_3 = \gamma_m \approx 33\%$. In the same conditions and reception of the

horizontal component we have $U_h \approx 1.2$ mv (see para 9, Chapter XI),
 $\frac{\Delta H_h}{H_h} = 5.6\%$, $U_{m.i}^h \approx 135$ mcv, $\gamma_3 \approx 11\%$. For the Canadian
apparatus with parameters of source and the field receiver similar
to AERI-2 $U_h = 1.57$ mv, $\frac{\Delta H_h}{H_h} = 0.24\%$, $U_{m.i.} \approx 4$ mcv and
 $\gamma_3 \approx 0.25\%$.

From appropriate formulas and tables, determination of the
methodical error for induction methods is made in the same way, in
which the signals of components, picked up by two field receivers, are
subtracted one from another. In this case, the methodical error is
determined from Table 17 for the version of the rotating magnetic field
and, from Table 18, for the linearly polarized field.

For the first version, with distance between planes $r = 200$ m,
 $U_y = U_z = 125$ mcv(234) and the deflection angle $\Delta \theta = \Delta \varphi = 2^\circ$
we have $\Delta \% \approx 0.72$ (see Table 17), $U_{m.i} \approx 0.9$ mcv, $\gamma_3 \approx 0.7\%$.

For the second version, with the same values of r , U_z and $\Delta \theta$
for the horizontal oscillating frame with the measuring of signal
ratio we get $\Delta \approx 19\%$ (see Table 18), $U_{m.i} \approx 24$ mcv and

$\gamma_3 \approx 19\%$; with the measuring of signal difference - $\Delta \approx 14.7\%$,
 $U_{m.i} \approx 18$ mcv and $\gamma_3 \approx 15\%$; for the vertical oscillating frame with
the measuring of signal ratio $\Delta \approx 9.9\%$, $U_{m.i} \approx 12$ mcv and $\gamma_3 \approx 10\%$;
with measuring of the difference of signals - $\Delta = 7.3\%$ $U_{m.i} \approx 9$ mcv
and $\gamma_3 \approx 7\%$.

Thus, the error, caused by methodical interference for certain
versions of the aerial induction method, specially for those with one
plane and helicopter with the outboard gondola, is fundamental; in many

cases it is quite considerable. In the BDK (infinitely long cable) method with the outboard gondola variation of the system's geometry, caused by the bumping of the gondola, the same results, as in the induction method, in the appearance of pseudoanomalies, i.e., actually in the methodical error. This question is discussed in detail in (148).

In the application of the BDK method, pseudoanomalies from the bumping of the gondola are of two types: anomalies due to deviation of the field receiver from the preset horizontal position in a vertical plane, and anomalies, obtained with deviation of the receiver from the line of profile in the horizontal plane. The anomalies of the first type are characteristic for the zone directly adjacent to the cable, in which the intensity of the vertical component exceeds that of the horizontal or is commensurable with it, whereas the direction of the total field vector is almost vertical. This bumping of the gondola is hardly noticeable from the helicopter. The usual indication is the slow (with a period 5-10 sec) forward swaying of the gondola in the flight direction. The characteristic feature of such pseudoanomalies is the alternation of relatively flat field peaks, low in amplitude and with sharply pointed troughs, corresponding to moments of intersection by the field receiver of regions with low and high gradients of the field.

The pseudoanomalies of the second type appear usually in marginal parts of the survey area where the groundings begin to affect the non-uniformity of the field parallel to the cable. The same conditions could be due to geological irregularities in the cable zone. The magnitudes

of anomalies are proportional to the cosine of the angle, formed by peak intensity vector of the field in this plane with the axis of the field receiver.

Investigations show (148) that on low frequencies the pseudoanomalies (with disorientation of the field receiver in the horizontal plane) could sometimes be commensurable with the anomalies caused by geological objects (10-20% of normal field); on high frequencies (976 cps and higher) they become insignificant (2-3%).

A rigid attachment of the field receiver sharply reduces error due to its incorrect orientation, as the deviation of the aircraft during flight from the preset course is less than the deviations of the gondola.

Connected directly with the error, caused by the variations of the system's geometry, is an error specified by the non-linear polarization of the primary field by the metal mass of the aircraft. In the metal mass, which is in the high intensity field of the oscillating frame, eddy currents, generating secondary field are being induced which generally do not coincide in phase with the field of the oscillating frame. This may result in the appearance of elliptical polarization of the primary field, thereby causing an additional error, specially in phase measuring. However, the experience of working with AERI-2 has shown that on frequencies below 1.5-2 kcps, when the conductivity of the metal mass of the aircraft may be assumed to be purely active, the appearance of reactive component is hardly likely. This can be seen from Fig. 195: on frequency 1949 cps, the phase variation of the signal does not exceed $3-3.5^{\circ}$, and on frequency 243 cps, it is practically

non-evident. On high frequencies this error could be compensated by transmitters and the compensating frame, generating the alternating magnetic field of corresponding phase and intensity, which compensates the field of eddy currents in the metal mass of the aircraft (6, 253).

The geological interferences of the induction and other methods of aerial electric prospecting are caused by the irregularity of surface layers, drifts and surrounding medium. These interferences are one of the chief sources of pseudoanomalies (measuring errors). The presence of geological interference results in reducing the penetrating capacity and resolving power of any method in aerial electric prospecting with the harmonic field.

It has been pointed out (see para 3, Chapter V) that one of the possible methods for reducing geological error is the simultaneous survey on two different frequencies (for instance, 250 and 1000 cps or 400 and 2000 cps). Other methods for reducing the interference of geological origin are sufficiently fully discussed in (69, 71, 117, 251). Some reduction of effect from the variation of the system's geometry can be obtained by measuring the difference or the sum of signal components from the two-frequencies field (127).

8. Appraisal of resultant measuring error in the main versions of the aerial induction method

After classification of the main interference sources in the induction method, quantitative evaluation of the chief ones and errors caused by them it would be possible to determine the resultant error in measuring and to recommend a selection of the optimum measurable parameters for one

or the other version.

Error of the first group, i.e., the summarized apparatus error, is natural to the apparatus in every version of the aerial induction method. Where the measuring systems belong to the medium accuracy class, it is on an average 4% in measuring the modulus, approximately 3% in measuring the components (due to higher interference-stability of phase-sensitive voltmeters) and $1-2^{\circ}$ in phase measuring. This kind of apparatus could be applied for exploration and mapping of extensive areas with the use of various induction methods (plane version with gondola let out on a cable of considerable length - 100-150 m; "Canadian" plane version of induction; one- and two-plane versions of VMP (rotating magnetic field); two-plane version of induction with linearly polarized field, i.e., according to Table 1 - versions 2;3 and 5 of first class and versions 1 and 2 of the second).

For the apparatus with sensitivity threshold over 10^{-7} a/m, meant for detailed investigations in limited and previously explored areas with the aim of discovering purely ore objects, error of the above order is unacceptable. This type of apparatus (versions 1 ; 4 ; 6 and 7 of first class) should be equipped with the measuring systems of higher accuracy, so that the summarized apparatus error would not exceed 1.5-2% in modulus measuring and $0.3-0.5^{\circ}$ in phase measuring.

Error of the second group, as shown by investigations, is not so important and is mostly of random nature. If it is taken into account that the sensitivity threshold of the apparatus in the aerial

induction method composes 10^{-7} a/m, the continuously active portion of this error could be assumed as 0.5-1.0%. This holds true for the apparatus of the induction method with spread out source and field receiver on the condition that the field receiver is located in the outboard gondola with the length of the cable not less than 15-20 m. In the apparatus of VMP and linearly polarized field, this error becomes reduced due to the automatic subtraction of signals.

The apparatus with combined frames, located directly on the aircraft, is more exposed to vibrations, acoustic noises rotating screws and electric noises from the electric equipment of the aircraft. With sensitivity threshold 10^{-7} a/m and effective protection from vibration, acoustic and electric noises, the constantly active portion of error of the second group still increases, comprising 1.0-1.5%. The peak of the error falls to low operating frequencies (100-250 cps), on which it could be upto 3-5%.

An analysis of the three groups of errors shows that the third group frequently determines the selection of the measurable component of the resulting field from the stand point of assuring the minimum error. From Tables 14 and 16, it is possible to determine which of the two components - horizontal or vertical - is preferable with the variation of the system's geometry for field reception in one or the other version of the first class induction method. If the drift angle of the gondola θ is zero or 90° , it would be more expedient to measure the vertical component, but if $\theta = 45^\circ$, - the horizontal component. With the application of combined frames, it is expedient to use the

horizontal component.

In the apparatus of the induction method with the drift angle of the gondola 0; 45 and 90°, it would be more rational to apply the simple method of electric compensation of the signal by a circuit of invariable initial phase of the compensating voltage, matched with the initial phase of the primary signal. As shown by Fig. 174, a, with penetrating compensation and insignificant variation of the system's geometry, it is also possible to measure, besides the modulus and orthogonal components of the signal, directly phase shift $\varphi_x \approx \varphi_2$. It is expedient also because, according to the curves in Fig. 56 and 57, it is possible to determine from the measured angle $\varphi_x \approx \varphi_2$ parameter γ^2 . In the other methods of electric compensation and other versions of the induction method, the implementation is of relative measuring and the results obtained cannot be directly used for determination of the absolute value of the phase parameter.

Thus, it may be assumed that the resulting error of the first and second groups ($\gamma_{res} = \sqrt{\gamma_1^2 + \gamma_2^2} \cdot 100\%$) has, on an average, the following values (132):

- a) for survey investigations with the measuring of modulus $\gamma_{res_m} = 5 \div 5.5\%$, component $\gamma_{res_m} = 4.5 \div 5\%$, $\gamma_{res_f} = 4 \div 4.5\%$ from the 45-degree scale of recorder;
- b) for detailed investigation with the measuring of modulus $\gamma''_{res_m} = 2 \div 3\%$, component $\gamma''_{res_m} = 2 \div 2.5\%$ $\gamma''_{res_f} = 1.7 \div 2.2\%$ from the 45 degree scale of recorder.

It should be mentioned that the versions of the induction method

systems, meant for geophysical survey investigations, may consist of a set of apparatus, permitting simultaneous recording of several parameters of the resultant field signal on two essentially different operating frequencies. It would also be expedient to supplement these systems with the apparatus of other aerogeophysical methods. The systems meant for detailed investigations in previously explored areas, due to the necessity of increasing the measuring accuracy, usually record one, the most effective, parameter of the signal and, as a rule, on one operating frequency.

Table 24 gives the values of average errors of the basic versions of practical induction methods and also the recommended methods of electric compensation of the primary field signal and the optimum measurable parameters of unbalanced signal.

9. Error in radio-transmission of the main signal.

Recording of φ_x and \dot{U}_x by the measuring apparatus of the BDK method requires transmission of the main signal \dot{U}_m from the ground generating unit to the mobile measuring unit. With absolute measuring of φ_x , it is necessary that the \dot{U}_m phase in relation to the circuit in cable \dot{I}_1 should be known (it is preferable to have $\varphi_m = 0$) and be constant in time.

The phase errors of radio-channel for the main signal $\Delta \varphi_m$ could be shown as the sum total of errors in its individual elements:

$$\Delta \varphi_m = \Delta \varphi_{t.s} + \Delta \varphi_{t.r} + \Delta \varphi_{c.k} + \Delta \varphi_{hec} \quad (\text{XIII. 65})$$

where $\Delta \varphi_{t.s}$ phase errors of comparative voltage take off system; $\Delta \varphi_{t.r}$ - phase errors of radio-transmitter; $\Delta \varphi_{c.k}$ - phase errors, caused by the

expansion time of the main signal in ether; $\Delta \varphi_{rec}$ - phase errors of radio-receiver.

As shown in (57), the phase errors of the system for taking off comparative voltage from the line with current I_1 are low - upto $\Delta \varphi_{e.s.} = 30-40$ min on all the operating frequencies.

The phase errors of radio transmitter $\Delta \varphi_{tec}$ are determined mainly by the non-uniformity of frequency and phase characteristics of the modulator and are quite high. To eliminate these errors, the set of ground apparatus includes high-frequency detector KD of control (see Fig. 251), indicator O and phase-inverter of radio-transmitter F-1. The inner phase shifts of the system are eliminated in calibration when the same signal is delivered at both its inputs.

The phase shift of control detector KD could be calculated from formula

$$\Delta \varphi_d = \text{arctg } 2 \pi F R_1 C_b, \quad (\text{XIII. 66})$$

where F - operation frequency of modulation; R_1 - load resistance of detector; C_b - blocking the condenser of the detector.

Phase characteristic of the detector is a straight line, the slope of which with low R_1 and C_b could be taken as quite insignificant.

Given below are the values of $\Delta \varphi_d$ at $R_1 = 50$ kohm, $C_b = 100$ pf and various modulation frequency F :

F , cps	81	244	488	976	1952
$\Delta \varphi_d$, rad . . .	$0^{\circ}09'$	$0^{\circ}26'$	$0^{\circ}53'$	$1^{\circ}46'$	$3^{\circ}30'$

In accordance with this data, the phase shifts upto frequency 976 cps are negligible and could be disregarded; only on frequency 1952 cps the phase error of the detector should be taken into account or, if possible,

compensated. The phase shifts of radio-transmitter $\Delta \varphi_{\text{rec}}$ could be compensated by phase-inverter F-1 with error $\Delta \varphi_d$; therefore, in further analysis, error $\Delta \varphi_{\text{rec}}$, included in formula (XIII. 65), need not be estimated.

The phase error of the main signal radio-receiver is composed of the errors of its individual stages:

$$\Delta \varphi = \Delta \varphi_{\text{hfa}} + \Delta \varphi_{\text{tr}} + \Delta \varphi_d + \Delta \varphi_{\text{lfa}} \quad (\text{XIII. 67})$$

where $\Delta \varphi_{\text{hfa}}$, $\Delta \varphi_{\text{tr}}$, $\Delta \varphi_d$ and $\Delta \varphi_{\text{lfa}}$ - the phase error respectively of the intermediate frequency amplifier and transformer, detector and low frequency amplifier.

By an appropriate selection of detector elements R_1 and C_b , the total phase error could be reduced to one constant value (for instance, to 90°) at all the operating frequencies F . Therefore, the phase errors, both on the transmitting side of the main signal radio-channel and on the receiving, could be reduced either to very low or to any known and time-constant value.

Returning to equation (XIII. 65), it can be noticed that only the phase error $\Delta \varphi_{\text{ef}}$ is found to be undetermined. It is well known (2, 72, 110, 247), with propagation through ether of the main signal as high-frequency modulated oscillations the latter are subjected to phase distortions, firstly, due to the final time of radio-wave propagation from the transmitter to the receiver and, secondly, due to the effect of the ground, above which the radio-wave is propagating. Since the main signal is received at small distances (30-50 km), i.e., the earth wave is being used, the effect of ionosphere is not estimated.

Table 24

Class of method type of system		Description of version	Averaged error, %				Method recommended for electric compensation	Perceptible field compon- ent. Optimum measurable parameters of unbal.sign.
			apparatus	external factors	methodic	resultant		
First (one aircraft).	Spread-out in space frames.	1. Helicopter version with source and receiver in one vertical plane ($\theta \approx 0^\circ$)	M 1,5-2 K 1,5 F 1,5	0,5-1	2	3	1st scheme of simple methods, 3rd of complex methods	Vertical. Modulus, phase or reactive component.
		2. "Canadian" (plane) version with outboard gond. ($\theta \approx 45^\circ$)	M 4 K 3 F 3,5-4		0,5-1	1	$\ll 4,5$	1st scheme of simple methods
		3. Plane with outboard gondola ($\theta \approx 65^\circ$)	M 4 K 3 F 3,5-4	0,5-1		< 33	< 34	1,2,3-d schemes of complex methods.
		4. Plane or helicopter with source and receiver at same altitude ($\theta \approx 90^\circ$)	M 1,5-2 K 1,5 F 1,5		1,0-1,5	3	4	1st scheme of simple methods. 3-d of complex.
		5. One plane VMP	M 3 K 2,5 F 3	0,3-0,5		$\ll 4$	$\ll 6$	--
	Combined frames	6. One generating, two receiving frames	M 1,5-2 K 1,5 F 1,5		1,0-1,5	2,5-3,5	4,5	--
		7. Coplanar or reciprocally perpendicular frames	M 1,5-2 K 1,5 F 1,5	1		2,5	1st simple, 3-d composite methods	Horizontal. React. comp. or modulus and phase
Second (two aircrafts)		1. Circular VMP	M 3 K 2,5 F 3	0,3-0,5	1,0-1,5	3,5	---	Mod., phase and compon. Mod. ratio of signals.
		2. Induction with linearly polarized. field	M 4 K 3 F 3,5-4	0,3-0,5	$\ll 12$	$\ll 13$	---	Mod. ratio of signals. Phase shift between them Modulus difference.

N.B: 1. Legend: M-modulus, K-component, F-phase. 2. In all the versions error in phase measuring is reduced to phasemeter scale 45° . 3. For the 2nd class version it would be expedient to apply vertical oscillating frame.

Thus

$$\Delta \varphi_{\phi} = \delta \varphi_t + \delta \varphi_a \quad (\text{XIII. 68})$$

where $\delta \varphi_t$ - the phase shift due to the propagation time of radio-wave; $\delta \varphi_a$ - the phase shift due to the ground effect.

The phase shift of modulating voltage $\delta \varphi_t$ depends on the ratio of carrying and modulating frequencies;

$$\delta \varphi_t = \delta \varphi_f \frac{F}{f} . \quad (\text{XIII. 69})$$

Here F - modulation frequency, f - carrying frequency, $\delta \varphi_f$ - phase shift of high-frequency oscillations.

$$\delta \varphi_f = 2 \pi f \frac{d}{c} , \quad (\text{XIII. 70})$$

where d - distance between transmitter and receiver; c - propagation velocity of light.

From equations (XIII. 69) and (XIII. 70) we get

$$\delta \varphi_t = 2 \pi \frac{dF}{c} , \quad (\text{XIII. 71})$$

i.e. the phase shift due to the propagation time depends only on distance d and the modulating frequency and does not depend on the carrying frequency.

Table 25 shows that the phase shift $\delta \varphi_t$ increases with increasing distance d and operating frequency F . In production determination of \dot{H}_x and φ_x at the ends of survey, traversed distance d may be upto 20-30 km; therefore in the interpretation of φ_x diagrams it is necessary to bring in corresponding corrections for $\delta \varphi_x$.

Table 25.

F, cps	d, m	$\Delta\varphi_t$, degr.
81	100	0,00972
	1000	0,0972
	10000	0,972
244	100	0,0293
	1000	0,293
	10000	2,93
488	100	0,0586
	1000	0,586
	10000	5,86
976	100	0,1172
	1000	1,172
	10000	11,72
1952	100	0,234
	1000	2,344
	10000	23,44

The additional phase shift due to the effect of the ground, above which the radio-wave is propagating, depends on its parameters - dielectric constant ϵ' and conductivity σ , and also on distance d and frequencies F and f . The emergence of this error the same as in the case of $\delta\varphi_t$, is explained by the phase shift of high-frequency oscillations:

$$\delta\varphi_q = \delta\varphi_{qf} \frac{F}{f} \quad (\text{XIII. 72})$$

where $\delta\varphi_{qt}$ - the phase shift of high-frequency oscillations due to the ground effect.

The expansion of function $\zeta(d, F, f, \epsilon', \sigma)$ involves a great number of mathematical operations. It may be mentioned that

in unsuitable conditions (with the radio-wave propagation above the dry ground $\epsilon' = 4$ and $\sigma = 10^{-3}$) at $d = 10$ km, $F = 10$ kcps, $f = 2$ Mcps we have $\delta\varphi_q = 45^\circ 30'$. With operations on the highest of the recommended frequencies for the BDK method (1952 cps the $\delta\varphi_q$ will accordingly be five times lower.

The additional phase shift $\delta\varphi_q$, caused by parameters of the medium, above which radio-wave of the main signal is propagating, is quite insignificant in respect of shift $\delta\varphi_t$. It decreases above a wet ground, is very low above fresh water and practically non-present above sea water. With a reduction in the carrying frequency, the magnitude of $\delta\varphi_q$ increases. However, the total value of $\Delta\varphi_q$, as pointed out, is insignificant and it may be assumed $\Delta\varphi_{ef} \approx \Delta\varphi_t$.

Thus, analysing the phase errors $\Delta\varphi_m$ of the main signal radio-channel/see formula (XIII. 65), it is possible to come to the conclusion that all apparatus errors could be either compensated, or they have a constant value and are accounted for in the interpretation of φ_x diagrams. With operation on low audio frequencies (81 and 244 cps) and short distances from the radio-transmitter of the main signal to the receiving and measuring apparatus the variable error $\Delta\varphi_{ef}$ is low and could be disregarded. With operations on high frequencies (976 and 1952) and long distances, an appropriate correction should be made in the interpretation of φ_x recording. It would be expedient to plot for this purpose either tables or curves of $\Delta\varphi_{of} = f(d, F)$.

10. Calibration of receiving-measuring channel

The receiving-measuring channel is usually calibrated for the checking and setting of the required working amplification factor of the

amplitude (modulus) measuring channel, the checking of working sensitivity of the magnetic field receivers and of good working order of individual blocks of apparatus. Calibration contributes to increase the accuracy of the measuring apparatus in productive conditions. This question has been thoroughly dealt with in (59, 90, 126).

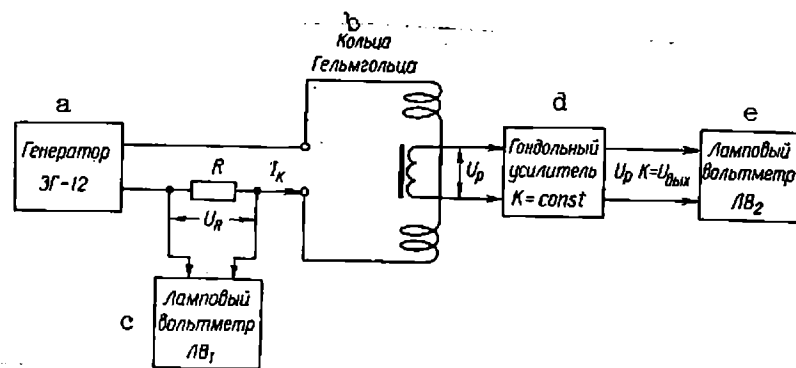
In AMRI-2, calibration is composed of three stages and includes, consecutively, the measuring amplifier, the transmission channel of the signal from the input of the gondola amplifier to the output of the measuring amplifier and the entire receiving-measuring channel (including the magnetic field receivers).

Calibration is implemented in the following order. As a preliminary, in the laboratory or at the base airport the working pickup of the magnetic field receivers is checked. The checking should be conducted in accordance with the diagram shown in Fig. 84 or Fig. 245. The sensitivity of field receiver S_r should be estimated from formula (VII. 26b and c). If there is an assurance that the sensitivity of the field receiver corresponds to the preset working value, the receiving-measuring apparatus could even be checked in productive conditions, i.e., during the flight.

The first to be calibrated is the selective measuring amplifier, after which the calibration signal, delivered to the receiving channel, acquires its nominal intensity.

Block diagram of the selective measuring amplifier in AMRI-2 with calibration elements is shown in Fig. 246. The calibration circuit includes resistance amplifier, which is fed comparative voltage used as calibration signal, and vacuum-tube voltmeter, previously graduated from a standard device. The error of the vacuum-tube voltmeter does not exceed

1-2%. Comparative voltage from the quartz master oscillator varies at various frequencies from about 2.9 to 3.9 v; therefore, to obtain nominal intensity, the calibration signal requires its adjustment, which is implemented in the resistance amplifier and is controlled by the vacuum-tube voltmeter. This amplifier raises the level of the calibration signal upto 15 v - optimum level of working voltage for the circuit of the tube voltmeter. By setting the calibration signal according to this voltmeter, the required calibration voltage, fed to the input of the selective circuit, is obtained automatically. In the resistance amplifier, the adjustment elements fix the required amplification factor of the selective measuring amplifier.



Key to Figure 245:
a, Generator 3Г-12;
b, Helmholtz coil;
c, VTVM, LV₁;
d, Gondola amplifier K = const;
e, VTVM, LV₂.

Fig. 245

Key to Figure 246:

a, To the gondola amplifier;
b, Resistive amplifier;
c, Reference voltage;
d, Selector circuit;
e, Cathode repeater;
f, Attenuator;

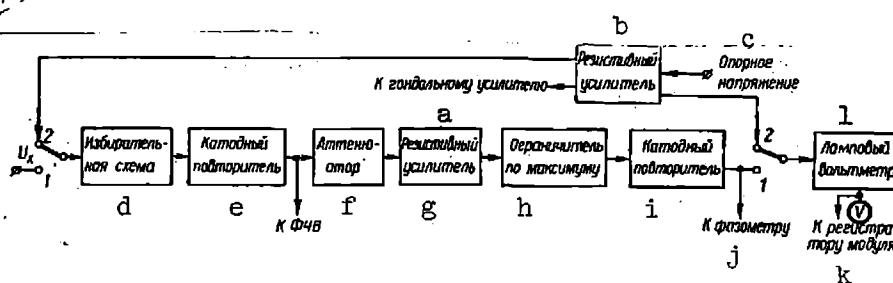


Fig. 246

g, Resistive amplifier;
h, Limiter with respect to maximum;
i, Cathode repeater;
j, To phase meter;
k, To recording module;
1, VTVM.

The receiving channel is calibrated separately on channels of low and high frequencies by feeding to the input of the receiving channel certain intensity of the calibrating signal with subsequent measuring of the output voltage from the gondola amplifier which, during calibration, should be the same on all the operating frequencies. Deviation of the output voltage from nominal may indicate, for instance, some defects in the receiving coils, in the input system or detuning of the magnetic field receiver. Depending on the magnitude of deviation, either the checking or adjustment of the channel is required. The method of this calibration for one channel is explained by the diagram shown in Fig. 247.

The comparative voltage U_{com_1} , used for calibration, arrives at the block of the selective measuring amplifier where, after the amplification, the calibration signal is measured by the vacuum-tube voltmeter of modulus meter (tumbler Bk_2 is in position 2). By means of potentiometer R_{89} , the comparative voltage is set at an intensity at which there is a complete deviation of the voltmeter's indicating needle. This voltage is the initial one for calibrating the whole of the receiving-measuring channel.

The active divider $R_{100} - R_{102}$ of sufficient accuracy serves for delivery at various points of the circuit of the calibration signal of different intensity. The first to be calibrated is the amplification in the selecting circuit and RC-amplifier (with tumbler Bk_1 in position 2, tumbler Bk_2 in position 1). A certain portion of the calibration voltage from divider $R_{100} - R_{102}$ is delivered to the input of the selective measuring amplifier. By means of potentiometer R_{63} the amplification factor is set in RC-amplifier of a value at which there is complete

deviation of voltmeter's needle.

- Key to Figure 247:
a, Selective measuring amplifier, channel I to FCHV Channel I;
b, Selection circuit;
c, RC-amplifier;
d, VTVM;
e, Calibrated signal amplifier;
f, Stabilized rectifier of gondola amplifier;
g, Channel I compensator;
h, Channel II compensator;
i, Connecting cable;
j, Gondola amplifier;
k, Receiving antennas.

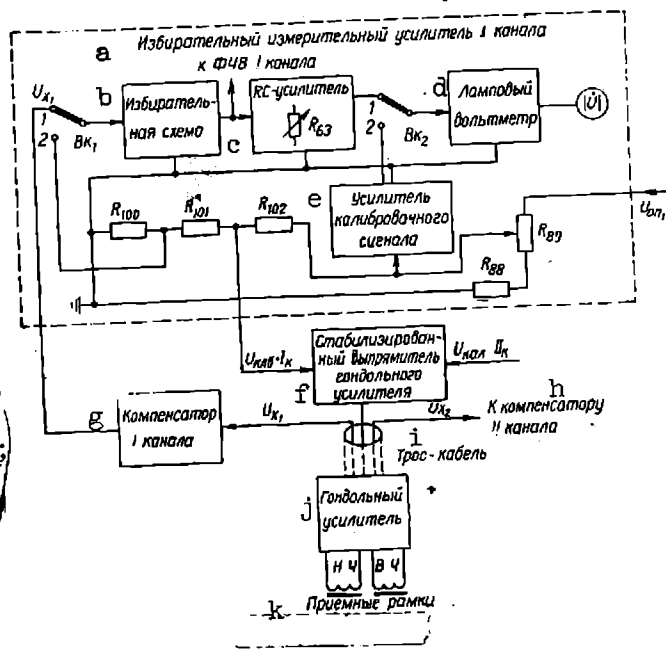


Fig. 247

For calibrating the measuring channel of the components, the phase-detecting voltmeter of the same channel is switched over to measuring the active component and the same measuring limit is set as for the modulus meter. By the adjustment of the FD-voltmeter through the amplification factor, total deviation of the needle is obtained in the direct counter of the component. (Prior to calibration with quadrant phase-inverter, zero adjustment of phasemeter should be made in the circuit of the main signal).

For calibration of the receiving channel, a portion of the calibrating voltage from divider $R_{100} - R_{102}$ ($U_{cal} = 0.5v$) is delivered into the stabilized rectifier block of the gondola amplifier remote energizing and hence into gondola amplifier. The tumblers Bk_1 and Bk_2 are in position 1. If the measured (i.e. calibrating) voltage deviates from the preset

intensity of 5 mv, its nominal intensity should be set by adjustment of the amplification factor in the whole measuring channel (in this case $K_{tot} = 1.5 \cdot 10^6$). The passing of the calibration signal through the stabilized rectifier block of the gondola amplifier is explained by the diagram shown in Fig. 248.

From the measuring group of channel I, the calibration signal is delivered on tumbler Bk_3 directly, and of channel II - on tumbler Bk_4 through voltage divider $R_{15} - R_{16}$.

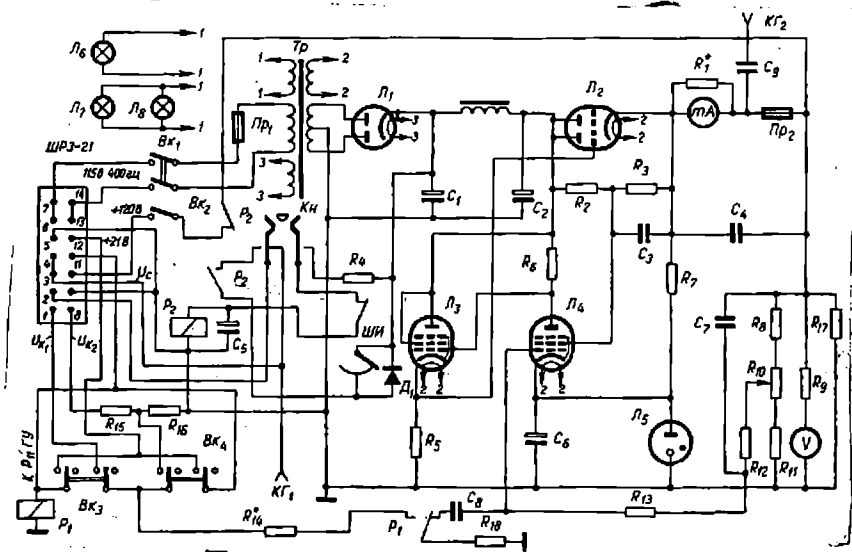


Fig. 248

The need to reduce the intensity of channel II calibration signal ten times in comparison to channel I is due to the fact that the sensitivity of the field receivers on high frequencies is considerably higher than on low frequencies; therefore, the voltage of these frequencies at the output of the gondola amplifier also differ considerably. The division of the calibrating signal of channel II immediately at the input of the gondola amplifier is rather difficult owing to the build-up of parasitic inductions on this divider.

During calibration the switching on is either of Bk_3 or Bk_4 ; and

relay P_1 , while operating, delivers the calibration signal by separating capacitance C_8 to unit controlling anode current of the stabilized rectifier with transmission factor of one. On direct current voltage 120v is superimposed the alternate voltage of the calibration signal for further transmission to the gondola amplifier.

Resistance R_{18} , cut-in to the unit of the anode current control, assures steady work of the stabilizer with the cut-out calibration, and resistance R_{14} , connected in series with the separating condenser C_8 assures steady work of the stabilizer during calibration.

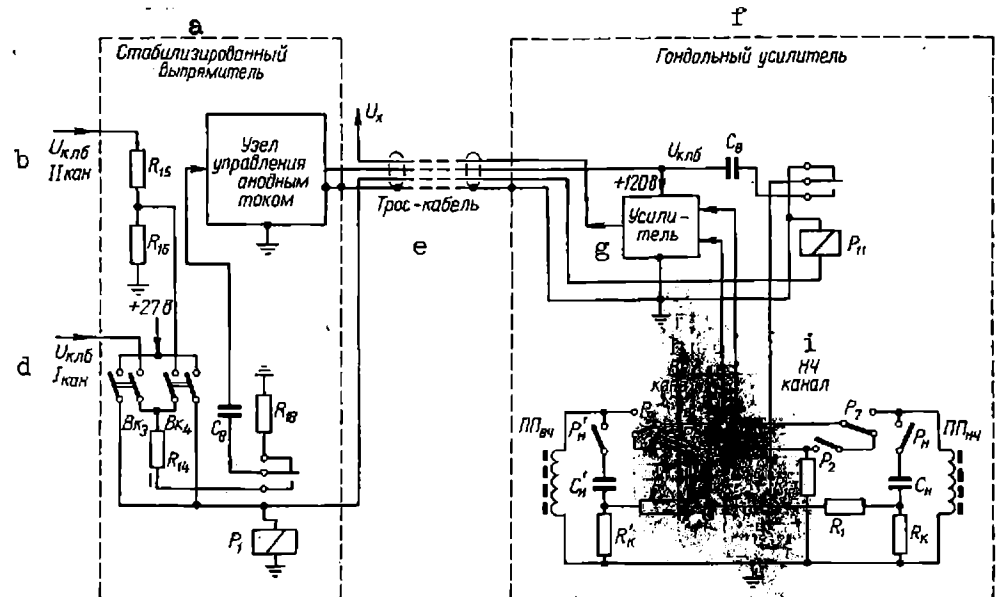
A detailed diagram of the whole receiving channel calibration is shown in Fig. 249. Simultaneously with relay R_1 in the stabilized rectifier block, operates relay R_{11} of the gondola amplifier (+ 27v is delivered to this relay by the third wire of the cable), which connects the branching node of dividers of the calibration signal to the calibration channel (see Fig. 117).

From divider $R_{14} - R_{48}$ (resistance R_{13} could be disregarded due to its low value) the calibration signal is delivered through the contacts of relay P_5 and P_9 to the input of the gondola amplifier channel II (position 9 of finder SHI_2 ; see para 2 Chapter X). If the brushes of finder SHI_2 are in position 10, the calibration signal from divider R_{13} , R_{48} , R_{14} gets delivered, through the contacts of relay P_2 and P_7 , to the input of channel I. The magnetic field receivers are cut out in both the cases.

To compensate for the partial voltage loss of the high frequency calibration signal on divider R_{15} , R_{16} in the stabilized rectifier block, divider R_{14} , R_{48} , R_{13} of the gondola amplifier divide this signal in the ratio 100: 1. Thus the delivery of calibration signals of the

same label is assured to both the inputs of the gondola amplifier. The latter's output voltages are then checked in the appropriate channels of the measuring group.

In positions 1-6 of the finder's brushes, the gondola amplifier is calibrated jointly with the field receivers.



a, Stabilized rectifier; b, U_{k1b} channel II; c, Anode current control unit; d, U_{k1b} channel I; e, Connecting cable; f, Gondola amplifier; g, Amplifier; h, HF channel; i, LF channel.

Fig. 249.

In calibration on channel I, the calibration signal gets delivered, through the contacts of relay P_{11} to the branching node of resistances R_1 , R'_1 and R_{14} ; relay P_7 and P_9 are both in working condition. In this case relay P_t operates also for tuning the magnetic antenna of low frequency to the operating frequency and, through divider R_1 , R_c , the calibration signal of the operating frequency is consecutively input into the antenna circuits. The calibration of channel II is carried out in the same way (relay P_9 and P'_t are in operating condition and divider R'_1 , R'_c

is cut in).

The value of resistance R_c (R'_c) for various operating frequencies is determinable from the condition of obtaining the required sensitivity of the field receiver with subsequent connection of this resistance into its circuit. The value of divider resistance R_1 , R_c (R'_1 , R'_c) (or division ratio) is so determined so that the calibrating signal input through this divider into the receiving circuit would activate in it similar for all working frequencies e.m.f., of 5 mv, and the output voltage of the gondola amplifier should be 0.5v on all the operating frequencies.

At the end of the calibration, relay P_{11} is de-energized and the common branching point of the calibration divider becomes closed on minus through the contacts of this relay, thereby protecting the input circuit from parasitic inductions from the anode chain.

The given scheme of calibration makes it possible to obtain constant equivalent sensitivity in respect of the field, regardless of the fact that, during the survey, some elements of the receiving-measuring channel may partially change their parameters and, moreover, it permits reduction to a considerable extent of the error of measuring of the apparatus. The shortcoming of this scheme is that the apparatus is calibrated not directly from the known magnitude of the magnetic field, as in the use of Helmholtz coils (111), for this purpose but from a known intensity of voltage, input into the oscillating circuit. In the scheme of Fig. 250, an artificial voltage ΔU is generated at the input of the gondola amplifier proportional to the required magnetic field \dot{H} and corresponds to the selected calibration range.

• U_c voltage, controlled by voltmeter, is fed to control the tube grid

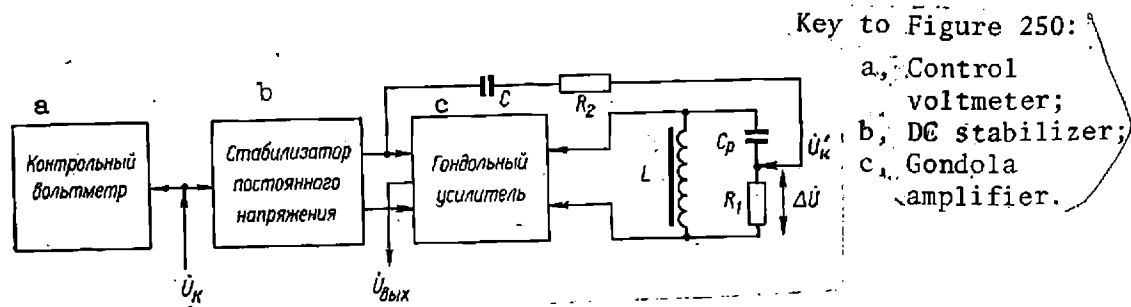


Fig. 250

in the stabilizer of the constant current voltage, which energizes the filament and the anode-screen circuits of the gondola amplifier. At the stabilizer output, simultaneously with the constant component, appears the alternate component of calibration voltage (59, 90):

$$\left| \dot{U}'_k \right| = K \left| \dot{U}_k \right| ,$$

where K - transmission factor of the stabilizer.

Calibration signal U'_c , through circuit $C R_2 R_1$ will enter the receiving circuit L, C_p as U voltage, causing appearance in the circuit of voltage

$$\dot{E}_1 = \Delta \dot{U} Q_c, \quad (\text{XIII. 73})$$

where Q_c - Q -factor of circuit $LC R_1$.

Under the effect of the vector component, the magnetic field for instance H_x , there is activation in the circuit of e.m.f.

$$\dot{E}_2 \approx S_0 Q_k \dot{H}_x, \quad (\text{XIII. 74})$$

where S_0 - initial sensitivity of the receiving coil on the operating frequency.

The transmission circuit of U_c signal could be made relatively stable and, thus, with an appropriate selection of divider CR_2R_1 , to calibrate the system on various operating frequencies according to the known magnitude of field H_x on one of the measuring ranges of the apparatus. Thus, in AMRI-2 and AMRA-2, calibration by this method is carried out on limit 10 mv.

The calibration of the measuring channel, in accordance with described method, could be implemented during flight and when the number of wires in the cable is limited to three.

The specificity of the combined zone method (BDK) (see para 5, Chapter III) does not permit the calibration of the measuring unit to be implemented as simply as in methods of the near zone. In the latter case, in the immediate vicinity to the receiving-measuring apparatus of the primary field exciter checking of the amplification channel from the magnetic field receiver to the recorder is not particularly difficult. In the BDK apparatus, the emitter and receiver of the field are spread out at considerable distance and the main signal, which reflects the current phase in the cable, is transmitted by radio-channel. The removal of aircraft from the sender of the main signal also introduces uncertainty in the initial phase reading, as the phase shift depends on this distance. Therefore, the correct choice of calibration for the receiving-measuring apparatus in the BDK method is of the utmost importance, specially the choice of calibration by phase.

One of the systems, permitting the carrying out of calibration by

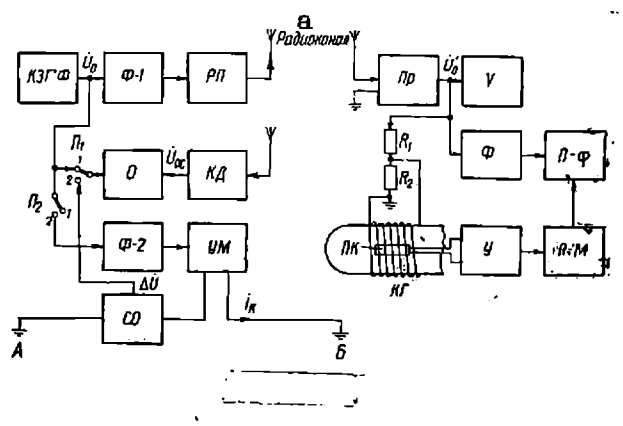
H_x with accuracy upto + 1% and by φH_x upto 1% directly during the flight, is shown in Fig. 251. The calibration is implemented by means of the induced field, generated by KG winding specially wound on the gondola, implementing function of Helmholtz coils. The current in KG winding is set by the comparative voltage of preset frequency U'_0 by means of voltage divider R_1, R_2 . From low-frequency master oscillator KZGF through phase-inverter F-1, the modulating voltage is delivered to radio-transmitter R and, in the form of high-frequency oscillations, modulated in amplitude, emits into the air. The phase of the main signal is controlled by control detector KD and control circuit O, which could be implemented as a zero indicator or oscillograph. Two voltages are fed to O circuit - U_0 and $U_{0.c}$ (from the control detector). It is assumed that the detector does not bring in phase errors in the demodulation of the main signal, or that if they do take place, they are previously got compensated in this block. The same requirements are extended to circuit O also. In the presence of the phase shift between the U_0 and $U_{0.c}$ voltages, it is eliminated by phase-inverter F-1. The position of switches P_1 and P_2 corresponds to the work of the apparatus for calibration, when into the grounded cable A-B no current is supplied from the power amplifier YH.

Phase characteristic of receiver π_p is corrected with an account of natural shifts in the elements of the receiver and additional phase shift due to the propagation time of radio-wave between the radio-transmitter and the main signal receiver. Therefore U'_0 voltage, at the moment of calibration may be taken as corresponding in phase to U_0 voltage on the transmitting side. As a result, the current in KG coil

reflects almost completely the state of ΔU_0 voltage at a given time, i.e., its phase, which is exactly what is required for the calibration.

In calibration by amplitude and phase, according to the scheme in question, it is necessary, for eliminating additional phase error due to the propagation time of radio-wave between the sender and receiver, that at the moment of calibration, the helicopter with measuring apparatus should be at a certain distance from the transmitter of the main signal. The radius of this circumference could be 5-10 km with deviation, during the flight, $\pm 1-2$ km.

Calibration procedure by phase is as follows: on the operating frequency, the KG coil generates the current, the intensity of which is controlled by voltmeter V, connected to divider R_1, R_2 with a preset division ratio. Thus in the receiving coil ΠK a certain e.m.f. is being induced from the magnetic field H_x . By phase-inverter, F, connected into the circuit of the main signal U_0 , phase recorder $\Pi - \varphi$ is adjusted at zero. The measured signal gets delivered to recorder $\Pi - \varphi$ from receiving coil ΠK through amplifier Y and modulus recorder $\Pi - M$.



Key to Figure 251:
a, Radio channel.

Fig. 251.

Calibration by amplitude is carried out simultaneously with calibration by phase. With this aim, the current amplitude in coil KG is controlled more carefully (by block V). Indication of recorder $\Pi - M$ to check the mark of the scale by varying the amplification factor of amplifier in the amplitude measuring channel.

The cable field, which has the current phase coinciding with the main signal phase, is generated by switching over of switches Π_1 and Π_2 into position 2. The operating current is input into A-B cable from amplifier YH . Phase-inverter $F-2$, by the control device of scheme 0, adjusts zero phase shift between voltages \dot{U}_c and $\Delta \dot{U}$. The $\Delta \dot{U}$ voltage is delivered to scheme 0 from the voltage take-off system CO, reflecting the same phase as current I in A-B cable.

The described calibration technique by phase and amplitude, eliminates the uncertainty of initial values φ_x and \dot{H}_x and permits the study of their variations within the survey area without additional apparatus distortions. Moreover, with this calibration there is no primary field of the cable which, in other cases, is an interfering signal (90, 118).

11. Reducing effect of interference impulses.

The measured signal in aerial electric prospecting may be superposed by considerable interference impulses, generated mostly by operating radio-stations and atmospheric discharges. In many cases, the level of the interference impulses is quite considerable, exceeding the level of the measured signal several times, which hampers the normal work of the apparatus and increases the variation error.

Key to Figure 252:

a, Input;
b, First linear spectrum converter;
c, Limiter

d, Second linear spectrum converter;
e, Output.

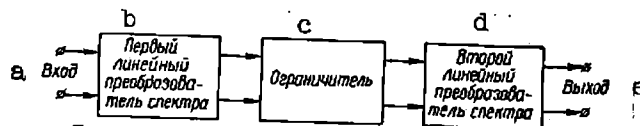


Fig. 252.

To reduce the effect of interference impulses, penetrating through the field receiver into the measuring apparatus, application is sometimes made of special systems for their limiting. These systems could be based on a higher system of protection against interference in radio-receivers consisting of a limiter and two linear transformers of spectrum (Fig. 252) (60). The operation of the system is based on transformation of the spectrum and taking into account the fact that the intensity of interference impulses of the spectral components within the operating frequency band of apparatus (300-5000 cps) is actually independent of frequency, whereas the intensity of working signals of the spectral components quickly decreases with its rise.

Fig. 253 shows the transformation structure of the working signal and interference impulse in the limiter of these interferences. Input oscillations, containing the working signal and interference impulses (Fig. 253, a), are fed into the input of the first linear spectrum transformer, the transmission factor of which increases with frequency. In the simplest way, this transformer could be assembled as a differentiating RC-chain. Due to this transmission factor of the first linear transformer, the useful signal at its output will be dampened to a greater extent than

the interference impulses. As a result, the level of the useful signal at the output of the transformer will drop noticeably, whereas the level of interference impulses will change very little (Fig. 253, b).

From the output of the first transformer the useful signal mixed with interference impulses gets delivered to the limiter, the limit threshold of which is higher than the maximum level of the useful signal, and hence - to the second linear spectrum transformer, with the transmission factor decreasing with the rise of frequency. The second transformer performs inverse to the first one transformation of the spectrum of oscillations and, as a result, the relative level of the useful signal increases to its normal value (Fig. 253, c). The simplest way to assemble the second linear transformer in the form of integrating RC-chain.

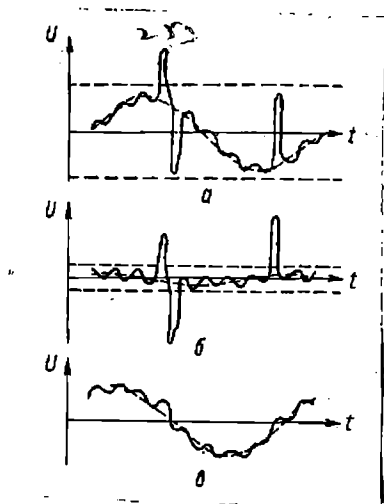


Fig. 253

Block diagram of limiter (ОЧП) of interference impulses worked out in application to the apparatus of aerial electric prospecting and which takes into account the specific nature of its work (fixed operating frequencies, high dynamic range of input signal), is shown in Fig. 254

The system's limiter is assembled with a follow-up limitation threshold. The principal diagram of ОМП, applied in the compensator of AERIS apparatus, is shown in Fig. 182.

The signal of operating frequency picked-up by the field receiver arrives at the ОМП input, where there is a ten-stage attenuator 1 with stage divisions 10 db each. Attenuator A is so estimated so that voltage taken off from it is about 500 mv with the variation of input signal from 500 mcv to 5 v. Since the level of 500 mcv is insufficient to assure normal work of the limiting circuit, a two-stage amplifier 2 is connected directly after the attenuator with the amplification factor 10^4 . L_4, L_5 in diagram in Fig. 182), encompassed by reverse feedback of 20 db ($R_{68} - R_{69}, C_{21}$). Thus, the signal with intensity 500 mcv is amplified 10^3 i.e. upto a level of 0.5 v. Interference impulses, on passing through the attenuator and amplifier, undergo the same level changes, as the useful signal (see Fig. 253). From the output of amplifier 2, voltage containing the useful signal and interference impulse, arrives at the differentiating RC-chain 3 - the first linear transformer of the spectrum. This chain for each operating frequency is composed of resistances $R_{75} - R_{77}$ and condensers $C_{26} - C_{28}$ and is held together by means of two plates of the five-position switch Π_1 (see Fig. 182). Elements of the chain are so matched so that the useful signal of any of the five operating frequencies is attenuated 15 times, whereas the level of interference impulses remains practically unchanged. Thus the noise/signal ratio at the output of the chain increases approximately 15 times. In order to obtain, the transmission factor of the first linear transformer of the useful signal close to one, a one-stage amplifier 4(L_6, a) with

amplification factor 12, is set up at its output. From the output of amplifier 4, voltage arrives at the limiter with the follow up threshold ($L_6, b; L_7; L_8$), assembled on a circuit of parallel diode limiting.

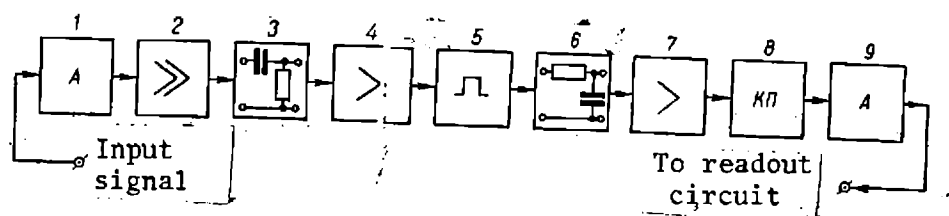


Fig. 254

The integrating chain 6 - the second linear spectrum transformer, connected after the limiter, is assembled as resistance R_{83} and a set of capacitances $C_{35} - C_{39}$, cut in by switch Π_1 in accordance with the operating frequencies. The integrating chain attenuates the level of noises, remaining after the limiting, in relation to the level of the useful signal (see Fig. 253, c). For a more effective suppression of noises, the elements of the chain are so estimated that its time constants correspond to the period of the operating frequencies.

From the output of the integrating chain, the signal arrives at amplifier 7 (L_9) with amplification factor 10, hence at cathode follower 8 (L_9), at the output of which is cut in attenuator 9, reverse in relation to attenuator 1. The last three elements of the circuit are meant for reducing the level of the useful signal at the output of $0 \text{ H } \Pi$ to the same level as at the input. Moreover, amplifier 7 compensates the 180-degree shift, brought in by amplifier 4 to the useful signal. Thus, the

common transmission factor of 0.97 is obtained almost one, which assures the transmission of the useful signal practically without damping with the highly attenuated level of interference impulses.

CHAPTER XIV - EXAMPLES OF CONSTRUCTION OF
APPARATUS FOR AERIAL ELECTRIC PROSPECTING

1. AERI-2 apparatus of induction aeromethod

AERI-2 apparatus was devised and produced in two sets on the order of the Ministry of Geology, USSR, on the basis of results obtained with the first test apparatus of the induction aeromethod AERIS. The AERIS (Fig. 255) was meant for the confirmation of theoretical postulates and for proving the effectiveness of this method; therefore, it was not quite a complete apparatus, suitable for productive operations. However, method testing and some productive operations have proved its sufficiently high metrological qualities and confirmed the value and effectiveness of the aerial induction method.

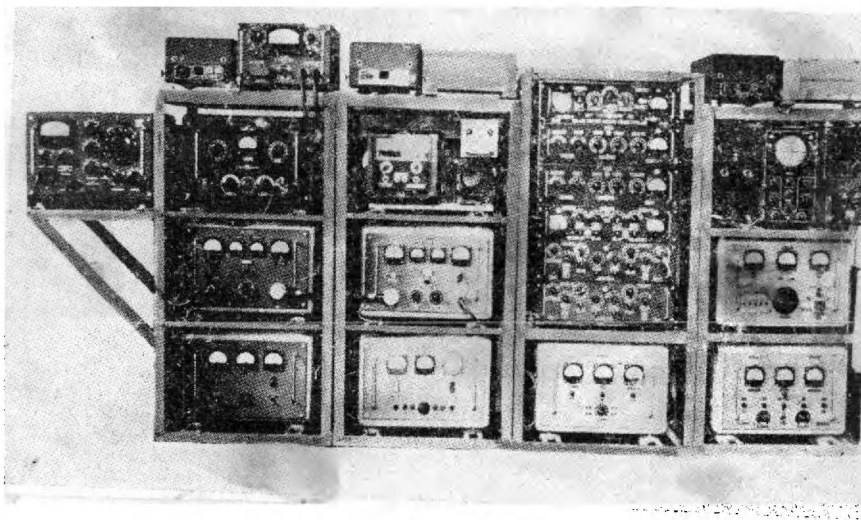


Fig. 255

The scheme of the AERIS apparatus (Fig. 256) permits the

measuring and recording, simultaneously on two frequencies of the following parameters of the resultant field: modulus, phase and active or reactive component of the signal, induced in the field receivers, and the difference of components on two operating frequencies. The main signal could be combined with current phase in the oscillating frame. The double-frequency operations were implemented on the following combinations of operating frequencies: 488-976; 488-1953; 488-3906; 488-7812; 976-1953; 976-3906 cps.

The low-frequency section of the oscillating frame was tuned into resonance, and the output power of the amplifier was 400 watts. The amplifier of the high-frequency signal provided power on an active load of about 250 watts. The sensitivity of the receiving frame on low operating frequency was approximately $12.4 \frac{V}{a/m}$; on high - it increased considerably, comprising on frequency 7812 cps $73 \frac{V}{a/m}$. The lower measuring limit of the signal amplitude (modulus) was 5 mcv.

As a result of a number of method testing and productive operations the following main defects were defined in the AERIS apparatus:

1. Non-presence of frequency division filters in the supply circuit of the oscillating frame does not make it possible to perform reliable double-frequency survey due to overstrain in the output circuits of the generating system.
2. Circuit coherence of measuring and recording the channels of the modulus and components does not permit their simultaneous

measuring and recording.

3. Comparatively high altitude of light (180-200m), specified by the safety technique of piloting and insufficient power of the generating system for this altitude limit the extent of the survey.

4. The application of recorders CK-100 and CG-17, inadaptable for operating in flying conditions, makes servicing of the apparatus difficult and lowers the quality of recording.

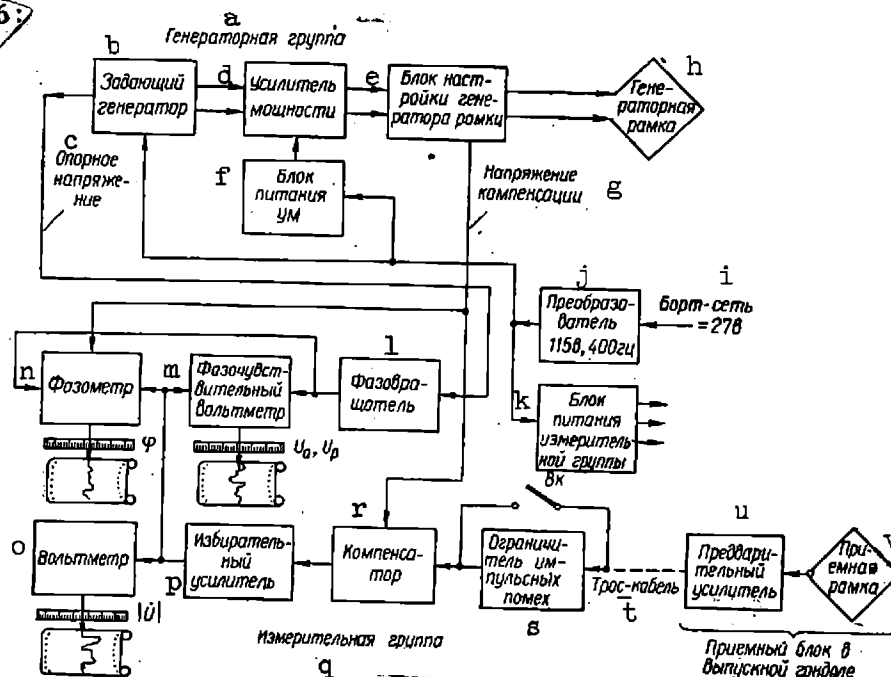
Thus, one of the main technical requirement of the newly developed apparatus was to make possible simultaneous operations of two frequencies with higher magnetic moments of the oscillating frame. The first part of this requirement in AERI-2 was met by the application of dividing filters, cut in between outputs of a two-channel generating system and sections of the oscillating frame. Increment of magnetic moments of the oscillating frame in two-frequency operations, with preset area and number of turns, was attained by increasing the power of the whole generating system and currents in sections of the frame, and also by tuning these sections to the corresponding frequencies in operations on two frequencies simultaneously.

Developed block diagram. The simplified block diagram for single-frequency operations is shown in Fig. 257. For a possible operation on the second frequency, a similar channel has been provided. The activation of one- or two-frequency magnetic field is effected by the generating system (generating group and oscillating frame) which, moreover, should supply to phase-

sensing blocks of the measuring group comparative voltage, and to the compensator - the compensating voltage. Provision has been made for matching these voltage phases with the current phase of each operating frequency in the oscillating frame.

Key to Figure 256:

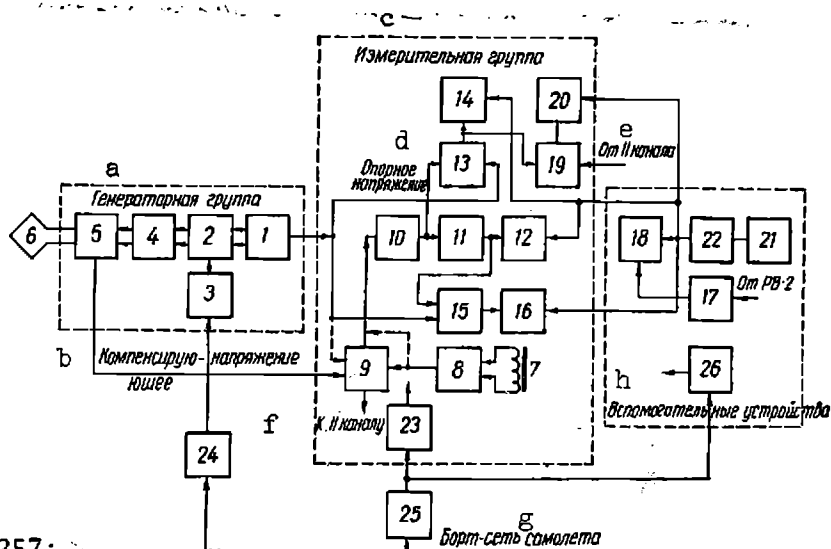
- a, Generator group;
- b, Transmitting generator;
- c, Reference voltage;
- d, Power amplifier;
- e, Unit for adjusting frame generator;
- f, Power block UM;
- g, Compensation voltage;
- h, Antenna;
- i, On-board current = 27V;
- j, Converter 115V, 400Hz;



- k, Power unit for measurement group, Bk;
- l, Phase converter;
- m, Phase-sensitive voltmeter;
- n, Phase meter;
- o, Voltmeter;
- p, Selective amplifier;
- q, Measurement group;
- r, Compensator;
- s, Limiting device for pulse noise;
- t, Connecting cable;
- u, Preamplifier;
- v, Receiving antenna;
- w, Receiving block in the extended gondola.

Fig. 256

The generating group is composed of the master oscillator 1, the power amplifier 2, the supply block 3, the dividing filter 4, the tuning block 5, the oscillating frame 6 and the standard aviation transformer 24 for the supply of current to the apparatus from the aircraft network.



Key to Figure 257:
a, Generator group; b, Compensating voltage; c, Measurement group; d, Reference voltage; e, From channel II; f, To channel II; g, On-board circuit of aircraft; h, Auxiliary devices.

Fig. 257

The master oscillator with quartz crystal control of frequency, generates oscillations of high frequency of 3898 cps with its subsequent division for obtaining the preset low frequencies (1949; 974; 487 and 243 cps). The output signal of the corresponding frequency is amplified by the power amplifier and delivered to the oscillating frame through the dividing filter and tuning block. The dividing filters assure a stable two-frequency operation of the generating group; by means of the tuning block, the corresponding section of the oscillating frame is tuned into resonance.

The measuring block is meant for measuring and recording, on two frequencies of modulus, phase, the active and reactive

components of signals, induced in the receiving elements by the anomalous magnetic field, and also of difference or sum total of the active or reactive components of signals from two operating frequencies.

The main blocks of one channel of the measuring group and of auxiliary devices are the following: common for both frequencies the receiving frames (magnetic antennas) 7 and preamplifier 8, placed in the trailing gondola, the electric compensation block 9, the selective amplifier 10 with gauge 11 and the modulus recorder 12, the phase-detecting voltmeter 13 with recorder 14, the phase-meter 15 with recorder 16, the system 17 for the matching radio-altimeter PB-2 with flight altitude recorder 18, common for both the channels the gauge of difference (sum total) of components 19 with recorder 20, the current supply block 23 and the standard airborne transformer 25 for current supply to the apparatus from the aircraft network; the time marks generator 21 and the system for matching this generator with the aerophoto camera 22.

The gondola is suspended from the aircraft by means of a three-core wire cable KTB-5M, which serves for the supply of current to the gondola amplifier, remote control and transmission of measured signals.

Picked up by the receiving frames and amplified by the preamplifier, the two-frequency signal is divided in the block of electric compensation and gets compensated to the extent required by the voltage obtained from the master oscillator or

taken off from resistance, connected in series with the oscillating frame. The isolation of the useful signal from noises is implemented in the selective amplifier, after which the signal is delivered to the modulus, phase and components gauge. The main signal for phase meter and the components gauge is taken off from the master oscillator.

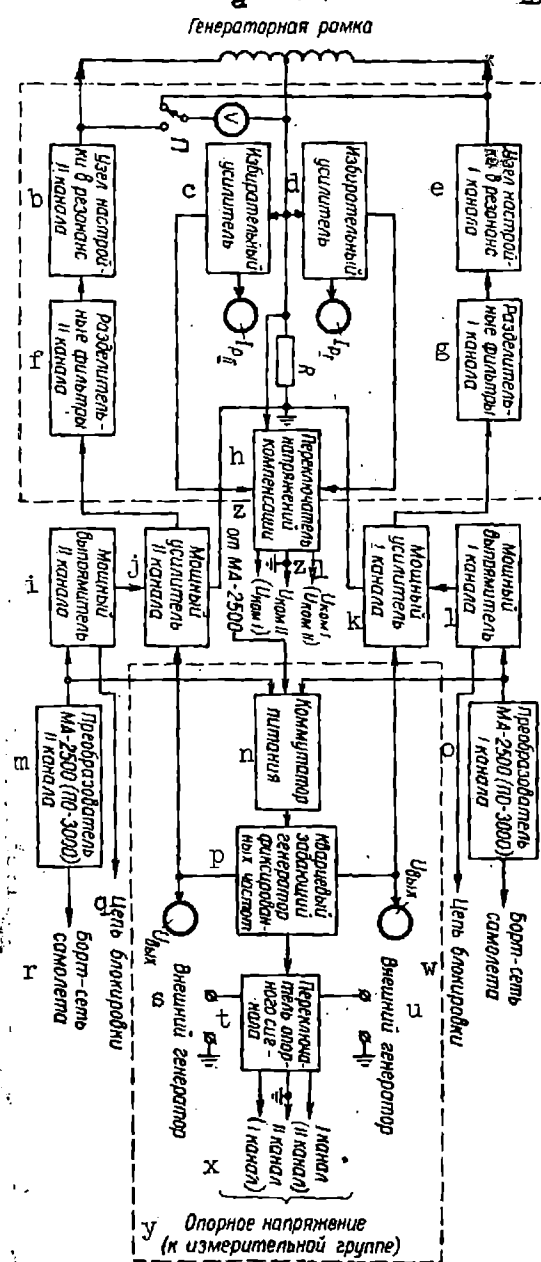
During the investigations of normal fields (flying at high altitudes) the measured signal could be fed from the gondola amplifier without compensation directly to the selective amplifier.

The block diagram of a two-channel generating system of AERI-2 is shown in Fig. 258. The two-channel output of the master oscillator (KZGF) assures the achievement of operating combinations of the two-frequency signal of the required amplitude and power for activating the power amplifiers of channels I and II. At the channel output of the master oscillator and power amplifiers, it is also possible to obtain the signal of any working frequency. The master oscillator is fed by voltage 115 v, 400 cps from one of the three transformers (MA-2500 or PO-3000), applied in the apparatus, connection to which is effected by means of the current supply commutator, fitted in the same block. The master oscillator effects the delivery of signal 2.9-3.9 v to phase-sensing blocks of the measuring group. The same voltage is used for the calibration of the receiving-measuring channel.

The power amplifier of channel I is meant for working on low operating frequencies (243, 487 and 974 cps), and of channel II -

on high (974; 1949; 3898 cps). The amplifiers are fed from competent rectifiers, which get their current supply from transformers MA-2500 or PO-3000.

- Key to Figure 258:
- a, Generator antenna;
 - b, Unit for adjustment of resonance in channel II;
 - c, Selective amplifier;
 - d, Selective amplifier;
 - e, Unit for adjustment of resonance, channel I;
 - f, Separating filters, channel II;
 - g, Separating filters, channel I;
 - h, Compensating voltage switch;
 - i, Power rectifier, channel II;
 - j, Power amplifier, channel II;
 - k, Power amplifier, channel I;
 - l, Power rectifier, channel I;
 - m, Converter MA-2500 (PO-3000) Channel II;
 - n, Power switch;
 - o, Converter MA-2500 (PO-3000) Channel I;
 - p, Quartz supply generator of fixed frequencies;



- q, Block circuit;
- r, On-board circuit of aircraft;
- s, External generator;
- t, Reference signal switch;
- u, External generator;
- v, On-board circuit of aircraft;
- w, Block circuit;
- x, Channel I, channel II, channel II, channel I;
- y, Reference voltage (to measurement group).
- z, From MA - 2,500;
- z₁, U_{com}.

Fig. 258

The outputs of power amplifiers are cut in through the matching block to the corresponding sections of the oscillating frame; the output of channel I to low-frequency section, composed of 11 loops, the output of channel II - to high-frequency section, consisting of 9 loops. The matching block assumes by means of dividing filters, reliable, stable, simultaneous two-frequency operation of the generating system on the magneto-couples sections of the oscillating frame and their tuning jointly with dividing filters to the operating frequency of the appropriate channel with the following combination of frequencies: 243-974; 243-1949; 243-3898; 487-1949; 487;3898 and 974-3898 cps. The combination of two adjacent frequencies is not effective and is not used in the apparatus. With single-frequency operation of the apparatus, any working section is also tuned to the required frequency.

To the middle wire of the oscillating frame is cut in active resistance R , from which compensating voltage is taken off for the measuring group, which shows the current phase of two operation frequencies in sections. The same voltage is used for the devices of measuring the currents I_{pI} and I_{pII} in the channels of the generating system, cut in at the inputs of the selective amplifiers of the corresponding channels of the matching blocks. The output voltages of the selective amplifiers could be used as compensation for the corresponding channels of the measuring group; however, in this case, the stability of the compensation will be low, since the

parameter variation of amplifiers will affect adversely the stability of compensating voltages. The voltage intensity on sections of the oscillating frame is controlled by voltmeter V (through change-over switch P).

The necessary condition for efficient working of the induction method apparatus is that the receiving channel should be highly noise-proof. This is achieved by concentrating selectivity in individual units and blocks of the entire receiving-measuring system in a way that would produce the required selectivity.

The block diagram of the receiving-measuring system in AERI-2, which operates simultaneously on two frequencies, is shown in Fig. 259, which also shows the auxiliary units and elements. The receiving system has two coils (magnetic antennas) for receiving and converting into e.m.f. the vertical component of tension vector of the magnetic field on an appropriate operating frequency or combination of working frequencies. To assure high preliminary selection, the receiving coils are tuned to operating frequencies 243; 487 and 974 cps (LF channel) and to 974; 1949 and 3898 cps (HF channel). The received working signals are mixed in a single-channel aperiodic amplifier (amplification factor 100), which brings up their level to a volume, exceeding the noise level in the cable and at the input of the measuring system.

Field receivers and preamplifier are placed in the trailing gondola; therefore; the change-over of operating frequencies, the current supply of the gondola amplifier and its calibration are

carried out remotely along a three-core cable. Field receivers have high field sensitivity; therefore, they assure the reception of quite weak signals.

From the maximum possible reduction of internal and vibration noises, most effective measures were adopted for shock-proofing the receiving coils, the gondola amplifier tubes, and of the whole reception system. Low-noise details were used in the amplifier and the system was carefully shielded for the elimination of external inductions. From the low-ohmic output of the gondola amplifier signals of operating frequencies are transmitted along the cable into the measuring unit. By means of the frequency change-over switch, set up in the stabilized rectifier block of the gondola amplifier, it is possible to carry out remote current supply to the amplifier and control of the receiving system and the gondola amplifier.

The received and amplified signals from the cable arrive at filters of compensation blocks of channel I and II, where they are divided, undergo additional selection and are amplified ten times. In measuring without compensation, the working signal is delivered, through the compensator of an appropriate channel, directly to the selective amplifier (amplification factor 10), in which the main selectivity of the measuring unit is concentrated. After the final filtering of noises and the rising of level of the working signal by one order in relation to the output signal (this is necessary to exclude the effect of parasitic inductions on the working signal

with its further distribution in the measuring blocks) it is delivered to all the subsequent measuring units of the apparatus. This makes it possible to measure independently the modulus and components.

From the output of the selective amplifier, the signal of the operating frequency arrives at the resistance amplifier (amplification factor 150), at the output of which is an indicator for direct reading of the received signal modulus. From the output of the same amplifier, the measured parameter is fed to the diagram tape for recording. The selective and measuring amplifiers are combined into one measuring selective amplifier. At the input of the measuring amplifier is the attenuator, by means of which the measuring range of the modulus is changed independently of other measured parameters.

After amplification, the operating frequency signal arrives in the measuring channel of the phase meter, and the master oscillator voltage - at the channel of the main signal. The comparative voltage passes preliminarily through quadrant ($0-360^{\circ}$) and octant ($0-90^{\circ}$) phase-invertors. The quadrant phase-invertor is required for zero adjustment of circuit for measuring the phase and components and for combining the main signal phase with the current phase in the oscillating frame. By means of this phase invertor, the phase may be evenly adjusted within each quadrant ($0-90^{\circ}$). The octant phase-invertor (at every 45°) is meant for expanding the measuring range of the phase. The measured phase

angle is controlled by the indicator; the recorder records its values on the diagram tape. From the output of the selective amplifier operating frequency the signal is fed to the phase-detecting voltmeter (FHV) which measures and records the active or reactive component. The signal at the phase-detecting voltmeter arrives from the master oscillator through the quadrant phase-inverter of the phase meter block. At the input of FHV is set up an attenuator for selecting the required measuring range of the component.

The measured and main signals from the phase-detecting voltmeter blocks of channels I and II are also delivered to the individual block - differential phase-detecting voltmeter (DFHV), which measures the difference or sum total of the reactive or active components of signals from two operating frequencies.

The output currents of the inner phase detectors DFHV of each channel are added up or subtracted, depending on what is being measured - the sum total or the difference of the components. The measured quantity is controlled by the indicator and record by the recorder.

The signal compensation of the primary field could be implemented by voltage, arriving from the matching block of the generating system, rigidly coupled in the phase with the current in the oscillating frame, as well as by the comparative voltage from the master oscillator. The selection of one or the other of

the indicated voltages and its delivery to the subtracting circuit of the compensator is effected by the commutator of compensating voltage of the compensation block.

In the second set of AERI-2, compensation could be performed directly by the received signal according to the scheme with the follow-up phase (see para 4, Chapter XI). For this, the commutator switch of the compensation block has a corresponding position (see Fig. 184). However, in Fig. 256 the compensation block is assembled for simplification in accordance with the usual scheme. In measuring with compensation the residual voltage (decompensation voltage) is also delivered to the measuring blocks.

The blocks of the receiving-measuring groups get the current supply from rectifiers (stabilized and unstabilized anode voltages, bias and filament voltages), which in their turn are energized by voltage 115 v, 400 cps from the transformer of the aircraft network (plane MA-2500 separate for the measuring group).

Both the channels of the measuring group are identical in their parameters and could work on any working frequency. Fig. 260 shows the developed block diagram of one channel in the receiving-measuring system with main commutation elements and nodes and blocks common for both the channels. The nodes, which in the matter of construction, form one whole (functional blocks), are shown in this figure by the dotted line.

By means of stepwise adjustment of the recorders pass band, a

675-B

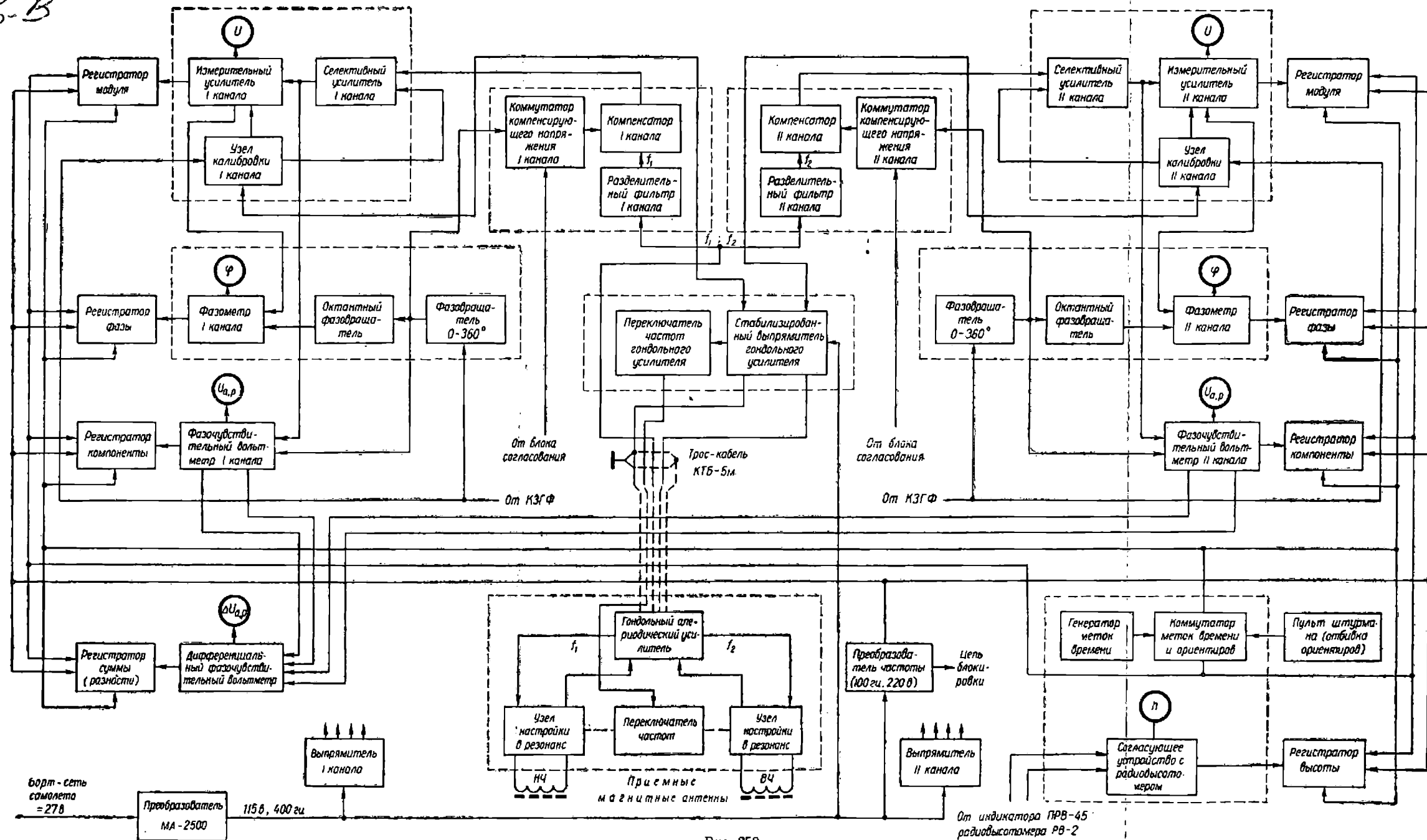


Рис. 259

FOLDOUT FRAME

FOLDOUT FRAME

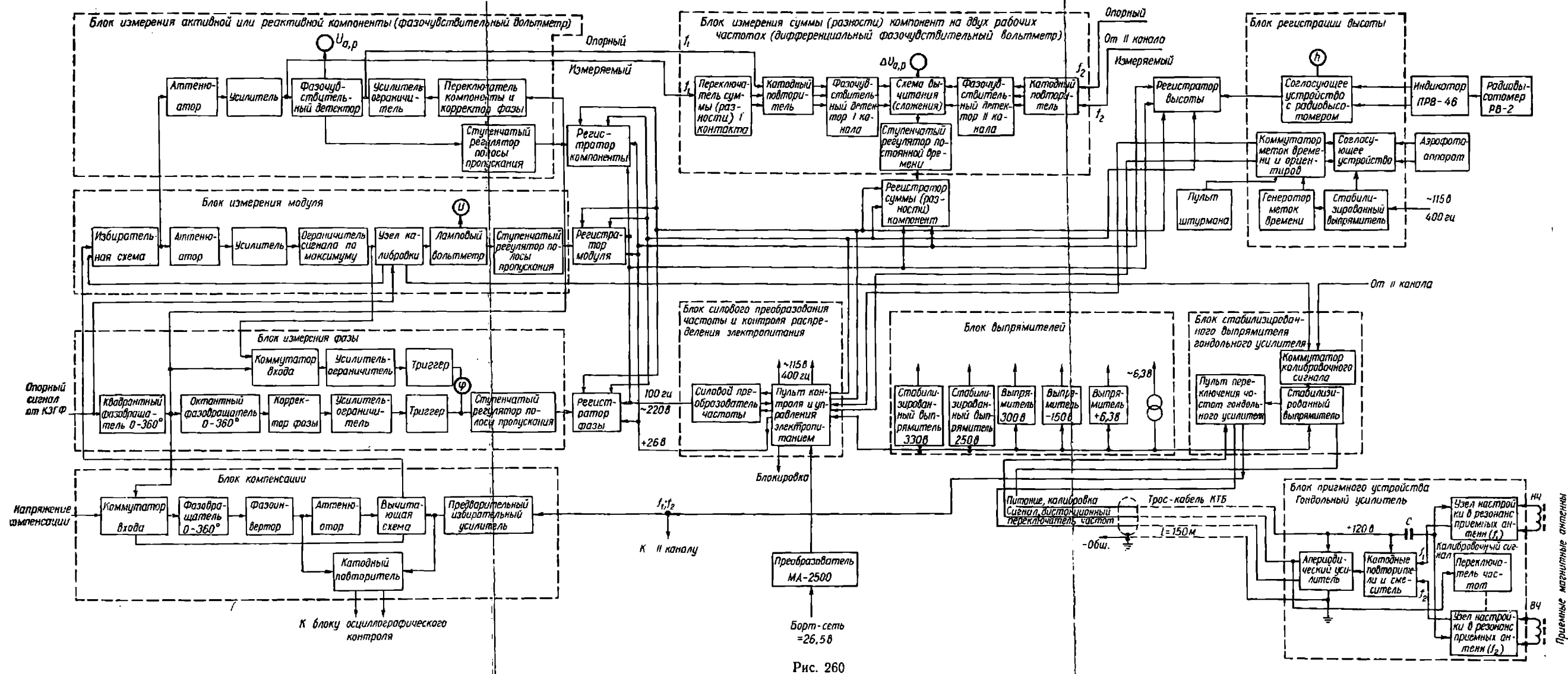


Рис. 260

variation of the recording's time constant occurs in parameter measuring blocks, which is equivalent to the measuring scale travel time of the recorder. Input into the compensation block is a dividing cathode follower, by means of which the measured and compensated signals are delivered to the oscillographic control block for visual observation of the compensation process.

The flight altitude recorder connects, through the matching system, to indicator PRV-46 of radio-altimeter RV-2. For a more precise recording of the flight altitude in the range 200 ± 30 m division is provided for of the standard range 0-1200 m into two non-standard ranges of recording 0.300 and 0.1200 m.

The auxiliary systems of the apparatus are meant for checking the efficiency of the apparatus, the measurements, the plotting of time breaks and guides on the diagram tapes of recorders etc. These systems include also the oscillographic control block, which permits checking the shape of the signal at the control nodal points of the generating and measuring groups, and also observing visually the compensation process separately in channels I and II of the measuring group.

Placed in the altitude indicator block is an electronic generator of marks, producing periodic electric impulses every $60 (\pm 1)$ sec for controlling the operation of digital markers on the recorder's tapes. By means of the commutator of time breaks and guides and the system for matching with the aerophoto camera, it is possible to mark the guides automatically, at the moment

of opening the camera's shutter. If aerial photo-survey is conducted only along the route guides, the operating is of markers with signs 0,1,2,.....,9, A and B; but if the survey is continuous throughout the route, the operation is of time break markers, which serve simultaneously as marks of the used recording range; in these cases the electronic generator of marks is cut off from the printing mechanism.

The panel located in the pilot's cabin makes it possible for the navigator to carry out remote marking of the guides during the flight of the plane above it and the setting of the next mark. The panel has an indicator of guide marks, operating synchronously with all the printing mechanisms of recorders. Electric cut in of the navigator's panel to these mechanisms is effected by the commutator of time breaks and guides.

The recorders are assembled on a base of standard recording bridges (MC), in which reversive and synchronous electric motors are used, operating from the industrial network of alternate currents (127v, 50 cps). However, on board the aircraft there is no such network and, more over, the travel time of writers on the recorder scale should be low (1.2-1.3 sec); therefore, to meet these conditions, while maintaining the invariable value of torque, it is expedient to supply to these electromotors voltage of higher frequency. Estimates and tests have shown that the most suitable is frequency 100 cps with voltage 220 v. Since the AERI-2 apparatus does not have transformers with these parameters, an

electronic-ion transformer was devised for current supply to the recorders, electromotors, capable of transforming 400 cps into 100 cps with voltage 220 v and effective power 300 v-a. This transformer has been made into a separate block, common for both the channels of the measuring group. From this plot the control of transformer MA-2500 in the measuring group is carried out and also the control of voltages and currents consumed in circuits 115 v 400 cps and 27 v of the constant current (transit circuit of transformer MA-2500, used for current supply to the marker mechanisms, number of relays, etc.). Input to the block is a blocking circuit for failure cut-out of the apparatus from the board network of aircraft.

The elements of the auxiliary systems include calibration circuits of the receiving-measuring channel, in blocks of the selective amplifier. The circuits are meant for checking and adjustment in the case of common amplification factor of the receiving-measuring channel.

Main specifications of the apparatus. The output amplifiers in sections of the oscillating frame, tuned to working frequencies 243-974 cps, provide power upto 1000 wts, and on frequencies 974-3898 cps - upto 700 watts.

The oscillating frame has 20 (11+9) loops and an area of about 88 m^2 , which makes it possible to obtain the value of the magnetic moment on frequency 243 cps (the most difficult case) upto $18300 \text{ av} \cdot \text{m}^2$. In receiving block are two magnetic antennas tuned into resonance, the sensitivity of which is $(\frac{v}{a/m})$:

for LF antenna at $f = 243$ cps -5, at $f = 487$ cps - 15, at $f = 974$ cps - 25; for HF antenna at $f = 974$ cps -25, at $f = 1949$ cps -50, at $f = 3898$ cps - 62.5. The working field sensitivity of the whole apparatus in the actual flying conditions is $2.4 \cdot 10^{-5}$ a/m.

The measuring and recording range: by modulus - 10; 30; 100; 300 and 1000 mcv, 1;3;10 and 30 mv; by components the same as by modulus, except 10 and 30 mv; measuring range of phase $\pm 45^\circ$; $\pm 90^\circ$ and $\pm 180^\circ$, recording - $\pm 45^\circ$ with selection of any octant within the range of angles $0-360^\circ$.

The selectivity of the receiving-measuring channel on all operating frequencies has attenuation not less than 40 db with detuning $\pm 10\%$ of the operating frequency.

The natural level of noises of the measuring channel, reduced to the input of the gondola preamplifier, when short-circuited, does not exceed 0.5 mcv, the mean level of external and vibration noises at the input of the receiving channel in normal working conditions is not over 20 mcv. The measuring error: of modulus and component upto 5%, in phase upto 2° . Consumption of energy from the board network is about 13k-watts. The apparatus is set up on plane IL-14P with power of board network increased upto 18 k-watt.

Construction of generating and measuring units. The AERI-2 apparatus is a composite complex, which has to operate reliably in flying conditions; therefore, during construction, the demands

imposed on it corresponded to the aviation radio-technical apparatus.

The principal co-efficient, which determine the construction of the aviation radio-technical apparatus, are (3) considerable vibrations within comparatively a wide range of frequencies (from one to some hundreds cps with amplitudes upto 1 mm), prolonged, as well as short-period accelerations, caused by the plane's motion in the air, with take-off and landing, impact loads, possible during the landing of the plane, especially in field aerodromes, extensive variation range of surrounding temperature, high relative humidity of air (upto 100%), etc. The apparatus should have minimum weight and overall size, consume as little as possible electric energy, and when it is switched on, the setting of working conditions should be quick. It should be convenient for tuning, control, repairs, etc. The enumerated requirements and the necessity of simultaneous operation on two frequencies, considerable power of the two-channel generating system and the number of recordable parameters determine the selection of the individual elements and nodes of the circuit as well as of dimensions and construction of functional blocks and of the set as a whole.

The outside view of the apparatus is shown in Fig. 261. AERI-2 consists of generating and measuring units, auxiliary systems, the oscillating frame, the measuring gondola and a system for its letting down and pulling up.

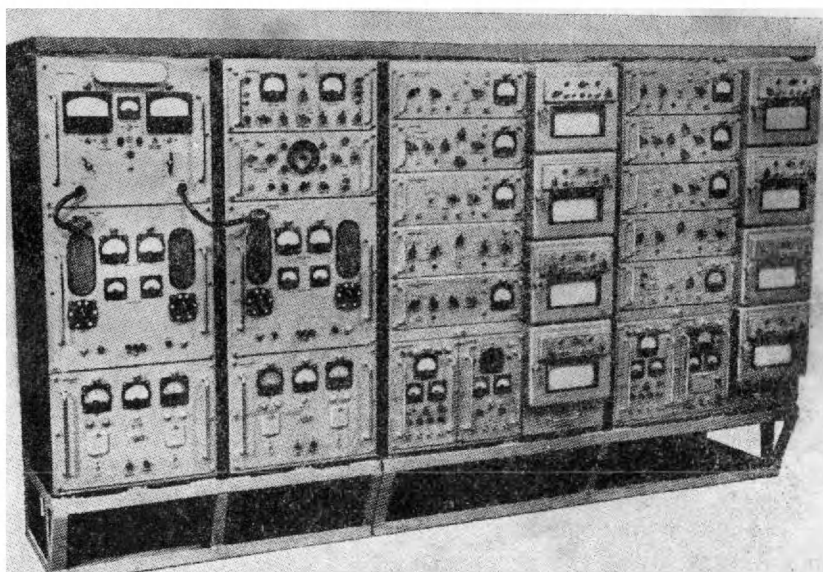


Fig. 261

The construction of the generating and measuring units is based on a system of cabinets. Four cabinets were provided for - two for each of the indicated units. The cabinets are divided into separate compartments for separate withdrawal of the functional blocks. This type of construction provides for the rational distribution of the weight of the apparatus, concentration in individual cabinets of blocks and nodes, pertaining to the same channel which is most convenient during transportation outside of the plane, since it simplifies servicing, repairs and adjustment.

Special attention is given in construction to the identity of blocks in overall size, as well as to the disposition of similar control and measuring devices.

The apparatus block consists of a front panel and a box-type chassis of pickled steel. Almost in all the blocks, the size of the chassis is 425x450 mm (with the exception of four blocks, which are 195x450 mm), whereas the depth of the cellars, according to the designation of the block, is 50, 60 and 90 mm. A similar length of the chassis considerably simplifies constructive execution of electrical and mechanical connections within the cabinets, and a similar width (in the majority of blocks) permits arranging them in monotypic cabinets. Moreover, a pair of blocks with chassis 195x450 mm is equivalent to the size of the standard block. Dimensions of cabinets: for generating unit 470x550x1200 mm; for measuring - 780x550x1200 mm.

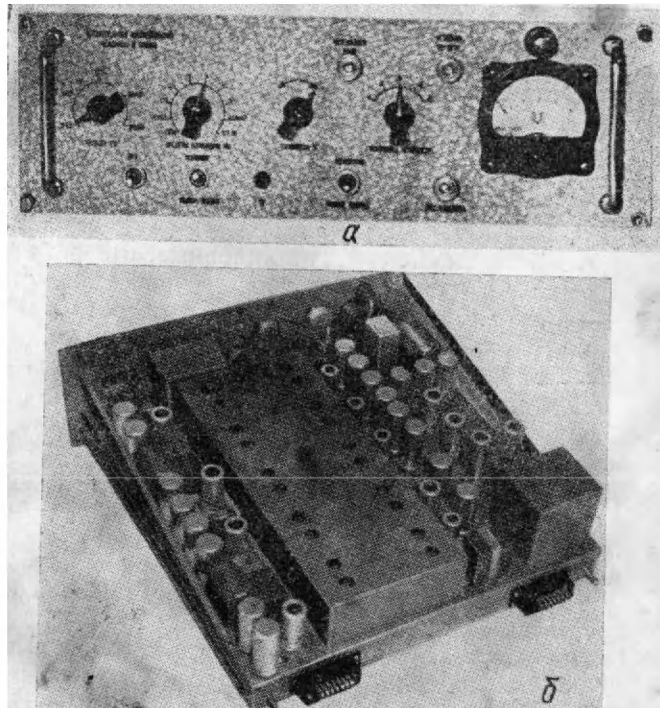


Fig. 262

Inspite of the specific properties of an individual block or a pair of blocks (the assumption is of two channels) it was possible to remain confined to the main standard sizes of front panels: three for the generating and two for the measuring units. The outside view of one of the standard blocks is shown in Fig. 262 (a - side view of the front panel, b - view from the top).

Functional blocks by means of two guiding sliders, two dowel pins and four (or six) non-falling out screws on the front panel are reliably fixed in compartments.

In the first cabinet of generating unit, there are three functional blocks, in the second - four; in each cabinet of the measuring unit, there are 11 compartments (on the left side are the functional blocks, on the right - the recorders).

The cabinets of the generating and measuring units are set up by means of 24 rubberized shock-absorbers on the two main base frames, which are rigidly fixed by bolts to the plane floor and one with the other. For convenient setting and servicing of the apparatus within the plane, the front portions of the frames are beveled towards the floor. In the first set of AERI-2 is additional top frame, to which the top surfaces of the cabinets are fastened by means of 16 rubberized shock absorbers. The top frame is fastened to the ceiling by brace wire. In the second set of AERI-2, instead of the top frame a longitudinal angled plate for sidewise attachment of the cabinets has been applied (by

eight rubberized shock absorbers, set up in the rear top angles). Attached by bolts to the longitudinal angled plate are three vertical and three sloping posts, joined by bolts to the bottom frames, thus forming a single rigid construction. The sloping posts pass between the cabinets of the apparatus. Every cabinet is attached to the base frame by eight shock-absorbers. Brace wires keep the angled plate fixed to the ceiling. Thus, each cabinet in both the sets of the apparatus is held by 10 shock-absorbers, which protect the apparatus from vibrations and shocks during the flight, as well as during the landings (79). The ventilation gratings are in the planking of the cabinets. Since the recorder mechanisms almost never get heated during operation, their compartments do not have gratings. By means of hinged brackets the recorders are attached to a vertical angled stand. Because of this each recorder, turning around the axle, comes out from the compartment and its mechanism is handy for checking, tuning or repairing. The recorders are closed with removable covers with glazed doors.

For a convenient access to intrablock connections, doors have been made at the back of each cabinet: single ones in the cabinets of the generating group, double in those of the measuring group. The doors are closed by rotary locks. At the base of the rear side of the cabinets are fixed panels, on which the plug sockets are set up for external and intracabinet connections .

The apparatus is cooled by forced air draft and outside air. The central air line, connected with the air collector, is placed on the bottom frame on the floor. The cabinet airlines are connected with the central air line by means of nipples and flexible hoses.

Each block of the apparatus is electrically connected with the general scheme by means of plug sockets and, where necessary, by special high-voltage transits. The inside plug jacks are of RSHA type (intrablock with cases for 6 and 14 contacts). The recorders are connected with the general scheme by flexible cables with socket plugs.

To exclude mutual coupling and to provide protection against the external electromagnetic field, many details (transformers, choke coils, etc.) and individual nodes of blocks are shielded by steel screens. The front panels have engraved description of blocks and the designation of control sections.

The weight of the four cabinets with blocks, bottom and top frames, is about 950 kg, and the weight of the whole set is about 1400 kg. The overall size of the apparatus is 2620x1590x1590 mm.

The trailing measuring gondola is meant for the disposition of receiving magnetic antennas and preamplifier; it is electrically connected with the measuring apparatus by a three-core cable KTB-5M, which at the same time functions as a towing cable. By means of a winch and letting-out system, the gondola could be let out from the plane to a working length of cable, 150 m.

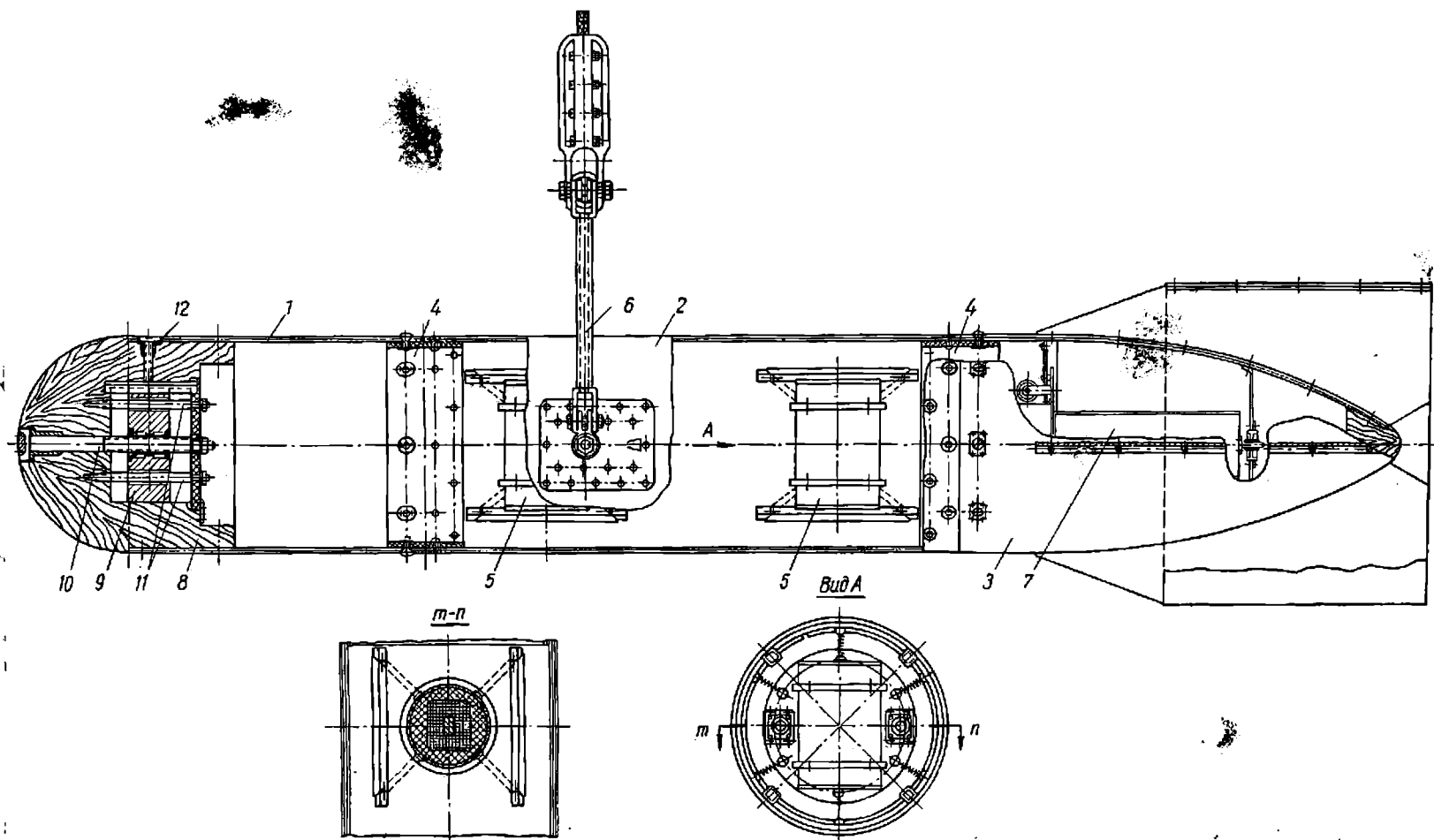


Fig. 263

The gondola is a stream-lined aerodynamic shell of cigar shape, consisting of the following main parts (Fig. 263): case with stabilizer and balance weight, suspension and shock-absorbing devices for receiving antennas.

The gondola case is made of high-quality ply-wood, impregnated with antimoisture compound. Its outside is pasted by two layers of perkale and colored by red nitre-dyes. The case consists of three parts: nose 1 with balance weight, middle 2 with attached suspension and the tail part 3 with ring stabilizer, where the gondola amplifier 7 is located. For connecting all the indicated parts there are in the middle portion of the gondola two landing rings 4 made of plastic glass, rigidly joined to this portion of the gondola by rivets. Through the screw bushing, riveted to the rings, eight brass screws are screwed in, thus assuring a sufficiently close setting and strength of the assembly.

The overall size of the gondola: OD = 290 mm, L = 1830 mm, stabilizer dia. d = 420 mm, length of the stabilizer ring 1 = 345 mm. The total weight of the gondola with suspension, magnetic reception antennas and gondola amplifier is about 55 kg.

The nose portion of the gondola is a hard ply-wood cylinder, in front of which is glued in a wooden knob 8 of spherical shape with inner boring for placing the balance lead weight 9 and transporting mechanism. By means of a duralumin screw 10 and two guides 11, the lead weight could be shifted within limits along the gondola axis for exact balancing. The weight is fixed in the required position by means of a brass press plank and screw 12. The head of the screw is in a seat on the cylinder's surface.

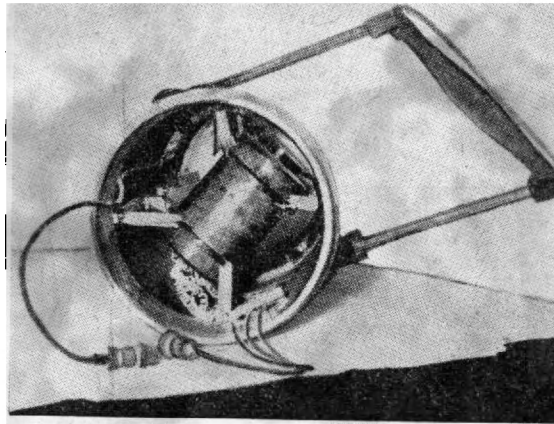


Рис. 264.

Fig. 264

Suspended on tape rubber in the middle portion of the gondola are the receiving magnetic antennas 5. The rubbers are attached to the top and bottom rings, set up on the plastic cylinders of the antennas (Fig. 264). Such is the rigidity of the selected rubbers that the natural frequency of the system would comprise a few cps. The fixing points of the rubber tapes of one antenna appear to form the apexes of a cube. This provides an approximately similar rigidity of the system in the direction of all the three coordinate axes. On the inside of the gondola case above and below the cylinders porolon pads are fixed to serve as dampers with considerable amplitude of antennas oscillations, built up during the impacts.

On the sides of the middle portion of the gondola there are two steel axles with two tractions with a cross-member, which make the suspension 6. For a reliable fixing of the axles riveted

inside and outside the cylinder there are brass facings. In the middle of the cross-member fixed on hinges is duraluminum knob, the sides of which are joined by screws with nuts. Inside the knob is an edgewise grooving, into which a steel bushing with embedded end of the cable with plug connector is inserted. The cross bars and connecting rods, which are hollow, are used for laying wires of gondola amplifier electric connection with cable cores.

For eliminating noises, which arrive at receiving antennas with the friction of metal against metal, capron (resin and fiber) bushing and washers have been put up in every hinge of the suspension.

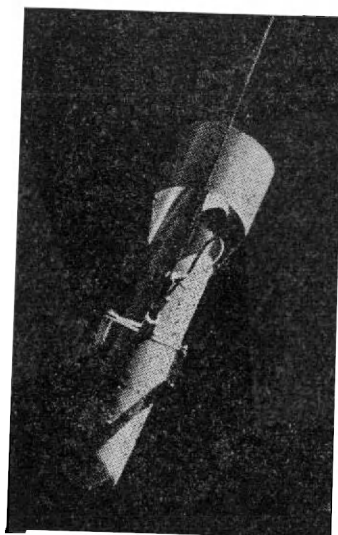


Fig. 265

Fig. 265 shows the photograph of a let-out gondola, which is additionally shock-proofed by a rubber shock-absorber. The wire-cable has a loose-fitting loop at the point of connection

with the link.

Setting up of apparatus in the aircraft. Fig. 266 shows a simplified diagram of the plane IL-14P with arranged apparatus, transformers, hatch with aerial photo-camera and let-down system. Also shown is the position and attachment of the oscillating frame.

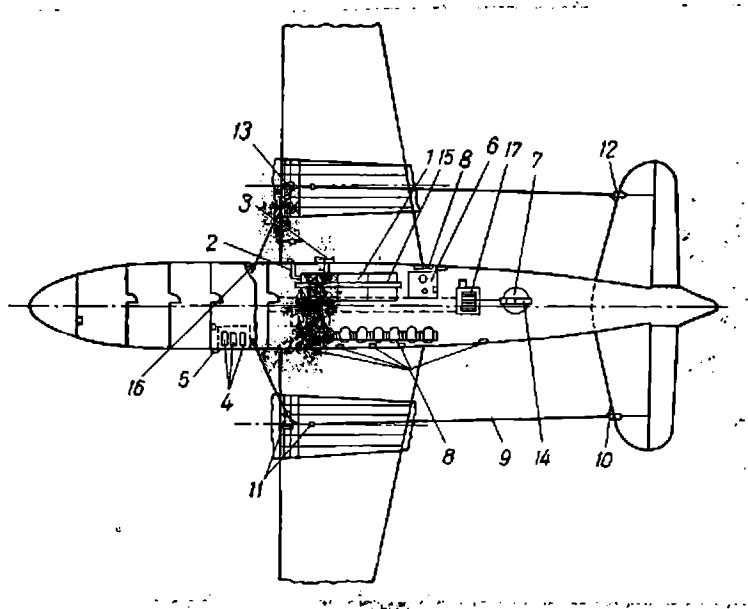


Fig. 266

The cabinets with apparatus 1 are arranged in the middle portion of the plane's center (in passenger cabin) and slightly closer to the right side. The cabinets face the left side, against which the operator's seats are placed. On the ceiling of the cabin is a beam 15 for the swinging of the top frame of the apparatus. The bottom frames are bolted to the floor of the plane.

The apparatus and transformers are cooled by outside air

by means of standard aviaional air collectors 2 and 5. Air-collector 2, set up in the right-hand forward window of the passenger cabin, connects with the apparatus by a rigid central air line and flexible hoses, fitted on nozzles of the central air line and the cabinets of the generating and measuring groups. For a better cooling of the generating group cabinets, the right-hand window has an exhaust system 3 of ejection type, joined to the cabinets by durite hose.

The transformers 4, placed into the sound-absorbing box, are set up in the forward luggage section. The air-collector 5 is joined to this box by means of a rigid metal sleeve. For the exit of heated air the box has holes at the top. On the right side of the baggage compartment, the transition block 16 is set up for bracing the turns and connection of the oscillating frame 9, as the turns of the frame are cut in its forward portion.

Fig. 266 shows the setting of the photo-hatch 6, meant for the setting of the aerial photo-camera for taking pictures of the locality along the route of the air-borne geophysical survey and optical viewer for observing the drift angle of the gondola.

In the rear of the passenger cabin is a winch with electric drive 17, in the floor of a cabin a hatch 7 is cut for the let-out system 14 with guide shaft and a device for fixing the gondola in the flying position. Along the left side of the cabin, at the working points of the operators and at the let-out system, there are the main stations of the talking system for inter communication

of the operators and for communicating with the crew during the carrying out of a survey.

The oscillating frame is made in the shape of a braid by MCSL wire 4 mm^2 in cross section. For a better streamlining in air flow and for the protection of wires from moisture the braid of the frame is covered by a plastic tube. In order that the frame may have an appropriate strength, it is suspended from the plane together with steel wire 10 (TOG 3-5 mm in diameter). The rear branch of the frame is laid on the front edge of the stabilizer and is attached to it by means of clamps. The braids of the side branches are set up jointly with the steel wire, stretched between the special plates of the stabilizer 12 and stands 13 on the motor gondolas. The wire should not form a closed loop. Therefore, it is stretched through intermediate nut insulators 11, set up near the stands of the motor gondolas.

The front branches of the frame, jointly with wire, are fixed to stands 13 on the motor gondolas, and after passing through holes in the wainscoting of the luggage compartment in the centre of the plane - to a bracket fixed in the floor. By means of rubber-bushing, the braid of the frame is insulated from the fuselage at the points of its input into the centre of the plane. Branches of the oscillating frame are fixed to the wire by means of cotton bandages.

The let-down system (Fig. 267) consists of logging winch LK-650 with stacker (not shown in the figure), electric drive 1,

guide blocks 2, shaft 3, clamps 4 for the fixing of the gondola device 5 for its reliable clamping during the flight and outlet hatch 6.

The logging winch, besides the electric drive, has a hand drive with drum brake. Onto the receiving drum of the winch 160-170 m of wire-cable KTB-5M is wound. The electric motor of the winch 0.6-0.8 k.watt with reducer, estimated for the supply of direct current from the board network, is set up on a special bracket 7, joined to the winch frame. The reducer is connected with the axle of the drive mechanism of the winch by means of a geared electric clutch, which enabless the gondola to be raised either by hand or by means of the electric drive.

In the flying position gondola enters into clamps 4, fitted on the fuselage and which center the gondola under the outlet hatch.

In order to soften the impacts and vibrations of the gondola in flying position, the clamps are lined with felting. A special device has been provided for a better fixing of the gondola, which keeps it reliably clamped. This device consists of a small hoisting block 5 with section grooving and stem for its rotation and a rubber shock-absorber 8 with hook 10. The hook catches the cross-member and by a turn of block 5 the required tension of the rubber shock absorber is obtained. The block is retained in the preset position by pin 9, which is inserted in its side holes.

Under the little guide block there is a device for releasing the gondola in case of failure. The device has a knife, the

cutting edge of which corresponds to the profile of the guide block groove. The knife is activated by an explosion of two pyro-cartridges and instantly cuts all cores of the cable. The button for switching on the pyro-cartridges (operating voltage 27 v) is in the pilot's cabin.

To prevent the friction of the cable against the plane-body during its let-down and hoisting, the bottom portion of the hatch is equipped with roller 3, which is a pair of truncated cones, joined by the smaller bases. This also helps obtain the centering of the cable in respect of the let-out system. The hoisting speed of the gondola by the electric drive is 40-50 m/min.

Electric circuit for connecting the apparatus with the board network of the plane. The primary source of power for AERI-2 is the direct current network of the IL-14P plane. Current supply in the board network is provided by two generators GSR-9000 with total power 18 k.watts. Total power consumption from the network by transformers - three MA-2500 or two PO-3000 and one MA-2500 - at nominal working conditions of the apparatus does not exceed 13.5 k-watt. The board network also supplies current for the electric drive of the winch with power 0.6-0.8 k-watt, which is, invariably, cut in with the apparatus off.

Through the transit circuit of transformer MA-2500 in the first set voltage from the board network is supplied to the apparatus for energizing some of its elements - frequency switching relay, electromagnets of mechanism for marking measuring range, time breaks and guides, recorder illuminators,

etc. In the second set, the transit circuit of transformers PO-3000 is used for the supply of voltage from board network to the generating group for energizing frequency switching relay.

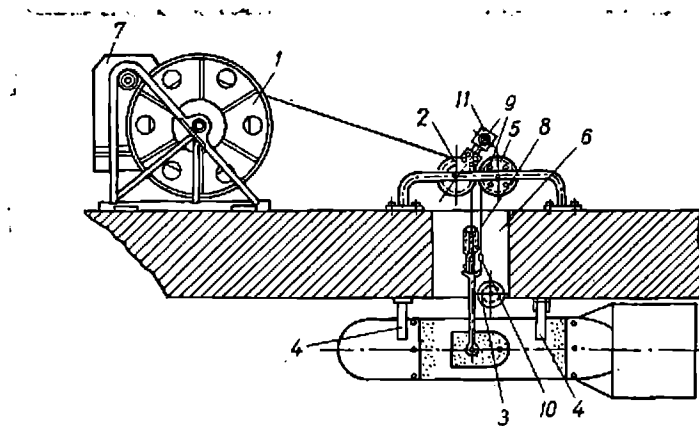


Рис. 267.

Fig. 267

The block diagram of the apparatus connection with the board network is shown in Fig. 268. The same diagram shows in a simplified form the main units of the electric system of the plane (generators GSR-9000, their protective system, current and voltage control node, etc.) The board network is "grounded" by minus to the plane's body.

The positive of the transformers 2 (MA-2500 or PO-3000) is connected with the bus bar of the left side through fuse 1 IP-200 type, the negative - directly with the plane mass. The section of each feeder should be approximately 70 mm^2 . The transformers are connected by means of hoses with appropriate cabinets of the apparatus, from which the remote control of transformers is being effected.

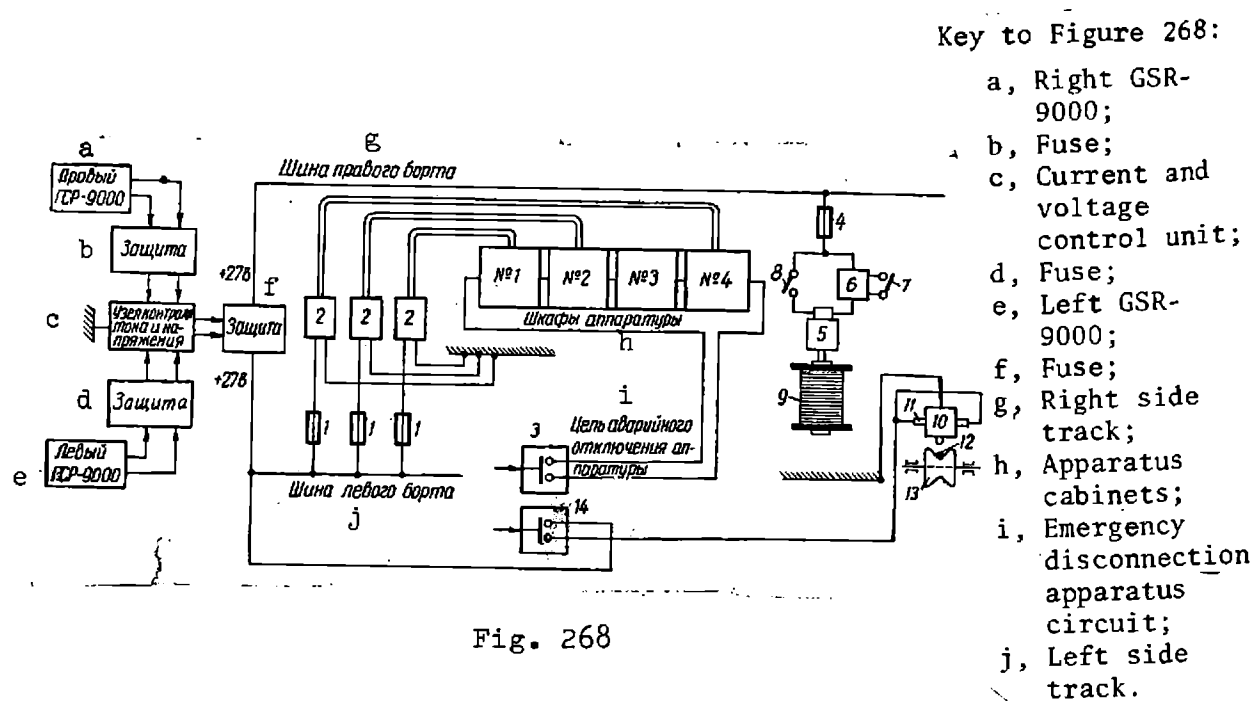


Fig. 268

The electric drive 5 of the winch 9 is cut in to the bus bar of the right side through IP-100 fuse 4. By means of the tumbler 8 it is possible to control electromagnetic coupling of electromotor, which starts by contactor 6, switched on by the tumbler 7. The contactor and tumbler are fitted in a special box attached to the winch frame. The electric drive is switched on only for the hoisting of the gondola, but its lowering is effected directly by the winch. Feeders for the electric drive should have a section of approximately 35 mm².

The emergency uncoupling of the apparatus is implemented by simultaneous de-energizing of all transformers by locking the tumbler 3 in the pilot's cabin. The emergency drop of the gondola is effected by pressing the button 14, through the normally open contacts of which voltage + 27 v gets delivered to pyro-cartridges 11 of the device for cutting cable (10, 12, 13).

2. Apparatus of VMP (rotating magnetic field) method, developed by VITR

The first set of apparatus for the VMP method was made in 1960 in VITR and was designed for application on plane LI-2. The second, more perfect, set, developed in 1961, was installed on plane AN-2; in 1962, it was modernized and recommended as a test sample for introducing the apparatus of the VMP method.

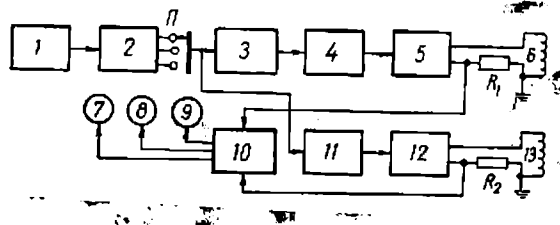


Fig. 269

Generating set. The block diagram of the generating set is shown in Fig. 269. Quartz master oscillator 1 ($f = 9800$ cps). Magnetic frequency dividers 2 applied for obtaining other operating frequencies (2450, 1225 and 612.5 cps). The required frequency is selected by switch P. The working signal from the output of the master oscillator arrives through a 90-degree phase-invertor 3 at the preamplifier 7 and terminal repeater 5. The same signal, but without the phase shift, is delivered to the preamplifier 11 and terminal repeater 12.

Terminal repeaters 5 and 12 are loaded onto tuned oscillating frames 6 and 13, into the circuit of which are connected, in series, control resistances R_1 and R_2 . The voltage taken off

these resistances is delivered to the control block 10, in which by the zero method preservation of the preset amplitude ratio of currents in the frame (indicator 7) and of the fixed phase shift (indicator 9) is checked. Indicator 8 permits controlling the intensity of the current in each oscillating frame.

Terminal power amplifiers are assembled on semi-conducting triode 1 and their power is supplied directly from the board network of the plane by voltage 26 v. This increases the efficiency of the amplifiers and reduces power consumption from the board network. The output power of each amplifier is 250 watt. The master oscillator is also energized from the board network of the plane and for obtaining anode voltage there is a semi-conductor transformer. The weight of the generating set is not over 45 kg, total power consumption does not exceed 1 kwt. The outside view of the generating block was shown in Fig. 10, a.

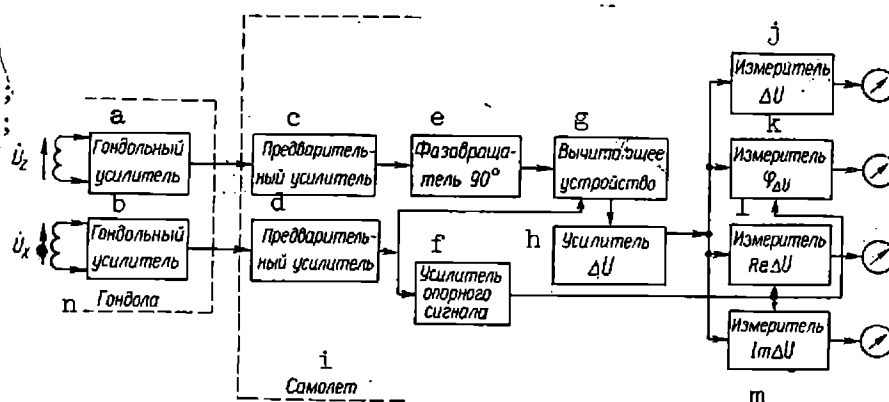
Added to the generating set is a device for checking circular polarization of the primary magnetic field. This device is a receiving frame, which can revolve around vertical and horizontal axis. The frame with ferrite core is tuned to the operating frequencies. The frame stage has a level and two goniometers. The whole device is set up on a tripod. The circular nature of the rotating magnetic field is checked on the ground. The output voltage of the device is measured vacuum-tube voltmeter (LV-9).

The vertical oscillating frame is attached to the fuselage of the plane; the upper branch is uplifted above the centre of the aeroplane wing and retained in the set position by two brackets;

the rear portion of the frame is attached to the tail fin of the plane. The lower branch of the frame is confined in a durite tube and attached directly to the center of the plane wing. The side branches of the horizontal frame are slightly removed from the center of the plane wing and fixed by six (three on each side) uniform brackets. To impart the required strength to the frame braid, a steel wire is embedded within it.

Key to Figure 270

- a, Gondola amplifier;
- b, Gondola amplifier;
- c, Preamplifier;
- d, Preamplifier;
- e, Phase converter 90° ;
- f, Reference signal amplifier;
- g, Readout device;



- h, Amplifier ΔU ;
- i, Aircraft;
- j, Meter ΔU ;
- k, Meter $\varphi \Delta U$;
- l, Meter $Re \Delta U$;
- m, Meter $Im \Delta U$;
- n, Gondola.

Fig. 270

If investigations are carried out by means of plane LI-2, the magnetic moment of the oscillating frames comprises about 1600 av.m^2 (each frame has 18 turns of wire LPRGS-2.5 and area $S \approx 30 \text{ m}^2$, if plane AN-2 - about 800 av.m^2).

The receiving-measuring set of the VMP method apparatus has two channels and could be constructed according to various block diagrams. Let us analyse three such diagrams (132, 234).

First Diagram (Fig. 270) is not highly noise-proof apparatus because of the fact that noise signals, received by both the frames, are geometrically added in the subtracting circuit, and the peak

noise is estimated as doubled magnitude of noises, active in each channel (assuming, that the noises are approximately of similar magnitude and shifted in the phase by 90°). Since the unbalance signal ΔU is very low in comparison with $(U_x) \approx (U_z)$, the instability of the preamplifiers, made with a narrow band, increases the error in ΔU determination. Therefore, in the given scheme, the main requirements of the measuring apparatus are high stability and selectivity, which cannot both be resolved simultaneously and completely, hence there is usually a compromise.

To increase the noise-proof it is expedient to measure directly the amplitude difference of both the signals $A = (U_x) - (U_z)$ (amplitude parameter) or their ratio and the phase shift between them $\Delta\varphi = \varphi_{U_x} - \varphi_{U_z}$ (phase parameter)(234). These measurements are assured by the second scheme (Fig. 271). Due to the detection of measured signals U_x and U_z and separation of envelope on the meter of A parameter, the signals will be the sum of average level noises. Hence the error will depend only on the difference of average value of the noises and not on their absolute magnitude. Therefore, the given scheme has a high noise-proofing than the first. Here also the measuring of the phase parameter is more simple, since the possible variations of the signal phase do not take up a wide angular range. However, due to the presence in this scheme, like that in the other, of two separate preamplifiers it is impossible to obtain high stability with high selectivity.

Key to Figure 271:

- a, Gondola amplifier;
- b, Gondola amplifier;
- c, Preamplifier;
- d, Preamplifier;
- e, Detector;
- f, Detector;
- g, Meter A;
- h, Gondola;

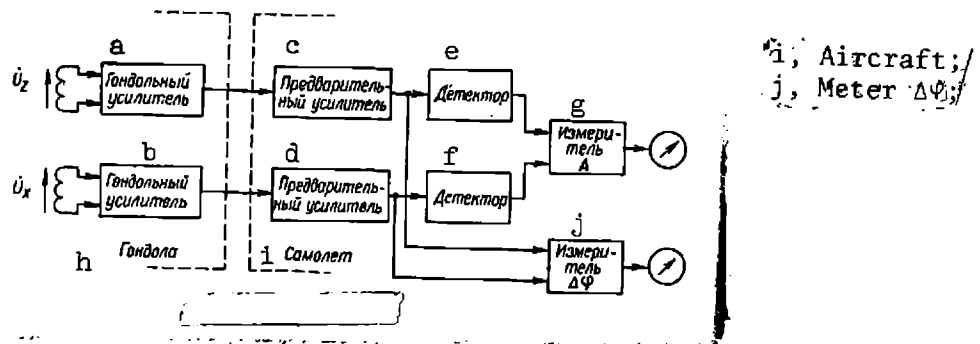


Fig. 271

The stability of measurements could be enhanced by the application of a scheme, in which the amplitude difference is measured by means of the commutator, which connects alternately with the input of the preamplifier voltage U_x or U_z (Fig. 272). After leaving the preamplifier these voltages arrive at the detector. If the amplitudes of the compared signals are uniform, their envelope at the output of the detector will be in the shape of a straight line. In other cases it will be stepwise. By means of filter separation of voltage is effected with the amplitude proportional to the difference of signals $(U_x) - (U_z)$, and with frequency equivalent to that of the commutating voltage.

Fig. 272 shows that the preamplifier and detector are common for both the compared signals. Although these units have their natural instability, in this case they do not cause any appreciable error in measurements (i.e. pseudoanomalies), as they are compensated through separation by the envelope. Therefore, in this system it is possible to apply for the selective circuit

of the preamplifier with narrow pass band without deterioration of the stability of the entire measuring system (12). Commutation phase measurements similar to commutation amplitude measurements may also be implemented.

In the test sample of the apparatus for the VMP method, the last block scheme of the measuring apparatus, shown in greater detail in Fig. 273 has been used. Here the signals U_x and U_z are taken off the receiving frames 1 and 2, which are tuned to the operating frequency of the apparatus and have field sensitivity about $7.5 \frac{V}{a/m}$. The receiving frames are placed in the trailing gondola; therefore, the operating frequencies are switched over by means of remote switch relay. Both signals are amplified by the gondola preamplifiers 3 and 4, having a comparatively wide pass band and high stability amplification factor (see para 2, Chapter X).

Key to Figure 272:

- a, Gondola amplifier;
- b, Switch;
- c, Preamplifier;
- d, Detector;
- e, Meter A
- f, Gondola amplifier;

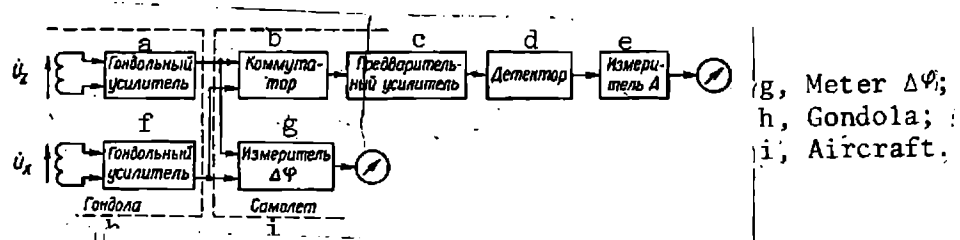


Fig. 272

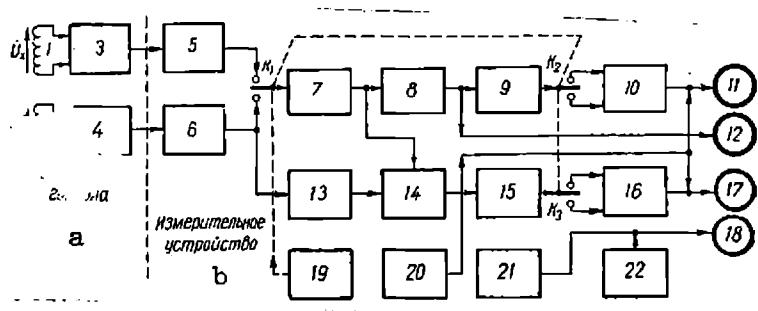
The amplified signals U_x and U_z are delivered along the cable into the measuring apparatus; at the input of which provision has been made of matching and calibrating stages 5 and 6. Hence the signals arrive at the electronic commutator K_1 , which alternately cuts them in to selective amplifier 7. The selective amplifier is followed by amplitude detector 8;

its output voltage has a stepwise shape and is proportional to the difference $(U_x) - (U_z)$; moreover, this voltage does not depend on the absolute values of U_x and U_z . The stepwise voltage is amplified by selective amplifier 9, tuned to the frequency of commutation $f_k = 30$ cps, and through output commutator K_2 , operating synchronously with the input one, arrives at the difference recorder 10 with writer 11. By means of the special divider in stage 5, the scale of writer 11 is calibrated in percentage ratio of the mean level of the primary field. Therefore, the measuring is of the relative amplitude parameter.

$$A = \frac{(U_x) - (U_z)}{U_o},$$

where

$$U_o = \frac{1}{2} ((U_x) + (U_z)).$$



Key to Figure 273:
a, Gondola;
b, Measuring device.

Fig. 273

Besides the stepwise voltage with commutation frequency f_k at the output of the amplitude detector there is a build-up of a constant component U_o , proportional to the mean level of the primary field. This voltage is used for the distance control

between the planes ($m_0 = \text{const}$) and gets recorded by writer 12.

In this scheme, phase measurements are also carried out by the commutation method. The measurable voltage is the signal U_z , which by means of amplifier-limiter 13 acquires a shape close to rectangular. The comparative voltage on phase-sensing detector 14 is supplied from the output of selective amplifier 7. Since the phases of voltages U_x and U_z are rectified in the measuring system by the additional 90-degree phase-inverter, with deviation from the preset phase shift of 90° between signals U_x and U_z , a stepwise voltage with frequency f_k will appear at the output of the phase detector (FHD). The output voltage of FHD, proportional to phase shift $\Delta\varphi$, is amplified by the selective amplifier 15 (tuned to frequency f_k) and through the output commutator K_3 arrives at difference recorder 16 with writer 17. For the calibration of the phase meter, there is a special device in the input stage 6.

Commutators $K_1 - K_3$, assembled on semi-conductor triodes, have a low noise level and are practically non inertial. They are energized from a separate low-power RC-generator 19.

In the measuring system, provision has been made for recording of the flight altitude h by pen 18, which gets the signal from the plane radio-altimeter 22. At the moment of tying in the aerial photographs, synchronizing impulses from photo-camera 21 are fed to pen 18, where they are recorded in the shape of narrow ejections. The pens 11 and 17 receive from system 20 time-breaks at 1 min. intervals (in the shape of shot ejections with positive polarity) and navigating marks of guides (long ejections of negative polarity).

For the recording of measured parameters the pen is type ASGM-25, the same as in the aeromagnetic station. The entire measuring system, with the exception of commutators, is assembled on electronic tubes; its weight is about 40 kg. The outside view is shown in Fig. 17,b. The power consumed is about 0.2 k-wt.

3. Apparatus of the BDK method worked out by FMI AN Ukr. SSR.

The developed block diagram of measuring and auxiliary apparatus of the mobile group in station AERA-58 is shown in Fig. 27⁴. The measuring apparatus is tuned and operates in relation to the position of the switch for the type of work 4 (calibration, operation of receiving system in the gondola, or with the receiving system in the tail). The measured signal is picked up by receiving ferrite coils 1 and 11, each of which is tuned to the operating frequency. The transition from one operating frequency to another is effected by the switching of resonance capacitances, commutable in systems 2 or 12. Depending on which receiving device is in operation, the measured signal is amplified by preamplifier 3 or 13 and then transmitted by the connecting cable to the measuring system - input of the type of work switch 4. Hence the measured signal arrives at selective amplifiers 5, where it is amplified upto the required intensity. Between the two selective amplifiers - a and c - is a stepwise voltage divider 5 b, serving as a switch of the measuring range.

The remote control of the measuring range is attained by switching over from the panel of components 41 to the terminals of

corresponding relay coils. In the retuning of the operating frequencies in selective amplifiers, the use is made of the switch connecting RC-filters, tuned to pertinent frequencies (the switch is not shown in Fig. 274).

The axis of the switch is brought out on the front panel of the measuring block. The amplified measured signal arrives at the FHD 6 and 32 in the channels of the component and phase recorder.

Let us trace the passage of the main phase signal. In transmitter UKV, included in the apparatus of the ground group, the operating frequency is modulated by voltage, the phase of which coincides with the current phase in the cable. This signal is picked up on the helicopter by the receiving antenna 23 and amplified by the radio-receiver of main signal 24. After detecting the separated modulation, voltage is amplified by LF-amplifier 25. From the output of the LF-amplifier, the voltage arrives at the input of the quadrature phase-inverter 26, hence to the auxiliary phase-inverter 27 (by $\pm 15^\circ$), and to the input of automatics block 39. At the output of the auxiliary phase-inverter 27, the main signal is directed into the circuit for measuring and recording of the components and phases. In the phase-recording channel, the main signal passes consecutively through stepwise phase-inverter-phase measuring range switch 28, the even graduated phase-inverter 29, amplifier 30, two-sided limiter 31, after which it arrives at the input of FHD 32. The voltage at the output of FHD

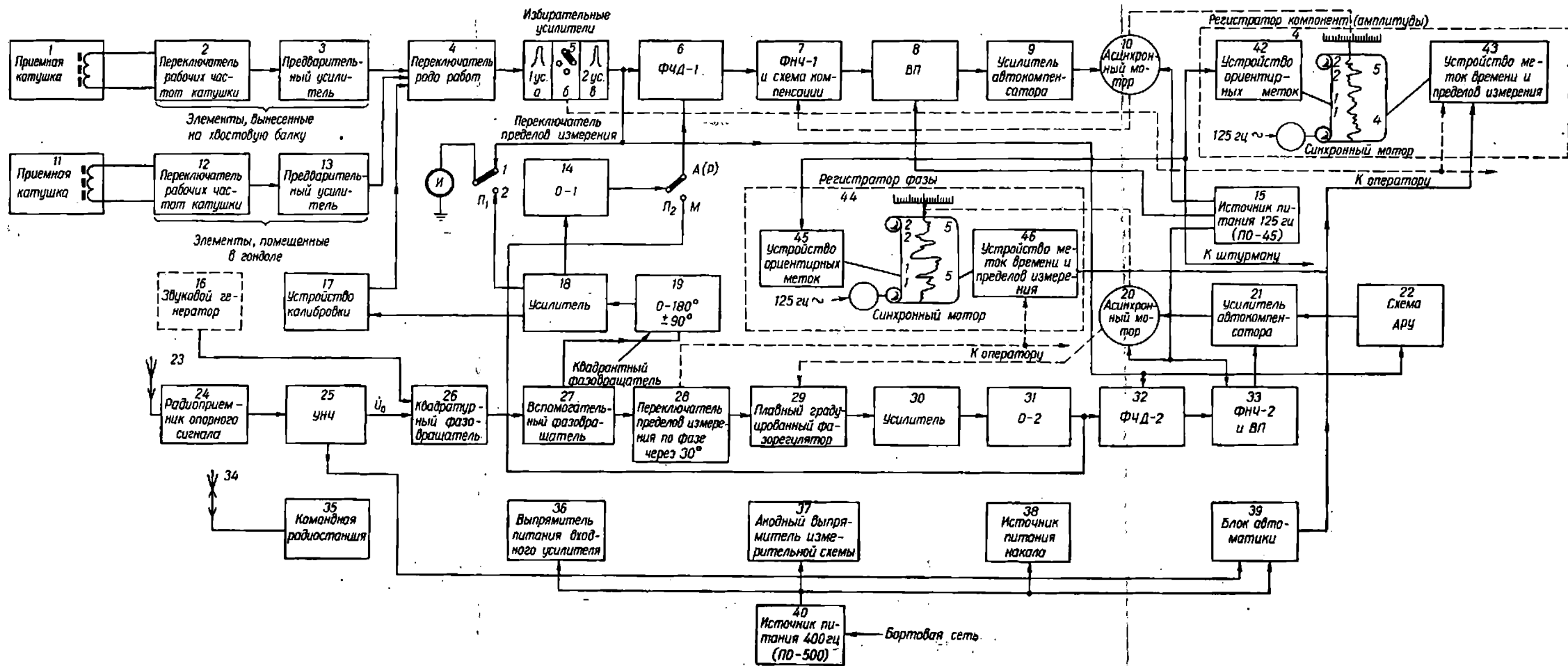


Рис. 274

FOLDOUT FRAME

FOLDOUT FRAME

705-B

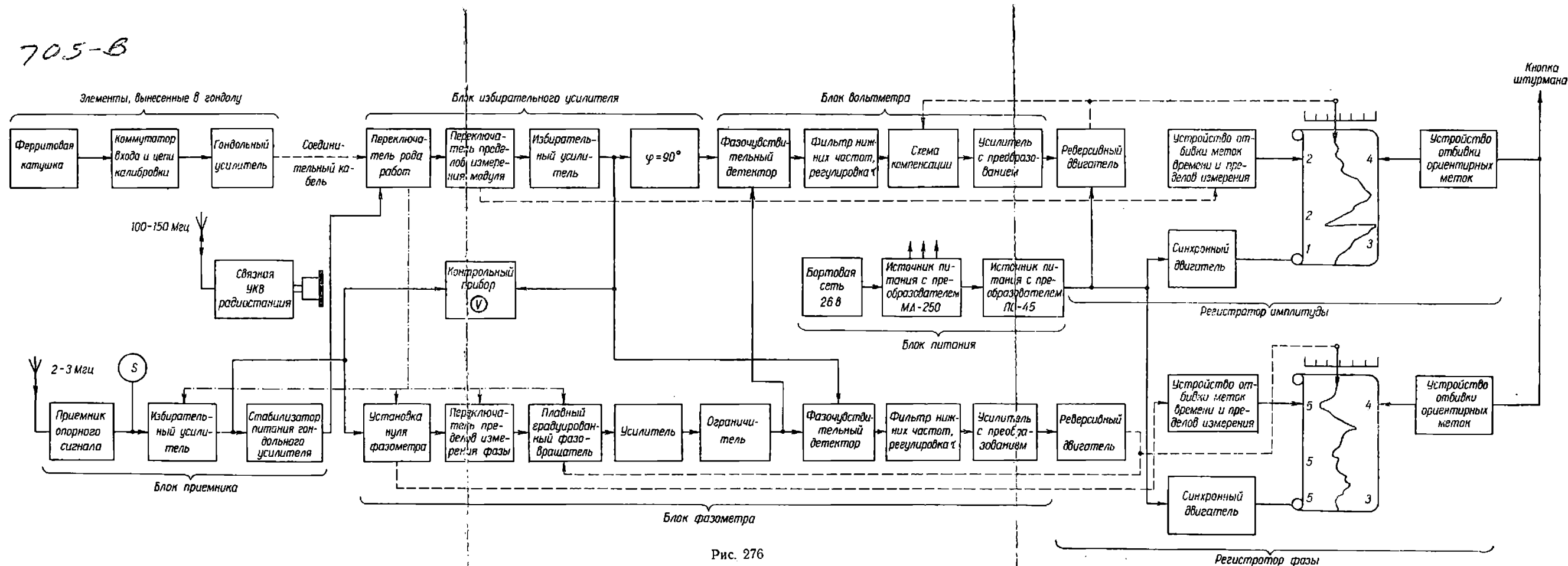


Рис. 276

is filtered by LF-filter 33, gets transformed into alternate voltage of 125 cps and is amplified by the electronic amplifier of the automatic compensator with transformer 21. The transformed signal activates the reversible synchronous motor 20, which revolves the even graduated phase-inverter 29 until quadrature (angle $\frac{\pi}{2}$) is set between the measured and main signals at the output of FHD 32. The smooth phase-inverter is graduated within the measured angles of the phase shift. The reversible motor is rigidly coupled with the recorder's carriage and fitted by means of pen, in the carriage phase variations between the measured and main signals are marked on the tape. To provide for a uniform sensitivity of the phase recorder there is AGC circuit 22.

From the output of the auxiliary phase-inverter 27 in the channel for recording components, the main signal arrives at the quadrant phase-inverter 19, in which the main signal vector is turned by $n \cdot 90^\circ$ ($n = 1 \div 4$) in relation to the original position of coordinates. Further on, the signal is amplified by amplifier 18, gets limited by the two-sided limiter 14 of 0-1 type and, in the shape of rectangular impulses, arrives at the input of FHD 6. The output voltage of FHD is filtered by LF-filter and compensated in circuit 7. The uncompensated portion of the voltage gets transformed, by means of the electronic amplifier of automatic compensator 9 with vibro-transformer (VP) 8, into alternate voltage of 125 cps and is delivered to reversible motor 10. The latter operates voltage in compensation circuit 7 and records on the diagram tape the value of one of the quadrature components.

If the main signal at the output of quadrant phase-inverter 19 is in phase with the measured signal at the output of selective amplifier 5 c, the measuring and recording is of the active component; but if with shift at 90° - of reactive. The recorders of component 41 and of phase 4 are provided with devices 42 and 45 for the printing of guide marks on diagrams and with devices 43 and 46 for printing the time breaks and measuring limits.

Above an orienting point, the navigator presses a button for the supply of current to the electromagnetic coils of devices for printing guide marks. The operator on an order from the navigator sets the next position of the guide-marks switch, getting the marking device ready for printing. The marks are printed simultaneously on both the recorders.

The device for the time breaks and measuring limits operates in the following way. From the output of LF-amplifier 25 the main signal arrives at the automatics block 39. Depending on the frequency of the main signal, the frequency is correspondingly divided in the circuit of the automatics block to 40.6 cps. The voltage of 40.6 cps is amplified upto a certain level and arrives at the winding of synchronous electrometer SD-2, which revolves the indicating needle at 1.62 rpm. At every 37 sec. the needle locks a pair of contacts and delivers the current supply to the electromagnet winding of mechanisms 43 and 46 for printing the time breaks and measuring limits. As a result, after every 37 sec, the imprint of figures for the corresponding measuring limits of the component

and phase appears on the diagrams. During the switching of the measuring range the operator fixes additionally its conventional number by pressing a special knob, thereby activating the printing mechanism at both the recorders. The apparatus also makes it possible to print the measuring range separately. On diagrams, left of the shifting, are printed the guide marks, on the right - the time break and marks of the switching measuring range.

The power supply to the measuring and auxiliary apparatus of station AERA-58 on helicopter comes from rectifiers with electronic stabilizers 36 and 37, and also from the current supply source of filament circuit 41. The source of supply voltage 40 of 400 cps is the mechanical transformer PO-500, and of 125 cps - PO-45; these transformers get their current supply from the helicopter's network.

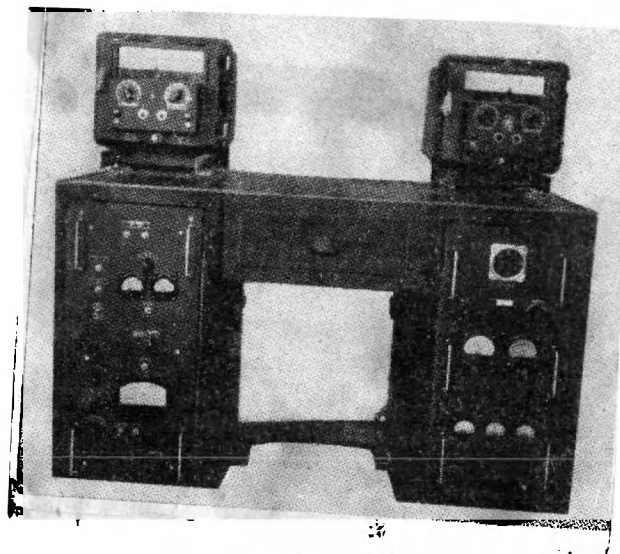


Fig. 275

The signal level at the output of the selective amplifier (5 c) and at the input of the two-sided limiter is controlled

by meter I in calibration mechanism 17. The meter is on the front panel. Position 1 of the switch P_1 corresponds to the level of the measured signal, position 2 - to the level of the main signal. The calibration of the measuring system is done in the same position.

For a two-way coupling with the ground unit, the application on the helicopter is of master radio-station 34 and 35 of RSIU-3M type.

The outside view of the measuring apparatus AERA-58 is shown in Fig. 275. The entire apparatus is mounted in the two cabinet legs of the table, on which on the left is the component recorder, on the right - the phase recorder.

The disposition of the measuring apparatus AERA-58 in helicopter MI-4 is shown in Fig. 104. The measuring apparatus 1 with recorders 2 is set up in the forward part of the helicopter cabin. At the side, through an opening in the floor, the antenna of the main signal receiver 3 can be brought out. The trailing gondola 4 with winch 5 for the lowering of the gondola are placed to the right of the helicopter's gravity center. Set up in the trailing gondola are the magnetic field receiver and preamplifier. Similar units are fitted inside the tail vibro-proof system 6.

The experience of using station AERA-58 and the improvement of exploration methods by its help have made it possible for the

Institute of Mechanical Science and Automatics of AH Ukr. SSR, jointly with L'vov Experimental Production of AH UkrSSR, to develop and issue in 1960 a small series of the modernized set of AERA-2 apparatus. By means of this apparatus, it is possible to measure and record the amplitude and phase of e.m.f. in the receiving coil (in relation to the comparative voltage). This apparatus has been provided with the stepwise adjustment of frequency pass band in the channels of amplitude and phase recording, which raises the quality of parameter recording on diagram tapes, calibration system, described in para 10 of Chapter XIII, automatic frequency switching in the gondola system. The construction of the mobile and ground apparatus has also been improved, reliability of the operation enhanced, etc.

The block diagram of the measuring apparatus is made by using synchronous reception circuits on FHD base. The recorders of complex values are constructed on the principle of the block diagram, shown in Fig. 213. The expanded block diagram of apparatus AERA-2 is shown in Fig. 276. The entire apparatus is made in the form of separate functional units - receiver block, phase meter block, etc.

The measured field induces e.m.f. in the magnetic field receiver (ferrite coil), signal from which arrives at the input commutator and calibration circuits and at the input of the gondola amplifier. Further on, the measured signal arrives at the block of the selective amplifier and phase-shifting

circuit. The type of work switch commutates the measuring circuit automatically. It has 12 positions (see para 10, Chapter X): 1-4- operating frequencies; 5 - short-circuiting of the gondola amplifier input; 6-9 calibration on four operating frequencies; 10-11 - active resistances equivalent to resonance resistance of receiving coils (100 kohm and 1.2 Mohm); 12 - synchronisation of step-by-step finders. The dash line shows coupling of the type of work switch assembled on the step-by-step finder, with similar finders in other blocks.

The comparative voltage is received by radio-channel from the ground unit on one of the two frequencies in the apparatus in the range 2-3 M-cps. The signal of carrier frequency, modulated by the voltage of one of the four operating frequencies, arrives at the receiver block, consisting of the main signal receiver, selective amplifier and current stabilizer of the gondola amplifier. Here this signal is demodulated and isolated as a comparative voltage of the operating frequency. The two-way coupling with the ground unit, required for quick work, is effected by means of the master radio-station of the helicopter.

From the output of the receiver's block, the comparative voltage is delivered to the phase meter block, consisting of zero setting device (non-graduated phase-inverter), measuring range switch (graduated phase-inverter), amplifier, FHD limiter, LF-filters and amplifier with transformation. The comparative voltage, in the shape of rectangular impulses, controls FHD from the output of the limiter circuit, thus providing for impulse-work.

The voltmeter block consists of phase-detector (FHD), LF-filter (FNH), adjustment circuit of time constant τ , amplifier with transformer and compensation circuit (rheochord, energized by direct-current stabilized voltage). The blocks of amplitude (modulus) and phase recorders are identical. They have reversible and synchronous motors, marking the mechanisms of time breaks, measuring range and guide marks. The mechanical coupling of recorders with rheochords in the compensation circuit with the even graduated phase-invertor and also with the measuring ranges of the amplitude and phase, are shown in the diagram by dashes. The levels of comparative voltage and measured signal are fixed by meter V.

The phase and amplitude recorders operate in the same way as in AERA-58. However, here the follow-up system of the phase recorder, due to less extensive variation range of the input signals, does not have the AGC circuit. Proportionality of amplitude indication in the circuit of the amplitude recorder with FHD is obtained when the voltage on it is in phase. With this aim the block of selective amplifier is provided by phase-invertor at 90° .

The calibration circuit, applied in AERA-2, is described in para 10 of Chapter XIII (see Fig. 250). Used for calibration is a control device with V_1 , current supply stabilizer of the gondola amplifier and the switch for the type of work.

The measuring unit of AERA-2 apparatus is made up as a single cabinet, which can be easily carried over and set on the frame-support 1 (Fig. 277). Into the cabinet, blocks 2-6 (2 - supply

block; 3 - selective amplifier; 4 - phase meter; 5 - voltmeter; 6 - receiver) are inserted in the connectors. Each block in the cabinet is fixed by four screws. Electric connections between the blocks are made as braids, fitted in the rear of the cabinet. here are also the connectors, through which the signals are fed to the apparatus from the gondola amplifier (measured signal) and from the radio-channel (main signal).

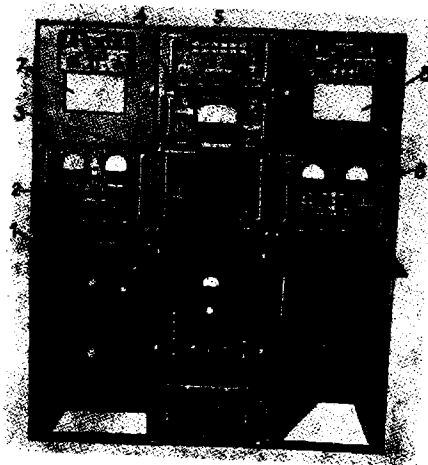


Fig. 277

The recorders of amplitude 7 and of phase 8 - are single-channel. The covers on recorders are removable for convenient servicing.

The disposition of AERA-2 measuring apparatus in helicopter MI-4 is identical to that of AERA-58. The only difference is that AERA-2 has a mechanized winch with cable-cutter and the construction of the gondola is to some extent improved. The winch control is interblocked and can be effected both from the measuring cabinet and from the winch itself. In the pilot's cabin

is the switch for an emergency drop of the gondola. The receiving system in the tail is not used in AERA-2.

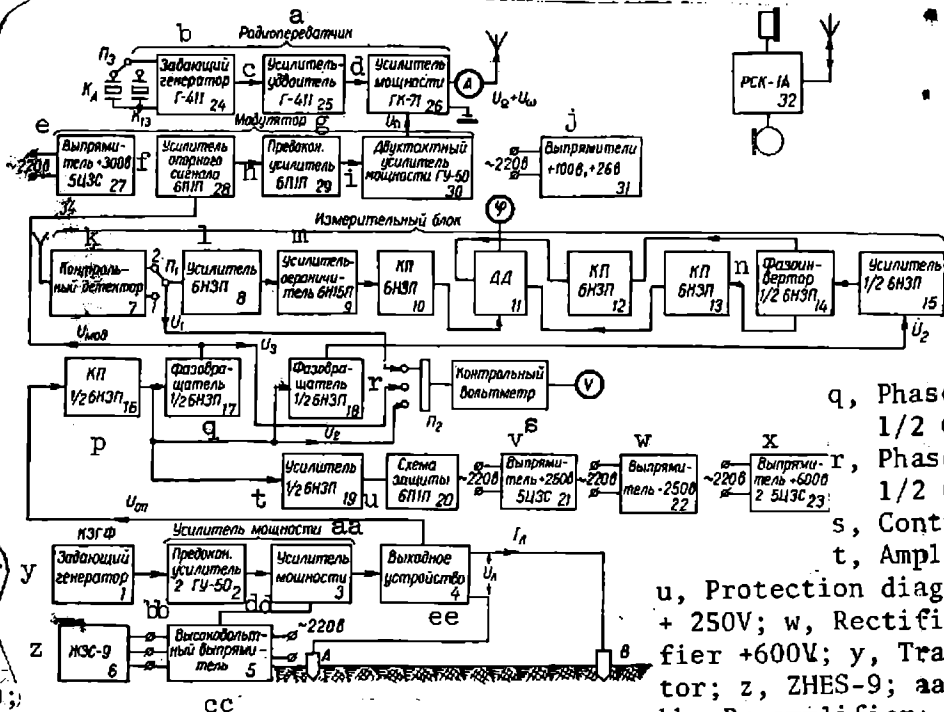
The ground generating apparatus, with signal transmitter of the main phase in AERA-2 and AERA-58, differs very little. In respect of construction, it is more successful in AERA-2. The composition of the ground unit of AERA-2 includes additionally: the control of the main signal phase, master radio-station for communication with the captain of the helicopter, electric power-plant, etc. Fig. 278 shows the expanded functional diagram of the ground unit. The output power amplifier 3 is cut in through the output system 4 (resistance matching transformer, capacitances and inductance box, take-off circuit of the main signal) to loading grounded line AB. The amplifier 3 is activated pre-terminal follower which receives the signal from the master oscillator of fixed frequencies 1.

The main signal is emitted into ether by means of a short-wave transmitter, consisting of a master oscillator 24, amplifier-doubler 25 and output power amplifier 25. The transmitter frequency is stabilized by means of quartz K_A and K_B . Anode screen modulation is effected in the output stage 26. The modulator consists of the preamplifier 28, the pre-terminal amplifier 29 and the push pull power amplifier 30. The main signal (U_{mod}) is fed to the modulator from the output system 4 through the cathode follower 16 and phase-inverter 17. The level of the modulator's main signal $U_{\text{mod}} = U_3$ is controlled by a special voltmeter, which is also used in the measuring circuit of the main signal.

The circuit for phase control of the main signal consists of FHD (11-14) with zero indicator. One FHD input receives the main signal, picked-up from the other by the detecting control receiver 7, which then passes through the amplifier 8, the limiter 9 and the cathode follower 10 to the circuit of the differential detector DD 11. To the second input of FHD is delivered signal U_2 , received from line AB and which consecutively passes through the cathode follower 16, the phase-invertor 18, the amplifier 15, the phase-invertor 14 and the cathode followers 12 and 13. The amplifier 19 and system 20 ensure automatic cut-out of line AB with its breaking.

Key to Figure 278:

- a, Transmitter;
- b, Transmitter generator G-411;
- c, Amplifier divider G-411;
- d, Amplifier, power GK-71;
- e, Rectifier + 300V 5TSZS;
- f, Reference signal amplifier 6PP;
- g, Modulator;
- h, Preamplifier 6PP;
- i, Two-cycle amplifier, power, GU-50;
- j, Rectifiers + 100V, + 26V;



- k, Control detector;
- l, Amplifier 6N3P;
- m, Amplifier, reference, 6N15;
- n, Phase inverter 1/2 6N3P;
- o, Amplifier 1/2 6N3P;
- p, KP 1/2 6N3P;
- q, Phase converter 1/2 6N3P;
- r, Phase converter 1/2 6N3P;
- s, Control voltmeter;
- t, Amplifier 1/2 6N3P;
- u, Protection diagram; v, Rectifier + 250V; w, Rectifier -250V; x, Rectifier +600V; y, Transmitting generator; z, ZHES-9; aa, Power amplifier; bb, Preamplifier; cc, High voltage rectifier; dd, Power amplifier; ee, Output device.

Fig. 278

The radio-station 32 maintains communication with the captain of the helicopter. The ground apparatus AERA-2 gets

its current supply from an independent electric power plant 6 of JES-9 type through rectifiers 5;21;22;23;27;31.

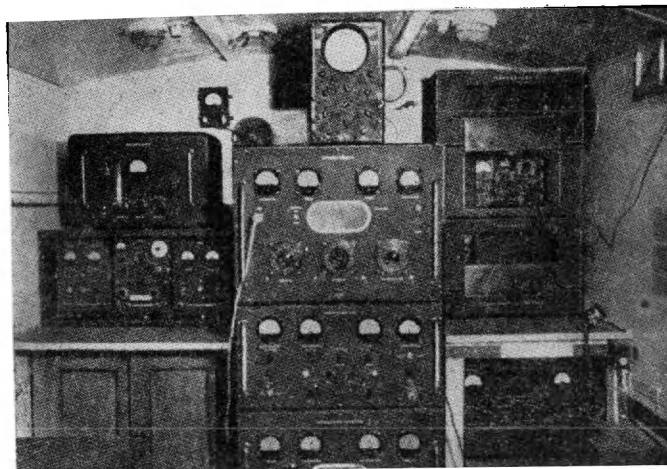


Fig. 279

The disposition of the ground apparatus AERA-2 in the van of truck ZIL-151 (without power plant) is shown in Fig. 279. In the middle of the forward side of the van is placed the cabinet with the power amplifier, the measuring block and the high-voltage rectifier. To the right of the cabinet is the communicating radio-station PSK-1A, to the left - the transmitter of the main signal and master oscillator KZGF. The telescopic antenna for the main signal transmitter is fitted outside in the front portion of the van. The antennas of the radio-station and the controlling detecting receiver are fitted on the roof of the van.

The basic technical specifications of the modernised set of AERA-2 differ considerably from those of AERA-58 (Table 26).

4. Apparatus for the BDK method, worked out by IAE SO AN USSR

In the development of the apparatus for the BDK method, the

aim was to modernize the available AERA-58 apparatus and to improve its stability against noise. In this connection, the individual elements and units of systems were investigated, new principal diagram worked out, as well as the construction of the measuring apparatus, the basic technical specifications of which are shown below was carried out.

Ground Unit: Operating frequencies of the generating system: 81, 244, 488, 976, 1953 cps. Power of the generating unit at each operating frequency with active load resistances 50; 100; 150; 200 and 300 ohm not less than 2 kw. The radio-transmitter of the main signal operates in the frequency range 36.0 to 46.1 Megacycles with output power about 20 watts providing for the transmission of this signal to the helicopter with its removal from the ground unit to a distance of upto 40 km. There is a communicating radio-station.

Mobile Group; The horizontal component of the magnetic field is measured by means of low-frequency reception antenna with ferrite core tuned to the operating frequency. The antenna and the preamplifier are meant for working in the temperature range $-25^{\circ} - + 35^{\circ}$ with relative humidity of the surrounding medium upto 80%.

The measuring system provides for the measuring and recording of the modulus and phase shift related or components of the signal from the horizontal component of the magnetic field of the relative main signal coinciding in the phase with the cable current. The minimum values of the magnetic field intensity, measured on operating frequencies, are as follows: for 81 cps - $4 \cdot 10^{-5}$ a/m for 244 cps - $4 \cdot 10^{-6}$, for 488; 976 and 1953 cps - $8 \cdot 10^{-7}$ a/m. The maximum

TABLE - 26

Charateristics.	AERA-58	AERA-2	Remarks
<u>Ground Unit</u>			
Operating frequencies, cps	81; 244; 976; 3904	244; 488; 976; 1952	In AERA-58 with frequency 3904 and length of cable over 5 km matching of power amplifier with load is very poor.
Nominal output power (on active load), Upto 1.8 k-watt		Upto 2.4	
Operating frequencies of main signal transmitter Megacycles	38.3 and 39.4	2.21 and 3.33	
Emitting power in antenna, v	80	100	
Total power consumption, K-watt	6	6	
Constructive features	Transporting in-trailers. Construction not sectional, hence not portable manually.	May be set and transported in vans GAZ-63 or ZIL-151. Possible to be carried by hand and transported by helicopter.	
<u>Mobile (Airborne) Unit.</u>			
Operating frequencies, cps	81; 244; 976; 3904	244; 488; 976; 1952;	In AERA-58, due to the noise, level frequency 81 cps was not used because of the non-matching of cable with out-put power amplifier; frequency 3904 cps was also not used.

Measurable quantities	Phase angle and component (active or reactive).	Phase angle and modulus.	
Resonance sensitivity			
$S_r, \frac{v}{\frac{\sigma}{m}}$ of reception			
circuit on operating frequencies, cps:			
81	0.44	-	The receiving element in AERA-2 is a coil with ferrite 200 (ferrite has a manganese addition).
244	3.75	4.63	
488	-	7.13	
976	15.0	21.25	
1952	-	20.0	
3904	18.0	-	
Q-Coefficient of reception circuit on operating frequencies, cps:			
81	8	-	
244	35	25	
488	-	30	
976	50	50	
1952	-	50	
3904	50	50	
Lower working range in modulus (component) measuring on operating frequencies, mcv.	15	10	
Upper working range of modulus (component) measuring, mv.	5	100	
Non-working zone in cable, km	2	1	
Operating frequency switching during survey	Impossible	Possible.	
Possibility of calibration during helicopter flight.	Without estimate of amplification coefficients of elements in gondola	With estimate of amplification coefficient of elements in gondola.	

Reduced error of modulus (components) recording	3% (with ratio of active and reactive components less than 3)	3 %	
Ranges of modulus recording	6	9	
Working range of phase recording, degr.	0 - 40	- 30-0 - +30	
Reduced error of phase recording, degr.	1.5	1	
Ranges of phase recording	6.2	12	Range switching by $\pm 30^\circ$
Phase characteristics drift with temp- erature variation of surrounding medium by 10°C , degr.	1	0.1- 0.15	
Power consumed from board network, k-watt.	1.2	1.0	Let-down of gondola during helicopter flight: for AERA-58 - by hand, For AERA-2 - electric winch and by hand.
Weight of apparatus without gondola and winch, kg.	300	250	

measuring range of the magnetic field intensity on all operating frequencies $4 \cdot 10^{-2}$ α/m . The reduced fundamental error in any measuring range does not exceed 3% in the modulus and 2° in the phase. The apparatus provides for the measuring of the phase shift within $0-360^\circ$.

The scale travel time of the pen-carriage in the phase and components recorders does not exceed 1 sec. The measuring unit has a device for graduating the measuring channels of the phase and components. The selectivity of the measuring unit is not below 40 db with detuning by 10%.

The current supply of the apparatus is from the network of the helicopter 26 v; the maximum consumed power is not over 1 k-watt. The weight of apparatus is about 300 kg.

The phase characteristic of the main phase radio-receiver in the low-frequency demodulated signal is stable - phase drift not over 0.5° during 2 hrs of work. The error in phase transmission of the main signal in relation to the current phase in the cable is within 1° .

Each of the two independent output voltages of the master oscillator, adjustable by means of adjusting resistances within 0-20 v, is measured by the detecting voltmeter of mean values. The master oscillator gets current supply through its own stabilized rectifier.

The power amplifier is a four-stage, assembled on push-pull circuit. The actuating voltage for obtaining nominal output power should be about 250 v. The secondary winding of the output

transformer is sectional and is estimated for matching with the active load 50; 100; 150; 200 and 300 ohm. In series with the grounded end of the secondary winding is the cut-in ammeter with measuring range 7 a for current control in the cable. Since cable resistance has inductive nature on operating frequencies, the power amplifier is provided with a set of capacitance, connected in series with the cable for compensating reactive load resistance.

The transmitter of the main phase signal in the BDK apparatus is the standard UKV radio-station, working on fixed operating frequencies 36.0 - 46.1 megacycles. The same radio-station is set up on the helicopter for reception of the main signal. To provide an assured reception of the signal at any point of the survey area, an antenna with a circular directional characteristics is used in the horizontal plane.

All the elements included in the ground unit are energized by 220 v voltage with frequency 50 cps from the power plant of the three-phase current with petrol engine.

The block diagram of the apparatus is shown in Fig.280. The ground unit includes mobile power plant of three-phase current 1, the master oscillator with quartz control of frequency 2, the vacuum-tube power amplifier 3, the radio-transmitter of main signal 4 and the radio-station for a two-way communication with the helicopter 5. The ground unit does not have a device for the phase control of comparative voltage, by means of which it is possible to determine and then to eliminate the additional phase shifts, emerging in the radio-channel with the transmission of the main phase. Compensation for these shifts in the apparatus is provided only by means of elements, included in the mobile group.

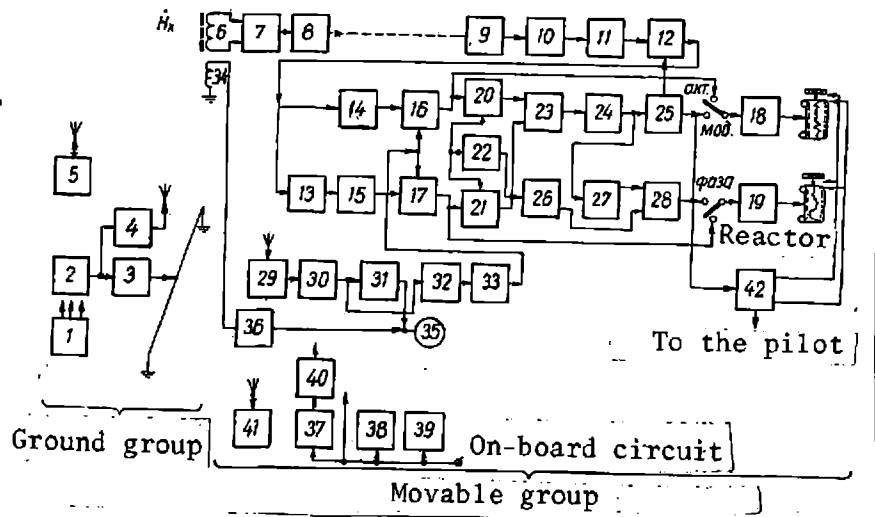


Fig.280

The signal of the operating frequency from the output of the master oscillator is delivered to the input of the power amplifier and to modulator YKV-4M of the main signal radio-transmitter. The circuit of the master oscillator permits adjustment of each voltage separately. The fundamental frequency of the quartz master oscillator is 7812 cps; the other operating frequencies are obtained by deviding the main frequency by four in the first divider (to obtain frequency 1953 cps and by two in the second, third and fourth dividers. In the fifth divider with division ratio three, the working frequency of 81 cps ($\frac{244}{3} \approx 81$ cps) is obtained. Also used as dividers are the relaxation synchronized oscillators-multivibrators.

The measured signal, received by the ferrite antenna 6 and amplified by the preamplifier 8, is transmitted by wire-cable to the input of the first amplifying stage 9. Block 7 serves to tune into resonance the receiving ferrite antenna.

The geophysical efficiency of the apparatus depends on its actual sensitivity, determinable not only by the sensitivity of the circuit adopted, i.e., by the minimum signal which could be reliably recorded, but also by the extent of its being noise-proof. To obtain greater sensitivity to the field a high-sensitive field receiver is required which should be provided with high stability against noises with vibration nature and external electromagnetic interference. The measuring channel should have the lower possible level of fundamental noises.

As a magnetic field receiver, the application of a coil with ferrite core is made tuned to the operating frequency for enhancing its sensitivity and selectivity. However, in the tuning of the antenna, control of the input phase errors is required, and also the checking of the circuit's sensitivity from the voltage of the measured field.

Bringing out of the field receiver and preamplifier into the gondola, trailing during the survey at the length of the cable (20-30m), makes it possible to reduce to a considerable extent the level of vibration noises. Placed into the gondola is also a remote control device 7, permitting the operator to switch-over the tuning capacitances of the frame into resonance.

After the selective amplifier 11 (10-measuring range switch), the signal is additionally amplified by amplifier 12, having linear or logarithmic curve. The presence of the logarithmic amplifier in the measuring channel simplifies the operator's work and improves the obtainable data, specially in measurements, carried out near

the laying of the cable, i.e., where the normal cable field sharply varies in intensity.

For the measuring phase, active or reactive components of e.m.f., induced in the field receiver, and also for the building up of coordinates, the radio-channel is used for transmitting the main signal.

Due to the fact that, for obtaining high stability of the apparatus against interference on low frequencies of the frequency filters with high Q-coefficient and stability of the parameters (52) is difficult, in these conditions the application for enhancing interference-stability of the apparatus is of the correlation method (synchronous detection). The synchronous detector with high time constant of the output LF filter permits the attenuation of the non-synchronous noise to a considerable extent ; this, however, reduces the quick action, which is undesirable for the measuring apparatus, set up on a moving object. Therefore, the time constant of the filter has been selected with an estimate of the helicopter's speed. In this measuring circuit, the positive properties of synchronous detecting are utilized, and to exclude the noise effect from the frequencies, lying beyond the pass band, prefiltering of the signal has been applied to commutation condition of the detector, i.e., in this apparatus, as in others, provision is made for the suppression, by filtering, of noises remote from the working frequency and for the near ones - by correlation method.

The application of synchronous detecting proposes the recording of results in rectangular coordinates, as the voltage

at the output of the synchronous detector is proportional to the active or reactive component. In order to obtain the measuring results in polar coordinates, while maintaining high interference stability, assured by the synchronous detector, a scheme for the conversion of Cartesian coordinates into polar ones, by means of the device for mean-square adding (53), was adopted. With this aim the direct voltage at the output of the two synchronous detectors gets transformed into alternate current voltages (one of them turns in the phase at 90°). Since the voltages delivered at the accumulator are in quadrature, the amplitude of the output signal will be proportional to the square root from the sum of components square, and the voltage phase at the output of the summing circuit in respect of transformed voltage of the active component will be equivalent to the phase of the measured signal. To measure the phase shift of the signal, it is sufficient to measure the phase shift between the commutating voltage and the voltage at the output of the summing circuit.

From the output of the amplifier 12, two signals, one of which is turned in the phase at 90° by the phase-inverter 13, arrives simultaneously through the phase-inversion circuits 14 and 15 at the synchronous detectors 18 and 17, controlled by the comparative voltage of rectangular shape. The output direct current voltages of synchronous detectors are proportional to the active and reactive components of the measured signal. Low-frequency filters at the output of the detectors provide a pass band on any operating frequency in the order of a few cps. The output voltages of the detectors are measured and recorded by two automatic

electronic compensators 18 and 19, based on standard automatic bridges MSI-01.

In measuring the modulus and phase, the constant current output voltages of synchronous detectors get transformed into alternate ones by means of semi-conductor transformers 20 and 21, controlled by voltage from the output of the multivibrator 22, operating on a frequency of about 750 cps. The alternate current voltage with transformation frequency is separated, after the summation, the application is of the automatic compensator 18 which, in this case, is cut out from the synchronous detector 16 of the active component.

The direct voltage, proportional to the signal module, is used for the automatic gain control of the logarithmic amplifier, and also for the automatic switching of the measuring range.

The phase shifts are measured by the phase meter, based on the phase detector 28. The voltages from the multivibrator and summation circuit are put into the detector after the limiters 26 and 27. The recording of the phase is effected by switching over the automatic compensator of the reactive component.

The comparative voltage, transmitted from the ground apparatus to the helicopter, is received by the radio-receiver 29, from the output of which after amplification by the selective amplifier 30 it arrives at the two phase-adjusters 31 and 32, constructed on the base of the VTM type revolving transformers. The phase-adjusters assure even phase variation of the received main signal within $0-360^{\circ}$. At the synchronous detectors, the main signal arrives from the output of the phase-adjuster 32 after

the limiter 33.

The phase meter is estimated to measure the phase shifts within the range $0-30^{\circ}$. For measuring higher angles, the use of the phase regulator 32 is made, by means of which it is possible to bring in a prefixed phase shift (for instance of 30° and hence every 30°). With its use, it is also possible to combine the phase of the main signal with the current phase in the cable.

To enhance the accuracy of measurements, the apparatus is provided with a special graduating device, consisting of an auxiliary frame 34, inductively coupled with the receiving frame 6, the graduated phase regulator 31, connected in the channel of the comparative voltage, the voltmeter 35 and the attenuator 36. By means of this system, a field with a known phase is generated and the intensity and the amplitude and phase characteristics of the measuring channel as a whole are checked for measuring with an error in the amplitude upto 2% and in the phase upto 1° .

The current supply of the entire measuring unit is obtained from the helicopter's network with voltage 27 v, filament circuits - directly from the network, other circuits through transformers 37, 38 and 39. The transformers 38 and 39 (frequency 125 cps) are used for the current supply of vibrotransformers and synchronous motors of recorders. The aviation transformer 37 with power 500 va, voltage 115 v and frequency 400 cps, serves to supply the current for the stabilized rectifier 40 (supply of anode-screen circuits of measuring apparatus).

The communication of the mobile unit with the ground one is through the radio-station of the helicopter 41. For automatic

fixing of time breaks on recorder tapes, indicating simultaneously the measuring range, guide marks and automatic switching of measuring range, block 42 is used. The control of recording guide marks is brought out on the navigator's panel.

The principal circuits of the main units of the apparatus are described in sufficient details in (118), therefore they are not discussed here. All the functional blocks of the measuring apparatus in the mobile group (measuring of main signal, rectifier, automatics and two recording blocks) are set up in a special cabinet and field to the floor by means of bolts and antidrag wires. Near the crew cabin the winch and the lowering system are set up. The supply block is placed above the battery compartment, and the next transformer PO-500. The antenna of the main signal receiver is fixed on the tail beam of the helicopter. The measuring cabinet is joined to other elements of the mobile group by means of flexible hoses and connectors.

For an emergency drop of the gondola, there is a cable-cutter, controlled from the cabin by the pilot. The pilot can also cut out the supply of the entire measuring apparatus and of the winch.

5. Correlation of survey results to locality

In geophysical investigations, the main practical interest and definite value are only of the data connected with the coordinates of the selected ground points or completely correlated with the locality of aerial electric prospecting.

The apparatus of aerial electric prospecting usually carries out continuous recording of measured parameters, shown in the form of curves. Therefore, all the points of the curve should refer to the corresponding points in the locality and, moreover, the altitude of the survey should be known. This means that, in aerial electric prospecting, as in the other aerogeophysical methods of mineral prospecting, it is necessary to carry out planimetric and altitude tying to the locality.

The chief methods of planimetric tie-in are visual tying, aerial photo-survey and radio-navigation. The first is usually carried out by the navigator of the aircraft in visual orientation from topographic of the locality or directly in the locality with the use of navigation devices of low accuracy; the second, by tying prints of photosurvey of the locality and the third - by means of special radionavigation devices.

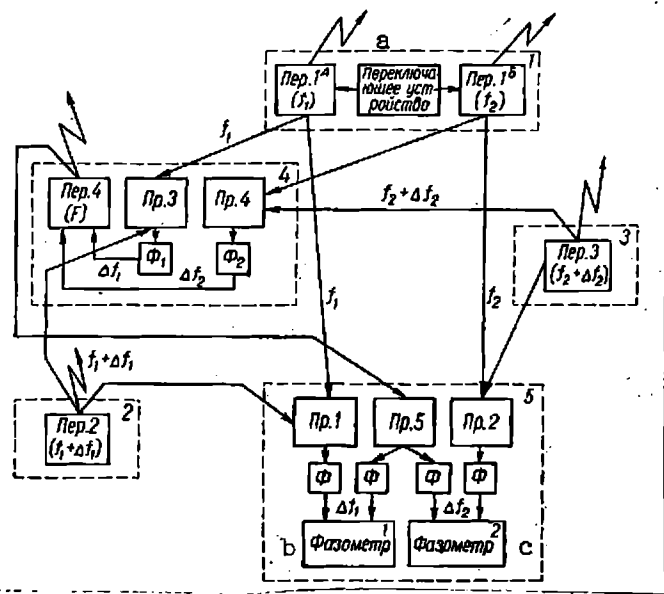
As a result of planimetric tying, regardless of how it was effected, a map of the route, travelled by the aircraft during the operation of the airborne electric prospecting apparatus, is obtained. Plotting of recorded parameters, synchronizing time break and guide marks on the curve permits referring the curves to certain segments of the aircraft route and to reduce them to the scale of the map of the survey area.

With visual tying the instants of passing above the landmarks are fixed by the navigator, as a rule, visually. The navigator presses the button switch of the remote marker of landmarks and on the tape of the recorder a corresponding mark appears. The passed

landmarks, the time of passing them and their number are entered in the plane log-book and marked on the field map. The geophysicist operator usually records on the tape the main points about the landmark.

The technique and methods of visual tying are, on the whole, simple, require attention and effort of the navigator. The reading errors in visual tying are at best 10-30 m.

In the absence of special radio-navigation means for piloting, there are frequently considerable deviations of the actual aircraft route from the course preset on the map, i.e., there are navigational errors during the flight along the profile. These errors are specially appreciable when the aerial survey is carried out in the taiga, open steppes without any landmark mountain areas, in survey with rounding of relief and intensive turbulence of air masses. Photo-tying has the best indicating quality. In comparison with visual photo-tying, taking photo prints of a locality, has a number of advantages the possibility of recording all the landmarks along the survey route and considerably greater accuracy of having them fixed the objective documentation of tying the possibility of controlling the results of the photosurvey and the use of differences imperceptible to the eye, in the coloring of the locality (spectrozoal film). Photo-tying is effected by wide-angle cameras, since it is highly important to obtain the maximum possible "capture" of the locality and small scale aerial photographs. This constitutes its difference from the usual aerial photo-survey.



Key to Figure 281:

- a, Switch;
- b, Phase meter 1;
- v, Phase meter 2.

Fig: 281.

However, in composite geographical conditions photo-tying without the guide marks is practically inapplicable. In this condition the only method for direct tying of the aircraft routes and data of airborne electric prospecting apparatus, set up on it, is the radio navigation method or the method of radio-geodesical tying. Radio-navigation means for planimetric tying are, naturally, more complicated than the above indicated, as a rule, they are costly and bulky, require a considerable number of serving personnel and their accuracy as far is comparatively low.

An example of radio-geodesic tying, which is most popular and could be used in aerial electric prospecting, is the radio-navigation system (142), the block diagram of which is shown in Fig: 281. The system consists of three ground base transmitting radio-stations and one retransmitting installation and also of the apparatus set up on the aircraft.

The operating principle of the system consists of the following. The central doubled base transmitter 1 emits alternately high-frequency oscillations of two different fixed frequencies f_1 and f_2 , with average switching frequency 6 cps. Two other single basic transmitters 2 and 3 continuously emit corresponding frequencies $f_1 + \Delta f_1$ and $f_2 + \Delta f_2$, where Δf_1 and Δf_2 - low frequencies. Thus, at $f_1 = 2510$ k-cps we have $\Delta f_1 = 400$ cps, at $f_2 = 2600$ k-cps $\Delta f_2 = 600$ cps. Coordinates of the ground installation of the three transmitters should be known.

At some land point, the coordinates of which should be known even approximately, is installed a retransmitter 4, consisting of two receivers Pr. 3 and Pr. 4, tuned respectively to frequencies f_1 and f_2 and transmitter Per.4, the carrier frequency F of which is quite distinct from frequencies f_1 and f_2 .

The retransmitting installations 4 serves to obtain the main phase. During the intervals when the central station 1 emits oscillations with frequency f_1 , the receiver Pr.3 receives simultaneously signals with frequencies f_1 and $f_1 + \Delta f_1$ and separates at the output oscillations with differential frequency Δf_1 , which after passing through low-frequency filter F_1 are delivered to modulator stage of retransmitter Per.4.

Thus, the carrier frequency F of the retransmitter Per.4 is alternately modulated by frequencies Δf_1 and Δf_2 . Set up on the aircraft is a mobile station 5 with three receivers (Pr.1, Pr.2, Pr.5) tuned respectively to frequencies f_1 , f_2 and F . At the output of the receivers are cut in low-frequency filters F , which separate the signals of differential frequency Δf_1 , and Δf_2 arriving therefore into two recording phase meters.

At the moment of send-off by the central transmitter Per. 1^A of the signal with frequency f_1 the receivers Pr.1 and Pr.5 separate oscillations with differential frequency Δf_1 , which are compared in the phase in the first phase meter. At the instant of send-off by the central transmitter Per. 1^B of the signal with frequency f_2 receivers Pr.2 and Pr.5 separate oscillations with differential frequency Δf_2 , which are also compared by the phase in the second phase meter.

The difference of phases measured in phase meters depends on the difference in the distance between the mobile object and ground base stations. With the motion of the aircraft, in the field of base stations continuous increment of phase shifts occurs, which phase-shift are recorded by phase meters. Then all the obtained data are plotted by a special method on the working map of the locality.

This system of radio-geodesical tying is bulky; therefore, development of more compact, comparatively simple systems, not requiring the spread of ground stations, is being carried out. Apparently the systems based on doppler effect (26, 165), will become the most widely adopted in aerial electric prospecting.

Altitude tying in aerial electric prospecting is usually effected by means of barometric or radio-technical altimeters, which fix barometric or true altitude respectively in the form of continuous or periodic recordings (curves) on the tapes of recorders.

BIBLIOGRAPHY:

1. Aleksandrovskaya G.V.-V kn. Voprosy razvedochnoi geofiziki
Gostoptekhizdat, Moskva, 1962.
2. Alpert Y.L., V.L.Ginsburg and E.L. Feinberg Rasprostranenie radiovoln (Propagation of
radio waves) --- Gostekhizdat, Moskva,
1953.
3. Andrievsky M.N. Konstruirovaniye elementov radioperedat-
chikov, ustanavlivaemykh na podvizhnykh
ob'ektakh (Construction of radio-trans-
mitters, set up on a mobile object).---
Oborongiz, Moskva, 1959.
4. Anisimev A.B. Odnopolosnaya radiosvyaz (One-band radio-
communication) --- Voenizdat, Moskva, 1961.
5. Apparatura firmy ABEM dlya vozduшной
razvedki (ABEM apparatus for aerial survey).
--- Sb. Perevodov. Izd. ONTI OKB MG i ON,
L., 1959, 25, 19-24.
6. Artamonov L.V., G.S. Razvedka i okhrana neдр, 1958, 1.
Frantov, N.M. Shuval-Sergeev
7. Artamonov L.V. and N.M. Sovetskaya geologiya (Soviet geology) ---
Shuval-Sergeev 1961, 2.
8. Artamonov L.V. - V kn. Metodika i tekhnika razvedki, 26. Izd.
ONTI VITR MG i ON SSSR, L., 1961.
9. Artamonov L.V., and Sovetskaya geologiya (Soviet Geology),
L.A. Rivosh 1962, 8.

10. Aseev V.P. Fazovye sootnosheniya v radiotekhnike
(Phase relations in radio-technique) ---
Svyaz'izdat, Moskva, 1959.
11. Bazhenov A.S.-V kn.: Byulleten' nauchno-tekhnicheskoi informatsii, ONTI VIMS MG i ON SSSR, 6/94,
Gosgeoltekhizdat, Moskva, 1961.
12. Bal'sen M.R.- V kh.: Byulleten tekhnicheskoi informatsii ONTI
OKB MG i ON SSSR. Gosgeoltekhizdat,
Moskva, 1958.
13. Belichenko A.I. Radiotekhnika, 1960, 15, 3.
14. Belichenko A.I.-V kn.: Apparatura aroelektrozvedki, Izd.-vo
AN USSR, Kiev, 1963.
15. Belichenko A.I. Radiotekhnika, 1964, 19, 11.
16. Berkman R.Ya., and V.N. Mikhailovsky Izv. AN SSSR, seriya geofiz., 1959, 6.
17. Berkman R. Ya. i dr. -V.: Avtomaticheskii kontrol i izmeritel'naya
tekhnika, 8. "Naukova dumka", Kiev, 1964.
18. Besonov L.A. Teoreticheskie osnovy elektrotekhniki
(Theoretical fundamentals of electro-
technique) "Vysshaya shkola", Moskva,
1964.
19. Blazhkevich B.I.-V kn.: Sb. trudov sovsshchaniya v IMA AN USSR.
Izd.-vo AN USSR, Kiev, 1953.
20. Blazhkevich B.I., and S.K. Kuzovkin. - V kn.: Avtomaticheskii kontrol i izmeritel'naya
tekhnika, 6. Izd.-vo AN USSR, Kiev, 1962.
21. Blazhkevich B.I., S.K. Kuzovkin and A.I. Belichenko
- V kn.: Apparatura aroelektrozvedki, Izd.-vo
AN USSR, Kiev, 1963, 5-17.

22. Blazkhevich B.I., and S.K. Kuzovkin. -V kn.: Apparatura aereolectrorazvedki, Izd-vo AN USSR, Kiev, 1963, 18-27.
23. Bonch-Bruevich A.M. Primenenie elektronnykh lamp v eksperimental'noi fizike (Application of electronic tubes in experimental physics) --- Gostekhzdat, Moskva, 1956.
24. Bonch-Bruevich A.M. and V.I. Shirkov ZhTF, 1955, 25.
25. Bosyi N.D. Elektricheskie filtry (Electric filters) --- Gostekhzdat, Kiev, 1959.
26. Boshnyakovich I.K. and Yu. S. Glebovskii Fotoprivyazka geofizicheskikh marshrutov i anomalii (Photo-tying of geophysical routes and anomalies). --- Gostekhzdat, Moskva, 1963.
27. Boshnyakovich I.D. Razvedka i okhrana neдр, 1959, 3.
28. Broyd I.D. and B. Roberts - V kn.: Geofizicheskie metody pazvedki i apparatura, 36, Gostoptekhzdat, Leningrad 1963, 36-45.
29. Bronshtein I.N. and K.A. Semendyaev Spravochnik po matematike, "Nauka" Moskva, 1964.
30. Bursian V.R. Teoriya electromagnitnykh polei, primenyayemykh v elektrorazvedke (Theory of electromagnetic fields applied in electric prospecting), ch. II. Izd-vo LGU, 1936.
31. Van'tyan L.L. and L.Z. Borovnikov Electrorazvedka po metody stanovleniya magnitnogo polya (Electric Prospecting by method of settled magnetic field) --- Gosgeoltekhizdat, Moskva, 1963.

32. Vasil'eva V.P. and A.I..i dr. Gorskii Raschet elementov impul'snykh radio-tekhnicheskikh ustroystv (Estimate of elements in radio-technical impulse systems) --- Gosenergoizdat, Moskva, 1963.
33. Vasil'ev P.I. .Opyt primeneniya aeroelektrozvedki metodom induktsii na Kol'skom poluostrove (Experiment of apply in aerial electric prospecting by induction method on Kolsky Peninsula). --- Izd. ONTI VIEMS, Moskva, 1964.
34. Vasil'ev P.I.- V kn.: Uchenye zapiski LGU, 324, seriya fiz.i geol. nauk, 15. Izd-vo LGU, Leningrad, 1964.
- 35 Vasil'ev P.I., and M.N. Molotkova - V kn.: Uchenye zapiski LGU, 324, seriya fiz. i geol. nauk, 15, Izd-vo LGU, Leningrad, 1964.
- 36 Watson G.N. Teoriya besselevykh funktsii (Theory of Bessel's function), ch. 1, IL, Moskva 1949.
37. Vvedenskii B.A. Vestnik teoreticheskoi i eksperimental'noi elektrotekhniki, 1928, 12, 439.
38. Velikin A.B.i and G.S. Frantov Elektromagnitnye polya, primenyaemye v induktivnykh metodakh elektrozvedki (Electromagnetic fields, applied in inductive methods of electric prospecting) --- Gostoptekhnizdat, Leningrad, 1962.

- 39 Velichko Yu.T. - V. kn.: Haukovi zapiski LPI, 27, seriya raditekhnichna, 1. Vid-vo LPI, L'viv, 1955.
- 40 Verzunov M.V., I.V. Lobanov and A.M. Semenov Odnopolosnaya modulyatsiya (Single-band modulation) Svyazizdat, Moskva, 1962.
- 41 Veshev A.V., E.V. Lyubtseva G.P. Somosyuk - V kn.: Uchenye zapiski LGU, 14, 15. Izd-vo LGU, Leningrad, 1963, 1964.
- 42 Veshev A.V. Elektroprofilirovanie na postoyannom i peremennom toke (Electric Profiling on direct and alternate current) --- "Nedra", Moskva, 1965.
- 43 Vishenchuk I.M., A.F. Kotyuk and L.Ya. Mizyuk Elektromekhanicheskie i elektronnye fazometry (Electro-mechanical and electronic phase meters) --- Gosenergoizdat, Moskva, 1962.
- 44 Voishillo G.V. Usiliteli nizkoi chastoty ha elektronnykh lampakh (LF-amplifiers on electric tubes) --- Svyaz'isdat, Moskva, 1959.
- 45 Volin M.L. Parazitnye svyazi i navodki (Parasitic couplings and inductions) --- "Sovetskoe radi", Moskva, 1965.
- 46 Vovutskii V.S. Korelyatsionnyi metod obnaruzheniya i izmereniya slabykh signalov (Asinkhronnee nakoplenie) (Correlation method of detecting and measuring weak signals) (Asynchronous stacking) --- "Nedra" Moskva, 1965.
- 47 Gasanonko L.B. - V kn.: Uchenye zapiski LGU, 10. Izd-vo LGU, Leningrad, 1958.

48. Gasanenko L.B.,
M.N. Molotkova and
V.G. Sapozhnikov. - V kn.: Uchenye zapiski LGU, 15. Izd-vo LGU,
Leningrad, 1964.
- 49 Ginkin G.G. Spravochnik po radiotekhnike , Gosener-
goizdat, Moskva, 1948.
- 50 Gitis E.I. Preobrazovateli informatsii dlya elektro-
nykh tsifrovyykh vychislitel'nykh ustroystv
(Information transformers for digital
computers) --- Gosenergoizdat, Moskva,
1961.
- 51 Glebovskii Yu. S. - V kn.: Buletten naychno-tekhnicheskoi informatsii
ONTI VIEMS MG i ON SSSR, 2(30). Gosgeolte-
khizdat, Moskva, 1961.
- 52 Govorkov V.A. Elektricheskie i magnitnye polya (Electric
and magnetic fields) --- Gosenergoizdat,
Moskva, 1960.
- 53 Gol'dgefter V.I., and
L. Ya. Mizyuk - V kn.: Trudy konferentsii po avtomaticheskomu
kontrolyu i elektricheskim izmereniyam
Izd-vo SO i AN SSSR, Novosibirsk, 1961.
- 54 Gol'dgefter V.I. - V kn.: Geofizicheskaya apparatura, 24, "Nedra",
Leningrad, 1965.
- 55 Gol'dgefter V.I. - V kn.: Teoriya i elementy sistem ob'bora
geofizicheskoi informatsii, "Naukova
dumka", Kiev, 1965.
- 56 Gonorovsky I.S. Osnovy radiotekhniki (Fundamentals of
radio-technique) --- Svyaz'izdat, Moskva,
1957.
- 57 Goncharskii V.N. - V kn.: Avtomaticheskii kontrol i izmeritel'naya
tekhnika, 4. Izd-vo AN USSR, Kiev, 1960.

- 58 Goncharskii V.N. -V kn.: Avtomaticheskii kontrol i izmeritel'naya tekhnika, 5. Izd-vo AN USSR, Kiev, 1961.
- 59 Goncharskii V.N. and N.I. Kalashnikov. V kn.: Teoriya i elementry sistem otbora geofizicheskoi informatsii, "Naukova dumka", Kiev, 1965.
- 60 Gorbachev A.A. Radiotekhnika, 1957, 12, 6.
- 61 Grinevich F.B. and L.Ya. Mizyuk. Izv. SO AN SSSR, Seriya geofiz., 1962, 1.
- 62 Gutkin L.S. ZhTF, 1945, 15, 10.
- 63 Daev D.S. - V kn.: Voprosy razvedochnoi geofiziki, 2. Izd-vo SO AN SSSR, Novosibirsk, 1961.
- 64 Dekhtyarenko P.I. Experimental'ne viznachennya chastotnykh kharakteristik sistem avtomatichnogo regul'yuvannya (Experimental Separation of frequency characteristics in automatic adjustment systems). Vid-vo AN USSR, Kiev, 1961.
- 65 James H., N. Nichols and R. Phillips Teoriya sledyashchikh sistem (Theory of follow-up systems). --- IL, Moskva, 1954.
66. Dikmarova L.P. Izv. AN SSSR, Seriya Geofiz., 1965, 8.
- 67 Dikmarova L.P. - V kn.: Teoriya i elementry system otbora geofizicheskoi informatsii "Naukova dumka", Kiev, 1965.
- 68 Dmitriev V.I. Izv. AN SSSR, Seriya Geofiz., 1959, 4.
- 69 Dmitriev V.I. Avtoreferat kand. diss. Moskva, 1959.
- 70 Dmitriev V.I. Izv. AN SSSR, Seriya Geofiz, 1960, 8.
- 71 Dmitriev V.I. Izv. AN SSSR, Seriya Geofiz., 1961, 1.

- 72 Dolukhanov M.P. Rasprostranenie radiovoln (Propagation of radio-waves) --- "C'yaz", N₁., 1965.
- 73 Evteev F.G. and V.A. Zhukov Tekhnologiya radioapparatury (Technology of radio-apparatus) --- Gosenergoizdat, Moskva, 1952.
- 74 Ermakov A.N., A.N. Klepikova and L.D. Yudina Usilenie malykh izmenenii sdviga faz mezhdu dvumya elektricheskimi signalami, Izv. vuzov, seriya radiotekhnika, 1962, 5.
- 75 Zaborovskii A.I. Elektrorazvedka (Electric Prospecting) --- Gostoptekhzdat, Moskva, 1963.
- 76 Zamekhovskii V.S. and S.K. Kuzovkin. - V kn.: Apparatura aereoelktorazvedki, Izv. AN SSSR, Kiev, 1963.
- 77 Zakharov V., Kh. Izv. AN SSSR, Seriya Geofiz., 1961, 12.
- 78 Ignat'ev G.P. Abt. svid., klass 21 d, 30₀₃, No.139750, Bulletin izobretenii, 1961, 14.
- 79 Il'shinskii V.S. Voprosy izolyatsii vibratsii i udarov (Problems of isolating vibration and impacts) --- "Sovtskoe radio", Moskva, 1960.
- 80 Iorish Yu. I. Zashchita samoletnogo oborudovaniya ot vibratsii (Protection of plane equipment from vibration) --- Oboronizdat, Moskva, 1960.
- 81 Iorish Yu. I. - V kn.: Sostoyanie sovremennogo priborostroeniya v oblasti izmeritel'noi tekhniki, Izd-vo MDNTI im. F.E. Dzerzhinskogo, Moskva, 1956.
- 82 Itskhoki Ya. S. Impul'snye ustroistva (Impulse systems) --- "Sovetskoe radio", Moskva, 1959.

- 83 Kalantarov P.L. and L.P. Neiman Teoreticheskie osnovy elektrotekhniki (Theoretical fundamentals of electro-technique) --- Gosenergoizdat, Moskva, 1954.
- 84 Kalantarov P.L. and A.A. Tseitlin Raschet induktivnostei. Gosenergizdat, 1965.
- 85 Kalashnikov N.I. Abt.svid., klass 21 d, 30₀₂, No.140130
Bulletin izobretenii, 1961, 15.
- 86 Kalashnikov N.I. - V kn.: Avtomaticheskii kontrol i izmeritel'naya tekhnika, 5. Izd-vo AN USSR, Kiev, 1961.
- 87 Kalashnikov N.I. and V.N. Goncharskii "Radio", 1962, 5.
- 88 Kalashnikov N.I. - V kn.: Avtomaticheskii kontrol i izmeritel'naya tekhnika, 7. Izd-vo AN USSR, Kiev, 1963.
- 89 Kalashnikov N.I. Avtoreferat kand.dissertatsiya. L'vov, 1963.
- 90 Kalashnikov N.I. i dr. Apparatura aeroelectrorazvedki. Izd-vo AN USSR, Kiev, 1963, 93-105.
- 91 Kalashnikov N.I., V.N. Goncharskii and V.A. Nichoga - V kn.: Apparatura aroelektrozvedki. Izd-vo AN USSR, Kiev, 1963, 122-128.
- 92 Kalashnikov N.I. and P.M. Sopronyuk - V kn.: Apparatura aroelektrozvedki, Izd-vo AN USSR, Kiev, 1963, 58-63.
- 93 Kalashnikov N.I. - V kn.: Trudy mezhvusoovskoi nauchnoi konferentsii po induktivnym metodam pudnoi geofizidi, (22-26 Noyabrya 1961 g.) "Nedra", Moskva, 1964.
- 94 Kalashnikov N.I. - V kn.: Avtomaticheskii kontrol i metody elektricheskikh izmerenii, 1. Izd-vo SO AN USSR, Novosibirsk, 1964.

- 95 Kalashnikov N.I. - V kn.: Avtomaticheskii kontrol i izmeritel'naya tekhnika, 8. Izd-vo AN USSR, Kiev, 1964
- 96 Kalashnikov N.I. - V kn.: Teoriya i elementy sistem otbora geofizicheskoi informatsii "Naukova dumka", Kiev, 1965.
- 97 Kalnyn R. and G.Sermans Izv. AH Latv. SSR. 1963, 3.
- 98 Kamenetskii F.M., A.A. Kaufman and Yakubovskii Yu. V. - V kn.: Izv. AN SSSR, Seriya Geofiz., 1957, 24.
- 99 Kamenetskii F.M., A.A. Kaufman and Yu. V. Yakubovskii - V kn.: Trudy MGRI, 36. Gosgeoltekhizdat, 1959.
- 100 Karandeev K.B and L.Ya. Mizyuk - v kn.: Voprosy avtomatiki i izmeritel'noi tekhniki Naychnye zapiski IMA AH SSSR, 4,3. Izd-vo AN SSSR, Kiev, 1955.
- 101 Karandeev K.B. and L.A. Sinitskii Avtomatika i telemekhanika 1958, 9.
102. Karandeev K.B. and L.Ya. Mizyuk Izv.SO AH SSSR, 1959, 7.
103. Karandeev K.B. & L.Ya. Mizyuk Izv. AH SSSR, Seriya Geofiz., 1960, 6.
- 104 Karandeev K.B. and G.A. Shtamberger Elektrichestvo (Electricity), 1962, 12.
105. Karandeev K.B. and G.A. Shtamberger - V kn.: Trudy mezhvuzovoi nauchnoi konferentsii po induktivnym methodam rudnoi geofiziki (22-26 Nov. 1961), "Nedra", Moskva, 1964
- 106 Karandeev K.B. and G.A. Shtamberger - V kn.: Doklady k seminaru po teme "Vnedrenie novoi metodiki i tekhniki elektrorasvedochnykh rabot v geolgo-razvedochnuyu sluzhbu", 34. Izd. ONTI VIEMS, Moskva, 1964.
- 107 Karandeev K.B. i dr. Izv. AH SSSR, Seriya Geofiz., 1964, 2.
- 108 Karandeev K.B. and G.A. Shtamberger - V kn.: Geofizicheskaya apparatura, 24. "Nedra", Leningrad, 1965.

- 109 Kashprovskii V.E. - V kn.: Teoriya i elementy sistem otbora geofizicheskoi informatsii (Theory and elements of systems for selection of geophysical information) " Naukova dumka", Kiev, 1965.
- 110 Kessenikh V.N. Rasprostranenie radiovoln (Propagation of radio-waves). --- Gostekhizdat, Moskva, 1952.
- 111 Kifer N.I. and V.S. Pantyushina Ispytanie ferromagnitnykh materialov (Tests of ferromagnetic material) --- Gosenergoizdat, Moskva, 1955.
- 112 Kleimenova N.G. Izv. AN SSSR, Seriya Geofiz, 1963, 12.
- 113 Kobrinskii M.P. - V kn.: Sostoyanie sovremennogo priborostroeniya v oblasti izmeritel'noi tekhniki (The state of instrument making at present in the sphere of measuring technique). --- Izd-vo MDNTI im. F.E. Dzerzhinskogo, Moskva, 1956.
- 114 Kovalev V.P. Pribory i tekhnika eksperimenta, 1958,2.
- 115 Koganov P.D. - V kn.: Trudy mezhvuzovskoi konferentsii po induktivnym metodam rudnoi geofiziki, (22-26 noyabrya 1961 g.). "Nedra", Moskva, 1964.
- 116 Kolosov A.A. Rezonansnye sistemy i rezonansnye usiliteli (Resonance systems and resonance amplifiers) --- Svyasizdat, Moskva, 1949.

- 117 Kotyuk A.F. Analiz skhem aereoektrorzvedki methodom inductsii (Circuit analysis of aerial electric prospecting by induction method) --- Izd-vo SO AH SSSR, Novosibirsk, 1962
- 118 Kotyuk A.F. i dr. Apparatura dlya aereoektrorazvedki methodom beskonechne dlinnogo kabelya (Apparatus for aerial electric prospecting by method of infinitely long cable) --- Izd-vo SO AN SSSR, Novosibirsk, 1962
- 119 Kraev A.P. Osnovy geoelektriki (Fundamental principles of geoelectricities) --- ch. 1. Gostekhzdat, Moskva, 1951.
- 120 Krivitskii B.H. Impul'snye skhemy i ustroistva (Impulse circuits and systems). --- "Sovetskoe radio", Moskva, 1955.
- 121 Krivitskii B.H. Avtomaticheskie sistemy radiotekhnicheskikh ustroistv (Automatic systems of radio-technical devices) --- Gosenergoizdat, Moskva, 1962.
- 122 Kuzovkin S.K. and P.V. Prots Avt. svid., klass NO 5d, 21d, 30₀₂, No.155887, Bulletin izobretonii i tovarnykh znakov, 1963, 14.
- 123 Kuzovkin S.K. and N.I. Kalashnikov - V kn.: Metodika i tekhnika razvedki, 26. Izd-vo ONTI VITR MG i ON SSSR, Leningrad, 1961.
- 124 Kuzovkin S.K. Izv. AN SSSR, Seriya Geofiz., 1963, 10
- 125 Kuzovkin S.K., A.I. Belichenko and R.V. Prots - V kn.: Apparatura elektrorazvedki. Izd-vo AN SSSR, Kiev, 1963, 28-34.

- 126 Kuzovkin S.K., A.I. Belichenko and R.V. Prots. - V kn.: Apparatura aerboelektrovozvedki Izd-vo AN SSSR, Kiev, 1963, 35-48.
- 127
- 128 Kuzovkin S.K. Izv. AN SSSR, Seriya Geofiz. 1964, 10
- 129 Kuzovkin S.K. - V kn.: Geofizicheskoe priborostroenie "Nedra", Leningrad, 1964.
- 130 Kuzovkin S.K. - V kn.: Avtomaticheskii kontrol i izmeritel'naya tekhnika, 8. Izd-vo AN SSSR, Kiev, 1964, 119-124.
- 131 Kuzovkin S.K. - V kn.: Avtomaticheskii kontrol i izmeritel'naya tekhnika, 8. Izd-vo AN SSSR, Kiev, 1964, 125-129.
- 132 Kuzovkin S.K. Avtoreferat kand. diss., L'vov, 1965.
- 133 Kuzovkin S.K. - V kn.: Teoriya i elementy sistem otbora i peredachi geofizicheskoi informatsii (Theory and elements in selection and transmission systems of geophysical information) --- "Naukova dumka", Kiev, 1965, 74-79.
- 134 Kuzovkin S.K. - V kn.: Teoriya i elementy sistem otbora geofizicheskoi informatsii. "Naukova dumka", Kiev, 1965, 84-89.
- 135 Kuzovkov N. Teoriya avtomaticheskogo regulirovaniya, osnovannaya na chastotnykh metodakh (Theory of automatic control, based on frequency methods). --- Oborongiz,

- Moskva, 1958.
- 136 Kulikovskii A.A. Lineinye kaskady radiopriemnikov
(Linear cascades of radio-receivers) ---
Gosenergoizdat, Moskva, 1958.
- 137 Kulikovskii L.F. and A.M. Melik-Shakhnazarov Kompensatory peremennogo toka (Compensators of alternate current) ---
Gosenergoizdat, Moskva, 1960
- 138 Kuflevskii E.F. Elektrosvyaz, 1962, 6.
- 139 Labutin V.K. Radio, 1958, 11.
- 140 Landsberg G.S. Optika (Optics) --- OGIz, Moskva, 1947.
- 141 Lindov V.I., V.B. Mal' and N.V. Sergeeva, - N kn.: Izmereniya v provodnoi svyazi (Measurements in line) --- 1(7). Izd. MRTP, Leningrad, 1956.
- 142 Lozinskaya N.M. and L.E. Mindlin - V kn.: Prikladnaya geofizika, 24, Gostoptekhi-
zdat, Moskva, 1960.
- 143 Landi R. i dr. Spravochnik radioinzhenera, Gosenergo-
izdat, Moskva, 1961.
- 144 Maierov F.V. Elektronnye regulatory (Electronic
regulators) --- Gostekhnizdat, Moskva,
1956.
- 145 Malinin R.M. Kondensatory i soprotivliniya (Condensers
and resistances) --- Voenizdat, Moskva,
1959.
- 146 Malyarevskii K.V. and V.K. Rybin. - V kn.: Geofizicheskaya apparatura, 20 "Nedra",
Leningrad, 1964.
- 147 Malyarevskii K.V. and V.K. Rybin. - V kn.: Geofizicheskaya apparatura, 23. "Nedra",
Leningrad, 1965.
- 148 Malyarevsky K.V. and V.K. Rybin. - V kn.: Geofizicheskaya apparatura, 24, "Nedra",
Leningrad, 1965.

- 149 Mandel'shtamp L.I. and P.D. Papaleksi Interferentsionnye metody issledovaniya rasprostraneniya radiovoln i ikh primemenie k izmereniyu rasstoyanii (Interference method of investigating propagation of radio-waves and their application for measuring distances) --- Polnoe sobranie trudov, t. II. Izd-vo, AN SSSR, Moskva, 1947.
- 150 Meerovich A.A. and L.G. Zelichenko Impul'snaya tekhnika (Impulse technique) --- "Sovetskoe radio", Moskva, 1954.
- 151 Mizyuk L.Yu Elektronni pokazchiki zminnoi naprugi (Electronic indicators of alternate current) --- Gostekhvidav, Kiev, 1960.
- 152 Mizyuk L.Ya Izv. SO AH SSSR, 1961, 7, 8.
- 153 Mizyuk L.Ya, & V.M. Podzharyi Izv. AH SSSR, Seriya Geofiz., 1963, 7.
- 154 Mizyuk L.Ya. Vkhodnye preobrazovateli dlya izmereniya napryazhennosti nizkochastotnykh magnitnykh polei (Input transformers for measuring tension of low-frequency magnetic fields). --- "Naukova dumka", Kiev, 1964.
- 155 Mizyuk L.Ya. & V.A. Nichoga - V kn.: Geofizicheskoe priborostroenie, 20. "Nedra" Leningrad, 1964.
- 156 Mikhailova G.A. Geomagnetism i aeronomiya (Geomagnetism and aeronomics), 1962, 2, 2.
- 157 Molochnov G.V. - V kn.: Geofizicheskoe priborostroenie, 20. "Nedra", Leningrad, 1964.

- 158 Nel'tner P. & G.P. Lafarg. - Vkn.:
Metodika i tekhnika razvedki, 16.
- 159 Nekhoroshev V.P. Razvedka nedr (Exploration of mineral resources), 1937, 3.
- 160 Nikitenko V.I. and A.A. Ivanov Izv. vyzov, seriya radiotekh, 1959, 2,4.
- 161 Nikitenko V.I. & A.A. Ivanov Izv. LETI, 1957, 37.
- 162 Nikol'skii V.V. Teoriya elektromagnitnogo polya
(Theory of electromagnetic field) ---
"Vysshaya shkela", Moskva, 1961.
- 163 Ogil'vi N.A., O.M.Myaskovskii and V.R. Laptev. - V kn.:
Bulletin ONTI Gosgeolkoma SSSR, 1.
Gosgeoltekhizdat, Moskva, 1961.
- 164 Orantskii P.P. Avtomaticheskie izmeritel'nye pribory,
analogovye i tsifrovye (Automatic
measuring devices, analog and digital)
--- "Tekhnika", Kiev, 1965.
- 165 Postryakov V.V. Radionavigatsionnye uglomernye sistemy
(Radio-navigational goniometric systems)
--- Gosenergoizdat, Moskva, 1955.
- 166 Peterson N.R. - V kn.: Geofizicheskie metody razvedki i apparatura,
34. Gostoptekhizdat, Leningrad, 1962.
- 167 Peterson N.R. Aeroelektrozrazvedka s gelikopterom nad
rudnym telom Modren v Nopande (Aerial
electric prospecting with helicopter
above ore body Mobren in Nopanda), 22.
Izd. ONTI VIMS MG i ON SSSR, Moskva, 1962.
- 168 Petrovskii A.A. Izv. IPG, 1925, 1.
- 169 Plotnik R.I. Obzor sostoyaniya metodiki i tekhniki

- elektrorazvedochnykh rabot na tverdye
poleznye iskopaemye za rubezhom (Review
of methods and technique of electric
prospecting for hard mineral abroad)---
38. Izd. ONTI VIEMS GKG SSSR, 1964.
- 170 Politsin N.D. and A.V.
Dolivo-Dobrovol'skii. - V kn.: Aerometody izucheniya prirodnkh resurso
Geografiz, Moskva, 1962.
- 171 Ponevitskii K.K. and
E.K. Stolyarova Avt. svid. No.119017, 1959. Bulletin.
- 172 Pris G.N. Izv. AN SSSR, Seriya Geofiz., 1961, 11.
- 173 Rasprostranenie dlinnykh i sverkhdlinnykh
radiovoln (sb. pod red V.B. Pestryakova).
IL, Moskva, 1960.
- 174 Reikh G.J. Teoriya i primeneniye elektronnykh
priborov (Theory and application of
electronic devices)---Gosenergoizdat,
Moskva, 1948.
- 175 Remez G.A. Kurs osnovnykh radiotekhnicheskikh
izmerenii (Course of fundamental radio-
technical measurements)---Svyaz'izdat,
Moskva, 1956.
- 176 Rizkin A.A. Osnovy teorii usilitel'nykh skhem
(Fundamental principles of measuring
circuits) --- Svyaz'izdat, Moskva, 1958.
- 177 Rogachev V.V. and
A.A. Flaksman - V kn.: Geofizicheskoe priborostoenie, 12.
Gostoptekhizdat, Leningrad, 1962.
- 178 Rosenblat M.A. ZhTF, 1954, 24, 4.
- 179 Roitman M.S. i dr. Izmeritelnaya tekhnika, 1961, 9.

- 180 Roks A.T. - V kn.: Geofizicheskaya apparatura, 23.
"Nedra", Leningrad, 1965.
- 181 Ronka V. - V kn.: Geofizicheskie metody razvedki i apparatura, 38. Gostoptekhnizdat, Leningrad, 1963.
- 182 Ryazanov B.I. Elektrosvyas, 1958, 2.
- 183 Saakov E.O. Teoriya i raschot izbiratel'nykh RC-sistem (Theory and estimate of selective RC-systems). --- Gosenergoizdat, Moskva, 1954.
- 184 Saturin A.A. Bulletin nauchno-tekhnicheskoi informatsii MG i ON SSSR, 8 (42), 1962.
- 185 Svetov B.S. Avtoreferat kand. diss., Moskva, 1960.
- 186 Svetov B.S. Razvedka i okhrana nedr, 1964, 11.
- 187 Sigorskii V.P. and I. Yu. Spektor - V kn.: Voprosy avtomatiki i izmeritel'noi tekhniki, 4. Izd-vo AN SSSR, Kiev, 1955.
- 188 Skripnik Yu. A. Avt. svid. No.124540, 1959 i No.135537, 1960. Bulletin izobretenii i tovarnykh znakov, 1959, 23; 1961, 3.
- 189 Smait V. Elektrostatika i elektrodinamika (Electrostatics and electrodynamics) --- IL, Moskva, 1954.
- 190 Smirnova I.A. and G.S. Frantov - V kn.: Geofizicheskoe priborostroenie, 21.
"Nedra", Leningrad, 1964.
- 191 Sogolovskii E.P., B.I.Shvedskii and G.A. Shevtsov - V kn.: Voprosy elektronnoi izmeritel'noi tekhniki, 1. Izd. LPI, L'vov, 1958.
- 192 Solov'ev N.N. Osnovy izmeritel'noi tekhniki provodnoi

- svyazi (Fundamental principles of line-measuring technique), --- ch. II. Gosenergoizdat, Moskva-Leningrad, 1957.
- 193 Sorkin I.M. Osnovy radioizmeritel'noi tekhniki (Fundamental principles of radio-measuring technique) --- Gosenergoizdat, Moskva, 1962.
- 194 Spravochnik po radiotekhnike, pod obshch. red. Smirenina B.A. Gosenergoizdat, Moskva, 1950.
- 195 Stekol'nikov I.S. Molniya i grom (Lightning and tender). --- Voenizdat, Moskva, 1964.
- 196 Stepanenko I.L. Spetsial'noe ispol'zovanie elektronnykh lamp v avtomatike i priborostroenii (Special use of electronic tubes in automatics and device construction) --- Gosenergoizdat, Moskva, 1956.
- 197 Stretton J.A. Teoriya elektromagnetizma (Theory of electromagnetism) --- Gostekhzdat, Moskva, 1948.
- 198 Tamm I.E. Osnovy teorii elektrichestva (Fundamental principles of electricity theory) --- Gosenergoizdat, Moskva, 1956.
- 199 Tartakovskii G.P. Dinamika sistem avtomaticheskoi regulirovki usileniya (Dynamics of automatic gain control systems) --- Gosenergoizat, Moskva, 1954.

- 200 Tarkhov A.C. Geofizicheskaya razvedka methodom induktsii (Geophysical prospectin by induction method) --- Gosgeoltekhizdat, Moskva, 1954.
- 201 Tarkhov A.G. Izv. AN SSSR, seriya geofiz., 1957, 8.
- 202 Tarkhov A.G. Osnovy geophysicheskoi razvedki metodom radioskop (Fundamentals of geophysical prospectinb by radio control and measuring instruments) --- Gosgeoltekhizdat, Moskva, 1961.
- 203 Tarkhov A.G. - V kn.: Trudy mezhvuzovskoi konferentsii po induktivnym metodam rudnoi geofiziki. "Nedra", Moskva, 1964.
- 204 Trkhanov A.G. and A.D. Frolov - V kn.: Vysokochastotnaya elektrorazvedka Method radioskop) --- 23. Izd-vo ONTI VIEMS GKG SSSR, Moskva, 1964.
- 205 Temnikov F.E. Avtomaticheskie registriruyushchie pribory (Automatic recorders) --- Mashgiz, Moskva, 1954.
- 206 Terent'ev B.P. Radiopere dayushchie ustroistva (Radio transmitting systems). --- Svyas'izdat, Moskva, 1963.
- 207 Termen F.I and J. Pettit. Izmeritel'naya tekhnika v elektronike (Measuring technique in electronics) --- IL, Moskva, 1955.
- 208 Tikhonov A.N. & V.I. Dmitriev Izv. AN SSSR, seriya geofiz., 1959, 9.

9

- 209 Tikhonov A.N. and V.I. Dmitriev Izv. AN SSSR, Seriya Geofiz. 1959, 10.
- 210 Temov K. Tekhnika melodezhi, 1964, 8.
- 211 Tornkvist G.N. Resul'taty vozdushnoi elektrorazvedki v Shvetsii, 25. Izd. OKB MG i ON SSSR, Leningrad, 1959.
- 212 Uil'yam D. Doklad na mezhdunarodnom seminare po vosdushnym geofizicheskim metodam s'emki (Paper read at the International Symposium on Aerial Geophysical Methods of Survey) --- Delhi, 1960.
- 213 Fok V.A. and V.R. Bursian Zhurnal russkogo fiz.-khim.obshchestva, ch. fiz., 1926, 8, 2.
- 214 Fok V.A. Izv. AN SSSR, Seriya geofiz., 1948, 12, 2
- 216 Frantov G.S. and N.M. Shuval-Sergeev Aeroelektorazvedka metodom beskonechno dlinnogo kabelya (Metodicheskoe rukovodstvo), 45. Izd. ONTI VITR, Leningrad, 1961.
- 215 Frantov G.S. and N.M. Shuval-Sergeev Razvedka i okhrana neдр. 1960, 1.
- 217 Frantov G.S. and N.M. Shuval-Sergeev Bulletin nauchno-tekhnicheskoi informatsii MG i ON SSSR, 1962, 1 (35).
- 218 Frantov G.S. - V kn.: Geofizicheskaya apparatura, 24. "Nedra", Leningrad, 1965.
- 219 Freinberg E.L. Rasprostranenie radiovoln vdol zemnoi poverkhnosti (Propagation of radio-waves along the earth surface) --- Izdvo AN SSSR, Moskva, 1961.
- 220 Frokin N.T. Indikatornye ustroistva (Indicating systems) --- Oborongiz, Moskva, 1956.

- 221 Frolov A.D. "Sovetskaya geologiya", 1960, 6.
- 222 Frolov A.D. - V kn.: Trudy mazhvuzovskoi konferentsii po inductivnym metodam rudnoi geofiziki. "Nedra", Moskva, 1964.
- 223 Kharkevich A.A. Ocherki obschei teorii svyazi. Gostekhzdat, Moskva, 1955.
- 224 Kharkevich A.A. Elektrosvyas, 1956, 5.
- 225 Kharkevich A.A. Teoreticheskie osnovy radiosvyazi (Theoretical fundamentals of radio-communication) --- Gostekhzdat, Moskva 1957.
- 226 Kharkevich A.A. Spektry i analiziz (Spectra and analysis) --- Fizmatgiz, Moskva, 1962.
- 227 Khomenyuk Yu.V. Izv. AN SSSR, Seriya Geofiz., 1961, 12.
- 228 Khomich V.I. Priemnye ferritovye anteny (Receiving ferrite antennas) --- Gosenergoizdat, Moskva, 1963.
- 229 Tsykin G.S. Elektronnye usiliteli (Electronic amplifiers). --- Svyaz'izdat, Moskva, 1960.
- 230 Shaub Yu. B. Izv. AN SSSR, seriya geofiz., 1961, 10.
- 231 Shaub Yu.B. - V kn.: Metodika i tekhnika razvedki, 26. Izd. Izd. ONTI VITR MG i ON SSSR, Leningrad, 1961
- 232 Shaub Yu.B. - V kn.: Geofizicheskoe priborostroenie, 8. Gostoptekhzdat, Leningrad, 1961.
- 233 Shaub Yu.B. Izv. AN SSSR, seriya geofiz., 1962, 2.

- 234 Shaub Yu.B. Osnovy aéroelektrorazvedki metodom vrashchayushchegosya magnitnogo polya (Fundamentals of aerial electric prospecting by method of rotating magnetic field) --- Gostoptekhnizdat, Leningrad, 1963.
- 235 Shaub Yu.B. Izv. AN SSSR, seriya geofiz., 1962, 7.
- 236 Shaub Yu.B. - V kn.: Geofizicheskoe priborostrosnie, 18. "Nedra", Leningrad, 1964
- 237 Shaub Yu.B. - V kn.: Geofizicheskoe priborostroenie, 21, Leningrad, 1964.
- 238 Shevtsov G.A., I.M. Vishenchuk and R.S. Kravtsov - V kn.: Doklady LPI, 1, 1. Izd. LPI, L'vov, 1955.
- 239 Sheinmann S.M. and G.S. Prantov - V kn.: Trudy VITR, 11. Izd. ONTI VITR, Leningrad, 1958.
- 240 Shirokov A.S. and A. Sh. Bogdanov Razvedka i okhrana neдр, 1954, 3.
- 241 Shirokov A.S., A.G. Tarkhov and A. Sh. Bogdanov - V kn.: Sostoyanie i puti razvitiya metodiki i apparatury elektricheskikh metodov poiskov i rasvedki tverdykh poleznykh iskopaemykh i inzhenerno-gidrogeologicheskikh izyskanii, 16. Izd. ONTI VIEMS GGK SSSR, Moskva, 1964.
- 242 Shuval-Sergeev N.M. and G.S. Frantov Sovetskaya geologiya, 1959, 1.
- 243 Shuval-Sergeev N.M. and G.S. Frantov - V kn.: Bulletin nauchno-tekhnicheskoi informatsii ONTI VIEMS MG i ON SSSR, 6(23). Gosgeoltekhizdat, Moskva, 1959.

- 244 Shuval-Sergeev N.M. and L.V. Artamonov V - kn.: Metodika i tekhnika razvedki, 26. Izd-vo ONTI VITR MG i ON SSSR, Leningrad, 1961.
- 245 Shtein B.B. and N.A. Chernyak Odnopolosnaya modulyatsiya s pomosh'yu fazovykh skhem (Single band modulation by means of phase circuits) --- Svyaz'izdat, Moskva, 1959.
- 246 Shumilovskii N.N. and V.Yu. Kneller Izv. vuzov, seriya priborostroeniya, 1958, 3.
- 247 Shchukin A.I. Rasprostranenie radiovoln (Propagation of radio-waves) --- Svyaz'izdat, Moskva, 1940.
- 248 Elektrovakuumnye pribory (spravochnik). Gosenergoizdat, Moskva, 1956.
- 249 Erlis K.E. and I.P. Stepanenko Elektronnyye usiliteli (Electronic amplifiers) --- Fizmatgiz, Moskva, 1961.
- 250 Yakubovskii Yu. V. - V kn.: Trudy MGRI im. Ordzhonikidze, 28. MGRI, 1955.
- 251 Yakubovskii Yu. V. Induktivnyi metod elektrorazvedki (Inductive method of electric prospecting) --- Gosgeoltekhizdat, Moskva, 1963.
- 252 Yanovskii B.M. Semnoi magnetizm (Earth magnetism) O--- Gostekhhizdat, Moskva, 1953.
- 253 Anderson W.C.U.S. patent No. 2697186, Official Gazette, 689, 2, 1954.
- 254 Barringer A.R. Mining Congress J., 1962, 48, 10.
- 255 Cloos E. Amer. J. Sci. 19/34, ser., V, 28, 166.
- 256 Canadian Mining J., 1959, 2,

- 257 Geophysics, 1955, 20, 2.
- 258 Helicopterborne electromagnetometer
test. Prospect of "Aeromagnetic surveys
LTD", Canada, 1957.
- 259 Kitai Electronic and Radio Eng., 1957, 34, 4.
- 260 Lundberg H. Canadian Mining J., 1959, 80, 4.
- 261 March H.W. Geophysics, 1953, 18, 3.
- 262 Pemberton R.H. Mining Eng., 1961, 13, 1.
- 263 Pemberton R.H. Geophysics, 1962, 27, 5.
- 264 Ruddock J., and
A.B. Clarcadall U.S. patent, No.2837650, Application,
May, 4, 505386, 1955.
- 265 Snellie D.W. Canadian Mining J., 1958, 79, 2.
- 266 Spiecker E.M. Bull. Amer. Petrol. Geol., 19
- 267 Torngquist. Geopgysik, 1956, 28, Oktober.
- 268 Ward S.H. et. al. Canadian Mining and Metallurg
1958, 51, 556.
- 269 Ward S.H. Geophysics, 24, 4, 1959.
- 270 Watt A.D. Maxwell E.L. - PJRE, 1957, 6.
-